GEOLOGICAL SURVEY OF CANADA
COMMISSION GÉOLOGIQUE DU CANADA

PAPER 78-1B

CURRENT RESEARCH
PART B

Energy, Mines and Resources Canada
Énergie, Mines et Ressources Canada

1978

Notice to Librarians and Indexers

The Geological Survey's thrice-yearly "Current Research" series contains many reports comparable in scope and subject matter to those appearing in scientific journals and other serials. All contributions to the Scientific and Technical Report section of "Current Research" include an abstract and bibliographic citation. It is hoped that these will assist you in cataloguing and indexing these reports and that this will result in a still wider dissemination of the results of the Geological Survey's research activities.

Technical editing and compilation
R.G. Blackadar
P.J. Griffin
H. Dumych
E.R.W. Neale

Production editing and layout
Leona R. Mahoney
Lorna A. Firth
Michael J. Kiel

Typed and checked by
Debby Busby
Janet Gilliland
Suzanne Lalonde
Janet Legere
Sharon Parnham

GEOLOGICAL SURVEY
PAPER 78-1B

CURRENT RESEARCH
PART B

1978

available by mail from

Printing and Publishing
Supply and Services Canada,
Hull, Québec, Canada K1A 0S9,

and

The Geological Survey of Canada
601 Booth St., Ottawa, K1A 0E8

or

Through your bookseller.

Catalogue No.	M44/78-1B	Price: Canada:	$5.00
ISBN -	0-660-01536-6	Other Countries:	$6.00

Price subject to change without notice

I : SCIENTIFIC AND TECHNICAL REPORTS

II : SCIENTIFIC AND TECHNICAL NOTES

III : DISCUSSIONS AND COMMUNICATIONS

INTRODUCTION

The fundamental role of the Geological Survey of Canada is to provide a comprehensive inventory and understanding of Canada's geological framework so that any activity that depends on geology is supplied with the necessary information. The principal aims are to supply geoscientific information necessary:

- to facilitate the discovery of mineral and energy resources.
- to evaluate the energy and mineral resources available to Canada.
- to identify geological hazards.
- to determine the capability of the landmass to withstand various types of use particularly in response to resource development and the disposal of wastes thereby assisting in conserving our natural environment.

The Geological Survey's work forms part of three EMR programs. In 1978-79 the bulk of the Survey's work is in the Geological Services Activity of the Earth Science Services Program whose objective is to "ensure the availability of geological information, technology and expertise concerning the description, understanding and evolution of the structure, composition, properties and processes of the earth's surficial deposits, crust and upper mantle, necessary for the identification of the resource base of Canada and the effective exploitation of mineral and energy resources".

Although the resources (dollars and man-years) assigned by the Geological Survey to the Energy and Mineral Programs are small compared to those assigned to the Earth Science Services Program, the information provided by the latter is critical to the success of the other two. Regional geological information is necessary before oil, gas, coal, uranium and mineral resource evaluations can be undertaken. Information on land stability must be in hand before pipelines can be planned and thus is essential when estimates of future supply are made. The geological environment of mineral and energy resources and the ways in which they accumulated must be understood before precise estimates of metallic mineral potential can be made.

The Energy Program is designed to ensure the availability and to promote effective use of the mineral resources available to Canada. As part of this program the Geological Survey participates in preparing assessments of oil and gas, coal and uranium resources.

The Mineral Program is designed to ensure adequate supply and to promote effective use of the mineral resources of Canada. The Geological Survey provides much of the information needed to facilitate the exploration and exploitation of such resources and to encourage their orderly development.

The Geological Survey of Canada is a branch of the Science and Technology Sector, Department of Energy, Mines and Resources. It currently has 780 man-years comprising 725 permanent staff of which 345 are university graduates with 195 holding doctorate degrees, mainly geologists, geophysicists and geochemists. The Geological Survey is the most decentralized branch of the department, having units in Ottawa; Dartmouth, Nova Scotia; Calgary, Alberta; and Vancouver and Patricia Bay, British Columbia. The branch is currently organized into 7 divisions based on major functions and to a lesser extent on geography.

Institute of Sedimentary and Petroleum Geology, Calgary, Alberta provides up-to-date information on the sedimentary basins of western and Arctic Canada. These areas contain most of Canada's oil, natural gas, and coal resources. It is also responsible, primarily, for making national assessments of petroleum and coal resources and for studying the nature and occurrence of these commodities.

Atlantic Geoscience Centre, Dartmouth, N.S., is concerned with studying all aspects of the marine geology of the Atlantic, and the central and eastern Arctic offshore areas and for providing the petroleum potential assessment for the Atlantic offshore.

Regional Economic Geology Division, Ottawa and Vancouver, is responsible for all aspects of the bedrock geology of Canada, excluding the Western Canada and Arctic sedimentary basins. Work in the Precambrian Shield and Appalachian regions is based in Ottawa whereas studies of Cordilleran geology are centred in Vancouver. A marine geology unit of the Cordilleran Subdivision at the Pacific Geoscience Centre, Patricia Bay, B.C., is responsible for studying the bedrock and unconsolidated sediments of the Pacific and Western Arctic offshore areas. The division is also concerned with establishing the conditions under which metallic mineral deposits occur and for describing and assessing their potential abundance and probable distribution.

Resource Geophysics and Geochemistry Division, based in Ottawa, provides geophysical and geochemical information needed for the exploration and evaluation of Canada's uranium and mineral resources. National systematic surveys such as the Federal-Provincial Uranium Reconnaissance Program (started in 1975) and the Federal-Provincial Aeromagnetic Program (active since 1961) are the responsibility of this division. As part of a national commitment the division undertakes the development, testing, calibration and standardization of geophysical and geochemical technology. Most of the Geological Survey's external activities (e.g. CIDA) are managed by this division.

Terrain Sciences Division, based largely in Ottawa, is concerned with the surficial geology of Canada. It undertakes systematic surveys as well as more detailed studies. An important part of the work is the assessment of the occurrence and magnitude of natural terrain hazards and the capability of the landmass for use. Engineering and environmental geology investigations are also undertaken by this division.

Geological Information Division, based in Ottawa, is responsible for the communication of results of the scientific work of the Geological Survey in the form of reports, maps, charts, and data released to users and potential users; the maintenance of the scientific library and associated data systems as an earth science information base; and the provision of geoscience information to the public. In support of these objectives the division maintains capabilities and facilities in scientific editing and information, cartography, and the library.

Central Laboratories and Administrative Services, based in Ottawa, provides chemical, mineralogical and technical support, mainly to Ottawa-based units, and the co-ordination of administrative, financial and personnel services.

The senior branch management staff is in Ottawa as are the Branch Program and Evaluation Office, the Data Systems Group and Special Projects related to national and international activities.

The reports and notes that make up this publication all contribute to one or more of the departmental programs and are planned and carried out by the various divisions. The variety of topics reflects the wide range of subjects studied as part of the Geological Survey's program but because this publication is issued three times each year no single volume is likely to cover the full range of activity.

Public interest and attention was drawn to one aspect of the Geological Survey's work when the branch was asked to participate in "Operation Morning Light" - the recovery of the remains of the Soviet satellite Cosmos 954 which disintegrated over northern Canada on January 24, 1978. Report 24 describes the results of the search carried out by various Canadian and United States organizations.

The nature and distribution of uranium deposits must be understood if reliable estimates are to be made of Canada's resources of this source of energy. Reports 21 and 23 describe the geology of deposits in Cape Breton and in the district of Mackenzie. Report 22 presents results of a study designed to assist in understanding the formation of uranium deposits and Report 8 gives results of a radiometric survey carried out near North Bay, Ontario.

As part of its contribution to the discovery of mineral resources the Geological Survey carries out studies of new exploration techniques. Indeed it has a leading role in developing geophysical and geochemical methodology. Reports 7 and 18 give results of two such studies.

In order to investigate and map the geology and near surface structure of rocks on the eastern continental shelf, studies such as those reported in reports 3 and 19 are carried out. This work is facilitated by geophysical studies some of which have been the subject of earlier reports. The continental margins are assuming an increasing importance in the search for oil and gas resources. A fuller understanding of the geology of these areas is essential for making more accurate estimates.

Information on bedrock and surficial geology is obtained through systematic surveys. Such information is basic to many of the activities carried out by the Geological Survey. Mineral and energy resources cannot be evaluated unless the regional geological framework is understood. Potential damage to the environment cannot be assessed unless the nature of the surficial materials is known. Report 2 presents the interim results of a study of a part of the Canadian Shield in the district of Keewatin. The area was mapped on a reconnaissance scale in the early 1950's but much more information is needed concerning the structure and stratigraphy of the metasedimentary and metavolcanic rocks and their relationships to the gneissic rocks. Such information contributes to an understanding of the presence or absence of mineral deposits from certain geological associations. Report 20 describes the surficial geology of an area west of Montreal. The results will be useful to those responsible for planning urban growth as well as to those involved in environmental matters. The study is part of a continuing study of the surficial deposits of the Ottawa Valley Lowlands designed to map, describe and explain the unconsolidated deposits and landforms of the area in order to provide the geological and terrain information pertinent to land use planning, agriculture, urban and industrial development, forestry and engineering construction.

The addition of a "Discussion and Communications" section to "Current Research, Part A" in January 1978 has been well received. Contributions are welcome and, subject to editorial acceptibility, will be published in the first issue following their receipt. A note to Contributors accompanies Part III of this publication. Manuscripts for inclusion in this volume were accepted until April 18.

Ottawa, May 1, 1978

R.G. Blackadar
Chief Scientific Editor

Separates

A limited number of separates of the papers that appear in this volume are available by direct request to the individual authors. The addresses of the Geological Survey of Canada offices follow:

601 Booth Street,
OTTAWA, Ontario
K1A 0E8

Institute of Sedimentary and Petroleum Geology,
3303-33rd Street N.W.,
CALGARY, Alberta
T2L 2A7

British Columbia Office,
100 West Pender Street,
VANCOUVER, B.C.
V6B 1R8

Atlantic Geoscience Centre,
Bedford Institute of Oceanography,
P.O. Box 1006,
DARTMOUTH, N.S.
B2Y 4A2

When no location accompanies an author's name in the title of a paper, the Ottawa address should be used.

ERRATUM

Current Research, Pt. A, Geol. Surv. Can., Paper 78-1A.
The text on pages 226 and 227 has been interchanged.

1. OCCURRENCE OF A LARGE PHYLLOCARID CRUSTACEAN OF LATE DEVONIAN-EARLY CARBONIFEROUS AGE FROM YUKON TERRITORY

Project 720072

M.J. Copeland and W.D. Ian Rolfe[1]

Abstract

Copeland, M.J. and Rolfe, W.D. Ian, Occurrence of a large phyllocarid crustacean of Late Devonian-Early Carboniferous age from Yukon Territory; in Current Research, Part B, Geol. Surv. Can., Paper 78-1B, p. 1-5, 1978.

*Two specimens of a large archaeostracan phyllocarid (**Dithyrocaris**? sp.) are reported from unnamed strata of Famennian-Early Mississippian age in northeastern Yukon Territory. The morphology of the carapace is unknown, but, for the first time, the presence of eight thoracic somites and seven pretelson abdominal somites can be demonstrated for a rhinocaridid, as well as the area originally occupied by anal integument, beneath the telson head.*

Introduction

Through the courtesy of Mr. John Senyk, Canadian Forestry Service, two fossil phyllocarid specimens were submitted for examination. These archaeostracans occur in three pieces of rock, one showing a telson with furcal rami (Pl. 1.1, fig. 2) 6 inches (15 cm) long and two comprising the 'part' of the anterior and the 'counterpart' of the posterior of another specimen 17.5 inches (44.5 cm) long (Pl. 1.1, fig. 1). Neither specimen is intact, but the larger individual, if complete, would have been about 27 inches (69.5 cm) in length, making it one of the largest phyllocarids yet reported.

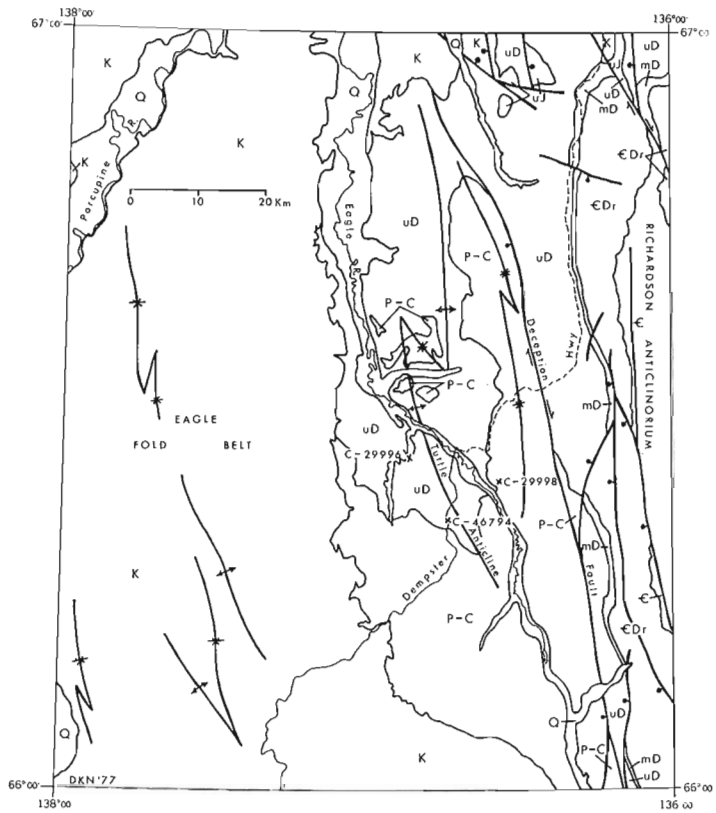

Figure 1.1. Geological map of Eagle River area (116 I), Yukon Territory, showing the stratigraphic and structural setting of GSC loc. C-46794 from which the two phyllocarid specimens were recovered.

LEGEND

QUATERNARY
Q — Undifferentiated fluviatile and lacustrine clay, silt, sand and gravel.

CRETACEOUS
Upper and Lower Cretaceous
K — Sandstone, siltstone and shale (includes Eagle Plain Formation).

JURASSIC
Upper Jurassic (mainly)
uJ — Sandstone, siltstone and limestone (includes strata of possible Late Triassic age).

PERMIAN and CARBONIFEROUS
P-C — Undifferentiated unnamed shale, Hart River, Ettrain and Jungle Creek formations.

DEVONIAN
Upper Devonian
uD — Unnamed sandstone, siltstone and shale, partly coeval with the Imperial Formation.

Middle and/or Lower Devonian
mD — Unnamed siltstone, shale and limestone.

DEVONIAN, SILURIAN, ORDOVICIAN and CAMBRIAN
Lower Devonian, Silurian, Ordovician, and Upper Cambrian Road River Formation
€Dr — Shale, limestone, chert and breccia conglomerate.

Upper and Middle Cambrian
€ — Undifferentiated shale, siltstone and sandstone.

Geology by D.K. Norris (unpubl.). Based on field observations by D.K. Norris, E.W. Bamber, J.A. Jeletzky, E.W. Mountjoy, B.S. Norford, A.W. Norris and G.R. Turnquist.

[1]Hunterian Museum, The University, Glasgow, Scotland.

The specimens were obtained by Mr. Senyk from debris at the base of a forty foot high (12 m) road cut near milepost 230 along the southeast side of Dempster Highway at 66°21'30"N, 136°45'W, 6.8 miles (12 km) southwest of Eagle River Crossing, Yukon Territory (GSC loc. C-46794). They are from a light brown siltstone bed that contained other, uncollected, fossil remains.

D.K. Norris, Geological Survey of Canada, provided the accompanying map (Fig. 1.1) and following stratigraphic information:

> "The locality is on the west flank of Richardson Anticlinorium adjacent to Eagle Fold Belt" (Fig. 1.1). "There, near the nose of south-plunging Tuttle Anticline, the fresh bedrock exposures along Dempster Highway appear to lie intermediate in stratigraphic position between dark grey shale with thin, resistant interbeds of fine grained sandstone (GSC loc. C-29996) on the west flank of the anticline, and dark grey, earthy weathering mudstone (GSC loc. C-29998) on the east flank. According to W.W. Brideaux (Internal Report, 1974) the shale at loc. C-29996 contains spores, often highly carbonized, of Late Devonian, probably Famennian age. The mudstone at loc. C-29998 contains abundant, moderately well preserved spores of Early Carboniferous age, according to D.C. McGregor (Internal Report, 1974). If field mapping is correct and the paleontological ages are representative, therefore, the roadside exposures containing the phyllocarids may be no older than Late Devonian, Famennian, and no younger than Early Carboniferous".

The specimens are preserved as flattened impressions. In order to reconstruct the figure of the larger individual (GSC 47803) the photographic negative of the 'counterpart' (B) of the specimen (Pl. 1.1, fig. 1) was reversed to obtain an image conforming in orientation with that of the anterior 'part' (A). Several inches of overlap occur between the two pieces of rock, permitting reliable determination of their relative positions. A reconstruction based on this photographic restoration is shown in Figure 1.2.

The smaller specimen containing a telson and furcal rami in ventral aspect (GSC 47804) was cut along the dotted lines shown on Plate 1.1, figure 2. Samples (A_1, B_1) were submitted to D.C. McGregor and T.T. Uyeno, Geological Survey of Canada, for palynological and conodont analyses respectively. Neither sample provided identifiable microfossils, conodonts were absent, and palynological preparations revealed only the presence of much macerated plant debris.

Discussion

The presence of the median dorsal plate of the carapace in specimen GSC 47803 confirms the assignment of these specimens to the Archaeostraca but does not permit exact determination of their generic identity within the Rhinocarididae. Such identification depends primarily on carapace shape and the nature of surface ornamentation — characteristics mostly lacking here. Even so, comparison with other fossil crustaceans would seem to indicate that these are extremely variable characteristics on which to base generic relationships. The specimens described here are extremely large, possibly slightly longer than **Hebertocaris** (= ?**Dithyrocaris**) **wideneri** Stumm and Chilman (Kesling and Chilman, 1975, p. 157) from the Middle Devonian Silica Formation of Ohio. Both species have typical, striate posterior abdominal ornamentation and the furcal rami are proximally broad (Pl. 1.1, fig. 2; Kesling and Chilman, 1975, Pl. 35). Restoration of **H.** (= ?**D.**) **wideneri** indicates that at

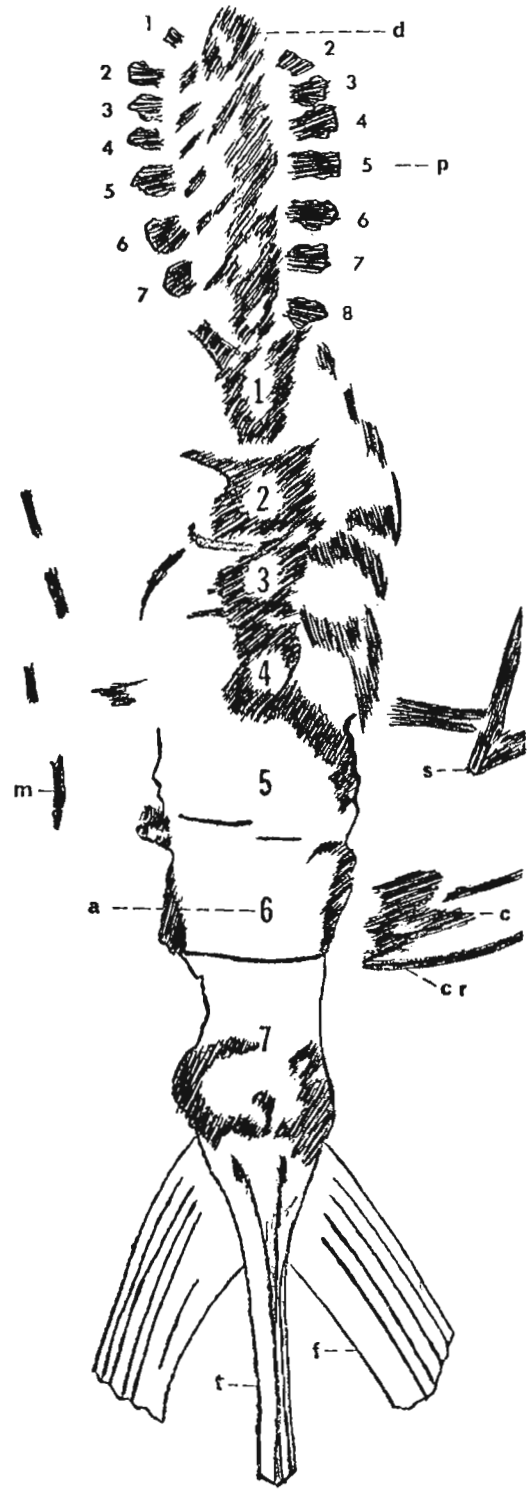

a - abdominal somite
c - carapace
cr - carapace rim
d - median dorsal plate
f - furcal ramus
t - telson
m - mesolateral carina of carapace
p - pereiopods
s - posteroventral spine of carapace

Figure 1.2. **Dithyrocaris**? sp. (GSC 47803), length 44.5 cm.

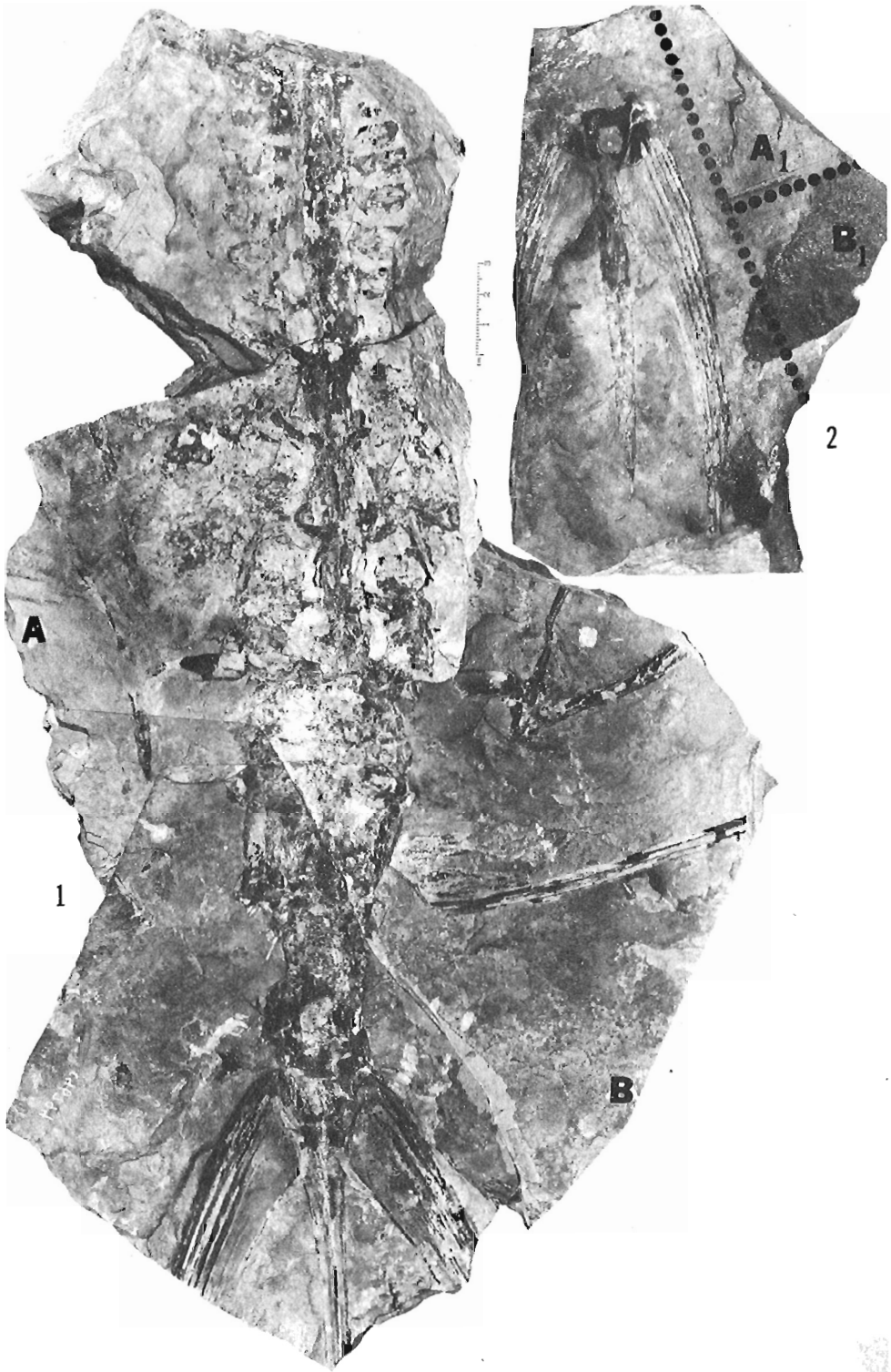

Plate 1.1. **Dithyrocaris**? sp. (scale in centimetres)

Figure 1. Photographic reconstruction of GSC 47803.

Figure 2. Ventral view of telson and furcal rami, showing hole formerly occupied by anal integument, GSC 47804.

least part of the proximal constriction in width of the furcal rami could be seen in dorsal view if the rami were preserved in laterally extended position. It is possible that general size and ornamentation of the furcal rami may prove of certain specific taxonomic value. Notwithstanding Bowman (1971) the terminology of Rolfe (1969) has been adhered to for telson and furca.

As previously observed (Rolfe, 1969, p. R312) "Recent Leptostraca are differentiated mainly by their limb structure, and if found fossil they would be separated into only two genera on the basis of carapace form...". Taxonomic grouping based on body divisions and associated appendages will probably also prove valid for dividing the Archaeostraca, but the degree to which these criteria may be applied will depend on the discovery of sufficiently well preserved material. The importance of the present collection rests in the fact that two tagmata with some appendages can be distinguished in the trunk of an individual rhinocaridid (Pl. 1.1, fig. 1). From specimen GSC 47803 it is possible to determine (Fig. 1.2) with some accuracy the posterior 16 of the probable 22 somites comprising the body divisions of an archaeostracan – 8 thoracic, 7 pretelsonal abdominal and telson with furcal rami. Such a succession of body divisions, though anteriorly incomplete, is compatible with that of modern phyllocarids but is the first reliable demonstration for a species of the Rhinocarididae (cf. Rolfe, 1969, fig. 122). No appendiculate pre-thoracic somites are preserved as that portion of the specimen is missing. The 8 thoracic somites are determinable by the presence of paired lamellar pereiopods 1-7 on the left side as illustrated and 2-8 on the right side, in proximity to the median dorsal plate. The complete structure of the thoracopods, however, is unknown. There are seven distinct pretelson abdominal somites, although the five most anterior somites are somewhat obscured by the median dorsal plate. Distinction of this abdominal segmentation would be much facilitated if pleopods were present, but none is preserved.

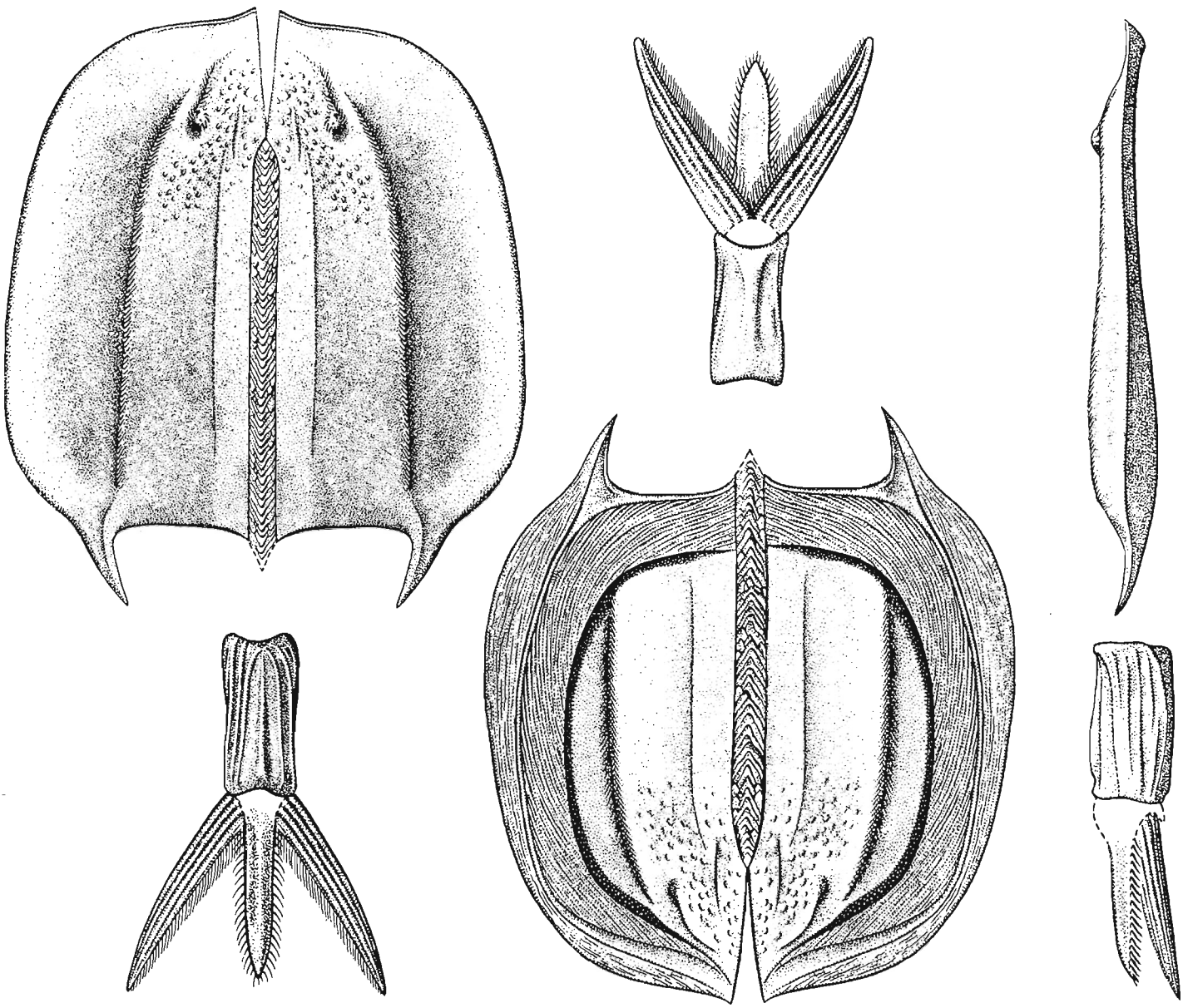

Figure 1.3. Reconstruction of **Dithyrocaris paradoxides** (De Koninck), Viséan, Belgium, showing dorsal, ventral and right lateral views of carapace, pretelson somite and telson with furcal rami. (The posteriorly convergent striae have been omitted by the artist from the ventral surface of the pretelson somite.) Total length, c. 13 cm (after Rolfe, 1969).

The telson is long and thin, about two thirds the length of the furcal rami (Pl. 1.1, fig. 2) and bears a strong median carina. For the first time in any rhinocaridid it is possible to demonstrate (Pl. 1.1, fig. 2) the aperture on the ventral surface of the telson head, formerly occupied by the anal integument (Rolfe, 1969, p. R303, fig. 126). A similar aperture may be detected on **Hebertocaris** (= ?**D.**) **wideneri** in the ventral aspect of the telson shown in Stumm and Chilman (1969, Pl. 6, fig. 4). The furcal rami are stout, broad, tapering distally, with 7 strong longitudinal ribs. The exterior ribs commence proximally on the ramus, whereas the interior ribs are progressively shorter and commence distally up to one third along the length of the furcal ramus, leaving the proximal interior surface of each ramus relatively unornamented.

The following approximate measurements (in centimetres) of **Dithyrocaris**? sp. have been derived from examination of specimens GSC 47803, 47804 and extrapolation from published figures of **Hebertocaris** (= ?**D.**) **wideneri**:

Prethorax (including cephalon and anterior part of the carapace)	ca. 18.5
Thorax	9
Abdomen	23.5
segment 1	2.0
2	2.75
3	2.25
4	2.75
5	3.75
6	4.50
7	5.50
Telson from anterior of telson head to tip of furcal ramus	18.5
	69.5

If these approximations are valid, the median carapace length (with rostrum) would be 35.5 cm, with the exsert portion of the abdomen (by analogy with **Nahecaris**, ca. last 41/2 somites) being 34 cm, giving a total body length of 69.5 cm. This considerably exceeds the length of **Hebertocaris** (Stumm and Chilman, 1969, p. 64) and is perhaps the largest rhinocaridid known. It is slightly shorter than the largest archaeostracan, **Schugurocaris**, which attains 75 cm (Rolfe, 1969, p. R297), but larger than known specimens of **Schugurocaris**? **cornwallisensis** (Copeland) of Silurian age from the Canadian Arctic (Copeland, 1960, 1971).

Remarks

The genera of Rhinocarididae require revision on a worldwide basis. Until this has been done the erection of new genera may be unwarranted. **Hebertocaris** Stumm and Chilman, 1969 may only be based on old instars of **Dithyrocaris** cf. **D. neptuni** (sensu Stumm and Chilman, 1969, p. 60) – the cuspate ornamentation of the carapace is reminiscent of that which appears only on what are interpreted as old individuals of **Ceratiocaris papilio** (Rolfe, 1962, p. 916, Pl. 132, fig. 5-7). Also, large, old individuals of **Montecaris** show proliferation of carapace ornament (Rolfe, in Brunton, Miles and Rolfe, 1969, p. 81). It would be expected that a range of smaller instars representing immature stages of these large individuals would be found. The posteriorly convergent striae of the pretelson somite of **Hebertocaris** appear to be on the ventral surface (Stumm and Chilman, 1969, Pl. 6, fig. 2) not on the dorsal surface (ibid., cf. text-fig. 3, text-fig. 1, 2 and corresponding plates), as in most **Dithyrocaris** species and many other phyllocarids, and this removes one purportedly distinctive feature (Fig. 1.3). The spinose rostral and ?median dorsal plates and the broad, weakly striated furcal rami are perhaps distinctive enough to warrant retention of the genus **Hebertocaris**, but these features require reviewing over the entire **Dithyrocaris** species complex before their significance, generic or otherwise, can be interpreted. **Mesothyra** Hall (in Hall and Clarke, 1888) has often been similarly regarded as a discrete genus, but it only differs from **Dithyrocaris** in having a tubercle, or hinge node, at the junction of the carapace valves (Rolfe, 1962, p. 917), and in having less prominent ridges on the caudal furca. The internal setation of the furcal ramus of **Mesothyra** is of questionable diagnostic significance as the type species of **Dithyrocaris** shows bases of setae in a similar position. It was for this reason that **Mesothyra** was placed in synonymy with **Dithyrocaris** (Copeland, 1967; Rolfe, 1969, p. R321; and previous authors), and why **Dithyrocaris** is used here in such an omnibus sense.

References

Bowman, T.E.
1971: The case of the non-ubiquitous telson and the fraudulent furca; Crustaceana, v. 21, p. 165-175.

Brunton, C.H., Miles, R.S., and Rolfe, W.D.I.
1969: Gogo Expedition 1967; Proc. Geol. Soc. London, no. 1655, p. 79-83.

Copeland, M.J.
1960: New occurrences of **Ceratiocaris** and **Ptychocaris** (Phyllocarida) from the Canadian Arctic; Geol. Surv. Can., Bull. 60, p. 49-54.

1967: A new species of **Dithyrocaris** (Phyllocarida) from the Imo Formation, Upper Mississippian, of Arkansas; J. Paleontol., v. 41, no. 5, p. 1195, 1196.

1971: Additional Silurian Arthropoda from Arctic and eastern Canada; Geol. Surv. Can., Bull. 200, p. 19-26.

Hall, J. and Clarke, J.M.
1888: Palaeontology: Vol. VII. Text and Plates. Containing descriptions of the trilobites and other Crustacea of the Oriskany, Upper Helderberg, Hamilton, Portage, Chemung and Catskill Groups; Geol. Surv., New York.

Kesling, R.V. and Chilman, R.B.
1975: Strata and megafossils of the Middle Devonian Silica Formation; Univ. Michigan, Mus. Pal., Papers on Paleontology no. 8.

Rolfe, W.D.I.
1962: Grosser morphology of the Scottish Silurian phyllocarid crustacean, **Ceratiocaris papilio** Salter in Murchison; J. Paleontol., v. 36, no. 5, p. 912-932.

1969: Phyllocarida; in Moore, R.C., Treatise on Invertebrate Paleontology, Part R, Arthropoda 4, p. R296-R331.

Stumm, E.C. and Chilman, R.B.
1969: Phyllocarid crustaceans from the Middle Devonian Silica Shale of northwestern Ohio and southeastern Michigan; Univ. Michigan, Contrib. Mus. Paleontol., v. 23, no. 3, p. 53-71.

2. STRATIGRAPHY AND STRUCTURE OF THE NORTHERN AMER GROUP (APHEBIAN), CHURCHILL STRUCTURAL PROVINCE, DISTRICT OF KEEWATIN

Project 760025

Clinton R. Tippett[1] and W.W. Heywood
Regional and Economic Geology Division

Abstract

Tippett, Clinton R., and Heywood, W.W., Stratigraphy and structure of the northern Amer group (Aphebian), Churchill Structural Province, District of Keewatin; in Current Research, Part B, Geol. Surv. Can., Paper 78-1B, p. 7-11, 1978.

Aphebian supracrustal rocks of the Amer group, exposed in a west-southwest trending synclinorium, have been subdivided into seven informal lithological units. They were deposited on a basement complex of probable Archean age. Discontinuous basal feldspathic sandstone and muscovite schist are overlain by orthoquartzite which locally may be differentiated into basal red, middle white and upper grey divisions. Above it, a thin, impure and commonly iron-rich clastic unit is followed by a pervasively crossbedded pink feldspathic quartzite. These lower clastic units are separated from the overlying clastic assemblage by a dolomitic limestone unit containing abundant laminae of cherty orthoquartzite. The carbonate unit is transitional upwards into a pelitic unit in which beds of impure brown carbonate alternate with slates and phyllites. The highest and thickest unit is a complex red sandstone-siltstone-phyllite assemblage which contains scattered beds of calcareous sandstone and carbonate pebble to boulder conglomerate.

The lower Amer group is affected by thrusts producing slices of lower Amer group rocks and thin slivers of basement rocks. The dolomitic limestone unit appears to have acted as a plane of décollement within the sediments as it locally forms soles of thrust faults and contains recumbent isoclinal folds and boudins, in contrast to the adjacent, apparently rigidly translated quartzite slices. Upright folding, which, in the central part of the belt may be related to thrusting, was followed by a phase of subvertical compression producing a subhorizontal crenulation cleavage. The latest phase of deformation resulted in a set of northwest-southeast normal faults which have systematically reduced the exposed width of the southwest plunging Amer group.

Metamorphic grade increases towards the south and west. To the east the orthoquartzite contains kyanite-bearing quartz veins, to the west both kyanite and sillimanite are present in quartz pebble conglomerate in the basal part of the supracrustal section.

Introduction

The area of Keewatin discussed in this paper (66H N1/2) was covered by reconnaissance mapping in 1954 (Wright, 1955). This mapping defined a belt of metasediments dominated by orthoquartzites, which was correlated with the Hurwitz Group. More detailed systematic work on the overall structure and stratigraphy of the Amer group began with the 1:250 000 mapping of the Amer Lake map area in 1976 (Heywood, 1977). This paper presents the stratigraphy of the Amer Group and an interpretation of the structural complexities of the area.

Stratigraphy

Basement Complex

The Amer group overlies a heterogeneous assemblage of rocks collectively referred to as the basement complex. This heterogeneity, together with locally observed discordance of trends between the lowermost unit of the Amer group and the basement complex suggests an unconformable relationship. The basement is chiefly a composite of four rock associations, namely:

1. the assemblage of metamorphosed intermediate to mafic volcanogenic rocks, ultramafic rocks, and diorite (along the southern margin);

2. granitoid rocks including lineated augen gneisses (mainly along the southeast and east margins) and medium grained granodioritic to granitic gneisses (along the east, northeast and north margins);

3. layered mafic schists containing variable combinations of hornblende, plagioclase, garnet and biotite (as small pods within the granitoid rocks along the northern margin); and

4. dark grey to orange, thinly to moderately layered biotite-hornblende schists and paragneisses with minor carbonate, amphibolite and iron formation (along the western end of the northern margin).

Locally, a distinct decrease in grain size was noted in some granitoids near the basement-cover contact. There the rocks are red, very fine grained and contain nebulous biotite wisps and quartz pod schistosity. Minor muscovite is present in some basement rocks near the contact. The basement-cover contact is generally well defined, however, in many places the relations are obscured by metamorphism and deformation.

Basement rocks of types 2 and 3 are intercalated with the Amer group on the north side of the belt along thrust faults which cut the basement and may be traced back to the main basement exposures along the fault traces. In one area a thrust slice of basement varies from type 2 to type 3 along strike.

The Amer group

The Amer group consists of seven units exposed along the northern margin of the belt (Fig. 2.1). In general two thick clastic subdivisions are present. The transition between them is a series of somewhat variable thin units (Fig. 2.2). At higher grades of metamorphism and greater degrees of

[1] Department of Geological Sciences, Queen's University, Kingston, Ontario, K7L 3N6.

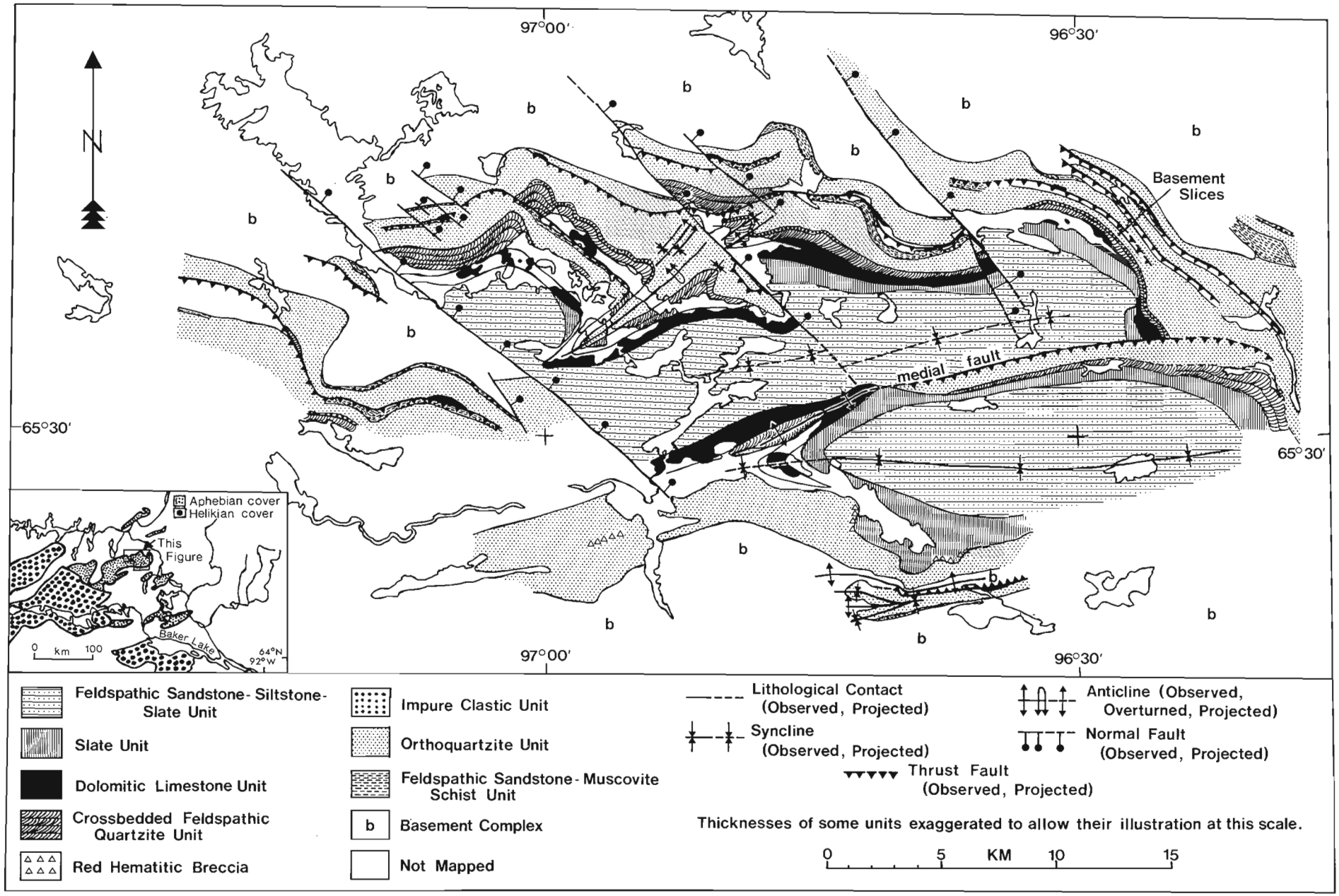

Figure 2.1. Lithological and structural map of the eastern Amer Lake synclinorium.

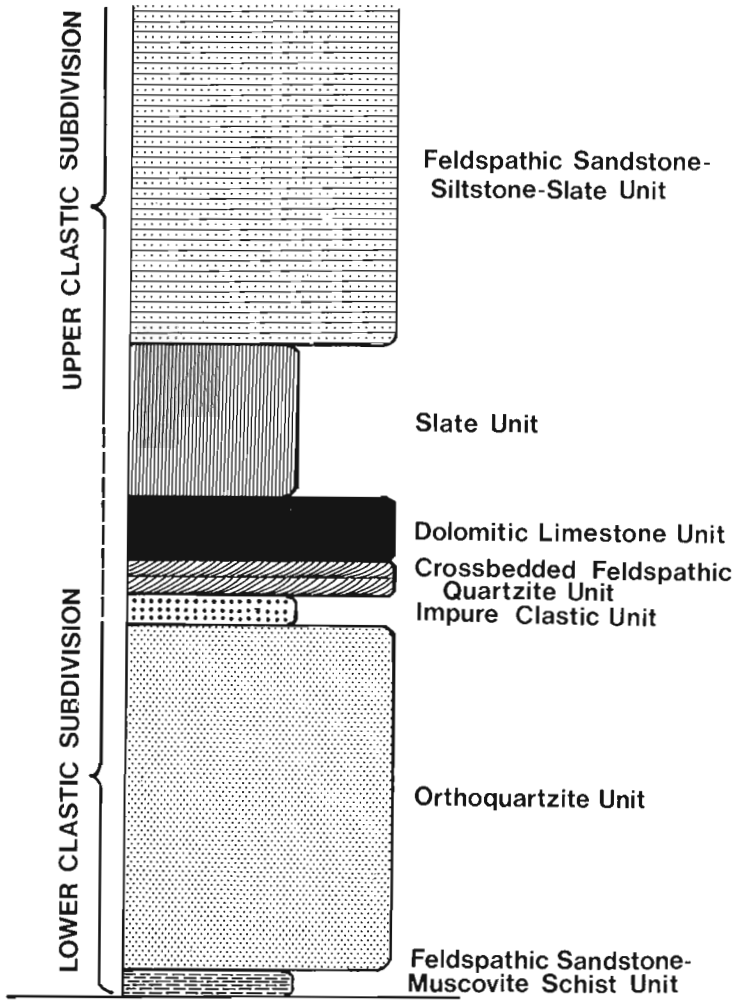

Figure 2.2. Stratigraphic column of the Amer group. Unit thicknesses not to scale.

higher grades of metamorphism and greater degrees of deformation in the west, finer details are lost but the overall sequence is similar.

1. Basal feldspathic sandstone and muscovite schist unit (0-30 m). The lowest unit of the Amer group is a somewhat discontinuous assemblage of slightly muscovitic schist layered on a scale of 1 mm to 2 m, averaging 5-30 cm. Grain size ranges from 0.5 to 4 mm, and averages 1 mm. Boudinaged and tightly folded medium to coarse grained quartz veins are common. Along the southern margin of the belt several tens of metres of quartz and, more rarely, granite and mafic pebble conglomerate occur within the basal unit. Where thrust faults have penetrated the basal section of the metasediments, the zone of schistose quartzite is expanded by the development of a pervasive fracture cleavage.

2. Orthoquartzite unit (400-1000 m). Light grey to white orthoquartzite forms the most prominent unit of the Amer group. Grain size averages 0.5 to 1 mm although some lenses along the southern margin contain granules and pebbles as much as 1 cm in diameter. Laterally discontinuous and sparsely distributed lenses of pebble conglomerate as much as 20 m thick consist predominantly of medium grained vein quartz pebbles and cobbles from 1 to 10 cm in diameter. Mafic chips are locally present in the lenses. Bedding is poorly defined and, where recognizable, takes the form of faint colour laminations from 1 to 10 cm thick. Plane bedded subunits containing rare current ripples dominate with scattered 10 to 20 cm thick crossbeds present near the top of the unit.

Colour variations locally useful in the subdivision of the unit, are present along the northern edge of the belt but fade out to the east and west. Blotchy to uniformly coloured, reddish to mauve quartzite is overlain by white quartzite which is capped by grey quartzite. Elsewhere, greenish and brownish variations are present.

3. Impure clastic unit (5-20 m). The orthoquartzite unit is overlain by a thin but laterally continuous unit which commonly contains a large amount of iron in the form of oxides, sulphides or silicates. Along the northern margin it is usually a fine grained, massive to flaggy, dark grey to black biotite siltstone or sandstone with some zones of sintery pyritiferous slate or red hematitic garnetiferous siltstone. The underlying quartzite passes rapidly into this unit with local development of a pyritiferous quartzite or dark grey quartzite interbedded with pelite on the scale of 5 to 10 mm.

Along the southern margin, the interval between the upper and lower clastic subdivisions is marked, at least locally, by a distinctive red conglomerate or breccia. This unlayered mixture is made up of a very fine grained red shaly matrix with angular to subangular clasts of fine grained quartzite comprising 10 to 95 per cent of the rock, ranging from matrix size up to 50 cm and averaging 1 to 2 cm in diameter. Vugs in the rock contain millimetre-sized crystals of specular hematite. Bounding lithologies are commonly white orthoquartzite and thinly laminated red mudstone. The fact that it outcrops below the quartzite in several places near the southern margin would seem to eliminate the possibility mentioned by Bell (1969) that it is a basal member of the Helikian Dubawnt Group. It may be a fault mélange of the white orthoquartzite and the thinly laminated red mudstone, or it could equally well be a brecciated quartzite recemented with a red mudstone matrix near the time of deposition.

4. Crossbedded feldspathic quartzite unit (10-30 m). The second unit in the transition between lower and upper clastic subdivisions is typically a pink feldspathic quartzite with an average grain size of 0.5 to 1 mm,containing 5 to 8 per cent unimodal pink, white and orange feldspar grains whose concentration defines compositional layering. The unit is pervasively crossbedded on the scale of 10 to 30 cm and, where the impure clastic unit is absent, may appear to be gradational to the slightly crossbedded upper part of the orthoquartzite unit. In the centre of the belt, as exposed along the "medial fault", the unit contains 3 to 5 cm black laminations which are probably correlatives of pelitic interbeds present along the southern margin. As well, crossbedding in the central zone is poorly developed, probably transitional to the plane bedded assemblage to the south. Towards the west the unit becomes more heterogeneous, such that north of Amer Lake the unit is a mixture of strongly crossbedded feldspathic quartzite, pink nonfeldspathic quartzite, red quartzose schist and quartzite with rare 0.5 to 20 cm muscovite lenticles.

5. Dolomitic limestone unit (30-50 m). Light buff weathering, fine grained dolomitic limestone occurs above the feldspathic quartzite but does not appear to be gradational with it. Thin, fine grained quartzite layers 0.1 mm to 1 m thick comprise 5 to 80 per cent, and average 35 per cent

of the unit. They are clustered into quartzite-dominated and dolomite-dominated bands on the outcrop scale, however, there does not appear to be any consistent regional variation in relative proportions. Although more or less continuous, quartzite layers are extensively boudinaged and/or isoclinally folded by the intense deformation localized in the unit. Locally abundant pre- and post-tectonic quartz veins may represent remobilized silica from the quartzite layers. At one location, calcitic and dolomitic marble interlayered on the scale of 3 to 5 cm were observed. The bulk of the unit is an alternation of monomineralic dolomite and quartz layers with minor amounts of metamorphic minerals such as tremolite, diopside, phlogopite, talc and calcite. Schistose tremolite-phlogopite layers are abundant along the traces of thrust faults.

The dolomite unit is most abundant along the northern margin; its relative absence to the south may reflect tectonic control rather than original distribution. Pale red to pink carbonate associated with the red laminated mudstone, however, may be equivalent to the main dolomitic unit, suggesting a facies change to the south. The unit passes upwards into the overlying pelites with an increase in micaceous and clastic components.

6. Slate unit (50-300 m). The slate unit is the uppermost unit of the transition between the upper and lower clastic subdivisions. Along the northern margin it is generally a dark grey to black, locally pyritiferous, slate to phyllite containing a variable component (usually 20 to 30 per cent) of boudinaged dark chocolate brown-weathering carbonate beds 1 to 30 cm thick. To the south thinly laminated red and grey slates and mudstones may be equivalent to this unit. The transition to the overlying unit occurs with the appearance of millimetre to metre thick beds of pink feldspathic detritus.

7. Feldspathic sandstone-siltstone-slate unit (3000 m +). This upper unit is a heterogeneous assemblage of clastic rocks arranged in lensoidal fashion, within which subunits are often distinguishable along a single traverse but in which correlations between adjacent traverses are difficult. There does not appear to be a regional pattern to the distribution of the dominant pink, red and grey feldspathic sandstone, orange to green siltstone, and grey to black slates although unrecognized folding in the core of the synclinorium where the unit is exposed, as well as poor outcrop, may account for the apparent lack of order. In the northern half of the area, overall impressions are of a dominantly feldspathic sandstone middle subunit grading into more pelitic rocks both above and below. To the south, the laminated mudstones grade upward into a fine to locally medium grained feldspathic sandstone which is the highest unit exposed.

Compositional layering in the dominantly feldspathic part of the unit apparently mimics the overall nature of the unit with abundant pinch and swell structures. Beds range from 1 mm to 2 m, average 20 to 30 cm thick and contain faint colour laminations measureable in millimetres. Sedimentary structures include rare current ripples, sandstone dykes, small scale ripples, and at least one large scale crossbed 2 m thick. Commonly a web of slaty wisps constituting 20 per cent of the rock encloses centimetre-sized pods of red sandstone. Elsewhere these isolated wisps define bedding even in sandstones containing less slate.

Light pink, slightly friable calcareous feldspathic sandstone beds 1 cm to 1 m in thickness form 5 to 10 per cent of the outcrops of this unit and locally exhibit graded bedding and basal scours. In some places purplish weathering calcareous sandstone beds contain blocks of buff dolomitic limestone as large as 25 by 50 cm, averaging 5 by 10 cm, as well as blocks of possibly more locally derived calcareous feldspathic sandstone. The resemblance of the dolomitic blocks to the dolomitic limestone unit (division 5) suggests that the latter was being eroded during deposition of the upper unit. It is not known whether the upper clastic subdivision is separated from the transitional units by an unconformity or, alternatively, whether the slumping of carbonate-rich detritus of this unit occurred from a contemporaneous carbonate accumulation.

Structural Geology

Geometry

The Amer group is exposed in a complexly faulted west-southwest-plunging synclinorium outlined by the high-standing orthoquartzite unit which encloses a tightly folded core (Fig. 2.1). The basement complex and the lower units of the Amer group, up to and including the dolomitic limestone unit, have been intercalated by means of thrust faulting around the margins of the synclinorium, producing an exaggerated quartzite outcrop width. Reasons for this interpretation follow:

- Rock types which occur in the basement complex away from the Amer group are present within the orthoquartzite unit along distinctive concordant valleys which may be traced back into the basement complex proper. In one case the transition between two basement types along a single lineament was observed. Basement exposures are consistently thin, suggesting thrust, rather than normal fault control.
- Colour variations in the orthoquartzite unit are repeated in the same order above each exposure of basement. The symmetry expected in folding is not present in the monoclinally dipping sequence.
- Muscovite schist and minor feldspathic sandstone of the basal unit consistently occur above the basement slices.
- Slivers of dolomitic limestone occur along these lineaments, below the basement exposures, or simply within the orthoquartzite unit, suggesting that the limestone has acted as a plane of detachment within the sedimentary sequence. This hypothesis is supported by the isoclinal folding and extensive boudining of the carbonate as opposed to the relatively undeformed adjacent orthoquartzite.

Figure 2.1 shows the traces of the thrust faults, as presently interpreted. Correlation across the major cross-faults is difficult in view of the differences in levels exposed.

The major east-northeast medial fault in the east-central part of the belt separates a syncline cored with medium grained feldspathic sandstone to the south from a complexly folded schistose assemblage to the north. It is probably a thrust fault as it places south-dipping red basal quartzite over the uppermost units of the Amer group. This fault appears to pass into a fold closure along the strike to the west and to merge with other thrusts to the east (Fig. 2.1).

Thrusting involving the more competent basal units may be correlative with the upright to north-northwest verging, doubly plunging folds affecting rocks of all units in the centre of the synclinorium, especially to the west. Poles to quartzite bedding define a single cluster to the east but broaden to form a great circle whose pole corresponds to mesoscopic fold hinges in the west. An increasing scatter of this great circle reflects increasingly variable fold plunges. The generally low plunges of the folds of this generation produce an isoclinal aspect due to the low angle of intersection between their hinges and the ground.

Given its overall west-southwest plunge, the Amer group synclinorium should logically broaden to the west. This tendency is counteracted by what are here considered to be normal faults which trend roughly northwest, repeatedly narrowing the width of the belt at the present level of erosion and exposing the lower units of the group. The faults may be hinged in the central or southern part of the belt or the medial fault may postdate them as offset along the southern margin is minimal. Sense of offset appears to be sinistral along the south-dipping northern margin. Normal fault movement with the southwest side up implies northeast-dipping fault surfaces. Conjugate joints observed along one fault confirm this interpretation.

Fabrics

Pervasive jointing is characteristic of the basal units of the group along the northern margin except near the basement where a penetrative subhorizontal schistosity is present. Along the southern margin a shallow to moderate south-southeast-dipping schistosity crosscuts both basement and cover. Its relationship to major structures is unknown although it could be axial planar to the regional synclinorium. Folds in the central part of the belt have strong axial planar schistosity in slaty layers which is locally related to transposition of layering. The expression of this phase in carbonate-rich units in the feldspathic sandstone-siltstone-slate unit is pressure solution producing a ribbed appearance whose intersection with bedding suggests crossbedding at first glance. Crenulations of all the above mentioned fabrics are locally developed with a continuous range from vertical to horizontal axial planes being consistently perpendicular to the older fabric. If thrusting and upright folding are related, these crenulations may be simply a late tectonic relaxation feature. They are most strongly developed in the central part of the belt where they have a subhorizontal orientation of axial planes and consistently plunge gently to the west-southwest.

The relationship of recumbent isoclinal folds and extensive boudinage in the dolomitic limestone to thrusting is inferred.

A pervasive fabric developed in both basement complex and cover along the northern margin is a shallow schistosity and quartz flattening fabric (averaging 165/25SW) usually at 25° to bedding (averaging 100/25SW) producing a down-dip intersection lineation (averaging 220/20SW) plunging 10 to 40° to the southwest. This is colinear with a diverse assemblage of biotite, quartz, feldspar and hornblende mineral and pebble elongations. The fabric expresses itself as a "fracture cleavage" in the quartzites. The relationship to major structures is unknown.

Metamorphism

Diagnostic mineral assemblages are poorly developed in rocks of the Amer group.

The dolomitic limestone unit at low grade is made up of alternating layers of dolomite and quartz which at higher grade produce tremolite-calcite reaction zones along the dolomite-quartz interfaces. Phlogopite is commonly present as a disseminated phase throughout the area. To the west, and particularly near crossfaults, diopside replaces quartz in the centre of boudins. Talc is locally developed.

Sky blue kyanite blades up to 1 x 1.5 x 0.1 cm occur in quartz veins and in quartzite along the northern margin of the belt. In the westernmost exposures and just north of Amer gake, muscovite-tourmaline-K feldspar-quartz pegmatites crosscut the basal Amer group. Locally they are accompanied by sillimanite in the basal units. One quartz pebble conglomerate contains sillimanite in pebbles and matrix and kyanite in veins, while others contain both kyanite and sillimanite in the matrix. The coexistence of kyanite and sillimanite under conditions of granitoid anatexis is significant in that it implies pressures whose origins, whether stratigraphically or tectonically produced, are enigmatic.

In terms of the sequence of deformation and metamorphism, the peak of mineral growth appears to have postdated the major deformations. Boudins of quartzite in the limestone are rimmed with tremolite and calcite and garnets in basement slices overgrow the penetrative schistosity. Minor boudinage of tremolite rosettes and crenulation of the schistosity outside the garnets are the only evidence of post-metamorphic deformation.

Conclusions

The Amer group is made up of two dominantly clastic sequences, separated by a transitional series of thin but distinctive lithologies. Stratigraphic repetition and involvement of basement rocks along the northern margin of the belt has been interpreted in terms of thrust faulting. Sinistral northwest faults are interpreted as northeast-dipping normal faults with southwest-sides-up-movement repeatedly constricting the west-southwest-plunging Amer Lake synclinorium. As a result, progressively higher grades of metamorphism in the basal units are exposed.

References

Bell, R.T.
1969: Study of the Hurwitz Group in the Eastern Part of the Rankin-Ennadai Belt, District of Keewatin (65 H (East Half), 65 I (East Half)); in Report of Activities, Part A, Geol. Surv. Can., Paper 69-1A, p. 147-148.

Heywood, W.W.
1977: Geology of the Amer Lake Map-Area, District of Keewatin; in Report of Activities, Part A, Geol. Surv. Can., Paper 77-1A, p. 409-410.

Wright, G.M.
1955: Geological notes on central District of Keewatin; Geol. Surv. Can., Paper 55-17.

1967: Geology of the southern barren grounds, parts of the districts of Mackenzie and Keewatin; Geol. Surv. Can., Mem. 350.

3. MARINE GEOLOGICAL-GEOPHYSICAL INVESTIGATIONS IN 1977 OF THE SCOTT INLET AND CAPE DYER – FROBISHER BAY AREAS OF THE BAFFIN ISLAND CONTINENTAL SHELF

Project 760015

Brian MacLean
Atlantic Geoscience Centre, Dartmouth

Abstract

MacLean, Brian, Marine geological-geophysical investigations in 1977 of the Scott Inlet and Cape Dyer – Frobisher Bay areas of the Baffin Island continental shelf; in Current Research, Part B, Geol. Surv. Can., Paper 78-1B, p. 13-20, 1978.

Geological-geophysical investigations were undertaken from ***C.S.S. Hudson*** *in 1977 in the Scott Inlet and the Cape Dyer – Frobisher Bay areas of the Baffin Island shelf.*

The walls of the Scott Inlet submarine trough consist mainly of more or less flat lying strata, whereas strata forming its floor have been folded and faulted. A structural high appears to underlie the outer part of the south wall. A calcareous concretion of late Eocene age was recovered by dredging across benches on the trough wall. A persistent oil slick in the area may be caused by seepage from the rock formations.

Bedrock geology of the southeastern Baffin Island shelf was further defined by geophysical profiling and the recovery between Cumberland Sound and Frobisher Bay of shallow drill cores of Precambrian gneiss and limestone of probable Ordovician age.

Introduction

Geological and geophysical investigations of the bedrock underlying the continental shelf adjacent to the east coast of Baffin Island were concentrated in 1977 in the vicinity of Scott Inlet, where an oil slick possibly from a natural seep was reported by Loncarevic and Falconer (1977), and at various localities between Cape Dyer and Frobisher Bay. The cruise tracks and stations occupied are indicated in Figures 3.1 and 3.2. This work was undertaken from **CSS Hudson** during cruise 77-027 as part of an on-going program to determine the extent, age, physical properties, and structural framework of the main bedrock units of the continental shelf in this region. Reconnaissance data on the surficial sediments of the shelf, and underway geophysical data and soft sediment samples en route across Baffin Bay from Thule, Greenland, and on two tracks across Davis Strait, were also obtained. This report deals with the bedrock studies on the Baffin Island shelf which were the primary objectives of the cruise.

The studies of the continental shelf geology were carried out by means of continuous seismic reflection (655 cm^3 air gun source), Huntec deep tow high resolution seismic, magnetic and gravity profiling in conjunction with collection of bedrock samples principally by shallow corehole drilling, and to a lesser extent, by dredging. The drilling was done with the Bedford Institute of Oceanography underwater electric rock core drill (Fowler and Kingston, 1975), which cuts a 25 mm diameter core and penetrates to a maximum of 6 m below the seafloor. The drilling procedure was similar to that used in this area (MacLean et al., 1977; in press).

Samples of consolidated and semiconsolidated rock considered representative of the underlying material were recovered at six localities, five by drilling, and one by dredging (Fig. 3.2; Table 3.1). Rock fragments obtained at other localities were all judged to be from erratics in the overburden. Failure to obtain bedrock cores at other drill sites resulted from several factors: (1) numerous electrical and mechanical problems with the drill that limited both penetration and number of drilling attempts at several stations; (2) difficulty in retaining cores of semiconsolidated material; (3) limited bedrock penetration at some localities due to fragments jamming in the core barrel; and (4) generally fairly thick overburden and the inherent difficulties in positioning the drill on the prime target area.

Table 3.1

1977 bedrock sample station* data

Station	Location lat.	Location long.	Water depth (m)	Seafloor penetration (cm)	Results
9	71°19.5'N	70°22.1'W	dredged interval 658-475 m		calcareous concretion recovered
25	64°01.4'N	63°55.9'W	197	414	370 cm biotite gneiss core
26A	63°39.5'N	63°38.1'W	373	354	83 cm limestone core
27	63°35.5'N	63°47.3'W	219	113	15 cm semiconsolidated sandstone core
28	63°11.8'N	63°00.9'W	179	277	100 cm limestone core
29	62°58.3'N	63°00.8'W	182	544	108 cm garnet gneiss core

* Drill stations, except No. 9 which was a dredge station.

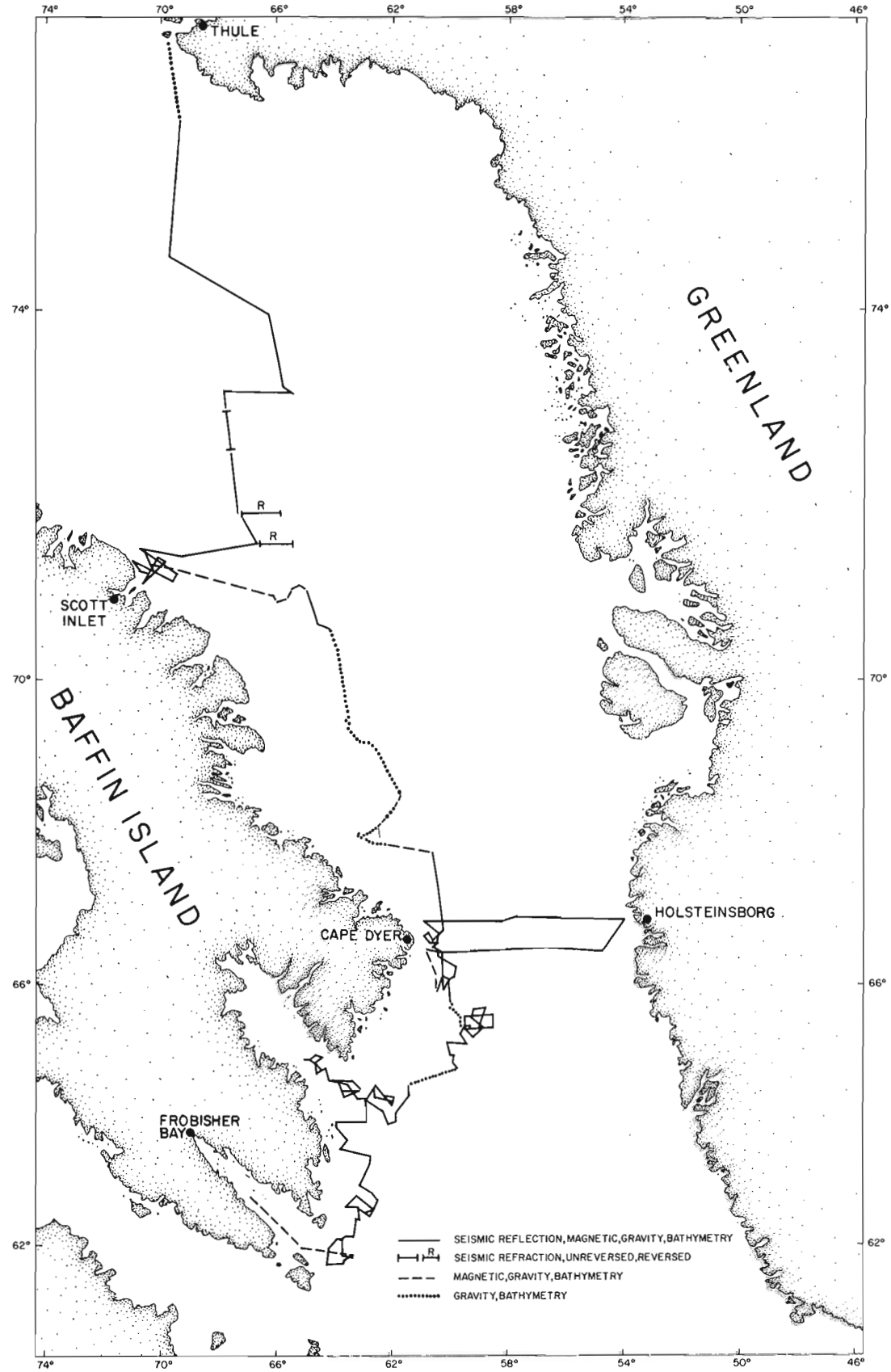

Figure 3.1. Tracks along which data were collected on cruise 77-027, **CSS Hudson** September 18 – October 13, 1977.

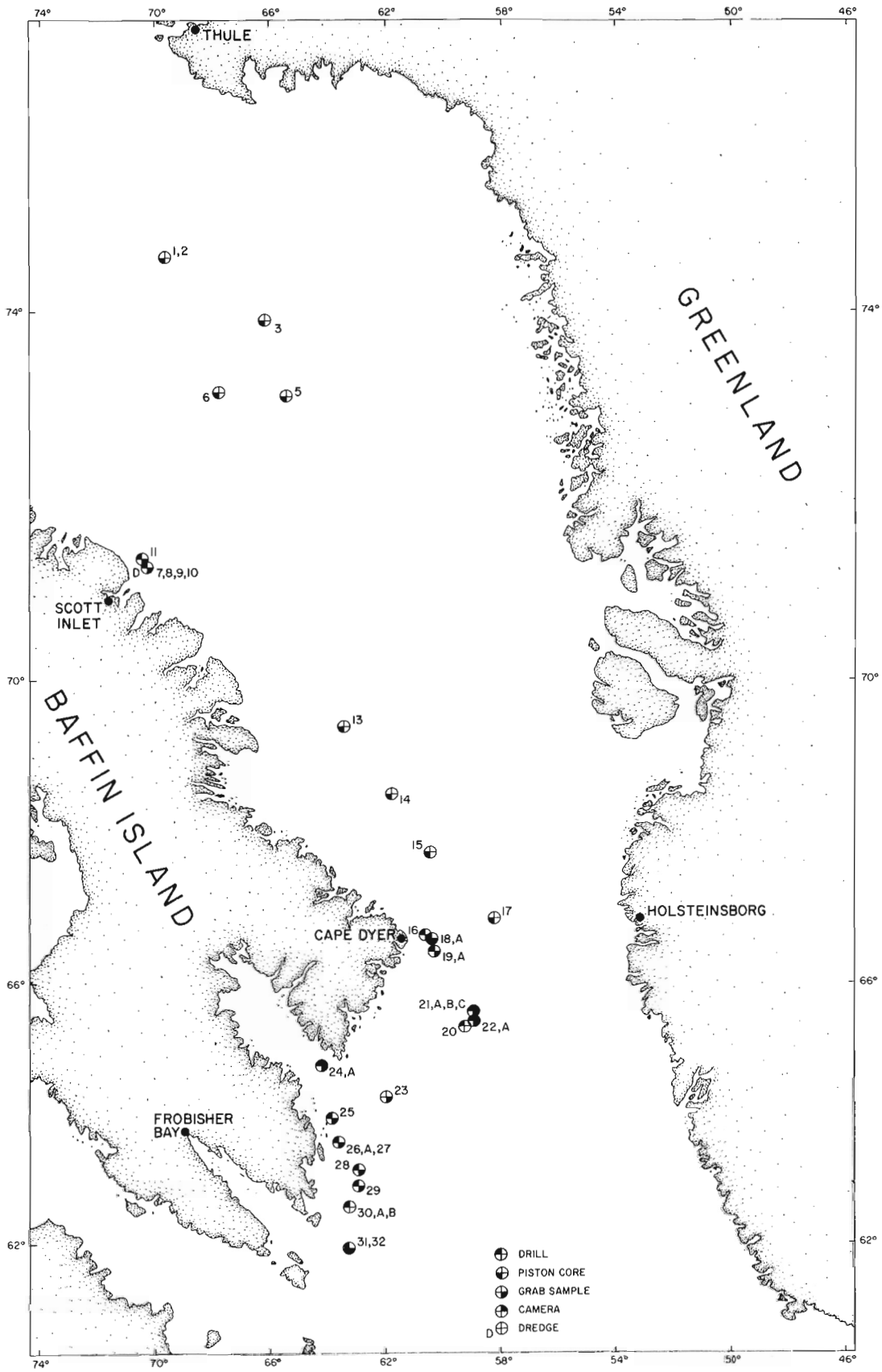

Figure 3.2. Geological stations occupied during cruise 77-027.

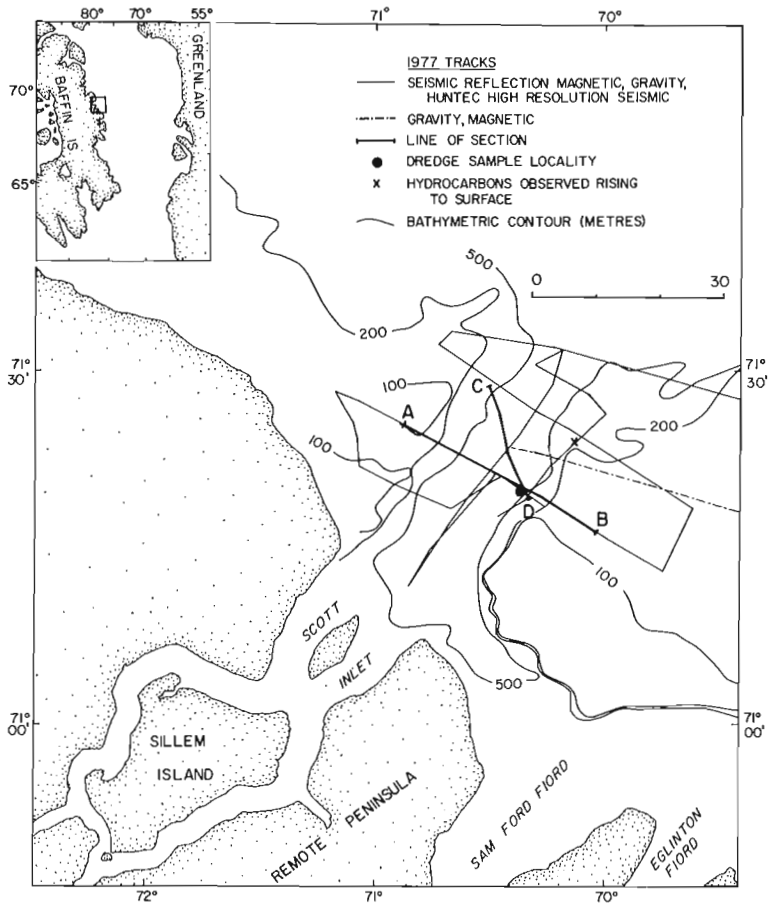

Figure 3.3. Index map of Scott Inlet area showing bathymetry, tracks along which geophysical data were collected in 1977, dredge sample location, and locality where hydrocarbon particles were seen coming to surface.

Strong currents, particularly between Cape Dyer and Frobisher Bay caused the ship to lose station and drilling to be terminated on two occasions. Unusually severe ice conditions prevented carrying out a planned reconnaissance of parts of the shelf between Scott Inlet and Cape Dyer and seriously hampered work from Cape Dyer to Cumberland Sound where drilling and towing of geophysical equipment were impractical in an ice-bound area that in places extended seaward for nearly 110 km from the coast.

Satellite navigation and Loran-C systems were used for navigational positioning.

Scott Inlet area

The occurrence of an oil slick in the vicinity of the submarine trough seaward from Scott Inlet was observed on two occasions in 1976 (Loncarevic and Falconer, 1977) and again in 1977 on September 5, 6, and 22. More extensive traversing of the area in 1977 revealed that the extent of the slick was greater than the limited observations in 1976 had indicated. Its observed extent on September 5 and 6 is shown by Levy (1978), who gives results of chemical studies of the hydrocarbon material. The slick was recognizable from a vessel only during calm sea conditions. Its persistence in time and space indicates that it originates from a source in this area and observations of hydrocarbon particles and gas bubbles rising to the surface (Loncarevic and Falconer, 1977; Levy, 1978) support this. The composition of the slick, its wide extent and the lack of known man-made causes suggest it may be caused by natural seepage of hydrocarbons from strata exposed at the seafloor. Work in this area in 1977 was directed to obtaining additional data on geological conditions as a prelude to more extensive studies planned for 1978.

The Scott Inlet submarine trough extends across the shelf in a northeasterly direction and represents a seaward continuation of Scott Inlet fiord (Fig. 3.3). Water depths in the trough reach more than 800 m, and it has some 700 m relief. The shores of Scott Inlet consist principally of precipitous cliffs rising several hundred metres from the sea. Løken and Hodgson (1971) reported and discussed the morphology of Scott Inlet and the submarine trough. The Scott Inlet fiord (and trough) are considered to have been carved by glacial erosion possibly along a pre-existing drainage system as suggested by Fortier and Morley (1956) and Ives and Andrews (1963).

Scott Island and the cliffs that form the shores of Scott Inlet are composed of a gneissic complex of Archean or Aphebian age (G.D. Jackson, pers. comm., 1978). Quaternary marine sediments form a narrow coastal lowland fringe to the north of Scott Inlet and less extensively to the south. Offshore, the walls of the submarine trough consist mainly of truncated beds of a more of less flat lying sedimentary sequence (Fig. 3.4 and 3.5) except the outer 15 km of the south wall where a structural high with associated positive gravity and magnetic anomalies occurs. A 100 milligal (F.A.) gravity low occurs over the central and inner part of the trough. Hood and Bower (1973) and Jackson et al. (1977) identified a sedimentary basin at least 6 km deep, and probably structurally controlled, along this section of the shelf on the basis of aeromagnetic and seismic refraction data. Strata forming the floor of the trough are folded and contain faults (Fig. 3.5). Data from a few profiles suggest that disturbed strata possibly extend beneath the younger flat lying strata of the walls, as for example along the northern part of profile C-D (Fig. 3.5) where an angular unconformity appears to exist between the beds of the lower part of the wall and flat lying strata higher in the section. Regionally, however, these relationships have not yet been well identified.

Dredging of the south wall between 658 m and 475 m water depth (Fig. 3.4) yielded a boulder sized dark grey calcareous concretion composed mainly of fine grained calcite together with some angular silt-to-sand sized quartz grains and minor other detrital components. Some sponge and a few other fossil fragments are present, mainly replaced by sparry calcite, but in general the rock contains few macrofossils. L.F. Jansa (pers. comm., 1978) believes the presence of ferroan sparry calcite replacing skeletal grains indicates that the concretionary material was influenced in later diagenetic stages by formation waters derived from argillaceous strata. The sample material might therefore be associated with a shaly sequence.

Examination of seismic profiles suggests that lithological variations among the strata forming the walls of the trough may be expected. For example, the rocks of the lower portion of the south wall on profile A-B (Fig. 3.4) give rise to stronger reflections of seismic energy than those higher in the sequence and also form benches on the trough wall. This suggests that harder and more resistant rocks occur along the lower section of the wall in this area with apparently softer (and possibly thinner bedded) material higher in the section. Petrologic inferences drawn by Jansa relating to the possibility of the limestone being in association with shale appear compatible with this tentative interpretation from the seismic data.

On the basis of a study of dinoflagellates in the sample, G.L. Williams (pers. comm., 1978) considers the rock to be of late Eocene age. Some Senonian species also were identified but their presence is attributed to reworking of material from older strata.

The lithological and faunal composition of the rock suggest that deposition took place in a neritic environment.

The nearest known occurrence of Eocene strata on the adjacent land is some 330 km to the north on Bylot Island at the northern end of Baffin Island where a thin sequence of molasse type sediments is preserved in northwest-southeast trending grabens (Jackson et al., 1975; Jackson and Davidson, 1975).

The locality some 15 km from the seaward end of the south wall where Loncarevic and Falconer (1977) and Levy (1978) observed blobs and bubbles coming to surface (Fig. 3.3) is approximately coincident with the flank of the structural high. This suggests that this area is a source of the slick material, but if as suspected, the hydrocarbons originate through natural seepage from seabottom strata, other source areas may exist. The truncated beds forming the trough walls and the folded and apparently faulted strata of the floor present numerous opportunities for escape of fluids or gasses should these be present in the rock formations. Possible deflections due to tidal currents acting on a stream of particles rising through the water column must also be considered in attempting to relate sea surface observations with seabed geology.

Occurrence of the slick north of the Scott Inlet trough (Levy, 1978) is also significant because water currents along the coast are southbound. Sources of the slick therefore may also exist elsewhere on the shelf, for example, seaward from Buchan Gulf where a submarine trough is cut into the shelf 87 km northwest of Scott Inlet.

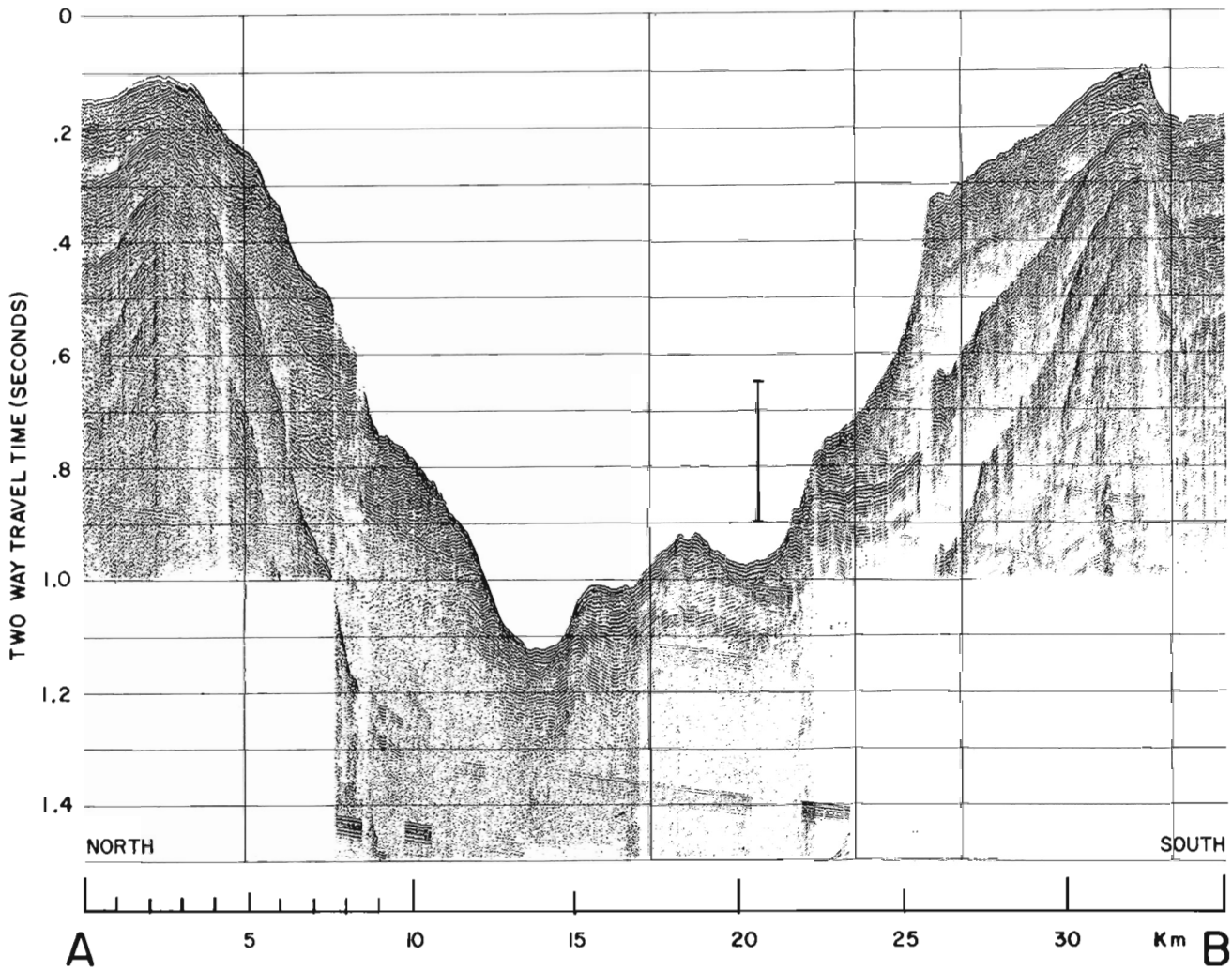

Figure 3.4. Profile A-B (see Fig. 3.3 for location). Seismic reflection record across Scott Inlet submarine trough illustrating the shape of the trough and the stratigraphic sequence through which it has been cut. The strong seismic reflectors in the lower part of the south wall approximately 22-26 km along the profile apparently are associated with more resistant strata that form benches on the trough wall at this locality. The vertical bar slightly to the right of centre indicates the approximate interval dredged. The seismic reflection data appear to support Løken and Hodgson's (1971) interpretation that the narrow ridge at the top of the south wall is a lateral moraine. The vertical exaggeration is approximately 23 times.

Cape Dyer – Frobisher Bay area

Volcanic rocks occur in a narrow discontinuous belt that extends northwestward from Cape Dyer for 85 km along the coast of eastern Baffin Island (Clarke and Upton, 1971). MacLean et al. (1978) reported on offshore basalt occurrences southeast of Cape Dyer on the basis of a petrological study of core samples, and seismic and magnetic data. Existence of basalt offshore in this area previously had been inferred by Grant (1975) and Hood and Bower (1973, 1975). Additional geophysical data acquired in 1977 further define the contact between the volcanics and the sediments adjoining them to seaward. A 12.5 cm core of dark grey, fine grained basalt was recovered at a locality 152 km southeast of Cape Dyer (Fig. 3.2, Stn. 21B) where the presence of basalt was inferred from geophysical data, but it is not clear whether or not the sample was in situ. The rock units closer to shore between Cape Dyer and Cumberland Sound were inaccessible for sampling and geophysical profiling due to ice.

Additional corehole drilling and geophysical profiling were carried out on the shelf between Cumberland Sound and Frobisher Bay to further define the rock units underlying that area and results from these studies are incorporated in the geological map (Fig. 3.6). The new data extend and refine information presented earlier on this area by MacLean et al. (1977). Table 3.1 summarizes the drill station data.

Drill station 25, where a 370 cm core of biotite gneiss was recovered, is situated just west of the boundary with Paleozoic strata at the south side of the entrance to Cumberland Sound. On the eastern side of the boundary and 44 km to the south, station 26-A yielded an 83 cm core of grey limestone composed of fine crystalline calcite. A core of dark brown micritic limestone was obtained at station 28 just north of the boundary with the Precambrian gneisses of the basement high (Fig. 3.6). This rock contains radiolariacasts and finely disseminated organic material and closely resembles rocks sampled previously 22 km to the west described by Jansa (1976) and MacLean et al. (1977). On the basis of lithologic, seismic and magnetic similarities the limestone rocks from stations 26A and 28 are considered part of the middle – late Ordovician sequence cored previously east and southeast of Cape Murchison (MacLean et al., 1977). Ordovician strata are also thought to occur in two small structural depressions in the basement southeast of Lady Franklin Island on the basis of seismic and magnetic data.

The Precambrian rocks of the basement high extending through Monumental and Lady Franklin islands are now considered, on the basis of a core of garnet-biotite gneiss recovered at station 29 and complementary seismic and magnetic data, to constitute the bedrock eastward to the boundary with the Mesozoic-Cenozoic strata that lap on them

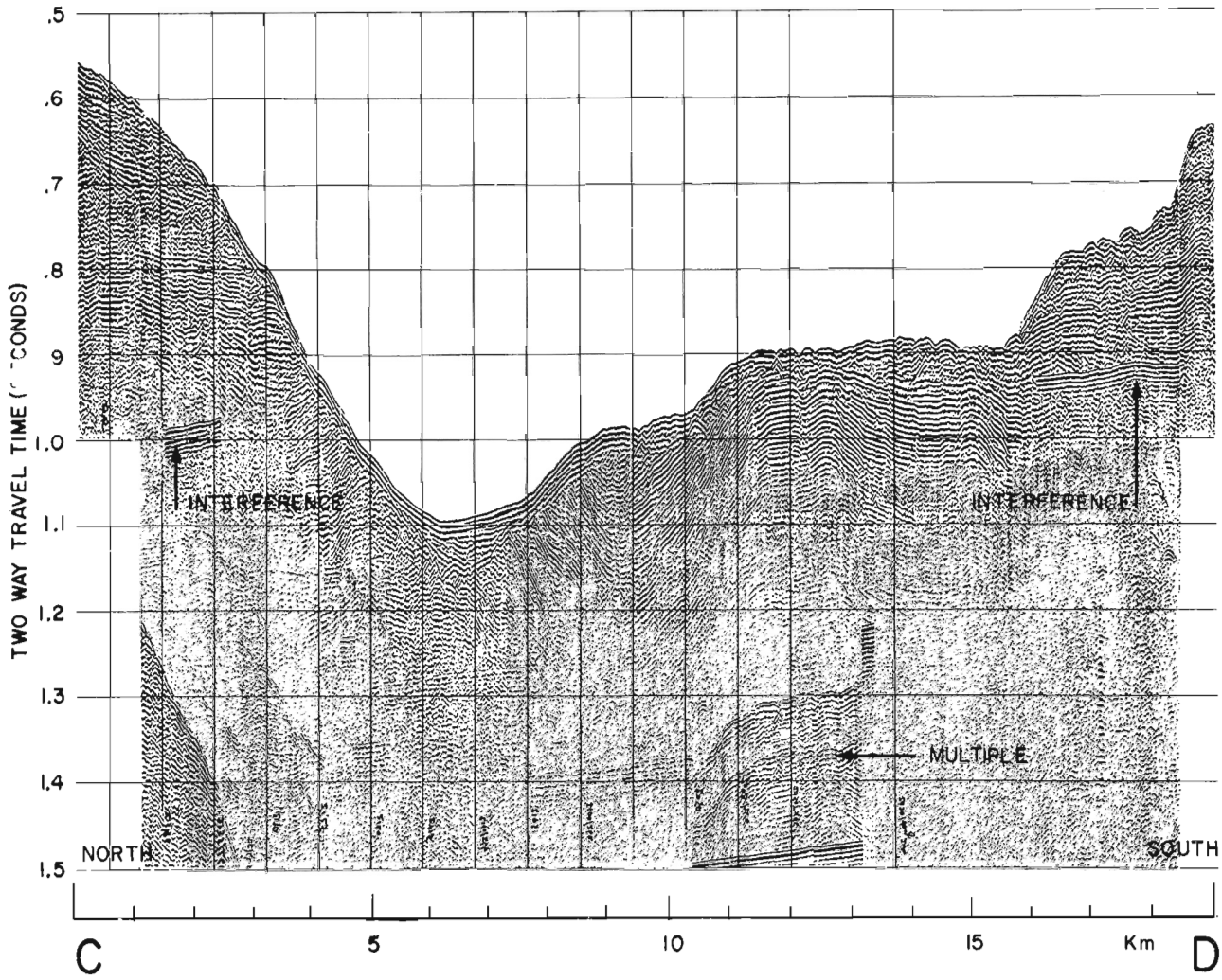

Figure 3.5. Profile C-D (see Fig. 3.3 for location). Seismic reflection record across part of Scott Inlet submarine trough illustrating folded and probably faulted strata in the floor of the trough and flatter lying strata higher on the walls. The vertical exaggeration is approximately 19 times.

to seaward. Lacking sample control MacLean et al. (1977) previously had tentatively mapped the eastern part of this Precambrian area simply as Ordovician or earlier.

A small sample of semiconsolidated sandstone with scattered gravel fragments was recovered from the cutting head of a piston corer at station 32 (Fig. 3.2) off the etrance to Frobisher Bay, 59 km southwest of a locality where similar sediment was drilled in 1976 (MacLean and Falconer, 1977). Foraminifera in the sample were studied by F.M. Gradstein who (pers. comm. 1978) considers the material to be of Pliocene-Quaternary age and deposition to have occurred in a normal salinity open marine environment. Gradstein correlates the foraminiferal assemblage in the sample with the uppermost assemblage in wells drilled on the Labrador Shelf (Gradstein and Williams, 1976). The sample locality is underlain by a sequence of apparently regularly bedded strata that dip gently seaward at an angle of about 2° and attain a thickness of 600 m or more at the core station. Difficulty has been experienced in obtaining satisfactory samples of this material with the drill and this has been attributed mainly to the strata being poorly lithified, though the thickness of surficial cover is also a factor. As a consequence, it is uncertain whether or not the material recovered by the piston corer is representative of the strata seen on the seismic records to underlie that locality.

In view of the foregoing, as well as analogies drawn with lithological and paleontological data from the Labrador Shelf (McWhae and Michel, 1975; Gradstein and Williams, 1976; Gradstein, pers. comm. 1978) and a sample of late Albian-Cenomanian age recovered at a drill station off Cumberland Sound (MacLean and Falconer, 1977), the sequence of sedimentary rocks on the outer part of the southeastern Baffin Island shelf (Fig. 3.6) is thought to be mainly of Cenozoic age and occurrences of Mesozoic strata at the bedrock surface are thought to be more localized.

A short core of semiconsolidated sandstone similar to material in the bottom of the piston core from station 32 was recovered from a thin layer covering the older rocks at station 27 east of Brevoort Island.

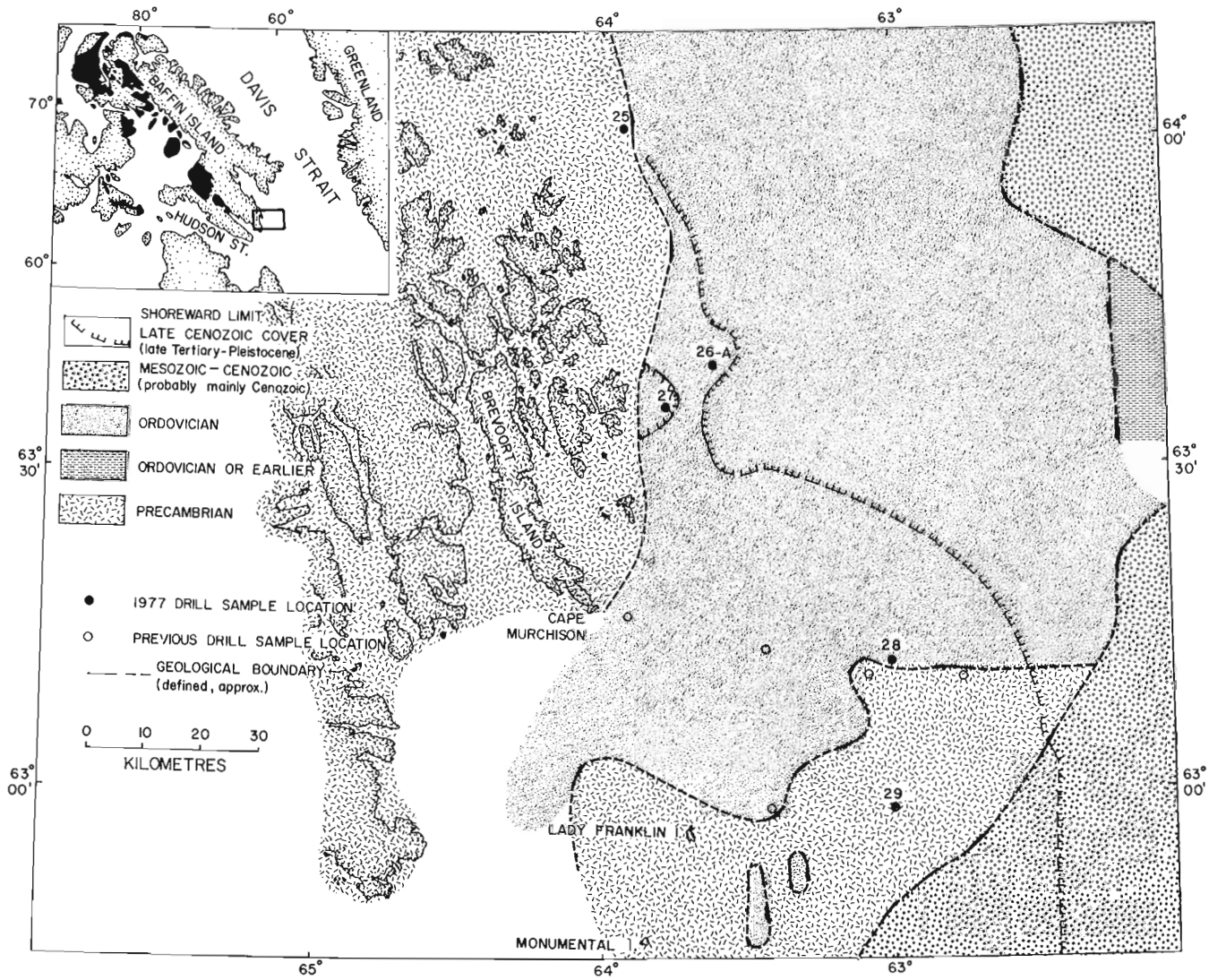

Figure 3.6. Geological map of the continental shelf seaward from Hall Peninsula, southeastern Baffin Island. This extends and updates information in Figure 3 of MacLean et al. (1977). Solid dark areas on inset map indicate known on-shore occurrences of Ordovician rocks (including undivided Ordovician-Silurian strata) in the Baffin Island region.

Acknowledgments

Grateful acknowledgment is made to Captain L. Strum, officers and crew of **CSS Hudson** and members of the scientific staff for their excellent co-operation and assistance in carrying out the field program; to P. Girouard for thin section preparation; to F.M. Gradstein and G.L. Williams for paleontological studies and age assignments; to L.F. Jansa, for petrological examination and comments on the samples; and to R.K.H. Falconer, R.T. Haworth, L.F. Jansa, and M.P. Latremouille for critical review of the manuscript.

References

Clarke, D.B. and Upton, B.G.J.
1971: Tertiary basalts of Baffin Island: field relations and tectonic setting; Can. J. Earth Sci., v. 8, p. 248-258.

Fortier, Y.O. and Morley, L.W.
1956: Geological unity of the Arctic Islands; Trans. Roy. Soc. Can., ser. 3, p. 3-12.

Fowler, G.A. and Kingston, P.F.
1975: An underwater drill for continental shelf exploration; Soc. Underwater Technol., v. 1, no. 4, p. 18-22.

Gradstein, F.M. and Williams, G.L.
1976: Biostratigraphy of the Labrador Shelf, Part 1; Geol. Surv. Can., Open File 349, 39 p.

Grant, A.C.
1975: Geophysical results from the continental margin off southern Baffin Island, **in** Canada's Continental Margins and Offshore Petroleum Exploration, C.J. Yorath, E.R. Parker and D.J. Glass, eds., Can. Soc. Pet. Geol., Mem. 4, p. 411-431.

Hood, P.J. and Bower, M.E.
1973: Low-level aeromagnetic surveys of the continental shelves bordering Baffin Bay and the Labrador Sea; **in** Earth Science Symposium on Offshore Eastern Canada, P.J. Hood, ed.; Geol. Surv. Can. Paper 71-23, p. 573-598.

1975: Aeromagnetic reconnaissance of Davis Strait and adjacent areas; **in** Canada's Continental Margins and Offshore Petroleum Exploration, C.J. Yorath, E.R. Parker, and D.J. Glass, eds.; Can. Soc. Pet. Geol., Mem. 4, p. 433-450.

Ives, J.D. and Andrews, J.T.
1963: Studies in the physical geography of north-central Baffin Island, N.W.T.; Geogr. Bull. no. 19, p. 5-48.

Jackson, G.D. and Davidson, A.
1975: Bylot Island map-area, District of Franklin; Geol. Surv. Can., Paper 74-29, 12 p.

Jackson, G.D., Davidson, A., and Morgan W.C.
1975: Geology of the Pond Inlet map-area Baffin Island, District of Franklin; Geol. Surv. Can., Paper 74-25, 33 p.

Jackson, H.R., Keen, C.E., and Barrett, D.L.
1977: Geophysical studies of the eastern continental margin of Baffin Bay and in Lancaster Sound; Can. J. Earth Sci., v. 14, p. 1991-2001.

Jansa, L.F.
1976: Lower Paleozoic radiolaria-bearing limestones from the Baffin Island shelf; in Report of Activities, Part B, Geol. Surv. Can., Paper 76-1B, p. 99-105.

Levy, E.M.
1978: Visual and chemical evidence for a natural seep at Scott Inlet, Baffin Island; in Current Research, Part B, Geol. Surv. Can., Paper 78-1B, rep. 4.

Løken, O.H. and Hodgson, D.A.
1971: On the submarine geomorphology along the east coast of Baffin Island; Can. J. Earth Sci., v. 8, p. 185-195.

Loncarevic, B.D. and Falconer, R.K.H.
1977: An oil slick occurrence off Baffin Island; in Report of Activities, Part A, Geol. Surv. Can., Paper 77-1A, p. 523-524.

MacLean, B. and Falconer, R.K.H.
1977: Baffin Island Shelf – Shallow corehole drilling, 1976; in Report of Activities, Part B, Geol. Surv. Can., Paper 77-1B, p. 125-127.

MacLean, B., Falconer, R.K.H., and Clarke, D.B.
1978: Tertiary basalts of western Davis Strait: bedrock core samples and geophysical data; Can. J. Earth Sci., v. 15, no. 5.

MacLean, B., Jansa, L.F., Falconer, R.K.H., and Srivastava, S.P.
1977: Ordovician strata on the southeastern Baffin Island shelf revealed by shallow drilling; Can. J. Earth Sci., v. 14, p. 1925-1939.

McWhae, J.R.H. and Michel, W.F.E.
1975: Stratigraphy of Bjarni H-81 and Leif M-48, Labrador Shelf; Bull. Can. Pet. Geol., v. 23, p. 361-382.

4. VISUAL AND CHEMICAL EVIDENCE FOR A NATURAL SEEP AT SCOTT INLET, BAFFIN ISLAND, DISTRICT OF FRANKLIN

E.M. Levy[1]

Abstract

Levy, E.M., Visual and chemical evidence for a natural seep at Scott Inlet, Baffin Island, District of Franklin; in Current Research, Part B, Geol. Surv. Can., Paper 78-1B, p. 21-26, 1978.

A visual reconnaissance of the sea surface off Scott Inlet in 1977 demonstrated the presence of slicks in an area where they were observed in 1976, although their extent was very much greater than previously thought. An extensive hydrochemical investigation was carried out, and elevated concentrations of dissolved and/or dispersed petroleum residues both at the surface and in the water column provided strong evidence for natural seepage of petroleum from the seabed.

Introduction

On two occasions during the 1976 **CSS Hudson** cruise to the Arctic, what appeared to be oil slicks were observed in the vicinity of Hecla and Griper Bank off Scott Inlet, Baffin Island (Loncarevic and Falconer, 1977) (Fig. 4.1). Water samples were taken from the surface and at depths of 50 and 300 m, and a sample of the slick was collected by swabbing the sea surface with cheesecloth. Direct high temperature gas chromatographic analysis of a scraping of the material on the cheesecloth revealed a broad spectrum (140 to 350°C) of aliphatic hydrocarbon peaks protruding from an unresolved envelope. This is typical of the chromatograms obtained by this procedure for partially weathered crude oils. Although more volatile compounds might have been present in the sample, they would not have been detected under these analytical conditions. In addition, the ultraviolet absorbance ratio (2.72) was in the range of those found for a variety of crude oils and the lighter residual fuel oils (Levy, 1972a). The water samples contained fluorescing substances (primarily aromatic hydrocarbons) as measured by fluorescence spectrophotometry (Levy, 1977a) in concentrations equivalent to 33 to 890 $\mu g\ L^{-1}$ of Bunker C fuel oil from the **Arrow** at the surface and 2 to 7.6 $\mu g\ L^{-1}$ in the water column. On the basis of the background levels previously observed on the Scotian Shelf and in the Gulf of St. Lawrence (Levy, 1971, 1972b; Levy and Walton, 1973), the concentrations in the water column and particularly those at the surface at Scott Inlet were very much higher than would have been anticipated for such a remote area and suggested that the elevated concentrations were the consequence of a local source on the seabed.

In addition to the information obtained from the 1976 cruise, floating petroleum residues were collected near Scott Inlet in 1971 during a study of the distribution of tar in the North Atlantic (Levy and Walton, 1976). This was one of only four areas throughout the Eastern Arctic where floating residues were encountered, but the possible significance of these observations was not appreciated at the time. Subsequently, these other areas – the entrance to Lancaster Sound north of Bylot Island, the northern Labrador Sea, and the Labrador Shelf – have attracted the attention of the oil industry for their potential as petroleum resource regions. In any event, the slick observed off Scott Island in 1976 and the floating residues collected in 1971 suggested that the source in this area had been active for a number of years. Because of the possibility that this source might be submarine seepage of petroleum from the seabed, and not merely the consequence of some anthropogenic input, a more detailed visual reconnaissance of the area and a more extensive hydrochemical survey was carried out in 1977.

Field Observations (September 5-6, 1977)

Because of ice conditions, **Hudson** approached the Scott Inlet area from the northeast (Fig. 4.2) under conditions that were ideal for visual observation of the sea surface. With excellent lighting and only a very light breeze, damping of capillary waves by surface-active substances was readily detected. An extensive slick was sighted at 1537 GMT and photographs were taken before crossing the boundary (Fig. 4.3). The slick was virtually continuous for 9 km along the ship's track and extended in a northwest-southeast direction as far as it was possible to see. Water samples were collected for the determination of salinity, oxygen, dissolved 'petroleum residues', volatile hydrocarbons, alkalinity, nutrients, and stable isotopes of carbon and oxygen. The surface microlayer was sampled with a stainless steel screen sampler (Garrett, 1965) while bottom sediments were collected with a Shipek grab and floating particulate matter was collected with a neuston net. While these operations were underway, two short excursions were made in the ship's launch for a closer inspection of the slick. At one location it had the appearance of an oily film with iridescent interference colours and a small patch of "chocolate mousse" was observed. Samples were collected. At a nearby location gas

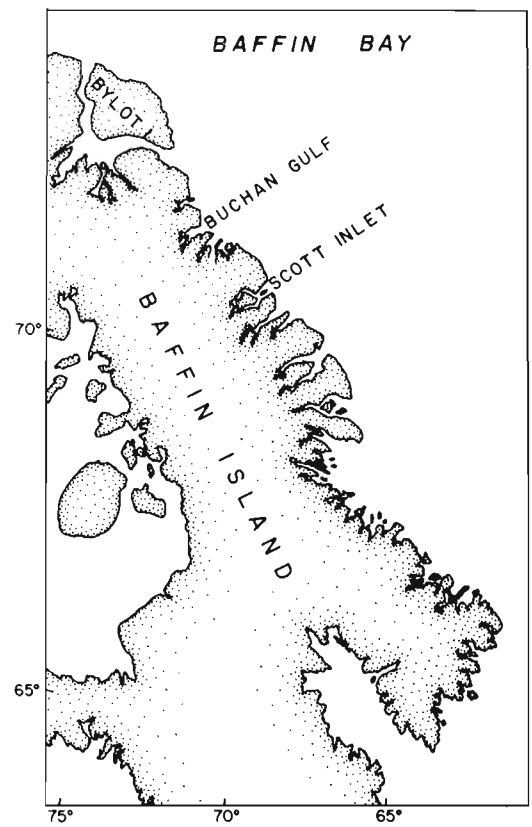

Figure 4.1. Map of Eastern Arctic.

[1]Atlantic Oceanographic Laboratory, Bedford Institute of Oceanography, Dartmouth, N.S., Canada B2Y 4A2.

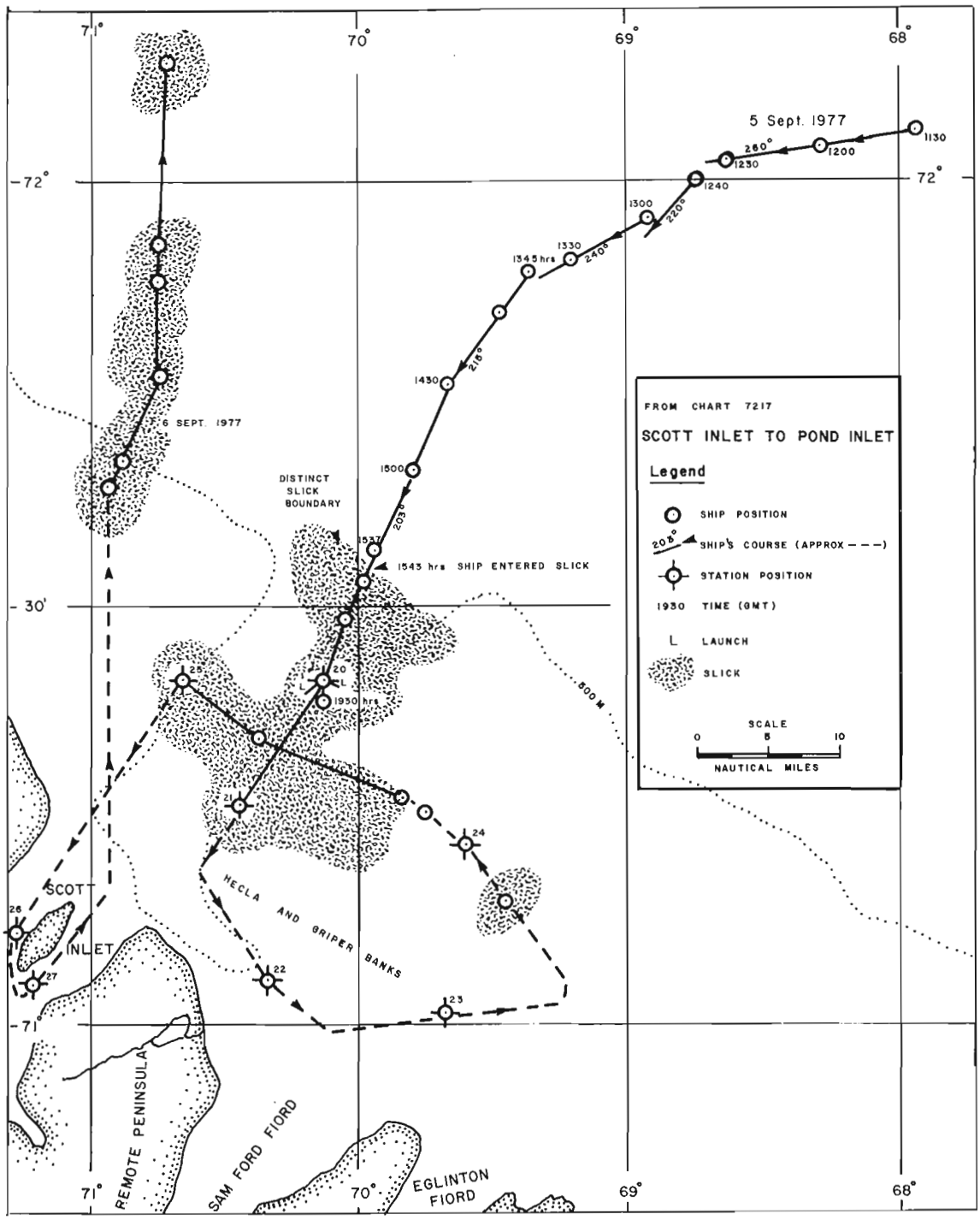

Figure 4.2. Map of Scott Inlet region ship's track and location of slick observed in September 1977.

bubbles were observed to be erupting through the sea surface, and samples of surface water were collected. Shortly afterwards a light wind arose, and light conditions changed slightly so that it was difficult to observe the slick from the launch. However, it was still plainly visible from **Hudson.** An almost continuous slick extended between Stations 20 and 21 in an undetermined distance to the northwest and southeast. Careful watch was maintained until nightfall, although conditions for observing the slicks deteriorated and finally ice was encountered. The ship did not get out of the ice until 1041 GMT on September 6. An almost continuous slick to the northeast of Hecla and Griper Banks extended between the edge of the ice field and Station 25, a distance of about 40 km. Its width, or its extension beyond the ice and north of Station 25, was not determined.

In order to establish whether the slick-forming material was entering the coastal waters via Scott Inlet from a source on land, Scott Island was circumnavigated. However, no slicks were observed in Scott Inlet, nor was there any other evidence of a terrestrial source for the slick-forming material (Levy, 1977b).

The **Hudson** left the area in late afternoon of September 6 and proceeded in a northerly direction. At that time there was sufficient ripple on the water that slicks were not observed. Towards evening, however, the breeze abated and the ship passed through an area of continuous slick which was at least 40 km long.

Unfortunately, time was not available to map out in more detail the extent of the slick or to locate the source (or sources?) of the slick-forming material. Nevertheless, this reconnaissance not only confirmed the presence of slicks in the Scott Inlet area as observed during 1976 but also demonstrated that the slick area is much more extensive than previously believed. In view of the southward currents in this region, the slick observed on the northward passage from Scott Inlet suggests that there might be a number of other sources on the Baffin Shelf.

Analytical Results

Qualitative. The extracts from the surface microlayer samples collected in the Scott Inlet area were combined and analyzed by high-temperature gas chromatography using a procedure developed for the analysis of tar balls and other high-boiling petroleum residues (Column: 2 m x 3 mm stainless steel, 3% Dexsil-300 on 100-120 Chromosorb W; Temperature program: 6°C/min to 350°C; Levy et al., 1973). The chromatogram revealed the presence of a broad spectrum of saturated hydrocarbon peaks protruding from an unresolved envelope. Such chromatograms are typical of crude oils which have undergone weathering in the marine environment. Since there was no indication of either a narrow range of specific hydrocarbons or of an odd-carbon preference, the slick-forming material is not of recent biosynthetic origin. Although this analysis is not capable of unequivocally identifying the nature of the slick-forming material, it does provide strong evidence that the slick originates from petroleum which is seeping from the seabed. A submarine trough extends seaward from the fiord at Scott Inlet across the Baffin Island continental shelf and, as shown by the seismic records (MacLean, 1978), the strata exposed on the walls and floor of this trough provide geological conditions favourable for seepage to occur. Similar bathymetric conditions are present at Buchan Gulf and at some of the fiords farther south. These would seem also to be potential sites of seepage of petroleum from the seabed.

Quantitative. A total of 55 samples was collected from the water column at Stations 20 to 27 in the environs of Scott Inlet (Fig. 4.2). These samples were extracted with carbon tetrachloride on board **Hudson** and subsequently analyzed by fluorescence spectrophotometry (Levy, 1977a) at the Bedford Institute of Oceanography. The data (Table 4.1) demonstrate that, although the concentrations of dissolved and/or dispersed petroleum residues[1] at most of the locations and depths sampled in the Scott Inlet area were at the background level[2] measured for Eastern Arctic waters in 1977, concentrations at some sampling sites were very much higher. These 'anomalies' were well beyond the experimental variability and were not observed elsewhere in the region surveyed in 1977. Further, there was no correlation between the concentration anomalies in the Scott Inlet samples and depth, salinity, dissolved oxygen, or other chemical parameters measured on the same sample of water. This would be expected if seepage was occurring sporadically from the exposed strata on the walls of the submarine canyon with the sporadic injections of petroleum being swept along by the water movements at the same time as they were rising under the force of their own buoyancy. The variability in the concentration data, then, represents the statistical chance of capturing in a 5-litre sampler, at a certain depth and at a particular instant in time, one or more of these discrete and non-homogeneously distributed injections of oil.

Concentrations of oil in the surface microlayer (Table 4.2) as sampled by the screen technique and analyzed by fluorescence spectrophotometry in the Scott Inlet area were 22 to 42 $\mu g\ L^{-1}$ (arithmetic mean 30.2 $\mu g\ L^{-1}$) except in seven areas where deliberate attempts were made to sample the slick-forming material when concentrations ranging from 85.7 to 1726 $\mu g\ L^{-1}$ (arithmetic mean 424 $\mu g\ L^{-1}$) were encountered. The sample with the highest concentration of oil was taken from a small patch of thin "chocolate mousse" floating on the surface. The concentration in the surface microlayer at one location in Scott Inlet was 14.6 $\mu g\ L^{-1}$ and this provides further evidence that the slick which was present offshore was not derived from a source in the inlet itself. By way of comparison the surface microlayer concentrations throughout Baffin Bay, with the exception of values at the entrance to Lancaster Sound and in the slick off Scott Inlet, were 3.5 to 11.4 $\mu g\ L^{-1}$ (arithmetic mean 7.0 $\mu g\ L^{-1}$). It is notable also that the concentrations in the surface microlayer in Baffin Bay were about an order of magnitude higher than those in the water column below and that this is well within the range of enrichment factors reported for surface-active organic substances in the ocean (MacIntyre, 1974).

Although a large number of water samples were collected throughout the Eastern Arctic and analyzed shipboard for light hydrocarbons (C_1-C_6), the data have not yet been processed. In addition, grab samples of surficial bottom sediments were collected and frozen but the chemical analyses have not yet been completed.

Conclusions

On the basis of the field observations and the analytical data which resulted from the 1977 **Hudson** cruise to the Eastern Arctic, the following conclusions may be drawn:

- Slicks were present off Scott Inlet during early September 1977 in the same general area where they were observed in 1976. However, in 1977 the slick covered a much more extensive area.
- Existing observations and analytical data indicate that the source of the slick is seepage of petroleum from the seabed. However, a detailed compositional analysis of the slick-forming material remains to be done.
- The presence of extensive slicks to the north of Scott Inlet during 1977 suggests that there may be other locations where seepage occurs.

---

[1] All concentrations of dissolved and/or dispersed petroleum residues are expressed in terms of Bunker C fuel oil taken from the tanker, **Arrow**, which grounded off Nova Scotia in 1970. This oil has been used as the reference material throughout our studies of petroleum in the North Atlantic (Levy, 1971, 1972b; Levy and Walton, 1973) and ensures that our data remain internally consistent and intercomparable.

[2] This background level is taken as the geometric mean of the concentrations of dissolved and/or dispersed petroleum residues measured in 563 water samples collected at 46 stations and at all standard oceanographic depths throughout the northern Labrador Sea, Davis Strait, Baffin Bay, Lancaster Sound, Jones Sound and Smith Sound in 1977. Samples from Scott Inlet were not included. Because the distribution of the data very closely approximates a lognormal distribution, the geometric mean (0.46 $\mu g\ L^{-1}$) is a more appropriate measure of central tendency than the arithmetic mean (0.70 $\mu g\ L^{-1}$). The 95% confidence ranges are 0.43 to 0.49 $\mu g\ L^{-1}$ and 0.60 to 0.80 $\mu g\ L^{-1}$ for the geometric and arithmetic means respectively. Whichever approach is taken, the general background level in Eastern Arctic waters during 1977 was appreciably less than 1 $\mu g\ L^{-1}$.

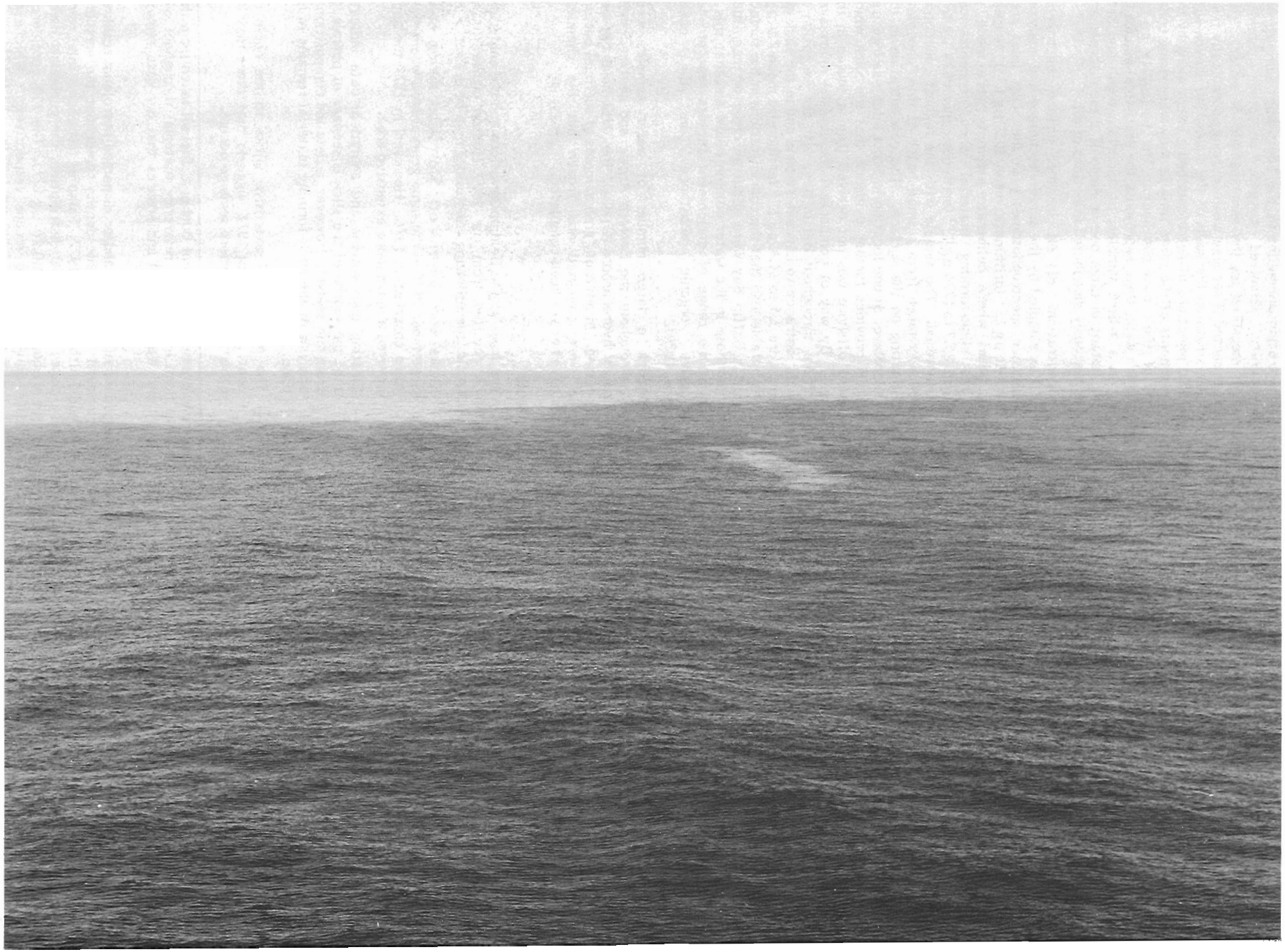

Figure 4.3. Photograph of slick off Scott Inlet.

Table 4.1

Concentrations of petroleum residues in the water column at Scott Inlet (September 1977)

Station	Depth (m)	Concentration ($\mu g\ L^{-1}$)
20	1	0.40
20	10	0.55
20	20	0.50
20	50	0.40
20	75	0.50
20	100	0.05
20	150	0.40
20	200	0.80
20	335	0.35
21	1	0.30
21	10	0.40
21	20	0.40
21	30	0.30
21	75	1.70
21	100	0.35
21	150	0.40
21	200	0.80
21	410	0.30
22	0	0.35
22	1	0.90
22	10	0.70
22	20	0.60
22	30	87.50
22	50	10.00
22	75	0.70
22	100	0.75
22	150	0.40
22	200	10.00
22	235	0.05
23	1	0.55
23	10	0.20
23	20	0.15
23	30	5.55
23	50	0.05
23	75	0.10
23	119	0.20
24	1	0.20
24	10	1.40
24	20	0.20
24	30	0.10
24	50	0.15
24	75	0.40
24	100	0.55
24	150	1.90
25	1	0.40
25	10	57.50
25	20	0.40
25	50	0.40
25	75	0.40
25	100	0.40
25	150	0.40
25	200	0.35
25	275	0.40
26	1	0.15
27	1	0.50

Table 4.2

Concentrations of petroleum residues in the surface microlayer at Scott Inlet (September 1977)

Station	Concentration ($\mu g\ L^{-1}$)
20*	85.7
	154.4
	1726.2
	212.0
	488.4
	202.0
21	22.8
24	26.3
25	41.6
26	14.6

*Samples collected from launch.

Future Work

Because of the potential economic and environmental importance of natural seepage of petroleum on the Baffin Island shelf and since the seep provides a natural laboratory for a study of the long term effects of chronic inputs of petroleum into an Arctic marine environment, a multidisciplinary chemical, biological and geological/geophysical investigation of the Scott Inlet seep and an exploratory survey of the Buchan Gulf region are being planned for the 1978 field season. Attempts will be made to map the slick areas more fully and to locate the source or sources of the slick-forming materials, to obtain a sufficient sample for detailed chemical analyses by modern analytical techniques including computerized gas chromatography-mass spectrometry, to collect and analyze the gases which are escaping from the sea surface in some areas, and to gather more extensive chemical data concerning the concentrations of petroleum-derived substances in the water column, on the sea surface and in the surficial bottom sediments. The biology program will focus on long term sublethal effects of petroleum on the physiology of Arctic phytoplankton and zooplankton and higher marine organisms and on the effects in carbon fluxes. Studies of primary production under Arctic conditions will also be carried out. The geology/geophysical program will be a continuation of the studies of the Baffin Island continental shelf already under way (MacLean, 1978). Together, these investigations should provide much more complete information concerning natural seepage on the Baffin Island shelf as well as an appreciation of the environmental consequences of exploration and production of oil in the Arctic.

Acknowledgments

Grateful acknowledgment is made to Captain D. Deer, officers and crew of **CSS Hudson,** and members of the scientific complement for their co-operation and assistance in carrying out the field program, to J. Moffatt and D. Conrad for their technical excellence in performing the laboratory analyses, to R. Belanger for his photographic support both during the cruise and afterwards, and to B. MacLean and R. Pocklington for critically reviewing the manuscript.

References

Garrett, W.D.
1965: Collection of slick-forming materials from the sea surface; Limnol. Oceanogr., v. 10, p. 602-605.

Levy, E.M.
1971: The presence of petroleum residues off the east coast of Nova Scotia, in the Gulf of St. Lawrence and the St. Lawrence River; Water Res., v. 5, p. 723-733.

1972a: The identification of petroleum products in the marine environment by absorption spectrophotometry; Water Res., v. 6, p. 57-69.

1972b: Evidence for the recovery of the waters off the East Coast of Nova Scotia from the effects of a major oil spill; Water, Air and Soil Pollution, v. 1, p. 144-148.

1977a: Fluorescence spectrophotometry: principles and practice as related to the determination of dissolved/dispersed petroleum residues in sea water; BIO Report Series/BI-R-77-7, July 1977.

1977b: Scott Inlet slick: an Arctic oil seep?; Spill Technology Newsletter, November/December, 1977.

Levy, E.M. and Walton, A.
1973: Dispersed and particulate petroleum residues in the Gulf of St. Lawrence; J. Fish. Res. Bd. Can., v. 30, p. 251-257.

1976: High seas oil pollution: particulate petroleum residues in the North Atlantic; J. Fish. Res. Bd. Can., v. 33, p. 2781-2791.

Levy, E.M., Webber, L.R., and Moffatt, J.D.
1973: A method for high temperature gas chromatographic analyses of petroleum residues; J. Chromatographic Sci., v. 11, p. 591-593.

Loncarevic, B.D. and Falconer, R.K.
1977: An oil slick occurrence off Baffin Island; in Report of Activities, Part A, Geol. Surv. Can., Paper 77-1A, p. 523-524.

MacIntyre, F.
1974: Chemical fractionation and sea-surface microlayer processes; in The Sea, ed. E.D. Goldberg, v. 5, p. 245-299.

MacLean, B.
1978: Marine geological-geophysical investigations of the Scott Inlet and Cape Dyer-Frobisher Bay areas of the Baffin Island Continental Shelf in 1977; in Current Research, Part B, Geol. Surv. Can., Paper 78-1B, rep. 3.

5. INTERNAL CORRELATIONS AND THICKNESS TRENDS, JURASSIC BUG CREEK FORMATION, NORTHEASTERN YUKON AND ADJACENT NORTHWEST TERRITORIES

Project 750067

T.P. Poulton
Institute of Sedimentary and Petroleum Geology, Calgary

Abstract

Poulton, T.P., Internal correlations and thickness trends, Jurassic Bug Creek Formation, northeastern Yukon and adjacent Northwest Territories; in Current Research, Part B, Geol. Surv. Can., Paper 78-1B, p. 27-30, 1978.

The Jurassic Bug Creek Formation and equivalent parts of the Kingak Formation to the northwest, considered together, form a clastic package that thickens more or less regularly, and becomes more argillaceous, northwestward from the contemporaneous Aklavik Arch. A small uplift was present in the vicinity of White Mountains in Early or early Middle Jurassic time. It was overstepped by Middle Jurassic sandstones, which also transgressed southward beyond the limits of Lower Jurassic sediments. Except for the basal sandstone member which occurs only locally, the five members of the Bug Creek Formation at its type section, together with two others not present there, can be recognized throughout most of the northern Richardson Mountains.

This report presents a summary of the results obtained following two seasons (1975, 1976) of field work in northern Richardson Mountains. Detailed descriptions of stratigraphic sections, formal naming of certain of the units, and documentation of the paleontological dating of the units and their environmental interpretation are in preparation. The additional regional data support and elaborate on the results of the preliminary report on the Lower and Middle Jurassic rocks by Poulton and Callomon (1976).

The Jurassic rocks of northern Richardson Mountains (Fig. 5.1) are a series of interbedded sandstones and argillaceous rocks comprising: the Bug Creek Formation (mainly sandstone) and its western argillaceous equivalent, the Kingak Formation; the lower part of the Husky Formation (shale); the Porcupine River Formation (sandstone); and the lower part of the North Branch Formation (mainly sandstone) (Fig. 5.2).

The Husky Formation is in part the eastern argillaceous equivalent of the Porcupine River Formation to the west and it is overlain by the North Branch Formation in the vicinity of the North Branch of Vittrekwa River, approximately 70 km south of McDougall Pass (Jeletzky, 1967, 1975, 1977).

The Bug Creek Formation represents the arenaceous, relatively thin, southern and eastern facies of a sedimentary sequence which thickens and becomes shalier to the north and west (Jeletzky, 1967, 1975; Poulton and Callomon, 1976), where it was originally described as the Kingak Formation in northeastern Alaska (Leffingwell, 1919; Detterman et al., 1975). Tongues of the Kingak Formation extend into the northern Richardson Mountains, where two of them were included as argillaceous members of the Bug Creek Formation in its original description by Jeletzky (1967). The correlation of these argillaceous tongues with the members of the Bug Creek Formation and the fossil occurrences on which the correlations largely are based are shown in Figures 5.2 and 5.5. The Bug Creek Formation is interpreted to represent two major deltaic lobes which prograded northward and westward into the Beaufort-Mackenzie Basin from the Aklavik Arch (Jeletzky, 1967). The sandstone portions of these deltaic complexes are the upper sandstone member and the lower of the two units that Jeletzky (1967) originally called together the intermediate sandstone member. An unconformity within the intermediate sandstone member at its type locality at Bug Creek is now known to separate different sandstone units: the one above of Bajocian age, and the other below, of Early Jurassic, possibly Pliensbachian age

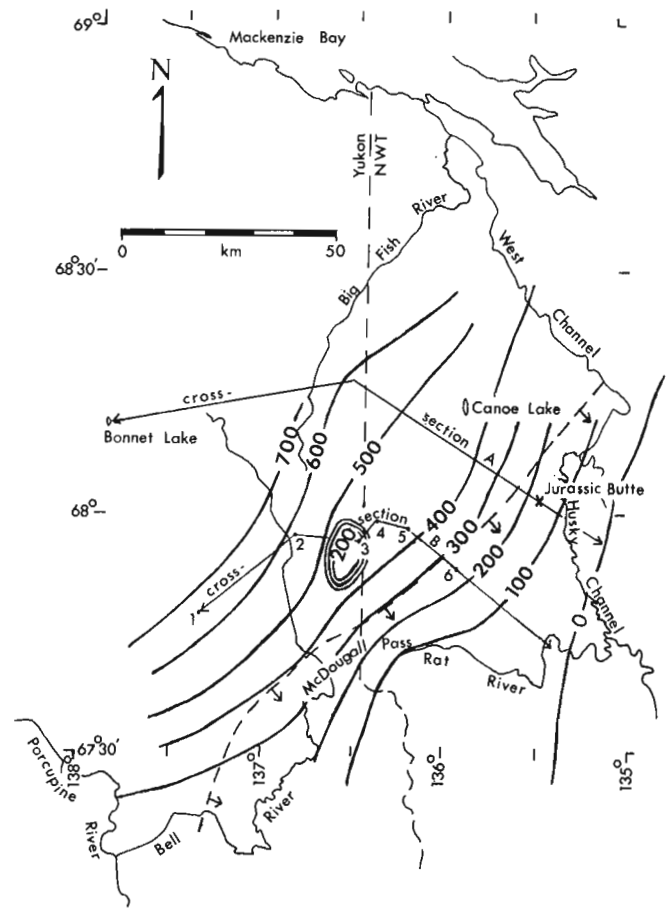

Figure 5.1

Index map, northern Richardson Mountains and vicinity. Locations of stratigraphic cross-sections A (Fig. 5.2) and B (Fig. 5.3), and stratigraphic sections 1 to 6 of cross-section B are shown. Isopachs, in metres, are for the Bug Creek Formation and equivalent parts of the Kingak Formation to the west. The Jurassic manifestation of the White Mountains Uplift is indicated by closely spaced contours north of McDougall Pass. The effect of the Aklavik Arch on the Jurassic rocks is expressed most strongly southeast of the dashed line.

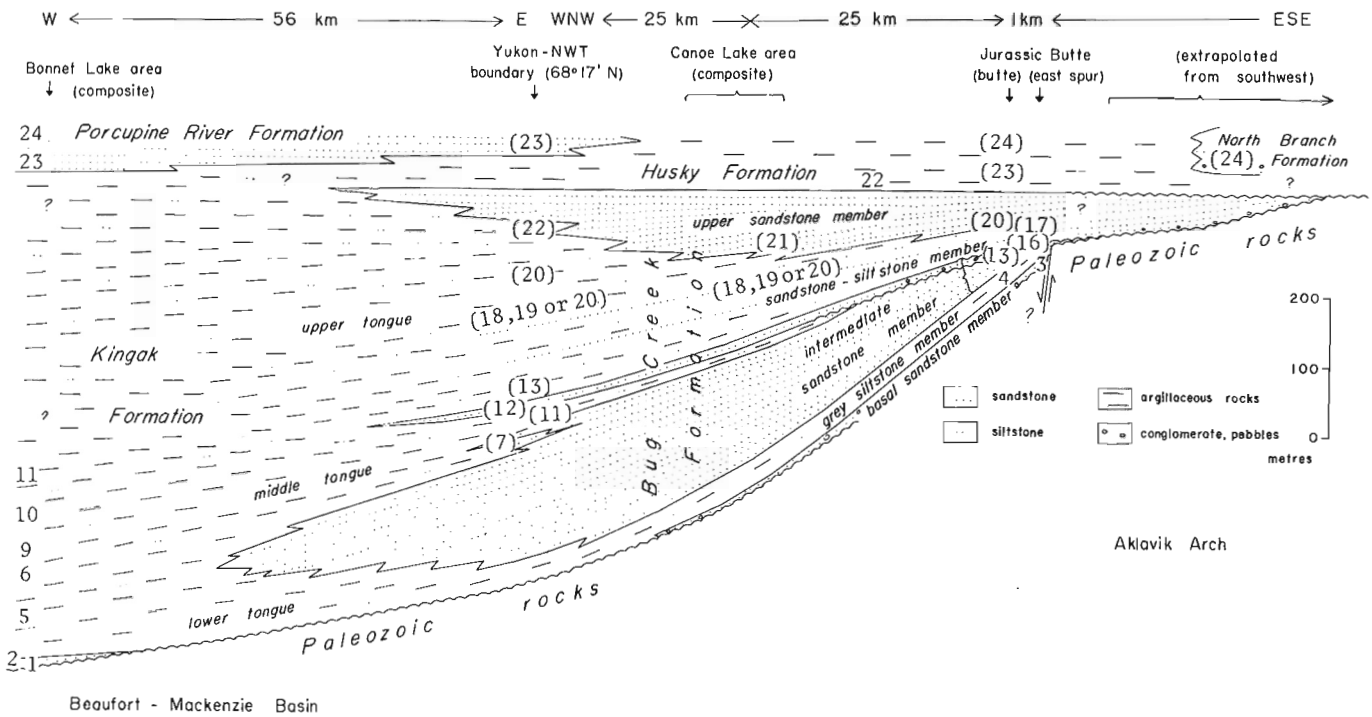

Figure 5.2. Generalized east-west stratigraphic cross-section A of Jurassic rocks, northern Richardson Mountains and as far west as Bonnet Lake (see Fig. 5.1). Terminology for the members of the Bug Creek Formation follows Jeletzky (1967). The numbers on the diagram indicate occurrences of diagnostic ammonites, most of which were identified by H. Frebold, or **Buchia** species, identified by J.A. Jeletzky. Those in brackets are extrapolated into the cross-section from nearby localities. The fossils and their ages are shown in Figure 5.5; a summary of the biostratigraphic data is given by Poulton (in press).

(Poulton and Callomon, 1976). The argillaceous middle Kingak tongue of Toarcian and Early Bajocian age occurs between these two sandstone units in sections north and west of Bug Creek, in the basinward succession off the Aklavik Arch. The upper, Bajocian, part of the intermediate sandstone is a thin, laterally persistent unit (Fig. 5.1) interpreted to be the basal unit of a southeasterly transgressive sea. The upper part of the Bug Creek Formation (sandstone-siltstone and upper sandstone members of Jeletzky (1967)) extends considerably farther southward than do the lower units of the Bug Creek Formation, overstepping Paleozoic rocks from McDougall Pass southward beyond Mount Millen. They are fluvial in character in their southern development (Jeletzky, 1967). Most of the sandstones are well cemented, and two major sandstone units, the upper sandstone member and lower part of the intermediate sandstone member, most commonly are hard, resistant orthoquartzites. This character reduces the potential for hydrocarbon discovery in the Bug Creek Formation.

The southeastward thinning of the Bug Creek Formation indicated in Figures 5.1 and 5.2 appears to have been accomplished both by original depositional thinning and by removal of part of the succession at the unconformity within the formation. The thinning, together with lithological, and to a lesser extent, paleontological facies variations, indicates approach to shorelines and sediment source areas to the southeast in Jurassic time. The exposures at Jurassic Butte, for example, are therefore unusually thin, rich in sandstone and conglomerate, and lack certain of the members developed in more complete, basinward successions. The Jurassic Butte outcrops are instructive, nevertheless, because they reveal the short lateral distance over which thinning and disappearance of units onto Aklavik Arch take place (Fig. 5.3).

The Bug Creek Formation forms most of the main bluff of Jurassic Butte itself and is also exposed in the small spurs extending eastward into Mackenzie Delta. The lower contact of the Bug Creek Formation with underlying Permian beds is difficult to locate precisely in the face of Jurassic Butte proper, partly because fossils have not been found there. It is tentatively placed at a conspicuous angular unconformity, both below and above which pebble-bearing sandstones occur. The basal sandstone member of the Bug Creek Formation here is unusually thin (1.5 m).

The Upper Permian sandstone unit that outcrops in the Aklavik Range to the north and west is absent on the spurs 1 to 2 km (approx.) east of Jurassic Butte and the Bug Creek Formation rests directly on red Permian(?) conglomerate beds. The contact is a fault in some exposures. The basal sandstone of the Bug Creek Formation is thicker (7.5 m approx.) here. The unconformity, above which lie probable Bajocian beds of the intermediate sandstone member, is probably located just above (west of) a 0.3 m thick (approx.) hard red sandstone bed which formed an erosion-resistant surface near the preserved top of the grey siltstone member. Belemnites and **Inoceramus**, together with chert-argillite pebbles, fossil wood and glauconite, characterize the lower beds of the intermediate sandstone member here. The bluff-forming sandstones of the upper sandstone member, which cap Jurassic Butte proper, may be missing on the spurs to the east due to a fault that juxtaposes lower beds of the sandstone-siltstone member against younger Upper Jurassic or Lower Cretaceous rocks (Jeletzky, 1967).

A small syn-Jurassic uplift in the vicinity of White Mountains has resulted in apparent removal of the lower part of the Bug Creek Formation (Fig. 5.4) below the unconformity within it (Poulton and Callomon, 1976). The northward

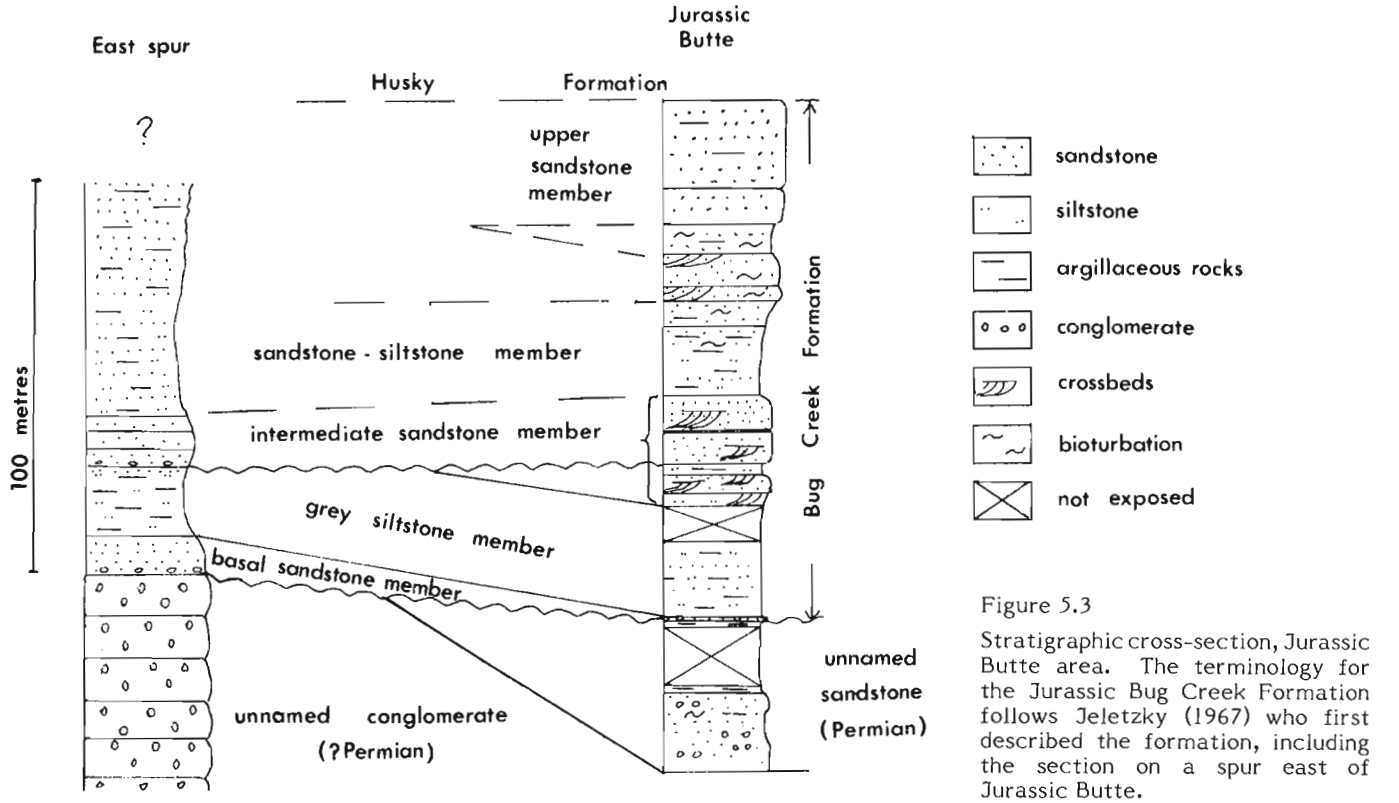

Figure 5.3

Stratigraphic cross-section, Jurassic Butte area. The terminology for the Jurassic Bug Creek Formation follows Jeletzky (1967) who first described the formation, including the section on a spur east of Jurassic Butte.

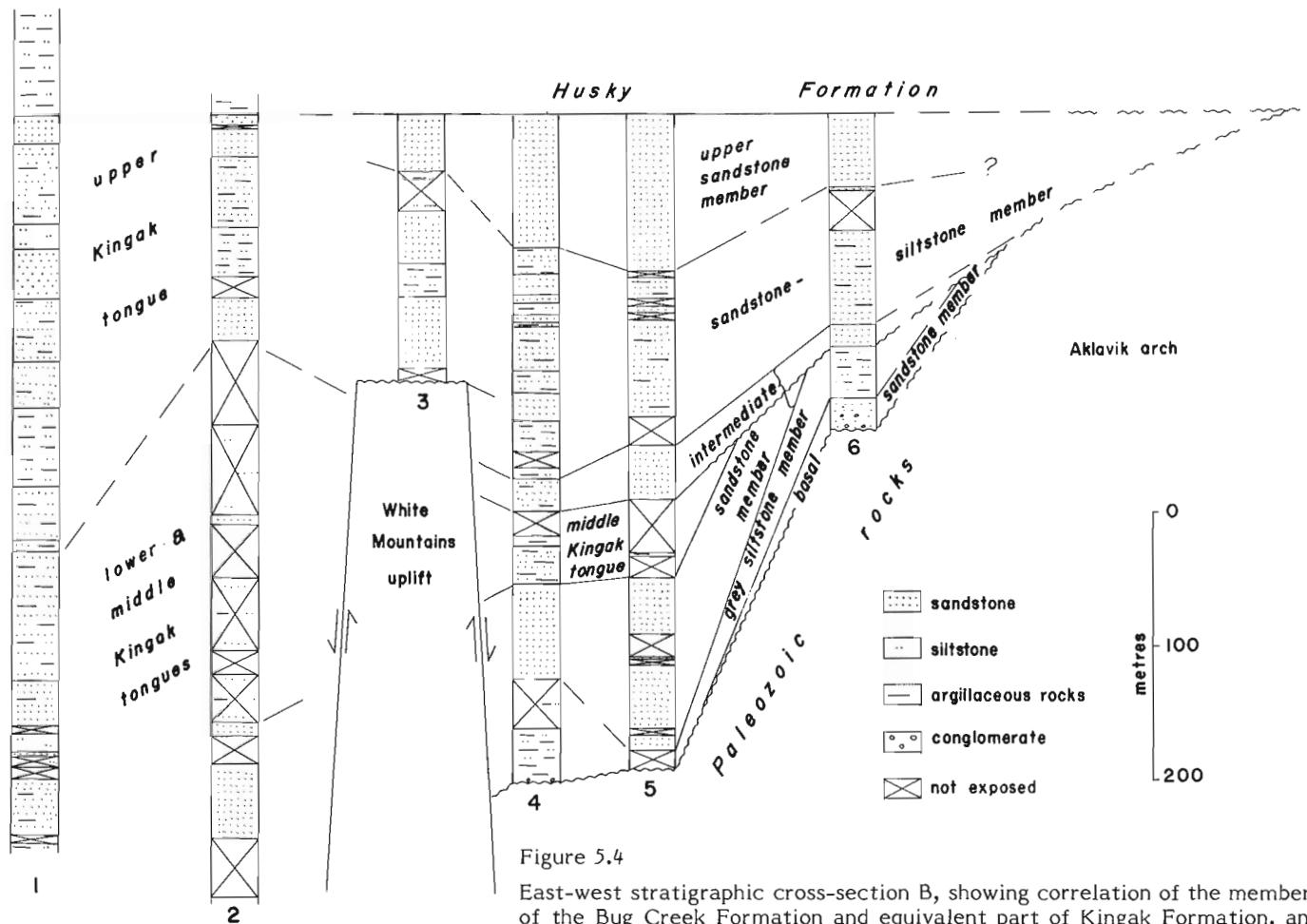

Figure 5.4

East-west stratigraphic cross-section B, showing correlation of the members of the Bug Creek Formation and equivalent part of Kingak Formation, and the White Mountains Uplift (location shown on Figure 5.1).

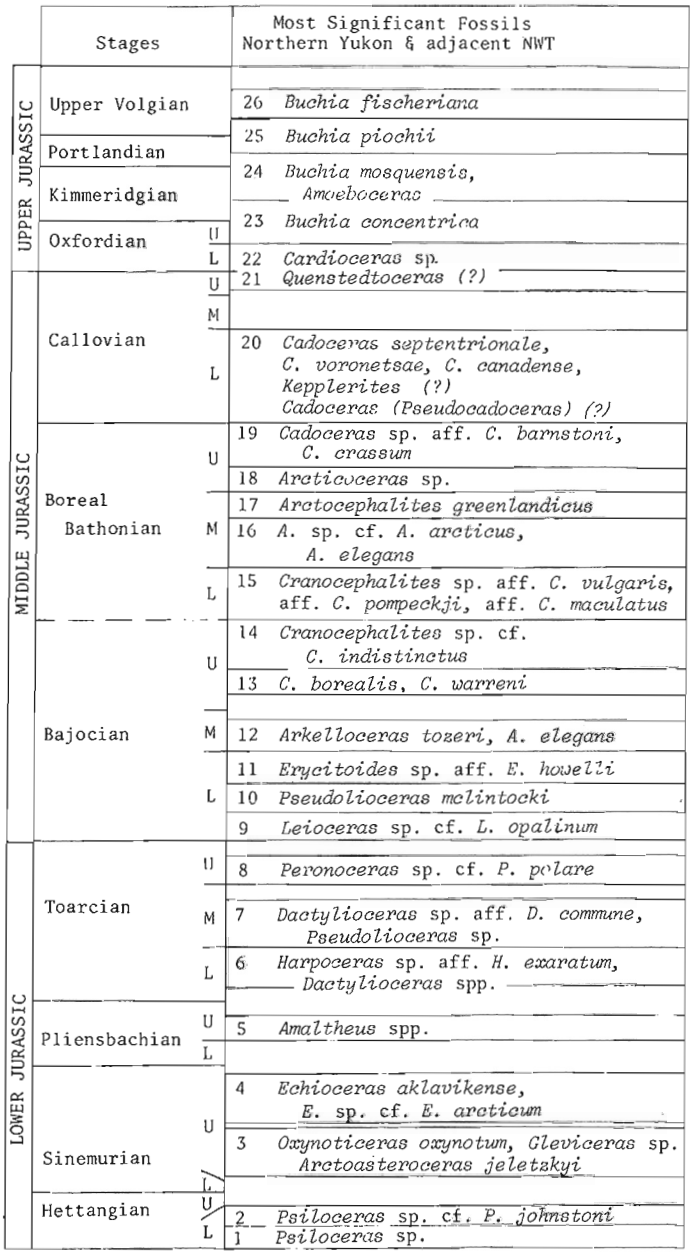

Figure 5.5. Summary of diagnostic Jurassic macrofossil occurrences and the ages they indicate based on correlations with northwestern Europe and eastern Greenland. Numbers refer to fossil occurrences shown in Figure 5.2.

extension of this uplift does not appear to be as great as Poulton and Callomon (1976) suggested, however, unless it was expressed in, but subsequently eroded from, the core of the present Cache Creek Uplift which appears to be offset by left-lateral movement northwestward from the White Mountains Uplift (D.K. Norris, pers. comm.). Relatively thick Jurassic sections between White Mountains and McDougall Pass indicate that the White Mountains Uplift was not continuous with the Aklavik Arch as previously stated (Poulton and Callomon, 1976). The precise nature of the boundaries of the White Mountains Uplift in the Jurassic remains unknown. They are interpreted as steep faults bounding a horst because of the short distance separating the essentially different successions adjacent to and within the uplift area. Steep post-Jurassic faults that may be primarily transcurrent in style (Norris and Yorath, in press) may have had significant vertical displacement as well (Young et al., 1976, Fig. 27). There is no evidence within the Jurassic rocks of slope deposits adjacent to the uplift or of sediment transport away from it.

The subdivisions of the Jurassic rocks shown in Figures 5.2 and 5.3 are not easily recognizable in the southwestern part of the area, between Bell and Porcupine rivers (Fig. 5.1). This is due in part to the lack of distinctive sandstone members in the basinward successions, and in part to complexity which may be due to the effects of the Aklavik Arch, as at Porcupine River near its confluence with Bell River, or of landmass source areas farther west (see Jeletzky, 1975).

References

Detterman, R.L., Reiser, H.N., Brosgé, W.P., and Dutro, J.T., Jr.
1975: Post-Carboniferous stratigraphy, northeastern Alaska; U.S. Geol. Surv., Prof. Paper 886.

Jeletzky, J.A.
1967: Jurassic and (?) Triassic rocks of the eastern slope of Richardson Mountains, northwest District of Mackenzie, 106M and 107B (parts of); Geol. Surv. Can., Paper 66-50.

1975: Jurassic and Lower Cretaceous paleogeography and depositional tectonics of Porcupine Plateau, adjacent areas of northern Yukon and those of Mackenzie District, N.W.T.; Geol. Surv. Can., Paper 74-16.

1977: Porcupine River Formation; a new Upper Jurassic sandstone unit, northern Yukon Territory; Geol. Surv. Can., Paper 76-27.

Leffingwell, E. de K.
1919: The Canning River region, northern Alaska; U.S. Geol. Surv., Prof. Paper 109.

Norris, D.K. and Yorath, C.J.
The North American Plate from the Arctic Archipelago to the Romanzof Mountains in The Ocean's Basins and Margins, v. 5, The Arctic Ocean, Chap. 3, F.G. Stehli et al., eds.; Plenum Press. (in press)

Poulton, T.P.
Notes on the pre-Late Oxfordian Jurassic biostratigraphy of northern Yukon and adjacent Northwest Territories; Geol. Assoc. Can., Spec. Paper. (in press)

Poulton, T.P. and Callomon, J.H.
1976: Major features of the Lower and Middle Jurassic stratigraphy of northern Richardson Mountains, northeastern Yukon Territory, and northwestern District of Mackenzie; in Report of Activities, Part B, Geol. Surv. Can., Paper 76-1B, p. 345-352.

Young, F.G., Myhr, D.W., and Yorath, C.J.
1976: Geology of the Beaufort-Mackenzie Basin; Geol. Surv. Can., Paper 76-11.

6. PALYNOLOGY OF THE LOWER PART, TYPE SECTION, TENT ISLAND FORMATION, YUKON TERRITORY

Project 770045

A.R. Sweet
Institute of Sedimentary and Petroleum Geology, Calgary

Abstract

Sweet, A.R., Palynology of the lower part, type section, Tent Island Formation, Yukon Territory; in Current Research, Part B, Geol. Surv. Can., Paper 78-1B, p. 31-37, 1978.

An assemblage of pollen, megaspores and fungal spores is described from fifteen samples of the Cuesta Creek Member and three outcrop samples of the Mudstone Member of the Tent Island Formation. The overall character of the assemblage and the presence of ***Aquilapollenites conatus*** *and* ***Wodehouseia*** *spp. indicate a Maastrichtian age.*

Introduction

The purpose of this paper is to record and describe pollen and spores from the Cuesta Creek Member and basal 6 m of the Mudstone Member of the Tent Island Formation at their type locality in the northwestern bank of Big Fish River near its junction with Boundary Creek, northern Yukon (68°30'30"N, 136°23'50"W). The Cuesta Creek Member was proposed by Young (1975) for a succession of sandstones, conglomerates and mudstones in the basal part of the Tent Island Formation. The member comprises the same strata as Unit 1 of Holmes and Oliver (1973). The contact between the Cuesta Creek Member and the underlying Boundary Creek Formation is not exposed at the type locality (Young, 1975). The writer estimated this contact to be about 4 m below the base of the exposed section at a slight change in slope. The Cuesta Creek Member lies conformably below the Mudstone Member of the Tent Island Formation.

Figure 6.1 illustrates the lithostratigraphic succession at the type locality based on the writer's field work of 1975 when he and D.C. Hope measured the Cuesta Creek Member as 106.5 m thick. This agrees closely with Young's (1975, p. 54, 55) measurement of equivalent units as 110.6 m.

Rouse and Srivastava (1972), McIntyre (1974), Doerenkamp et al. (1976) and Wilson (1977) have described palynological assemblages that are relevant to this study by virtue of their ages and their proximity to the Yukon Coastal Plain.

Method

The pollen and spores in the Cuesta Creek Member and contiguous strata are poorly preserved (Pl. 6.1, 6.2) because of thermal alteration (organic maturation) or weathering, and possibly also because of an unfavourable depositional environment. Fifteen to 20 g of rock were processed for miospores and an additional 100 g for megaspores. The acid insoluble organic residues were oxidized in Schulze's solution at room temperature for 8 to 48 hours, then for 3 to 5 minutes in Schulze's solution at 100°C.

The observed number of specimens of biostratigraphically significant species is listed in Figure 6.1. These numbers are based upon the complete scanning of at least six 22 x 40 mm coverslips per sample containing representative size-fractions of residue up to the plus 45 µm size fraction. In addition, up to 4 slides per sample were examined from a plus 45 µm size fraction obtained from the megaspore preparations. All but 4 of the specimens of **Wodehouseia** sp. A, one half of the recorded number of **Aquilapollenites** cf. **A. sentus** Srivastava 1969, and most of the megaspores are obtained from the latter. Therefore the numbers of specimens given in Figure 6.1 are disproportionately high for the larger taxa and are given only to reflect the relative scarcity of identifiable specimens.

Palynological Assemblage

In addition to the taxa listed in Figure 6.1, other probably indigenous palynomorphs in the basal part of the Tent Island Formation include: bisaccate pollen (dominant); pollen of the Cupressaceae-Taxodiaceae complex; **Pulcheripollenites** sp. (Pl. 6.1, fig. 20, Pl. 6.2, fig. 5), **Ulmipollenites** sp., miscellaneous tricolpate (Pl. 6.2, fig. 6,7),

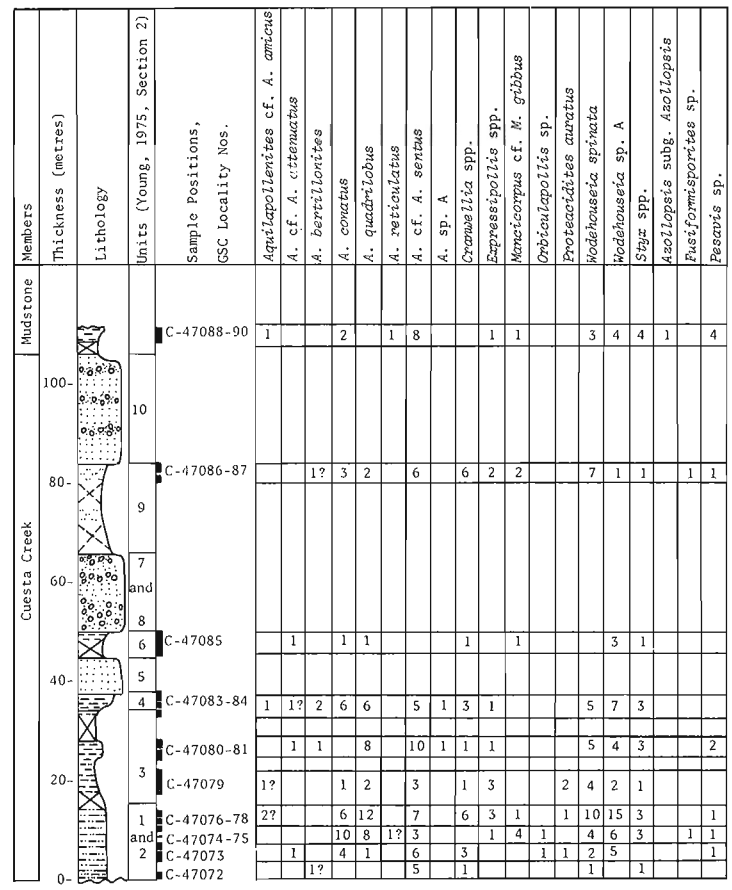

Figure 6.1. Chart of selected pollen, megaspores and fungal spores showing stratigraphic occurrences.

monocolpate (**Liliacidites** sp., Pl. 6.2, fig. 4) and triporate pollen; species of **Cicatricosisporites, Deltoidospora, Laevigatosporites, Lycopodiumsporites, Stereisporites, Taurocusporites** and **Zlivisporis** (Pl. 6.2, fig. 10); fungal spores (Pl. 6.2, fig. 14-17) and miscellaneous dinoflagellates. Also encountered were single specimens of **Ovoidites ligneolus** (Potonié) Thomson and Pflug 1953 (Pl. 6.2, fig. 8) and **Operculites** sp. (Pl. 6.2, fig. 19); several of **Schizophacus parvus** (Cookson and Dettmann) Pierce 1976 (Pl. 6.2, fig. 9), **Palambages** sp. and **Pediastrum** sp. (Pl. 6.2, fig. 20); and many specimens of **Horologinella** sp. (Pl. 6.2, fig. 21) showing a wide range of morphological variation.

Reworked palynomorphs in the basal part of the Tent Island Formation include Early Devonian and Carboniferous miospores; probable Permo-Triassic striate bisaccate pollen; Early Cretaceous dinoflagellates (W.W. Brideaux, pers. comm., October, 1977); and a typical Late Albian to Cenomanian assemblage of megaspores including **Arcellites disciformis** Miner emend. Ellis and Tschudy 1964, **A. reticulatus** (Cookson and Dettmann) Potter 1963 and **Balmeisporites holodictyus** Cookson and Dettmann 1958. A few specimens of **Bacutriletes** sp., **Erlansonisporites** sp., and **Costatheca** sp., which may or may not be reworked, were also recovered.

Pollen Grains

Aquilapollenites cf. **A. amicus** Srivastava 1968

Plate 6.1, figure 4

Remarks. Two specimens similar to **A. amicus** were observed. The figured specimen lacks sculpturing on its equatorial projections, perhaps reflecting its poor state of preservation. **Aquilapollenites amicus** occurs in the lower part of the Edmonton Group of Alberta (Srivastava, 1970) and in the Frenchman Formation (upper Maastrichtian) of Saskatchewan (unpublished data).

Aquilapollenites cf. **A. attenuatus** Funkhouser 1961

Plate 6.1, figure 6

Remarks. The sparsely spinose, isopolar to subisopolar aquiloid grains encountered in this study are comparable with **A. attenuatus** in their pattern of spine distribution, their relatively large size and their prominent endexinal thickenings. Similar forms were referred to **A. asper** Mchedlishvili 1961 and **A. aucellatus** Srivastava 1969 in McIntyre (1974). **Aquilapollenites** of this general type range from the Campanian to the top of the Maastrichtian (Tschudy and Leopold, 1970).

Aquilapollenites bertillonites Funkhouser 1961

Plate 6.1, figures 2 and 3

Occurrence. Hell Creek and Lance formations of midcontinental USA, Maastrichtian (Tschudy and Leopold, 1970); Frenchman Formation (Maastrichtian) of Saskatchewan (unpublished data).

Aquilapollenites conatus Norton 1965

Plate 6.1, figure 1

Remarks. Because of the reduced striae on the equatorial projections, the specimens seen in this study are better referred to **A. conatus** than to another otherwise similar species, **A. parallelus** Tschudy 1969, from undifferentiated Upper Cretaceous strata in Alaska.

Occurrence. Upper portion of the Hell Creek and Lance formations of midcontinental USA, middle to upper Maastrichtian (Tschudy and Leopold, 1970); between the 'mauve shale' (Battle Formation) and Nevis coal seam (lower part of the Scollard Formation; Gibson, 1977), of Alberta, upper Maastrichtian (Srivastava, 1970); and the upper Maastrichtian of the Alaskan North Slope (Wiggins, 1976, p. 54).

Heteropolar, spinose forms of **Aquilapollenites**

Plate 6.1, figures 7-9

Remarks. In some specimens from the Cuesta Creek Member, the diameter of the major polar dome approaches that of the equatorial projections (of the **A. pulcher** Funkhouser 1961 type; Pl. 6.1, fig. 7, 8), whereas in others the diameter of the major polar projection greatly exceeds that of the equatorial projections (of the **A. quadrilobus** type; Pl. 6.1, fig. 9). Because of taxonomic confusion and differences in interpreting species within this group, a reliable age range for individual species is often difficult to extract from literature. Tschudy and Leopold (1970) indicate that heteropolar forms of **Aquilapollenites** range throughout the Campanian and Maastrichtian.

Plate 6.1

Figures x1000 unless otherwise stated. (ISPG 1059-2)

Figure 1. **Aquilapollenites conatus** Norton 1965: C-47074, GSC Type No. 48961.

Figures 2, 3. **Aquilapollenites bertillonites** Funkhouser 1961: equatorial view, C-47072, GSC Type No. 48962; polar view, C-47080, GSC Type No. 48963, respectively.

Figure 4. **Aquilapollenites** cf. **A. amicus** Srivastava 1968: C-47083, GSC Type No. 48964.

Figure 5. **Aquilapollenites reticulatus** (Mchedlishvili) Tschudy and Leopold 1970: C-47090, GSC Type No. 48965.

Figure 6. **Aquilapollenites** cf. **A. attenuatus** Funkhouser 1961: C-47085, GSC Type No. 48966.

Figures 7-9. Heteropolar, spinose forms of **Aquilapollenites:** C-47083, GSC Type No. 48967; C-47085, GSC Type No. 48968; C-47080, GSC Type No. 48969, respectively.

Figures 10, 11. **Aquilapollenites** cf. **A. sentus** Srivastava 1969: C-47083, GSC Type No. 48970; C-47084, GSC Type No. 48971, respectively. Both x500.

Figures 12, 13. **Aquilapollenites** sp. A: C-47083, GSC Type No. 48972; C-47081, GSC Type No. 48973, respectively.

Figure 14. **Mancicorpus** cf. **M. gibbus** Srivastava 1968: C-47076, GSC Type No. 48974. x500.

Figures 15-19. **Cranwellia** spp.: C-47077, GSC Type No. 48975; C-47087, GSC Type No. 48976; C-47085, GSC Type No. 48977; C-47087, GSC Type No. 48978; C-47084, GSC Type No. 48979, respectively. Figure 19, x500.

Figure 20. **Pulcheripollenites** sp.: C-47076, GSC Type No. 48980.

Figure 21. **Proteacidites auratus** Srivastava 1969: C-47073, GSC Type No. 48981.

Figure 22. **Orbiculapollis** sp.: C-47074, GSC Type No. 48982.

Figures 23-26. **Expressipollis** spp.: C-47079, GSC Type No. 48983; C-47080, GSC Type No. 48984; C-47080, GSC Type No. 48985; C-47081, GSC Type No. 48986.

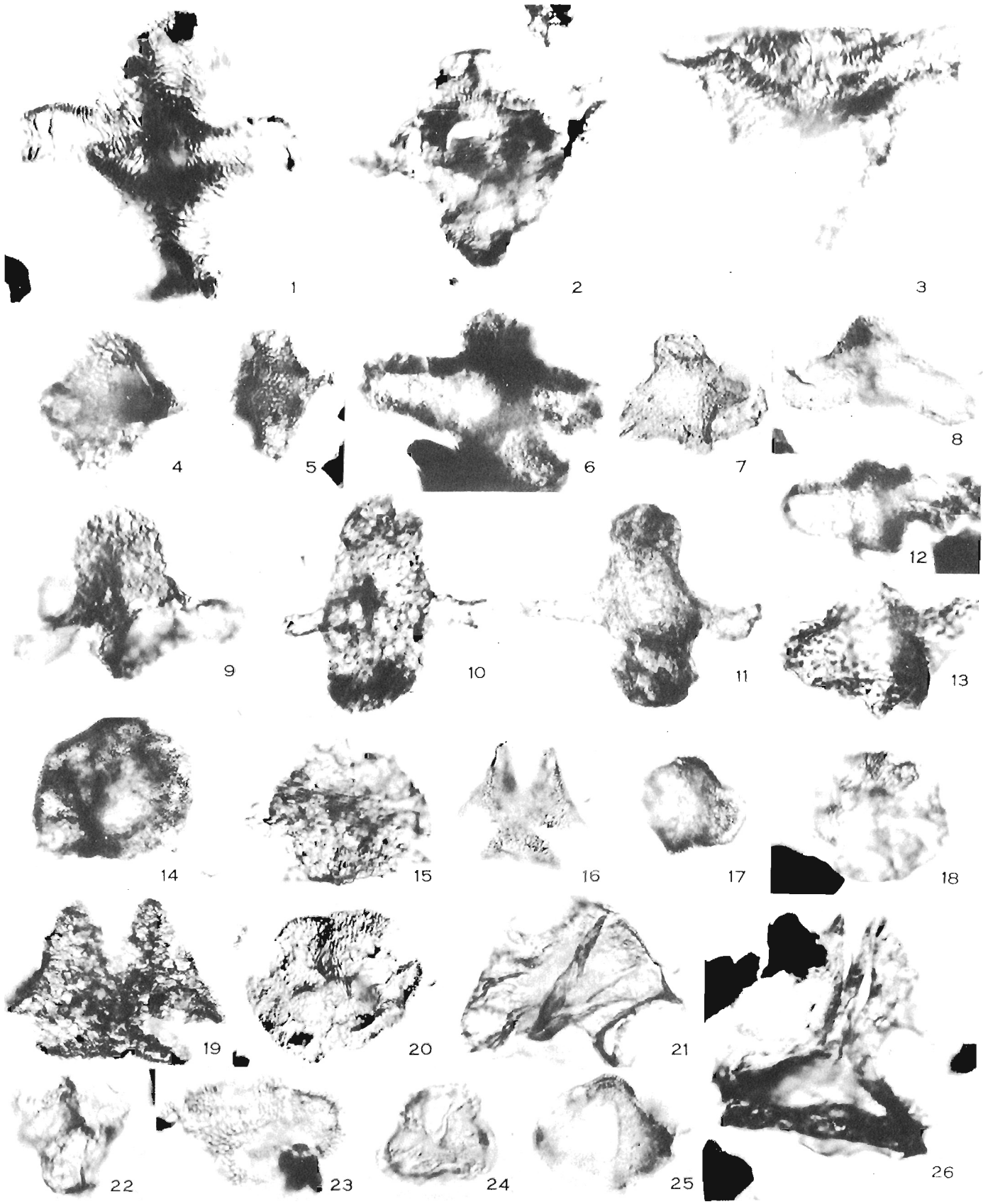
1
2
3
4
5
6
7
8
9
10
11
12
13
14
15
16
17
18
19
20
21
22
23
24
25
26

Aquilapollenites reticulatus (Mchedlishvili)

Tschudy and Leopold 1970

Plate 6.1, figure 5

Remarks. Only a single specimen referrable to this species was seen.

Occurrence. This species has been widely reported from upper Campanian to upper Maastrichtian strata (Tschudy and Leopold, 1970). In Saskatchewan it ranges into the base of the Ravenscrag Formation of Paleocene age (unpublished data).

Aquilapollenites cf. **A. sentus** Srivastava 1969

Plate 6.1, figures 10, 11

Remarks. The size (polar axis 68.5 (80) 95.6 µm long; equatorial diameter including projections 63 (83.5) 106 µm; equatorial projections 16 (27.6) 34.7 µm long) and the constriction of the polar projections immediately above the equatorial region (Pl. 6.1, fig. 11) in some specimens are much the same as in **A. sentus.** However, the spines of **A. sentus** are considerably larger (4-7 µm long, 1.5-3.5 µm wide at base) than those observed in **A.** cf. **A. sentus** (1-4.5 µm long, 0.8-1.2 µm wide). Srivastava (1970) reports **A. sentus** as occurring in the lower and middle parts of the Edmonton Group (Horseshoe Canyon Formation) of Early and Middle Maastrichtian age.

Aquilapollenites sp. A.

Plate 6.1, figures 12, 13

Remarks. Iso- to subisopolar grains with a relatively short polar axis and numerous spines distributed over the entire surface are referred to this species.

Cranwellia spp.

Plate 6.1, Figures 15 to 19

Remarks. Over twenty specimens of striate, tricolp(or)ate pollen were encountered exhibiting variation in size and shape. One striate, tetracolpate specimen, possibly **Cranw edmontonensis** Srivastava 1966, was recorded (Pl. 6.1, ..g. 18). **Cranwellia** has frequently been reported from Campanian to Maastrichtian strata but is also known to range into the Tertiary and may have affinity with the extant genus **Elytranthe** (Srivastava, 1966).

Expressipollis spp.

Plate 6.1, figures 23-26

Remarks. Several specimens, all poorly preserved, are referrable to **Expressipollis.** These include forms having affinity with the **Expressipollis accuratus** Chlonova 1961 complex of Felix and Burbridge (1973) (Pl. 6.1, fig. 23) and possible specimens of **Expressipollis ocliferius** Chlonova 1961 (Pl. 6.1, fig. 26). Although the identity of these species is uncertain, the recognition of **Expressipollis** indicates that the Cuesta Creek flora probably has affinities with the floras described from the lower Eureka Sound Formation (Felix and Burbridge, 1973), the upper shale member of the Kanguk Formation (Doerenkamp et al., 1976) and the Mason River Formation of the Horton River Section (McIntyre, 1974).

Mancicorpus cf. **M. gibbus** Srivastava 1968

Plate 6.1, figure 14

Remarks. All observed specimens are badly preserved. **Mancicorpus gibbus** is known from strata below the 'mauve shale' (Battle Formation) of Alberta (Srivastava, 1970) and has been observed in the Frenchman Formation of Saskatchewan (unpublished data). Both occurrences are Maastrichtian.

Orbiculapollis sp.

Plate 6.1, figure 22

Occurrence. **Orbiculapollis** has been widely reported in the Upper Cretaceous boreal floral complex of western Siberia and Arctic Canada (Doerenkamp et al., 1976).

Proteacidites auratus Srivastava 1969

Plate 6.1, figure 21

Occurrence. Lower to middle part of the Edmonton Group of Alberta, Maastrichtian (Srivastava, 1970); Bonnet Plume Formation of northeastern Yukon Territory, Maastrichtian (Rouse and Srivastava, 1972).

Wodehouseia spinata Stanley 1961

Plate 6.2, figure 1

Remarks. Fourteen specimens gave a size range of 44 (50) 57 µm (long equatorial, pollen b axis) by 30 (35) 40 µm (polar, pollen c axis), a fifteenth specimen, 68 x 48 µm, resembled the smaller specimens in all but size.

Plate 6.2

Figures x1000 unless otherwise stated. (ISPG 1059-1)

Figure 1. **Wodehouseia spinata** Stanley 1961: C-47087, GSC Type No. 48987.

Figures 2, 3. **Wodehouseia** sp. A: C-47076, GSC Type No. 48988; C-47080, GSC Type No. 48989, respectively. Both x500.

Figure 4. **Liliacidites** sp.: C-47081, GSC Type No. 48990.

Figure 5. **Pulcheripollenites** sp.: C-47074, GSC Type No. 48991.

Figures 6, 7. Tricolpate pollen: C-47087, GSC Type No. 48992; C-47072, GSC Type No. 48993, respectively.

Figure 8. **Ovoidites ligneolus** (Potonié) Thomson and Pflug 1953: C-47086, GSC Type No. 48994; x500.

Figure 9. **Schizophacus parvus** (Cookson and Dettmann) Pierce 1976: C-47076, GSC Type No. 48995.

Figure 10. **Zlivisporis** sp.: C-47075, GSC Type No. 48996.

Figures 11-13. **Styx** spp.: C-47081, GSC Type No. 48997; C-47090, GSC Type No. 48998; C-47080, GSC Type No. 48999. Figure 11, x500. Figures 12 and 13, x400.

Figure 14. **Fusiformisporites** sp.: C-47086, GSC Type No. 49000.

Figure 15. **Pesavis** sp.: C-47074, GSC Type No. 49001.

Figure 16. Fungal spore: C-47081, GSC Type No. 49002.

Figure 17. **Pluricellaesporites** sp.: C-47088, GSC Type No. 49003; x500.

Figure 18. **Azollopsis** massula: C-47090, GSC Type No. 49004, x500.

Figure 19. **Operculites** sp.: C-47086, GSC Type No. 49005.

Figure 20. **Pediastrum** sp.: C-47076, GSC Type No. 49006; x500.

Figure 21. **Horologinella** sp.: C-47081, GSC Type No. 49007.

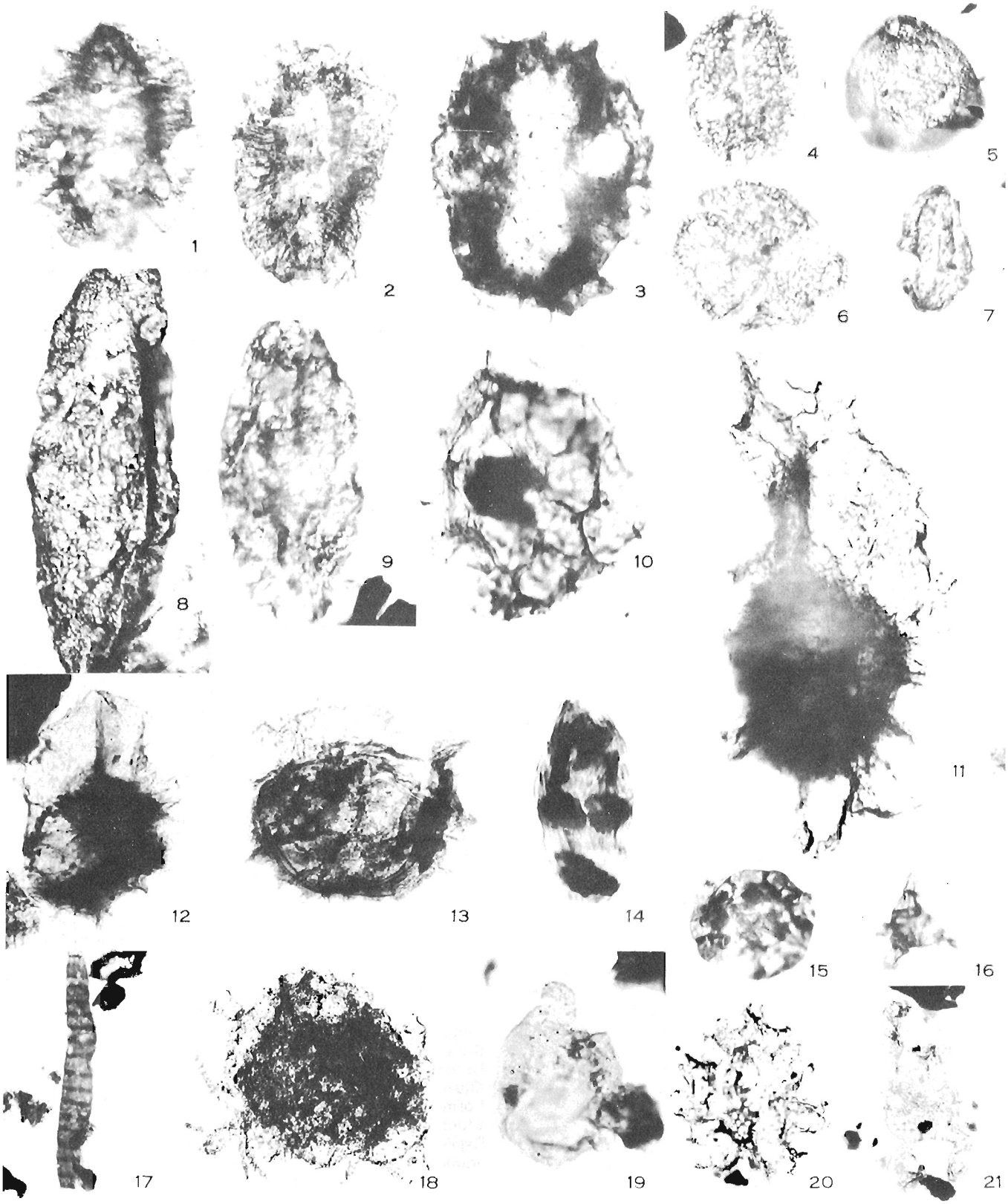
1
2
3
4
5
6
7
8
9
10
11
12
13
14
15
16
17
18
19
20
21

Occurrences. **Wodehouseia spinata** occurs widely in strata ranging from Maastrichtian to Paleogene in age (for known occurrences see Wiggins, 1976). Adjacent to the Cuesta Creek type section it is abundant in the upper Maastrichtian of the Alaskan North Slope and southern Alaska, with specimens locally occurring in the Paleocene of the Alaskan North Slope (Wiggins, 1976). It first occurs 51.8 m above the base of McIntyre's H3 division in the Horton River Section, District of Mackenzie (McIntyre, 1974) and is known also from the CVI zone (CVIc subdivision) and CVII zone in the shale member of the Kanguk Formation, Banks Island (Doerenkamp et al., 1976) and from the Zone 2 of the Bonnet Plume Formation of northeastern Yukon Territory (Rouse and Srivastava, 1972).

Wodehouseia sp. A.

Plate 6.2, figures 2, 3

Description. Based on 30 specimens – Long equatorial, pollen b axis 66 (89.5) 112 µm, S.D. 11.8 µm; polar, pollen c axis 50 (70.8) 98 µm, S.D. 11.8 µm. Pollen grain with a 3-zoned sculpture pattern: aperture region reticulate, devoid of apiculate sculptural elements except for a single spine or cone set on the distal side of each colp (observed on two specimens); central body-flange transition region fimbriate or with relatively fine, radially oriented plicae, and lacking prominent apiculate sculpture; outer flange-flange meridian region reticulate, with prominent 5 to 9 µm long, 1.5 to 3 µm wide at base, apiculate sculptural elements projecting above the general ektexinal surface and beyond the flange margin. Apiculate elements are generally spinose, some are baculate with blunt terminations. The distance between colpi is 30 µm (one specimen), which if typical of the population would imply that the colpi were inserted in from the ends of the grain approximately one third length of long equatorial axis. The inner outline of the flange on some specimens (Pl. 6.2, fig. 3) suggests that the central body is dumbbell shaped. The flange is constricted at the terminus of the long equatorial axis.

Remarks. The terminology above is that of Wiggins (1976). **Wodehouseia** sp. A probably is a new species or subspecies but is not formally named because of its poor preservation.

Four previously described taxa, **Wodehouseia fimbriata** Stanley 1961, **W. fimbriata** subsp. **constricta** Wiggins 1976, **W. excelsa** (Samoilovitch) Wiggins 1976, and **W. vestivirgata** Wiggins 1976 share with **Wodehouseia** sp. A a relatively large size and a 3-zoned sculpture pattern with a fimbriate medial zone. Of the four listed above only **W. fimbriata** subsp. **constricta** and **W. vestivirgata** have, like **Wodehouseia** sp. A, a conspicuously constricted flange in the equatorial region. The density and length of the apiculate elements in the outer flange-flange meridian zone in **Wodehouseia** sp. A are more similar to those illustrated for **W. vestivirgata**, whereas the mostly spinose form of the sculpture elements, the spacing of the colpi and the probable dumbbell shape of the central body are similar to those of **W. fimbriata** var. **constricta**. **Wodehouseia vestivirgata** is known from the upper Maastrichtian and **W. fimbriata** subsp. **constricta** from the upper Maastrichtian to lower Paleocene of the Alaskan North Slope (Wiggins, 1976).

Megaspores

Styx spp.

Plate 6.2, figures 11-13

Remarks. The several specimens of **Styx** recovered appear to represent at least three species, **Styx minor** Norton 1967, **Styx canadensis** (Srivastava and Binda) Sweet 1978, and a rugulate form possibly of the **Styx rara** (Kondinskaya) Srivastava 1971 type. Most reported occurrences of **Styx** are confined to the Upper Cretaceous.

Azollopsis subg. **Azollopsis**

Plate 6.2, figure 18

Remarks. One massulae with multibarbed glochidia characteristic of subg. **Azollopsis** was recovered. This subgenus ranges in age from Campanian to ?Eocene (Sweet and Hills, 1974).

Fungal Spores

Fusiformisporites sp.

Plate 6.2, figure 14

Occurrence. Elsik (1976) considers the range of **Fusiformisporites** to be from mid-Paleocene to Recent.

Pesavis sp.

Plate 6.2, figure 15

Remarks. This form of conidiospore was given the preliminary name **P.** "parva" by Jansonius (1976). It may be conspecific with the specimen in Elsik and Jansonius (1974, Pl. 1, fig. 10), from Paleogene strata of the Mackenzie delta.

Age Interpretation

The maximum age of the Cuesta Creek Member is inferred to be Maastrichtian based on the combined occurrence of **Wodehouseia spinata**, **Wodehouseia** sp. A and **Aquilapollenites conatus**. If one accepts that the pollen spectrum represents an indigenous assemblage, the probable minimum age can be determined as late Maastrichtian based on the character of the total assemblage and in particular the occurrence of a relatively diverse assemblage of aquiloid pollen together with **Cranwellia**, **Expressipollis** and **Styx**.

The occurrence of **Pesavis** and **Fusiformisporites** might be considered indicative of a Paleocene age. This interpretation would require that much of the recovered pollen be considered reworked. The relatively poor documentation that is currently available for the total stratigraphic ranges of fungal spores weakens the argument for a Paleocene age.

The assemblages from Zone 2 of the Bonnet Plume Formation (Rouse and Srivastava, 1972), from Division H3 of the "pale shale zone" (McIntyre, 1974), and from the shale member of the Kanguk Formation (Doerenkamp et al., 1976) all bear similarities to that in the lower Tent Island Formation. The latter assemblage has in common with the Zone 2 assemblage of the Bonnet Plume Formation spinose, heteropolar and spinose, isopolar aquiloid pollen, **Cranwellia**, **Pulcheripollenites**, **Proteacidites auratus** and **Wodehouseia spinata**. However, **Expressipollis** and **Orbiculapollis** were not reported by Rouse and Srivastava (1972).

The middle part (51.8-125 m) of McIntyre's (1974) Division H3 contains a closely comparable flora to that in the lower Tent Island Formation. This interval encompasses the upper part of the Lower Member and the lower part of the Middle Member of the Mason River Formation (Yorath et al., 1975). Doerenkamp et al. (1976) compared their CVIc subzone flora from the upper part of the shale member of the Kanguk Formation with that of the middle part of McIntyre's Division H3 defined above. In common with these Kanguk and Mason River assemblages, that from the lower Tent Island Formation contains **Wodehouseia spinata**, **Wodehouseia** sp. A which bears some morphologic similarity to **W. fimbriata** s.l., **Expressipollis** spp., **Orbiculapollis** sp., and an assemblage of aquiloid pollen that encompasses a variety of morphotypes. Hence it is probable that the exposed part of the Cuesta Creek Member at its type locality and the base of the Mudstone Member, or the lower Tent Island Formation, is correlative with a horizon at least 51.8 m above the base of the Mason River Formation and with some portion of the upper part of the shale member of the Kanguk Formation.

Acknowledgments

The author thanks S. Pickering for extracting palynomorphs from unpromising samples and E. O'Keefe for processing the megaspore samples. The capable field assistance of D.C. Hope is gratefully acknowledged as are the helpful discussions with F.G. Young on the stratigraphy of the Yukon coastal plain. W.W. Brideaux obliged with a critical reading and W.A.M. Jenkins with a constructive dissection of the paper.

References

Doerenkamp, A., Jardiné, S., and Moreau, P.
1976: Cretaceous and Tertiary palynomorph assemblages from Banks Island and adjacent areas (N.W.T.); Bull. Can. Pet. Geol., v. 24, p. 372-417.

Elsik, W.C.
1976: Microscopic Fungal remains and Cenozoic palynostratigraphy; Geosci. Man., v. 15, p. 115-120.

Elsik, W.C. and Jansonius, J.
1974: New genera of Paleogene fungal spores; Can. J. Botany, v. 52, p. 973-958.

Felix, C.J. and Burbridge, P.P.
1973: A Maestrichtian age microflora from Arctic Canada; Geosci. Man., v. 7, p. 1-29.

Gibson, D.W.
1977: Upper Cretaceous and Tertiary coal-bearing strata in the Drumheller-Ardley region, Red Deer River Valley, Alberta; Geol. Surv. Can., Paper 76-35, p. 41.

Holmes, D.W. and Oliver, T.A.
1973: Source and depositional environments of the Moose Channel Formation, Northwest Territories; Bull. Can. Pet. Geol., v. 24, p. 435-478.

Jansonius, J.
1976: Paleogene fungal spores and fruiting bodies of the Canadian Arctic; Geosci. Man., v. 15, p. 129-132.

McIntyre, D.J.
1974: Palynology of an Upper Cretaceous section, Horton River, District of Mackenzie, N.W.T.; Geol. Surv. Can., Paper 74-14, p. 1-56.

Rouse, G.E. and Srivastava, S.K.
1972: Palynological zonation of Cretaceous and Early Tertiary rocks of the Bonnet Plume Formation, northeastern Yukon, Canada; Can. J. Earth Sci., v. 9, p. 1163-1179.

Srivastava, S.K.
1966: Upper Cretaceous microflora (Maestrichtian) from Scollard, Alberta, Canada; Pollen Spores, v. 8, p. 497-552.

1970: Pollen biostratigraphy and paleoecology of the Edmonton Formation (Maestrichtian) Alberta, Canada; Paleogeogr. Paleoclimatol. Paleoecol., v. 7, p. 221-276.

Sweet, A.R. and Hills, L.V.
1974: A detailed study of the genus **Azollopsis**; Can. J. Botany, v. 52, p. 1625-1642.

Tschudy, B.D. and Leopold, E.B.
1970: **Aquilapollenites** (Rouse) Funkhouser – Selected Rocky Mountain taxa and their stratigraphic ranges; Geol. Soc. Am., Spec. Paper 127, p. 113-167.

Wiggins, V.D.
1976: Fossil Oculata pollen from Alaska; Geosci. Man., v. 15, p. 51-76.

Wilson, A.M.
1977: Palynology of three sections across the uppermost Cretaceous-Paleocene boundary in the Yukon Territory and District of Mackenzie, Canada; unpub. M.Sc. thesis, Dep. Geol. Sci., Univ. Saskatchewan.

Yorath, C.J., Balkwill, H.R., and Klassen, R.W.
1975: Franklin Bay and Malloch Hill map-areas, District of Mackenzie; Geol. Surv. Can., Paper 74-36, p. 1-35.

Young, F.G.
1975: Upper Cretaceous stratigraphy, Yukon Coastal Plain and northwestern Mackenzie Delta; Geol. Surv. Can., Bull. 249, p. 1-83.

7. EVALUATION OF He AND Rn GEOCHEMICAL URANIUM EXPLORATION TECHNIQUES IN THE "KEY" LAKE AREA, SASKATCHEWAN

Project 720067

W. Dyck, R.A. Campbell, and J.C. Pelchat
Resource Geophysics and Geochemistry Division

Abstract

Dyck, W., Campbell, R.A., and Pelchat, J.C., Evaluation of He and Rn geochemical uranium exploration techniques in the "Key" Lake area, Saskatchewan; in Current Research, Part B, Geol. Surv. Can., Paper 78-1B, p. 39-44, 1978.

To determine the strength and extent of various geochemical signals, particularly those of He and Rn, emanating from the U deposits in the "Key" Lake, Saskatchewan area several drillhole waters, detailed lake bottom water samples, and 100 lake water samples from an 800 km² area surrounding "Key" Lake were collected, and analyzed in the field laboratory for He, Rn, O_2, Eh, pH and conductivity.

Generally the lakes are shallow (less than 10 m) and well mixed in the summer as indicated by near equilibrium O_2 values and uniform temperatures down to 7 to 10 m. Mixing has resulted in small values for the dissolved gases Rn and He and much lower values (up to a factor of 8) in the summer than in the winter under the ice.

Regional Rn and He values, determined in the field, ranged from 0 to 293 picocuries/L (pc/L) and 43 to 92 std nanolitres/litre (nL/L) respectively, with background values of about 1 pc/L for Rn and 43 nL/L for He. By comparison, waters from drillholes into the main ore zone yielded up to 300,000 pc/L Rn and 20,000 nL/L He.

The semidetailed and detailed follow-up confirmed two anomalous Rn areas, one at "Zimmer" Lake and the other at "Seahorse" Lake. On these scales of exploration both He and Rn in lake waters detected the radioactive boulder fields and the ore below several of the lakes. Concentrations were relatively low. Rn seemed more stable and gave larger contrasts than He but took longer to measure.

Introduction

The recently discovered high grade U deposits at "Key" Lake, Saskatchewan (Dahlkamp and Tan, 1977) provide excellent sites for the testing of U exploration techniques. Although drilling has already caused some disturbance of the natural environment at "Key" Lake, it is important that as many tests as possible are carried out prior to mining, for it has been the authors experience that mining activities have a profound effect on the distribution of elements in the surficial environment.

To determine the usefulness of He, Rn and U in lakes and groundwaters, in particular He for U exploration, a series of tests were designed and carried out during the 1977 field season in the "Key" Lake area. For logistic reasons the 3 man Geological Survey of Canada party joined a University of Regina team which was carrying out detailed geochemical studies in the "Key" Lake area under the direction of Dr. Parslow. The main objectives of the field tests were: (1) to see what kind of He signal could be observed in the waters over the ore deposits relative to barren country; (2) to test a semiportable He analyzer under field conditions; and (3) to compare Rn, U, and He levels obtained in the summer to those in the winter under the ice. To evaluate the effectiveness of the He method relative to the Rn and U methods of prospecting, lake waters and sediments were also collected for Rn and U analysis at selected sites. This report describes in summary form the actual field work carried out, the preliminary analytical results obtained in the field laboratory, and presents some tentative conclusions.

Field Investigations

The field investigations can be divided into 5 interrelated tests:-

1. Regional lake water and sediment survey
2. Semidetailed lake water follow-up
3. Detailed lake water follow-up
4. Seasonal comparison of lake waters
5. Drillhole water tests

1. Regional lake water and sediment survey

About 400 lake sites within an 800 km² rectangle in the southwest corner of map sheet 74 H were sampled by helicopter during the period of June 10-20, 1977. The sample area surrounded the "Key" Lake ore deposits and was bounded by U.T.M. co-ordinates 6 352 700N-442 500E; 6 352 700N-478 500E; 6 300 000N-442 500E and 6 300 000N-478 5000E. (Fig. 7.1) From each of these sites two lake sediment samples, one for the Geological Survey of Canada and one for the University of Regina, one lake surface water and one lake bottom (1 m from the bottom) water were collected. In addition two lake bottom waters were collected from every fourth site for analysis in the field laboratory. The sediment samples were collected in an Ekman dredge and contained in two 450 mL plastic bags. A Wildco acrylic water sampler was used to collect the lake bottom waters. The bottom water collected at each site was poured into a 200 mL aluminum container and the water collected at every fourth site was poured into two 300 mL glass bottles. The surface water samples were collected by hand in 220 mL plastic bottles.

To check on the sampling and analytical accuracy one blank (distilled water), one control reference (multi-trace element standard) and one duplicate were inserted in every group of 17 samples collected during the regional lake water survey.

2. Semidetailed lake water follow-up

A semidetailed lake water follow-up was performed in two areas where interesting Rn results were obtained during the regional lake water and sediment survey. Altogether 57 lake water sites were sampled using helicopter and boat support between June 20 and 23, 1977. Fourteen samples were collected in a 5 km² area at "Zimmer" Lake and 33 water samples were collected in a 15 km² area at "Seahorse" Lake (Fig. 7.2). At each site a water sample was collected 1 m from the bottom using a Wildco acrylic water sampler

and two 300 mL glass bottles were filled. These samples were analyzed in the field laboratory and at the Geological Survey geochemistry laboratory in Ottawa.

3. Detailed lake water follow-up

From June 22-25, 1977, ninety-six sites were sampled in a detailed lake bottom water follow-up to the regional and semidetailed surveys. These samples were collected by boat along 13 traverses in four lakes (Fig. 7.3). These particular traverses were picked either because of their relative position to the two orebodies (Gaertner and Deilmann) or because of interesting results obtained during the semidetailed survey. All the lines were run in a northwest direction with 3 lines (20 sites) on "Karl Ernst" Lake, 4 lines (27 sites) on "Dieter" Lake, 3 lines on "Key" Lake (37 sites) and 3 lines on "Upper Seahorse" Lake (12 sites). The lake traverses were positioned 100 m apart and the samples were collected at 30 m intervals. At each site two 300 mL glass bottles were filled with waters collected 1 m above the lake bottom by the Wildco acrylic water sampler. The samples were then analyzed in the field laboratory and in the Ottawa laboratory.

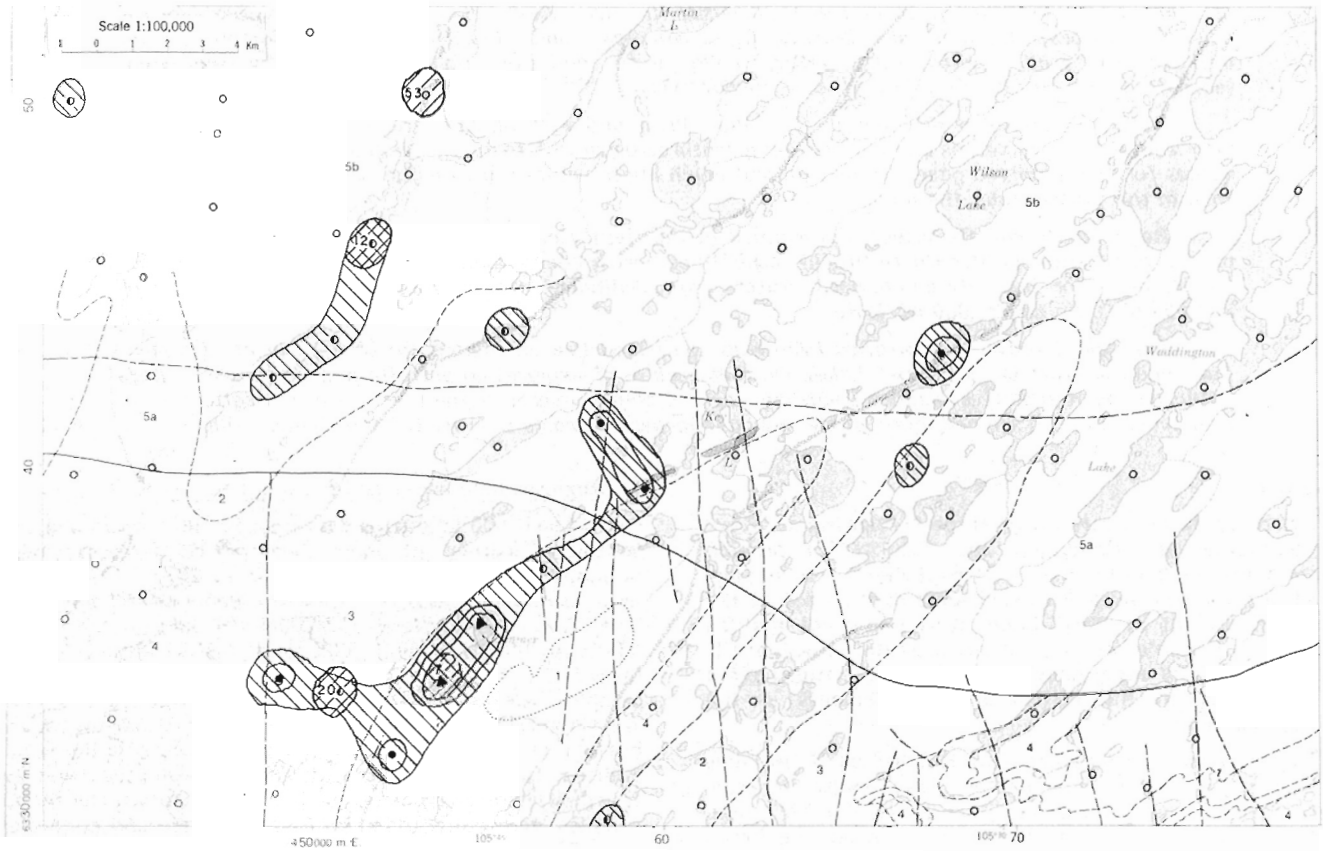

LEGEND

Compiled from maps produced by
Baer (1968), Ramaekers (1975) and Ray (1976)

HELIKIAN

5 ATHABASKA FORMATION
5a Coarse conglomerate
5b Medium conglomerate and sandstone

APHEBIAN

4 WOLLASTON GROUP
Meta-arkose

3 WOLLASTON GROUP
Pelitic and semi-pelitic schists and gneisses

ARCHEAN

2 Biotite granite-adamellite gneiss

1 Charnockitic rocks

Rn, PC/L
- o 0 – 3
- • 11 – 50
- ◦ 4 – 10
- ▲ >50

He, NET NL/L

- Approximate edge of Athabaska Formation
- Size grain boundary within Athabaska Formation
- Area containing numerous outcrops
- Fault of major joints
- Shear with mylonite
- Location of the "Key" Lake U-Ni deposits

Figure 7.1. He and Rn in lake bottom water samples from regional survey.

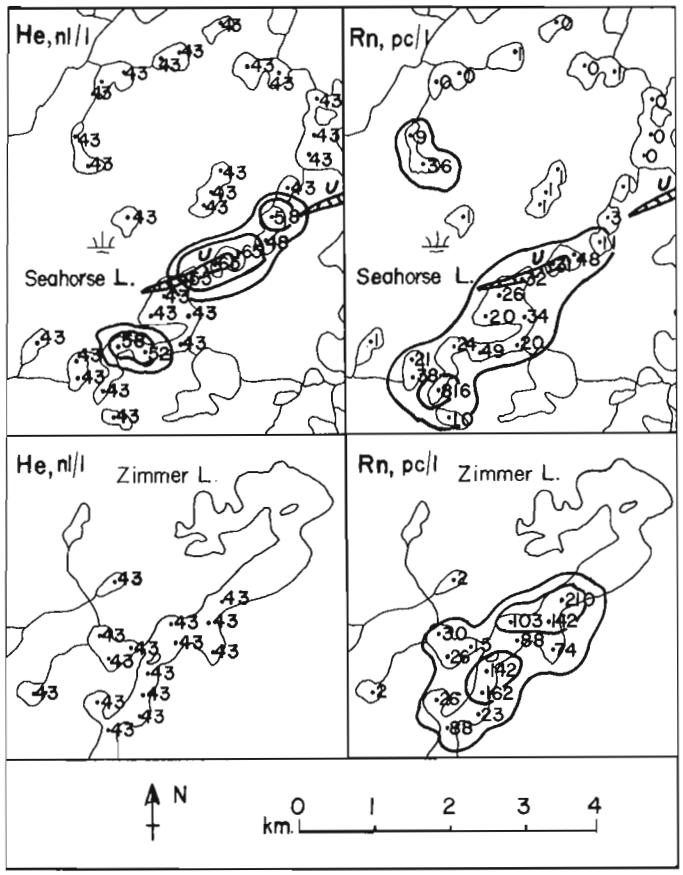

Figure 7.2. He and Rn in lake bottom water samples from semidetailed survey.

4. Seasonal comparison of lake waters

Eighty-six lake water samples from 36 sites, 4 well water samples from 2 sites and 1 stream water sample were collected between June 28-30, 1977. These sites were chosen to coincide with sites sampled in March of 1977. The 86 lake water samples were collected by boat in 8 lakes within a 16 km^2 area of the Uranerz camp at "Key" Lake, the stream water from a stream between "Hourglass" and "Upper Seahorse" lakes, and the well waters were collected from 2 wells located in the Uranerz camp. In the lake and stream water sampling an acrylic Wildco depth sampler was used to collect 45 samples (top, bottom, middle) from 15 sites, 40 samples (top and bottom) from 20 sites and 2 samples (bottom) from 2 sites. The top samples were collected 1 m from the surface, the bottom samples 1 m from the lake bottom and the middle samples were collected halfway between the surface and lake bottom. For each sample three, 300 mL glass bottles were filled for analysis in the field and in Ottawa.

5. Drillhole water tests

On June 27, 27 water samples were collected from 10 holes drilled for hydrological studies. On July 4, 35 samples were collected from 7 U exploration drillholes in or near U mineralization. The samples were taken at arbitrary intervals of from 15 m to 20 m. Maximum depths encountered were: 59 m for hydrological holes and 98 m for exploration holes. From each site two 300 mL glass bottles were filled for analysis in the field and in Ottawa.

Field Laboratory

The field laboratory was set up in a 25 foot trailer which was trucked into the "Key" Lake area over a winter road from La Ronge during the winter of 1976-77. The mobile laboratory was equipped with a heating system, a water supply system a radiophone and an air conditioner. Electricity was generated by two portable generators; a gasoline driven MacCulloch and a diesel driven Koeler.

In the field laboratory the water samples were analyzed for He, Rn, pH, Eh, conductivity and O_2. He was analyzed with an Alcatel ASM 10 helium leak detector while radon was determined by degassing a 120 mL aliquot into a ZnS cell and measuring the alpha particle emanation rate with a Rn counter (Dyck and Pelchat, 1977; Dyck, 1968).

General Geology

The "Key" Lake area is at the southeastern margin of the Athabasca basin at the contact between the Athabasca Formation and the crystalline basement. In the southeastern part of the study area Aphebian metasediments (gneiss and schists) of the Wollaston Group lie unconformably on an Archean basement of foliated granitic and charnockitic rocks. In the north the Aphebian and Archean rocks are unconformably overlain by the poorly exposed Athabasca Formation consisting of sandstones, grits and conglomerates (Ramaekers, 1975). The basement rocks and those of the Athabasca Formation are almost completely covered by up to 90 m of glacial deposits (eskers, kames, outwash sands and various tills). The main structural features in the "Key" Lake area are the pre-to-post Athabasca faults. These basement faults trend northeast-southwest and one of these faults is associated with the mineralization at "Key" Lake.

To date two orebodies have been discovered at "Key" Lake; the Gaertner and Deilmann orebodies (Fig. 7.1). The Gaertner orebody is 1500 m in length, 80 m thick and ranges in width from 10 to 40 m while the Deilmann orebody has a minimum length of 800 m, a width of 10 to 100 m and a depth of 150 m. Dahlkamp and Tan (1977) report grades of up to 45% U_3O_8 and 45% Ni in the Gaertner orebody and up to 20% U_3O_8 and 25% Ni in the Deilmann orebody. The U-Ni mineralization consists of U oxides and silicates and nickel sulphides and arsenides and is found in both the Athabasca Formation and the underlying gneiss close to their unconformable contact.

Results and Discussion

As stated in the introduction, the main purpose of this study was to test the He method of prospecting for U. However, for purposes of comparison and in order to obtain as much background data as possible on what may well prove to be one of Canada's richest U deposits, the regional survey included also centre lake surface water and centre lake sediment samples. These samples as well as the He analyses of 400 lake bottom water samples await processing. But the 99 additional lake bottom water samples taken at every fourth site during the regional survey were analyzed in the field laboratory and are discussed here, as are the semidetailed and detailed lake water field data. It should be stressed here that the authors do not recommend such a wide sample density (1 site/8 km^2) for routine He and Rn surveys for U exploration. The reason for this set of 99 samples was mainly to obtain a background reading from the area and test the recently assembled He analyzer (Dyck and Pelchat, 1977). Even at such wide spacing two areas with higher than background Rn values were outlined. One in the "Zimmer" Lake area where up to 292 pc/L were found relative to about 1 pc/L for background and the other in a small lake 1.5 km northwest of "Seahorse" Lake were 45 pc/L were found. The

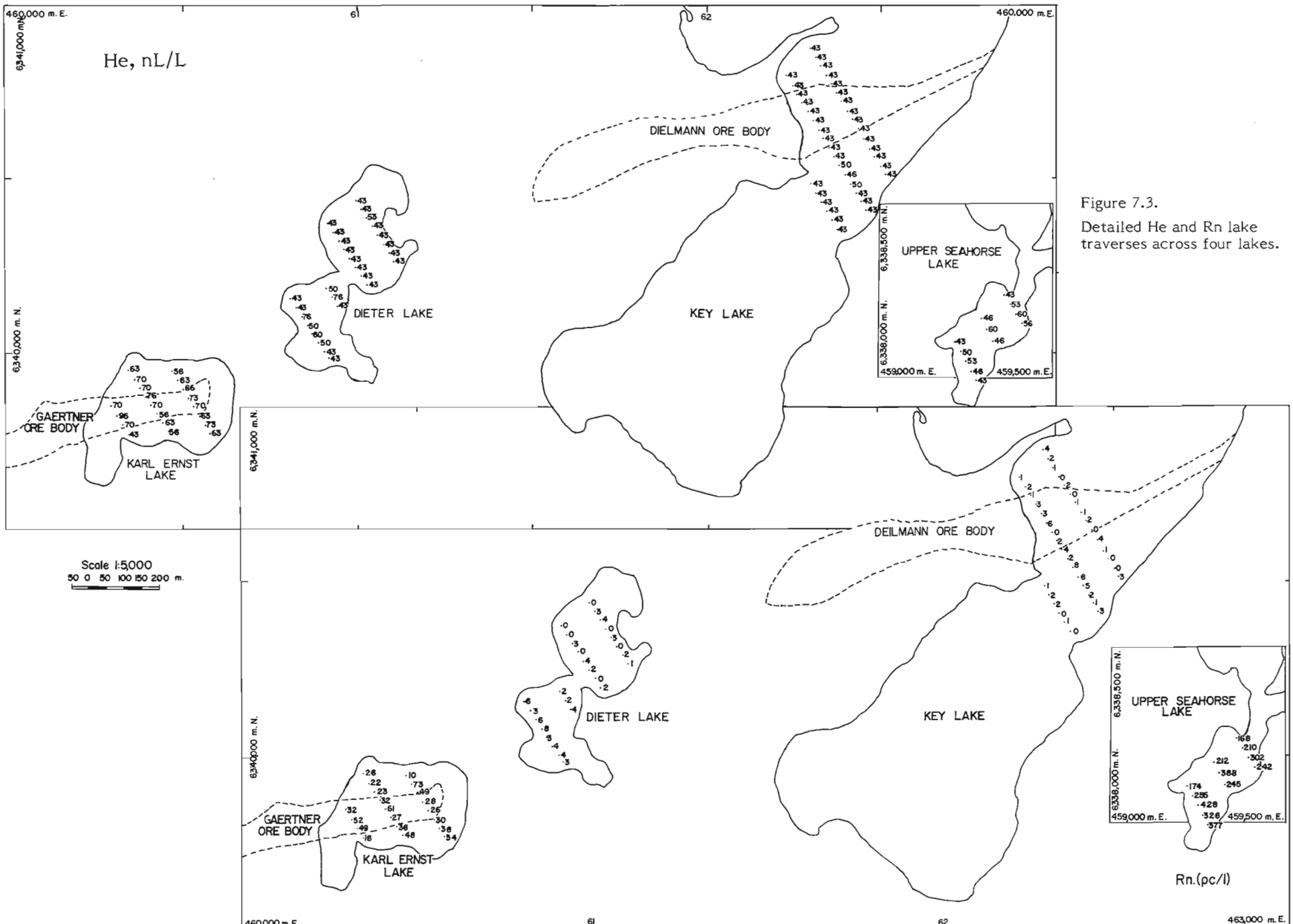

Figure 7.3.

Detailed He and Rn lake traverses across four lakes.

one "Seahorse" Lake site chosen for this survey had only 12 pc/L even though there is ore some 50 m below this lake. The 45 pc/L value in the small shallow lake was confirmed in the semidetailed follow-up. It is in an area of thick overburden and sandstone cover but a preliminary geological map (Ray, 1976) shows a north-south trending fault under this lake. The semidetailed follow-up also confirmed Rn in "Zimmer" Lake and "Seahorse" Lake with the highest value of 816 pc/L in the south end of "Seahorse" Lake. It is thought that these Rn values reflect primarily the radioactive boulder train in the area.

Only four of the 99 regional sites contained higher than background He values; background in this case being the equilibrium value determined by the He content of the air and the solubility of He in water at the prevailing temperature and pressure. This value is about 45 nL/L (Weiss, 1971). For this work calibration curves for the He analyzer used in the field gave a value of 43 nL/L. Two of the high He sites were in the "Zimmer" Lake area and two in two adjacent larger lakes about 12 km northwest of "Key" Lake. Here the highest value of 96 nL/L was observed, but neither of these sites had much above background Rn values. Most likely these values reflect a structural feature with groundwater influx, for the water had also a higher than background conductivity (25 micromhos/cm vs a 10 mmh/cm background). As evident in Figure 7.2 no He readings above equilibrium were observed in "Zimmer" Lake samples taken in the semidetailed follow-up even though all the samples had anomalous Rn and two sites sampled in the regional survey had higher than background He and Rn. Perhaps a few windy days between the two sampling times had depleted the excess dissolved He but not Rn. Also Rn is able to build up quicker than He to detectable levels. However, "Seahorse", "Karl Ernst" and "Dieter" lakes gave a positive He response during the semidetailed survey.

In Figure 7.3 the detailed lake bottom traverses are shown. The traverse locations and site spacings were obtained by estimating distances from points on shore and hence are very approximate. Over the ore zone in "Karl Ernst" Lake up to 73 pc/L Rn and 95 nL/L He were observed. With all the drilling in this lake one would expect much higher values than that from contamination alone. That contamination plays only a small part is evident from the "Key" Lake He and Rn values over the ore zone; they are virtually zero even though drillholes puncture the ore zone. While the depth of lakes is believed to play a role in controlling He and Rn concentrations it does not appear to be a strong factor when a temperature gradient exists. Note the absence of both He and Rn from the two northern traverses in "Dieter" Lake in spite of the fact that some of these sites were among the deepest (up to 20 m) of all the detailed sites. These sites also indicate that nonmineralized parts of the ore bearing contact, presumed to continue from "Karl Ernst" Lake through "Dieter" Lake to "Key" Lake, do not produce He and Rn as do the drilled, mineralized parts. The higher than background He and Rn values in the southern part of "Dieter" Lake are probably produced by the ore under "Karl Ernst" Lake and groundwater moving from "Karl Ernst" Lake to "Dieter" Lake.

The detailed traverses at the south end of "Seahorse" Lake yielded up to 428 pc/L Rn and 60 nL/L He. This part of the lake reaches a depth of only 4 m so that He escape will be more pronounced. The relatively high Rn levels suggest that the source is nearby. No drilling was evident here. Most likely a concentration of radioactive boulders near the surface gives rise to this anomaly, similar to the ones in the "Zimmer" Lake area.

The winter-summer comparison tests will be described in detail elsewhere. Qualitatively speaking both Rn and He levels in the lakes were significantly lower in the summer than in the winter. For example Rn and He values in the two "Karl Ernst" Lake bottom sites in the winter under the ice were 147 and 183 pc/L and 137 and 152 nL/L, respectively. In the summer the same sites gave 29 and 19 pc/L and 65 and 76 nL/L, respectively. The reduction in the Rn concentration at first glance appears much more drastic than the He drop but with a subtraction of the He contribution of atmospheric air of 42 to 45 nL/L one can see that the net He is reduced by a factor of 4. Three factors may explain this summer-winter contrast namely temperature, water level and flow, and wind action. Wind action, in summer was probably the most dominant factor in stirring up the water thus prohibiting the build up of a gradient. The lack of a gradient in lakes less than 7 m deep was quite evident from the constant temperature and O_2 content between surface and bottom lake samples in the summer. However, the spring run-off dilution effect of trace element concentrations may also be important. This factor should become evident when ionic species are measured. The gentle relief precludes extensive upwelling of groundwaters through faults. Regional movement is estimated to be about 3 m/year in a northeasterly direction even though the sandy overburden contains about 25% voids. Hence, groundwaters do not contribute significantly to the dissolved gas content of the lakes. This lack of communication between the groundwater and lake water regimes is also evident from the absence of U, Rn and He in "Key" Lake even though part of one orebody lies directly underneath it. Also, the mining camp wells have a conductivity of 30 micromhos/cm as compared to 10 in the lake which is about 100 metres away.

Drillhole Samples

By far the highest Rn and He values were obtained from water samples from drillholes. The results from two of these holes are shown in Figure 7.4. The highest values of about 300 000 pc/L Rn and 20 000 nL/L He were obtained at the bottom of hole 1061 which penetrates the main ore zone at about 50 m. Hole 1161 shows only a small gamma ray signal between 90 and 95 m. Contrary to expectation the Rn concentration is lower in the mineralized zone than in the sandstone above it. He behaves as expected in both holes. The lowest Rn and He values encountered in the drillholes were 300 pc/L and 43 nL/L and can be taken as typical near surface groundwater background values. None of the holes tested gave background values for Rn and He coincidentally. However, more tests, much farther from ore are needed to establish typical background values for these gases in groundwaters of the Athabasca sandstones. One interesting and clear correlation from the drillhole data emerges; low or equilibrium He values correspond to high O_2 values, indicating the strong effect atmospheric contact has on the concentration of these two gases in water. This correspondence is much less evident with Rn and O_2 resulting in poor correspondence between He and Rn in some instances. No mineralogical data were available from these holes when this report was prepared so a comparison between U in the ground and He or Rn in the water is not possible at this time. A rough comparison between the gamma ray logs and Rn or He shows a rather diffuse correspondence suggesting complex groundwater flow patterns and Ra, Rn, and He migration. Work is continuing in the hope of learning something about these patterns and establishing useful criteria and procedures for prospecting.

The high pH and conductivity values have doubtless resulted from the additives in the drilling mud which was still present in all holes as a gel when sampled. The slightly higher pH and conductivity values observed in the lakes where drilling had taken place are probably also due to these additives. The high O_2 and Eh in hole 1161 relative to that in hole 1061 may be due to the fact that hole 1161 was completed several days and hole 1061 several weeks before

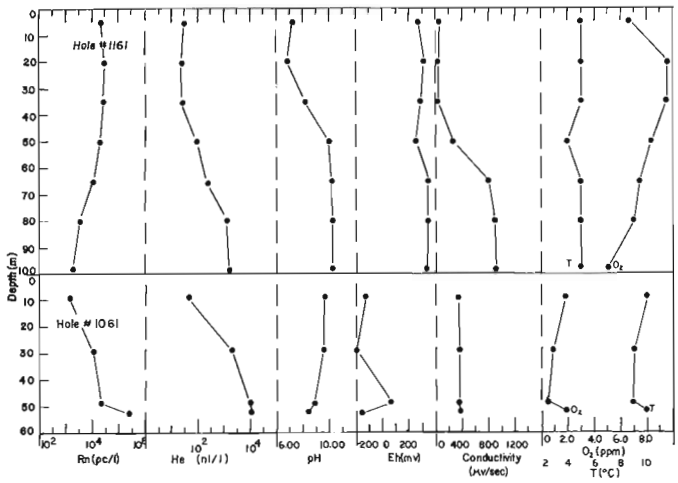

Figure 7.4. He and Rn profiles of two drillholes in mineralized ground.

sampling. The highly reducing environment in the main ore zone may also be a factor in this contrast. It is tempting to ascribe the higher temperature in hole 1061 to the nearness of the main ore zone. However, an equally likely explanation is the fact that lake water from "Seahorse" Lake moves through the ground past 1061 into "Karl Ernst" Lake. Lake waters at the time of sampling were about 17°C down to a depth of 7 to 10 m depending on the size of the lake.

Conclusions

Barring possible contamination as a result of drilling, the U ore deposits and the radioactive boulder fields in the "Key" Lake area, Saskatchewan give rise to He and Rn anomalies in lake bottom water samples, particularly when studied in detail. "Key" Lake itself, even though underlain by U ore, gives virtually zero He and Rn signals suggesting a rather tight seal between ore and lake bottom. The anomalies generally are subtle and absolute concentrations low, hence good equipment and competent operators are essential.

The He analysis facility, set up during the winter, was tested for the first time under true field conditions and found to perform well, detecting relative He concentrations of 5 nL/L and producing up to 120 analyses per man day. Although He measurements are more difficult than Rn measurements they are more quickly performed with the procedures and equipment adapted by the Geological Survey.

The presence of highly anomalous He and Rn in drillhole waters in and near U ore zones suggest that their routine measurement during exploratory drilling may indicate proximity and thereby increase the probability of detecting a deposit.

The tests as carried out during the summer revealed no obvious advantage of the He method over the Rn method for U prospecting. In fact, Rn contrasts between background and anomaly were generally higher and Rn anomalies more dispersed than He. The generally weaker He signal in lake bottom waters indicates its greater mobility and its mode of occurrence suggests that He in lakes is more suitable for detailed prospecting for U mineralization. However, in winter under the ice, lake bottom water samples from "Key" Lake itself had anomalous He but no anomalous Rn. This, plus the fact that no anomalous U is found in this lake, suggests that under the conditions prevailing at this lake He is the one tracer that is mobile enough to enter the lake and accumulate under the ice.

Acknowledgments

The authors would like to acknowledge the valuable assistance rendered by the staff of Uranerz Exploration and Mining Ltd. in the selection of test sites and background information and in providing transportation for men and equipment when required.

Provision of food and lodging and other field camp facilities by the University of Regina field party were greatly appreciated.

References

Baer, A.J.
1969: Precambrian geology of Geikie river map-area, 74 H, Saskatchewan; Geol. Surv. Can., Paper 68-41, 11 p.

Dahlkamp, F.J. and Tan, B.
1977: Geology and mineralogy of the Key Lake U deposits, northern Saskatchewan, Canada; in Proceedings of an International Symposium on the Geology, Mining and Extractive Processing of U., Inst. Mining Met. London, 1977, ed. Jones, M.J., p. 145-157.

Dyck, W.
1969: Field and laboraory methods used by the Geological Survey of Canada in geochemical surveys. No. 10. Random determination apparatus for geochemical prospecting for uranium; Geol. Surv. Can., Paper 68-21, 30 p.

Dyck, W. and Pelchat, J.C.
1977: A semi portable helium analysis facility; in Report of Activities, Part C, Geol. Surv. Can., Paper 77-1C, p. 85-87.

Ramaekers, P.P.
1975: Athabasca Formation, Southeast edge (74 H): I Reconnaissance Geological Survey; in Summary of Investigations 1975, eds. Christopher, J.E. and MacDonald, R.; Sask. Dep. Min. Resour., p. 18-23.

Ray, G.E.
1975: Foster Lake (NE) and Geikie River (SE) areas; in Summary of Investigations 1975, eds. Christopher, J.E. and MacDonald, R.; Sask. Dep. Min. Resour., p. 13-18.

1976: Foster Lake (NW) - Geikie River (SW) areas; in Summary of Investigations 1976, eds. Christopher, J.E. and MacDonald, R; Sask. Dep. Min. Resour., p. 18-23.

Weiss, R.F.
1971: Solubility of helium and neon in water and sea water; J. Chem. Eng. Data, v. 16, no. 2, p. 235-241.

8. A RECONNAISSANCE CAR-BORNE RADIOMETRIC SURVEY OF GRENVILLE METASEDIMENTS, NORTH BAY AREA, ONTARIO

Project 750010

N. Prasad and J.A. Kerswill
Regional and Economic Geology Division

Abstract

Prasad, N. and Kerswill, J.A., A reconnaissance car-borne radiometric survey of Grenville metasediments, North Bay area, Ontario; in Current Research, Part B, Geol. Surv. Can., Paper 78-1B, p. 45-48, 1978.

A car-borne total count scintillometer survey conducted in the North Bay region of the Grenville Structural Province did not detect any anomalies greater than 1.5 times background in the paragneisses. It has been suggested that such gneisses could be metamorphic equivalents of Huronian sediments such as those that host uranium deposits at Elliot Lake and Agnew Lake. Furthermore, the different paragneiss units did not differ in terms of their radiometric expression as measured by the total count scintillometer although in situ measurements suggested that such differences do exist. More detailed work is recommended in the coarse clastic metasediments adjacent to the Grenville Front. An anomaly related to a shear zone and probably to alkalic intrusive activity was found in Springer township.

Introduction

A reconnaissance radiometric survey by car-borne scintillometer was conducted in the North Bay – Sturgeon Falls area of the Grenville Province (parts of NTS 31F and 41I). The area is bounded to the north by the Grenville Front and to the south by Highway 17 (Fig. 8.1). The objective of this study was to survey the metasediments within this part of the Grenville Structural Province for radiometric anomalies.

Twenty-three traverses totalling about 560 km were completed over an area of approximately 5000 km^2 (Fig. 8.1). The geology of the area is covered by Ontario Department of Mines and Northern Affairs compilation maps 2216 (North Bay – 1 inch to 2 miles) and 2271 (Burwash – 1 inch to 2 miles); preliminary maps P678 (Tomiko West – 1 inch to 1 mile), P679 (Tomiko East – 1 inch to 1 mile) and P844 (River Valley – 1 inch to 1 mile). Ontario Geological Survey compilation map 2361 (Sudbury-Cobalt – 1 inch to 4 miles) was used as a base map.

The original scintillometer traces of traverses and corresponding 1:50 000 topographic sheets with traverse data are with the authors in Ottawa at 601 Booth St. and are available for viewing.

General Geology

Metasedimentary gneisses, the most abundant rocks of the study area, have been subdivided into three principal types (OGS Map 2361). These are:

(1) biotite gneiss derived from greywacke, siltstone, immature sandstone and minor calcareous siltstone and sandstone;

(2) quartz feldspathic gneiss including muscovitic quartzose and feldspathic gneisses derived from orthoquartzite, subarkose, aluminous claystone, arkose and ferruginous arkose and;

(3) gneissic coarse clastic metasediments derived from pebbly to bouldery coarse grained greywacke, immature sandstone, arkose, and minor conglomerate.

Lumbers (ODMNA Map P678) notes that gneissic meta-conglomerates within the coarse clastic metasediments occurring near the Grenville Front unconformably overlie the Early Precambrian rocks in the Grenville Province and form the basal part of the metasedimentary sequence in the Grenville. Felsic plutonic rocks ranging in composition from granite to granodiorite and in age from Early to Late Precambrian and rocks of the Late Precambrian anorthosite suite intrude the paragneisses of the study area (Fig. 8.1).

Roscoe (1969), Lumbers (1971) and others have proposed that certain paragneisses of the Grenville may be metamorphic equivalents of basal Huronian sediments that host uranium mineralization at Elliot Lake, Agnew Lake and within the Cobalt Embayment. Several uranium showings occur near the study area in basal Huronian sediments just north of the Grenville Front (Fig. 8.1). East of traverse 1 in Vogt Township uranium and gold occur in quartz-pebble conglomerate and quartzite unconformably overlying Archean greenstone and iron-formation (Thomson, 1960). West of Traverse 1 in Pardo Township uranium occurs in basal quartz-pebble conglomerate (Thomson, 1960). Uranium and gold mineralization occurs northeast of the study area in the vicinity of Hunters Point, Quebec and is within a band of metaquartzite in Grenville gneisses (Roscoe, 1969). Similar muscovitic and quartzose gneisses outcrop near the eastern boundary of the study area (Lumbers, 1971). Also occurring within the Grenville Province of the study area is a uraniferous pegmatite (just north of the end of Traverse 6).

Method

Equipment used during the survey included a Nuclear Enterprises Model NE970 total count scintillometer and an Esterline-Angus Model AW chart recorder mounted in a 4-wheel drive light truck. The scintillometer contains a phosphor detector measuring six inches in diameter by three inches in thickness. It was placed unshielded in the middle of a vehicle as far above the road as practically possible. A time constant of 0.5 second, the shortest and most sensitive available on the scintillometer, a range setting of 0-400 counts per second, suitable for recording up to five times background, and a chart speed of three inches per minute, equivalent to six inches per mile at thirty miles per hour, were used throughout the work. Traverse speeds were held as constant as possible averaging 25 miles per hour on paved highways and less than 5 miles per hour on back roads. Fiducial points, reference mileages, outcrop lithologies and comments on speed and type of terrain were tape recorded while on traverse and later transcribed onto the scintillometer traces. All anomalies were checked by running a minitraverse in both directions over the anomaly and by

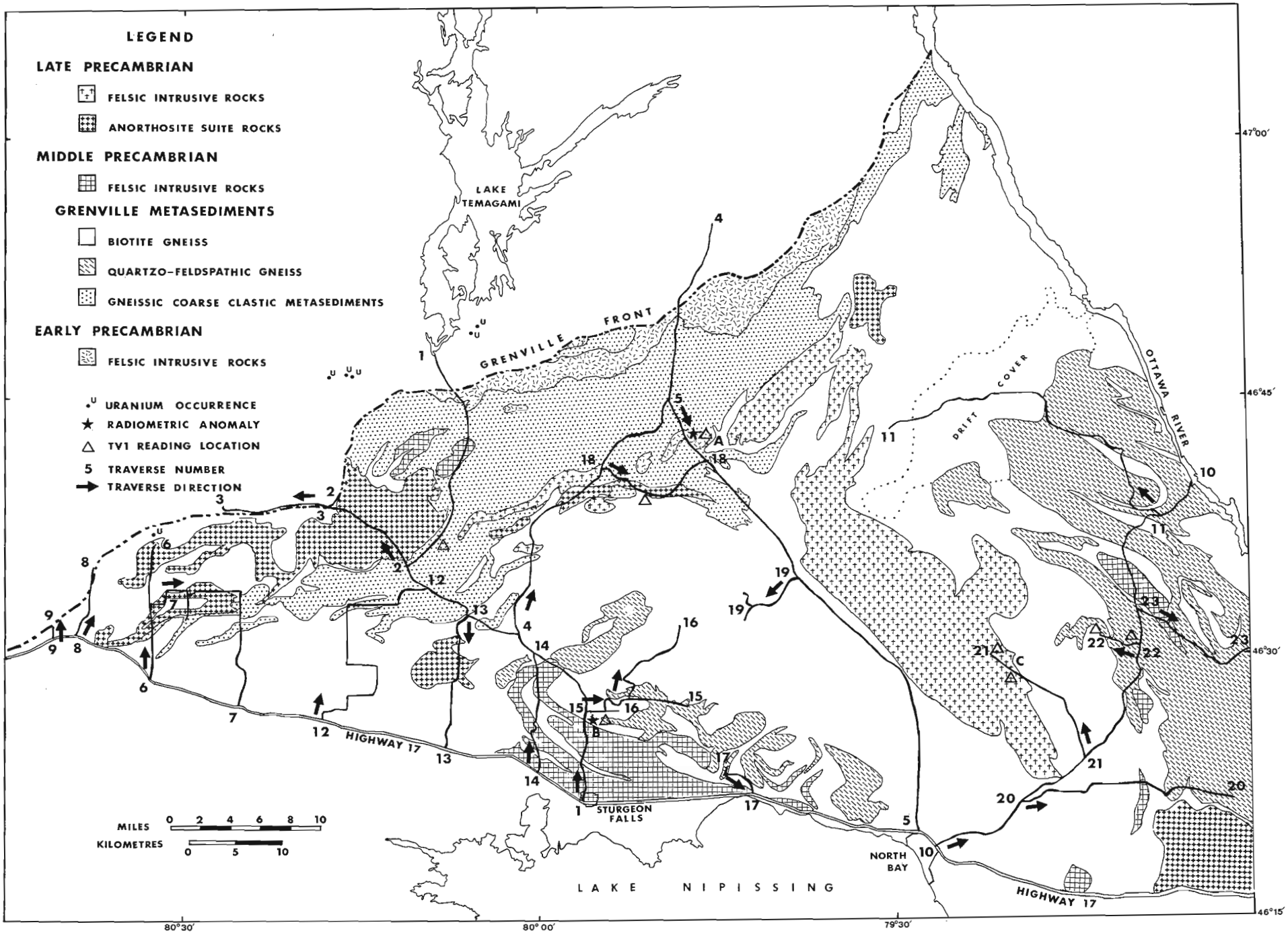

Figure 8.1. Generalized geological map of the study area (modified after OGS Map 2361).

Table 8.1

Summary of TV-1 readings in counts per minute* where T_1 = total counts, T_2 = counts due to U and Th, and T_3 = counts due to Th

Rock Type	Township	Traverse	T_1	T_2	T_3
Biotite gneiss	Springer	1	1500	60	20
Biotite gneiss	French	22	1750	85	20
Biotite gneiss	Mulock	21	2000	150	20
Quartz feldspar gneiss	French	22	3250	200	35
Coarse clastic metasediment	Gibbons	1	3500	200	30
Mixed gneiss	McLaren	18	3500	250	45
Gneissic granite	Springer	1	3000	200	45
Granite	Mulock	21	3500	225	35
Quartz monzonite	Sisk	5	8000	425	100
Feldspar porphyry dyke	Springer	1	7500	600	125
Shear zone	Springer	1	9500	650	150

*After background correction for T_2 and T_3 leading to T_2' and T_3' the counts due to U equal $T_2'-3.5T_3'$; the counts due to Th equal T_3'.

ground followup using a McPhar TV-1 gamma-ray spectrometer. This instrument contains a 1.25 by 1.0 inch sodium iodide crystal. TV-1 readings were all taken on relatively flat outcrop surfaces (2π geometry).

Results

Background readings over metasediments of the study area varied from 60 to 90 counts per second as measured by the car-borne scintillometer. No readings greater than 1.3 times local background were found in the paragneisses traversed by the survey. The two greatest readings in such rocks were about 1.2 times the local background and occurred in roadcuts of gneissic metaconglomerate (ODMNA Map P678) along Highway 11 in Sisk Township just north of the Marten River bridge. Examination of the car-borne scintillometer traces revealed no consistent differences in background among the three principal metasedimentary rock types. Generally traces over drift covered terrain were indistinguishable from traces over outcrop, particularly where the outcrops were flat lying.

Readings[1] taken on outcrop by the TV-1 throughout the course of the work (Table 8.1) suggest that differences in background may exist between the principal metasedimentary rock types even though such differences were not apparent in the scintillometer traces. The readings indicate background ranges in the metasediments as follows: T_1 = 1500-3500, T_2 = 60-200 and T_3 = 20-35. Biotite gneiss seems to have a lesser background than either the quartz-feldspar gneiss or the gneiss derived from coarse-clastic sediments.

A roadcut through quartz monzonite in Sisk Township immediately south of the Marten River bridge on Highway 11 gave readings of about 125 counts per second on the car-borne scintillometer (Loc. A, Fig. 8.1). Ground followup by TV-1 gave readings on outcrop of $T_1 \simeq 8000$, $T_2 \simeq 425$ and $T_3 \simeq 100$. Thus, the radiometric expression of the quartz monzonite was about two to three times the regional background of the metasediments.

Significant radioactivity was detected in a roadcut of gneissic granite in contact with biotite gneiss just south of Brûlé Creek on Highway 64 in Springer Township (Loc. B, Fig. 8.1). Radioactivity was found to be associated with a northerly trending mylonitic shear zone and a northeasterly trending hematitic feldspar porphyry dyke both of which crosscut the gneissic intrusion. Biotite gneiss and minor amphibolite at the south end of the roadcut gave TV-1 readings of $T_1 \simeq 1500$, $T_2 \simeq 60$, and $T_3 \simeq 20$. TV-1 readings on gneissic granite not immediately near the shear zone or the dyke were $T_1 \simeq 3000$, $T_2 \simeq 200$ and $T_3 \simeq 45$. In contrast, readings on the steeply easterly dipping shear zone, which contains hematite and carbonate were $T_1 \simeq 9500$, $T_2 \simeq 650$, $T_3 \simeq 150$ and readings on the steeply westerly dipping 10 m thick dyke were $T_1 \simeq 7500$, $T_2 \simeq 600$ and $T_3 \simeq 125$.

Higher than background TV-1 readings were also found to be associated with several relatively flat lying outcrops of Mulock granite in Mulock Township (Loc. C, Fig. 8.1) although background fluctuations on the car-borne scintillometer trace masked this phenomenon. TV-1 readings were $T_1 \simeq 3500$, $T_2 \simeq 225$ and $T_3 \simeq 35$ which compare to a background on nearby drift of $T_1 \simeq 1500$, $T_2 \simeq 100$ and $T_3 \simeq 15$.

Discussion

In the planning stages for this work it was believed that indications of anomalous uranium and thorium content might be detected in the Grenville metasediments of the study area. The two targets were the gneissic coarse clastic rocks along the Grenville Front and the muscovitic to quartzose gneisses northeast of North Bay. An apparent lack of anomalies in these metasediments suggests that abnormal amounts of uranium and thorium if present in Huronian conglomerates and sandstones before the Grenville orogeny, were either lost during metamorphism and deformation or concentrated in granite and/or pegmatite derived from anatexis of the sediments.

The greater than regional background readings associated with the quartz monzonite in Sisk Township reflect a greater background in these intrusive rocks and may not indicate anomalous concentrations of uranium with respect to typical granitic rocks. The shear zone in Springer Township (Loc. B) resembles radioactive shear zones associated with

[1]All TV-1 readings in the text are not adjusted for background.

alkalic complexes in the Chapleau area (Ruzicka, 1978). The porphyry dyke may also be genetically related to the intrusion of an alkalic complex. Lumbers (1971, p. 53, 85) notes that a drillhole put down in granitic rocks about one kilometre west of Locality B revealed a wide zone of altered and shattered fenitic rock containing carbonate veins but no radioactivity. He suggested the presence of a small alkalic complex in the area or alternatively that the veins and fenitization could be only one of several localized zones of shattering and fenitization within a regional rift system.

It was previously stated that visual examination of the car-borne scintillometer traces indicates the three principal metasedimentary rock types have similar backgrounds. If this conclusion is valid then it is possible to state that radiometric expression as measured by a total count car-borne scintillometer of the type used in this survey cannot be used as an aid to geological mapping of metasediments in the study area. However, TV-1 readings taken on a number of metasedimentary outcrops suggest that at least local differences in background do exist and that these can be detected by in situ measurements.

It is important to recognize that the essentially negative results of the survey may be because background fluctuations over areas of drift and over outcrop were generally great enough to mask subtle differences in background that may indeed exist. Different positioning of the scintillometer, the use of a longer time constant to smooth out the traces, or the placement of a lead shield beneath the detector to reduce the influence of road building material might have been useful. Several traverses at different speeds and with different settings of the time constant were made over the Sisk Township quartz monzonite in an effort to determine which conditions lead to the most interpretable scintillometer response. The results of this indicate that the placement of the scintillometer, the speed of the traverse and the time constant employed during the survey were adequate.

Limitations

Two significant limitations affect the interpretation of results from this survey. These are the lack of roads in large parts of the study area and the predominance of drift cover in the areas that were traversed. At least 80 per cent of the total traversing was done over drift.

A further limitation inherent in all car-borne radiometric surveys relates to the complexity of factors which contribute to the scintillometer trace. Random fluctuations in source radioactivity, variations caused by different distances between the source and detector, changes in geometry of source with respect to the detector, variable radioactivity in the roadbed, differing thicknesses of overburden and even contrasts in weather must be considered when attempting to correlate radiometric expression with bedrock lithology.

Conclusions

Differences in background radiation among the metasedimentary rock types of the study area were not sufficient to be detected by this total count car-borne survey. Anomalous radioactivity was not found in the paragneisses but was detected in Springer Township in rocks probably associated with alkalic intrusive activity. Felsic intrusive rocks in Sisk and Mulock townships were found to possess backgrounds greater than the metasediments.

Recommendations

The greatest car-borne scintillometer readings in metasediments which could perhaps be interpreted as small anomalies occurred in gneissic coarse clastic rocks just north of the Marten River bridge. Ground followup in these metasediments which geologically may be the most favourable for the occurrence of uranium is strongly recommended. Such followup was not done during this survey.

A more detailed radiometric survey involving in situ measurements on outcrops of the study area is also recommended. The readings from such a study should be more interpretable than those of this survey because the number of complicating factors would be greatly reduced. Such a survey would be particularly useful if a three threshold scintillometer or equivalent instrument were used.

Exploration for uranium in the coarse clastic metasediments along the Grenville Front might be warranted if it can be established that these rocks have a greater background radioactivity than the other Grenville metasediments.

Acknowledgments

We would like to thank V. Ruzicka of the Uranium Resource Evaluation Section, Geological Survey of Canada, for suggesting and supervising this project. Help was also received from J.A. Robertson of the Geological Branch, Ontario Division of Mines.

References

Lumbers, S.B.
1971: Geology of the North Bay area, districts of Nipissing and Parry Sound; Ont. Dep. Mines Northern Affairs, Geol. Rep. 94, 104 p.

Roscoe, S.M.
1969: Huronian rocks and uraniferous conglomerates in the Canadian Shield; Geol. Surv. Can., Paper 68-40, p. 107, 117-118.

Ruzicka, V.
1978: Evaluation of selected uranium-bearing areas in Canada; in Current Research, Part A, Geol. Surv. Can., Paper 78-1A, p. 273.

Thomson, J.E.
1960: Uranium and thorium deposits at the base of the Huronian System in the District of Sudbury; Ont. Dep. Mines, Geol. Rep. 1, p. 33-37.

9.

MINERALOGY OF RADIOACTIVE OCCURRENCES IN THE GRENVILLE STRUCTURAL PROVINCE ONTARIO AND QUEBEC: A PRELIMINARY REPORT

Project 770061

J. Rimsaite
Regional and Economic Geology Division

Abstract

Rimsaite, J., Mineralogy of radioactive occurrences in the Grenville Structural Province: A preliminary report; in Current Research, Part B, Geol. Surv. Can., Paper 78-1B, p. 49-58, 1978.

Metamorphic and pegmatitic types of uranium mineralization in the Bancroft area, Ontario and in the Mont-Laurier – Cabonga area, Quebec were visited during the field season in 1977. Four types of occurrences were identified on the basis of uranium/thorium ratios and rare earth element content: (1) prospects containing predominantly uranium; (2) those containing both uranium and thorium close to 1:1 ratio; (3) radioactive showings containing predominantly thorium; and (4) those having abundant rare earths minerals, in addition to uranium and thorium. Preliminary results on uranium distribution between radioactive pegmatites, their host rocks, and some rock-forming minerals indicate that the uranium, thorium and rare earths are present mainly in radioactive minerals, such as uraninite, uranothorite, betafite, allanite, radioactive titanite and cyrtolite. Although micas and amphiboles commonly host radioactive minerals, the uranium content in structures of the rock-forming minerals is insignificant, ranging from 0.4 to 7.7 ppm. The principal differences between the occurrences in Ontario and Quebec are the higher metamorphic grades and the presence of calcite, fluorite, anhydrite as well as abundant heavy minerals and albite in mineralized rocks of the Bancroft area, Ontario.

Introduction

The radioactive occurrences were examined in the field (Fig. 9.1 and 9.2) and representative specimens were collected for mineralogical laboratory studies in an attempt to determine favourable environmental conditions for uranium mineralization in the Grenville Structural Province. The 15 occurrences visited in the Mont-Laurier – Cabonga radioactive area, Quebec, are between Mont St. Michel (46°47'N, 75°20'W) and Pond Lake (47°N, 74°45'W) NTS areas 31J/14E, W and 31J/15W and include the following prospects (Fig. 9.1): PP-1 and PP-2, Pond Lake prospect; NL, cleared and bulldozed areas north of Norman Lake; JMV-1 to 4, four properties owned by Johns-Manville Co., west and north of Patibre (Axe) Lake; TD, TDN-1 and TDN-2, three properties owned by the Mont-Laurier Uranium Mines Ltd. east of Lièvre River, between Patibre Lake and Tom Dick Creek; RFR, radioactive pegmatite east of Lièvre River trending in northeasterly direction across the road to La Force Lake; G, two prospects drilled by Gulf Minerals Ltd. in La Force Lake area, southeast of Patibre Lake; H-50, radioactive Hanson Lake zone, and RPL occurrences of the principal rock types were examined in Pierre Lake area.

Former mining properties and the operating Madawaska uranium mine (45°N, 78°W) were visited in the Bancroft area, Ontario (NTS area 31F/4) and include the following sampling localities (Fig. 9.2):

"A" Faraday granite that hosts Madawaska mine at its southern margin was examined in roadcuts and blastings along highway 500, 1.5 km and 3.5 km north of Bancroft;

"B" Bicroft mine;

"C" Cardiff mine;

"D" Dyno mine;

"E" Radioactive granite and granite pegmatite south of Madawaska mine were examined in roadcuts along highway 28;

"F" Madawaska uranium mine (former Faraday mine);

"GH" Greyhawk mine;

"I" Mafic rocks and crystalline limestone, cut by granite, exposed along highway 28 west of Bancroft;

"SC" Silver Crater mine.

This report describes geological setting, mineralogical characteristics of principal rock units, preliminary results on the distribution of uranium in radioactive pegmatites and surrounding rocks (Table 9.1), and relative abundance of the heavy fraction in selected rocks (i.e. with a specific gravity greater than 3.3, Table 9.2).

Geological Setting and Mineralogical Characteristics of Radioactive Showings and Surrounding Rocks

Mont-Laurier – Cabonga area, Quebec

Parts of the area were studied by Allen (1971), Tremblay (1974), and Kish (1977). The principal rock types were collected for this study following the lithological-stratigraphic subdivision provided by Kish (1977) on his preliminary geological map, DPV 487 (Fig. 9.1). The principal rock units and their mineralogical characteristics determined in thin sections of the collected rocks are as follows.

Unit 1: Grey and pink gneiss of Patibre Formation underlies paragneiss of the Grenville Group and thereby represents the oldest pre-Grenville metamorphic rocks in this area. Samples collected west of Patibre Lake are composed of leucocratic gneiss with melanocratic, hornblende-rich clusters. The leucocratic gneiss comprises cataclastic quartz, twinned albite, clouded by fine grained alteration products, interstitial microcline, and rare disseminated chloritized biotite. The melanocratic portions consist of pleochroic dark green to pale brown hornblende that is intergrown with partly altered biotite, blue-green tourmaline, and titanite. The mafic minerals are disseminated in fairly fresh, medium grained mosaic of plagioclase, quartz, and minor microcline. Accessory minerals are apatite, titanite, rare radioactive allanite, and zircon. The characteristic features are narrow bands of potassic feldspar overgrown on partly chloritized biotite (as in Rimsaite, 1967a, Plate III, Fig. VII-21). Leucocratic gneiss near Pierre Lake contains less than one per cent mafics. It is composed of medium grained mosaic of

microcline, quartz, and plagioclase, rare disseminated biotite laths, zoned titanite, and allanite. The radioactive titanite, allanite and small zircon crystals produce prominent black halos in biotite. The interstitial plagioclase has altered centres that are overgrown by clear albite rims.

Unit 2: Banded paragneiss of the Grenville Group (La Force Formation) is made up of well-sorted clastic and chemical sediments. These include quartzites, calc-silicate rocks, marble, biotite gneiss, arkose, and white metamorphosed pegmatite. Rocks representing various members of La Force Formation were examined in most of the mineralized areas (Fig. 9.1). The lower quartzite members are exposed in showings north of Norman Lake and bands of crystalline calcite in JMV-3 prospect. The quartzite exibits local variations in mineralogical composition. It consists predominantly of irregular strained quartz intergrowths and variable quantities of feldspar and disseminated laths of brown biotite. Some biotite laths are partly altered to chlorite and replaced by muscovite. Feldspar grains are clouded by alteration and locally overgrown by clear albite rims. The quartzite adjacent to mineralized U-Mo-bearing pegmatite at the JMV-1 prospect contains irregular bands of rounded, probably detrital, plagioclase grains that are clouded by alteration and partly replaced by white mica. Quartzites in Norman Lake area form prominent ridges and consist predominantly of cataclastic recrystallized quartz and minor interstitial biotite. Accessory minerals include rare disseminated apatite, sphene, and zircon.

The white metamorphic pegmatites (2f) contain xenoliths of biotite gneiss that vary in abundance, size, and

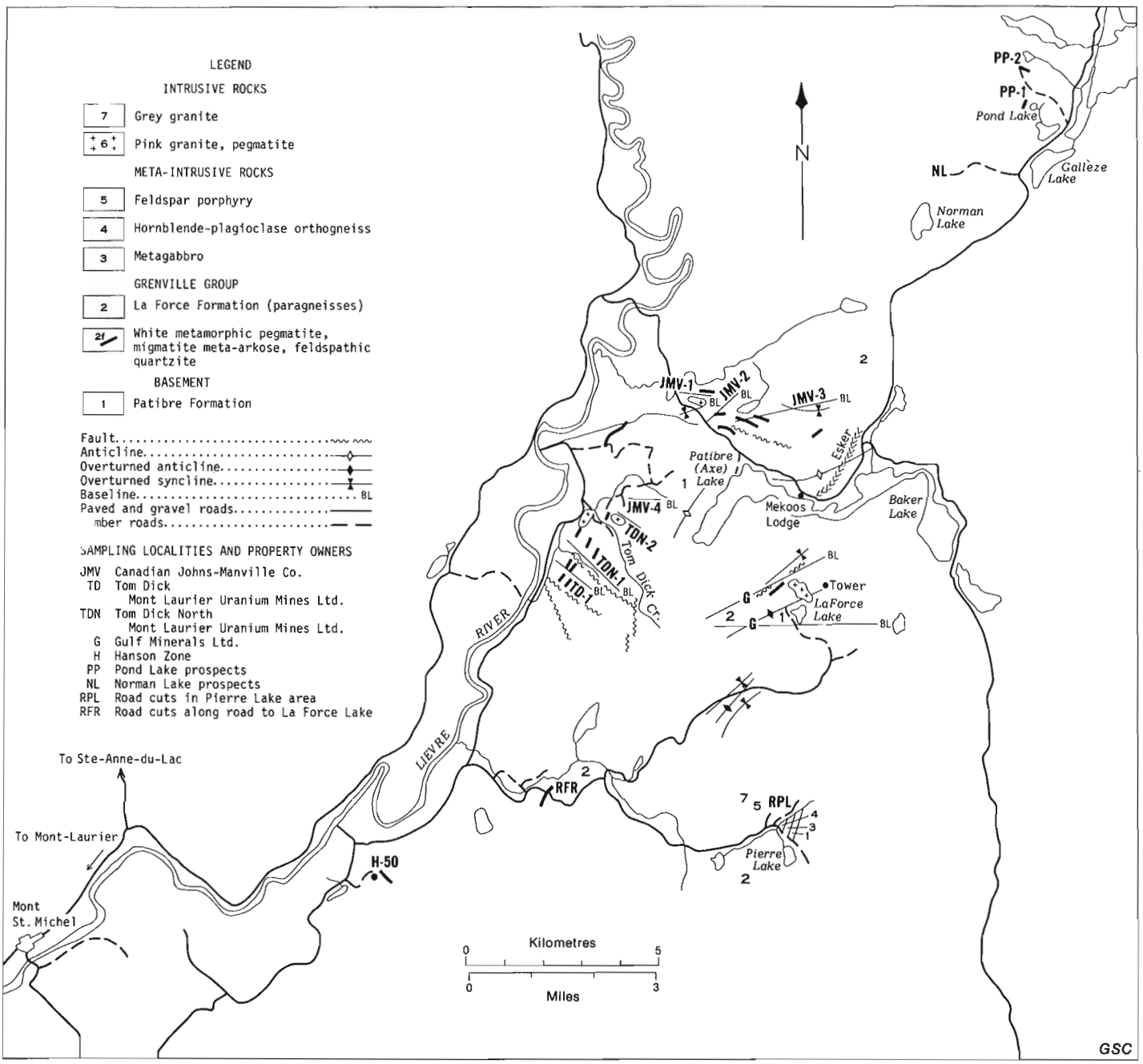

Figure 9.1. Sketch map showing radioactive occurrences and location of samples in the Patibre Lake area, 60 km north of Mont-Laurier, Quebec (after L. Kish, 1977, map DPV-487, and Tremblay, 1974).

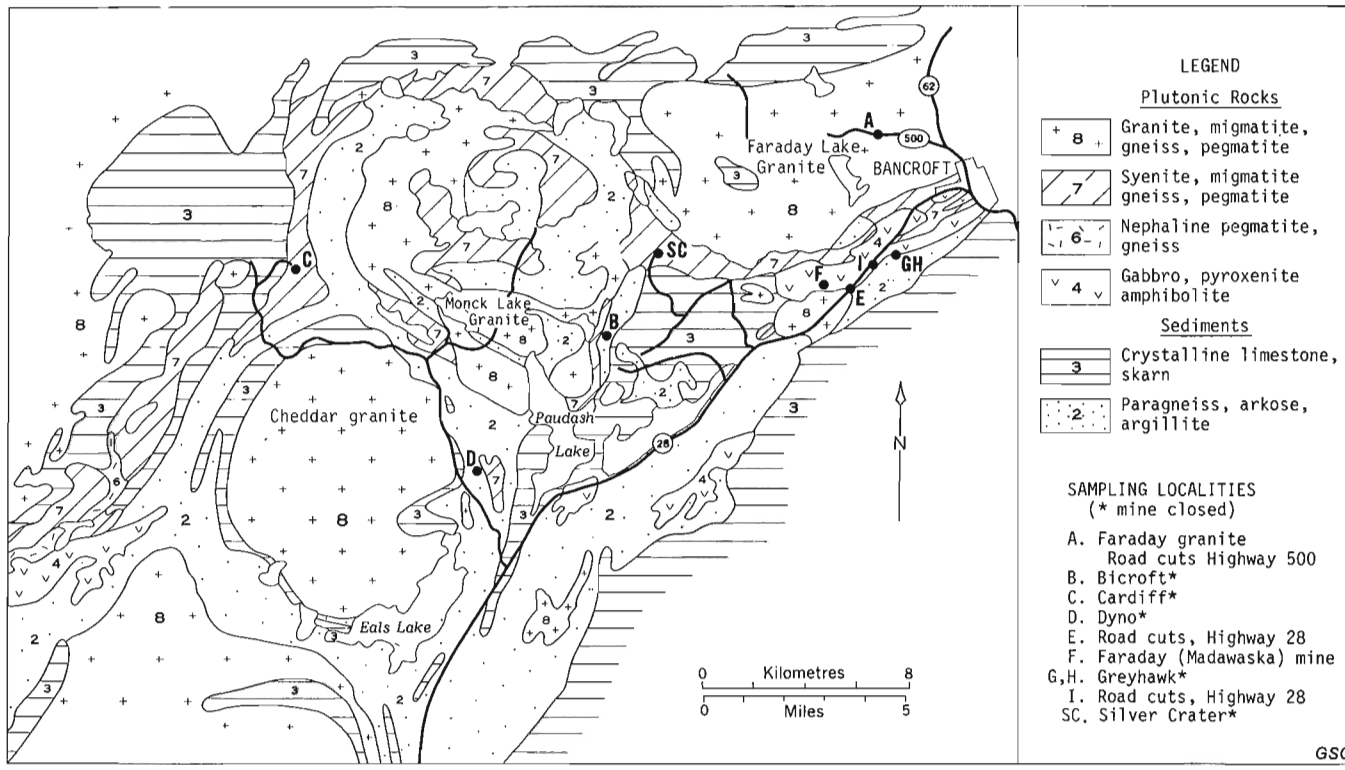

Figure 9.2. Geological sketch map showing location of samples in the Bancroft area, Ontario (after Ontario Department of Mines, Map 1957b, Haliburton-Bancroft area, Ontario).

degree of resorption. The radioactivity of the pegmatites is erratic, the most radioactive spots being associated with remnant gneiss and fractures. The fractures are probably contaminated with secondary radioactive minerals containing remobilized uranium. The leucocratic portions of the pegmatite consist of recrystallized cataclastic quartz and perthitic microcline with variable quantities of albitic plagioclase and biotite. The large, porphyroblastic minerals are surrounded by medium grained graphic intergrowths of quartz, albite, and fresh microcline. The gneissic xenoliths are commonly finer grained than the host pegmatite and contain more abundant mafic minerals. The biotite varies in colour from greenish brown in less resorbed xenoliths to pleochroic reddish brown to straw-yellow in recrystallized xenoliths. Accessory minerals are more abundant in xenoliths and include green pleochroic tourmaline, graphite, uraninite, uranothorite, titanite, allanite, zircon, cyrtolite, and locally minor sulphides, molybdenite, pyrite, and chalcopyrite. The radioactive minerals produce prominent pleochroic halos in biotite. Titanite, allanite, apatite, uranothorite, and uraninite occur usually in groups at the edges of biotite laths or singly in quartz and albite. Radioactive minerals in feldspar and quartz are surrounded by radiating fractures that are commonly filled by red and black alteration products.

Unit 3: Metagabbro was observed in radioactive prospect JMV-1 and near Pierre Lake, RPL. It occurs as dense, very hard bands, commonly associated with coarser grained mafic orthogneiss of unit 4. In thin section the black metagabbro of unit 3 appears granular and fresh. It is composed of 40 per cent mafic metamorphic minerals, including subhedral green hornblende, minor biotite, and opaque grains that are uniformly disseminated in a leucocratic groundmass. The leucocratic minerals are mainly lamellar plagioclase (as in Rimsaite, 1967a, Plate I, Figs. II-4 and 5) and minor quartz that crystallizes in fractures. The rock contains abundant fine grained apatite and rare radioactive zircons surrounded by dark pleochroic halos in biotite.

Unit 4: Hornblende-plagioclase orthogneiss varies in grain size, texture, and biotite content. Mineralogically the orthogneiss is similar to metagabbro, but melanocratic and leucocratic parts of the rock are less evenly distributed than in the metagabbro of unit 3. The biotite-rich variety of the orthogneiss contains abundant sphene and locally graphic intergrowths of hornblende and quartz, in addition to minerals observed in the metagabbro.

Unit 5: Feldspar porphyry collected near Pierre Lake, RPL, exhibits a seriate-porphyroblastic texture and marked variations in grain size. Coarse grained porphyroblasts of microcline-perthite are surrounded by medium grained myrmekitic quartz-albite intergrowths, clear microcline, and brown biotite bands. Apatite, radioactive sphene, allanite, and zoned zircon are associated with biotite.

Unit 6: Pink granite and pegmatite were observed in several radioactive prospects, including PP-1, JMV-4, TDN-2, and H-50. They occur as small bodies commonly within paragneiss of La Force Formation. Pink pegmatites consist of coarse grained strained quartz, antiperthitic albite, less abundant microcline, biotite, and fine grained myrmekitic quartz-albite intergrowths. Biotite is locally replaced by minor muscovite and carbonate, and contains prominent pleochroic halos surrounding zircon, allanite, titanite, and uranothorite. The antiperthite is altered to patches of fine grained sericite and unidentified specks that give the rock a pink appearance.

Unit 7: Grey granite intrudes and replaces gneiss of unit 1 along fractures in sampling location RPL north of Pierre Lake. This rock is fine to medium grained microcline granite containing minor clouded albite grains, overgrown by clear rims, and minor disseminated green-brown biotite. The biotite is intergrown with sphene, allanite, apatite, and muscovite.

Table 9.1. Distribution of uranium in selected minerals and rocks form the Grenville Structural Province, determined by neutron activation analyses*

Occurrence (Fig. 9.1, 9.2)	Rock Unit	Description of rock and mineral samples	Analysis No.	U ppm
Area North of Mont-Laurier, Fig. 9.1				
PP-2	2f	White pegmatite and xenoliths of biotite gneiss	9	1360
JMV-1	2	Migmatite xenolith in U-ore, feldspathic	10	53.8
JMV-1	2	Migmatite xenolith in U-ore, biotite-rich	11	76.1
JMV-1	6	Pink pegmatite	25	5.7
JMV-1	2	Biotite gneiss surrounding uraniferous pegmatite	26	33.9
JMV-3	2f	Boulder of white radioactive pegmatite	29	45.7
JMV-3	2f	Weathered earth from pegmatite boulder (29)	30	16.9
RFR	Ic	Xenoliths of grey gneiss in white pegmatite	31	4.7
RPL	3	Metagabbro	32	1.4
RPL	4	Plagioclase-hornblende-biotite orthogneiss	33	4.6
RPL	5	Pink porphyry	34	4.0
RPL	7	Grey granite filling fractures in gneiss of unit 2	35	3.4
H-50	6	Pink Th- and U-bearing pegmatite	36	690
H-50	6	Altered feldspar from Th- and U-bearing pegmatite	37	127
TDN-2	2f	Fine grained white pegmatite	38	404
TDN-2	2f	Medium grained white pegmatite	39	243
TDN-2	2f	Rusty stained fracture fillings in pegmatite	40	61
RFR	2f	White pegmatite with migmatite xenoliths	41	19.2
RFR	2	Migmatite xenoliths in pegmatite (41)	42	5.7
RFR	Ic	Gneissic xenoliths in pegmatite (41)	43	5.3
Bancroft Area, Fig. 9.2				
Madawaska mine underground				
F	2	Hornblende-biotite gneiss near shaft at 7th level	1	3.6
F	2	Hornblende from gneiss 1	44	1.2
F	2	Biotite from gneiss 1	45	3.3
F	8	Granite pegmatite	2	119
F	8/3	Metasomatic granite pegmatite, containing anhydrite	3	31.4
F	8/3	Hornblende from anhydrite-calcite pegmatite (3)	50	2.3
F	8	Anhydrite from anhydrite-calcite pegmatite (3)	49	0.6
F	8	Massive pegmatite composed of red feldspar	4	419
F	8	Pegmatite containing purple-stained feldspar	5	927
F	8	Radioactive pegmatite	6	16 920
F	7	Radioactive pegmatite containing rare earths	27	23 440
SC	2	Mica schist, host rock in Silver Crater mine	7	23.9
SC	7	Muscovite separated from albite and betafite	28	7.7
C	3	Crystalline limestone with purple fluorite and mica	8	7.5
C	3	Phlogopite from crystalline limestone (8)	46	0.4
B	8	Brown ore containing red halos, Bicroft mine	12	1330
B	7	Ore composed of red feldspar and mafic minerals	13	4090
B	2	Migmatitic paragneiss from Bicroft mine	14	35.7
B	8	Pegmatite containing abundant mafic minerals	15	6370
B	8	Granite with melanocratic xenoliths	16	231
GH	8	Granite pegmatite with melanocratic xenoliths	17	2510
E	8	Red granite pegmatite south of Madawaska mine	18	123
E	8	Fine grained granite, south of Madawaska mine	19	6.6
E	2/4	Dark gneiss, host rock of granite (19)	20	7.1
I	3	Impure limestone containing phlogopite, sphene	21	7.2
A	2/8	Hornblende-biotite-rich bands in migmatite	22	7.1
A	2/8	Feldspar-quartz-rich bands in migmatite	23	2.8
A	2/8	Hornblende from melanocratic bands in migmatite (22)	47	1.7
A	2/8	Biotite from melanocratic bands in migmatite (22)	48	3.0
A	8	Red pegmatite in Faraday granite	24	4.5

*Analyses made at the Atomic Energy of Canada Ltd., Order No. 1420091.

Table 9.2

Abundance of heavy mineral fraction (specific gravity >3.3) in selected rocks

Uranium Analysis No. from Table 9.1	Location (Fig. 9.1, 9.2)	Description of rock	Weight of rock grams	Sieve fractions */	Weight of sieve fraction grams	Weight of heavy fraction grams
Area North of Mont-Laurier						
9	PP-2	White pegmatite (unit 2f)	4000	1	1000	3.5
				2	150	<0.5
				3	350	<0.5
				4	1000	
10	JMV-1	Migmatite, feldspathic part	6000	1	1000	2.5
				2	200	<0.5
				3	500	<0.5
				4	800	
11	JMV-1	Migmatite, micaceous part	6000	1	800	6.0
				2	200	<0.5
				3	300	<0.5
				4	500	
25	JMV-1	Pink pegmatite	2200	1	500	1.0
				2	150	<0.5
				3	200	<0.5
				4	400	
26	JMV-1	Mo-bearing pegmatite	2500	1	500	3.0
				2	200	<0.5
				3	250	<0.5
				4	500	
Bancroft Area						
1	F (mine)	Gneissic host rock	6000	1	1500	33.0
				2	300	4.0
				3	1000	8.0
				4	1500	
23	A (Faraday granite)	Migmatite, feldspathic part	8000	1	3000	9.0
				2	500	<0.5
				3	100	<0.5
				4	3000	
22	A	Migmatite, melanocratic part	5000	1	1400	14.0
				2	500	3.0
				3	500	1.0
				4	1200	
24	A	Pegmatite in granite	8000	1	3000	200.
				2	300	11.
				3	500	12.
				4	1000	
2	F (mine)	Granite pegmatite	4000	1	1000	3.
				2	100	<0.5
				3	300	<0.5
				4	1000	
3	F	Metasomatic pegmatite	3000	1	500	1.5
				2	180	<0.5
				3	300	<0.5
				4	800	
4	F	Massive pegmatite		1	500	3.0
				2	200	<0.5
				3	150	<0.5
				4	500	
5	F	Purple pegmatite	3500	1	850	120.
				2	300	9.
				3	200	4.
				4	900	
6	F	Radioactive pegmatite	2200	1	900	300.
				2	200	40.
				3	600	100.
				4	500	
13	B	Ore, feldspar and mafics	4500	1	500	250.
				2	200	8.
				3	300	5.
				4	1000	

*Sieve fractions (mesh) 1: (-100 to 200); 2: (-200 to 250); 3: (-250 to 325); 4: (-325)
corresponding grain size: 150-75 µm; 75-60 µm; 60-45 µm; <45 µm

Figure 9.3. Showing high grade rare earth and uranium ore from the Bancroft area (F). The ore is composed of allanite (dark prisms); cyrtolite (pale grey zoned grains); titanite (grey, wedge-shaped crystals); tourmaline (dark poikilitic patches in the lower field, centre of the photograph); and minor biotite in albite groundmass. This specimen contains 23 440 ppm U, Table 9.1, analysis 27. (GSC 203226-L)

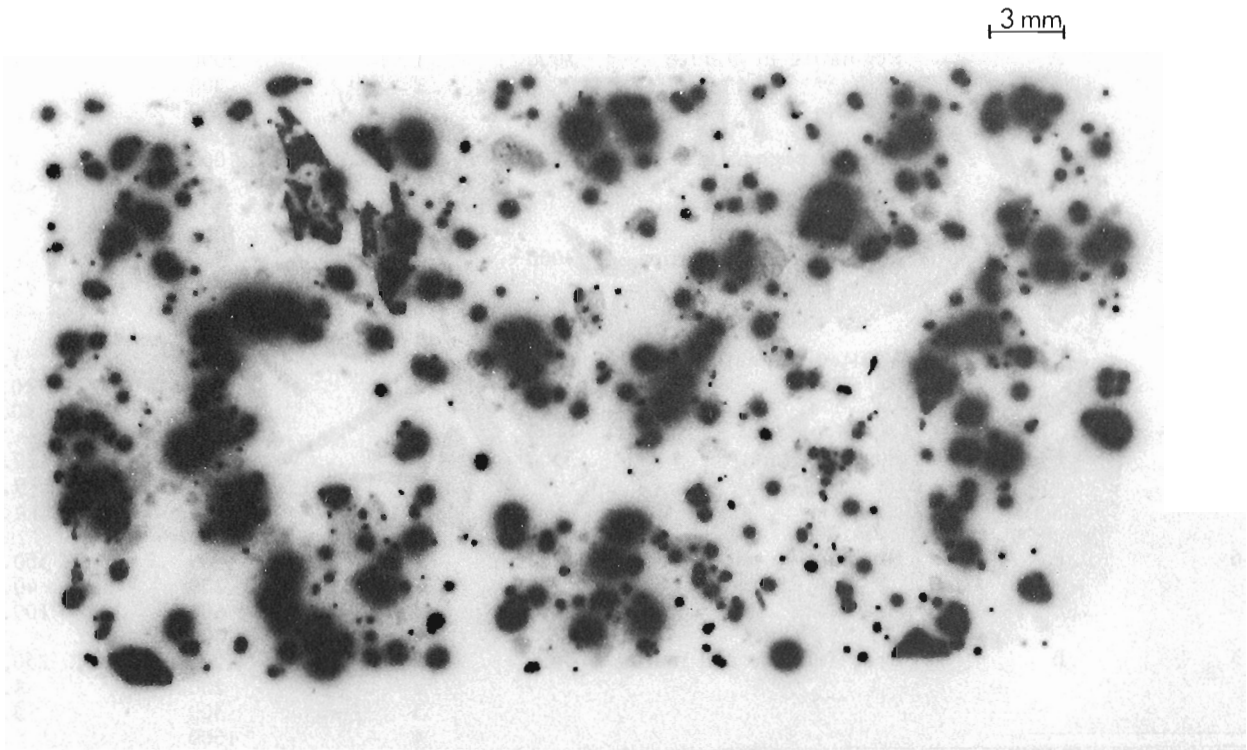

Figure 9.4. Autoradiograph of high grade ore in Figure 9.3, showing distribution of weakly radioactive allanite (pale grey prisms) and strongly radioactive uraninite and uranothorite (black spots). (GSC 203226-Q)

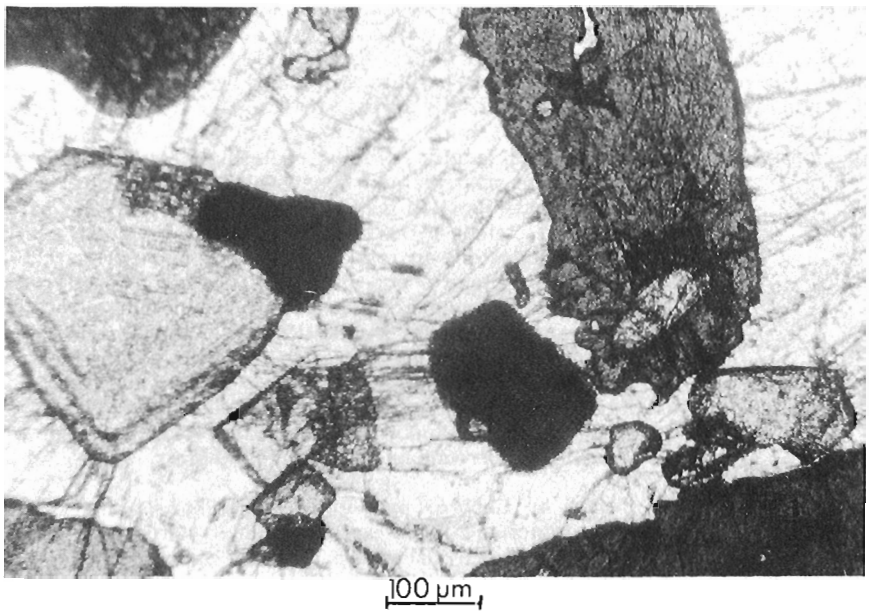

Figure 9.5.

Showing details of ore in Figure 9.3. Allanite with inclusions of zircon, uraninite and uranothorite (dark grey prism with white and black inclusions, right); black euhedral uraninite (centre) and zoned cyrtolite containing black specks of uraninite (left) in fractured albite (white groundmass).

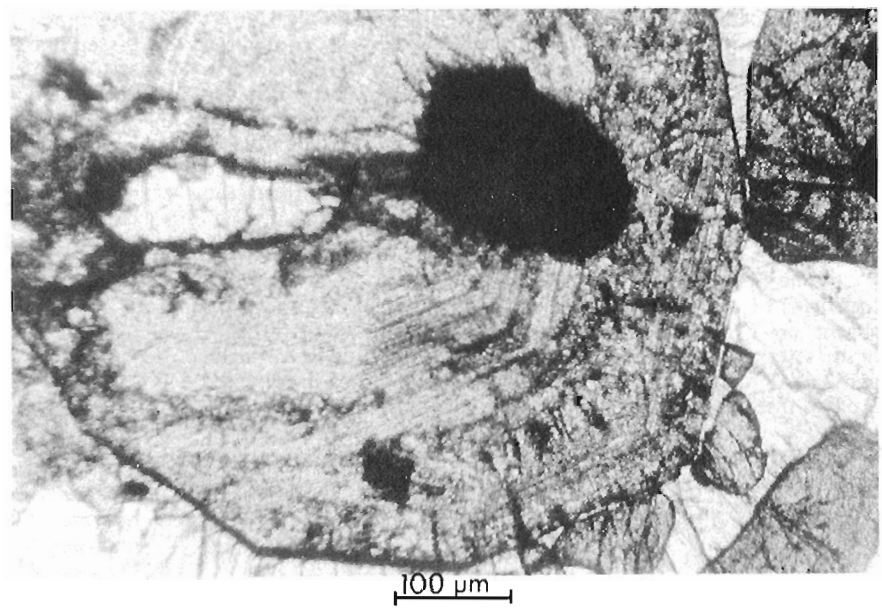

Figure 9.6.

Zoned cyrtolite composed of isotropic and anisotropic bands containing black radioactive inclusions.

All rocks examined in thin sections exhibit cataclastic textures, followed by recrystallization and replacements of minerals. The main difference between the rocks is in the contents of mafic minerals, potassic and sodic feldspars, and accessory minerals.

According to Kish (1977) rocks of units 1 to 5 are folded, faulted and affected by regional metamorphism of amphibolite facies. Radioactive mineralization occurs predominantly in white pegmatites, feldspathic and biotite-bearing quartzites, in biotite paragneiss of La Force Formation of unit 2, and in pink pegmatites that are probably related to pink granites of unit 6. In bulldozed areas, the radioactive pegmatites are cleared of glacial debris and exposed to weathering. The exposed surfaces of feldspar-rich rocks are altered to fine grained white clay crusts.

Three types of radioactive mineralization have been distinguished by scintillometer readings in the field:

(1) white pegmatites and quartz-feldspar-biotite gneiss containing more uranium than thorium. In these rocks uranium is present mainly in uraninite crystals. The radioactive belts having predominantly uranium mineralization include the Pond prospects, PP-1 and 2; properties owned by Johns-Manville Co. north of Patibre Lake, JMV-1 to 3; white pegmatites north of Tom Dick creek, TDN-2, and prospects north of La Force Lake, G, in Figure 9.1;

(2) white pegmatites containing relatively fresh inclusions of biotite gneiss and approximately equal average concentrations of uranium and thorium. These include prospects in Tom Dick area, TD and TDN-1 (Fig. 9.1) and

(3) radioactive pegmatites associated with pink granites of unit 6 containing more thorium than uranium. These were examined in prospects JMV-4 and in Hanson zone, H-50.

The uranium and thorium contents and Th/U ratios determined by Tremblay (1974, Table III) for pink pegmatite show considerable variations. The thorium contents range

from 75 ppm to 5000 ppm, the uranium contents from 16 ppm to 2300 ppm, and Th/U ratios vary from 1.1 to 8.1 for the nine reported determinations. Uranium concentrations, determined by neutron activation in the present study (Table 9.1) are comparable with those reported by Tremblay (1974, Table III). The lowest concentrations were found in the metagabbro, 1.4 ppm U, and the highest in pink pegmatite, 690 ppm U, and in white pegmatite, 1360 ppm U.

In an attempt to increase uranium concentration by separating light minerals, heavy mineral fractions were prepared from a few selected rock samples (Table 9.2). Preliminary results in Table 9.2 indicate low heavy mineral contents in the selected rocks from PP-2 and JMV prospects. The best recovery of heavy minerals was in the coarser, 150-75 μm fraction, and the highest concentration of heavy minerals (0.75%) was obtained from a melanocratic portion of a migmatitic xenolith in a white pegmatite. Mineralogical and chemical studies of the heavy fractions are not yet completed.

Bancroft Area, Ontario

Mineralogical studies of rare and radioactive minerals in pegmatites and skarns enclosed in, and surrounding, granite and syenite bodies in the Bancroft area commenced over 50 years ago (Ellsworth, 1932). General geology and numerous mining properties in the area have been described by Hewitt (1957) and Satterly (1957), and summarized in geological map 1957b Haliburton-Bancroft area, Ontario, by the Ontario Department of Mines. Results of isotopic age determinations on micas and uranium- and thorium-bearing minerals have been interpreted by Robinson (1960). Detailed isotopic studies of pleochroic halos in micas and fluorite are being conducted by R.V. Gentry using an ion probe on specimens from the Bancroft area in order to further investigate polonium ^{218}Po decay to ^{206}Pb, (Gentry, 1974, and pers. comm.).

The radioactive occurrences visited and sampling localities of the principal ores and rock types in this study are shown on Figure 9.2. Mineralogical and petrological characteristics of samples representing rock units on the geological map 1957b of the Haliburton-Bancroft area, were studied in thin sections. Results are as follows:

Unit 2: Paragneiss, arkose, and argillite are associated with crystalline limestone (unit 3) and occur as rims and bands between granite and syenite bodies. The biotite-hornblende gneiss collected in the Madawaska uranium mine near the shaft at the seventh level consists of 50 per cent mafic minerals evenly disseminated in quartz-feldspar matrix. The predominant feldspar is oligoclase. It is medium grained, fresh, and exhibits lamellar twinning. Minor microcline fills interstitial spaces between biotite and oligoclase. Quartz is less abundant than oligoclase. Locally quartz and oligoclase exhibit undulatory extinction and strain effects. The mafic minerals, in decreasing order of abundance, are green pleochroic hornblende, brown biotite, cordierite, and irregular opaque grains of magnetite that crystallize along grain boundaries of biotite and hornblende. Accessories are commonly associated with mafic minerals and include abundant apatite and sphene. Sphene commonly occurs in intergrowths with magnetite. Euhedral zircon and small prisms of apatite are scattered in feldspar and quartz. This rock contains 2.2 wt. per cent of heavy minerals in the 150-75 μm fraction (Table 9.2). The uranium contents in the whole rocks and in hornblende and biotite concentrates are 3.6, 1.2 and 3.3 ppm U (Table 9.1). Paragneiss in roadcuts of highway 28 contain abundant interstitial calcite and minor fluorite, in addition to quartz, feldspars, hornblende, biotite and accessory titanite, apatite and zircon.

Unit 3: Crystalline limestone was examined in Cardiff mine, C; in Silver Crater mine, SC; in Madawaska mine, F; and in roadcuts along highway 28, I, (Fig. 9.2). In Madawaska mine, xenoliths or patches of coarse grained calcite and anhydrite occur locally in pegmatites. The crystalline limestone in Cardiff mine consists of calcite, purple fluorite, phlogopite, and locally contains radiating white amphibole, green euhedral apatite, and honey-yellow chondrodite. The fluorite appears mottled purple and white and shows a pale discoloration along fractures and grain boundaries. Crystalline limestone in roadcuts, I, contains rusty patches and bands of silicate impurities that are composed predominantly of phlogopite surrounded by sphene and abundant accessories, apatite and pyrite. Rusty limonitic stains are attributed to decomposing pyrite. At the contact with granite and pegmatite, crystalline limestone is altered to skarn and locally contains diopside and disseminated uranium and rare earths minerals. Radioactive marbles are pink and contain rusty-red halos surrounding radioactive minerals.

Unit 4: Gabbro, pyroxenite, amphibolite, and other mafic metamorphic rocks were examined in roadcuts along highway 28 between Madawaska uranium mine and Bancroft, underground in the Madawaska mine, and along southern edge of Faraday granite. Fine grained dense rocks in roadcuts occur as black bands and sheets resembling diabase dykes. The black metadiabase contains 60 per cent mafic minerals disseminated in plagioclase groundmass. The mafic constituents are disintegrating pyroxene surrounded by blue-green amphibole. The rock contains accessory carbonate, titanite, epidote, and opaque grains consisting mainly of magnetite, minor pyrite, and pyrrhotite. The hornblendites consist of 90 per cent hornblende interbanded with 10 per cent magnetite. In thin section hornblende crystals appear pale green, granular, subhedral to euhedral and vary from 50 μm to 400 μm in diameter. Bands of coarse grained and fine grained amphibolite are separated by thin seams of opaque magnetite. Hornblende crystals adjacent to magnetite streaks are filled with opaque specks thereby appearing dark green or mottled grey. Accessory minerals include abundant apatite and minor carbonate in fine grained hornblende bands. Bright green spinel and/or garnet occurs in intergrowths with magnetite, and orange-red iron oxides produce reddish stains along fractures. Metagabbro differs from melanocratic hornblendite by segregations of mafic minerals and leucocratic portions consisting of plagioclase and minor quartz. The metagabbro contains remnants of pyroxene enclosed in amphibole, abundant titanite, apatite, and locally biotite. All gradations from evenly grained melanocratic rocks to coarse grained patchy and banded white-black rocks have been observed. Some melanocratic rocks resemble migmatites consisting of alternating dark and white bands. Melanocratic rocks are common xenoliths in granite and syenite pegmatites. In radioactive pegmatites, mafic minerals such as hornblende and biotite from partly-resorbed xenoliths are common hosts for uraninite and uranothorite.

Unit 6: Nepheline pegmatite and gneiss occur west of Cheddar granite in association with metagabbro and syenite.

Unit 7: Syenite rocks are associated with granitic rocks. They also occur in crystalline limestone and along the margins of granitic bodies. Syenite rocks consist predominantly of sodic feldspars and are important hosts for uranium ore. Specimens of radioactive albite-rich pegmatites were collected in Bicroft and Madawaska mines (uranium analyses 13 and 27 in Table 9.1). The radioactive syenitic pegmatites are medium to coarse grained and consist essentially of albite, minor quartz, and interstitial microcline. They contain variable amounts of carbonate, anhydrite, and mafic xenoliths that locally make up 60 per cent of the rock. Quantities of heavy accessory minerals

apparently increase with increasing content of radioactive minerals. In mineralized rock from Bicroft mine, heavy minerals reach 50 wt. per cent in 150-75 μm fraction, analysis No. 13 in Table 9.2. In high grade ore, albite and quartz are fractured, exhibiting characteristic curved cracks and radial fractures surrounding radioactive inclusions that are coated with reddish brown crusts giving the rock a brownish appearance. The partly-resorbed mafic xenoliths consist of recrystallized bright green amphibole, pleochroic reddish brown biotite, abundant titanite, apatite, allanite, cyrtolite, and locally fluorite. In uranium-rare earths ore, heavy accessory minerals can exceed in abundance ferromagnesian minerals, hornblende, and biotite. The biotite, hornblende, allanite, and cyrtolite are common hosts for uranium and thorium minerals. A specimen representing high grade rare earth-uranium ore is illustrated in Figures 9.3 to 9.6. It consists of brownish fractured albite (50 per cent), minor interstitial quartz, and microcline (5 per cent), abundant heavy minerals (40 per cent) including allanite, titanite, zoned cyrtolite, uraninite, thorianite, uranothorite, and local segregations of biotite, tourmaline, apatite, fluorite and calcite. The biotite in the high grade ore contains inclusions of euhedral uraninite and has an uncommon structural formula:

Octahedral layer: $(Ti_{.07}Fe^{3+}_{.7}Fe^{2+}_{1.28}Mg_{3.12}Mn_{.06}Li_{.4}Zn_{.01})$

Tetrahedral layer: $(Si_{6.16}Al_{1.82}Ti_{.02})$

Interlayer: $(Na_{.04}Ca_{.02}K_{1.86}Ba\&Cs_{.01}Rb_{.06})$

Oxygen and hyrdoxyl group: $O_{20.5}OH_{1.29}F_{1.7}$ (Rimsaite, 1967b, Plate VIII, Figs. 8, 9, Table VI).

As can be seen from the complex formula, the biotite contains relatively high concentrations of ferric iron, lithium, rubidium (5000 ppm), and fluorine in its structure. The biotite apparently crystallized from highly differentiated residual pegmatitic liquids, enriched in rubidium, lithium, and fluorine. Note that the fluorine content in biotite exceeds that of hydroxyl. The dark green tourmaline locally forms large interstitial poikilitic masses enclosing and replacing all minerals. The presence of tourmaline porphyroblasts suggest boron metasomatism during the final stages of pegmatitic activity. The enclosed uraninite in allanite and associated boron activity in the Bancroft area are similar to those observed in the Mary Kathleen deposit in Australia (Hawkins, 1976).

Unit 8: Granitized gneiss grading to granites and pegmatites are the most abundant rocks in the Bancroft area. They are closely associated with syenites forming circular bodies in orthogneisses and metasediments. Migmatitic gneisses and granitized metasediments were examined in roadcuts and trenches along highway 500 north of Bancroft, location A, and in the Madawaska mine, F. Migmatitic gneisses consist of alternating thin melanocratic and porphyroblastic leucocratic bands. The melanocratic bands are composed of green pleochroic hornblende and biotite in quartz-plagioclase groundmass. Locally, hornblende forms poikiloblastic porphyroblasts. The biotite commonly replaces hornblende and contains dark pleochroic halos surrounding zircon inclusions. The leucocratic portions consist of coarse grained cataclastic quartz, clouded plagioclase, less abundant microcline, partly-resorbed greenish biotite, and epidote. Abundant titanite and apatite crystallize along the transition zone between melanocractic and leucocratic bands. The plagioclase, partly clouded by fine grained secondary minerals, produces the pink appearance of leucocratic bands. The melanocratic bands are more radioactive than the leucocratic bands, and the hornblende contains less uranium than the associated biotite (Table 9.1, analyses 22, 23, 47, and 48, and corresponding uranium values 7.1, 2.8, 1.7, and 3.0 ppm U). The uranium is probably associated with heavy mineral fraction which is more abundant in melanocratic bands (Table 9.2, analyses 22 and 23, and corresponding heavy fractions 1 per cent and 0.3 per cent). The pegmatitic granite consists predominantly of microcline perthite and variable proportions of plagioclase, quartz, and mafic xenoliths. Feldspars are deformed and exhibit interrupted twinning and patchy, recrystallized replacement textures (as in Rimsaite, 1967a, Plate II, Figs. V-13, and V-14). Granites, grading to coarse grained pegmatites are important hosts to uranium mineralization in the Madawaska mine. They differ in proportions of quartz, microcline, albite, carbonate, anhydrite, melanocratic xenoliths, and uranium-thorium contents (from 31.4 ppm U to 16920 ppm U, analyses 2 to 6 in Table 9.1). The uranium content apparently increases with increasing abundance of albite, melanocratic xenoliths, and heavy mineral fraction (Table 9.2, analyses 2 to 6). The uranium-rich pegmatite (analysis 6, Tables 9.1 and 9.2) contains more than 50 volume per cent hornblende interbanded with pink streaks of coarse grained titanite, anhydrite, apatite, abundant cyrtolite, heterogeneous uranothorite, and euhedral uraninite enclosed in reddish alteration rims. The reddish colour of granitic and syenitic rocks in the Bancroft area is probably related to partial alteration of ferromagnesian minerals and magnetite in recrystallized xenoliths. Quartz-rich residual pegmatite and metasomatic pegmatite containing abundant calcite and anhydrite contain only 119 ppm U and 31.4 ppm U; anhydrite and associated hornblende contain 0.6 ppm U and 2.3 ppm U (Table 9.1, analyses 2, 3, 49, and 50).

Summary

Specimens representing principal rock types and uranium mineralization in an area north of Mont-Laurier, Quebec, and in the Bancroft area, Ontario, were collected for laboratory studies in an attempt to determine favourable environments for uranium mineralization. Preliminary results based on thin section study and 50 neutron activation analyses for uranium in selected minerals and rocks indicated the following differences and similarities between the radioactive occurrences examined in Ontario and Quebec.

The uranium mineralization occurs mainly in granitic and syenitic pegmatites containing variable quantities of melanocratic xenoliths. The mineralized pegmatites that contain dominantly uranium in an area north of Mont Laurier, Quebec, are white. They are composed predominantly of quartz and microcline and contain variable quantities of biotite-rich xenoliths, plagioclase, trace amounts of heavy minerals, and very erratic distribution of uraninite and uranothorite. Only a few specimens collected in Bear Lake locality, JMV-3, containing marked quantities of heavy and radioactive minerals, including zoned cyrtolite, resembled the U, Th, rare earths pegmatites of the Bancroft area. According to the preliminary map by Kish (1976), the uraniferous white pegmatites occur in a stratigraphically lower unit 2 than the pink granite and related pink pegmatites (unit 6) which contain more thorium than uranium.

The radioactive occurrences in the Bancroft area include granite and syenite pegmatites and closely associated skarns. The pegmatites are pink to reddish and contain xenoliths of crystalline limestone, anhydrite, and hornblende-rich rocks. The presence of partly-resorbed and recrystallized limestone apparently resulted in the abundance of Ca-rich minerals, titanite, apatite and allanite and skarn-like mineralization. The uranium mineralizaton in the Bancroft area is related to late granitic and syenitic activity (rock units 7 and 8) that also produced metasomatic skarn rocks and fluorite-rich veins in the surrounding crystalline limestone. The surrounding limestones might possibly account for the presence of Si-deficient, Na-rich syenitic rocks that provided

favourable environments for crystallization of rare earths and radioactive minerals in the Bancroft area. The presence of remnant pyroxene and abundant hornblende indicate a greater abundance of original melanocratic rocks in the Bancroft area than in the area north of Mont-Laurier. The leucocratic rocks examined in Quebec contain biotite partly replaced by chlorite and muscovite thereby inferring effects of retrograde metamorphism. The area north of Mont-Laurier is characterized by potassium-rich rocks, whereas the Bancroft area represents a sodium-rich province. Chemical analyses of these specimens are being made. They may indicate more distinct differences between mineralized and common rocks in the uraniferous belt north of Mont-Laurier, Quebec, and in the Bancroft area, Ontario.

Acknowledgments

R.F. Kaltwasser of the Canadian Johns-Manville Company Limited provided valuable information concerning exploration results and acted as guide in prospects JMV-1 to 3 during our visit with L.P. Tremblay and N. Prasad in June 1977. The author was assisted in the field by N. Prasad (Quebec) and J. Kerswill (Ontario). The management and staff of the Madawaska uranium mine are thanked for their guidance at the mine site.

References

Allen, J.M.
1971: The genesis of Precambrian uranium deposits in eastern Canada, and the uraniferous pegmatites at Mont-Laurier, Quebec; unpubl. M.Sc. thesis, Queen's Univ., Kingston, Ontario, 83 p.

Ellsworth, H.V.
1932: Rare-element minerals of Canada; Geol. Surv. Can., Econ. Geol. Rep., 11, 212 p.

Gentry, R.V.
1974: Radiohalos in a radiochronological and cosmological perspective; Science, v. 184, p. 62-66.

Hawkins, B.V.
1976: Mary Kathleen uranium deposit; ed. Ryan, G.R., Excursion Guide No. 49 AC, 25th Int. Geol. Congr., Sydney, Australia, p. 37-39.

Hewitt, D.F.
1957: General geology; in Satterly, J.: Radioactive mineral occurrences in the Bancroft area, Ontario, Ontario Dep. Mines, 65th Ann. Rep., v. 65, pt. 6, 1956, p. 5-26).

Kish, L.
1977: Patibre (Axe) Lake area. Preliminary Report; Ministère des Richesses Naturelles, Service des Gites Mineraux, DPV-487, p. 13 and geological map 1:20 000 of DPV-487. (Placed on open file in January 1977.)

Rimsaite, J.H.Y.
1967a: Optical heterogeneity of feldspars observed in diverse Canadian rocks; Schweiz. Min. Petr. Mitt., v. 47, no. 1, p. 61-76.

1967b: Studies of rock-forming micas; Geol. Surv. Can., Bull. 149, p. 20-21.

Robinson, S.C.
1960: Note on the interpretation of U-Pb, Th-Pb and K-Ar ages in the Bancroft, Ontario region; Age determinations by the Geological Survey of Canada, Rep. 1. Isotopic ages, ed. Lowdon, J.A., Geol. Surv. Can., Paper 60-17, p. 41.

Tremblay, P.
1974: Mineralogy and geochemistry of the radioactive pegmatites of the Mont-Laurier area, Quebec; unpubl. M.Sc. thesis, Queen's Univ., Kingston, Ontario, 133 p.

10.

GEOLOGY AND COAL RESOURCES OF THE TERTIARY SEDIMENTS, QUESNEL-PRINCE GEORGE AREA, BRITISH COLUMBIA

Project 760056

Peter S.W. Graham
Institute of Sedimentary and Petroleum Geology, Calgary

Abstract

Graham, Peter, S.W., Geology and coal resources of the Tertiary sediments, Quesnel-Prince George area, British Columbia; in Current Research, Part B, Geol. Surv. Can., Paper 78-1B, p. 59-64, 1978.

Coal occurs in both the upper and lower members of the Oligocene-Miocene Fraser River Formation which outcrops along the Fraser River from Prince George to Alexandria Ferry, 38 km south of Quesnel, British Columbia. Deposition of sediments was controlled by an ancient south-flowing river system which drained a more subdued terrain under wetter and warmer conditions than those that presently prevail. Thicker coal seams, up to 21.9 m thick, are restricted to the lower Fraser River Formation. The coal is Subbituminous "B" to "C" in rank, contains many clay partings and has an inherently high ash content. Potentially economic areas are restricted to south of Quesnel.

Introduction

Throughout central British Columbia, many scattered Tertiary sedimentary basins occur in which coal or coaly material has been recorded. The Geological Survey of Canada, in co-operation with the British Columbia Department of Mines and Petroleum Resources, has initiated a study of some of these basins. This paper discusses geology and coal resource potential in the vicinity of Quesnel and Prince George, an area of more immediate economic interest. Previous work in this area has been done by Dawson (1877), Reinecke (1920), Cockfield (1932), Lay (1940, 1941), Mathews and Rouse (1963), McCallum (1969) and Piel (1971, 1977). Information for this study has been taken mainly from published and unpublished reports, supported by field observations of the writer.

General Geology

Figure 10.1 summarizes the geology as interpreted by Lay (1940), McCallum (1969) and others. Recent work on the palynology, vertebrate remains and potassium argon dating by Mathews and Rouse (1963), Piel (1971) and Hopkins (written comm.) has solved most of the time stratigraphic problems

Figure 10.1

Table of formations

Age	Group or formation	Members & Thickness (Lay 1940)	Members – Facies (McCallum 1969)	Members This Report	Lithology
Early Pliocene-Late Miocene	Endako Group (?) (Tipper 1960)	Upper Volcanics 15 m	Not Studied	Upper Volcanics	Olivine basalt, andesite
Early Pliocene to Late Miocene	Fraser River Formation (Reinecke 1920)	Diatomite Member 50 m	Tertiary C	Upper Fraser River Formation	Claystone, siltstone, sandstone, diatomaceous clays, minor coal
Mid- to Late Miocene		Gravel Member 150+ m	Tertiary B: Channel; Off Channel		Conglomerate, sandstone, occasional claystone
		UNCONFORMITY			
Early Oligocene		Australian Member 360+ m	Tertiary A: Arkose, Gritty clay, Gravel	Lower Fraser River Formation	Claystone, siltstone, sandstone, conglomerate, coal
UNCONFORMITY					
Eocene	Unit 4 (Tipper 1959)	Lower Lavas 600+ m	Early Tertiary Volcanics	Lower Lavas	Andesite, related tuffs and breccias, minor conglomerate and sandstone
UNCONFORMITY					
Penn-Permian	Cache Creek Group (Tipper 1959)				Chert, argillite, limestone, greenstone, minor greywacke and conglomerate

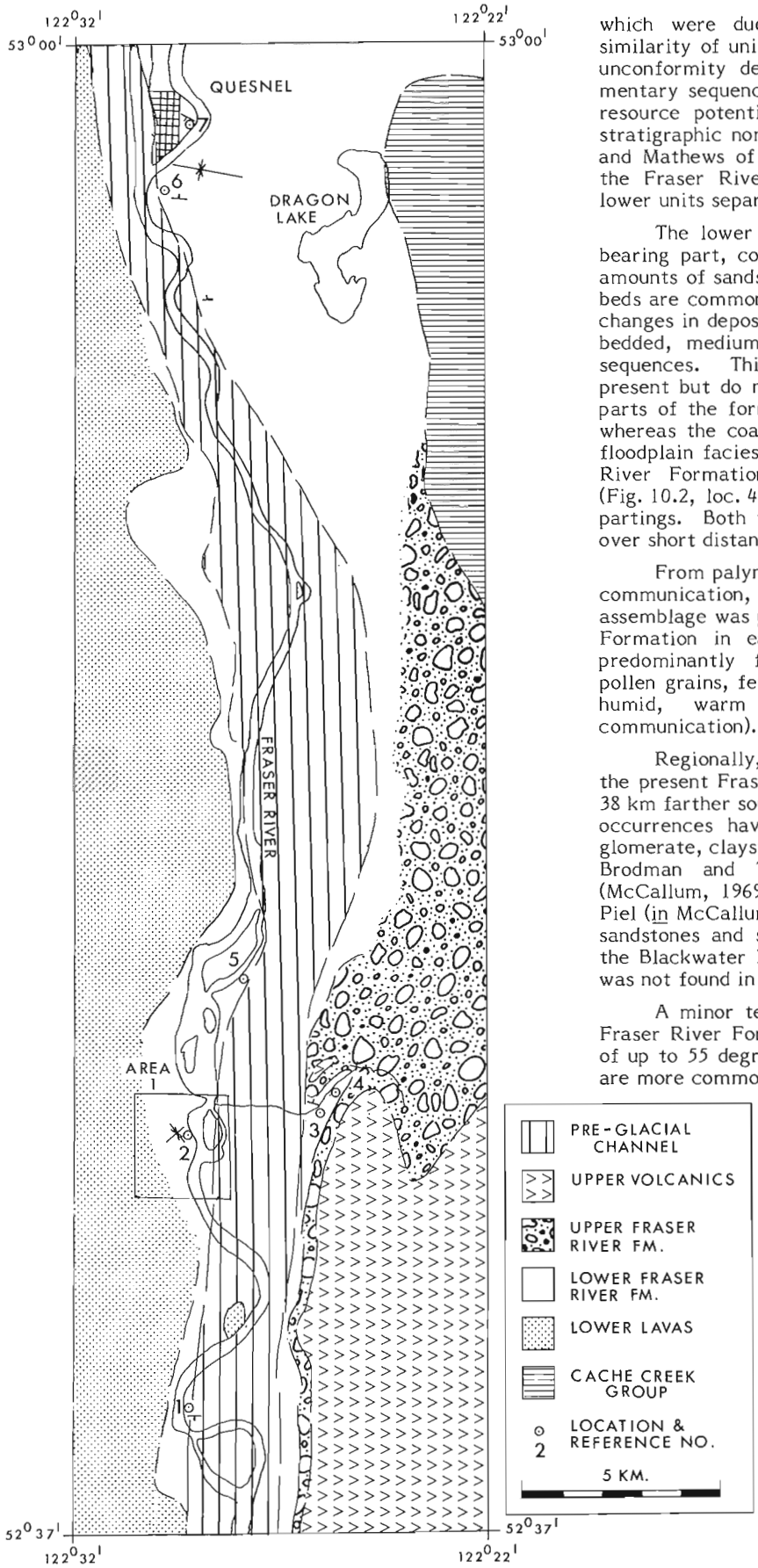

Figure 10.2. Generalized geology map, Quesnel area. Modified after Tipper (1959).

which were due to poor bedrock exposure and the lithologic similarity of units. A further stratigraphic problem is the angular unconformity described by Lay (1940) within the Tertiary sedimentary sequence. The present study deals mainly with the coal resource potential of the Tertiary sediments. Revision of the stratigraphic nomenclature is currently being undertaken by Rouse and Mathews of the University of British Columbia. Tentatively, the Fraser River Formation is treated informally as upper and lower units separated by the unconformity.

The lower Fraser River Formation, which is the main coal-bearing part, consists of at least 360 m of claystone with lesser amounts of sandstone, conglomerate and coal. Individual lithologic beds are commonly thin. Vertically they contain evidence of rapid changes in depositional environment. Generally sandstones are thin bedded, medium to coarse grained and occur in fining-upward sequences. Thicker sandstone-conglomerate sequences are also present but do not appear to be associated with the coal-bearing parts of the formation. They may represent main channel facies whereas the coal-bearing sequences may represent off channel or floodplain facies. Coals occur in several parts of the lower Fraser River Formation and have been reported up to 21.9 m thick (Fig. 10.2, loc. 4). These coal zones commonly contain many clay partings. Both the coal beds and the clay partings are lenticular over short distances.

From palynological evidence, Piel (1971) and Hopkins (written communication, 1978) have concluded that a large and varied floral assemblage was present during deposition of the lower Fraser River Formation in early Oligocene time. The flora observed was predominantly from angiosperms, conifers with non-bladdered pollen grains, ferns and lower plants, the taxa of which indicate a humid, warm temperate paleoclimate (Hopkins, written communication).

Regionally, the lower Fraser River Formation is restricted to the present Fraser River Valley from Quesnel to Alexandria Ferry, 38 km farther south (Fig. 10.2, loc. 1). However, two other possible occurrences have been reported. Interbedded sandstones, conglomerate, claystones and "thin beds of lignite" outcrop on Haggith, Brodman and Tabor creeks, 10 km south of Prince George (McCallum, 1969). This succession has been dated by Rouse and Piel (in McCallum, 1969) as early Oligocene. Another succession of sandstones and siltstones of possible Oligocene age was found on the Blackwater River 60 km northwest of Quesnel. Although coal was not found in place, it was observed as debris in the creek.

A minor tectonic event prior to the deposition of the upper Fraser River Formation caused tilting of the coal measures. Dips of up to 55 degrees have been reported (McCallum, 1969, p. 9) but are more commonly less than 20 degrees.

The upper Fraser River Formation consists of at least 200 m of massive conglomerates and sandstones grading up to siltstones, claystones with occasional diatomaceous clay, and coal. Separating the upper and lower units is an angular unconformity recognized by Lay (1940) at Big Bend, 11 km north of Quesnel. The upper unit characteristically dips less than 5 degrees. It is poorly indurated which makes it almost indistinguishable from some interglacial sediments located in the region.

Most exposures of the upper unit of the formation are located on the Fraser River between Prince George and Quesnel. It has also been observed in the upper reaches of Australian Creek (Fig. 10.2, loc. 4) and may cover a considerable area west of the Fraser River.

The upper unit was deposited during a much cooler period than the lower unit as indicated by a dramatic increase in the conifer population (Mathews and Rouse, 1963; Piel, 1971, 1977). These authors have assigned a mid-late Miocene age for the upper Fraser River Formation.

Coal seams have been recorded in the upper unit and except in one place are very thin, dirty and discontinuous (Reinecke, 1920; Laurence, 1953). On the Nechako River 20 km west of Prince George, however, Lay (1941, p. 35) described two coal seams 1.5 and 1.8 m thick. The age of these coals has not been well established and may prove to be Oligocene and, hence, within the lower unit.

Environments of Deposition

Tipper (1959) and McCallum (1969) state that deposition of sediments was from a north-flowing river system; however, Lay (1940) had previously shown convincing evidence for a southerly flow direction after Eocene time. Lay's interpretation was confirmed by the present author's observations of pebble imbrication. The upper Fraser River Formation was deposited by an ancestral river which drained a relatively subdued terrain. The river system occupied a valley along the trend of the present Fraser River Valley in this area. South of Quesnel, lateral river migration apparently did not exceed 6 km. Relatively humid conditions in the early Oligocene

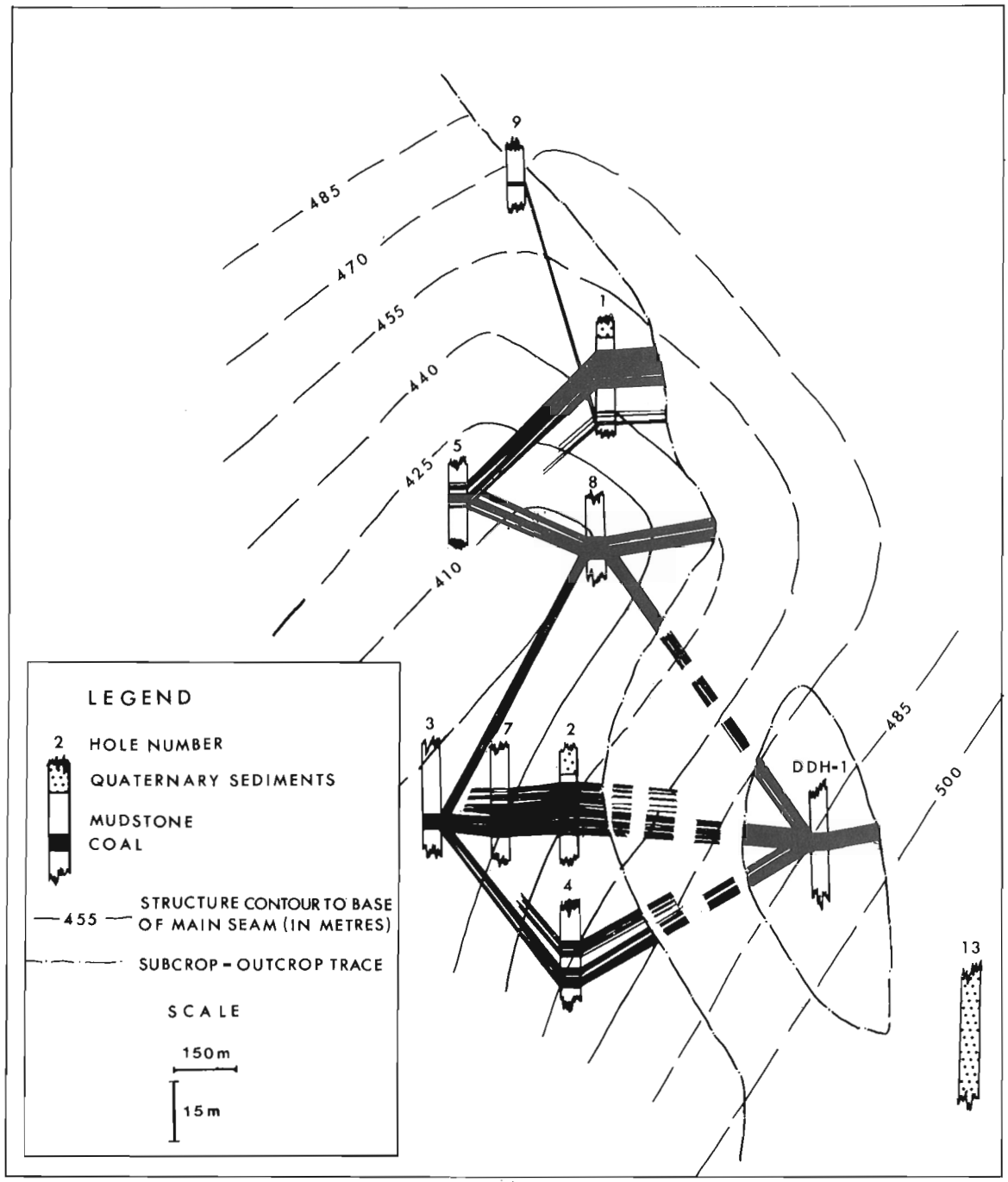

Figure 10.3. Fence diagram and structure contour map of main seam, Area 1. For location of area, see Figure 10.2.

may have been responsible for the abundance of local paludal and lacustrine conditions in the overbank areas. Occasional flood conditions could have caused the thin, fining-upward sandstone units. This type of environment should lead to rapid facies changes both perpendicular and parallel to the direction of stream flow. Subsequent to the deposition of the lower unit, mild tectonism caused local tilting of the strata before erosion and final deposition of the upper Fraser River Formation. Clasts in the conglomerate of the upper unit are predominantly composed of older quartzites and metamorphosed material (Reinecke, 1920) which indicates that the reactivation of the river system occurred after a period of tectonism rather than volcanism. Because of cooler climatic conditions and the higher fluvial energy regime in the upper unit, major peat accumulation would not be expected.

A short period of volcanism occurred during and after deposition of the upper unit (McCallum, 1969, p. 19). Subsequently, the river was re-established and cut a deep channel through the upper and lower units of the Fraser River Formation prior to Pleistocene glaciation (Fig. 10.2).

Deposition of fluvial sediments along the present Fraser River has occurred sporadically since early Oligocene time. This could indicate that the Fraser River fault zone recognized farther south by Trettin (1961) and others continues into the study area and runs close to the present river channel. Reactivation of the fault zone must have occurred from late Eocene to early Oligocene and also from mid-Oligocene to mid-Miocene time. This is indicated by the angular unconformities separating the sedimentary units.

Areas of Economic Interest

Except for two thick coals reported by Lay (1941, p. 35) west of Prince George, all other major seams reported occur south of Quesnel. These occurrences have been divided into four separate areas and are discussed individually.

1. Red Cliff

A cliff of reddish clays is located immediately south of the Quesnel townsite and was altered by the burning of an underlying coal seam. A series of holes drilled by the British

Figure 10.4

Coal seam data, Quesnel, B.C.

Location	Source of Data	Coal Thickness (metres)	Interval between seams	% Moisture	% Volatile Matter	% Fixed Carbon	% Ash	Sulphur	kCal/kg	Reference
1. Alexandria[1] Ferry	outcrop	1.07 1.22 1.22	0.6 0.46	6.9[3] 5.1 3.4	39.7 38.2 38.8	39.7 38.5 36.8	13.7 18.2 21.0			B.C. Rep. Minister 1924, p. A127
2. Doyle's Ranch	outcrop	min. 2.4		33.9	23.4	27.2	15.5	0.6	3300	Can. Dep. Mines Tech. Surv. Rep. Analyses 1940
	outcrop	min. 2.4		21.0[5] 0	25.5 42.8	31.8 57.2	21.7 0			B.C., Rep. Minister, 1931, p. A172
2. Doyle's Ranch	7 Rotary[2] Test holes 1 DDH	3.2 to 13.2 net coal		45.8 0	19.3 49.3	18.5 51.7	16.4 30.2[4]	0.23	2547	Yoon, 1972 Lakes, 1930
3. Australian Creek	Adit	1.13		11.5 0	30.6 49.8	28.5 50.2	29.4 0			Reinecke, 1920
4. DDH 3	diamond-drill hole	4.2 21.9	141.7							Lakes, 1930
5. Howard's Ranch	outcrop	1.3		3.6 0	40.2 52.0	35.6 48.0	20.6 0			B.C. Rep. Minister of Mines, 1924, p. A127
6. Red Cliff	15 auger holes B.C. Dep. of Highways	18 net 30 gross								B.C. Dep. Highways unpub. rep. on Plywood Hill Slide
7. Quesnel	3 rotary holes B.C. Dep. of Highways	2 to 6 m								B.C. Dep. Highways, unpub. rep. on Quesnel Bridge 1958

[1] Numbers represent locations on Figure 1.

[2] Analysis averaged from 8 samples.

[3] Analysis on an "as Received" basis.

[4] Ash calculated on a moisture free basis.

[5] Dry ash free analysis calculated using the Parr Formula.

Columbia Department of Highways (Fig. 10.2, loc. 6), 560 m southwest of this cliff, penetrated a possible 30 m coal zone containing an average of 60 per cent coal by volume. Further evidence of a major coal zone at least 18 m thick was found in a water well 800 m east of the drillholes. These three points give an approximate regional dip of 5 degrees north. At location 7 (Fig. 10.2), three shallow holes were drilled for bridge pilings, and penetrated a seam ranging from 2 to 6 m thick. A dip of 16 degrees southwest was calculated here. From additional surface evidence an east-west trending syncline is proposed (Fig. 10.2). The area between location 6 and Dragon Lake should have the highest potential for near-surface coal.

2. West Australian Creek

Master Exploration Ltd. (Yoon, 1972) drilled a series of rotary holes of which 7 penetrated a major coal zone on the west bank of the Fraser River west of Australian Creek (Fig. 10.2, Area 1). Results of the drilling (see Fig. 10.3) showed this zone to average 75 per cent coal and 25 per cent clay partings. Furthermore the zone is lenticular, ranging from 3.4 m (net) to 13.2 m (net) over a distance of 500 m. Measured, Indicated, and Inferred Resources have been calculated (by the writer) at 4, 10 and 14.5 million tonnes, respectively. Calculations were based on Cordilleran coal parameters established by the Department of Energy, Mines and Resources (EMR Rep. EP77-5). Erosion by the preglacial channel restricts the seam almost entirely to the west bank of the Fraser River. The coal measures have been folded into a southwest-plunging syncline with dips on the limbs of approximately 10 degrees (see Fig. 10.3).

3. East Australian Creek

A diamond-drill hole, 4 km east of Area 1, penetrated two major coal zones 4.2 and 21.9 m thick (Fig. 10.2, loc. 4). Records show that this coal contains numerous clay partings similar to coals in the other areas. Measured surface dips range from 15 to 25 degrees northeast, which should bring the lower, thicker seam nearer to the surface farther southwest. However, the seam may have been truncated and partially removed prior to the deposition of the upper Fraser River Formation.

4. Alexandria Ferry

An outcrop located just south of the old Alexandria Ferry (Fig. 10.2, loc. 1) contains several thin coal seams and one major coal zone with 3.5 m coal in a 4.7 m thick interval and dipping 15 degrees south (B.C. Department of Mines, 1924, p. A126). Immediately east of this outcrop is a deeply incised preglacial channel which eliminates the economic potential of much of the area. There is, however, a small area to the east and south of the Alexandria Ferry crossing which may be underlain by a major coal seam.

Coal Rank and Quality

Several coal analyses have been previously reported and are summarized on Figure 10.4. According to the Parr Formula (ASTM, 1973, p. 56), the coal ranks Subbituminous "B" to "C" on a moisture mineral matter free basis. Excluding the clay partings, the coal continues to display an inherently high ash content, averaging between 20 and 30 per cent on a moisture-free basis. Although rank and quality are low, they are comparable to the coal seams at Hat Creek 200 km farther south (Church, 1977).

Conclusions

The mid-Tertiary sediments in the Quesnel-Prince George area can be divided into two distinct stratigraphic units of which the lower has greater economic potential. Coal seams are lenticular and high in ash. Some of the subsurface data presently available are of dubious quality and further drill hole information is required to better determine the stratigraphy and obtain more accurate coal resource information.

References

American Society for Testing and Materials
1973: Book of ASTM Standards, Part 19, Gaseous fuels, Coal and Coke; Philadelphia, Pennsylvania, p. 56.

British Columbia Department of Mines
1924: Report to the Minister of Mines, 1923, p. A125-A127.

1931: Report to the Minister of Mines, 1930, p. A170-A172.

Canada, Department of Mines and Technical Surveys
1940: Report of Analysis No. 21401.

Canada, Energy, Mines and Resources
1977: 1976 Assessment of Canada's Coal Resources and Reserves, Rep. EP77-5.

Cockfield, W.E.
1932: Oil possibilities between Soda Creek and Quesnel, Cariboo district, British Columbia; Geol. Surv. Can., Summ. Rep. 1931, Pt. A, p. 58-65.

Church, B.N.
1977: Geology of the Hat Creek Coal Basin; B.C. Dep. Mines and Pet. Resour., Geology in British Columbia, 1975, p. 99-118.

Dawson, G.M.
1877: Report on explorations in British Columbia; Geol. Surv. Can., Rep. Prog., 1875-76, p. 255-260.

Lakes, A.
1930: Preliminary Report on the Cariboo Coal and Clay Syndicate Property; unpubl. rep., B.C. Dep. Mines Pet. Resour., Open File.

Laurence, R.H.
1953: Report on the Geological Survey of B.C. Petroleum and Natural Gas Permit 549, Quesnel Area; J.C. Sproule and Associates, unpubl. rep., B.C. Dep. Mines Pet. Resour., Open File.

Lay, D.
1940: Fraser River Tertiary Drainage History in relation to Placer Gold Deposits; B.C. Dep. Mines, Bull. 3.

1941: Fraser River Tertiary Drainage History in relation to Placer Gold Deposits, Part II; B.C. Dep. Mines, Bull. 11.

Mathews, W.H. and Rouse, G.E.
1963: Late Tertiary Volcanic Rocks and Plant Bearing Deposits in British Columbia; Bull. Geol. Soc. Am., v. 74, p. 55-60.

McCallum, J.A.
1969: Groundwater and geology of the South Prince George Area, Central British Columbia, ARDA Research Project No. 10014; unpubl. rep., of the Water Investigations Branch, B.C. Dep. Lands, Forests and Water Resour., April, 1969.

Piel, K.M.
1971: Palynology of Oligocene Sediments from central British Columbia; Can. J. Botany, v. 49, p. 1885-1920.

1977: Miocene Palynological assemblages from central British Columbia; Am. Assoc. Stratigr. Palynol., Contrib. 5A, p. 91-110.

Reinecke, L.
1920: Mineral Deposits between Lillooet and Prince George; Geol. Surv. Can., Mem. 118, p. 13-18, 80-81.

Tipper, H.W.
1959: Geology of the Quesnel area, Cariboo District, British Columbia; Geol. Surv. Can., Map 12-1959.

1960: Geology of the Prince George area, Cariboo District, British Columbia; Geol. Surv. Can., Map 49-1960.

Trettin, H.P.
1961: Geology of the Fraser River Valley between Lillooet and Big Bar Creek; B.C. Dep. Mines Pet Resour., Bull. 44, p. 95-99.

Yoon, T.N.
1972: Exploration Report on Quesnel coal properties. Master Explorations Ltd.; unpubl. rep., B.C. Dep. Mines Pet. Resour., Open File.

11. SOME WENLOCKIAN (SILURIAN) OSTRACODA FROM SOUTHWESTERN DISTRICT OF MACKENZIE

Project 720072

M.J. Copeland
Regional and Economic Geology Division

Abstract

Copeland, M.J., Some Wenlockian (Silurian) Ostracoda from southwestern District of Mackenzie; in Current Research, Part B, Geol. Surv. Can., Paper 78-1B, p. 65-72, 1978.

A widespread ostracode fauna representative of the Ural-Cordilleran subprovince has been reported from northwestern Canada. This fauna was previously presumed of late Wenlockian? or early Ludlovian? to Gedinnian age but, based on the complete faunal assemblage, is now demonstrated to be undoubtedly as old as Wenlockian and possibly early Wenlockian.

Introduction

Lenz (1968, 1972, 1977) and others have shown that brachiopod, trilobite, graptolite and conodont faunas may be used with varying degrees of reliability to determine the age of diverse early Paleozoic clastic and carbonate rock sequences in southern Yukon Territory and southwestern District of Mackenzie. Ostracodes are also good stratigraphic markers throughout this area (Berdan and Copeland, 1973; Copeland, 1974, 1977) but their usefulness in correlation with ostracode faunas elsewhere is limited because many taxa are new and no standard Paleozoic ostracode zonation exists. International zonation may not be possible, because, unlike some of the previously mentioned fossil groups, many Paleozoic ostracode faunas demonstrate a high degree of provincialism (Copeland and Berdan, 1977). This permits detailed local correlation but usually not zonation on worldwide or continental bases. Provincialism of many early Paleozoic ostracode faunas may result from facies control (Berdan, 1977) but also may be due to the shallow platform benthonic adaptations of many rapidly evolving leperditicopid and palaeocopid lineages (Copeland, in press) – groups that did not, for the most part, survive the Paleozoic. Failure of these ostracodes to adapt to even moderate environmental changes may have caused rapid extinction of taxa before their extensive distribution could be attained.

One of the most widespread early Paleozoic ostracode faunas appears to have existed in the northern hemisphere during the late Silurian and early Devonian within the Ural-Cordilleran subprovince (Boucot and Johnson, 1973). This was suggested earlier (Copeland, 1977, fig. 8) but the time of inception of this ostracode fauna was questionable due to lack of associated fauna on which to base exact correlation. Lenz (1977) recently presented evidence for the occurrence of Wenlockian faunas in eastern Selwyn Basin based on brachiopods, trilobites and conodonts from two collections which also contain silicified ostracodes. These collections are from calcareous strata 6 miles (10 km) east of Avalanche Lake (62°23'N; 127°03'W), 300-330 feet (90-99 m) and 675-685 feet (225-228 m) below the top of a section transitional between the Whittaker and Road River formations. Thirty brachiopod taxa occur in the stratigraphically higher collection (300-330 ft) and Lenz (1977, p. 1524) states that "the overall brachiopod evidence suggests a Wenlockian age, an age consistent with trilobite faunas". The stratigraphically lower interval (675-685 ft) contains only 6 brachiopod genera but has conodonts suggestive of "the **amorphognathoides** Zone of late Llandoverian and early Wenlockian age. In view of the presence of **Atrypella** and **Janius** in the fauna, an early Wenlockian age is tentatively suggested". Based on previously known occurrences of similar ostracodes from northwestern Canada, only a late Wenlockian? to early Ludlovian age could be assigned to these Avalanche Lake collections. Considering the faunal evidence presented by Lenz, however, a Wenlockian assignment is probable. This implies that the cosmopolitan late Silurian – early Devonian Ural-Cordilleran ostracode fauna was of longer duration in northwestern Canada than previously known, with several genera in the Avalanche Lake collections appearing earlier than their Ludlovian Uralian counterparts reported by Abushik (1968) and Abushik and Modzalevskaya (1973).

As more evidence becomes available it is probable that zonation of this ostracode fauna will become refined and more exact ages may be assigned to stratigraphic units containing this assemblage. At present it appears that a tentative faunal progression of **Beyrichia (Beyrichia) lenzi** n. sp. (Wenlockian – early Ludlovian), **B. (B.) henningsmoeni** McGill (Ludlovian) and **B. (B.) arctigena** Martinsson (Gedinnian) may prove of stratigraphic importance throughout northwestern and Arctic Canada.

Table 11.1

Occurrence of Wenlockian ostracodes, Avalanche Lake and Delorme Range, District of Mackenzie

Ostracode Species	Localities			
	Avalanche Lake		Delorme Range	
	300-330	675-685	C-47-150	C-47-100
*Ludvigsenites? sp.	X			
+Treposella sp.	X		?	
*Beyrichia (Beyrichia) lenzi	X		X	X
+Yukonibolbina sp. cf. Y. plana	X			
+Cornikloedenina lorangerae		X		
*Retisacculus? sp.	X			
Alaskabolbina sp.	X			
+Berdanopsis ursensis	X			
*'Ctenobolbina' mackenziensis	X			
'Aparchites' sp.	X			
+Undulirete mackenziensis	X		X	X
+Libumella sp. cf. L. ambigua	X		X	X
+Processobairdia delormensis	X	X	X	X
+Acanthoscapha subnavicula	X		X	X
+Cadmea acuta	X		X	X
+Cooperatia lacrimosa	X		X	X
+Silenis proteus	X	X		
*Arcuaria avalanchensis	X			
Ockerella? sp.	X	X		
*Antijanusella spinosa	X			
Camdenidea? sp.	X		?	

* species described here
\+ species described in Copeland, 1977

Collections similar to those from the Avalanche Lake Section in Selwyn Basin were obtained from calcareous strata of upper Whittaker and lower Delorme formations in Root Basin to the east (Copeland, 1977). These basins are separated by Redstone Arch, a positive structural feature that was transgressed intermittently during the early Paleozoic and served as a southward-trending barrier separating the deeper, open ocean Selwyn Basin from the shallower, possibly restricted Root Basin embayment. Lenz (1974, p. 1125) considered brachiopods from the uppermost Whittaker Formation of Root Basin as late Wenlockian or early Ludlovian. There, the Whittaker Formation is conformably overlain by lower beds of the Delorme Formation and the age of their contact may be equated approximately with the Wenlockian-Ludlovian boundary. In eastern Selwyn Basin, however, contact of the Whittaker and Delorme formations with the Road River Formation is highly diachronous, clastic strata of the Road River Formation to the southwest lying in juxtaposition with carbonate rocks of both the Whittaker and Delorme formations to the northeast. Correlation between these continental slope and platform rock sequences of Selwyn Basin may only be effected paleontologically and the Ostracoda seem to present one potential faunal solution to this problem.

Twenty-one ostracode species have been recovered from the two Avalanche Lake collections: 20 from the upper 300-330 foot interval and 4 from the lower 675-685 foot interval. Eleven of these species were reported previously (Copeland, 1977) in strata of late Wenlockian? to late Ludlovian age. Of the stratigraphic sections reported therein, greatest similarity exists between ostracode fauna of the 300-330 foot interval at Avalanche Lake and those 5 feet (1.5 m) above and 45 feet (13.5 m) below the conformable Whittaker-Delorme contact 75 miles (120 km) to the northeast in Root Basin at localities C-47-150 and C-47-100 of Section VI in Delorme Range (Table 11.1). The Avalanche Lake collection in Selwyn Basin occurs in Road River and Whittaker formations rocks some 300 feet (90 m) below the Whittaker-Delorme contact (Lenz, pers. comm.). If correlation based on ostracode fauna from these two sections is accepted, the Whittaker-Delorme contact at Avalanche Lake in eastern Selwyn Basin would appear to be somewhat younger than that same contact in Delorme Range of Root Basin.

Systematic Paleontology

Subclass Ostracoda Latrielle, 1806

Order Archaeocopida Sylvester-Bradley, 1961

Family Beyrichonidae? Ulrich and Bassler, 1931

Genus **Ludvigsenites** Copeland, 1974

Ludvigsenites? sp.

Plate 11.1, fig.3

Description. Valve elongate, postplete, with long, straight hingeline. Bilobate, S2 straight, long, deep, near mid valve. Anterior lobe with near marginal anterior hooklike process slightly below dorsum, and prominent, hemispherical node anterior of S2. Posterior lobe inflated, with prominent posteriorly directed posterodorsal tubercle obscuring posterior end of hinge in lateral view.

Length of right valve, 5.6 mm, height 3.0 mm.

Type. GSC 54764.

Occurrence. Avalanche Lake loc. 300-330, Wenlockian.

Remarks. This specimen differs from **L. mackenziensis**, the type species, in having a vertical instead of inclined S2, a prominent node on the anterior lobe anterior of S2 and the posterior tubercle higher on the posterior lobe. The shell is etched so that the surface texture of the valve and the possible presence of an 'eye tubercle' are unknown.

PLATE 11.1

(All specimens from locality 300-330, except figure 12)

Figures 1, 2. **'Ctenobolbina' mackenziensis** n. sp. left lateral views of two tecnomorphic? valves, x 40 and x 20, GSC 54762, 54763.

Figure 3. **Ludvigsenites**? sp., right lateral view of a valve, x 10, GSC 54764.

Figures 4, 5. **Retisacculus**? sp., right and left lateral views of two valves, x 40, GSC 54765, 54766.

Figure 6. **Udulirete mackenziensis** Copeland, right lateral view of a valve, x 40, GSC 54767.

Figure 7. **Treposella** sp., right lateral view of a valve, x 40, GSC 54768.

Figure 8. **Berdanopsis ursensis** Copeland, right lateral view of a tecnomorphic valve, x 40, GSC 54769.

Figures 9, 10, 13. **Alaskabolbina** sp., left lateral, ventral and right lateral views of three valves, x 40, GSC 54770-54772.

Figure 11. **Yukonibolbina** sp. cf. **Y. plana** Copeland, left lateral view of a valve, GSC 54773.

Figure 12. **Berdanopsis royalensis**? Copeland; right lateral view of a broken heteromorphic valve, x 20, loc. CH-27-770, GSC 54774.

Figures 14-23. **Beyrichia (Beyrichia) lenzi** n. sp., all figures x 20. 14, right lateral view of a tecnomorphic valve, paratype, GSC 54775; 15, right lateral view of a heteromorphic valve, holotype GSC 54776; 16, ventral view of a heteromorphic carapace, paratype GSC 54777; 17-19, left lateral views of three tecnomorphic valves, paratypes GSC 54778-54780; 20, right lateral view of a tecnomorphic valve, paratype GSC 54781; 21, ventral view of a right heteromorphic valve, paratype GSC 54782; 22, left lateral view of a tecnomorphic valve, paratype GSC 54783; 23, right lateral view of a tecnomorphic valve, paratype GSC 54784.

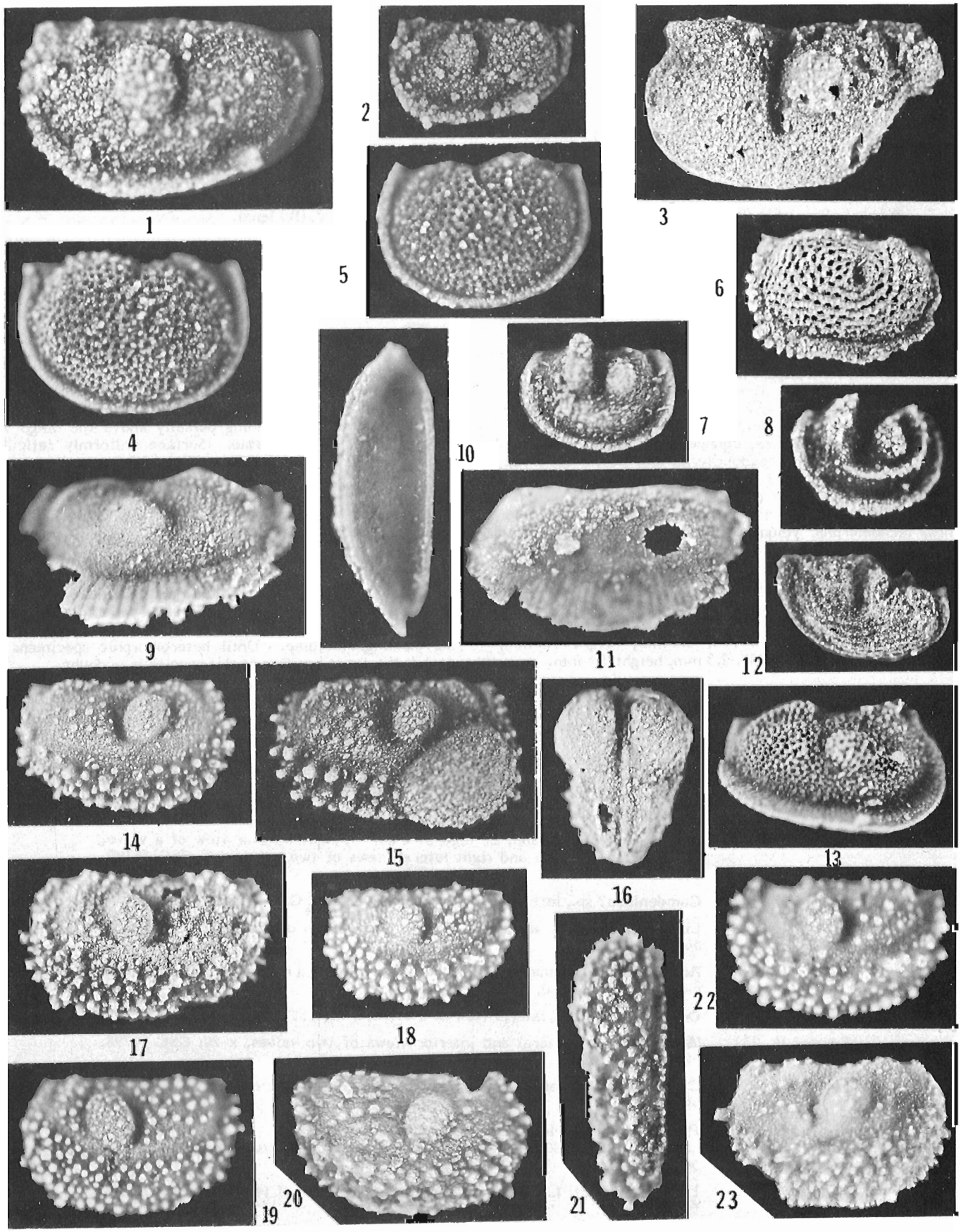
1
2
3
4
5
6
7
8
9
10
11
12
13
14
15
16
17
18
19
20
21
22
23

This specimen and those of the type species were recovered from strata near the continental shelf-continental slope deposits interface. Both may represent a deeper marine ostracode fauna that is presently unknown. The occurrence of a Wenlockian archaeocopid is of importance as it extends the range of the Archaeocopida from the Middle Ordovician (Esbataottine Formation) into the Middle Silurian.

Order Palaeocopida Henningsmoen, 1953

Family Beyrichiidae Matthew, 1886

Genus **Beyrichia** M'Coy, 1846

Subgenus **Beyrichia (Beyrichia)** M'Coy, 1846

Beyrichia (Beyrichia) lenzi n. sp.

Plate 11.1, figs. 14-23

Beyrichia (Beyrichia) sp. 1. Copeland, 1977, p. 20, pl. I, figs. 5, 6.

Description. Medium sized **Beyrichia** species, pronouncedly tuberculate with more numerous and undiferrentiated larger tubercles on the ventral part of the valve, separated from the less tuberculate dorsal part of the valve by the non tuberculate syllobial groove and non tuberculate furrow between the anterior lobe and anteroventral field. Anterior lobe and syllobium cuspate, connected beneath S2 without lobular differentiation. Preadductorial lobe pustulose, broad, low, feebly differentiated from anterior lobe. Adductorial sulcus short, in dorsal half of valve. Heteromorphic velum a low, tuberculate ridge with one major row of supravelar spines, tecnomorphic velum tuberculate with two or more rows of randomly distributed supravelar tubercles. Heteromorphic crumina well delimited dorsally, globular, with low tubercles or pustules, in anteroventral field. Marginal ridge tuberculate.

Length of holotype, GSC 54776, 2.5 mm, height 1.5 mm; length of paratype, GSC 54775, 2.2 mm, height 1.3 mm; length of paratype, GSC 54780, 2.3 mm, height 1.4 mm.

Types. Holotype, GSC 54776, paratypes, GSC 54775, 54777-54784.

Occurrences. Avalanche Lake, loc. 300-330; Section VI, locs. C-47-100, C-47-150; Section VIII, loc. S-2-795 (Copeland, 1977, p. 20).

Remarks. This species appears most nearly similar to **B. (B.) halliana** Martinsson of the Upper Visby-Slite beds of Gotland. **B. (B.) halliana** however, has more pronounced and discrete dorsal cusps, the anterior lobe is not dissected by a non tuberculate furrow continuous posteriorly with the syllobial groove, the crumina is ventrally striate not tuberculate as in **B. (B.) lenzi** and the marginal structure is a ridge, not denticulate as in **B. (B.) lenzi**.

Genus **Retisacculus** Martinsson, 1962

Retisacculus? sp.

Pl. 11.1, figs. 4, 5

Description. Valves semicircular in lateral view, hingeline straight about five-sixths greatest length, free margin evenly curved. Velar flange smooth, narrow. Anterior and posterior lobes evenly inflated, no evidence of L2, both lobes united broadly beneath thin, shallow S2 which lies in dorsal third of valve. Both lobes extending dorsally above the hinge with suggestion of dorsal cristae. Surface uniformly reticulate except for thin S2. Only tecnomorphs known.

Types. GSC 54765, 54766.

Occurrence. Avalanche Lake, loc. 300-330, Wenlockian.

Remarks. These tecnomorphic specimens are treposelline in appearance and seem to be most closely allied with **Retisacculus** because of the complete obsolescence of the preadductorial lobe. Unlike **R. commatatus** and **R. semicolonatus**, the median sulcus of **Retisacculus** sp. is very shallow and thread like, only one reticule wide and about as deep as the surrounding reticulae. Until heteromorphic specimens are found, the exact position of this species is in doubt.

PLATE 11.2
(All specimens from locality 300-330)

Figures 1-4. **Arcuaria avalanchensis** n. sp., all figures x 20. 1, right interior view of a valve, paratype GSC 54785; 2, 3, right lateral views of two carapaces, holotype GSC 54786, paratype GSC 54787; 4, dorsal view of a carapace, paratype GSC 54788.

Figures 5-7. **Cadmea acuta** Copeland, all figures x 20. 5, right interior view of a valve, GSC 54789; 6, 7, left and right lateral views of two carapaces, GSC 54790, 54791.

Figure 9. **Camdenidea**? sp., left lateral view of a valve, x 20, GSC 54793.

Figure 10. **Libumella** sp. cf. **L. ambigua** (Lundin), lateral view of a carapace, x 20, GSC 54794.

Figures 11, 12. **Acanthoscapha subnavicula** Abushik, dorsal view of a carapace and left lateral view of a valve, x 40, GSC 54795, 54796.

Figure 13. **Ockerella**? sp., left lateral view of a valve, x 40, GSC 54797.

Figures 14, 23. **'Aparchites'** sp., lateral and interior views of two valves, x 20, GSC 54798, 54807.

Figure 15. **Cooperatia lacrimosa** Copeland, right lateral view of a carapace, x 20, GSC 54799.

Figures 16-18. **Processobairdia delormensis** Copeland, all figures x 20. 16, dorsal view of a carapace, GSC 54800; 17, 18, left and right lateral views of two valves, GSC 54801, 54802.

Figures 19, 20. **Libumella** sp. cf. **L. ambigua** (Lundin), lateral views of two valves, x 40, GSC 54803, 54804.

Figures 8, 21, 22. **Antijanusella spinosa** n. sp., all figures x 20. 8, left lateral view of a valve, paratype GSC 54792; 21, 22, right lateral and dorsal views of two carapaces, paratype GSC 54805, holotype GSC 54806.

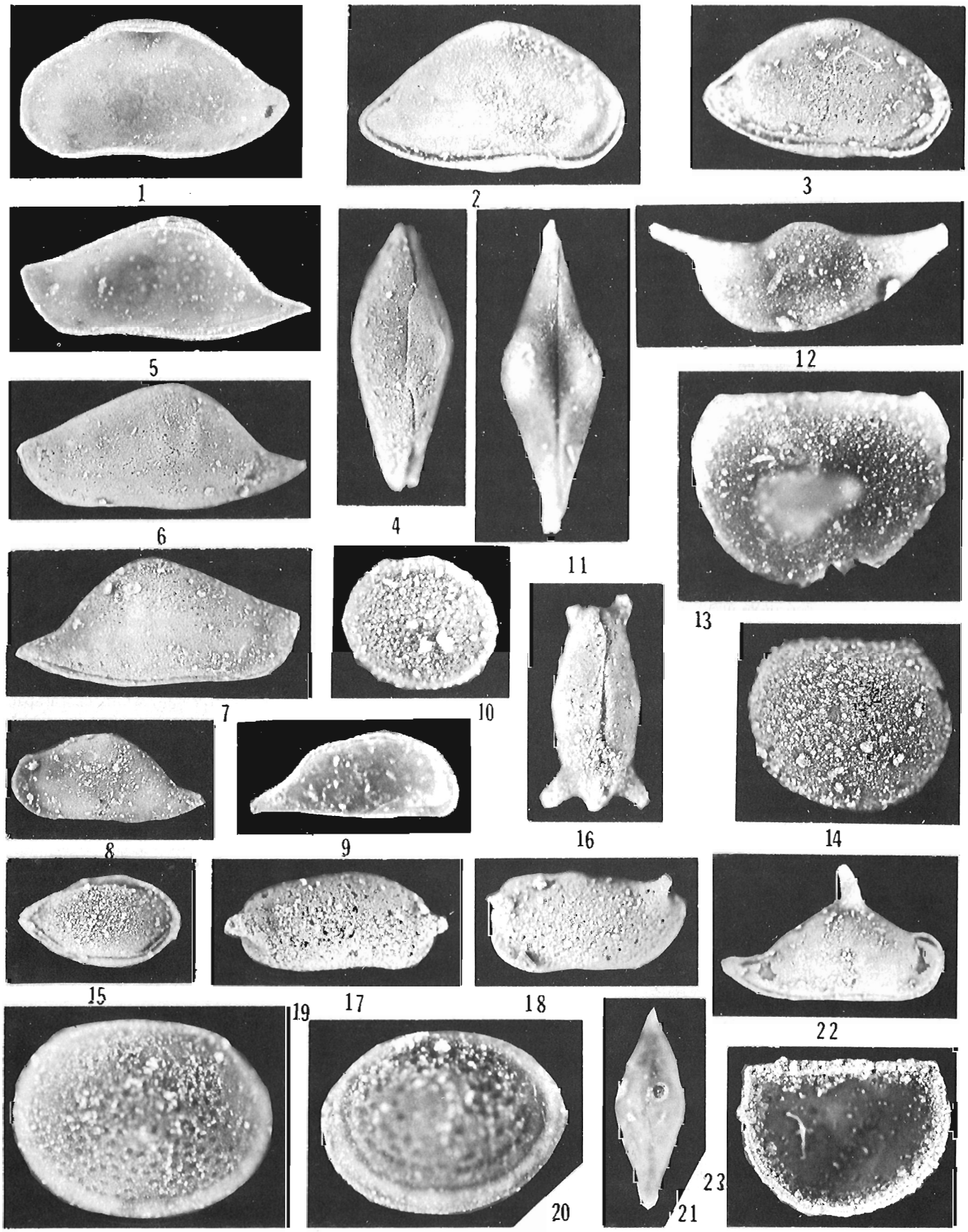
1
2
3
5
4
12
6
11
13
7
10
16
14
8
9
15
17
18
22
19
20
21
23

Family Hollinidae Swartz, 1936

Genus **Ctenobolbina** Ulrich, 1890

'Ctenobolbina' mackenziensis n. sp.

Pl. 11.1, figs. 1, 2

Description. Valves preplete; hingeline straight, four-fifths greatest length. Cardinal angles abrupt, obtuse. Anterior margin broadly curved, confluent with venter; posterior margin more narrowly rounded.

Bisulcate, S1 indistinct, joined to prominent S2 dorsal of large, hemispherical L2. S2 narrow, inverted comma-shaped, situated near mid valve. L3 broad, low. Domicilium surface covered with minute papillae.

Velar frill prominent, broadest anteriorly and antero-ventrally, produced into well developed posteriorly directed, hollow posteroventral spine and narrowing considerably across the posterior part of the valve as a low ridge curved parallel with the posterior margin. Velum of presumed tecnomorphic valves slightly flaring laterally. Subvelar field channeled to smooth marginal ridge. Presumed heteromorph unknown.

Length of holotype, GSC 54762, 1.6 mm, height 0.9 mm.

Types. Holotype, GSC 54762, paratype, GSC 54763.

Occurrence. Avalanche Lake, loc. 300-330, Wenlockian.

Remarks. This species is most similar to Ordovician species such as **'Ctenobolbina' punctata** Ulrich that lack an alate process on the domicilium. Those Ordovician species have a less pronounced preadductorial node, S2 is generally deeper and may extend as a shallow furrow to the velum on some species.

Order Podocopida Müller, 1894

Family Bairdiocyprididae Shaver, 1961

Genus **Arcuaria** Neckaja, 1958

Arcuaria avalanchensis n. sp.

Pl. 11.2, figs. 1-4

Description. Valves somewhat bairdiid in lateral view, dorsum highly arched, greatest height near mid length of valve. Hinge short, at greatest height, about one-fifth greatest length of valve. Posterodorsal slope straight to slightly convex, meeting posteroventral slope at slight angulation. Ventral margin gently curved, slightly convex in both valves in anterior half. Anterior margin narrowly rounded. Right valve with a dorsal protuberance that overreaches left valve at hinge; left valve completely overlapping right valve except along hinge.

Circular adductorial muscle scar visible on valve anterior, somewhat anterior of mid length and ventral of mid height; at about height of posterior angulation. Surface smooth.

Length of holotype, GSC 54786, 2.60 mm, height 1.50 mm; length of paratype, GSC 54787, 2.45 mm, height 1.30 mm.

Types. Holotype, GSC 54786, paratypes, GSC 54785, 54787, 54788.

Occurrence. Avalanche Lake, loc. 300-330, Wenlockian.

Remarks. **A. avalanchensis** is larger but very similar in lateral view and age to **A. delormensis** Copeland, 1977. The present species has a pronounced dorsal protuberance on the right valve in the position of the smooth dorsal overreach of **A. delormensis.**

Family Krausellidae Berdan, 1961

Genus **Antijanusella** n. gen.

Type species **Antijanusella spinosa** n. sp.

Included species **Spinobairdia**? sp. Copeland, 1977

Diagnosis. Subtriangular janusellid like ostracodes with L/R free marginal overlap and R/L dorsal overreach. Right valve with a pronounced spine at apex of dorsum. Both valves posteriorly acuminate.

Discussion. **Antijanusella** is similar to other genera of the Krausellidae only in that both valves are distinctly different and the left valve overlaps the right valve ventrally. Unlike **Krausella** and **Janusella** however, both valves of **Antijanusella** are acuminate posteriorly, the left valve extending past the right valve. As exemplified by the type species, the morphology of **Antijanusella** is fundamentally opposite to that of **Janusella** both in reversal of greatest posterior acumination and occurrence of the dorsal spine. Consideration of **Spinobairdia**? sp. Copeland, 1977 as an antijanusellid is possibly questionable as that species is based on an incomplete right valve which, however, bears a prominent dorsal spine.

Age. Wenlockian, ?Pridolian.

Antijanusella spinosa n. sp.

Pl. 11.2, figs. 8, 21, 22

Description. Subtriangular-bairdiid in lateral view, greatest height slightly anterior of mid length, greatest length in ventral half of valve. Hingeline short, at apex of dorsum, antero- and posterodorsal slopes straight, inclined, anterior margin compressed, narrowly curved to straight venter, posterior margin acuminate in both valves. Left valve overlapping right along free margin, right valve overreaching left dorsally and produced into a strong, dorsally directed spine. Surface smooth.

Length of holotype, GSC 54806, 2.1 mm, height 1.4 mm; length of paratype, GSC 54805, 1.9 mm, width of carapace 0.7 mm.

Types. Holotype, GSC 54806, paratypes, GSC 54792, 54805.

Occurrence. Avalanche Lake, loc. 300-330, Wenlockian.

Reference

Abushik, A.F.
1968: Ludlovian ostracodes of the Turkestan Range (Soviet Central Asia); Paleontol. J., v. 2, n. 3, p. 68-76.

Abushik, A.F. and Modzalevskaya, T.L.
1973: Silurian-Devonian boundary on the west slope of the subpolar Urals; Doklady Akad. Nauk. SSSR, v. 209, n. 5, p. 1171-1173.

Berdan, J.M.
1977: Early Devonian ostracode assemblages from Nevada; Geol. Soc. Amer., Abstr., 1977 Ann. Meetings, p. 894; also, Western North America Devonian, eds. M.A. Murphy, W.B.N. Berry and C.A. Sandberg, Univ. California, Riverside Campus, Mus. Contrib. 4, p. 55-64.

Berdan, J.M. and Copeland, M.J.
1973: Ostracodes from Lower Devonian formations in Alaska and Yukon Territory; U.S. Geol. Surv., Prof. Paper 825.

Boucot, A.J. and Johnson, J.G.
1973: Silurian brachiopods; in Hallam, A. (editor), Atlas of Paleobiogeography; Elsevier Sci. Publ. Co., Amsterdam, London, New York, p. 59-65.

Copeland, M.J.
1974: Middle Ordovician Ostracoda from southwestern District of Mackenzie; Geol. Surv. Can., Bull. 244.

1977: Early Paleozoic Ostracoda from southwestern District of Mackenzie and Yukon Territory; Geol. Surv. Can., Bull. 275.

Early Paleozoic ostracode assemblages, northwestern Canada; Geol. Assoc. Can., Sp. Paper. (in press)

Copeland, M.J. and Berdan, J.M.
1977: Silurian and early Devonian beyrichiacean ostracode provincialism in northeastern North America; in Report of Activities, Part B, Geol. Surv. Can., Paper 77-1B, p. 15-24.

Lenz, A.C.
1968: Upper Silurian and Lower Devonian biostratigraphy, Royal Creek, Yukon Territory, Canada; Int. Symposium on the Devonian System, Calgary, 1967, v. II, Alta. Soc. Pet. Geol., p. 587-599.

1972: Ordovician to Devonian history of northern Yukon and adjacent District of Mackenzie; Bull. Can. Pet. Geol., v. 20, n. 2, p. 321-361.

1974: Silurian Brachiopoda, upper Allen Bay Formation, Griffiths Island, Arctic Archipelago, and uppermost Whittaker Formation, Mackenzie Mountains, Northwest Territories; Can. J. Earth Sci., v. 11, p. 1123-1135.

1977: Llandoverian and Wenlockian brachiopods from the Canadian Cordillera; Can. J. Earth Sci., v. 14, p. 1521-1554.

12. LOWER PALEOZOIC CHITINOZOA AND ACRITARCHA FROM NEWFOUNDLAND

Project 690006

F. Martin[1]
Regional and Economic Geology Division

Abstract

Martin, F., Lower paleozoic Chitinozoa and Acritarcha from Newfoundland; in Current Research, Part B, Geol. Surv. Can., Paper 78-1B, p. 73-81, 1978.

Palynomorphs were recovered from samples collected principally from Upper Cambrian and Ordovician strata in western and eastern Newfoundland. Samples from central Newfoundland volcanic belt were barren. Palynomorphs are identified and related to previously described forms from Europe, North Africa and North America.

Introduction

In the course of two field seasons (1975; 1976), 105 samples intended for chitinozoan and acritarch study were collected in Newfoundland from rocks ranging in age from Middle Cambrian to Silurian, though principally Late Cambrian to Ordovician. For the purposes of this report the subdivision of Newfoundland into three parts - Western Platform, Central Volcanic Mobile Belt and Avalon Platform – proposed by Williams (1964) is followed (Fig. 12.1, 12.2).

Western Platform

The present collections relate to only Port au Port Peninsula, Cow Head Peninsula and the Table Point area; microfossiliferous localities and stratigraphic horizons are listed below by area but discussion of the microfossils is not subdivided. Few taxa of Chitinozoa and Acritarcha are present (Fig. 12.3). The latter, more than the former, particularly resemble those of the Baltic region.

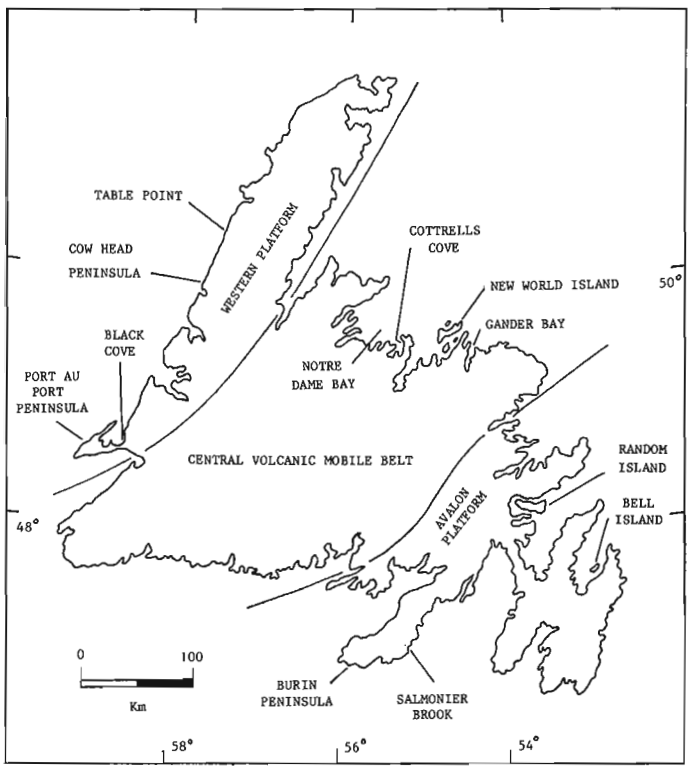

Figure 12.1. Sketch-map of Newfoundland, showing location of collecting areas.

Port au Port Peninsula

GSC Loc. 92983 and 94410. Long Point Group, Winterhouse Formation; old quarry immediately southeast of the fishing huts near the west end of Clam Bank Cove, 750 m northwest of Lourdes. Both samples are from jointed, slickensided, dark grey-green mudstone and shale which are overturned to the northwest. Loc. 92983 is from the stratigraphically youngest 1 m of strata (that is, in the lowest part of the quarry); Loc. 94410 is from a level 2.5 m stratigraphically older. The strata are in the higher part of the Winterhouse Formation as defined by Bergström et al. (1974) and lie above the 213 m (700 ft) omitted from their section by those authors (op. cit., p. 1630).

GSC Loc. 92987. Table Head Formation; shale in east side of excavation for the more northerly of the two fuel tanks situated west of road No. 59 leading to Fox Island River, and 3 km north-northeast of Port au Port village. The rocks correspond to part of the middle Table Head Formation as described for its type area by Whittington (1965, p. 286); the locality was noted by Kay (1967).

GSC Loc. 94409. Clam Bank Formation, lower part; headland at west end of Clam Bank Cove, 850 m northwest of Lourdes. The horizon is possibly in Bed 2 of the measured section given by Schuchert and Dunbar (1934, p. 106); the locality was noted also as "Stop 6-5" by Poole and Rodgers (1972, p. 96). The succession here is inverted and the sample is from a level 1 m 40 stratigraphically above the base of Bed 2. On the basis of their finding **Camarocrinus**, Schuchert and Dunbar (1934, p. 104) assigned an Early Devonian age to the Clam Bank Formation; Boucot (1969, p. 477) suggested that it belongs to the Přidoli Series, highest Silurian.

GSC Loc. 94417. Humber Arm Sequence. The sample is from cherty limestone on the north side of the small bay about 300 m south of Black Point, the northern extremity of East Bay and situated 5.5 km north-northeast of Port au Port Village. The horizon is probably in Bed 5 of Schuchert and Dunbar (1934, p. 92), and the locality is "Stop 6-3" of Poole and Rodgers (1972, p. 94). For additional notes see Morris and Kay (1966).

Cow Head Peninsula

The area is situated about 190 km northeast of Port au Port and the stratigraphy has been described by Kindle and Whittington (1958) whose numbered lithostratigraphic units are employed in the following account.

GSC Loc. 94384. Cow Head Group; lowest third of bed 11. The sample is from a calcilutite 1 to 2 m below the conglomerate of bed 12, on the east side of The Ledge and near the base of the cliff.

[1]Institut Royal des Sciences Naturelles de Belgique, rue Vautier, 31, B – 1040 Bruxelles

STRUCTURAL SUBDIVISION	GEOGRAPHIC LOCATION	LITHOSTRATIGRAPHIC SUBDIVISION		AGE	SAMPLES			
					Total Processed	Number Barren	Containing Chitinozoa	Containing Acritarchs
WESTERN PLATFORM	PORT AU PORT PENINSULA 1	Clam Bank Formation		Pridoli (= U.Silurian)	3	2	—	1
		Long Point Group	Winterhouse Formation	Caradoc (& ?U.Ashgill)	2	0	2	2
			Lourdes Limestone	Caradoc	3	3	—	—
		Humber Arm Sequence (in part)		Llanvirn - Llandeilo	2	1	—	1
		Table Head Formation		Arenig - Llanvirn	2	1	1	1
		St. George Formation		Tremadoc - Arenig	4	4	—	—
		Green Point Group		Tremadoc	3	3	—	—
	COW HEAD PENINSULA 3	Cow Head Group		Tremadoc - Llanvirn	11	8	3	0
	TABLE POINT 4	Table Head Formation	Green Bar	Llanvirn	2	2	—	—
			Upper		1	0	1	0
			Middle		5	4	1	0
			Lower		6	5	1	0
	5	St. George Formation		Tremadoc - Arenig	3	3	—	—

Figure 12.2. Geographic and stratigraphic distribution of samples containing chitinozoa and/or acritarchs. Leiospheres and undeterminable chitinozoa and/or acritarchs are not taken into account. Numbers in the Geographic Location column refer to the following:

1. Bergström et al., 1974;
2. Riley, 1962;
3. Units 6-14 of Kindle and Whittington, 1958;
4. Whittington and Kindle, 1963;
5. Schuchert and Dunbar, 1934;
6. Units 2-5 of Horne, 1976;
7. Cobbs Arm Limestone of Bergström et al., 1974;
8. Unnamed argillites of Bergström et al., 1974, p. 1651, fig. 9;
9. Localities along road 352, between 4.2 km and 15.45 km south of southern limit of Cottrells Cove village, Notre Dame Bay. Unit O_2 of Williams, 1967;
10. Hutchinson, 1962, Jenness, 1963, Dean, 1976;
11. Hayes, 1915, Rose, 1952, Dean and Martin, in press;
12. North bank of Salmonier Brook, c. 200 m east of its intersection with the Marystown - St. Lawrence road and 4 km northwest of Burin (see Hutchinson, 1962 for general notes, following unpublished work by T.N. Walthier).

STRUCTURAL SUBDIVISION	GEOGRAPHIC LOCATION	LITHOSTRATIGRAPHIC SUBDIVISION	AGE	SAMPLES			
				Total Processed	Number Barren	Containing Chitinozoa	Containing Acritarchs
CENTRAL MOBILE BELT	New World Island 6	Summerford Group	Tremadoc - Llandeilo	7	7	—	—
	7	Hillgrade Group	Llandeilo	2	2	—	—
	Gander Bay area 8	Unnamed	?Caradoc	1	1	—	—
	Notre Dame Bay area 9	Unnamed	Ordovician (s.l.)	7	7	—	—
AVALON PLATFORM	Random Island area 10	Clarenville Formation	Tremadoc	8	2	0	6
		Elliott Cove Formation	Upper Cambrian	15	0	0	15
		Manuels River Formation	late Middle Cambrian	5	3	0	2
	Bell Island 11	Wabana Group (in part)	Arenig	5	0	0	5
		Bell Island Group (in part)	Tremadoc	7	0	0	7
	Burin Peninsula 12	Manuels River Formation	late Middle Cambrian	1	1	—	—

Figure 12.2 (cont'd)

GSC Loc. 94386. Cow Head Group; top of bed 9 and 1 m below the conglomerate of bed 10 on the west side of The Ledge. The rock is dark shale containing numerous, well-preserved graptolites.

GSC Loc. 94387. Cow Head Group; shale in basal portion of bed 9; west side of The Head.

Table Point Area

Table Point, also known as Table Head, is a headland situated about 50 km north-northeast of Cow Head. The section was described by Schuchert and Dunbar (1934, p. 58, 63) and redescribed by Whittington and Kindle (1963, particularly Fig. 1), whose terminology is followed here.

GSC Loc. 94400. Top part of lower Table Head Formation. The sample is from a massive, nodular limestone in the highest portion of bed 8, the top of which forms Table Point itself.

GSC Loc. 94403. Middle Table Head Formation; dark shales 41 m above the contact with the lower Table Head Formation. South side of Table Point.

GSC Loc. 94408. Upper Table Head Formation. Dark shales in the gully on the shore at the north end of the "Beach Gravels" shown by Whittington and Kindle (1963). The locality is not accessible at high tide.

Discussion

Many samples from the Green Point Formation, Table Head Formation and Cow Head Group contain abundant larvae and fragments of Graptolithina as well as leiospheres (Pl. 12.1, fig. 5).

Shales of the Green Point Formation which outcrop in the foot of the cliff at Tea Cove, on the southeast side of the southwestern end of Long Point and 2.5 km east of Lourdes (see Riley, 1962, p. 16 for details of section), contain only dispersed leiospheres and larvae of dendroid graptolites. The large number and good preservation of these suggest that the absence of chitinozoa and non-leiospherid acritarchs is a primary feature.

Sampling was carried out in the St. George Formation at two sections: (1) southeast and southwest of The Gravels, close to Port au Port (respectively from Beds 27 and 7 of Schuchert and Dunbar, 1934, p. 47); and (2) the shore section immediately north of Table Point (Beds 21 and possibly 16 of Schuchert and Dunbar, 1934, p. 58). These samples were barren of palynomorphs.

In the Cow Head Group at Cow Head Peninsula, beds 9 and 11 of Kindle and Whittington (1958), attributed by them to the Arenig Series on the basis of graptolite evidence, yielded fairly numerous chitinozoa. GSC Loc. 94387, in the basal part of bed 9, from which **Tetragraptus approximatus** (Nicholson) is recorded, contains **Conochitina chydea** Jenkins, 1967 and numerous **Rhabdochitina usitata** Jenkins 1967. The uppermost part of bed 9 (GSC Loc. 94386), stated to contain **Tetragraptus quadribrachiatus** (Hall), yielded **R. usitata** and, moreover, numerous **Amphorachitina** sp. **R. usitata** is present to the exclusion of all other taxa in the lowest third of bed 11 (GSC Loc. 94384), from which **Tetragraptus fruticosus** (Hall) is recorded.

Conochitina chydea and **Rhabdochitina usitata** are known to range from the Llanvirn to the Caradoc Series in Shropshire (Jenkins, 1967) and are recorded from the Table Head Formation of Port au Port Peninsula and at the section between Three Rock Point and Cape Cormorant, southwest of Lourdes (Neville, 1974). The genus **Amphorachitina** Poumot, 1968 is found in the Tremadoc and lower Arenig Series of the Algerian – Tunisian Sahara.

The Table Head Formation at its type locality Table Point, where it has been correlated with the lower Llanvirn Series on the bases of graptolites and trilobites (Whittington and Kindle, 1963) and conodonts (Fåhraeus, 1970), contains some blackish chitinozoa, usually incomplete and showing lines of fracture (GSC Locs. 94400, 94403, 94408). They are assigned to **Lagenochitina** cf. **L. baltica** Eisenack, 1931, **Desmochitina** cf. **D. lata** Schallreuter, 1963 sensu Neville,

LITHOSTRATIGRAPHIC SUBDIVISION		GSC LOCALITY	CHITINOZOA									ACRITARCHS							
			Rhabdochitina usitata	Amphorachitina sp.	Desmochitina cf. D. lata	Conochitina chydea	Lagenochitina cf. L. baltica	Rhabdochitina turgida	Hercochitina aff. H. downiei	Kalochitina multispinata	Ancyrochitina alaticornis	Peteinosphaeridium micranthum	Peteinosph. cf. P. nanofurcatum	Goniosphaeridium polygonale	Actipilion aff. A. druggii	Peteinosphaeridium breviradiatum	Multiplicisphaeridium bifurcatum	Micrhystridium stellatum	Onondagaella sp.
CLAM BANK FM.		94409	—	—	—	—	—	—	—	—	—	—	—	—	—	—	—	2	1
WINTERHOUSE FM.		92983	—	—	—	—	—	—	26	5	2	—	—	8	1	6	11	—	—
		94410	—	—	—	—	—	—	38	3	1	—	—	7	—	4	5	—	—
HUMBER ARM SEQUENCE		94417	—	—	—	—	—	—	—	—	—	7	2	—	—	—	—	—	—
TABLE HEAD FM.	upper	94408	—	—	2	8	—	—	—	—	—	—	—	—	—	—	—	—	—
	middle	92987	—	—	6	5	1	1	—	—	—	—	—	—	—	—	—	—	—
		94403	—	—	—	—	2	—	—	—	—	—	—	—	—	—	—	—	—
	lower	94400	—	—	3	2	—	—	—	—	—	—	—	—	—	—	—	—	—
COW HEAD GROUP	unit 11	94384	27	—	—	—	—	—	—	—	—	—	—	—	—	—	—	—	—
	unit 9	94386	4	31	—	—	—	—	—	—	—	—	—	—	—	—	—	—	—
		94387	>200	—	—	2	—	—	—	—	—	—	—	—	—	—	—	—	—

Figure 12.3. Distribution chart for chitinozoa and acritarchs in the Western Platform, showing number of specimens per sample.

1974 and **Conochitina chydea.** These taxa, as well as **Rhabdochitina turgida** Jenkins, 1967, are better preserved in the middle Table Head Formation which outcrops to the north of Port au Port (GSC Loc. 92987) and is dated as early Llanvirn (Whittington, 1965, p. 268; 1968). The chitinozoa recorded above are among those described by Neville (1974) from the Table Head Formation exposed on the northwest coast of Port au Port Peninsula and they give no additional precision to the stratigraphic data already known for these outcrops. In West Shropshire **C. turgida** is known from the Llanvirn and Llandeilo Series (Jenkins, 1967).

In the strongly faulted rocks on the east side of East Bay, one sample (GSC Loc. 94417) from the Humber Arm sequence provided some acritarchs; all are referred to **Peteinosphaeridium micranthum** (Eisenack, 1959) and P. cf. **P. nanofurcatum** Kjellström, 1971.

The holotypes of both these species came from the Ordovician of the Baltic region; the first is from the "Unterer Glaukonitkalk B_2", the age of which is stated to be Arenig, and the second is from the Viru "Series", which has been correlated with the Zone of **Glyptograptus teretiusculus** (now equated with the lower Llandeilo Series).

At the west end of Clam Bank Cove, Port au Port Peninsula, the upper part of the Winterhouse Formation (Unit G, Area 3 of Fåhraeus, 1973, p. 1829), which lies stratigraphically below a reddish, palynologically barren series of conglomerates (the succession here is inverted), contains chitinozoa and acritarchs, both of which are relatively well preserved and translucent. More than 213 m (700 ft) below this horizon Riva (in Bergström et al., 1974, p. 1631) recorded **Climacograptus** cf. **C. manitoulinensis** Caley, 1936, on the basis of which he suggested this portion of the Winterhouse Formation to be of Cincinnatian age (i.e., highest Caradoc to Ashgill in terms of the British standard succession). A recent account (Dean, in press) of the stratigraphy and trilobites of the Long Point Group suggests that the Winterhouse Formation may be no younger than Barneveld in age, and that a large stratigraphic break separates the rocks from those of the overlying Clam Bank Formation. The two palynologically productive levels (GSC Loc. 92983 and 94410), which according to Bergström et al. (1974, fig. 7) would thus be of an age equivalent to the **Pleurograptus linearis** Zone or **Dicellograptus complanatus** Zone, contain similar chitinozoa. The assemblage, different from that known from the **D. complanatus** Zone of Anticosti Island (Achab, 1977), indicates a Caradoc rather than an Ashgill age. It contains the following, listed in order of decreasing frequency: **Hercochitina** aff. **H. downiei** Jenkins, 1967, **Kalochitina multispinata** Jansonius, 1964 and **Ancyrochitina alaticornis** Jenkins, 1967. Elsewhere **H. downiei** is known only from the Onnian Stage, higher Caradoc Series, of South Shropshire (Jenkins, 1967). **Kalochitina multispinata** is described from the Meaford and Dundas formations of Late Ordovician age, in Ontario (Jansonius, 1964) and is abundant in some levels of the Viola Limestone and Sylvan Shale of Oklahoma (Jenkins, 1969; 1970), strata assigned, respectively, to the Caradoc and Ashgill Series; its frequency is variable in the Trenton and Utica groups in the central part of the St. Lawrence Platform (author's unpublished data). In South Shropshire **Ancyrochitina alaticornis** occurs abundantly from the Longvillian Stage to the Actonian Stage of the Caradoc Series (Jenkins, 1967). One damaged specimen has been recorded from the Table Head Formation of the Port au Port Peninsula (Neville, 1974) and the species may be locally abundant in the Trenton Group around Montreal (author's unpublished data). The acritarchs from the upper part of the Winterhouse Formation do not permit a precise age assessment. **Multiplicisphaeridium bifurcatum** Staplin et al., 1965 is known from the Middle Ordovician of Anticosti Island (Trenton Group, Staplin et al., 1965, p. 182) and Gotland (Viruan "Series", Kjellström, 1971), as well as from the Caradoc and ?Ashgill Series of Belgium (Martin, 1974). **Goniosphaeridium polygonale** (Eisenack) Eisenack, 1969 and **Peteinosphaeridium breviradiatum** (Eisenack) Kjellström, 1971 are long ranging species in the Ordovician and Silurian of Europe (Martin, 1974). In addition **P. breviradiatum** is found in the Chazy, Trenton and Utica groups of the central St. Lawrence Platform (author's unpublished data). Only one specimen of **Actipilion** aff. **A. druggii** Loeblich, 1970 was found in the Winterhouse Formation; the types of this species were described from the Sylvan Shale of Oklahoma.

According to Boucot (1969, p. 477) the Clam Bank Formation probably represents the Přidoli Series, the topmost subdivision of the Silurian, a conclusion based upon brachiopod evidence. The lower part of the formation at Clam Bank Cove (GSC Loc. 94409) contains spores, the alga **Tasmanites** and very rare acritarchs. Among the last named, **Micrhystridium stellatum** Deflandre, 1945 is particularly long ranging and has been reported from Ordovician to early Mesozoic sediments (Martin, 1969; Lister, 1970). The genus **Onondagaella** Cramer, 1966 is recorded from upper Silurian and Lower Devonian rocks (Playford, 1977).

Central Volcanic Mobile Belt

The samples, all of Ordovician age, from this region were obtained from localities at New World Island, Gander Bay and Notre Dame Bay (for list of localities see Fig. 12.2). None yielded determinable Chitinozoa or Acritarcha.

Avalon Platform

This region has yielded the most productive samples. At Bell Island, Conception Bay (Fig. 12.1) three successive acritarch assemblages, of Tremadoc to Arenig age, were found in the upper part of the Bell Island Group and the exposed portion of the Wabana Group as interpreted by Rose (1952; Dean and Martin, in press). The two latter groups contain few macrofossils with the exception of inarticulate brachiopods, which may be locally abundant; the youngest outcrops of the Wabana Group contain rare graptolites and trilobites indicating an Early Arenig age.

At Random Island, Trinity Bay (Fig. 12.1) progressive changes in the composition of acritarch assemblages permit the recognition of six microfloras (Martin, in prep.) in the Manuels River, Elliott Cove and Clarenville formations. The latter have been attributed respectively to the Middle Cambrian, Upper Cambrian and Lower Tremadoc Series, principally upon the evidence of the trilobites (Hutchinson, 1962; Jenness, 1963; Dean, 1976), though the precise location of the Cambro-Ordovician boundary is not yet known. The numerous acritarch taxa from the Avalon Platform show affinities with those from Shropshire, Bohemia, Belgium and southwestern France.

Palynological Notes

CHITINOZOA

Genus **Amphorachitina** Poumot, 1968

Amphorachitina sp.

Plate 12.1, figure 23

Figured specimen. GSC No. 56684.

Remarks. The specimens vary in length from 450 to 600 µm. They differ from **Amphorachitina conifundus** Poumot, 1968 in having a more distinct oral tube. The ogival shape of the oboral pole distinguishes the genus from **Lagenochitina** Eisenack, 1931.

Plate 12.1

Figures 1, 2, 4, 9, 15, 18. **Rhabdochitina usitata** Jenkins, 1967. Fig. 1: GSC 56661, GSC Loc. 94384, x 110. Figs. 2, 4, 9, 15, 18: GSC Loc. 94387, x 100. Fig. 2: GSC 56662. Fig. 4: GSC 56663. Fig. 9: GSC 56664. Fig. 15: GSC 56665. Fig. 18: GSC 56666.

Figure 3. **Actipilion** aff. **A. druggii** Loeblich, 1970. GSC 56667, GSC Loc. 92983, x 500.

Figure 5. Graptoloid sicula and leiosphere; there is no evidence of biological connection between the two. GSC 56668, GSC Loc. 92987, x 100.

Figures 6, 8. **Desmochitina** cf. **D. lata** sensu Neville, 1974. Fig. 6: GSC 56669, GSC Loc. 94400, x 200. Fig. 8: GSC 56670, GSC Loc. 92987, x 200.

Figures 7, 17, 24. **Hercochitina** aff. **H. downiei** Jenkins, 1967. Fig. 7: aboral part, GSC 56671, GSC Loc. 92983, x 1100. Fig. 17: GSC 56672, GSC Loc. 92983, x 200. Fig. 24: GSC 56673, GSC Loc. 94410, x 200.

Figure 10. **Rhabdochitina turgida** Jenkins, 1967. GSC 56674, GSC Loc. 92987, x 100.

Figure 11. **Ancyrochitina alaticornis** Jenkins, 1967. GSC 56675, GSC Loc. 94410, x 200.

Figure 12. **Goniosphaeridium polygonale** (Eisenack, 1931). GSC 56676, GSC Loc. 92983, x 200.

Figures 13, 19, 21. **Kalochitina multispinata** Jansonius, 1964. GSC Loc. 94410. Fig. 13: GSC 56677, x 200. Fig. 19: GSC 56678, x 200. Fig. 21: detail of the ornamentation, GSC 56679, x 2800.

Figure 14. **Conochitina chydea** Jenkins, 1967. GSC 56680, GSC Loc. 94408, x 200.

Figure 16. **Peteinosphaeridium** cf. **P. nanofurcatum** Kjellström, 1971. GSC 56681, GSC Loc. 94417, x 500.

Figure 20. **Peteinosphaeridium micranthum** (Eisenack, 1959). GSC 56682, GSC Loc. 94417, x 500.

Figure 22. **Lagenochitina** cf. **L. baltica** Eisenack, 1931. GSC 56683, GSC Loc. 94403, x 100.

Figure 23. **Amphorachitina** sp. GSC 56684, GSC Loc. 94386, x 50.

Figure 25. **Peteinosphaeridium breviradiatum** (Eisenack, 1959). GSC 56685, GSC Loc. 94410, x 500.


1

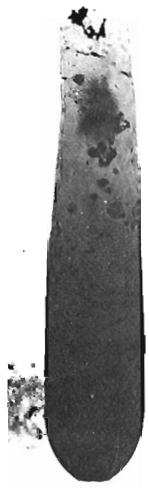
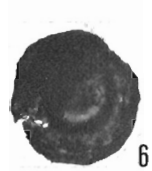
6


10


9

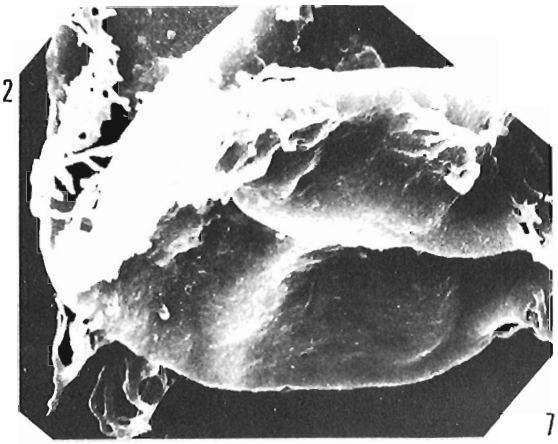
2
7

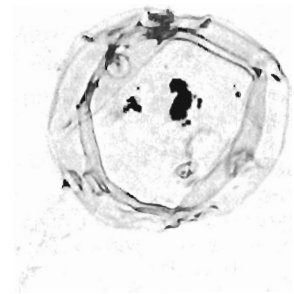
3


11


12


13

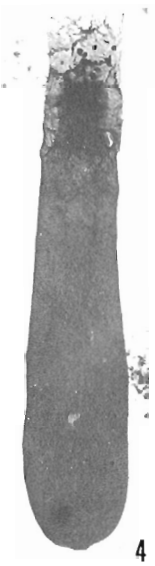
4

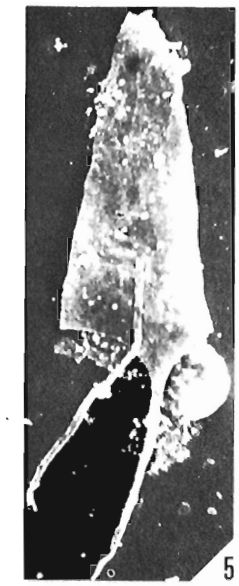
5


8


14


15

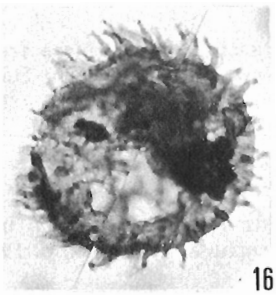
16


17


18


19

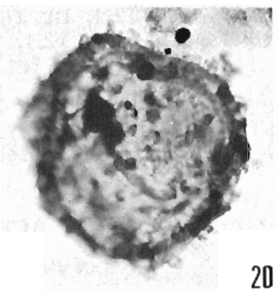
20

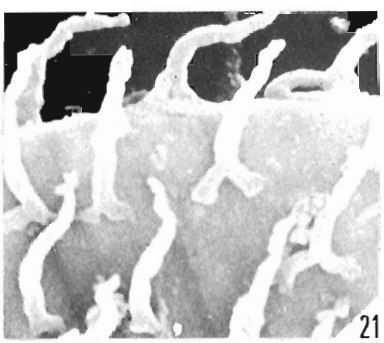
21


22


23


24

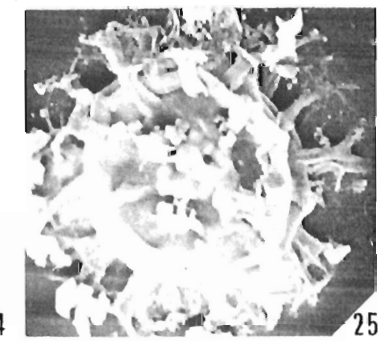
25

Genus **Hercochitina** Jenkins, 1967

Hercochitina aff. **H. downiei** Jenkins, 1967

Plate 12.1, figures 7, 17, 24

Figured specimens. GSC No. 56671 (Pl. 12.1, fig. 7), GSC No. 56672 (Pl. 12.1, fig. 17), GSC No. 56673 (Pl. 12.1, fig. 24).

Remarks. Length of the test varies from 130 to 225 µm; that of the somewhat compressed and often broken ornamentation is up to 22 µm. The processes are arranged in from about 10 to 15 longitudinal rows, and their distal extremities are interconnected on the same row, free from those laterally adjacent to them; they do not form a reticulum as in **Acanthochitina rashidi** Jenkins, 1970. Although the dimensions and proportions of the test and the number of longitudinal rows of processes agree with the diagnosis of **Hercochitina downiei**, the specific attribution is considered dubious because of the Newfoundland material's less developed ornamentation, which attains a length of up to 59 µm in the Shropshire specimens.

The oral tube is more distinct and cylindrical than in both **Acanthochitina rashidi** and **Kalochitina multispinata** Jansonius, 1964. The specimen of **K. multispinata** figured by Jenkins (1970, text-fig. 6d) shows an extreme example of variation of the ornamentation which is very far from that of typical representatives. The longitudinal disposition of the ornamentation recalls that of **Hercochitina** aff. **H. downiei** but the rows are closer together and the spines shorter. **Hercochitina crickmayi** Jansonius, 1964 is larger and bears more numerous longitudinal rows of processes.

Genus **Rhabdochitina** Eisenack 1931

Rhabdochitina usitata Jenkins, 1967

Plate 12.1, figures 1, 2, 4, 9, 15, 18

1967 **Rhabdochitina usitata** Jenkins, p. 468, Pl. 74, figs. 13-15, 20; Pl. 75, fig. 1.

1974 **Rhabdochitina usitata** Jenkins, Neville, p. 202, Pl. 7, figs. 12, 13, 16-18.

Figured specimens. GSC No. 56661 (Pl. 12.1, fig. 1), GSC No. 56662 (Pl. 12.1, fig. 2), GSC No. 56663 (Pl. 12.1, fig. 4), GSC No. 56664 (Pl. 12.1, fig. 9), GSC No. 56665 (Pl. 12.1, fig. 15), GSC No. 56666 (Pl. 12.1, fig. 18).

Remarks. Size variation is continuous and a little more important than previously described. Total length = 270 to 760 µm. Mucro rarely observed; wall always smooth.

ACRITARCHA

Genus **Actipilion** Loeblich, 1970

Actipilion aff. **A. druggii** Loeblich, 1970

Plate 12.1, figure 3

Figured specimen. GSC No. 56667.

Remarks. A single specimen from the Winterhouse Formation lacks the wall ornamentation of the type species, which comes from the Sylvan Shale of Oklahoma. The characteristics of the proximal part of the processes also permit the following Ordovician species from the Baltic region to be assigned to **Actipilion: A. (Baltisphaeridium) latiradiatus** (Eisenack, 1959, p. 195) n. comb. and **A. (Baltisphaeridium) constrictus** (Kjellström, 1971, p. 22) n. comb.

Genus **Goniosphaeridium** Eisenack, 1969

Goniosphaeridium polygonale (Eisenack, 1931)

Plate 12.1, figure 12

1931 **Ovum hispidum polygonale** Eisenack, p. 113, Pl. 4, figs. 16-20; Pl. 5, fig. 18.

1969 **Goniosphaeridium polygonale** (Eisenack, 1931), Eisenack, p. 257.

Figured specimen. GSC No. 56676.

Remarks. All the specimens have numerous processes, the distal ends of which are filled with an undetermined opaque substance, as shown by Eisenack (1963, Pl. 19, fig. 2).

References

Achab, A.
1977: Les chitinozoaires de la zone à **Dicellograptus complanatus**, Formation de Vauréal, Ordovicien supérieur, Ile d'Anticosti, Québec; Can. J. Earth Sci., v. 14, p. 413-425.

Bergström, S.M., Riva, J., and Kay, M.
1974: Significance of conodonts, graptolites and shelly faunas from the Ordovician of Western and North-Central Newfoundland; Can. J. Earth Sci., v. 11, p. 1625-1660.

Boucot, A.J.
1969: Silurian-Devonian of Northern Appalachians — Newfoundland; in Kay, M. (ed.), North Atlantic — Geology and Continental Drift. Am. Assoc. Pet. Geol., Mem. 12, p. 477-483.

Dean, W.T.
1976: Some aspects of Ordovician correlation and trilobites distribution in the Canadian Appalachians; p. 227-250 in Bassett, M.G. (ed.), The Ordovician System; Univ. of Wales Press and National Museum of Wales, Cardiff.

The correlation and trilobites of the Long Point Group (Ordovician), Port au Port Peninsula, southwestern Newfoundland. Geol. Surv. Can., Bull. (in press)

Dean, W.T. and Martin, F.
Lower Ordovician acritarchs and trilobites from Bell Island, eastern Newfoundland; Geol. Surv. Can., Bull. (in press).

Eisenack, A.
1931: Neue Mikrofossilien des baltischen Silurs. I.; Palaeont. Z., v. 13, p. 74-118.

1959: Neotypen Baltischer Silur-Hystrichosphaeren und neue Arten; Palaeontographica, v. 112, A, p. 193-211.

1963: Mitteilungen zur Biologie des Hystrichosphären und über neue Arten; N. Jb. Geol. Paläont. Abh., v. 118 p. 207-216.

1963: Zur Systematik einiger paläozoischer Hystrichosphären (Acritarcha) des baltischen Gebietes; N. Jb. Geol. Paläont. Abh., v. 133, p. 245-266.

Fåhraeus, L.E.
1970: Conodont-based correlations of Lower and Middle Ordovician strata in western Newfoundland; Geol. Soc. Am., Bull., v. 81, p. 2061-2076.

1973: Depositional environments and conodont-based correlation of the Long Point Formation (Middle Ordovician), western Newfoundland; Can. J. Earth Sci., v. 12, p. 1822-1833.

Hayes, A.O.
1915: Wabana Iron Ore of Newfoundland; Can. Geol. Surv., Mem. 78,

Horne, G.S.
1976: Geology of Lower Ordovician fossiliferous strata between Virgin Arm and Squid Cove, New World Island, Newfoundland; Geol. Surv. Can., Bull. 261.

Hutchinson, R.D.
1962: Cambrian stratigraphy and trilobites faunas of Southeastern Newfoundland; Geol. Surv. Can., Bull. 88.

Jansonius, J.
1964: Morphology and classification of some Chitinozoa; Bull. Can. Pet. Geol., v. 12, p. 901-918.

Jenkins, W.A.M.
1967: Ordovician Chitinozoa from Shropshire; Palaeontology, v. 10, p. 436-488.

1969: Chitinozoa from the Ordovician Viola and Fernvale Limestones of the Arbuckle Mountains, Oklahoma; Spec. Pap. Palaeontol., no. 5, p. 1-44.

1970: Chitinozoa from the Ordovician Sylvan Shale of the Arbuckle Mountains, Oklahoma; Palaeontology, v. 13, p. 261-288.

Jenness, S.E.
1963: Terra Nova and Bonavista map-areas, Newfoundland (2D, E1/2 and 2C); Geol. Surv. Can., Mem. 327.

Kay, M.
1967: Field Trip Guide -- Stephenville -- Port au Port Peninsula; Gander Conference, Columbia University, Field Trips, August-September, 1967.

Kindle, C.H. and Whittington, H.B.
1958: Stratigraphy of the Cow Head region, Western Newfoundland; Geol. Soc. Am., Bull., v. 69, p. 315-342.

Kjellström, G.
1971: Ordovician microplankton (baltisphaerids) from the Grötlingbo Borehole No. 1 in Gotland, Sweden; Sver. Geol. Unders., Ser. C, No. 655, p. 1-75.

Loeblich, A.R., Jr.
1970: Morphology, ultrastructure and distribution of Paleozoic acritarchs; North Am. Paleontol. Convention, Chicago, 1969, Proc. G, p. 705-788.

Lister, T.R.
1970: The acritarchs and chitinozoza from the Wenlock and Ludlow Series of the Ludlow and Millichope areas, Shropshire -- Part 1; Palaeontogr. Soc. [Monogr.], v. 124, p. 1-100.

Martin, F.
1969: Les Acritarches de l'Ordovicien et du Silurien belges. Détermination et Valeur stratigraphique; Mém. Inst. r. Sci. nat. Belg., No. 160 (dated 1968), p. 1-175.

1974: Ordovician supérieur et Silurien inférieur à Deerlijk (Belgique) -- Palynofacies et Microfacies; Mém. Inst. r. Sci. n. Belg., No. 174 (dated 1973), p. 1-71.

Morris, R.W. and Kay, M.
1966: Ordovician graptolites from the Middle Table Head Formation at Black Cove, Port au Port, Newfoundland; J. Paleontol., v. 40, p. 1223-1229,

Neville, R.S.W.
1974: Ordovician Chitinozoa from western Newfoundland; Rev. Palaeobot. Palynol., v. 18, p. 187-222.

Playford, G.
1977: Lower to Middle Devonian acritarchs of the Moose River Basin, Ontario; Geol. Surv. Can., Bull. 279.

Poole, W.H. and Rodgers, J.
1972: Appalachian geotectonic elements of the Atlantic Provinces and Southern Quebec; 24th Int. Geol. Congr., Field Exc. A63-C63.

Poumot, C.
1968: **Amphorachitina, Ollachitina, Velatachitina;** trois nouveaux genres de chitinozoaires de l'Erg oriental (Algérie-Tunisie); Bull. Centre Rech. Pau-SNPA, v. 2, p. 45-55.

Riley, G.C.
1962: Stephenville map-area, Newfoundland; Geol. Surv. Can., Mem. 323.

Rodgers, J.
1965: Long Point and Clam Bank Formations, Western Newfoundland; Proc. Geol. Assoc. Can., v. 16, p. 83-94.

Rose, E.R.
1952: Torbay map-area, Newfoundland; Geol. Surv. Can., Mem. 265.

Schuchert, C. and Dunbar, C.O.
1934: Stratigraphy of Western Newfoundland; Geol. Soc. Am., Mem. 1.

Staplin, F.L., Jansonius, J., and Pocock, S.A.J.
1965: Evaluation of some acritarchous hystrichosphere genera; N. Jb. Geol. Paläont. Abh., v. 123, p. 167-201.

Whittington, H.B.
1965: Trilobites of the Ordovician Table Head Formation, western Newfoundland; Harv. Univ. Mus. Comp. Zool., Bull., v. 132, p. 275-442.

1968: Zonation and correlation of Canadian and Early Mohawkian Series; in Zen, E-an et al. Ed., Studies of Appalachian Geology: Northern and Maritime, p. 49-60.

Whittington, H.B. and Kindle, C.H.
1963: Middle Ordovician Table Head Formation, Western Newfoundland; Geol. Soc. Am., Bull., v. 74, p. 745-758.

Williams, H.
1964: The Appalachians in northeastern Newfoundland -- a two-sided symmetrical system; Am. J. Sci., v. 262, p. 1137-1158.

1967: Island of Newfoundland; Geol. Surv. Can., Map 1231A, scale: 1:1 000 000.

13. COMPUTER PROCESSING OF GAMMA-RAY LOGS: ITERATION AND INVERSE FILTERING

Project 740085

John G. Conaway and P.G. Killeen
Resource Geophysics and Geochemistry Division

Abstract

Conaway, John G., and Killeen, P.G., Computer processing of gamma-ray logs: Iteration and inverse filtering; in Current Research, Part B, Geol. Surv. Can., Paper 78-1B, p. 83-88, 1978.

For nearly two decades an iterative computer technique has been used for processing gamma-ray logs to determine the distribution of uranium along a borehole. Recently an inverse filter technique has been developed for the same application. Analysis of the iterative technique shows that it approaches theoretical equivalence with the inverse filter technique as the number of iterations increases. In tests with gamma-ray borehole logs with a sampling interval of 10 cm there was little difference in the results produced by the two methods. In practice a sampling interval shorter than 10 cm should be used to improve resolution and reduce aliasing errors. In this case a smoothing filter is required with both techniques to reduce the high-frequency noise.

The inverse filter technique generally requires less than 5 per cent as much computing time as iteration, and may be accomplished using an 'open-ended' algorithm, thereby making possible on-line processing of the data using a minicomputer or microprocessor, concurrent with the logging of the borehole.

Introduction

An iterative computer technique for determining radioelement concentrations from gamma-ray borehole logs has been in routine use in the United States since it was first introduced by Scott et al. (1961), and Scott (1962; 1963). Recently an inverse filter technique has been presented by Conaway and Killeen (in press) which is intended for the same purpose – determining radioelement concentrations from gamma-ray logs. A number of questions regarding the two techniques immediately present themselves: Are the results from the two methods equivalent? Which is more efficient? What are the advantages and disadvantages of each? The answers to these questions can be obtained from theoretical considerations, computer studies, and tests with gamma-ray borehole logs.

First a brief review of the theory is necessary. Consider the case of an infinitesimally thin radioactive ore zone embedded in a thick sequence of barren rock (Fig. 13.1a). The function expressing the distribution of radioactive material with depth is an impulse or 'spike' (Fig. 13.1b) having a flat amplitude spectrum (Fig. 13.2, curve a). This is the desired output of a gamma-ray logging system in the presence of a thin ore zone – a spike proportional in height to the ore grade. The actual output which would be obtained under noise-free conditions using a point-detector would resemble Figure 13.1c. This curve, called the geologic impulse response or GIR (Conaway and Killeen, in press), has an amplitude spectrum similar to Figure 13.2, curve b.

The purpose of computer processing of the raw data is to convert the geologic impulse response (Fig. 13.1c) into the spike (Fig. 13.1b) within the limitations imposed by noise. In other words, in the ideal case the data are processed to make the amplitude spectrum of the GIR (Fig. 13.2b) flat, as shown in Figure 13.2a.

Inverse Filtering

Representing the geologic impulse response function (Fig. 13.1c) by the symbol s(z), the relationship between the noise-free gamma-ray log c(z), and the distribution of radioactive material along a borehole, g(z), is given by

$$c(z) = g(z) * s(z) \quad \ldots\ldots\ldots\ldots\ldots\ldots\ldots\ldots (1)$$

where the symbol * denotes convolution (see e.g. Kanasewich, 1973, for a discussion of convolution). In the frequency domain this is expressed as

$$C(\omega) = G(\omega) \cdot S(\omega) \quad \ldots\ldots\ldots\ldots\ldots\ldots\ldots\ldots (2)$$

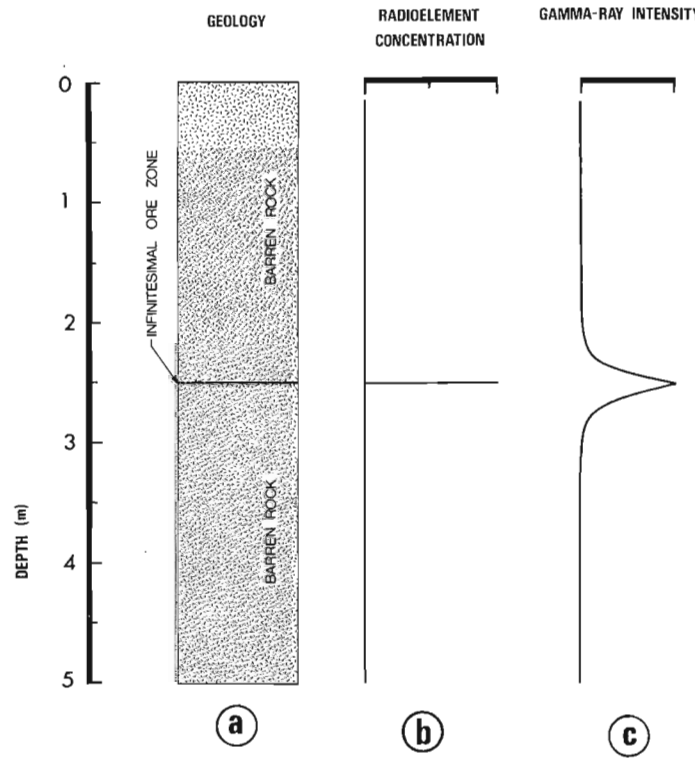

Figure 13.1

(a) Geologic column showing an infinitesimally thin radioactive ore zone sandwiched between two thick barren zones, a 'geologic impulse' of radioactive ore.

(b) Plot of radioelement concentration with depth corresponding to Figure 13.1a.

(c) Noise-free response of a point-detector to the thin ore zone, the 'geologic impulse response'.

where $C(\omega)$, $G(\omega)$ and $S(\omega)$ are the Fourier transforms of f(z), g(z), and s(z), respectively. Thus in the frequency domain the distribution of radioactive material is given by

$$G(\omega) = C(\omega) \cdot \left(\frac{1}{S(\omega)}\right) \quad \ldots\ldots\ldots\ldots\ldots\ldots\ldots\ldots (3)$$

Letting

$$F(\omega) = \frac{1}{S(\omega)}$$

then in the space domain

$$g(z) = c(z) * f(z) \quad \ldots\ldots\ldots\ldots\ldots\ldots\ldots\ldots (4)$$

where the inverse filter f(z) is the Fourier transform of $F(\omega)$.

In the special case of the infinitesimally thin ore zone (Fig. 13.1)

$$C(\omega) = S(\omega)$$

Therefore, from equation (3)

$$G(\omega) = S(\omega) \cdot \left(\frac{1}{S(\omega)}\right) = 1$$

In theory, then, the flat spectrum of the impulse has been recovered by inverse filtering, in the absence of noise.

The Iterative Algorithm

The heart of the computer program given by Scott (1962), as well as of the modern counterpart of that program, is an iterative algorithm which, in its simplest form, is shown in the flow chart given in Figure 13.3. The step enclosed in the dashed box, that of setting negative grade values equal to zero will be ignored for the present. Letting the contribution of the i^{th} step in the iteration to the value of g(z) be given by $b_i(z)$, from the flow chart we have:

initial state	$b_o(z) = c(z)$
contribution of first iteration	$b_1(z) = c(z) - c(z)*s(z)$
contribution of second iteration	$b_2(z) = c(z) - 2c(z)*s(z) + c(z)*s(z)*s(z)$
contribution of third iteration	$b_3(z) = c(z) - 3c(z)*s(z) + 3c(z)*s(z)*s(z) - c(z)*s(z)*s(z)*s(z)$

Expressing this in the frequency domain, where the contribution of the i^{th} step in the iteration is $B_i(\omega)$,

$$B_o(\omega) = C(\omega)$$

$$B_1(\omega) = C(\omega) - C(\omega)\, S(\omega)$$

$$B_2(\omega) = C(\omega) - 2C(\omega)\, S(\omega) + C(\omega)\, S^2(\omega)$$

$$B_3(\omega) = C(\omega) - 3C(\omega)\, S(\omega) + 3C(\omega)\, S^2(\omega) - C(\omega)\, S^3(\omega)$$

In general terms, then

$$B_i(\omega) = C(\omega)\ [1 - S(\omega)]^{\,i} \qquad \text{where } i = 0,1,2,\ldots, n$$

Thus, in the frequency domain the processed log after n iterations, $G_n(\omega)$, is given by

$$G_n(\omega) = \sum_{i=0}^{n} B_i(\omega) = \sum_{i=0}^{n} C(\omega)\ [1 - S(\omega)]^{\,i}$$

or

$$G_n(\omega) = C(\omega) \sum_{i=0}^{n} [1 - S(\omega)]^{\,i} \quad \ldots\ldots\ldots\ldots\ldots\ldots (5)$$

It can be shown that the series

$$\sum_{i=0}^{n} [1 - S(\omega)]^{\,i}$$

converges to $1/S(\omega)$ as n becomes large, for all values of $S(\omega)$ such that

$$0 \leq | 1 - S(\omega) | < 1 \quad \ldots\ldots\ldots\ldots\ldots\ldots\ldots\ldots (6)$$

(see e.g. Sokolnikoff and Sokolnikoff, 1941). As can be seen from Figure 13.2b, the condition given by equation (6) will be valid. Thus, after many iterations the value of $G_n(\omega)$ approaches

$$G_n(\omega) = C(\omega) \cdot \left(\frac{1}{S(\omega)}\right) \quad \ldots\ldots\ldots\ldots\ldots\ldots\ldots\ldots (7)$$

which is identical to equation (3). Thus it has been shown that the inverse filter technique and the iterative technique for processing gamma-ray logs are theoretically equivalent operations.

Referring once again to the flow chart for the iterative algorithm (Fig. 13.3) consider the step shown in the dashed box, that of setting negative ore grade values equal to zero. As will be shown more fully later, the iteration process amplifies high frequencies while exerting relatively little effect on low frequencies. Thus, the scatter in the iterated ore grade values is greater than the scatter in gamma-ray counts. This means that some of the processed ore grade values may be negative; however, the mean grade over a given zone will be correct. The act of setting negative grade values equal to zero introduces statistical bias, causing the mean calculated grade over the zone to be erroneously high. In general this is a small effect, but since this step in the processing of the log is unnecessary and invalid, it should be eliminated.

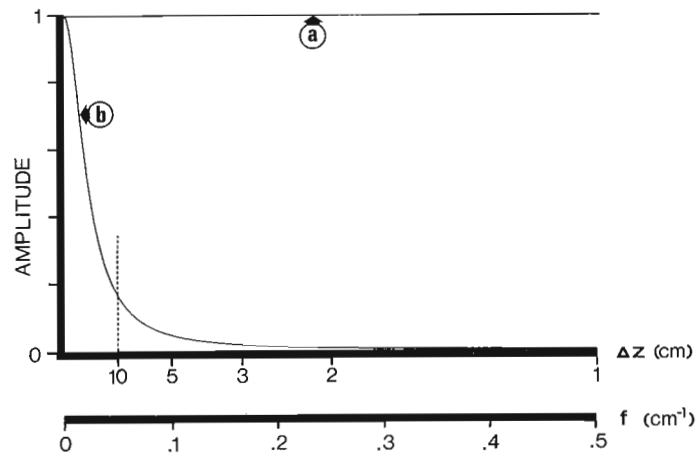

Figure 13.2

(a) Amplitude spectrum of a spike (Fig. 13.1b).

(b) Amplitude spectrum of the noise-free geologic impulse response (Fig. 13.1c). Two horizontal axes are shown for convenience. The lower one, spatial frequency (f), is given by $f = \omega/2\pi$. The upper scale is calibrated in sampling interval (Δz), to make it easy to study the amplitude spectra in relation to the Nyquist frequency f_N for various sampling intervals, where $f_N = 1/2\Delta z$. The amplitude spectrum is a plot of amplitude as a function of spatial frequency (f); the upper horizontal axis, Δz, is provided for reference only. Note especially the significant amount of energy at frequencies higher than the Nyquist frequency for $\Delta z = 10$ cm (dashed line).

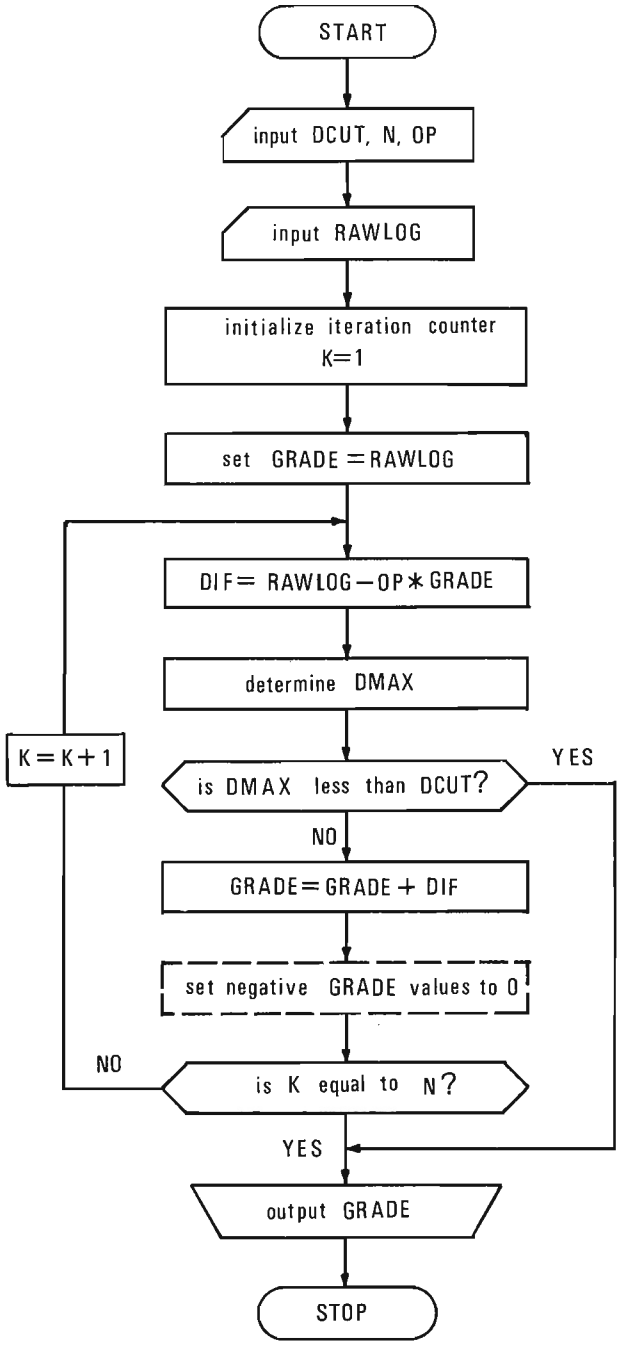

Figure 13.3. Flow chart for the iterative algorithm used for determining ore grade values from a gamma-ray log. The parameters used are:

- N – the number of iterations to be performed.
- OP – the digitized system impulse response function determined in a model borehole.
- RAWLOG – the array containing the raw gamma-ray log.
- GRADE – the array containing the approximate grade values being iterated.
- DIF – defined in flow chart.
- DMAX – maximum value of DIF.
- DCUT – assigned cutoff value of DMAX to stop processing before N iterations have been reached.

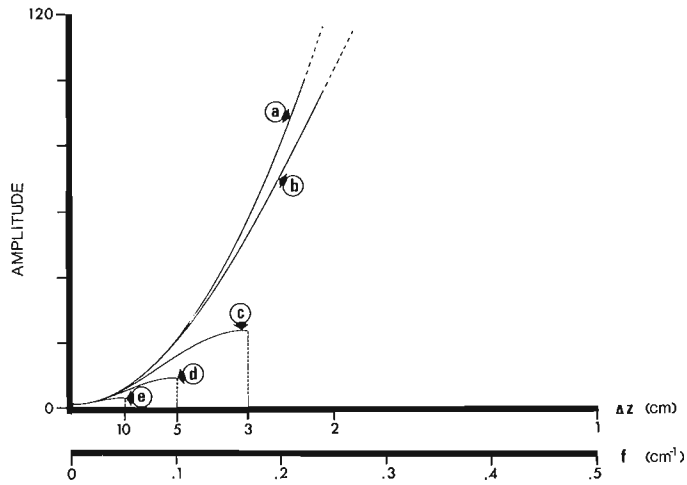

Figure 13.4. Amplitude spectrum of the theoretical inverse operator (curve a) and of the 3-point approximate inverse operators for sampling intervals of 1 cm (b), 3 cm (c), 5 cm (d), and 10 cm (e).

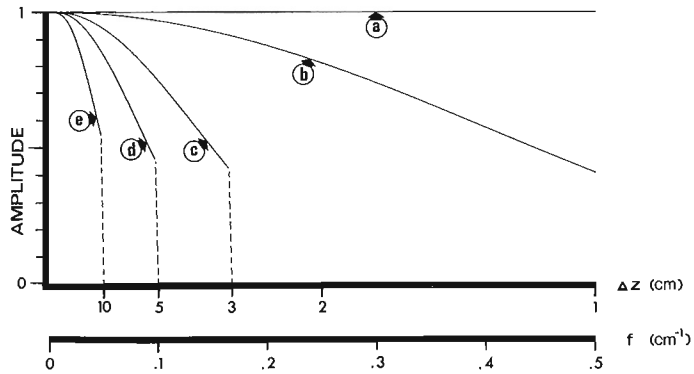

Figure 13.5. Amplitude spectrum of the noise-free geologic impulse response (shown in Fig. 13.2b) after application of the theoretical inverse operator (a), and approximate inverse operators corresponding to sampling intervals of 1 cm(b), 3 cm (c), 5 cm (d), and 10 cm (e).

Iteration and Inverse Filtering in Practice

The problem of developing an inverse filter operator for processing gamma-ray logs may be approached from many directions. Perhaps the simplest solution has been presented by Conaway and Killeen (in press), based in part on earlier work by Czubek (1971) and Davydov (1970). Here the GIR is approximated by the function

$$s(z) = \frac{\alpha}{2} e^{-\alpha|z|} \quad \ldots\ldots\ldots\ldots\ldots\ldots\ldots\ldots (8)$$

where the constant α is most easily determined in a model borehole. This function has been found to provide a reasonable fit to the experimentally determined response function with Geological Survey of Canada gamma-ray logging equipment. The amplitude spectrum of the theoretical inverse operator is shown as curve a in Figure 13.4. This theoretical inverse operator may be approximated by a simple 3-point operator given by

$$\left(-\frac{1}{(\alpha\Delta z)^2}, \quad 1 + \frac{2}{(\alpha\Delta z)^2}, \quad -\frac{1}{(\alpha\Delta z)^2}\right). \quad \ldots\ldots\ldots (9)$$

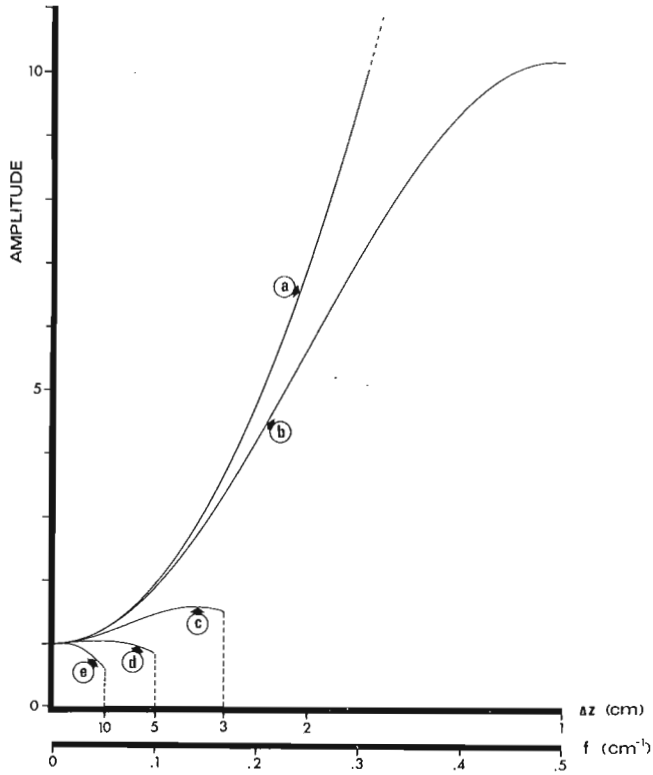

Figure 13.6. Amplitude spectrum of geologic impulse response with noise, after application of theoretical inverse operator (a), and approximate inverse operators corresponding to sampling intervals of 1 cm (b), 3 cm (c), 5 cm (d), and 10 cm (e).

The amplitude spectra for this operator for sampling intervals Δz = 1, 3, 5, and 10 cm are also shown in Figure 13.4 as curves b through e, respectively.

If the assumed shape of the GIR represents a good approximation in a given case, then the noise-free amplitude spectrum of the GIR processed with the exact inverse operator would resemble Figure 13.5 curve a. The approximate inverse operator would produce spectra resembling curves b through e, depending on the sampling interval. The effect of noise on the processed amplitude spectrum is shown in Figure 13.6 curves a through e. Two points are immediately apparent: (1) The operator performance improves as Δz decreases (Fig. 13.5) and (2) a low-pass filter will be required if a sampling interval much shorter than 10 cm is used (Fig. 13.6). It can be seen from Figure 13.2, curve b that a significant amount of information may be present at frequencies higher than the Nyquist frequency for Δz = 10 cm (vertical dashed line). Thus, to reduce errors due to aliasing of this high frequency information a sampling interval shorter than 10 cm should be used.

In the case of the iterative processing technique, Figure 13.7 curve a shows the noise-free amplitude spectrum of the GIR; curves b through h show the shape of the spectrum after 1, 2, 5, 10, 15, 20, and 30 iterations, respectively. Similarly, Figure 13.8 shows the iterative results with a noise level identical to that used in producing Figure 13.6. Here it can be seen once again that a smoothing filter is needed for sampling intervals significantly less than Δz = 10 cm. Although it may seem at first that the noise level of the processed log may be controlled sufficiently by stopping after fewer iterations when processing data obtained at smaller sampling intervals, in fact this technique

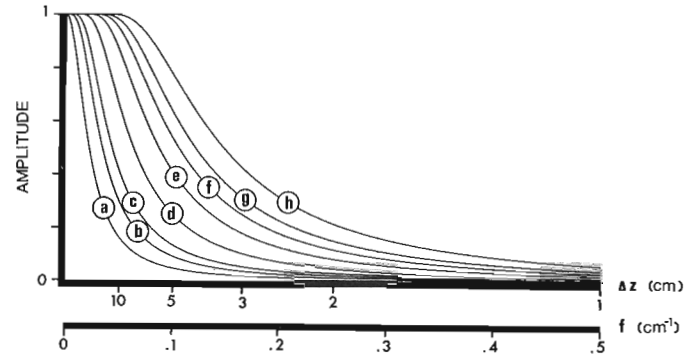

Figure 13.7. (a) Amplitude spectrum of the noise-free geologic impulse response. The other curves show the amplitude spectrum of the GIR after 1 iteration (b), 2 iterations (c), 5 iterations (d), 10 iterations (e), 15 iterations (f), 20 iterations (g), and 30 iterations (h).

does not give results as good as those which may be obtained by using more iterations and a smoothing filter. This latter technique gives more accurate information at low frequencies and a better cutoff at higher frequencies.

Two examples are presented to illustrate some of the points discussed above. Figure 13.9a shows a portion of a digitally recorded gamma-ray log run at v = 3 m/min with sampling interval Δt = 2 s (Δz = 10 cm). The log was processed iteratively (10 iterations) and is plotted as Figure 13.9b. The inverse filtered log (approximate operator) is given as Figure 13.9c. Figures 13.9b and 13.9c have been plotted on a scale of gamma-ray intensity rather than ore grade to facilitate comparison of the 3 curves. The agreement between the two processed logs, while not exact, is very close. In order to process the raw gamma-ray log (Fig. 13.9a), which has approximately 160 gamma-ray readings, the iterative technique required on the order of 14 500 multiplication operations and 18 000 additions or subtractions. The inverse filter method required only about 500 multiplications and 500 additions. Thus in this case inverse filtering is more efficient by a factor of about 30 in terms of computation time.

As a second example, consider the gamma-ray log shown in Figure 13.10a. This log is from the same section of the borehole as Figure 13.9, but run at a speed of 1 m/min with Δt = 2 s (Δz = 3.3 cm), thus giving similar counting statistics to Figure 13.9. Figure 13.10b shows the iterated log after 10 iterations. This processed log is rather noisy, and a smoothing filter should be used. The program as it stands now does not have a provision for smoothing, since it has traditionally been used with a sampling interval of 10-15 cm. Figure 13.10c shows the deconvolved and smoothed log produced using a 9-point combined smoothing and approximate inverse operator (see Conaway and Killeen, in press). The resolution here is somewhat better than in Figure 13.9, where Δz = 10 cm. To process the log shown in Figure 13.10 the inverse filter technique required about 4500 multiplications and a similar number of additions, while the iterative technique, even without smoothing, required about 135 000 multiplications and 145 000 additions or subtractions. Once again this represents a difference in computational efficiency of about 30:1 in favour of inverse filtering. Figure 13.10b can be smoothed to give results similar to Figure 13.10c, if a suitable smoothing routine is incorporated into the computer program. Selection of a suitable length of smoothing operator of a given type is a matter requiring some experience. This decision is perhaps best made on the basis

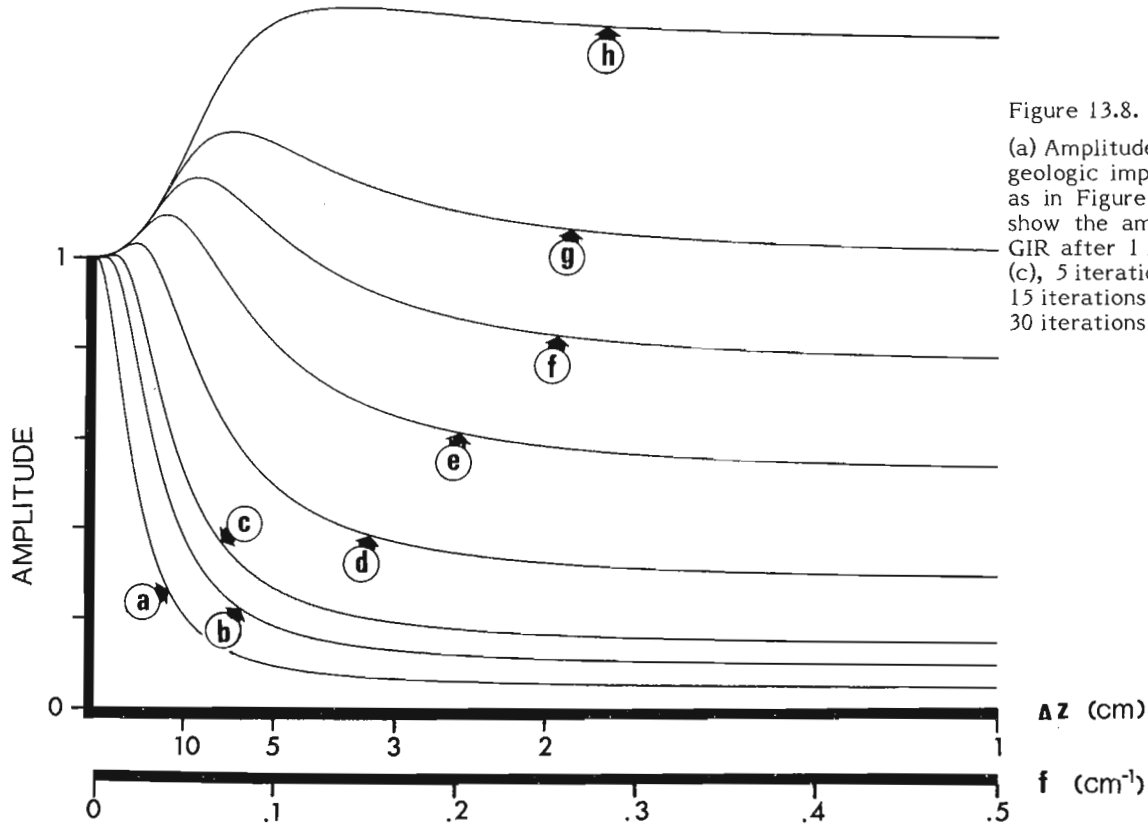

Figure 13.8.

(a) Amplitude spectrum of the geologic impulse response with noise as in Figure 13.6. The other curves show the amplitude spectrum of the GIR after 1 iteration (b), 2 iterations (c), 5 iterations (d), 10 iterations (e), 15 iterations (f), 20 iterations (g), and 30 iterations (h).

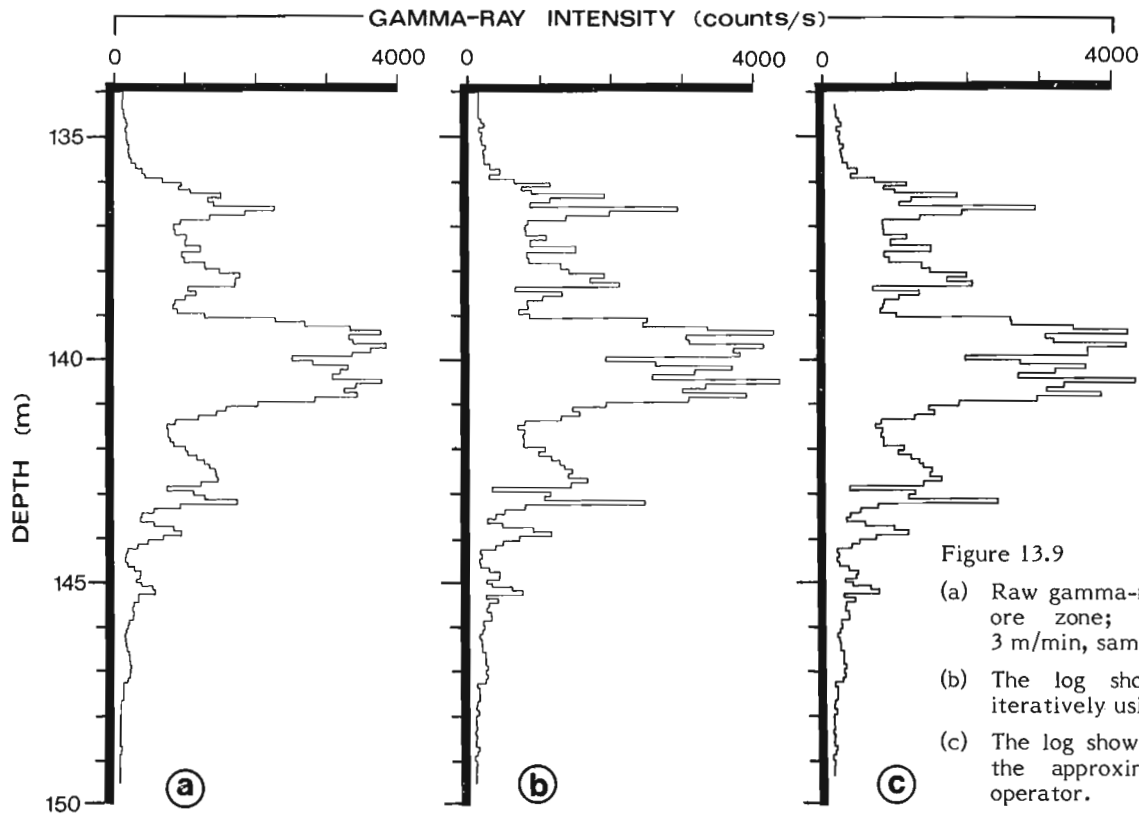

Figure 13.9

(a) Raw gamma-ray log from a uranium ore zone; logging velocity v = 3 m/min, sampling interval Δz = 10 cm.

(b) The log shown in (a) processed iteratively using 10 iterations.

(c) The log shown in (a) processed with the approximate 3-point inverse operator.

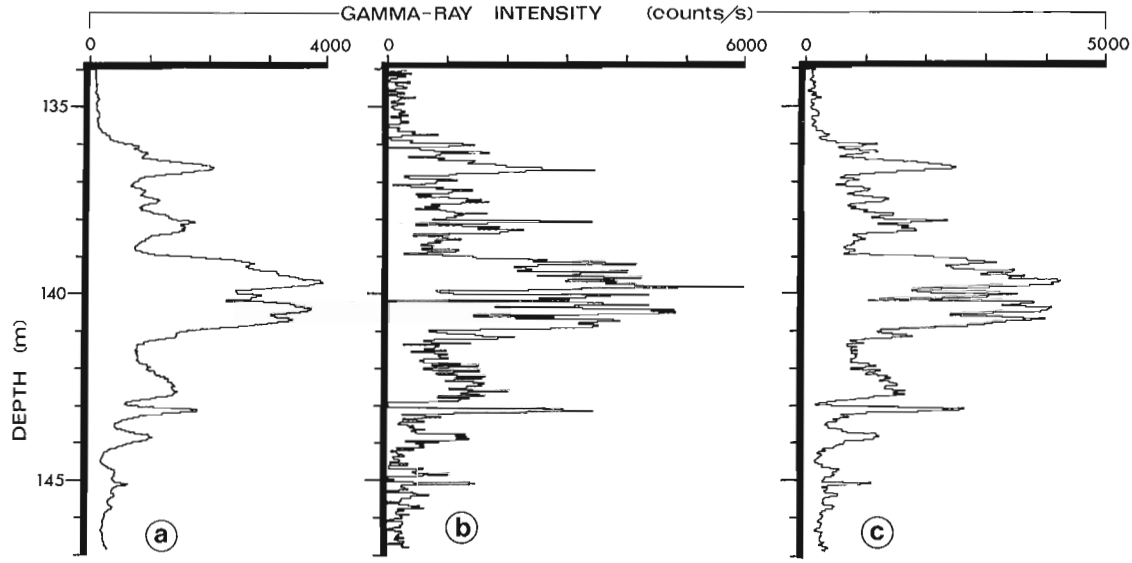

Figure 13.10

(a) Raw gamma-ray log from the same ore zone as in Figure 13.9; logging velocity v = 1 m/min, sampling interval Δz = 3.3 cm.

(b) The log shown in (a) processed iteratively using 10 iterations.

(c) The log shown in (a) processed with the approximate 3-point inverse operator.

of studies of the repeatability of several processed logs obtained in the same borehole under the same conditions. The best smoothing operator will be the shortest one which still produces results of acceptable repeatability.

Conclusions

It has been demonstrated that the iterative and inverse filter techniques for processing gamma-ray borehole logs are theoretically equivalent operations. From the example log with a sampling interval Δz = 10 cm (Fig. 13.9) it is clear that, while the approximate inverse filter and the iterative technique with 10 iterations give very similar results, the inverse filter method is many times more efficient computationally. From the amplitude spectra and the example log with Δz = 3.3 cm (Fig. 13.10) it can be seen that a sampling interval less than 10 cm should be used for improved resolution and to reduce aliasing errors; a smoothing filter is required with either method for the shorter sampling intervals.

Because discrete convolution is a sequential operation, the inverse filter technique requires little core memory, and allows the data to be processed on-line concurrently with the logging operations using a minicomputer or microprocessor. It is likely that the next generation of portable digital gamma-ray logging equipment will include such a facility. A proposed system of this type has been described by Killeen et al. (1978).

References

Conaway, J.G. and Killeen, P.G.
Quantitative uranium determinations from gamma-ray logs by application of digital time series analysis; Geophysics, v. 43 (in press).

Czubek, J.A.
1971: Differential interpretation of gamma-ray logs: I. Case of the static gamma-ray curve: Report no. 760/I, Nuclear Energy Information Center of the Polish Government Commissioner for Use of Nuclear Energy, Warsaw, Poland.

Davydov, Y.B.
1970: Odnomernaya obratnaya zadacha gamma-karotazha skvazhin (One dimensional inversion problem of borehole gamma logging): Izv. Vyssh. Uchebn. Zaved., Geol. i. Razvedka, no. 2, p. 105-109 (in Russian).

Kanasewich, E.R.
1973: Time sequence analysis in Geophysics; Calgary, University of Alberta Press.

Killeen, P.G., Conaway, J.G. and Bristow, Q.
1978: A gamma-ray spectral logging system including digital playback, with recommendations for a new generation system; in Current Research, Part A, Geol. Surv. Can., Paper 78-1A, p. 235-241.

Scott, J.H.
1962: The GAMLOG computer program; U.S.A.E.C. Report RME-143, Grand Junction, Colorado.

1963: Computer analysis of gamma-ray logs; Geophysics, v. 28, p. 457-465.

Scott, J.H., Dodd, P.H., Droullard, R.F., and Mudra, P.J.
1961: Quantitative interpretation of gamma-ray logs; Geophysics, v. 26, p. 182-191.

Sokolnikoff, I.S. and Sokolnikoff, E.S.
1941: Higher mathematics for engineers and physicists; McGraw Hill, New York.

14.

STRATIGRAPHY OF THE UPPER ORDOVICIAN - LOWER SILURIAN SEQUENCE IN THE AROOSTOOK-MATAPÉDIA ANTICLINORIUM, GASPÉ PENINSULA, QUÉBEC

E.M.R. Research Agreement 2239-4-9277

C. Hubert[1] and J. Béland[1]
Regional and Economic Geology Division

Abstract

Hubert, C. and Béland, J., Stratigraphy of the Upper Ordovician-Lower Silurian sequence in the Aroostook-Matapédia anticlinorium, Gaspé Peninsula, Québec; in Current Research, Part B, Geol. Surv. Can., Paper 78-1B, p. 89-90, 1978.

The stratigraphic sequence is as follows: a unit of mudstone at the base is overlain by ribbon limestone, followed upward by a thick assemblage of dominantly calcareous flysch and finally by more ribbon limestone. The strata are deformed by two sets of superimposed folds, oriented north-northwest and north-northeast respectively.

Introduction

This report is a preliminary report of an ongoing stratigraphic and structural study in the Upper Ordovician - Lower Silurian strata of the west-central part of the Aroostook - Matapédia anticlinorium in the Gaspé Peninsula (Fig. 14.1). The strata are dominantly calcareous and some have the characteristics of flysch deposits. The rocks show two phases of deformation.

The purpose of the study is to synthesize the petrologic and tectonic data in order to establish the regional setting of these rocks in the Appalachian orogen. Towards this goal, sequences of strata exposed along more than 60 km of roadcuts and riverbanks in the vicinity of the town of Matapédia have been examined in detail during the summer of 1977.

Stratigraphy

Four stratigraphic units have been thus far recognized in the Matapédia area. The oldest unit consists of thin to medium bedded, dolomitic and calcareous, greenish grey mudstone, and minor limestone. The limestone is a silty, blue-grey calcilutite and occurs at irregular intervals throughout the unit in subunits 1 to 20 m thick. Graptolites collected by J.P.A. Noble in 1976 indicate that the lower part of the unit is of Upper Hirnantian (latest Ordovician) age (J. Riva, pers. comm. 1977).

Upwards the mudstone unit grades into a blue-grey micritic ribbon limestone in beds, 2 to 10 cm thick, separated by a thin, dark grey shale.

Overlying the ribbon limestone unit is a very distinctive unit approximately 3100 m thick. It consists of silty and sandy limestones with minor greenish grey feldspathic sandstone and lithic conglomerate. The limestones are medium bedded calcisiltite and calcarenite, with 20 to 50 per cent detrital quartz, feldspar and minor igneous, sedimentary and metamorphic rock fragments. In some beds, allochthonous fragments of pelmatozoan, bryozoan, brachiopod, trilobite and ostrocode constitute the bulk of the transported fraction of the limestone. The feldspathic sandstone, medium to fine

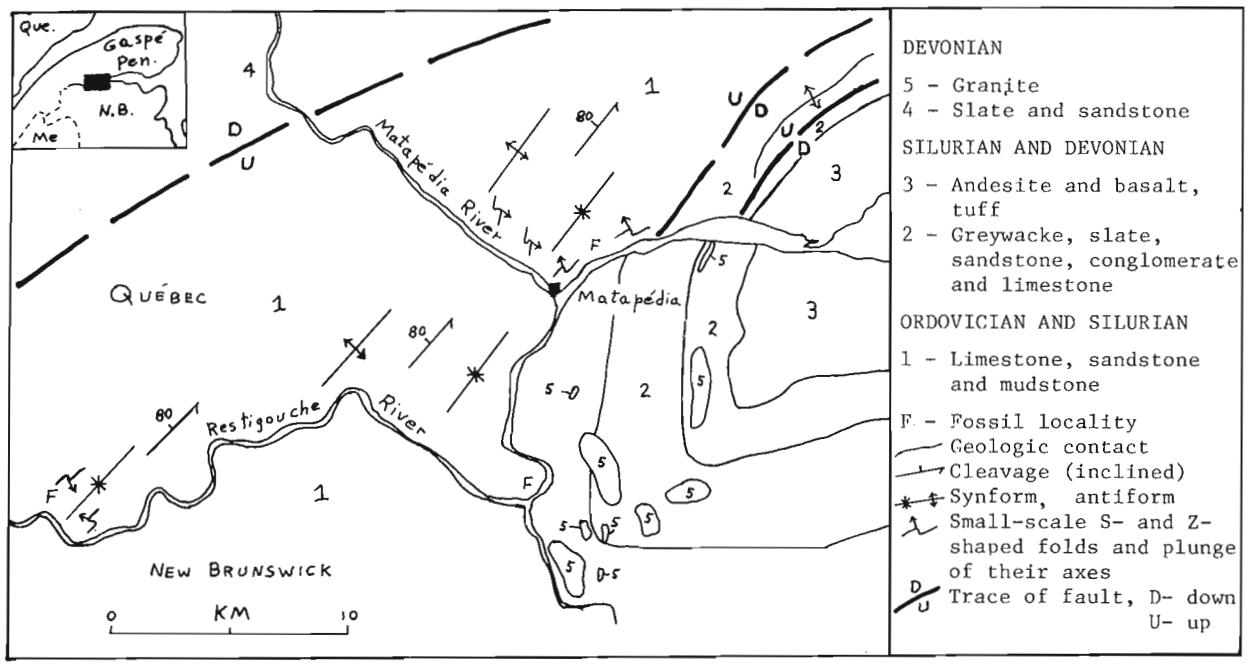

Figure 14.1 General geology of the Aroostook-Matapédia anticlinorium near Matapédia, Québec.

[1] Département de géologie, université de Montréal, Montréal, Québec, H3C 3J7.

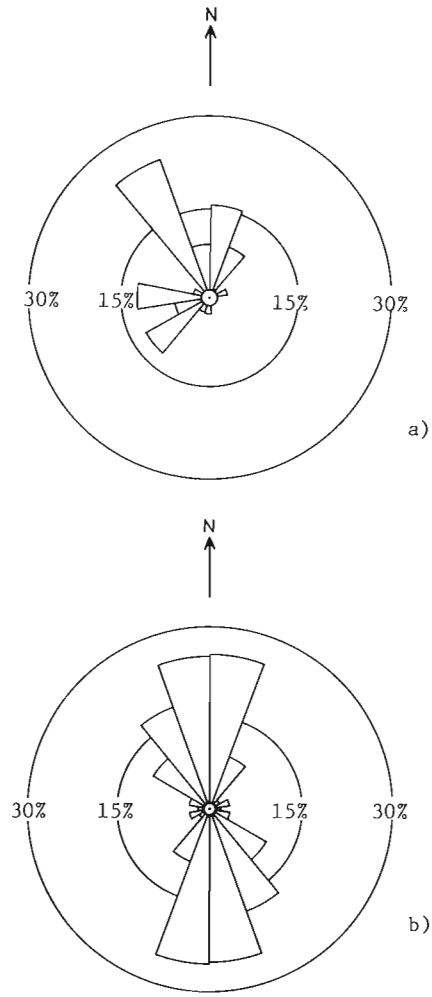

Figure 14.2 Rose diagrams of paleocurrent determination; 20° class interval;
a) flute cast and cross bedding (33 measurements)
b) groove and channel casts (55 measurements)

grained, occurs mainly in the lower third of the unit, in beds 10 to 30 cm thick, scattered throughout the limestone. Small lenses of lithic conglomerate fill wash-out channels at irregular intervals throughout the unit. These lenses, generally less than 10 cm thick, vary in width from 4 cm to 3 m. The conglomerates are composed of small pebbles and granules of rock fragments which, in decreasing order of abundance, are carbonate, sandstone, fossil debris, chert, volcanic, sericite and biotite schists, amphibolite and, possibly, serpentinite. This suite of rock fragments strongly suggests that material for this unit was derived from a nearby source similar in parent-rock content to that of the Taconian orogen. Most beds of conglomerate, sandstone and limestone display a Bouma sequence of turbidite structures with graded bedding, parallel lamination, cross and/or convolute lamination, and an upper division with parallel lamination. Wash-out channels, flute and groove casts are relatively common on the sole of the beds. Paleocurrent observations (Fig. 14.2) indicate that the material was transported from the south and southeast, probably from the Miramichi anticlinorium. Ostrocodes collected in the upper part of this unit by P.J. Lespérance and C. Hubert, indicate an Upper Llandovery age (M.J. Copeland, pers. comm. 1977).

The uppermost unit consists of thin and medium bedded, blue-grey micritic limestone alternating with a thin, dark grey shale.

Numerous felsic dykes and sills cut the sequence; they are probably of Devonian age (Béland, 1960).

The fourfold stratigraphic subdivision recognized here is in large part similar to that proposed recently by Lachance (1974, 1975 and 1977).

Structure

Two directions of folds are recognized. One system is generally oriented north-northwest although locally north or rarely west, and commonly lacks associated cleavage. Small-scale folds have S and Z shapes, and are useful in identifying limbs and hinges of major folds. The orientation of the second system of folds is uniform throughout the area. The folds trend north-northeast and are overturned towards the east. Congruent, small-scale parasitic folds are common on the limbs and in the hinge of larger folds. A coarse cleavage, with a 2 to 20 mm spacing, is present everywhere and a very steep lination results from the intersection of this cleavage with the primary bedding surface.

References

Béland, J.
1960: Région de Rimouski - Matapédia; Ministère des Mines Québec, R.P. 430, 20 p.

Lachance, S.
1974: Région de l'Ascension-de-Patapédia; Ministère des Richesses Naturelles Québec, D.P. 273, 19 p.

1975: Région de St-François d'Assisse; Ministère des Richesses Naturelles Québec, D.P. 328, 16 p.

1977: Région de St-Alexis-de-Matapédia; Ministère des Richesses Naturelles Québec, D.P.V. 458, 23 p.

15. COMPOSITIONAL VARIATION OF DEBRIS IN GLACIERS, BYLOT ISLAND, DISTRICT OF FRANKLIN

Project 770033

R.N.W. DiLabio and W.W. Shilts
Terrain Sciences Division

Abstract

DiLabio, R.N.W. and Shilts, W.W., Compositional variation of debris in glaciers, Bylot Island, District of Franklin; in Current Research, Part B, Geol. Surv. Can., Paper 78-1B, p. 91-94, 1978.

A pilot study to define variations in composition of glacial debris was carried out on outlet glaciers that flow from high-grade metamorphic terrane onto sedimentary terrane on the southwest side of Bylot Island. Preliminary observations indicate that 1) debris in lateral moraines of four of the five glaciers sampled has differing and distinct trace element geochemistry; 2) there are significant vertical compositional changes in debris bands in the glaciers; and 3) more than 99 per cent of the sand and coarser debris in the ice and moraines is derived from the metamorphic terrane.

Introduction

In 1977 reconnaissance and sampling of five glaciers and their end moraines were carried out on the southwest side of Bylot Island (Fig. 15.1). All glaciers drain basins within the central ice mass, which overlies rugged, highly metamorphosed Archean and/or Aphebian bedrock terrane (Jackson et al., 1975; Jackson and Davidson, 1975). Four of the glaciers studied extend as narrow, lobate bodies up to 15 km onto gently rolling terrain (Fig. 15.2) underlain by poorly consolidated Cretaceous and Tertiary sandstone and siltstone with some coal measures. The snout of the westernmost glacier studied overlies Helikian sandstone, shale, and dolostone. Major objectives of the study were to ascertain (1) at what distance down-ice from the gneiss-sedimentary rock contact the younger rock types became a significant part of the glacial load, (2) how the concentrations of various lithologic components varied vertically in the numerous debris bands in two of the five glaciers, and (3) how the composition of lateral moraines varied around the depositing glacier, as well as from one glacier to another, and how their composition and degree of weathering compared to those same properties of debris in transit in the ice of the two glaciers sampled in profile.

Preliminary Results

At present, trace element concentrations of clay sized (<4 μm diameter) particles have been determined by atomic absorption after a hot HNO_3-HCl leach* for lateral moraines of five glaciers and for several profiles collected from the debris bands (Fig. 15.3) of Aktineq and "Camp" glaciers (Fig. 15.1). In addition, trace element contents of heavy mineral separates (s.g. >3.3) from fine sand (0.063-0.250 mm) have been determined as well as preliminary textural parameters and X-ray diffraction data for samples collected in profile.

On the southeast side of the snout of Aktineq Glacier, a gully exposes several layers of peaty material lying in growth position on till (?) and fluvial and eolian sand and gravel. Dates on the lower organic beds are 7860 ± 100 and 7450 ± 230 ^{14}C years (GSC-2541, GSC-2577), and a date on the uppermost peaty layer, 2 m higher in the section, is 450 ± 70 ^{14}C years (GSC-2597). Because large boulders from the lateral moraine of Aktineq Glacier lie on sediment covering this uppermost unit, it is concluded that the glacier snout is as far out onto the lowlands as it has been in the past 7000+ years and that the till in the outer portion of the lateral moraine is very young.

From megascopic observations, all samples collected appear to be composed of more than 99 per cent Precambrian detritus, regardless of the distance of glacial flow over the younger bedrock. The debris bands on Aktineq and "Camp" glaciers show striking changes in colour and texture vertically; many debris bands contain clasts of highly deformed to virtually undeformed outwash, one piece of which was found more than 30 m above the base of "Camp" glacier. This clast of outwash was capped with fibrous peat which was dated at 120 ± 120 ^{14}C years (GSC-2529, uncorrected).

Trace element contents of clay from lateral moraines indicate that two glaciers drain chemically similar bedrock terrane but that significant differences exist among the other three, suggesting that the five glaciers drain four geochemically different bedrock basins (Fig. 15.4). Trace element contents of clay from samples of englacial debris from the two glaciers profiled are similar to the contents in clay from their lateral moraines. Although the profiles sampled are from glaciers less than 10 km apart, they show trace element concentrations that are distinctly different, "Camp" glacier being markedly enriched in Cr, Fe, and Ni and to a lesser extent in Cu and Zn (Fig. 15.5). Preliminary

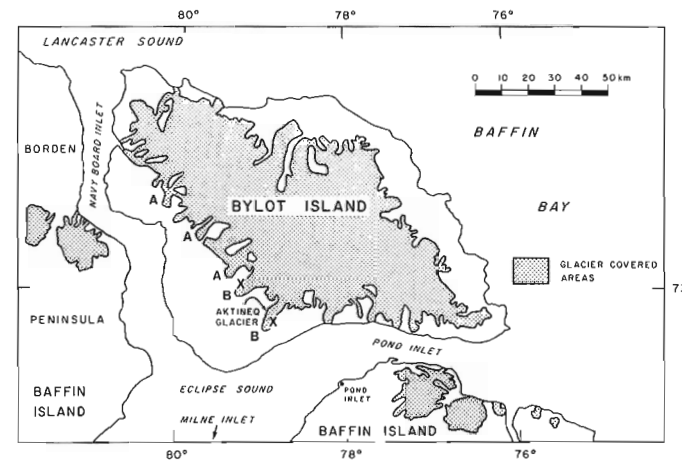

Figure 15.1. Location map of Bylot Island area. Glacier-covered areas also include many horns and nunataks. A = glaciers where till in moraines was sampled, B = glaciers where glacier ice and till were sampled, X = sites of peat samples collected for radiocarbon dating. Glacier labelled B to the northwest of Aktineq Glacier is "Camp" glacier.

* Analyses by Bondar-Clegg & Co., Ltd., Ottawa.

analysis of X-ray diffraction data for the <4 μm fraction of these samples suggests that there may be an enrichment in the mixed layer or expansible clay minerals (typical of Cretaceous and Tertiary terranes) in samples from Aktineq Glacier, although both suites of samples are dominated by a chlorite-10Å mica (illite?) clay mineralogy. Thus, the generally lower metal values of Aktineq Glacier may be caused as much by dilution by metal-poor clays of local (Cretaceous-Tertiary) derivation as by basic differences in the geology of the Precambrian source areas. Eight samples of the Cretaceous to Tertiary rocks (collected by H.R. Balkwill) contain less than 30 ppm Cu, Pb, and Ni, 5 ppm Co, 85 ppm Cr, 100 ppm Zn, and 2.8 per cent Fe. The presence of numerous, rusty weathering, sulphide-bearing gneissic boulders around "Camp" glacier, and the scarcity of these around Aktineq, however, tends to support the relationship of high metal levels to mineralization. Seventeen rusty boulders collected near "Camp" glacier contain up to 780 ppm Cu, 230 ppm Co, 240 ppm Cr, and 580 ppm Ni. Thirteen of the seventeen contain more than 300 ppm Cu.

These results support a suggestion made by E.B. Evenson (pers. comm., 1977) that englacial debris in alpine or outlet glaciers might be used to discover mineralization hidden beneath ice caps in their catchment areas, i.e. that till in moraines of present or past alpine glaciers or englacial sediment might be used in a fashion similar to stream sediments to map or discover the abnormal geochemical responses associated with mineralization within a drainage basin.

Heavy mineral (s.g. <3.3) content of the sand fraction from the lateral moraines of the five glaciers is very high in all samples (5 to 25 per cent by weight), and the heavy mineral suite is dominated by more than 90 per cent garnets and magnetic minerals with minor amounts of pyroxenes. Mineralogical and chemical analyses of these fractions are thus certain to reflect overwhelmingly the nature of the high-grade metamorphic Precambrian terrane from which these minerals predominantly were derived. Trace element analysis and visual scans of heavy mineral mounts of this fraction, however, suggest that sulphide or other labile components that may have been present in the lateral moraines have been destroyed in most samples by weathering. The variations in total contents (by weight) of heavy and magnetic minerals suggest that these, like the trace element values, vary in a systematic way from glacier to glacier.

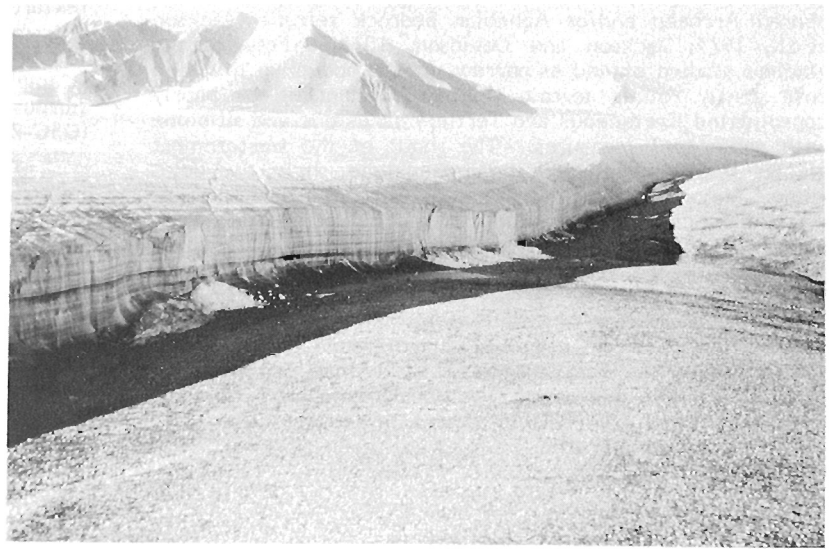

Figure 15.2.

East side of "Camp" glacier where it leaves the mountains and flows onto the gently rolling lowlands. Glacial flow is from upper right to lower left. (GSC 203226-F)

Figure 15.3.

Ice cliff on west side of "Camp" glacier. Glacial flow is from left to right. (GSC 203226-G)

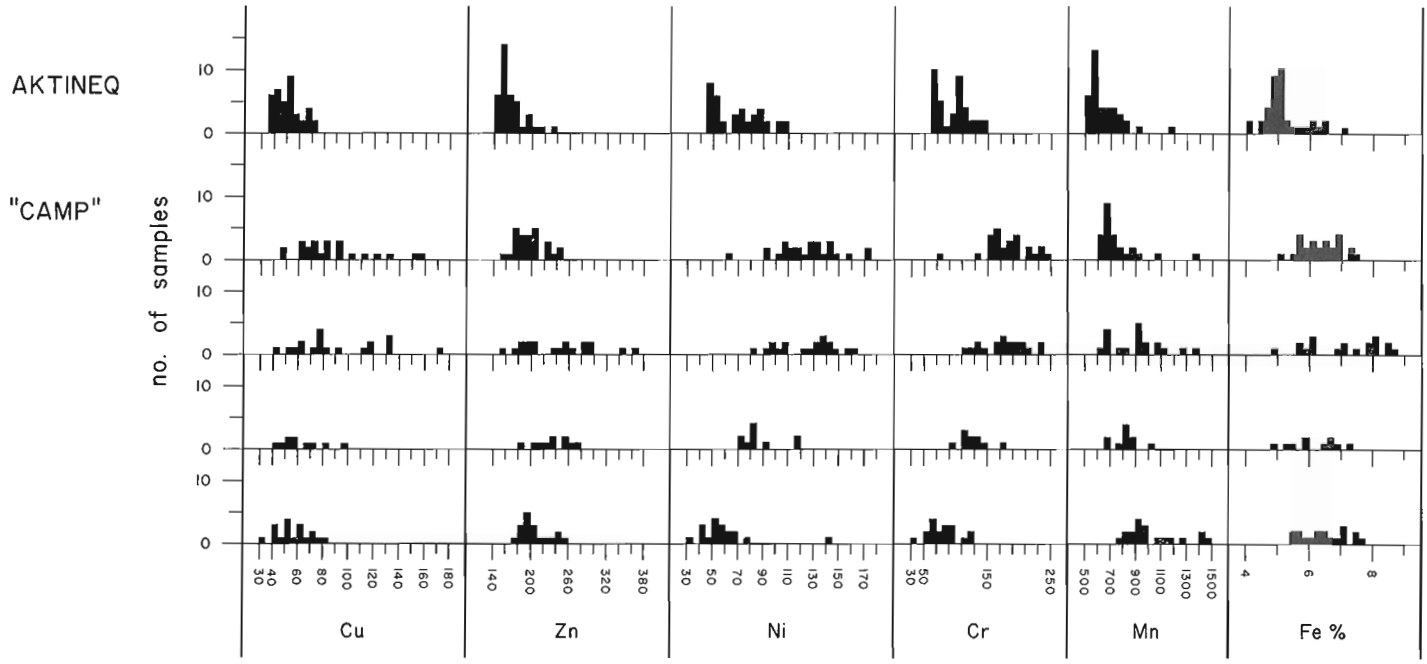

Figure 15.4. Frequency histograms of selected trace element distributions in the <2 μm fraction of till from lateral moraines of five glaciers. Horizontal scales are in ppm, except Fe, which is in per cent.

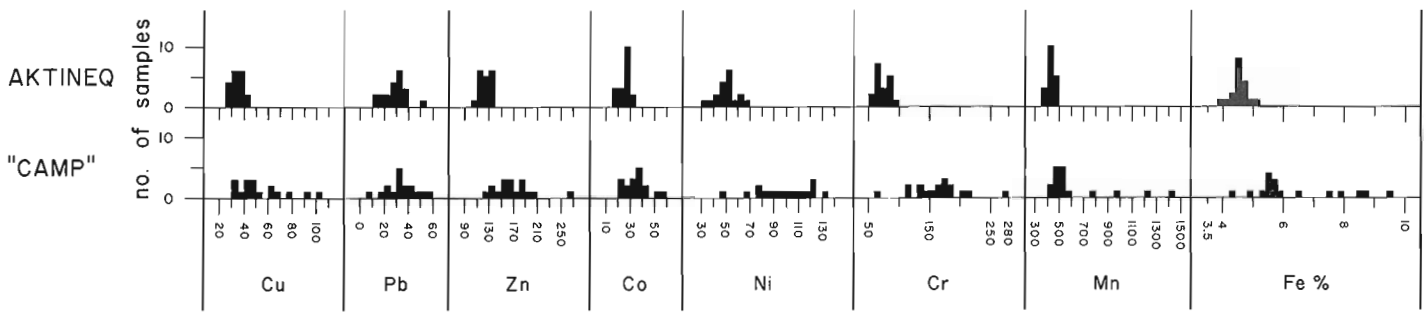

Figure 15.5. Frequency histograms of selected trace element distributions in the <4 μm fraction of debris in transport in Aktineq and "Camp" glaciers. Horizontal scales are in ppm, except Fe, which is in per cent.

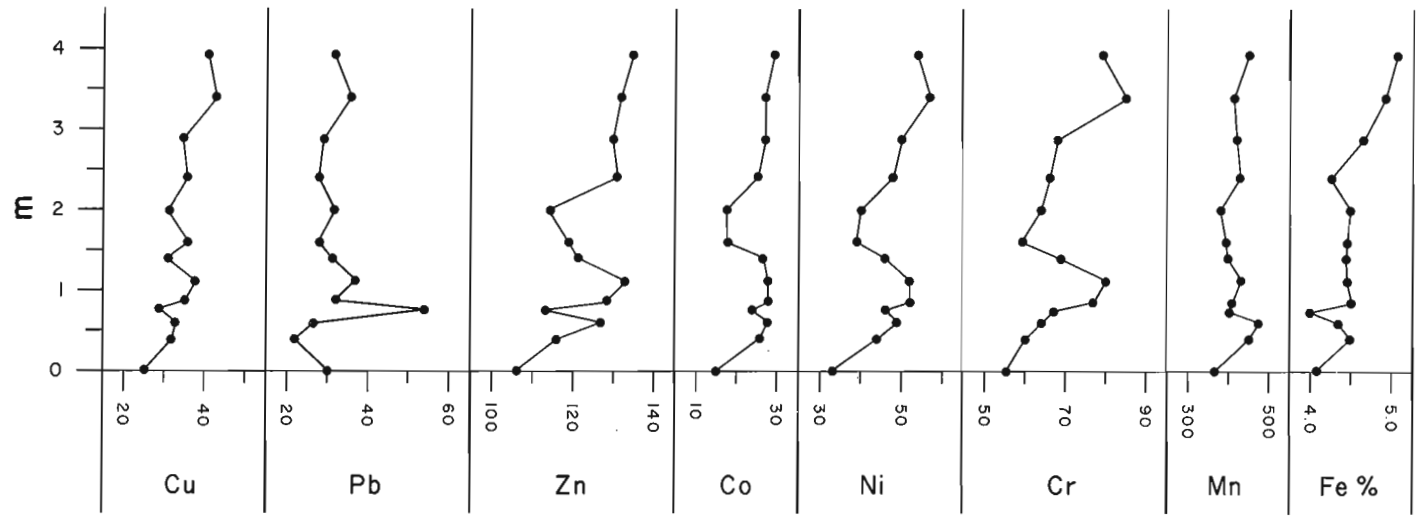

Figure 15.6. Vertical variations in trace element content of <4 μm fraction of debris in transport, east side of Aktineq Glacier. Vertical scale is true ice thickness above base of exposure. Horizontal scales are in ppm, except Fe, which is in per cent.

Analyses of clay from profile samples of "Camp" and Aktineq glaciers confirm what was evident from colour and textural contrasts in the field – that composition varies significantly vertically from debris band to debris band (Fig. 15.6). Similar variation has been noted by profile sampling of Wisconsinan till sections elsewhere in Canada (e.g. Shilts, 1976; Podolak and Shilts, 1978). It is probable that such regular vertical variations reflect stacking of debris bands of various thickness with minimal postdepositional disturbance. Furthermore, each debris band can represent the erosional tapping of some small part of the subglacial bed. This was illustrated strikingly by bright green debris bands located some 20 m above the base of "Camp" glacier and several kilometres down-ice from the nearest Precambrian source. The band was found to be markedly enriched in chlorite, Fe, and Mn relative to other debris bands above and below it.

Once formed, a debris band may persist for considerable distances downglacier with little or no addition of local material. In this connection it is of note that even the thick basal layers of debris-charged ice near the snout of Aktineq Glacier contain Precambrian detritus with no noticeable local component, even though exposures are more than 15 km from the nearest Precambrian outcrops. The expansible minerals found in the clay fraction of this debris indicate, however, that a local component is present and that provenance studies based on analysis of coarse debris (Boulton, 1970; Souchez, 1971) should be complemented by lithological analysis of fine fractions of the debris.

Conclusions

Because of the preliminary and incomplete nature of these data, conclusions from this phase of the glacier sedimentation study are general.

1) Bylot Island glaciers carry debris that can be related distinctly to their catchment areas in highly metamorphosed Precambrian terrane, despite the location of samples a few to 15 km onto chemically and lithologically dissimilar Cretaceous, Tertiary, and Helikian rocks.

2) Debris bands carry material that has been transported significant distances with little disturbance from adjacent bands or addition of debris from the base of the glacier.

3) The composition of debris bands varies vertically in a regular way, in much the same manner that previously deposited, apparently homogeneous till varies elsewhere in Canada. The variation within one glacier is, in this case, less than the significant compositional variation among glaciers.

4) Lateral moraines have compositional characteristics that are related closely to the debris in transit in adjacent glaciers. Some of the more labile minerals, such as sulphides, may have been removed from them by weathering.

5) Aktineq Glacier was as far advanced from the mountains during the past 500 years as at any time in the previous 7000 years.

References

Boulton, G.S.
1970: On the origin and transport of englacial debris in Svalbard glaciers; J. Glaciol., v. 9, p. 213-228.

Jackson, G.D. and Davidson, A.
1975: Bylot Island map-area, District of Franklin; Geol. Surv. Can., Paper 74-29, 12 p.

Jackson, G.E., Davidson, A., and Morgan, W.C.
1975: Geology of the Pond Inlet map-area, Baffin Island, District of Franklin; Geol. Surv. Can., Paper 74-25, 33 p.

Podolak, W.E. and Shilts, W.W.
1978: Some physical and chemical properties of till derived from the Meguma Group, southeast Nova Scotia; in Current Research, Part A, Geol. Surv. Can., Paper 78-1A, p. 459-464.

Shilts, W.W.
1976: Glacial till and mineral exploration; in Glacial Till, ed. R.F. Legget; R. Soc. Can., Spec. Pub. 12, p. 205-224.

Souchez, R.A.
1971: Ice-cored moraines in south-western Ellesmere Island, N.W.T., Canada; J. Glaciol., v. 10, p. 245-254.

16. MID-WISCONSINAN CLIMATES OF THE PACIFIC NORTHWEST

Project 740063

J.J. Clague
Terrain Sciences Division, Vancouver

Abstract

Clague, J.J., Mid-Wisconsinan climates of the Pacific Northwest; in Current Research, Part B, Geol. Surv. Can., Paper 78-1B, p. 95-100, 1978.

A controversy among earth scientists as to whether or not British Columbia and northwestern Washington were glaciated during mid-Wisconsinan time highlights the present uncertainty over late Pleistocene climates and environments in the Pacific Northwest. A review of relevant terrestrial lithostratigraphic and biostratigraphic information and selected paleoclimatic data from deep-sea cores shows that a lengthy nonglacial interval characterized by a sharply fluctuating, but generally cooler, climate occurred in the Pacific Northwest during mid-Wisconsinan time. Although remnant ice caps probably persisted in eastern and northeastern Canada during this interval, lowland areas adjacent to the presently glacierized mountains of western Canada were continuously ice free.

The Pleistocene Cordilleran glacier complex was controlled by different climatic factors from the Laurentide Ice Sheet. The precipitation and temperature regimes in the Cordillera, unlike those in other areas of Canada, are affected strongly by the Pacific Ocean. Both warm surface waters in the northeastern Pacific Ocean and reduced air temperatures probably were required for the growth of ice sheets in British Columbia, and these conditions apparently were not fulfilled during mid-Wisconsinan time.

Introduction

Although recent advances have been made in the regional correlation of Quaternary stratigraphic units in Canada (e.g., Dreimanis, 1975; Fulton, 1977), there is not yet a consensus as to the extent and timing of the climatic episodes that these units are thought to record. This probably is due, in part, to the difficulties of correlating lithostratigraphic units which are diachronous and which likely are deposited in response to nonclimatic, as well as climatic, factors. Furthermore, geologic responses to global climatic changes probably differed throughout Canada as a result of differences in oceanic and atmospheric circulation and continental geography. Thus, for example, the Canadian Cordillera was affected largely by the climatic regime of the northeastern Pacific Ocean, whereas the plains and Canadian Shield were influenced by air masses from the Arctic and Atlantic oceans and from the continental United States. Because ice masses in the Cordillera were responding to climatic factors different from those affecting the Laurentide Ice Sheet, detailed synchroneity of Quaternary geologic-climatic events is unlikely.

A general correlation, however, can be made of major late Quaternary stratigraphic units in western Canada (Fulton, 1977). The standard Wisconsinan stratigraphic succession in this region is a three-part sequence consisting of younger and older glacial deposits separated by nonglacial sediments. The nonglacial sediments were deposited during a lengthy interval, occupying much or all of middle Wisconsinan time, when glacier ice was absent from most plateaus, valleys, and lowland areas of the Cordillera and from the plains of western Canada. Early and late Wisconsinan times were dominated by glacial conditions, and ice covered much of the Cordillera at glacial maxima.

Inferences as to Wisconsinan climatic conditions in western Canada have been based largely on lithostratigraphy, with chronologic control provided by radiocarbon dates. Unfortunately, there is little published information on the paleoclimatic significance of fossil flora and fauna in Wisconsinan sediments of the region. The need for such information is highlighted by recent palynologic studies in western Washington (Heusser, 1972, 1977; Hansen and Easterbrook, 1974), from which it has been concluded that glacial conditions existed during part of the mid-Wisconsinan interval, in direct disagreement with paleoclimatic inferences from stratigraphic sequences in western Canada (Fulton et al., 1976; Fulton, 1977).

This paper summarizes the lithostratigraphic and biostratigraphic evidence pertaining to mid-Wisconsinan climates in the Pacific Northwest. The stratigraphic data are discussed in the context of global paleoclimatic trends deduced from selected deep-sea cores. It is shown that biostratigraphic data cited by some workers as evidence for mid-Wisconsinan glaciation in northwestern Washington do not necessarily contradict the lithostratigraphic evidence for continuous nonglacial conditions in southern British Columbia during mid-Wisconsinan time.

Mid-Wisconsinan Stratigraphy and Climates, British Columbia

Three nonglacial and two glacial sedimentary sequences are recognized in British Columbia (Fig. 16.1). Of interest here are middle Wisconsinan deposits, comprising stratified, nonglacial sediments with forest beds and, locally, the remains of large vertebrates (bison, horse, and mammoth). These include the Bessette sediments of south-central British Columbia and the Cowichan Head Formation of southwestern British Columbia. Finite radiocarbon dates from 43 800 ± 800 (GSC-740) to 19 100 ± 240 (GSC-913) years have been obtained on the former, and 58 800 $^{+2900}_{-2100}$ (QL-195) to about 24 000 years on the latter. A compilation of radiocarbon dates from these two units, from correlative strata, and from late Wisconsinan advance outwash (Quadra Sand) indicates that lowland areas, intermontane valleys, and plateaus in British Columbia were ice free continuously for several tens of thousands of years during middle and late Wisconsinan time (Fig. 16.2). A lengthy mid-Wisconsinan nonglacial interval also has been documented for other areas of western Canada (Fulton, 1977).

The presence of forest beds and large vertebrates suggests that the climate during at least part of the mid-Wisconsinan interval in British Columbia was not too different from the present (Fulton, 1971). Fossil beetles and pollen from the Cowichan Head Formation suggest a climate

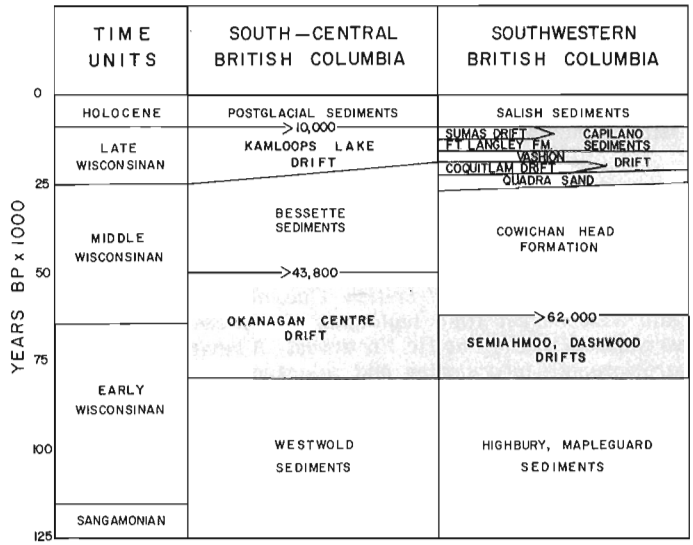

Figure 16.1. Late Quaternary stratigraphic framework of British Columbia. Drift units are stippled. References: south-central British Columbia, Fulton (1975); southwestern British Columbia, Fyles (1963), Armstrong (1975, 1977).

at times similar to, and at times colder than, the present (Armstrong and Clague, 1977). Palynologic analysis of an organic-rich silt in central British Columbia indicates that shrub-tundra conditions existed in that area during at least part of the mid-Wisconsinan interval (Harington et al., 1974). Alley and Valentine (1977), however, concluded from an examination of pollen spectra and a paleosol in the Bessette sediments that dry grassland environments occurred in some presently forested valleys in southern British Columbia between at least 42 000 and 25 000 years B.P. and that a major climatic deterioration commenced only after about 25 000 years B.P. Clague (1976, 1977), on the other hand, attributed the initial deposition of outwash sand (Quadra Sand) in coastal southwestern British Columbia to climatic deterioration accompanying the onset of late Wisconsinan glaciation at or before about 29 000 years B.P. Coastal lowlands, however, were not occupied by glacier ice until some time after 25 000 years B.P., and parts of the south-central part of the province were not covered by ice until after 19 000 years B.P.

In summary, several differing climatic reconstructions have been proposed for mid-Wisconsinan time in British Columbia (Fig. 16.3). Unfortunately, most of these are based on limited data or pertain to only a small part of the interval. It appears, however, that mid-Wisconsinan climates varied from cold to relatively warm. More detailed climatic reconstructions await combined studies of the flora and fauna of Bessette sediments and the Cowichan Head Formation.

Whatever the details of the paleoclimatic record, it is apparent that climatic conditions at no time during this interval were such that glaciers advanced far out of the alpine valleys into intermontane areas and coastal lowlands. Although this does not rule out mid-Wisconsinan glacier fluctuations in alpine areas, it does restrict the magnitude of such fluctuations.

Independent evidence for a lengthy Wisconsinan interstade is provided by calcium carbonate cave deposits from the Alberni area of Vancouver Island. Uranium-thorium dates on these deposits suggest that speleothem growth, and therefore nonglacial conditions, were continuous from some time before about 60 000 to about 32 000 years B.P. (M. Gascoyne, McMaster University, written comm., 1977).

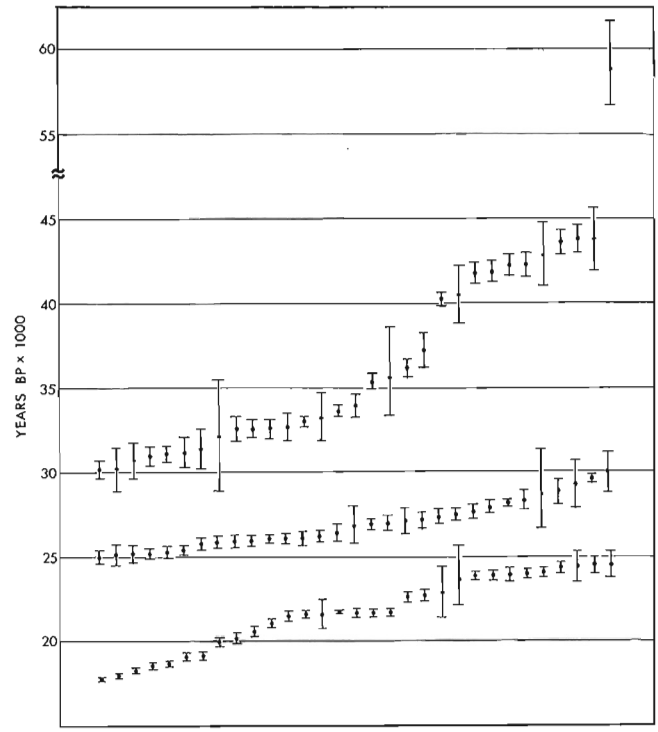

Figure 16.2. Finite radiocarbon dates from mid- and late-Wisconsinan stratified sediments (Bessette sediments, Cowichan Head Formation, Quadra Sand, and unnamed correlatives) in British Columbia. The bar indicates the possible range on either side of the date. The five youngest dates are from stratified sediments occurring between two late Wisconsinan tills in the Fraser Lowland east of Vancouver. Dates are from Anderson (1968), Fulton (1971), Harington et al. (1974), Clague (1975, 1977), Westgate and Fulton (1975), Fulton et al. (1976), Armstrong (1977), and Armstrong and Clague (1977).

The cessation in growth at about 32 000 years B.P., although possibly due to nonclimatic factors, may reflect climatic deterioration accompanying an early alpine phase of the late Wisconsinan (Fraser) glaciation.

Mid-Wisconsinan Climates, Washington State

Palynological data obtained from Wisconsinan sediments in the Puget Lowland (Hansen and Easterbrook, 1974) and Olympic Mountains (Heusser, 1972, 1974, 1977) in northwestern Washington bear on coeval climatic conditions in nearby British Columbia. Stratified sediments near the Wisconsinan glacial limit on the Olympic Peninsula provide a continuous record of late Quaternary vegetation and environments. A paleotemperature curve, constructed by comparing fossil pollen spectra with modern plant communities encountered at various altitudes in the Olympic Mountains near the studied sections, is shown in Figure 16.4. Heusser (1972, 1977) correlated pollen zones on which this curve is based with the various geologic-climatic units recognized in Puget Lowland to the east. For example, the cold interval between about 28 000 and 10 000 years B.P. was correlated with the Fraser Glaciation of late Wisconsinan time, and cold pollen spectra between about 40 000 and 34 000 years B.P. were assigned to a late stade of the penultimate (Salmon Springs) glaciation (Easterbrook, 1969). Hansen and Easterbrook (1974) examined pollen from peat beds in purported late Salmon Springs outwash in Puget Lowland and interpreted a cooler, moister climate than that of the present.

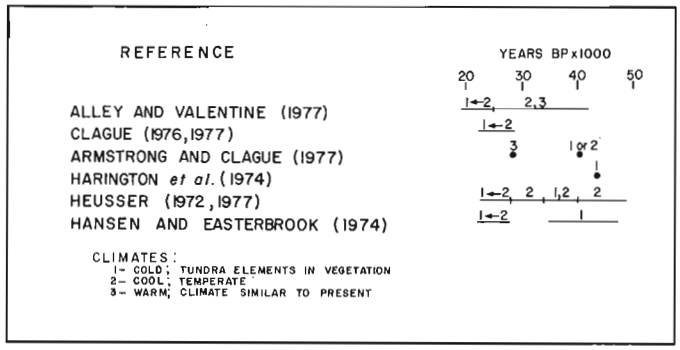

Figure 16.3. Mid- and late-Wisconsinan paleoclimates, British Columbia and northwestern Washington. See text for details.

These palynologic data suggest that much of mid-Wisconsinan time was cooler than at present (Fig. 16.3). It does not follow, however, that all cold phases (e.g., that from about 40 000 to 34 000 years B.P.) were accompanied by glacier expansion into lowland areas. Most of the mid-Wisconsinan cold phases were shorter in duration than the major late Wisconsinan cold interval and were separated by periods of climatic amelioration (Fig. 16.4). It is doubtful that glaciation of ice sheet proportions could be achieved during these shorter cold phases without accompanying significant increases in precipitation. Furthermore, lithostratigraphic and geochronologic data from southern British Columbia provide strong evidence against continental glaciation of the Cordillera at the time of deposition of the so-called late Salmon Springs till (Fig. 16.2).

The lithostratigraphic evidence cited in support of late Salmon Springs glacier invasion of Puget Lowland (Hansen and Easterbrook, 1974) has been questioned (Fulton et al., 1976), and a controversy continues to exist concerning alternative nonglacial modes of origin for sediments identified at critical localities as till and outwash.

In summary, the available biostratigraphic evidence from northwestern Washington indicates that mid-Wisconsinan climates were generally cooler than at present; however, lengthy intervals of relative warmth alternated with short cold phases. Temperature-precipitation regimes were such that glaciers in the Canadian Cordillera were restricted largely to mountain valleys until the end of mid-Wisconsinan time.

Unfortunately, the terrestrial stratigraphic record is too fragmentary and the fossil flora and fauna insufficiently investigated to outline in more detail mid-Wisconsinan climatic changes. Some additional constraints on the climatic character of this interval, however, are provided by deep-sea sediments.

Marine Paleoclimatic Data

Promising climatic reconstructions have been made from deep-sea cores using such parameters as oxygen isotope ratios and microfossil assemblages. These parameters often directly reflect water-temperature variations or changes in the total volume of ice on the earth's surface. A chronology for deep-sea cores has been established using radiometric age dates and magnetic and isotopic stratigraphy. An advantage of using marine sediments to assess paleoclimatic trends is that sedimentation rates at many ocean floor sites have been approximately uniform throughout the Quaternary; cores from these sites apparently lack hiatuses that are common in terrestrial stratigraphic successions.

The applicability of deep-sea sediment data in assessing mid-Wisconsinan climates of the Pacific Northwest is shown by three independent studies, one based on the oxygen isotope stratigraphy of a core from the equatorial Pacific Ocean, a second concerned with the isotope and pollen stratigraphy of cores off the northwestern United States, and a third dealing with the abundance of ice-rafted detritus in cores from the Gulf of Alaska.

Core V28-238

Core V28-238 from the equatorial Pacific is highly calcareous and is characterized by a uniform sedimentation rate and an absence of hiatuses. From the similarity in oxygen isotope ratios obtained from both planktonic and benthonic foraminifers, Shackleton and Opdyke (1973) concluded that water temperatures at the sea surface in this location have not varied significantly from the last interglaciation to the present. The isotopic differences in the core, therefore, can be attributed directly to fluctuations in the isotopic composition of seawater caused by the differential withdrawal of water molecules of different mass to form continental ice sheets. Shackleton and Opdyke thus were able to link isotope ratios directly to terrestrial ice volumes. Because ocean temperature changes may be related poorly to atmospheric temperature fluctuations, core V28-238 is superior to most cores from temperate latitudes as an indicator of global climatic trends.

The difficulty of relating local ocean temperatures to atmospheric parameters or global ice volumes is shown by late Quaternary changes in near-surface water temperatures in the north Pacific Ocean off the Oregon coast (Moore, 1973). Near-surface water temperatures in this area increased to their present values from minima about 24 000 years B.P. This warming apparently was not in phase with glacial fluctuations on the adjacent continent, because maximum late Wisconsinan glaciation of the Northern Hemisphere occurred between 20 000 and 16 000 years B.P., well after the surface water temperature minimum in the adjacent North Pacific. The apparent paradox of warming ocean waters co-occurring with advancing glaciers may be due to changes in patterns of divergence and coastal upwelling off northwestern North America. Perhaps the warming waters provided increased precipitation to glaciers in the adjacent Cordillera and thus facilitated their growth.

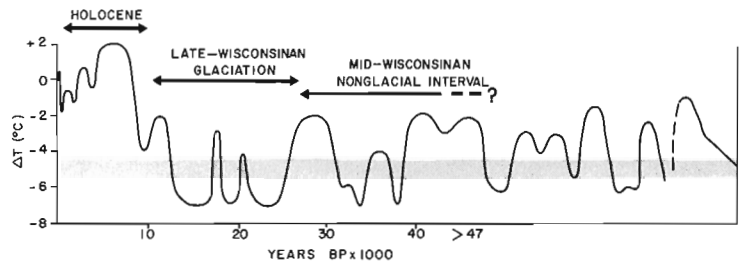

Figure 16.4. Late Quaternary temperature changes in northwestern Washington based upon palynological investigation of sediments on Olympic Peninsula. Temperature changes are amounts above or below the present July mean near sea level. Stippling indicates temperature interval at which transition from subalpine forest to alpine tundra would occur near sea level. Time spans of the Holocene and late Wisconsinan (Fraser) glaciation after Heusser (1972, 1977); that of the mid-Wisconsinan interval based upon stratigraphic successions in western Canada (Fulton, 1977). The temperature graph is from Heusser (1977, his Fig. 16).

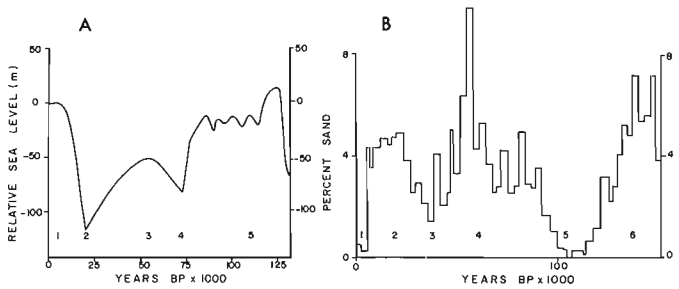

A. Glacio-eustatic sea level curve based on isotopic trends in core V28-238 (Shackleton and Opdyke, 1973, their Fig. 7).

B. Graph of dry weight per cent coarse sand in core V21-171 as a function of age (von Huene et al., 1976, their Fig. 4).

Figure 16.5. Selected data from two Pacific deep-sea cores illustrating the climatic fluctuations of late Quaternary time. The absence of a ramp at the beginning of graph B suggests that the top of the core either was not recovered or was badly disturbed. The mid-Wisconsinan nonglacial interval in both cores corresponds to isotope stage 3.

Because the isotopic differences in core V28-238 are due solely to variations in terrestrial ice volumes, the isotopic data were translated by Shackleton and Opdyke into eustatic sea levels relative to the present. The resulting glacio-eustatic sea level curve, shown in Figure 16.5A, is strongly supported by Barbados and New Guinea coral-terrace radiometric dates (Broecker et al., 1968; Veeh and Chappell, 1970; Shackleton, 1971).

Although short-duration changes in isotope ratios and, therefore, ice volumes may not be detected because of sampling limitations and stratigraphic mixing caused by faunal burrowing activity, the broad climatic trends of core V28-238 are evident. Maximum glacierization of the Northern Hemisphere occurred during isotope stages 2 and 4[1] at about 20 000 and 70 000 years B.P., respectively. Although there was considerable ice on the North American and Eurasian continents from about 70 000 years B.P. (perhaps as early as about 110 000 years B.P.) to the rapid melting at the end of stage 2 between 16 000 and 6000 years B.P. (Shackleton and Opdyke, 1973; Shackleton and Heusser, 1977), glaciation was less extensive during the middle of this interval from about 65 000 to 25 000 years B.P. Isotope stages 1, 3, and 5 correspond to postglacial, mid-Wisconsinan, and Sangamonian (plus part of early Wisconsinan) time, respectively.

Dates of isotope stage boundaries estimated from core V28-238 can be used as global averages for the boundaries of late Quaternary climatic intervals: 13 000 years B.P. (boundaries of stages 1 and 2, and postglacial and Wisconsinan time); 32 000 years B.P. (2-3, late-middle Wisconsinan[2]); 64 000 years B.P. (3-4, middle-early Wisconsinan); and 115 000 years B.P. (5d-5e, Wisconsinan-Sangamonian).

The glacio-eustatic curve (Fig. 16.5A) is in agreement with terrestrial stratigraphic data indicating that glacier ice remained over parts of eastern and northeastern Canada throughout mid-Wisconsinan time while much of western Canada was ice free (Prest, 1970; Dreimanis and Karrow, 1972; Fulton, 1977).

Marine Cores off Northwestern United States

Heusser and Heusser (1977) determined pollen spectra from isotopically analyzed marine cores off the northwestern United States and concluded that vegetation in the Pacific Northwest, in general, responded synchronously with fluctuations in global ice volumes during at least the last 127 000 years. Only during isotope stage 5 were air temperatures equal to or higher than at present. Pollen data suggest temperature depressions of 6°C and at least 7°C during isotope stages 4 and 2, respectively. Stage 3 was warmer than the immediately preceding or succeeding stages, but was cooler than at present.

Core V21-171

Core V21-171 from the Gulf of Alaska contains coarse detritus believed to have been rafted by icebergs (von Huene et al., 1976). The amount of sand and gravel at each level in the core is thought to be proportional to the abundance of icebergs calved from tidewater glaciers in southeastern Alaska. Small glacier advances in this area probably would lead to a substantial increase in berg ice in the North Pacific; thus the abundance of ice-rafted detritus in marine sediments may be a sensitive indicator of climatic change in southeastern Alaska. Furthermore, fluctuations of Pleistocene glaciers in the mountains bordering the Gulf of Alaska probably were broadly synchronous with those of the main Cordilleran glacier complex to the southeast, and thus the relative abundance through time of ice-rafted detritus in Gulf of Alaska sediments may provide direct information on paleoclimates of the Pacific Northwest.

A graph of the abundance of coarse terrigenous detritus in core V21-171 (Fig. 16.5B) indicates glacial maxima corresponding approximately in time to isotope stages 2, 4, and 6. The mid-Wisconsinan nonglacial interval corresponds to the coarse sand minimum correlated with stage 3. During this interval, more ice-rafted detritus was deposited than at present or during the last interglacial, suggesting that alpine glaciers in mountains bordering the Gulf of Alaska may have been more extensive during mid-Wisconsinan time than now. Variations in abundance of coarse sand in zone 3 sediments suggest that mid-Wisconsinan climates were unstable, an inference supported by biostratigraphic data from British Columbia and Washington.

It is hazardous to estimate the duration of the mid-Wisconsinan interval using the data from core V21-171, because there are no age control points in the part of the core illustrated in Figure 16.5B, and because sedimentation rates at the core site undoubtedly have varied. The one age shown in Figure 16.5B is based on a linear extrapolation at a constant sedimentation rate from control points near the base of the core, and therefore likely is in error. For example, the minimum in ice-rafted detritus estimated to have occurred from 115 000 to 105 000 years B.P. assuming uniform sedimentation represents isotope stage 5e which actually extended from about 129 000 to 115 000 years B.P. (Shackleton and Opdyke, 1973).

In conclusion, data from deep-sea sediments in different parts of the Pacific Ocean indicate a cool mid-Wisconsinan interval during which continental glaciers were smaller than during either early or late Wisconsinan time.

---

[1] Isotope stage nomenclature after Emiliani (1955).

[2] Many geoscientists place the boundary between late and middle Wisconsinan time at 22 500 to 25 000 years B.P. (e.g., Prest, 1970; Dreimanis and Karrow, 1972; Fulton, 1977). Dates chosen for this and other geologic-climatic boundaries vary according to the criteria used to define climatic change. These criteria include global ice volumes, local and regional lithostratigraphy, and biostratigraphy.

Conclusions

A review of lithostratigraphic and biostratigraphic information from the Pacific Northwest and relevant paleoclimatic data from selected deep-sea cores shows that a lengthy nonglacial interval characterized by a sharply fluctuating, but generally cooler, climate occurred in British Columbia during middle Wisconsinan time. Although a substantial ice cover probably remained in eastern and northeastern Canada during this interval, lowland areas adjacent to presently glacierized mountains in the Canadian Cordillera remained ice free.

The lack of an extensive ice cover in the Cordillera during the generally cool mid-Wisconsinan interval may be due in part to the existence of relatively cold surface waters in the adjacent Pacific. The warming of surface waters in late Wisconsinan time, due to changes in the regional oceanic circulation pattern, may have resulted in increased precipitation in the Cordillera. This, combined with further decreases in temperature, triggered an expansion of glaciers culminating in the inundation of most of British Columbia and northwestern Washington by ice.

Quaternary climates of the Pacific Northwest are controlled primarily by the adjacent Pacific Ocean. Because climates of other sectors of glaciated North America are controlled by different ocean bodies and air circulation patterns, detailed synchroneity of glacial events on a continental scale is unlikely.

References

Alley, N.F. and Valentine, K.W.G.
1977: Palaeoenvironments of the Olympia Interglacial (Mid-Wisconsin) in southeastern British Columbia, Canada; in Abstracts; Int. Assoc. Quat. Res., 10th Congr., Birmingham, England, p. 12.

Anderson, F.E.
1968: Seaward terminus of the Vashon continental glacier in the Strait of Juan de Fuca; Mar. Geol., v. 6, no. 6, p. 419-438.

Armstrong, J.E.
1975: Quaternary geology, stratigraphic studies, and revaluation of terrain inventory maps, Fraser Lowland, British Columbia (92G/1, 2, and parts of 92G/3, 6, 7, and H/4); in Report of Activities, Part A; Geol. Surv. Can., Paper 75-1A, p. 377-380.

1977: Quaternary stratigraphy of the Fraser Lowland; Geol. Assoc. Can., Ann. Mtg., Vancouver, Guideb., Field Trip no. 10, 20 p.

Armstrong, J.E. and Clague, J.J.
1977: Two major Wisconsin lithostratigraphic units in southwest British Columbia; Can. J. Earth Sci., v. 14, no. 7, p. 1471-1480.

Broecker, W.S., Thurber, D.L., Goddard, J., Ku, T-L., Matthews, R.K., and Mesolella, K.J.
1968: Milankovitch hypothesis supported by precise dating of coral reefs and deep-sea sediments; Science, v. 159, no. 3812, p. 297-300.

Clague, J.J.
1975: Late Quaternary sediments and geomorphic history of the southern Rocky Mountain Trench, British Columbia; Can. J. Earth Sci., v. 12, no. 4, p. 595-605.

1976: Quadra Sand and its relation to the late Wisconsin glaciation of southwest British Columbia; Can. J. Earth Sci., v. 13, no. 6, p. 803-815.

Clague, J.J. (cont'd)
1977: Quadra Sand: a study of the late Pleistocene geology and geomorphic history of coastal southwest British Columbia; Geol. Surv. Can., Paper 77-17, 24 p.

Dreimanis, A.
1975: Last glaciation in eastern and central Canada; in Quaternary Glaciations in the Northern Hemisphere, ed. V. Sibrava; Int. Union Geol. Sci. and Unesco, Int. Geol. Correlation Programme, Proj. 73/1/24, Rep. no. 2, p. 130-143.

Dreimanis, A. and Karrow, P.F.
1972: Glacial history of the Great Lakes — St. Lawrence region, the classification of the Wisconsin(an) Stage, and its correlatives; in Quaternary Geology; 24th Int. Geol. Congr., Montreal, sect. 12, p. 5-15.

Easterbrook, D.J.
1969: Pleistocene chronology of the Puget Lowland and San Juan Islands, Washington; Geol. Soc. Am., Bull., v. 80, no. 11, p. 2273-2286.

Emiliani, C.
1955: Pleistocene temperatures; J. Geol., v. 63, no. 6, p. 538-578.

Fulton, R.J.
1971: Radiocarbon geochronology of southern British Columbia; Geol. Surv. Can., Paper 71-37, 28 p.

1975: Quaternary geology and geomorphology, Nicola-Vernon area, British Columbia; Geol. Surv. Can., Mem. 380, 50 p.

1977: Late Pleistocene stratigraphic correlations, Western Canada; in Quaternary Glaciations in the Northern Hemisphere, ed. V. Sibrava; Int. Union Geol. Sci. and Unesco, Int. Geol. Correlation Programme, Proj. 73/1/24, Rep. no. 4, p. 204-217.

Fulton, R.J., Armstrong, J.E., and Fyles, J.G.
1976: Discussion [of Stratigraphy and palynology of late Quaternary sediments in the Puget Lowland, Washington]; Geol. Soc. Am., Bull., v. 87, no. 1, p. 153-155.

Fyles, J.G.
1963: Surficial geology of Horne Lake and Parksville map-areas, Vancouver Island, British Columbia; Geol. Surv. Can., Mem. 318, 142 p.

Hansen, B.S. and Easterbrook, D.J.
1974: Stratigraphy and palynology of late Quaternary sediments in the Puget Lowland, Washington; Geol. Soc. Am., Bull., v. 85, no. 4, p. 587-602.

Harington, C.R., Tipper, H.W., and Mott, R.J.
1974: Mammoth from Babine Lake, British Columbia; Can. J. Earth Sci., v. 11, no. 2, p. 285-303.

Heusser, C.J.
1972: Palynology and phytogeographical significance of a late-Pleistocene refugium near Kalaloch, Washington; Quat. Res., v. 2, no. 2, p. 189-201.

1974: Quaternary vegetation, climate, and glaciation of the Hoh River valley, Washington; Geol. Soc. Am., Bull., v. 85, no. 10, p. 1547-1560.

1977: Quaternary palynology of the Pacific slope of Washington; Quat. Res., v. 8, no. 3, p. 282-306.

Heusser, L. and Heusser, C.
1977: Quaternary climate of northwestern United States inferred from marine and continental pollen; in Abstracts; Int. Assoc. Quat. Res.,10th Congr., Birmingham, England, p. 206.

Moore, T.C., Jr.
1973: Late Pleistocene-Holocene oceanographic changes in the northeastern Pacific; Quat. Res., v. 3, no. 1, p. 99-109.

Prest, V.K.
1970: Quaternary geology of Canada; in Geology and Economic Minerals of Canada, ed. R.J.W. Douglas; Geol. Surv. Can., Econ. Geol. Rep. no. 1, p. 676-764.

Shackleton, N.J.
1971: New Guinea Reef Complex III; in The Phanerozoic Time-scale – A Supplement; Geol. Soc. Lond., Spec. Publ. no. 5, p. 106-107.

Shackleton, N.J. and Heusser, L.
1977: Oxygen isotope and pollen stratigraphy of a deep-sea core from the Pacific coast of North America; in Abstracts; Int. Assoc. Quat. Res., 10th Congr., Birmingham, England, p. 416.

Shackleton, N.J. and Opdyke, N.D.
1973: Oxygen isotope and palaeomagnetic stratigraphy of equatorial Pacific core V28-238: oxygen isotope temperatures and ice volumes on a 10^5 year and 10^6 year scale; Quat. Res., v. 3, no. 1, p. 39-55.

Veeh, H.H. and Chappell, J.
1970: Astronomical theory of climatic change: support from New Guinea; Science, v. 167, no. 3919, p. 862-865.

von Huene, R., Crouch, J., and Larson, E.
1976: Glacial advance in the Gulf of Alaska area implied by ice-rafted material; in Investigation of Late Quaternary Paleoceanography and Paleoclimatology, ed. R.M. Cline and J.D. Hays; Geol. Soc. Am., Mem. 145, p. 411-422.

Westgate, J.A. and Fulton, R.J.
1975: Tephrostratigraphy of Olympia Interglacial sediments in south-central British Columbia, Canada; Can. J. Earth Sci., v. 12, no. 3, p. 489-502.

17.

PHYSICAL CHARACTERISTICS AND SEASONAL CHANGES IN AN ARCTIC ESTUARINE ENVIRONMENT

Project 730021

S.R. Morison and R.B. Taylor
Terrain Sciences Division

Abstract

Morison, S.R. and Taylor, R.B., Physical characteristics and seasonal changes in an arctic estuarine environment; in Current Research, Part B, Geol. Surv. Can., Paper 78-1B, p. 101-106, 1978.

Cunningham Inlet exhibits distinct seasonal changes in water mass, primarily because of variable fluvial discharge resulting from limited source water, i.e. snowmelt. In summer there is a pronounced halocline at a depth of 1 to 3 m, with freshwater flowing over the more dense saline water. Suspended sediment from rivers is the main source of clayey silt covering much of the inlet bottom. Bedrock outcrops along the shallow entrance to the inlet and unconsolidated sediments along the shores are the other major sources of sediment found on the inlet bottom.

Introduction

Considerable information now is known about the oceanography and marine geology of large channels of the Canadian Arctic Archipelago, but few detailed studies have been conducted in the small shallow bays or inlets. A base camp located at Cunningham Inlet for a coastal morphology and process study of northern Somerset Island provided an opportunity to examine a semi-enclosed, shallow inlet. Observations of seasonal changes in water mass, sea ice breakup, and sampling of marine sediments were made during the summers of 1974 to 1976. This paper represents the results of an initial analysis of the data and essentially is a summary of observations made in 1976.

Cunningham Inlet is one of the two major inlets along the north coast of Somerset Island, Northwest Territories (Fig. 17.1). The inlet is 7.5 km long, 5.1 km at its widest point, and is approximately 120 km^2 in area. Steep plateau slopes of 150 m relief, fronted by a narrow beach, line the eastern shore of the inlet. Along the western shore the plateau is fronted by more gradual slopes veneered with gravel raised beaches. The mouth of the inlet is nearly completely closed by a tombolo, tombolo island, and another smaller island (Fig. 17.4), which have been built across a wide bedrock sill. A delta primarily deposited by Cunningham River lies across the head of the inlet. Cunningham River, with a drainage basin area of 2600 km^2 (Grey, 1976), is the largest of several rivers emptying into Cunningham Inlet.

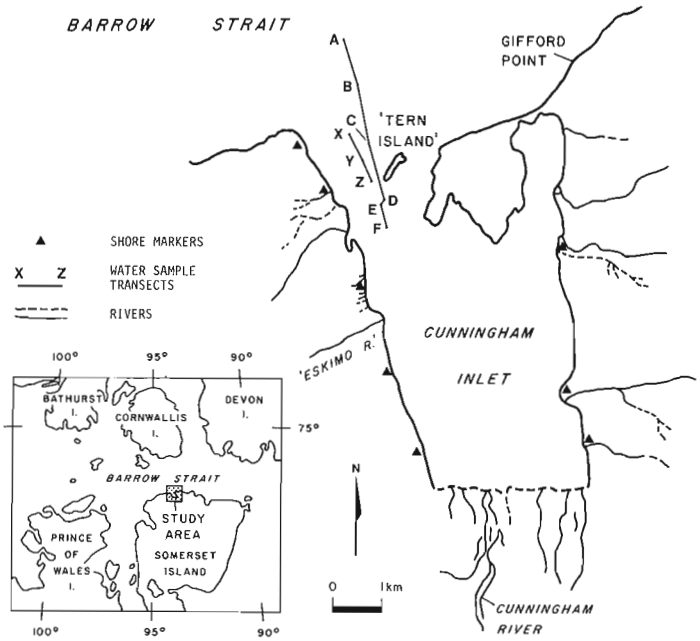

Figure 17.1. Location map of the study area.

At the northwest end of the inlet exposures of thin bedded, fine grained, argillaceous limestone with interbeds (1 to 30 mm) of siltstone were found as well as thick bedded blocky argillaceous limestone with no interbeds. The limestone is thought to belong to the Read Bay Formation of upper Silurian age previously mapped along northern Somerset Island (Fortier et al., 1963). The bedrock is unconformably overlain by unconsolidated Quaternary rubble, sand, and silt.

Methods of Study

Field Method

Water temperature and salinity were measured with a portable salinity-conductivity-temperature meter (Yellow Springs Instruments Co.), and water samples for suspended sediment analysis were collected with a horizontal alpha water bottle. Bottom sediments were collected using a Ponar and Petite Ponar grab sampler. Bathymetry and water depths at sampling stations were measured using a Raytheon DE719 Fathometer. Before sea ice breakup the measurements were made through seal holes, and after breakup they were made from a pneumatic boat. Horizontal control for the sampling stations was obtained using two theodolites at known shore markers to sight on the station. When the theodolites were not available, a sextant was used to obtain angles from the sampling station to known shore markers.

Laboratory Methods

Mechanical and mineral analysis of the bottom sediment samples was completed by Morison in the laboratory of the Department of Geology, Queen's University. For grain size analysis, 50 g of freeze-dried sample was disaggregated and split through a 62 µm wet sieve. The coarse fraction was dry sieved and the fine fraction was pipetted.

Physical Characteristics of Cunningham Inlet

Bathymetry

Echo sounding transects show that the inlet bathymetry closely resembles the topography of the adjacent shorelines. The eastern nearshore bottom slopes steeply to depths of 36 to 42 m. In contrast the western bottom slopes are more gradual, and depths are generally shallower than 24 m. A partially divided channel of 6 to 9 m depth runs north-south into the inlet between 'Tern Island' and the western shore. Elsewhere across the inlet mouth, depths are less than 3 m. Along the front of the Cunningham River delta depths varied from 6 to 18 m.

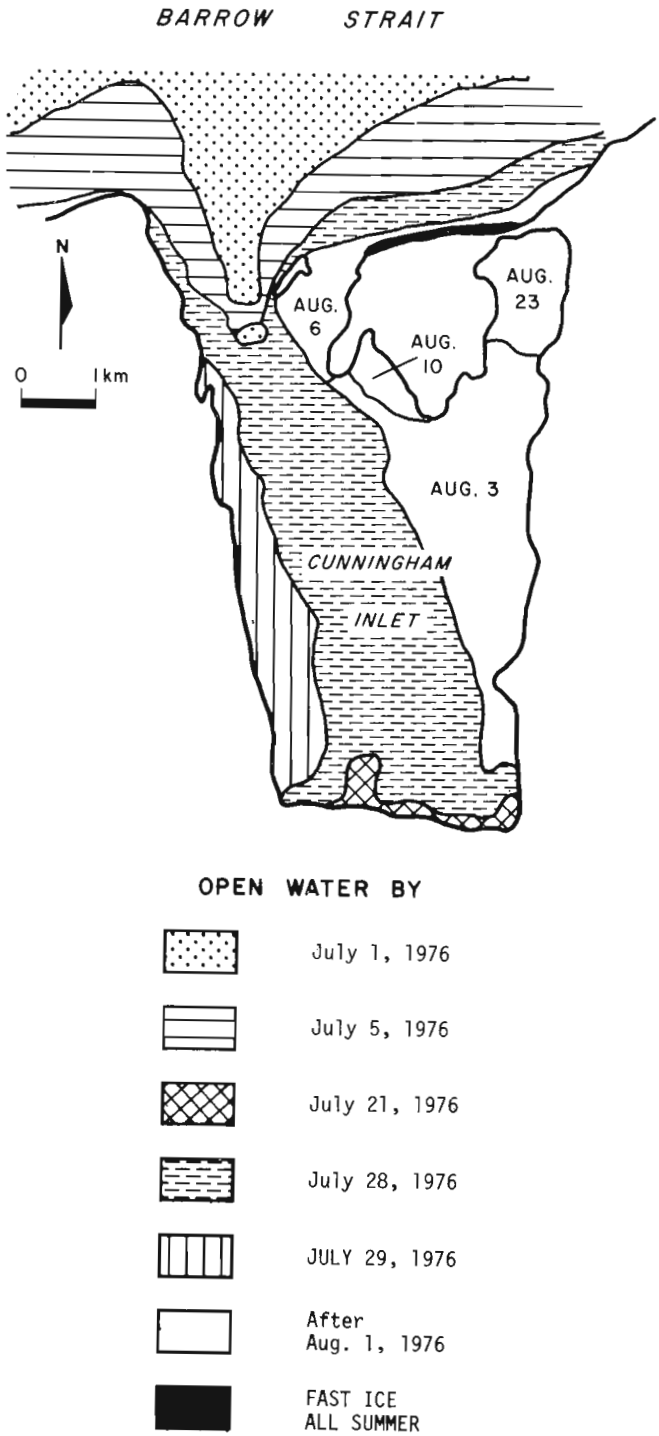

Figure 17.2. Sequence of sea ice breakup in Cunningham Inlet during 1976.

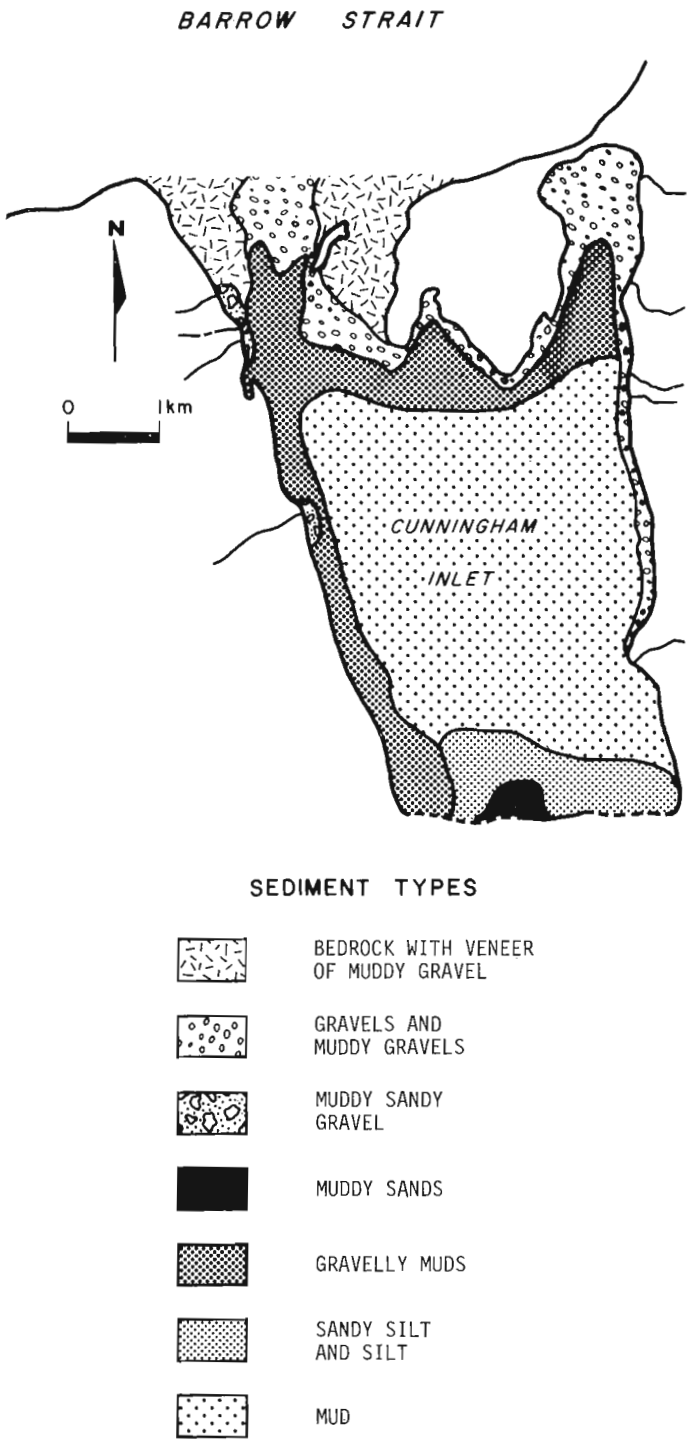

Figure 17.3. Distribution of surficial sediment by textural type (classification after Folk, 1954).

Figure 17.4. Aerial view of the mouth of Cunningham Inlet, July 20, 1976. (GSC 203216-L)

Tides

The tides recorded in Cunningham Inlet from July 27 to September 8, 1976 were mixed semidiurnal and had a mean tidal range of 1.2 m. The extreme range recorded was 2.1 m to 0.4 m.

Ice Conditions

Ice breakup progresses outward from an open water area, which develops early at the northern part of the inlet entrance, and from river mouths, especially Cunningham River. Tidal currents of estimated 0.4 to 0.7 m/s are responsible for the early ice breakup in the entrance channel. Melting of sea ice at the river mouths is associated with large inputs of warm freshwater during spring melt on land. Once a strip of open water extends from the entrance to the head of the inlet, the ice begins to break away from the east and west shores and lastly from the northeast corner of the inlet (Fig. 17.2).

Ice breakup in 1976 was later than in 1974 or 1975. Although open water extended into Cunningham Inlet from Barrow Strait on June 25, little change in ice cover occurred until after the rivers reached flood stage during July 18-24 (Fig. 17.2). On July 28 during a flood tide, west-northwest winds broke apart the rotted ice in the centre of the inlet, resulting in a continuous strip of open water along the length of the inlet. Sea ice left the rest of the inlet by the first week of August, except in the northeast corner, which became ice free by August 23. New ice began to form during calm nights in late August and early September.

Salinity and Temperature

Seasonal changes in water mass characteristics at Cunningham Inlet are caused by large volumes of freshwater which are introduced during the summer as a result of spring runoff. In 1976 measurements of water characteristics in the inlet were begun on July 3, which was after the start of spring melt but before the rivers reached flood stage during July 18-24.

Measurements recorded through seal holes across the middle of the inlet showed a pronounced halocline, from 2 to 3 ‰ at the surface to 28 to 30 ‰ at 3 m depth. Beneath this layer the marine waters became colder and more saline with depth. Salinity measurements made along a transect running north-south in the inlet entrance (Fig. 17.1) showed that the halocline decreased from a depth of 2 m at the south end of the entrance (the ice edge) to 0.5 m offshore of the inlet (Fig. 17.6). At the entrance to the inlet a distinct plume of turbid water was observed to move in and out of the inlet with tide. This phenomenon was most obvious during peak river discharge and when the area of open water at the inlet entrance was narrow. Water characteristics on either side of the plume edge indicated that it was the freshwater-saltwater interface. Waters on the seaward side of the interface were more saline, colder, and contained much less suspended sediment than waters on the inlet side (Fig. 17.5a,b).

Inaccessibility prevented measurements offshore of the Cunningham River delta until after ice breakup. On July 30 a pronounced halocline still existed at 1 to 2 m depth, but an even more pronounced thermocline occurred, from 6 to 8°C at the surface to 1 to 2°C at a depth of 3 m. Water temperature had ranged only between 0 and 3°C outside the delta area. The higher temperatures at the head of the inlet reflected the higher water temperature of Cunningham River, which on July 30 was also 6 to 8°C.

In August increased mixing of waters by waves and a steady decrease of freshwater emptying into the inlet led to less stratification of the surface waters. By August 29 the water column at the entrance to the inlet was isohaline, 26 to 27 ‰ , and temperatures hovered around 0°C. Elsewhere in the inlet salinities ranged from 24 to 30 ‰ with increased depth, and pockets of warm water, up to 2°C, were observed. During the summer the coldest, most saline, and most dense waters were found in the deeper parts of the inlet along the east shore.

Estuary Type

Cunningham Inlet cannot be classified as any one of the basic estuaries described by Pritchard and Carter (1971). This is because of the variable fluvial discharge resulting from limited source waters, i.e. snowmelt. Before spring melt the marine waters dominate, and the water mass of the inlet is nearly vertically homogeneous because of the sea ice cover and absence of freshwater. During summer the large inputs of freshwater are insufficient to push the larger mass of marine waters seaward, and the less dense freshwater flows across the surface causing a pronounced stratification in the water column. At this time the inlet resembles a highly stratified estuary. In late summer as the input of freshwater decreases and the marine waters become more dominant, the inlet inherits the characteristics of a partially mixed estuary. By freezeup the water mass returns to a nearly vertically homogeneous state. These water mass characteristics were observed during all three summers; however, the timing of the changes varied due to different dates of spring melt, river flood stage, and sea ice breakup in the inlet.

Suspended Sediment

Water samples were collected from the rivers emptying into Cunningham Inlet and from the inlet itself to determine seasonal changes in suspended sediment concentration. The total input of sediment from the rivers has not been calculated yet; however, comments can be made on the concentrations of suspended sediment carried within the inlet and through the entrance to the inlet.

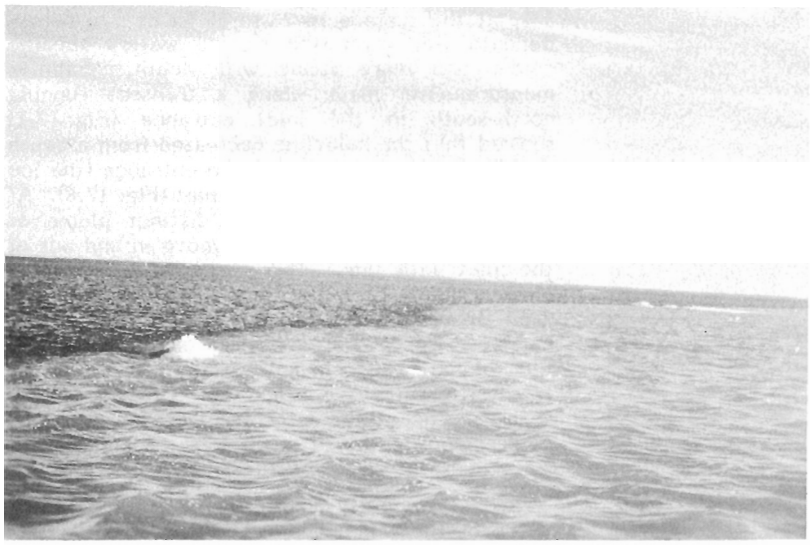

Figure 17.5a. The 'freshwater-saltwater interface' in the entrance to Cunningham Inlet on July 26, 1976. Barrow Strait is at the top of the photo. (GSC 203216-O)

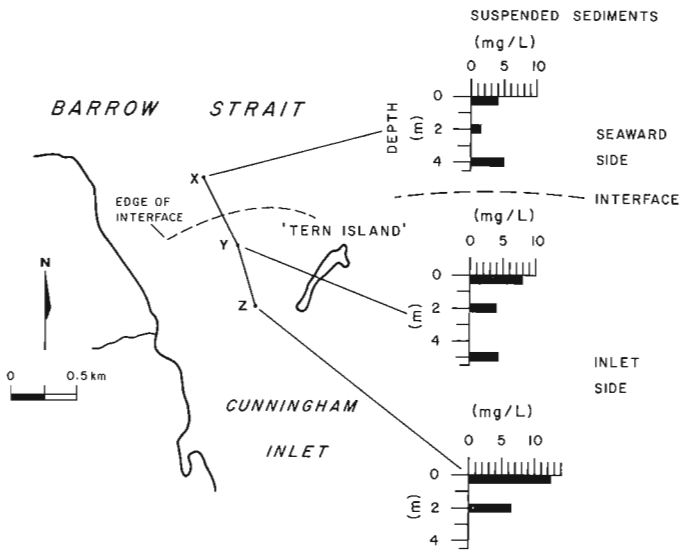

Figure 17.5b. Profiles of suspended sediment concentrations (mg/L) sampled on either side of the 'freshwater-saltwater interface' shown in Figure 17.5a. The location of the sampling stations is shown in Figure 17.1.

In early July there was less than 1 mg/L of suspended sediment in the waters sampled through the seal holes in the ice. After the rivers reached flood stage, however, 8 to 20 mg/L of suspended sediment was observed at the inlet entrance. The highest concentrations of suspended sediment were carried above 2 to 3 m depth, i.e. on top of the denser saline waters. Wright (1971) also observed that the seasonal thermohaline stratification of Alaskan fiords supported large concentrations of suspended sediment in the upper layer.

In late July, water samples were collected from along the length of the entrance channel and across the plume of sediment mentioned above (Fig. 17.5a). On July 21 sediment concentrations varied from 20 mg/L within the plume to 8 mg/L seaward of the plume. Samples collected from the same locations on July 26 also showed a decrease in suspended sediment concentrations in a south to north direction (Fig. 17.5b).

Water samples also were collected from Cunningham River on July 30, at one station just seaward of the delta and at another 1.1 km to the north. Sediment concentration in the river channels varied from 8 to 55 mg/L while just offshore 9 mg/L was observed at the surface and 24 mg/L near the bottom at 16 m. At the station 1.1 km north of the delta, the suspended sediment decreased from 12 mg/L at the surface to 5 mg/L at a depth of 30 m. Thus, it appears that some of the suspended sediment from Cunningham River quickly settles to the bottom and that some is dispersed from the delta in the near-surface waters of the inlet.

By August 29 the near stoppage of river flow was reflected in the suspended sediment concentration. At the head of the inlet 2 to 5 mg/L was observed, and at the entrance to the inlet there was only 2 to 3 mg/L. Occasionally during summer storms large concentrations of suspended sediment were entrained by waves breaking in the shallow entrance to the inlet, thus redistributing the finer sized sediments.

Marine Sediment Characteristics

Sixty-four sediment samples were collected from within the inlet during 1975 and 1976, and an additional 15 samples were collected from across the delta and along the shores of the inlet. Final analysis of the samples has not been completed; however, a preliminary map of sediment type has been prepared (Fig. 17.3). The textural classification and nomenclature assigned to the sediment types are those defined by Folk (1954).

Textural Characteristics

Bottom sediment within the central portion of the inlet is a soft, light brownish grey mud (Fig. 17.3). Ternary diagrams show that the mud is slightly richer in silt than clay (Morison, 1977). At the entrance to the inlet, the bedrock sill is overlain by a veneer of angular cobbles and pebbles mixed with the light brownish grey mud. Dark grey to black sandy silt and gravelly mud of high organic content were sampled across the southern end of the entrance channel. Hunter and Godfrey (1975) had conducted a shallow seismic refraction survey of the inlet and estimated this deposit to be 15 to 17 m thick. Across the south end of the tombolo island the topographic high, observed by Hunter and Godfrey (1975), was covered by gravelly muds. However, in the nearshore zone, as along the east and west sides of the inlet, muddy gravels predominate. It appears that the nearshore is a zone of transition between the gravel beaches and the muddy marine deposits. Silt, sandy silt, and muddy sand cover the delta foreslope whereas silts and sandy muds occur in tidal pools on the delta. Above high tide limit the sediments were rounded cobbles and pebbles mixed with medium to coarse sand.

Sediment Composition

The mineralogy of the sand fraction was as follows: calcite 10-80%, quartz 5-50%, amphibole 1-5%, pyroxene 1-5%, and mica (biotite) trace. The lithic fragments found in the inlet were limestone, probably from the Read Bay geologic formation. Fossil content in the samples included bivalves, foraminifera, ostracods, and sponge spicules.

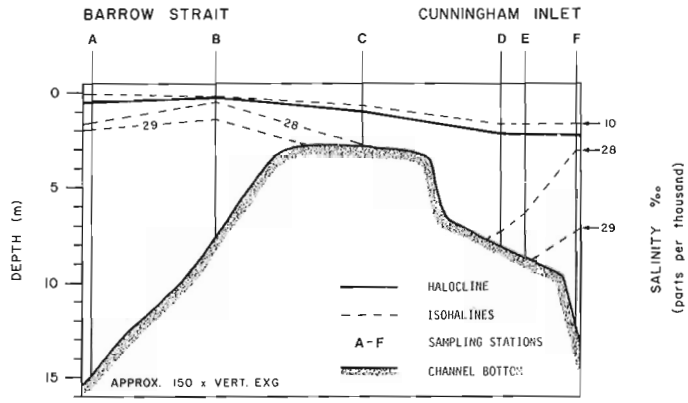

Figure 17.6. A profile of salinity values and the location of the halocline along the inlet entrance on July 21, 1976. Refer to Figure 17.1 for location of sampling stations.

Discussion of Sediment Distribution

The major contributors of sediment to Cunningham Inlet are the surrounding rivers. The large area of mud in the centre of the inlet reflects the suspended sediment dumped into the inlet by rivers. The large drainage area and length of Cunningham River make it the largest contributor.

The bimodal or polymodal bottom sediments in the nearshore reflect another source of sediment – the beach and low shore bluffs. The beaches are primarily gravel, with some bedrock outcrops. The low bluffs on the west shore are muddy sandy rubble with mudslides occurring as a result of rill wash during spring melt (Fig. 17.7a). During the summer locally generated waves erode the beaches, transporting beach sediments seaward. Gravel also is added to the nearshore zone by rivers during peak flood stage.

The shallow entrance to the inlet traps much of the suspended sediment leaving the inlet, and the main source of cobbles and pebbles at the entrance is the underlying bedrock or exposed bedrock on shore (Fig. 17.7b). Fractured bedrock, especially in intertidal and shallow water areas, provides slabs of rock which are easily dislodged by sea ice or short period, steep waves. The flatness of the rocks helps the waves to entrain them.

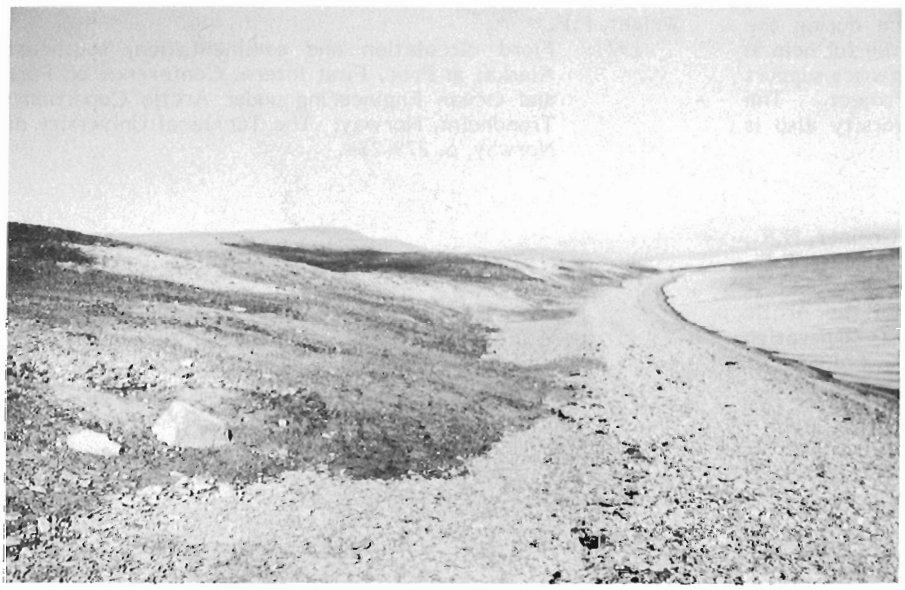

Figure 17.7a.

Gravel beaches are backed by low shore bluffs, some with mudslides across their slope. The photo shows the western shoreline of the inlet just north of 'Eskimo River' (Fig. 17.1). (GSC 165002)

Figure 17.7b.

Fractured bedrock and cobbles observed along the nearshore at the entrance to the inlet. (GSC 203216-N)

Summary

Cunningham Inlet is a semi-enclosed basin with only a narrow outlet to Barrow Strait. As a result, the water mass of the inlet is affected tremendously by the large input of freshwater from surrounding rivers during a very short period each summer. In summer, the inlet resembles a highly stratified estuary with a halocline from 2 ‰ at the surface to 31‰ at 3 m depth. Large amounts of suspended sediment also are emptied into the inlet by the rivers at this time. It is the 'fresh' surface water flowing on top of the denser saline water that transports and disperses the suspended sediment throughout the inlet. During late summer with the decrease in fluvial discharge the inlet resembles a partially mixed estuary and the suspended sediment concentrations become minimal.

The majority of bottom sediment is mud (clayey silt). Pebbles, cobbles, and boulders are found near the inlet shores, and both bedrock outcrops and bedrock fragments are found in the mouth of the inlet. The major sources of bottom sediment are rivers, bedrock outcrops both offshore and alongshore, and unconsolidated sediments along the shoreline.

Acknowledgments

The authors wish to thank Ross Cameron, Pat Newman, and Roland Wahlgren for invaluable assistance during the 1976 field season and John Legault and Jim Savelle for help in collecting bottom sediments in 1975. Superb logistics support was provided by Polar Continental Shelf Project. The assistance of Dr. G. Bartlett of Queen's University also is acknowledged.

References

Fortier, Y.O., Blackadar, R.G., Glenister, B.F., Greiner, H.R., McLaren, D.J., McMillan, N.J., Norris, A.W., Roots, E.F., Souther, J.G., Thorsteinsson, R., and Tozer, E.T.
1963: Geology of the north-central part of the Arctic Archipelago, Northwest Territories (Operation Franklin); Geol. Surv. Can., Mem. 320, 671 p.

Folk, R.L.
1954: The distinction between grain size and mineral composition in sedimentary rock nomenclature; J. Geol., v. 62, p. 344-359.

Grey, B.J.
1976: Hydrologic reconnaissance: Somerset Island, District of Franklin; Glaciology Div., Environment Canada.

Hunter, J.A. and Godfrey, R.J.
1975: A shallow marine refraction survey, Cunningham Inlet, Somerset Island, N.W.T.; in Report of Activities, Part B, Geol. Surv. Can., Paper 75-1B, p. 19-22.

Morison, S.R.
1977: Physical characteristics and seasonal changes in an Arctic estuarine environment; unpubl. B.Sc. thesis, Queen's University, Kingston.

Pritchard, D.W. and Carter, H.H.
1971: Classification of estuaries, classification according to physical processes; in The Estuarine Environment: Estuaries and Estuarine Sedimentation, ed. J.R. Schubel; Am. Geol. Inst., Washington, D.C., p. IV-1-17.

Wright, F.F.
1971: Fjord circulation and sedimentation, southeast Alaska; in Proc. First Intern. Conference on Port and Ocean Engineering under Arctic Conditions; Trondheim, Norway: The Technical University of Norway, p. 279-284.

18. METHODOLOGY FOR RADAR TRANSILLUMINATION EXPERIMENTS

Project 750037

A.P. Annan and J.L. Davis
Resource Geophysics and Geochemistry Division

Abstract

Annan, A.P. and Davis, J.L., Methodology for radar transillumination experiments; in Current Research, Part B, Geol. Surv. Can., Paper 78-1B, p. 107-110, 1978.

Transillumination measurements represent the optimum technique to determine the high frequency electrical properties of a material in situ. The methodology and a simple interpretation scheme for a transillumination experiment are presented. Data obtained with an impulse radar system, operating at a centre frequency of 80 MHz, in a potash mine are used to demonstrate the techniques developed. The experimental data yield a bulk dielectric constant estimate of 5.3 for the potash ore.

Background

Transillumination experiments provide estimates of the bulk high frequency electrical properties of a medium. In a radar transillumination experiment, the transmitting antenna is placed on one side of a block of material under study and the receiving antenna is placed on the other side. One antenna is then moved sideways with respect to the other. The basic transillumination geometry is shown in Figure 18.1.

In conjunction with extensive radar experiments conducted in a number of Saskatchewan potash mines, a series of transillumination experiments was carried out to provide background information on the bulk electrical properties of the salt beds. Almost ideal transillumination conditions were available in the mines. Large pillars of salt and potash ore were available and easily accessible. The purpose of this report is to outline the field technique and to illustrate how an estimate of the propagation velocity and the apparent dielectric constant of the material is derived. While a great deal more information can be extracted from the data, the primary emphasis here is a quick and relatively simple technique for providing estimates of the velocity and dielectric constant. More detailed analysis of the data is reserved for a later report.

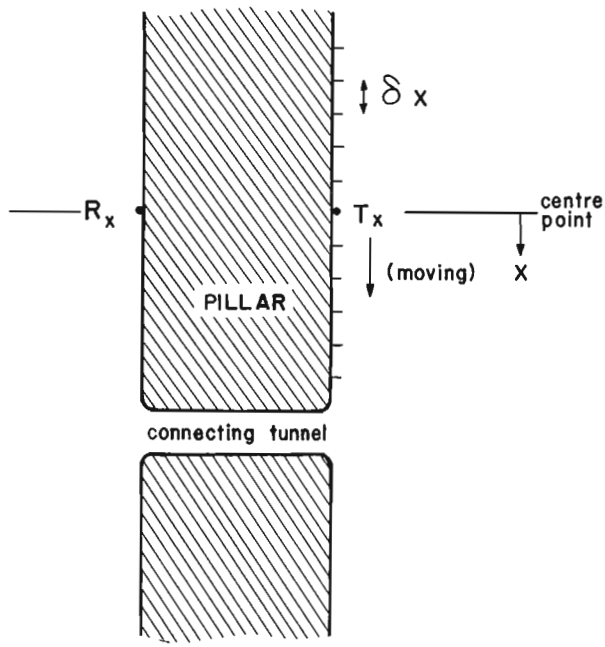

Figure 18.1 Illustration of transillumination experiment geometry.

Field Methodology

The field methodology of data collection is described here in order to document the procedure and to set the stage for data reduction. The following steps outline the field procedure for a transillumination experiment:

(a) A pillar with satisfactory dimensions and geometrical shape is chosen in a geologically significant area.

(b) A centre point (x = 0) for the array is picked at some practical distance from a passageway connecting both sides of the pillar under study (Fig. 18.1).

(c) One side of the pillar is chained off in increments, δ_x, both ways from the array centre point (Fig. 18.1). In practice, the value for δ_x should be less than 20 per cent of the pillar thickness. The maximum offset from the centre point should be 1 to 2 times the pillar thickness.

(d) One antenna is set up at the centre point of the array on the unchained side of the pillar. This antenna is enclosed with radio wave absorbing material to reduce spurious back scatter from other objects in the tunnel or adjacent walls. The receiving antenna is usually held fixed because wiring logistics are simpler in this mode.

(e) The other antenna is placed at the centre of the array on the chained side of the pillar. Ideally, this antenna should be enclosed with radio wave absorbing material but often this is not practical. The radar gains and ranges are then adjusted to the appropriate levels. This step provides the closest approach maximum signal level setting.

(f) The antenna on the chained side of the pillar is moved to the marked point farthest from the connecting tunnel. This position allows the radar system gains to be set for the minimum signal level.

(g) The moving antenna is then transported from marker to marker until the marker closest to the connecting passageway is reached. As the signal level approaches saturation or decreases below reasonably useful levels, the radar gain is adjusted appropriately up or down.

Estimation of Propagation Velocity

The radar record yields the travel times for the signal to pass through the pillar as a function of the position of the moving antenna. The time origin for the data is not easily determined. To determine the propagation velocity through the pillar it is necessary to allow for the unknown time origin as well as any misalignment associated with positioning errors.

A typical transillumination record is shown in Figure 18.2. The data were obtained with an impulse radar employing antennas constructed by the Geological Survey of Canada for this particular purpose. The antennas had a centre frequency of 80 MHz and about a 70 MHz bandwidth. The record shows a variable grey scale graphic recording of the radar signal as a function of the moving antenna position. The format of these records is discussed by Annan and Davis (1976). In this particular record the δ_x was 1.5 m (5 ft).

The travel time for the signal passing through the pillar decreases to a minimum at the centre point and then increases again. This record is readily reduced to a raw set of data points which give travel time relative to an arbitrary time origin as a function of the antenna position. This data set will be denoted (X_i, Y_i) where X_i is the position of the moving antenna with respect to the measured origin and Y_i is the travel time.

If the centre of the chained line is not aligned with the fixed antenna, the travel times will not be symmetrical as a function of X_i (i.e. $Y(-X_i) \neq Y(X_i)$). From the shape of the travel time curve it is possible to estimate the position of minimum travel time. This position allows an estimate of the misalignment error. The corrected position data, Z_i, is denoted by

$$Z_i = X_i - \varepsilon \qquad (1)$$

where ε is the alignment error.

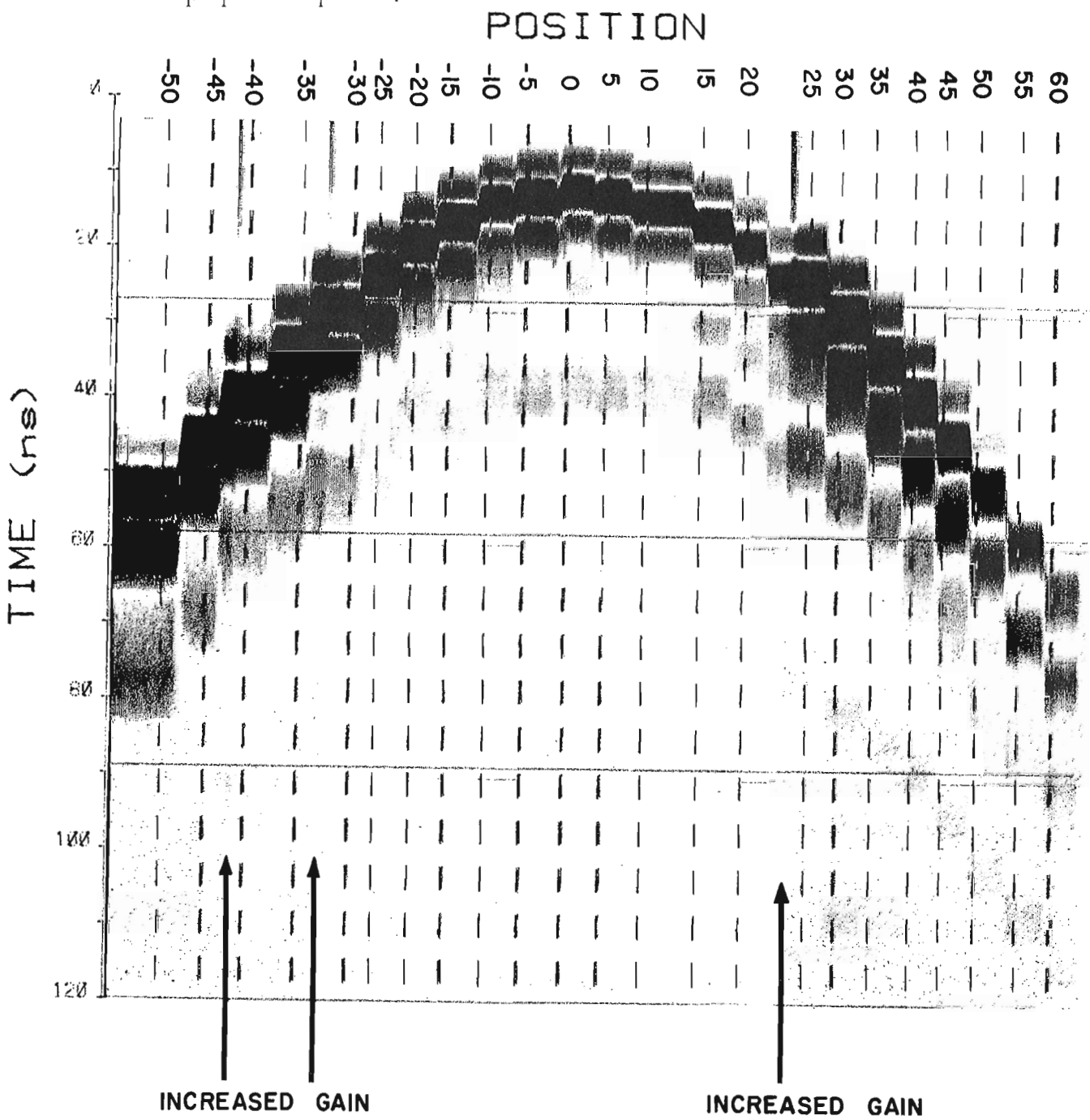

Figure 18.2 Typical transillumination record obtained in a potash mine. The position is indicated in feet.

The theoretical travel time through a plane surfaced pillar as a function of moving antenna position is

$$t_i = \frac{1}{V} (Z_i^2 + d^2)^{1/2} \quad (2)$$

where d is the pillar thickness and V is the propagation velocity in the pillar The true travel time for position t_i is related to the measured travel time Y_i by

$$Y_i = t_i - T_R \quad (3)$$

where T_R is the unknown origin offset time for the measured travel times. Combining expression (2) with (3) yields

$$X_i^2 = V^2 Y_i^2 + 2V^2 T_R Y_i + (V^2 T_R^2 - d^2) \quad (4)$$

Defining the equation

$$Z^2 = a_o + a_1 Y + a_2 y^2 \quad (5)$$

a least squares fit (Jenkins and Watts, 1969) to a parabolic form with the data set (Z_i^2, Y_i) yields the parameters

$$a_o = (V^2 T_R^2 - d^2) \quad (6)$$

$$a_1 = 2 V^2 T_R \quad (7)$$

$$a_2 = V^2 \quad (8)$$

Regrouping the equations yields

$$V = (a_2)^{1/2} \quad (9)$$

$$T_R = \frac{1}{2} \frac{a_1}{a_2} \quad (10)$$

$$d = (\frac{a_1^2}{4a_2} - a_o)^{1/2} \quad (11)$$

This analysis thus yields estimates of the velocity, the time origin, and the pillar thickness. Since a measurement of the pillar thickness is available, a check on the quality of the fit is available.

Interpretation of Field Example

The raw data for travel time versus position from the record in Figure 18.2 are listed in Table 18.1. The asymmetry of the data has been used to provide the estimate for ϵ of 1.2 m (4 ft). A standard least squares parabolic fit available for the HP-65 calculator was applied to the reduced data. The calculated values for a_o, a_1 and a_2 are

$$a_o = -27.76$$

$$a_1 = 0.63$$

$$a_2 = .017$$

which yield

$$V = 0.13 \text{ m/ns}$$

$$T_R = 18.4 \text{ ns}$$

$$d = 5.8 \text{ m}$$

The pillar in this example was not surveyed. An estimate of the pillar thickness, using a cloth tape and assuming that the pillar faces are parallel, is 6.2 m. The accuracy of this estimate like that of the centre point of the array is about 10 per cent. The propagation velocity yields an estimate of the bulk apparent dielectric constant, K_a, where

$$K_a = (\frac{c}{V})^2 \quad (12)$$

and c is the electromagnetic wave velocity in a vacuum (0.3 m/ns). The transillumination data yields an apparent dielectric constant of 5.3.

Table 18.1

Raw travel time versus position data derived from transillumination record shown in Figure 18.2.

X_i (feet)	Y_i (ns)
-45	125.2
-40	114.9
-35	105.3
-30	93.0
-25	85.1
-20	77.5
-15	70.8
-10	66.0
- 5	63.2
0	63.8
5	68.0
10	74.5
0	64.6
5	68.0
10	74.5
15	81.7
20	89.9
25	99.8
30	109.5
35	119.3
40	130.2
45	143.2
50	151.9

Practical Limits for Implementation and Interpretation

The interpretation method used here is very simplistic and implicitly requires several assumptions to be made. The most important assumptions are that the pillar walls are plane and parallel and that the velocity is constant throughout the pillar. For all experiments conducted in the potash mines the walls of pillars were sufficiently regular for the plane, parallel wall assumption to be made. If this assumption cannot be made, a revised interpretation scheme must be derived. An alternate scheme would most likely require some method for measuring the absolute time origin for the data. The assumption of constant velocity within the pillar is consistent with all our analysis to date. More detailed study, however, may reveal discrepancies which are associated with this assumption. We have not encountered any anomalous transillumination records which might indicate significant variations in V over the spatial distances covered by our experiments.

Another source of error can be associated with the unknown time origin for the data. In data with some finite error in the data points, analysis with a large origin offset T_R can lead to spurious results. In this case, $a_1 \gg a_2$ in the expressions. To minimize this source of error, a time origin should be picked for the data which is reasonably close to the true time origin. A practical manner for estimating the time origin is to set the travel at the closest approach equal to

$$Y(o) = \frac{d_{obs}}{V_{est}}$$

where d_{obs} is the thickness of the pillar observed in the field and V_{est} a reasonable estimate of the propagation velocity in the pillar. For potash data, the velocity estimate was chosen to be 0.12 m/ns (Davis and Annan, 1977).

Practical dimensions for a transillumination experiment are governed primarily by the availability of suitable sites. In addition, the smallest dimension should be significantly larger than the signal wavelengths, and the largest dimension sufficiently small that the signal is not all absorbed by the material illuminated. Additional geometrical constraints are imposed if highly directional antennas are employed.

Summary and Conclusions

A systematic procedure is developed for conducting transillumination experiments and deriving electromagnetic wave velocity and apparent dielectric constant of bulk materials. The technique has been successfully applied in a number of potash mines. In sylvite rich material the apparent dielectric constant of 5.3 determined here for the frequency band 40 to 120 MHz is similar to the value of 5.5 previously obtained with time domain reflectometry methods (Davis and Annan, 1977).

References

Annan, A.P. and Davis, J.L.
1976: Impulse radar sounding in permafrost; Radio Science, v. 11, no. 4, p. 383-394.

Davis, J.L. and Annan, A.P.
1977: Electrical properties of potash ore in situ; in Report of Activities, Part B, Geol. Surv. Can., Paper 77-1B, p. 75-76.

Jenkins, G.M. and Watt, D.G.
1969: Spectral Analysis and its Applications; Holden-Day Inc., San Francisco, 525 p.

19. CLAY MINERAL ANALYSIS OF MESOZOIC-CENOZOIC SEQUENCES, LABRADOR SHELF - A PRELIMINARY REPORT

Project 760037

D.C. Umpleby, G.R. Stevens[1], and J.A. Colwell[1]
Atlantic Geoscience Centre, Dartmouth

Abstract

Umpleby, D.C., Stevens, G.R., and Colwell, J.A., Clay mineral analyses of Mesozoic-Cenozoic sequences, Labrador Shelf; in Current Research, Part B, Geol. Surv. Can., Paper 78-1B, p. 111-114, 1978.

Clay minerals separated from Cretaceous and Tertiary sediments of the Labrador Shelf have been quantitatively analyzed to show the stratigraphic relevance of the clay mineral content. Kaolinite is prevalent in rocks of early Cretaceous age whereas montmorillonite is predominant in Upper Cretaceous and Paleocene rocks. In the deepest well, however, sediments of Paleocene age are dominated by illite, suggesting that diagenesis occurred under a relatively high thermal regime. Diagenetic processes are also indicated by other parameters.

Introduction

Since 1973, eight deep wells have been drilled on the Labrador Shelf (Fig. 19.1). Three of these wells encountered gas and condensate. At the present time, six of these wells, including the three discoveries, have been released from a confidential status.

In this study, cuttings from five nonconfidential wells, taken at variously-spaced intervals of the Mesozoic and Cenozoic sequences, have been quantitatively analyzed for clay minerals. Although the results of this analysis are of a preliminary nature, some degree of correlation has been found between the predominant clay mineral type and stratigraphy. In addition, the deepest well, Snorri J-90, was drilled into sediments which in the lower part show the effects of diagenesis characteristic of a relatively high thermal regime.

Purpose of the Study

The reasons for conducting this study are:

1. To determine if a clay-mineral stratigraphy exists and, if so, whether it follows the biostratigraphic framework;
2. To ascertain if the spectrum of clay minerals provides evidence of conditions prevailing in adjacent provenance areas during the Cretaceous and Tertiary;
3. To study the predominant clay minerals present in order to ascertain whether the release of hydrocarbons, given a favourable maturation history, may have occurred; and
4. To evaluate the degree of diagenesis under the combined effects of age and temperature – criteria essential for evaluating the hydrocarbon potential of the area.

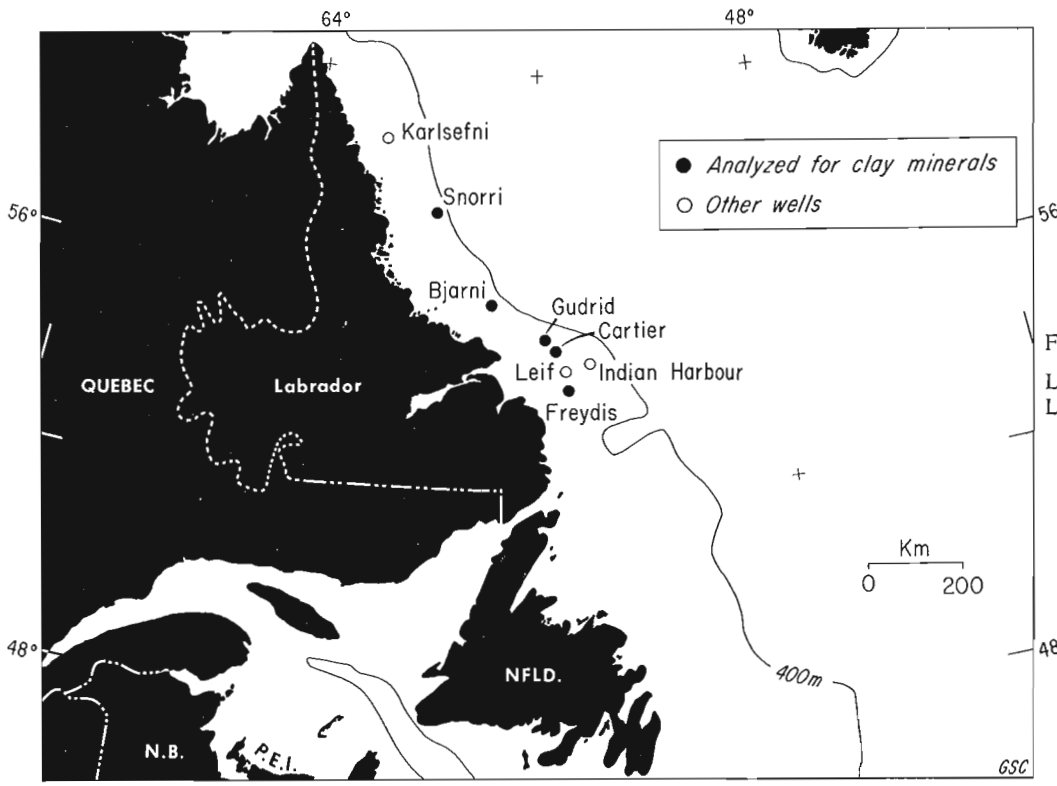

Figure 19.1.

Location of deep wells on the Labrador Shelf.

[1] Acadia University, Wolfville, Nova Scotia.

Stratigraphy

The Labrador Shelf is underlain by a thick clastic wedge which is nowhere exposed on the adjacent onshore areas. Stratigraphic studies (McWhae and Michel, 1975) show that this wedge can be divided into two parts. The lower part is restricted to a fault-bound basin beneath the eastern half of the shelf and contains the following sequences:

Early Barremian to Hauterivian subaerial basalt lavas and associated deposits (continental sands, shales, and aquagene tuffs).

Early Barremian to Albian continental sand.

Albian to late Paleocene or earliest Eocene shallow water sediments – mainly grey shales, locally including thick marginal to nonmarine sands.

The overlying sequence, of early Eocene and younger age, consists primarily of thick, variably silty and sandy turbidites which were rapidly deposited in relatively deep water. This younger sequence is exclusively marine, overlaps the older, geographically-restricted sequence and forms the bulk of the clastic wedge.

Clay Sample Techniques

A total of 184 samples was taken from the five wells. About half the samples were taken at specific horizons; the others were composites taken from a number of intervals. Drilling mud was removed from the cuttings by wet sieving through a 0.056 mm screen. Fragments larger than 2 mm (mainly cavings) were removed at the same time. After disaggregation, the clay minerals were separated and treated using a modification of the method described by Biscaye (1965). Two smear slides were prepared from the <2 µm fraction of each sample. One was glycolated overnight at 80°C in order to fully expand the montmorillonite and mixed clay minerals.

Diffraction Equipment and Methods

All slides were scanned on the same Phillips equipment using a nickel filtered-copper radiation generated from a normal-focus tube driven at 34 RV and 33 MA. Output from the proportional flow counter was further processed through a pulse-height analyser before scaling and recording. A time constant of 4 s was used for both fast (1° 2θ/min) and slow (1/4° 2θ/min) scans. Both glycolated and unglycolated slide mounts were scanned between 2 and 30° at 1° 2θ/min. The glycolated mounts also were re-scanned from 24 to 26° at slow speed (1/4° 2θ/min) to resolve overlapping peaks of kaolinite and chlorite.

Analysis of Diffractograms

The relative abundances of the four major clay minerals were determined from the areas of appropriate diffractogram peaks, essentially following the method of Biscaye (1965). The areas were weighted to correspond more closely to actual mineral abundances. The percentage of each mineral was calculated from the ratio weighted peak area to total peak area. The peaks and weighting factors used were:

1. the area of the 17 nm glycolated peak for montmorillonite;
2. four times the area of the 10 nm glycolated peak for illite; and
3. two times the area of the 7 nm glycolated peak for chlorite plus kaolinite.

The latter peak area was apportioned between chlorite and kaolinite. Biscaye (1965) had determined the areas of the 3.59 nm kaolinite and 3.54 nm chlorite peaks from a slow scan and used the ratio of the two areas to apportion the 7 nm peak area. We found that these peaks were often poorly resolved. After some experimentation with various mixtures

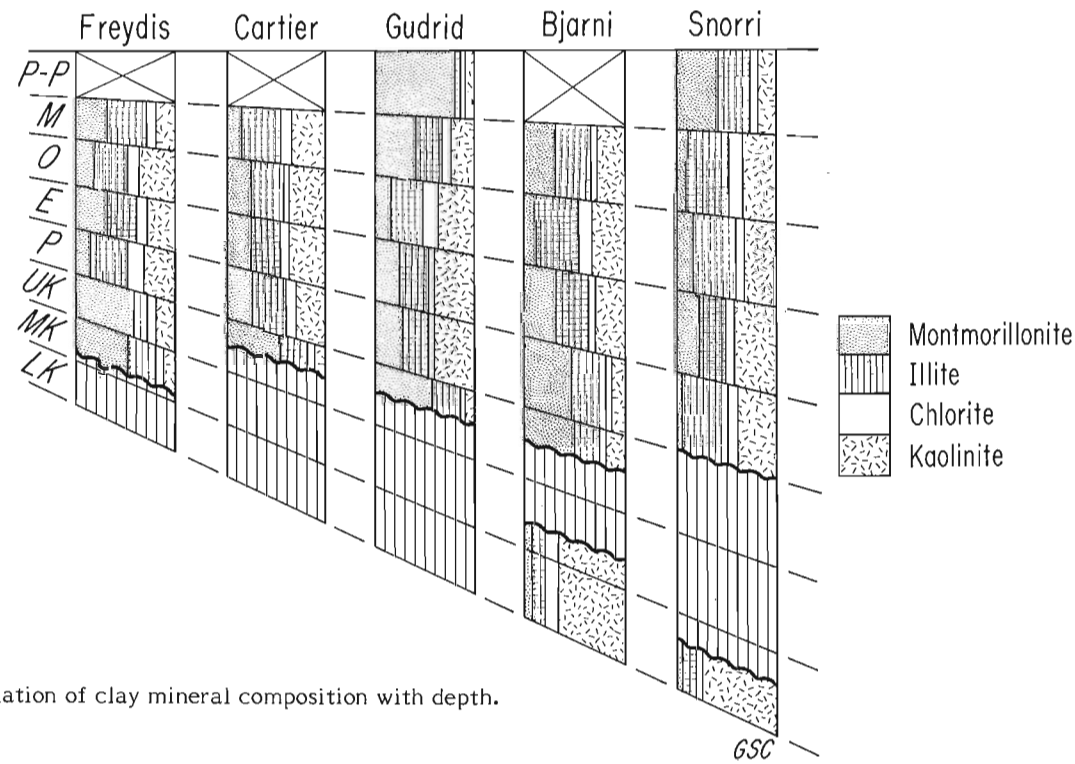

Figure 19.2. Variation of clay mineral composition with depth.

of pure kaolinite and chlorite we were able to calculate the relative amounts of these minerals using peak heights as follows:

1. the relative heights of the peaks at 3.58 nm (kaolinite) and 3.54 nm (chlorite) on the slow scan, and
2. the relative heights of the 4.7 nm peak and the 3.54-3.58 nm combined peak for chlorite plus kaolinite on the fast scan.

The average of the two determinations was used to apportion the 7 nm peak area to kaolinite and chlorite.

Clay Mineral Analysis Results

The plot of average clay analysis versus stratigraphic age (Fig. 19.2) shows a good correlation between clay mineral analysis and stratigraphy in the lower part of section.

The Early Cretaceous sandy sequence in Bjarni H-81 and Snorri J-90 is kaolinite-rich. Montmorillonite is generally predominant in the mid-Cretaceous to Early Paleocene dark shales. Snorri J-90 is an exception to this generalization as here, because of diagenesis in the Paleocene sequence, montmorillonite has been transformed to illite.

Sequences younger than Paleocene show a similar distribution of clay mineral type. In Eocene sediment, montmorillonite, illite, and kaolinite occur in approximately equal amounts; in the Oligocene sequence both illite and kaolinite exceed the proportion of montmorillonite, but in the Miocene sequence the distribution of clay minerals is erratic, illite is generally predominant though the proportions of both kaolinite and montmorillonite are only slightly smaller.

Interpretation of Results

1. The predominance of kaolinite in the clay fraction of early Cretaceous sediments suggest conditions in the source area were characterized by a warm pluvial climate.

2. In mid Cretaceous to early Paleocene sediments the clay fraction is dominated by montmorillonite suggesting that semi-arid, savanna-like conditions prevailed on adjacent provenance areas.

3. Late Paleocene and younger sequences show no preferred clay mineral which suggests a general instability of the clay minerals both in the developing regolith of provenance areas and in the adjacent basins.

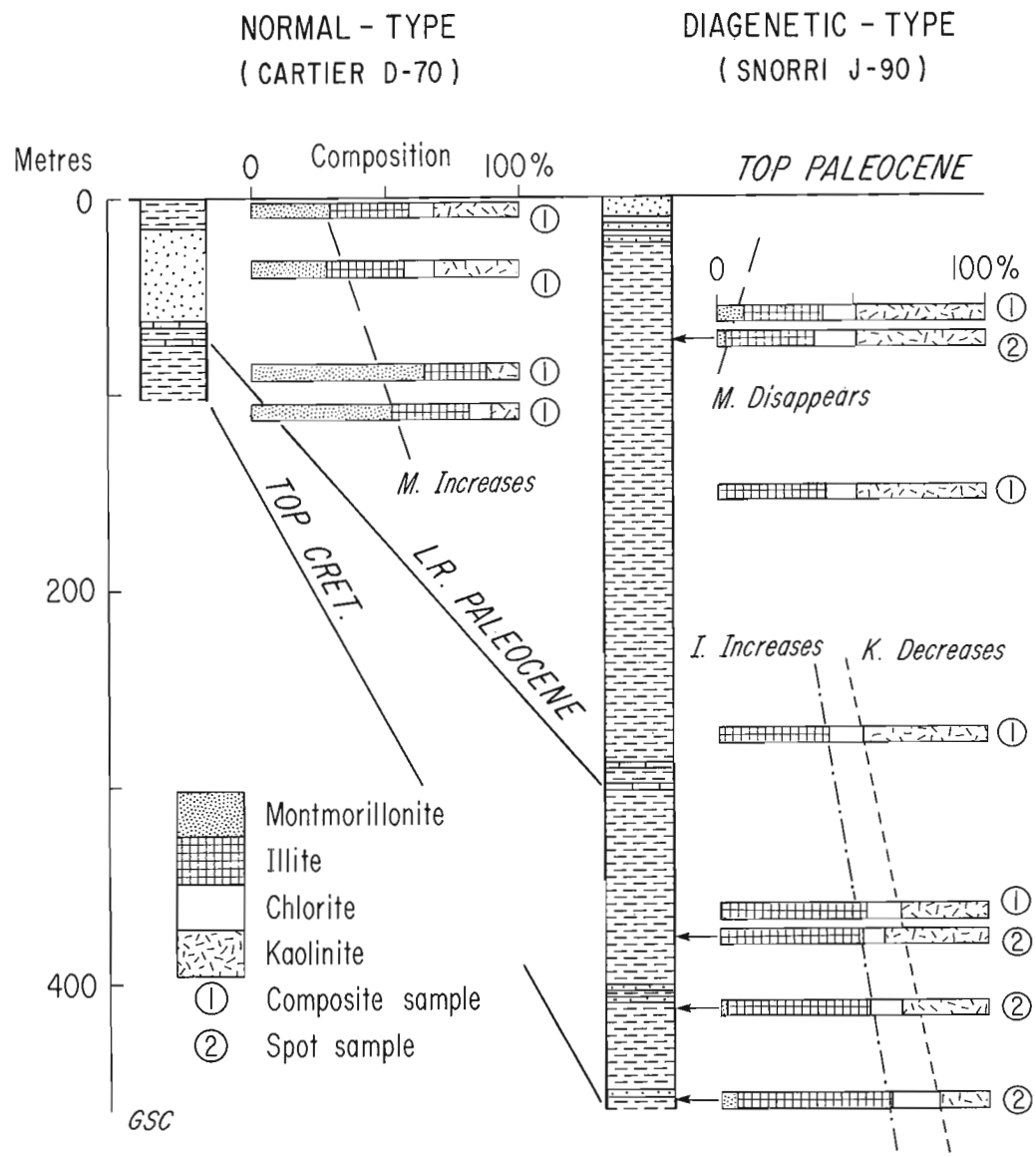

Figure 19.3. Comparison of clay mineral composition of normal and altered Paleocene sequences.

4. In the gas and condensate discoveries, Gudrid H-55 and Bjarni H-81, the reservoir horizon is adjacent to late Cretaceous and Paleocene shales. These shales are in a favourable thermal milieu for the generation of hydrocarbons and therefore are probable source beds. The clay fraction is dominated by montmorillonite. According to currently accepted theories on the relationship between the formation and migration of hydrocarbons and clay-mineral diagenesis, montmorillonite is the only clay mineral capable of expelling large amounts of lattice water. This expulsion of water provides a mechanism for moving hydrocarbons from source beds into adjacent reservoirs.

5. The diagenetic conversion of montmorillonite to illite may be demonstrated in Snorri J-90 (Fig. 3). This well is deeper and penetrated an area of relatively higher heat flow than the other wells (as evidenced by high Ro values of coals and by measured formation temperatures), so more advanced diagenesis is probable. In other wells, Paleocene sediments are dominated by montmorillonite. In Snorri J-90 Paleocene sediments are dominated by illite, the proportion of which increases with depth first at the expense of montmorillonite and with greater depth at the expense of kaolinite. The diffraction peak of illite becomes sharper with depth, another indication that diagenesis has occurred.

References

Biscaye, P.E.
1965: Mineralogy and sedimentation of recent deep-sea clay in the Atlantic Ocean and adjacent seas and oceans; Bull. Geol. Soc. Am., v. 76, p. 803-832.

McWhae, J.R.M. and Michel, W.F.E.
1975: Stratigraphy of Bjarni H-81 and Leif M-48, Labrador Shelf; Bull. Can. Petrol. Geol., v. 23, p. 361-382.

SURFICIAL GEOLOGY: LACHUTE-MONTEBELLO AREA, QUEBEC

Project 740068

S.H. Richard
Terrain Sciences Division

Abstract

Richard, S.H., Surficial geology: Lachute-Montebello area, Quebec; in Current Research, Part B, Geol. Surv. Can., Paper 78-1B, p. 115-119, 1978.

Unconsolidated Quaternary sediments of Lachute-Montebello area, Quebec consist mainly of glacial deposits abandoned by the Wisconsin glacier and of marine sediments deposited during the submergence of the lower parts of the area by the Champlain Sea. The presence of lodgment till overlying subaqueous marine outwash sediments in central Ottawa Valley near Pointe-Fortune is reported for the first time. Fossiliferous diamictons and glaciomarine deposits have been found in the Oka Mountains and in the Laurentian Highlands near Lachute either in the surface glacial deposits or underlying fossiliferous marine beach deposits. Marine sediments deposited in the Champlain Sea basin overlie the glacial deposits in the low-lying areas of the Ottawa-St. Lawrence Lowlands and in the valleys of the Laurentian Highlands. The highest marine shells recovered from these sediments at or near the marine limit were found near Montebello, Calumet, and Grenville at ca. 175 m elevation. The last shoreline of the regressing Champlain Sea was found at the foot of the Oka Mountains near La Trappe at ca. 70 m elevation. Late Champlain Sea deltaic sand plains were built by the early Ottawa River in the St. Lawrence Lowlands between Saint-Philippe-d'Argenteuil and Lachute and between Upper Lachute and Saint-Hermas just before final land emergence. This was followed by a phase of river channel and terrace downcutting through the soft sensitive marine clays and silts of Ottawa Valley and of the St. Lawrence Lowlands by the degrading early Ottawa River.

Field investigation and mapping of the surficial geology of the Lachute (31 G/9, 10, 15, 16) map area have been completed. Studies of the bedrock geology and mineral resources of parts of the map area were carried out intermittently between 1842 and 1925 by Logan (1863, 1864), Ells (1901), and Wilson (1920). Osborne and McGerrigle (1938) reinvestigated the geology of the major part of the map area and studied the unconsolidated Quaternary sediments. Wilson (1946) incorporated earlier works on the bedrock geology of the Ottawa and St. Lawrence Valley Lowlands. The most recent compilation of bedrock geology is provided by Douglas (1978).

Investigations and mapping of the surficial geology of parts of the Lachute map area were carried out by D.A. St-Onge (Kugler-Gagnon, 1977), Laverdière (1972a,b), Laverdière and Guimont (1973). These studies dealt with the area surrounding the International Airport at Mirabel which is located in the southeastern part of the Lachute map area.

The unconsolidated Quaternary deposits in the Lachute map area are well developed in surface extent and thickness over the Paleozoic limestone, dolomite, and sandstone platform of the Ottawa Valley Lowlands and over the Oka Mountains Upland in the south. In the north, however, bedrock outcrops nearly everywhere in the form of bare hilly rock knobs in the Precambrian Shield Uplands, and the unconsolidated deposits are restricted mainly to long, narrow valleys and smaller depressions developed between the intricate maze of bedrock hills and ridges that make up the Laurentian Mountains north of Ottawa and North rivers.

Glacial Deposits

In the Laurentian Highlands glacial deposits are the most widespread surficial deposits, but they make up only about 20 per cent of the land surface. They occur mainly as a discontinuous mantle of lodgment and melt-out till, bouldery and gravelly to sandy in texture, covering the floors and lower sides of valleys and depressions developed between the bedrock hills and knobs forming the major part of the Laurentian Highlands. A thin discontinuous mantle or veneer of till also commonly covers the top and flanks of the bedrock hills between the outcrops. A few morainal ridges have been observed in valleys, but these till deposits are generally hummocky to undulating surfaces without any well oriented features.

The valleys and depressions contain most of the glaciofluvial deposits found in the Precambrian basement Highlands. Fairly thick (>20 m) bodies of well sorted and bedded bouldery cobbly gravel and sand occur in the form of pitted outwash plains, pitted valley trains, and kame terraces in North River valley in three main areas: Sainte-Marguerite, Piedmont, and Saint-Jérôme areas; Rouge River valley around Arundel, McDonald Lake, and Herrington; Petite Rouge River valley between Lac des Plages and Namur and in the valley of its main tributary Petite Rouge River east. These extensive bodies of coarse waterlaid materials were deposited by glacial meltwater at and near the ice margin during the last stage of deglaciation when the remnants of ice were restricted to the main valleys and depressions after the bedrock hills and ridges had become ice free (Parry and MacPherson, 1964, p. 238-239, 242).

In the Ottawa Valley Lowlands, lodgment and melt-out till deposits are found in the form of gently undulating to moderately rolling till plains directly overlying bedrock, most generally in areas where the bedrock outcrops or is near the surface. These till areas make up about 40 per cent of the land surface and occur mainly between Grenville and Saint-Philippe-d'Argenteuil, between Lachute and Saint-Jérôme in a long low ridge south of North River valley, and around Saint Andrews East, Côte-Saint-Vincent and Sainte-Scholastique. The till is grey to brown where weathered and oxidized, compact, calcareous, silty to sandy, with 60 per cent of the clasts and boulders derived locally from the Paleozoic sediments and 40 per cent made up of clasts derived from Precambrian basement rocks of the Laurentian Highlands to the north. The till surfaces in the lowlands lying above 73 m (240 ft.) elevation all have been reworked and modified by the marine waters of the Champlain Sea during submergence of the area. The till surfaces lying below 73 m elevation have been exhumed from under their cover of marine sediments and have been modified by erosion of the early Ottawa River with main channels occurring between Saint-Eugène and

Figure 20.1.

Stratigraphy exposed in an active sand pit 2 km south of Pointe-Fortune on the Ontario-Quebec border. Photo shows 5 to 7 m of "marine" subaqueous outwash sands overlain by 3 to 4 m of till. (GSC 203332-D)

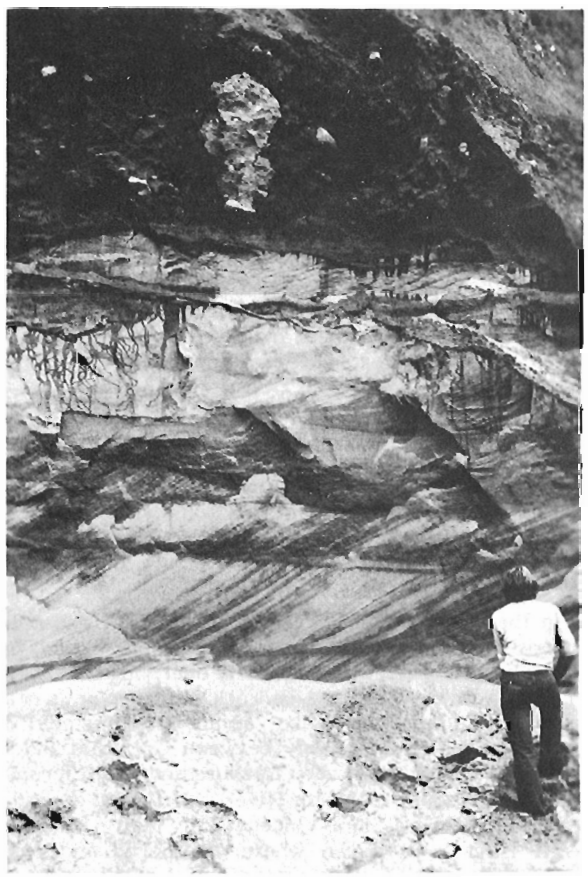

Figure 20.2. Close-up of the same units shown in Figure 20.1 showing contact between a lower unit of well sorted and crossbedded sands overlain by till. (GSC 203332-A)

Pointe-Fortune south of Ottawa River and between the Oka Mountains and the massive bedrock escarpment forming the edge of the Precambrian basement north of North River valley between Lachute and Saint-Jérôme. Only one well developed oriented till ridge was found 2 km east of Saint Andrews East running in a southwest-northeast direction between two Precambrian bedrock hills and barely rising above the cover of marine silty clay that lies over its southern flank.

At one locality 2 km south of Pointe-Fortune on Ottawa River a fresh exposure in an active sand and gravel pit on the Ontario-Quebec border shows a very compact, grey, calcareous, silty, basal or lodgment till, varying in thickness from 2 to 8 m, lying over a well sorted and bedded sand. Only the upper part of the sand is exposed and its thickness varies from 1 to 4 m (Fig. 20.1 and 20.2). No fossils were found in either the till or in the underlying sand, but the sand is believed to be subaqueous outwash deposited in a marine environment. Only one till has been found in Ottawa Valley and rests directly on bedrock at the base of the stratigraphic column: "The borings in Ottawa Valley reveal, on the contrary, that a single, thin till sheet discontinuously overlies bedrock. Since deposition of this till, the Ottawa Valley basin has received the apparently continuous suite of nonglacial sediments briefly described above" (Gadd, 1977, p. 379). The stratigraphy exposed in the Pointe-Fortune pit differs from this simple stratigraphic framework presented by Gadd for the sedimentological history of Ottawa Valley.

In the Oka Mountains, a grey, compact, calcareous, lodgment till with numerous clasts of striated blue Ordovician limestone mantles most of the ground surface between protruding bare rock knobs of the Precambrian basement and of remnants of eroded Cretaceous volcanic plugs. In all gravel pits and in roadside ditches up to 2 m deep this till unit, whether at the surface on the northern or western flanks of the Oka Mountains or under fossiliferous marine beach gravel and sand deposits, contains abundant specimens of marine macrofossil shells, either broken or whole, in its matrix. At eight localities west of Saint-Joseph-du-Lac and north of La Trappe, samples of this fossiliferous till have been recovered and have yielded numerous specimens of **Portlandia arctica, Hiatella arctica, Balanus hameri, Macoma balthica,** and **Mytilus edulis** (Fig. 20.3). The presence of marine shells in the matrix of the surface till at these localities suggests that the glacial deposits in the Oka Mountains were derived from

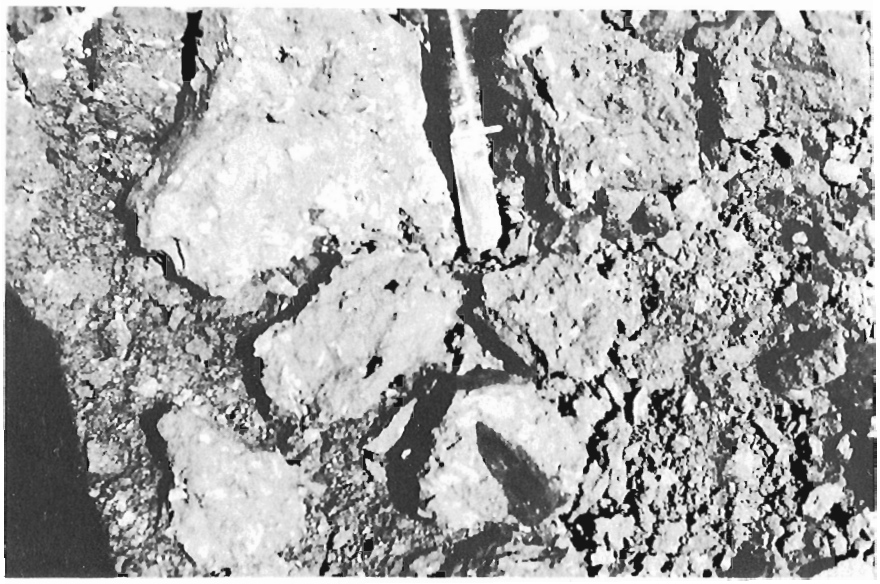

Figure 20.3.

Fossiliferous till showing shells of **Hiatella arctica** and **Balanus hameri** dispersed in the matrix of the till, 3 km west of Saint-Joseph-du-Lac. (GSC 203332-F)

fossiliferous marine beds overridden by the readvancing or fluctuating ice margin of the Laurentide Ice Sheet in the Champlain Sea. Radiocarbon dates on some of the marine shell samples recovered from this till unit will help to indicate the time when the event took place (Hillaire-Marcel, 1974, p. 409-410, 415-416).

In the Precambrian basement Highlands north of the lowlands, fossiliferous stony glaciomarine deposits have only been found 7 km northeast of Lachute, Quebec in a borrow pit under a Champlain Sea marine beach. This fossiliferous diamicton appears to consist of marine clay beds to which was added a mixture of boulders, pebbles, and deformed beds of marine shells by the advance or fluctuation of the ice margin. Marine shells identified include **Hiatella arctica** and **Balanus hameri.** The diamicton is underlain by unfossiliferous ice-contact gravels and cobbles (Fig. 20.4, 20.5) (Hillaire-Marcel, 1974, p. 409-411, 416).

In the lowlands, ice-contact and ice-marginal outwash deposits are not well developed as surface deposits. They are found mainly in the Oka Mountains west of Saint-Joseph-du-Lac and north of La Trappe in the same gravel pits that have yielded the fossiliferous diamictons described above and west of Saint Andrews East between North and Ottawa rivers. One possible interpretation of this paucity is that after the ice front abandoned its position against the northern flank of the Oka Mountains, where it remained well grounded and stabilized for a time resulting in the construction of concentrated and localized ice-marginal subaqueous outwash bodies on the Champlain Sea floor, it receded northward in standing marine waters mainly by calving without deposition of outwash until the ice margin reached the Precambrian basement Highlands north of Grenville, Lachute, and Saint-Canut.

Marine Sediments

Postglacial marine sediments deposited by the Champlain Sea, following the withdrawal of Laurentide ice, are less widespread than glacial deposits and make up only about 15 per cent of the land surface of the map area. The most important of these in area and size are grey, massive, calcareous, fossiliferous marine clays and silts. They are best developed in Ottawa Valley between Montebello and Saint-Placide and in the St. Lawrence Lowland between the Oka Mountains and the Laurentian Highlands where they were deposited in long, in places narrow, erosional depressions and wider basins developed in flat-lying Paleozoic limestones, sandstones, and dolomites. In the Laurentian Highlands deposition was restricted to the long narrow valleys of North, Rouge, Maskinongé, and Petite Rouge rivers and their main tributaries where the deposits are thick in places. In the Ottawa-St. Lawrence Lowlands, these primary surface deposits form gently sloping clay plains rising highest in the west (102 m, 335 ft.) near Montebello, 91 m (300 ft.) near Grenville and Brownsburg, 71 m (235 ft.) near Mirabel and Saint-Jérôme and 68 m (225 ft.) near Saint-Augustin and La Trappe. In the long narrow valleys of the Laurentian Highlands the small marine silty clay flats are at much higher elevations: in Petite Rouge River valley clay was found at 205 m (675 ft.) and near Namur at 216 m (710 ft.); in Maskinongé River valley at 205 m (675 ft.) near Boileau and 194 m (640 ft.) near Brookdale; in Rouge River valley at 190 to 194 m (625 to 640 ft.) near Gray Valley, at 194 m (640 ft.) at Huberdeau, 192 m (635 ft.) at Arundel, 197 m (650 ft.) near Bevin Lake, 192 m (635 ft.) at Batesville, 190 to 194 m (625 to 640 ft.) near Rouge Valley; and in North River valley at 205 m (675 ft.) near Sainte-Adèle, 205 m (675 ft.) near Mont-Rolland, 194 m (640 ft.) at Saint-Sauveur-des-Monts, and 194 m (640 ft.) near Shawbridge. In these valleys on the Laurentian Highlands the clay is grey, blocky, massive, and lacks fossils except in the southernmost parts of the valleys near Ottawa Valley. In the Ottawa-St. Lawrence Lowlands on the other hand, the marine clay is grey, blocky, and massive, but the upper part of the unit shows horizontal red bands alternating with grey bands. At one locality near Killowen, 5 km north of Saint-Placide, fossil marine shells of **Hiatella arctica** and **Macoma balthica** with their periostracum intact were found in situ along the locally sandy bedding planes separating the red bands from the grey bands. This proves marine deposition of these banded sediments.

In the Laurentian Highlands the narrow marine clay flats commonly are mantled by a coarser cover, which varies in texture from fine sand to fine gravel, and which is grey but weathers to orange buff near the surface. The cover is thickest where deltas were constructed at the heads of the narrow fiords created by the drowning of the lower parts of the valleys by the submergence of the Champlain Sea. The highest elevations at which deltaic deposits are found may be assumed to be the marine limit in each valley: in Petite Rouge Valley at 220 m (725 ft.) near Namur; in Maskinongé Valley at 220 m (725 ft.) near Lac-Rémi; in Iroquois Valley, tributary to Rouge River at 220 m (725 ft.) near Rockway Valley; in Rouge Valley at 220 to 225 m (725 to 740 ft.) near Arundel; and in North Valley at 225 to 228 m (740 to 750 ft.)

Figure 20.4.

Exposure 7 km northeast of Lachute, Quebec in an active gravel pit showing a fossiliferous unsorted clayey diamicton underlain by unfossiliferous gravel and cobbles. (GSC 203332)

Figure 20.5.

Fossiliferous clayey diamicton shown in Figure 20.4. Shells exposed include **Hiatella arctica** and **Balanus hameri.** (GSC 203332-E)

near Sainte-Adèle. No marine fossils have been found in these deltaic sands except in the southernmost parts of the valleys near Ottawa River where fossil shells of **Hiatella arctica, Balanus hameri, Mytilus edulis,** and **Macoma balthica** have been recovered at elevations varying from 145 to 160 m (475 to 525 ft.) from localities 5 km north of Montebello, 1.5 km north of Pointe-au-Chêne, and 3 km north of Calumet. The marine limit recorded by the highest fossiliferous beach deposits along the southern flank of the Laurentian Highlands between Montebello, Lachute, and Saint-Jérôme is much lower than that recorded by deltaic deposits farther north near the heads of the former fiords. Highest marine shell localities show that the marine limit lies at ca. 168 to 175 m (550 to 575 ft.) 5 km north of Montebello, 168 to 175 m (550 to 575 ft.) 3 km north of Calumet, 175 m (575 ft.) 7 km north of Grenville, and 182 m (595 ft.) 4 km northwest of Brownsburg.

In the Oka Mountains numerous well developed beach deposits were found over till or ice-marginal outwash deposits covering the northern flank between elevations of 160 m (525 ft.) for the highest one and 84 m (275 ft.) for the lowest one 2 km west of Saint-Joseph-du-Lac. Marine shells were recovered from all these shoreline features, and radiocarbon age determinations on the highest and lowest samples should help to date the first and last stands of the Champlain Sea in this area.

In the lowland, a few poorly developed fossiliferous beach deposits are present above 70 m (230 ft.) elevation. The best developed and lowest fossiliferous marine beach was found near La Trappe at 70 m elevation (Richard, 1976, p. 208). Abandoned deltas of early Ottawa River are well developed between Watson, Saint-Philippe-d'Argenteuil, and Lachute, between St. Andrews East and Lachute, and between Saint-Benoît and Lachute where extensive deltaic sand plains have been built at 70 to 77 m (230 to 255 ft.) over the primary marine clay surface. No fossils were found in these deltaic sand deposits. As a result of continued glacio-isostatic uplift of the land, this delta construction phase in the Ottawa-St. Lawrence Lowlands was followed by a phase of channel downcutting by the early Ottawa River. This resulted in the production of numerous unfossiliferous alluvial channel and terrace sand deposits east and south of Chute-à-Blondeau and between Cushing, Lachute, and Saint-Canut in North River valley which was used by the early Ottawa River

as its first channel across the lowlands. South and east of Lachute, the channelling phase of the early Ottawa River also produced several generations of now abandoned river channels and erosional terraces cut into the uplifted marine clay plains below 70 m (230 ft.) elevation. This river channelling through soft clay persisted across the lowlands north of Oka Mountains until the degrading early Ottawa River exposed underlying glacial drift and bedrock in each channel. The more resistant materials stopped channel downcutting causing successive abandonment.

The phase of channel downcutting by the early Ottawa River removed large quantities of marine clay from the lowlands and from a central belt on either side of Ottawa River and also produced a large number of abandoned river bluffs cut in sensitive marine clays. At least two massive slope failures and mass movements have occurred; one is 4 km northeast of Saint Andrews East and the other is 2 km southeast of Saint-Philippe-d'Argenteuil. They occur along the uppermost and highest abandoned river-cut bluff and have resulted in the production of aprons and fans of hummocky topography of tilted or slumped clay and sand blocks on the floor of the abandoned channels (MacPherson, 1967, p. 343-360).

Following deglaciation in the Highlands and land emergence in the lowland, a large number of marshes and peat bogs developed where swales of the undulating and uneven ground moraine, of the recently ice-freed rock basins and of the abandoned river channel floors were poorly drained.

References

Douglas, R.J.W. (general co-ordinator)
1978: Geology, Rivière Gatineau, Quebec-Ontario; Geol. Surv. Can., Sheet 31, Geological Atlas, Map 1334A, scale 1:1 000 000.

Ells, R.W.
1901: Geology, Grenville map-area; Geol. Surv. Can., Map no. 750, with Ann. Rep., v. XII, pt. J., map-sheet no. 121.

Gadd, N.R.
1977: Offlap sedimentary sequence in Champlain Sea, Ontario and Quebec; in Report of Activities, Part A; Geol. Surv. Can., Paper 77-1A, p. 379-380.

Hillaire-Marcel, C.
1974: La déglaciation au nord-ouest de Montréal: données radiochronologiques et faits stratigraphiques; Rev. Géogr. Montr., vol. XXVIII, no. 4, p. 407-417.

Kugler-Gagnon, M.
1977: The geoscientific information system for the North Montreal Region; Geol. Surv. Can., Paper 76-26, 15 p.

Laverdière, C.
1972a: Les paysages physiques; leur origine morphogénétique; Univ. Montréal, CREM (Ecologie de la Zone de l'Aéroport international de Montréal), 102 p., ill.

1972b: La carte géomorphologique; notes explicatives; Univ. Montréal, CREM (Ecologie de la Zone de l'Aéroport international de Montréal), 144 p., ill.

Laverdière, C. et Guimont, P.
1973: La roche en place; Univ. Montréal, CREM (Ecologie de la Zone de l'Aéroport international de Montréal), 152 p., ill.

Logan, W.E. (and others)
1863: Geology of Canada, 1863; Geol. Surv. Can., Rept. Prog. from its commencement to 1863, Montreal, Dawson Brothers.

1864: Atlas accompanying Geology of Canada, 1863; Geol. Surv. Can.

MacPherson, J.C.
1967: Raised shorelines and drainage evolution in the Montreal Lowland; Cah. Géogr. Qué., v. 23, p. 343-360.

Osborne, F.F. and McGerrigle, H.W.
1938: Lachute map-area. Part I General and applied geology, Part II The Lowland Area; Que. Bur. Mines, Ann. Rep., Pt. C, p. 5-68, Map 408 E/2 and W/2.

Parry, J.T. and MacPherson, J.C.
1964: The St. Faustin-St. Narcisse Moraine and the Champlain Sea; Rev. Géogr. Montr., v. XVIII, no. 2, p. 235-248.

Richard, S.H.
1976: Surficial geology mapping: Valleyfield-Rigaud area, Quebec; in Report of Activities, Part A; Geol. Surv. Can., Paper 76-1A, p. 205-208.

Wilson, A.E.
1946: Geology of the Ottawa-St. Lawrence Lowland, Ontario and Quebec; Geol. Surv. Can., Mem. 241, 62 p.

Wilson, M.E.
1920: Geology, Map 1680; Geol. Surv. Can.

21. BASE METAL AND URANIUM DISTRIBUTION ALONG THE WINDSOR-HORTON CONTACT, CENTRAL CAPE BRETON ISLAND, NOVA SCOTIA

Project 700059

R.V. Kirkham
Regional and Economic Geology Division

Abstract

Kirkham, R.V., Base metal and uranium distribution along the Windsor-Horton contact, central Cape Breton Island, Nova Scotia; in Current Research, Part B, Geol. Surv. Can., Paper 78-1B, p. 121-135, 1978.

Copper, lead, and zinc have been known for some time to occur in minor amounts at widely scattered localities along the Windsor-Horton contact and anomalous amounts of uranium have recently been discovered in rocks near this contact in the South Maitland area of mainland Nova Scotia. In some localities in central Cape Breton Island, geological and geochemical studies have demonstrated that copper, lead, and/or zinc contents in these rocks approach ore concentrations and warrant further investigation but that, in general, these rocks have lower uranium concentrations than similar strata in the South Maitland area of mainland Nova Scotia.

Base metal deposition probably occurred during early diagenesis and was related to ordinary, albeit rather specialized, early diagenetic, sedimentary processes.

Introduction

Over the past few years, as part of general investigations of copper deposits in Canada, the writer and various colleagues have studied the distribution of base metals along the Windsor-Horton or stratigraphically equivalent contacts throughout the Atlantic Provinces (e.g. Kirkham, 1974; Binney and Kirkham, 1974, 1975; Binney, 1975a, b; Worley, 1975; Geldsetzer, 1977). The main reason for concentrating effort on the Windsor-Horton contact is because these rocks show many similarities to the Permian Zechstein-Rotliegendes contact (Kupferschiefer) in central Europe and to many other important sedimentary copper deposits throughout the world. The Windsor-Horton contact affords an excellent opportunity to study such sedimentary environments in Canada.

Sparse base metal occurrences are widely distributed along the Windsor-Horton contact (e.g. Binney, 1975a; Binney and Kirkham, 1975) but to date none of these occurrences have proved to be of economic importance. Since 1973 an attempt has been made to document and sample as many outcrop localities and diamond drill cores as possible through the Windsor-Horton contact. Samples collected have been analyzed for a variety of elements but only Cu, Pb, Zn, and U are reported here. Data from central Cape Breton Island were chosen for publication because there are more sample sites in this region than elsewhere and significant new information has been obtained for the Yankee Line road area.

General Geology

The Windsor-Horton* contact is the focus of this study. Figure 21.1 shows the general distribution of Windsor Group and Horton Group rocks in central Cape Breton Island and Figure 21.2 shows sample sites and localities referred to in the text. Most of these localities have been described previously by Binney (1975a).

In most parts of the area under consideration, dark, algal-laminated, micritic basal A_1 (Macumber) limestone or dark, argillaceous, micritic limestone ("Frenchvale-Lake Enon facies") of the Windsor Group sits apparently conformably on coarse continental clastic rocks of the Horton Group (Fig. 21.3). Most upper Horton strata display shades of red with from 10 cm to 20 m of pale green-grey, "bleached" material immediately beneath the anoxic Windsor limestone. In most areas the uppermost Horton is conglomeratic and shows no signs of reworking. Nevertheless, at some localities, such as East Bay (loc. 10) imbricated, reworked (?), green cobble conglomerate, that conceivably might be beach deposits, occurs on top of the red conglomerate. If this green conglomerate has been reworked it should more properly be considered part of the Windsor Group. However, for this study all the coarse clastic rocks beneath the A_1 or basal micritic limestone in the central Cape Breton Island area are considered part of the Horton Group. At some localities outside the area, such as Findlay Beach and Lakevale (Binney, 1975a; Binney and Kirkham, 1975), thin, conformable, green-grey conglomerate units beneath the A_1 limestone sit unconformably on top of older, red clastic sedimentary rocks. These thin conglomerate units might be hiatal lag deposits or related to high energy environments that existed briefly during the initial Windsor transgression. Until their environments of formation can be ascertained, it is uncertain if these thin conglomerate beds belong to the Windsor or Horton Group. Except for the northwestern part of the study area, where arkosic sandstone underlies basal Windsor limestone, most of the upper Horton consists of pebble to boulder conglomerate with variable amounts of sand or silt matrix. In general the conglomerate thins and becomes finer grained to the north and west.

About 5 to 15 m of typical, algal-laminated, pelletal, micritic, slightly pyritic, medium grey A_1 limestone is the basal unit of the Windsor Group throughout most of the area northwest of a line extending from Squire Point (loc. 32) through Christmas Island (loc. 12 and 13) to Sugarcamp (loc. 6) (Fig. 21.2 and Geldsetzer, 1977). A thick section of typical A_1 limestone also occurs to the southeast of this line in the Soldier Cove (loc. 4) area. In the area extending from Frenchvale (loc. 11) through East Bay (loc. 10) to Lake Enon (loc. 3) (Fig. 21.2) the basal Windsor is characteristically a dark, slightly pyritic, micritic, argillaceous limestone ("Frenchvale-Lake Enon facies") that shows some similarities to typical A_1 limestone but is probably a distinct, argillaceous facies deposited closer to the main shoreline of the lower Windsor basin (Geldsetzer, 1977). Dark grey, micritic, fenestral limestone with scattered chalcopyrite and pyrite at Black River (loc. 5) and pale, brachiopod limestone at Englishtown (loc. 33) sit directly on basement.

* Horton in the Sydney area has previously been referred to as Grantmire (e.g. Bell and Goranson, 1938; Kelley, 1967; Weeks, 1954).

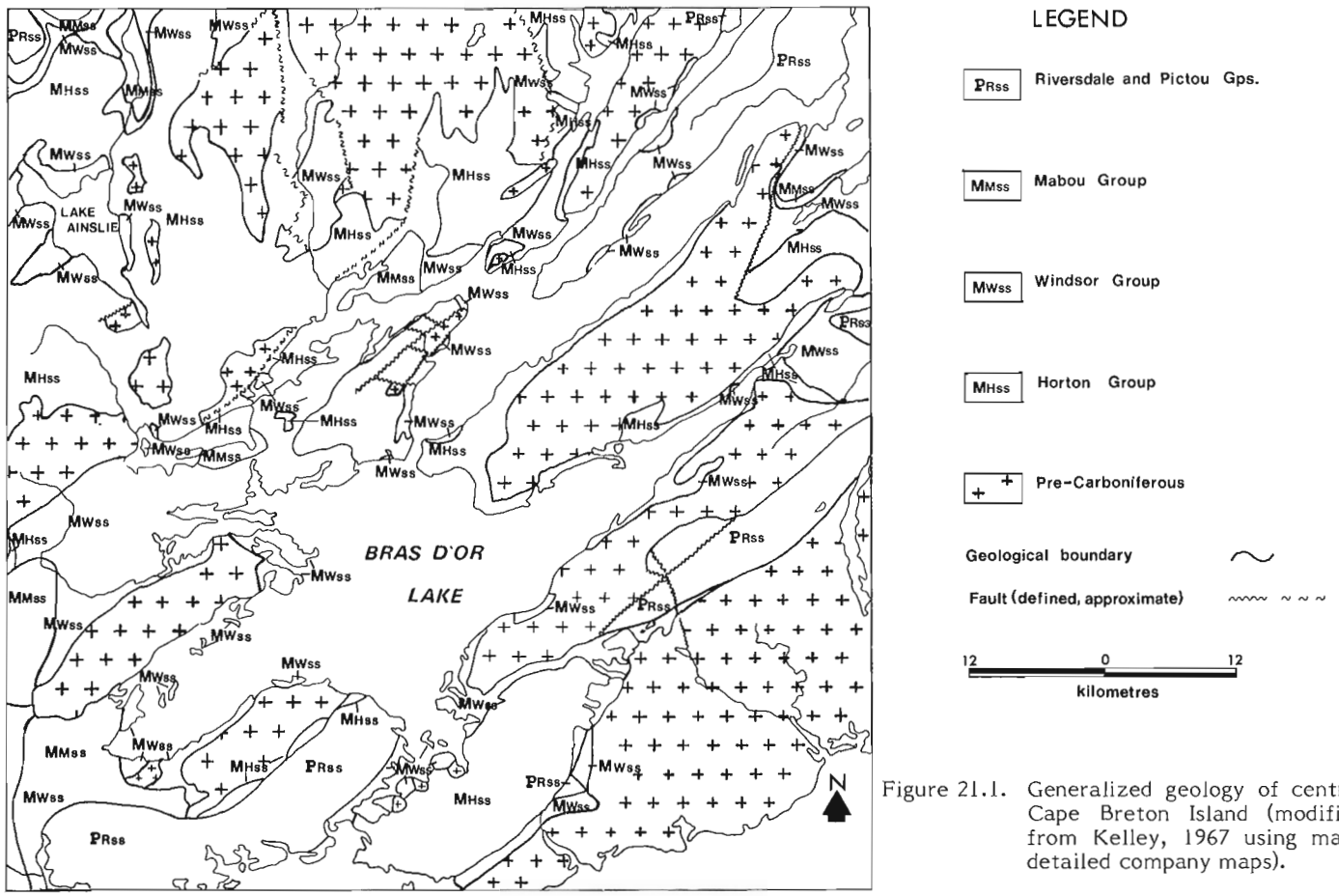

Figure 21.1. Generalized geology of central Cape Breton Island (modified from Kelley, 1967 using many detailed company maps).

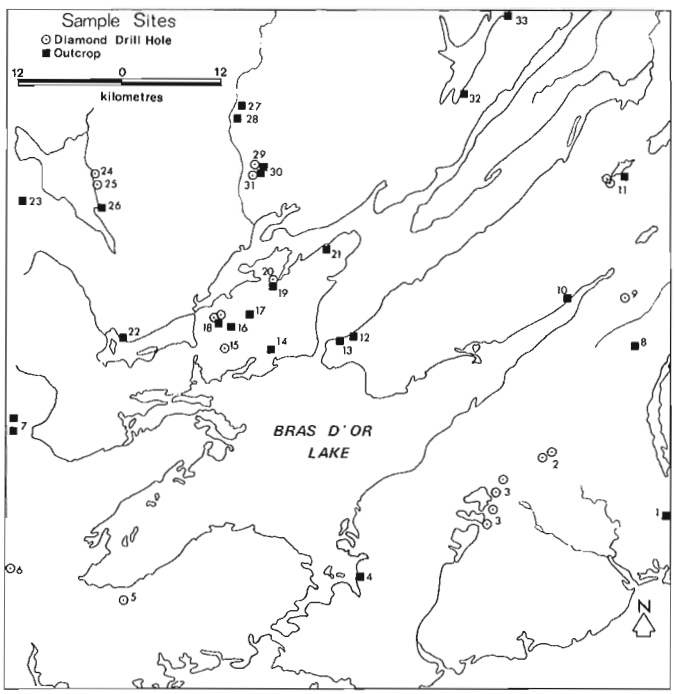

Figure 21.2. Map showing sample sites and localities referred to in text. Locality names are listed in Tables 21.1 and 21.2.

Information based on examination of diamond drill cores indicates that in most parts of central Cape Breton Island basal Windsor limestone is overlain directly by a thick sequence (about 300 m) of evaporites. In the Frenchvale-Lake Enon area the overlying strata consist of interlayered evaporites, carbonates, and fine grained clastic sediments with a few thin conglomerate units at Lake Enon and at Point Edward in the Sydney area (Bell and Goranson, 1938; Geldsetzer, 1977).

The A_1 limestone generally has been considered to be unfossiliferous and in recent years considerable debate has arisen as to whether lithologies of the A and B biostratigraphic subzones of Bell (1929) are time-equivalent or time-transgressive (Schenk, 1969). Mamet (1970) and Utting (1977, 1978) suggest, on the basis of microfauna and spores respectively, that the A and B subzones are probably time-equivalent.

During the course of the present investigation brachiopods were noted in basal Windsor limestones at East Bay (loc. 10), Frenchvale (loc. 11), Christmas Island (loc. 12, 13), Red Point Road (loc. 14), Walker Road (loc. 16), Cains Mountain Road (loc. 17), and Grass Cove Road (loc. 19) (Fig. 21.2). M.J. Copeland of the Geological Survey examined these fossils and described most of them as "indeterminate" (Report No. MP-8-1977-MJC). However, for the Christmas Island pit section (sample KQ-75-40; loc. 12, Fig. 21.2) he identified "**Composita** sp., echinoderm? debris"; for the Christmas Island shoreline section (sample KQ-75-41; loc. 13, Fig. 21.2), "**Composita** sp., trilobite? fragment", and Red Point Road (sample KQW-75-1H; loc. 14, Fig. 21.2) "**Composita**? sp.". In his report Copeland states: "The faunal list of Bell (1929, p. 66) does not show the presence of brachiopod or echinoderm? debris in Windsor Subzone A. **Composita**, however, is indicated as common in Subzone B".

Figure 21.3.

Typical A_1 (Macumber) limestone conformably overlying Horton conglomerate. Christmas Island, Nova Scotia (GSC 3-20-73).

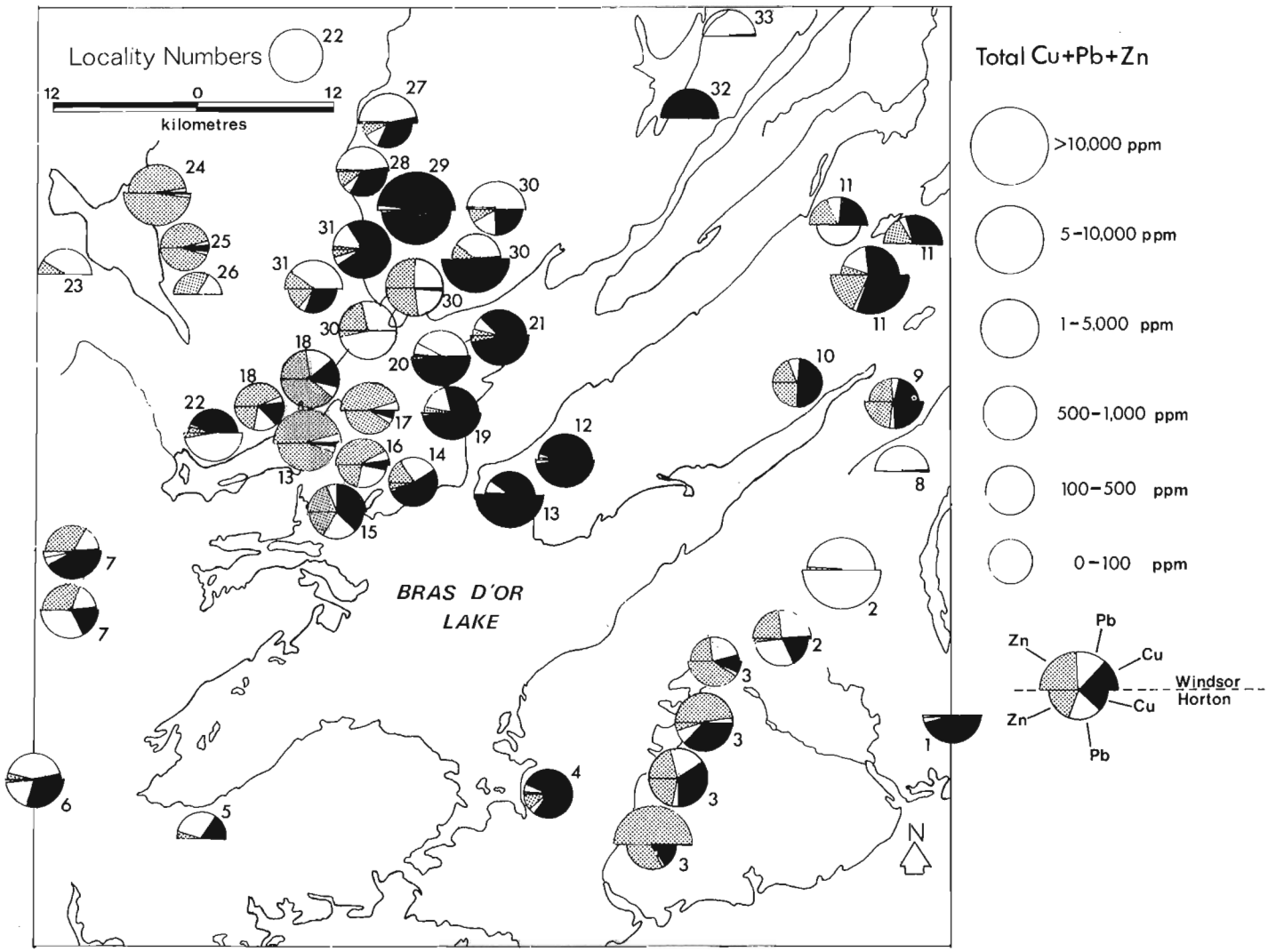

Figure 21.4. Diagram showing regional metal variations along the Windsor-Horton contact in central Cape Breton Island.

Table 21.1

Uppermost Horton Analysis

Loc. No.[1]	Locality	Sample No.[2]	Cu[3]	Pb[3]	Zn[3]	U[3]	R%Cu[4]	R%Pb[4]	R%Zn[4]	Description[5]
1.	McIntyre Lake	KQB-73-26C	1364	111	60	2.5	88.9	7.2	3.9	dark grey, limy ark; cp
2.	Big Barren	BB-74-3-705.8-706'(Amax)	210	360	30	4.8	35.0	60.0	5.0	grey, silty ark; py
		BB-74-23-322.3'(Amax)	30	25000	80	6.3	0.1	99.6	0.3	green-grey cg; gn
3.	Lake Enon	212-1-74-195' (Noranda)	20	57	100	2.1	11.3	32.2	56.5	green-grey ark; py
		212-2-74-167.2'(Noranda)	80	15	160	10.8	31.4	5.9	62.7	grey, gritty mudstone
		L.E.163-149' (Kaiser)	1200	190	1090	3.5	48.4	7.7	43.9	green cg
		L.E.124-240' (Kaiser)	3000	700	600	24.8	69.8	16.3	13.9	green cg
		212-11-74-560' (Noranda)	140	30	550	3.2	19.4	4.2	76.4	green cg; py
4.	Soldier Cove	KQB-74-66(-2')	158	29	58	2.7	64.5	11.8	23.7	green pebble cg
5.	Black River									
6.	Sugarcamp	S-1-384.5' (Rio Tinto)	2800	1800	200	10.7	58.3	37.5	4.2	green cg; py
7.	Diogeness Brook	KQ-77-20A	80	1775	3060	5.7	1.6	36.1	62.3	green ark cobble to boulder cg
		KQ-77-21B	1080	300	130	3.0	71.5	19.9	8.6	green ark pebble to cobble cg; py, mala
8.	Huntington Mtn.									
9.	Glen Morrison	GM-1-21' (Imperial)	595	68	588	7.5	47.6	5.4	47.0	
10	East Bay	KQB-73-1(8)	180	59	256	4.6	36.4	11.9	51.7	green-grey pebble to boulder cg; mala
11	Frenchvale (Coxheath)	67-10-212½' (Mariner)	3485	275	2225	13.0	58.2	4.6	37.2	green, silty pebble cg
		70-4-559' (Cerro)	11	2	31	1.5	25.0	4.5	70.5	pale green pebble cg
12	Christmas Island (Pit)	KQB-73-6B	4800	100	30	4.1	97.4	2.0	0.6	green ark and cg; mala
13	Christmas Is.(Shore RR)	KQB-73-7B	6500	14	30	6.3	99.3	0.2	0.6	green, ark cg; mala
14	Red Point Road	KQW-75-1B	430	18	50	4.5	86.3	3.6	10.0	green-grey, ark cg
15	Iona Rear	IR-74-2-134.2'-134.3' (Amax)	130	230	180	1.3	24.1	42.6	33.3	grey, ark cg
16	Walker Road	KQW-75-4B	40	255	200	1.5	8.1	51.5	40.4	green-grey cg; py
17	Cains Mtn. Road	KQW-75-3A	40	27	310	0.9	10.6	7.2	82.2	green-grey cg; py
18	Jubilee	TG-2-41' (Texas Gulf)	262	93	2880	1.4	8.1	2.9	89.0	pale green-grey, ark pebble cg; sp, gn, py
		TG-14-200.0'-200.8'(TG)	350	300	2200	3.9	12.3	10.5	77.2	medium green-grey, silty pebble cg; sp,gn,py
		ATG-8-398' (Amax-TG)	118	156	198	2.7	25.0	33.0	41.9	medium green-grey ark; py
19	Grass Cove Road	KQ-75-45A	1200	11	20	1.9	97.5	0.9	1.6	green, ark pebble cg; py
20	Iona Cross Road	141-3-552' (St. Joe)	1533	29	16	3.2	97.1	1.8	1.0	green-grey, ark pebble cg; mala
21	Washabuck	KQB-73-17B	950	18	60	9.1	92.4	1.8	5.8	green ark; cp, mala
22.	Whycocomagh	KQB-74-100 (-0')	4150	99	50	3.5	96.5	2.3	1.2	green cg
23.	Hay River									
24.	Glenmore	137-2-329' (St. Joe)	145	220	5420	1.4	2.5	3.8	93.7	medium grey ark; py
25.	East Side Brook	137-1-92 1/3' (St. Joe)	32	40	400	3.0	6.8	8.5	84.7	pale to medium grey ark
26.	Trout River									
27.	Upper Middle River	KQB-74-76A	75	28	20	1.0	61.0	22.8	16.3	green-grey ark
28.	McRae Brook	KQB-74-77A	150	25	50	1.8	66.7	11.1	22.2	green ark; py
29.	Yankee Line	Y.L.-3-207.2'(NSDM)	6540	34	44	3.5	98.8	0.5	0.7	grey, ark cg; cp, py, mala
30.	Yankee Line (Roadcut)	KQ-77-23B	260	180	100	1.3	48.1	33.3	18.5	weathered, green pebble cg
		KQB-73-19A	7100	26	40	1.6	99.1	0.4	0.6	green-grey ark cg; mala
30.	Yankee Line (Stream)	KQ-77-22DD	120	1420	1900	2.5	3.5	41.3	55.2	green-grey pebble cg; py, gn
		KQ-73-18A	25	930	70	-	2.4	90.7	6.8	grey, ark cg; py
31.	Yankee Line	MR-75-1-145'-145.3' (Getty)	910	125	98	2.0	80.3	11.0	8.6	pale green, ark cg
		MR-75-2-77½' (Getty)	230	16	107	4.0	65.2	4.5	30.3	medium green ark and pale green pebble cg
32.	Squire Point									
33.	Englishtown									
		AVERAGE	1263	879	592	4.4	46.2	32.2	21.6	

[1] Locations are shown on Figure 21.2.

[2] Footages are either drillhole depths or +or-stratigraphic distances from contact. Corporations responsible for drill holes are given in brackets.

[3] Cu, Pb, Zn, and U values in parts per million. Uranium analyses by neutron activation and most copper, lead, and zinc analyses by atomic absorption.

[4] R%Cu, R%Pb, R%Zn equal $\frac{Cu}{Cu+Pb+Zn} \times 100$; $\frac{Pb}{Cu+Pb+Zn} \times 100$; $\frac{Zn}{Cu+Pb+Zn} \times 100$, respectively.

[5] Abbreviations: ark = arkosic, arkose; bn = bornite; cc = chalcocite; cp = chalcopyrite; cg = conglomerate; gn = galena; ls = limestone; mala = malachite; py = pyrite; and sp = sphalerite.

Although faunal data are meagre for the three A_1 limestone localities referred to above, they lend support to the concept that A and B biostratigraphic subzones of Bell overlap in time.

Base Metal Distribution

Tables 21.1 and 21.2 list the base metal contents of samples collected from uppermost Horton and lowermost Windsor Rocks, respectively. Figure 21.4 illustrates the regional variations of metal values and ratios. Most samples represent a stratigraphic thickness of 2 to 10 cm. These samples should establish regional metal variations, if indeed such variations exist. These samples were chosen for analysis because the Windsor-Horton contact is easily recognized over a large area and because it represents a very diagnostic geological event, namely a rapid, extensive marine transgression over continental red beds, and because this is a prime stratigraphic site for sedimentary copper deposition. Samples for chemical analyses were collected from many stratigraphic profiles across the contact, but only chemical profiles for the Yankee Line road area are reported in this paper. Some such chemical profiles for the Lake Enon area have been reported by Binney (1975b).

Copper, lead, and zinc contents and ratios vary markedly along the Windsor-Horton contact from one locality to another (Tables 21.1, 21.2; Fig. 21.4). Detailed studies in some areas indicate that metal values tend to be erratic and vary widely on a local scale. For these areas the metal distribution probably is locally controlled and it is questionable whether these metal values conform to any broad-scale, regional pattern. Nevertheless, exploration work in other areas such as Frenchvale (loc. 11, Fig. 21.3) has indicated that reasonably consistent metal values (0.2 to 0.3% Cu) over a thickness of about 1 m can be traced for as much as 5 km along strike. In such areas controls on base metal distribution were of more regional extent.

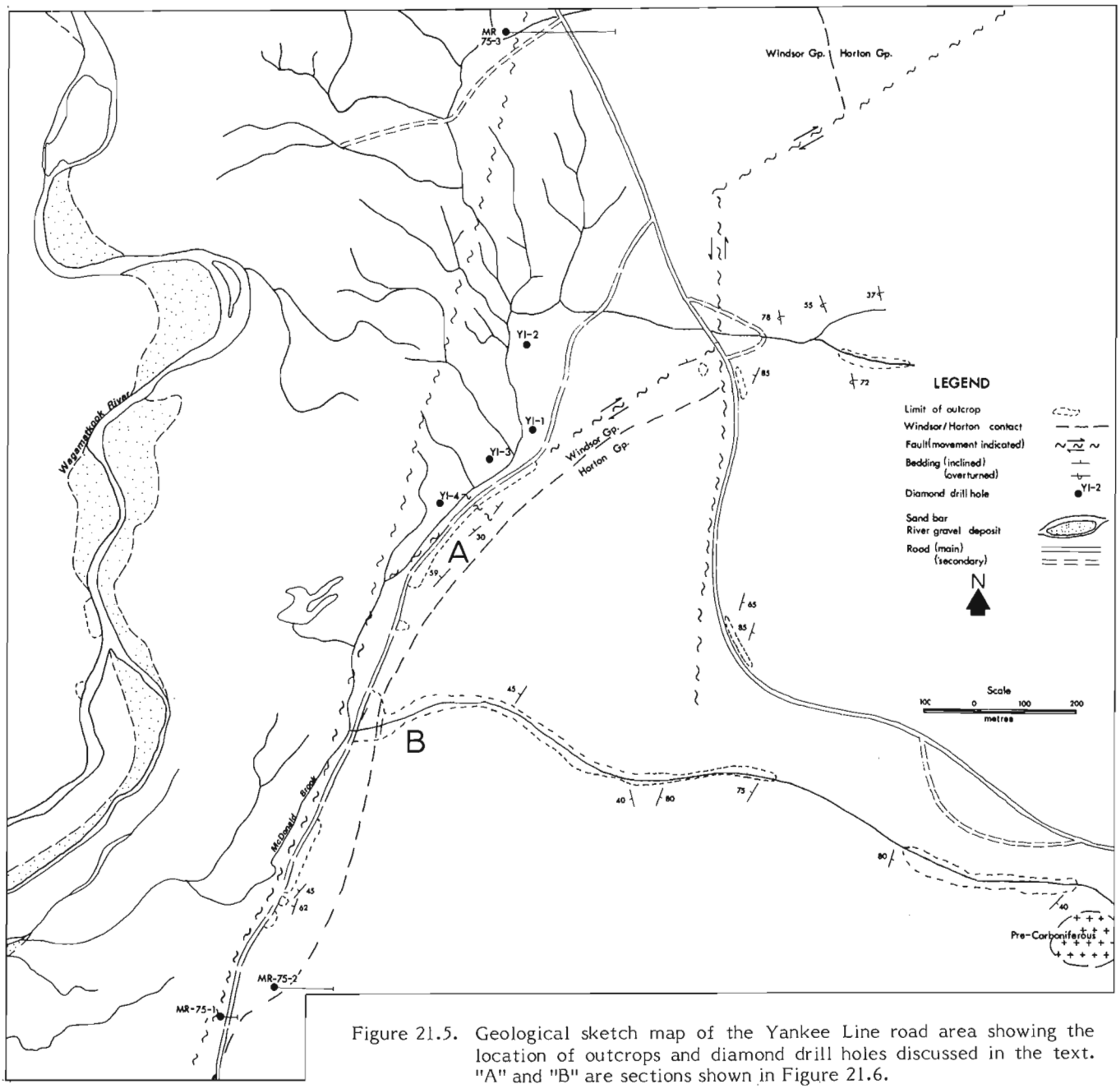

Figure 21.5. Geological sketch map of the Yankee Line road area showing the location of outcrops and diamond drill holes discussed in the text. "A" and "B" are sections shown in Figure 21.6.

Figure 21.6. Sections through the Windsor-Horton contact showing vertical copper, lead, and zinc variations. Yankee Line road area, Nova Scotia. Abbreviations are explained in Table 21.1 and Figure 21.8.

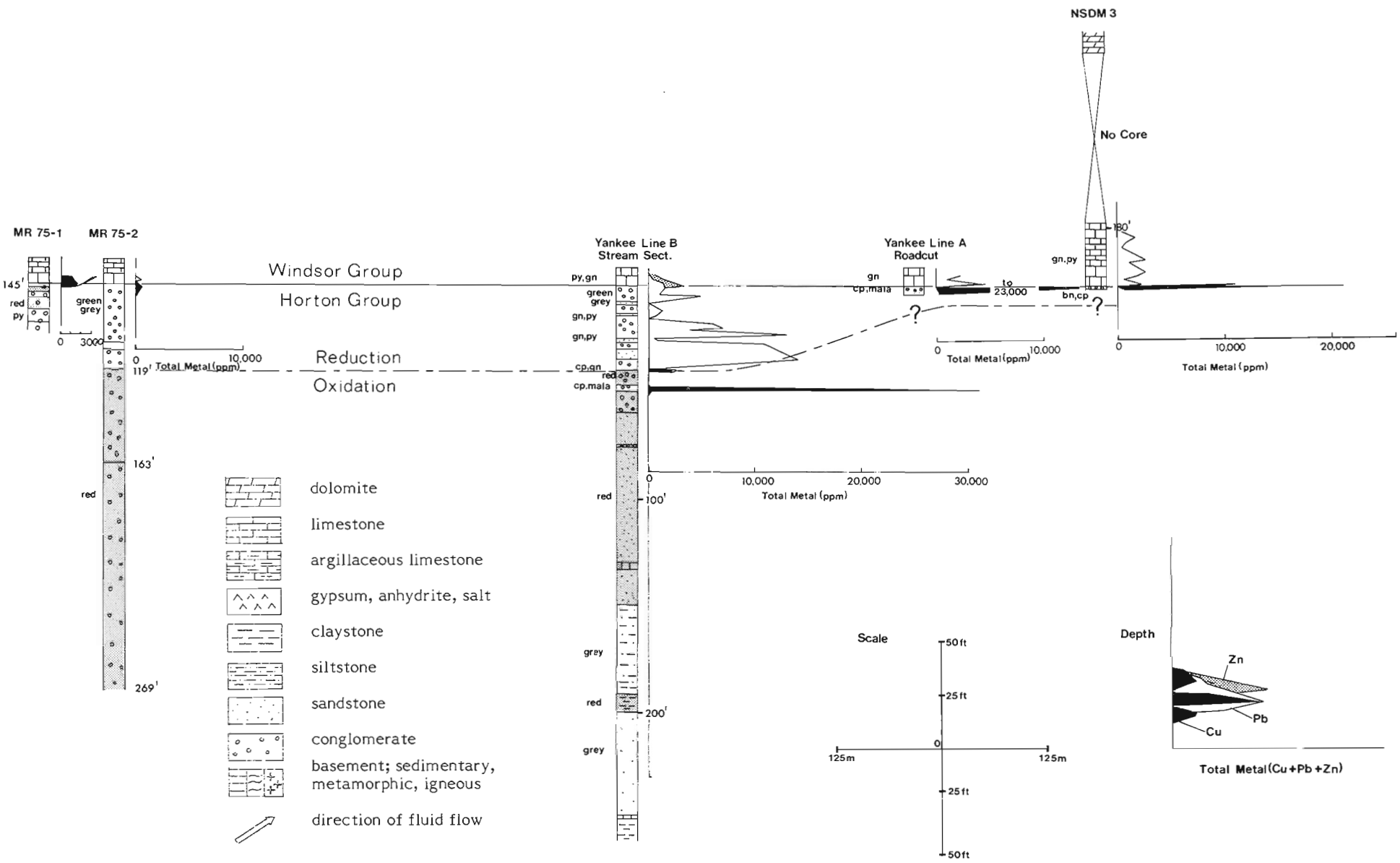

Figure 21.4 and Tables 21.1 and 21.2 show that one metal can be dominant over the other two or that any two of the three metals can be associated with each other and be dominant over the third. Few localities contain approximately equal amounts of copper, lead, and zinc. In the study area the uppermost Horton samples average 1263 ppm Cu, 879 ppm Pb*, and 592 ppm Zn, and the lowermost Windsor samples average 507 ppm Cu, 535 ppm Pb, and 795 ppm Zn. These values greatly exceed those for normal sedimentary rocks.

Uranium Distribution

The average uranium content of uppermost Horton beds is 4.4 ppm and lowermost Windsor beds is 5.0 ppm (Tables 21.1, 21.2). The U shows little relationship to the Cu, Pb, or Zn. Concentrations as high as those reported by Charbonneau and Ford (1977, 1978) in the South Maitland area of mainland Nova Scotia were not found along the Windsor-Horton contact in central Cape Breton Island. Nevertheless, some samples from the Lake Enon and other areas contain as much as 11 to 25 ppm uranium or about 3 to 10 times background values in the area. Although these data provide no indication of viable uranium deposits along the contact in the area, a deposit could have been easily missed because a scintillometer was not used in the field and these samples were not collected specifically for uranium studies.

Uraniferous A_1 limestone samples from the South Maitland area, collected by Charbonneau and Ford, are distinctively reddish and have been oxidized. Although few outcrops of the Windsor-Horton contact occur in the region, field studies have indicated that in a large area extending from South Maitland to Cheverie in the Windsor type area much of the basal A_1 limestone has been oxidized and has a reddish tint (Binney, 1975a and Worley, 1975). Smaller hematitic areas in basal Windsor rocks have been recognized in New Brunswick and Newfoundland (Binney and Kirkham, 1975). However, the uranium content of four samples collected from red-grey A_1 limestone in Johnson Cove (Cheverie area) average 3.1 ppm, indicating that uranium has not been particularly concentrated in these red "facies". Although uranium deposition in the basal Windsor carbonates in the South Maitland area might be related to oxidation, these analyses indicate that uranium deposition is not related to all oxidation of basal Windsor carbonates.

Charbonneau and Ford (1978) indicated that some of the highest uranium concentrations occur in the Pembroke Breccia near the top of the A_1 limestone (Macumber). Clifton (1963) has presented considerable evidence that the Pembroke Breccia is either late Triassic or post-Triassic. If this is true then the uranium in the breccia was probably also concentrated in the late Triassic or post-Triassic by processes that were unrelated to those that deposited base metals along the Windsor-Horton contact.

Yankee Line Road Area

Jones and Covert (1972, p. 115) reported that the Nova Scotia Department of Mines hole Y.L. 3, drilled in the Yankee Line road area (loc. 29, 30 and 31, Fig. 21.2), averaged 150 ppm Cu and 2300 ppm Pb from 195 to 200 feet; 300 ppm Cu and 2000 ppm Pb from 200 to 207 feet; and 1300 ppm Cu and 60 ppm Pb from 207 to 215 feet. The Nova Scotia Department of Mines kindly permitted access to the Y.L. 3 core, which was sampled and studied in detail. Results of chemical analyses are cited in Table 21.3. Instead of a grade of 1300 ppm Cu over 8 feet, more detailed sampling revealed about 11 300 ppm Cu over 1 foot from 206.8 to 207.8 feet (no core remained between 209 and 215 feet). The copper is present primarily as disseminated bornite and chalcopyrite and, at the time of analysis, this value represented the highest grade copper found anywhere along the Windsor-Horton contact.

Because of these encouraging results, the writer, with W.D. Sinclair, examined briefly the Yankee Line road area in the summer of 1977. In an excellent stream exposure immediately south of the road (Fig. 21.5), low grade galena was found disseminated in conglomerate, arkose, and limestone over 45 feet of section (footages are visual estimates) with a thin, erratic(?) copper (chalcopyrite and malachite) zone in conglomerate below. Analytical results indicate that, disseminated in conglomerate and arkose, there could be as much as 7000 ppm Pb over 17 feet with 10 000 to 20 000 ppm Cu over about 1 foot (Table 21.3). This mineralization was not mentioned by Jones and Covert (1972), Binney (1975a), or in any company report the writer has seen.

The copper and lead are obviously related to each other, with a lead zone positioned above a copper zone (Table 21.3, Fig. 21.6). In the stream section the boundary between the lead and copper zones occurs about 40 feet below the Windsor-Horton contact. At no other locality has this type of copper mineralization been found this far beneath the Windsor-Horton contact. The same copper-lead boundary may occur near the Windsor-Horton contact in the roadcut** and drill hole Y.L. 3 about 600 m northeast of the stream section.

After the field examination the writer learned of the Getty Mines Limited drill holes through the contact about 600 m southwest of the stream section (Fig. 21.5). Getty officials kindly permitted the writer to study and sample the core. Unfortunately, the core from these two holes is virtually devoid of visible chalcopyrite and galena. The reason for the abrupt termination of the copper and lead mineralization in this direction is not clear. Possibly mineralization in the area is related to an early fault system or, more probable, it is in some way related to facies changes in the upper Horton. Based on the Getty drill hole MR-75-2 and the stream section, the upper conglomerate unit of the Horton appears to be considerably thicker in the unmineralized core section than in the mineralized stream section. The possibility of a local paleohydrological control on base metal sulphide distribution should be investigated.

Environments of sedimentation

A knowledge of the environments of sedimentation is essential for detailed modelling of the controls of base metal distribution along the Windsor-Horton contact. Many explanations have been put forward for Horton and Windsor sedimentation but perhaps some of the more prominent, comprehensive recent proposals have been presented by Schenk (1967a, b, 1969, 1975a, b). Schenk (1969) proposed that thick, lower Carboniferous, mainly continental red beds, accumulated in a complex rift-valley system and that during the mid-Carboniferous, the basins were flooded repeatedly by hypersaline seas. Schenk (1967a, 1975a) suggested that the A_1 (Macumber) limestone is a strand-line carbonate that was deposited in the shallow subtidal to high intertidal zone. In

* Note that one high lead value for Big Barren strongly influences this average (Table 21.1).

** The single high copper value (KQ-77-23C) in Table 21.3 for the roadcut appears to be related to a minor fault block.

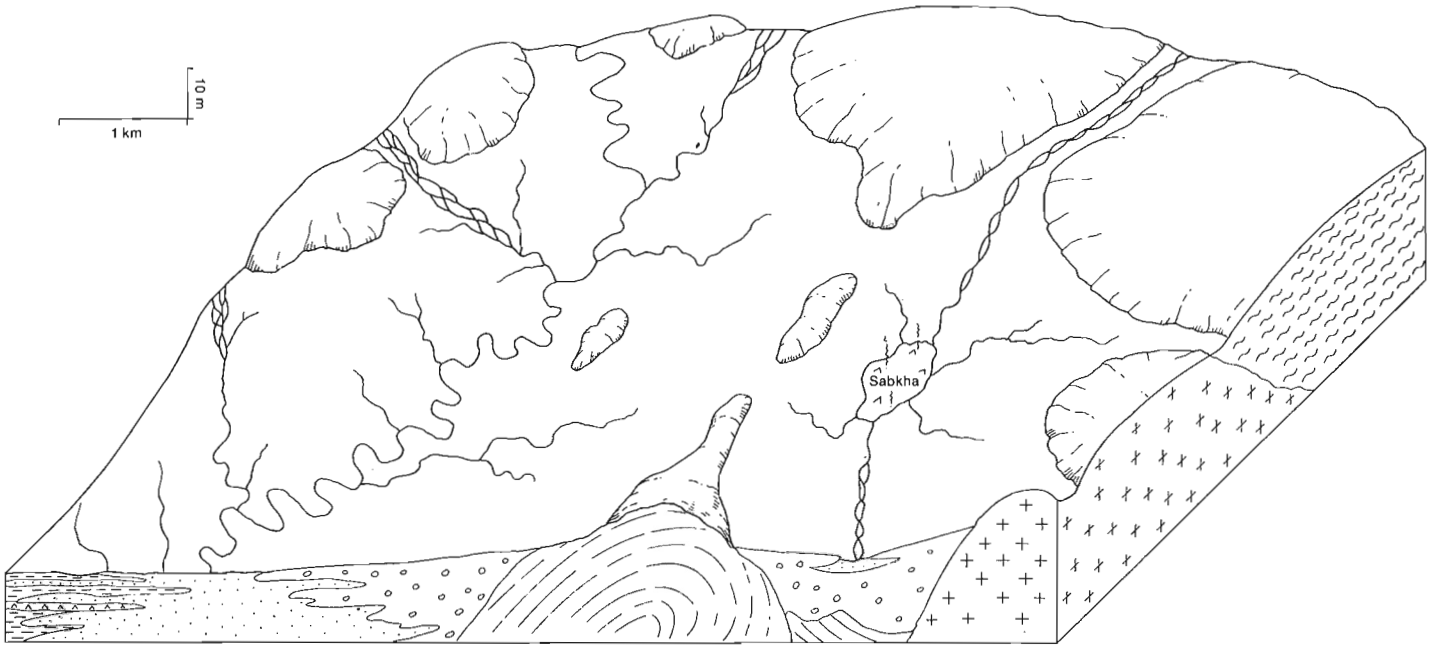

Figure 21.7. Block diagram depicting upper Horton sedimentary environments just prior to the Windsor transgression.

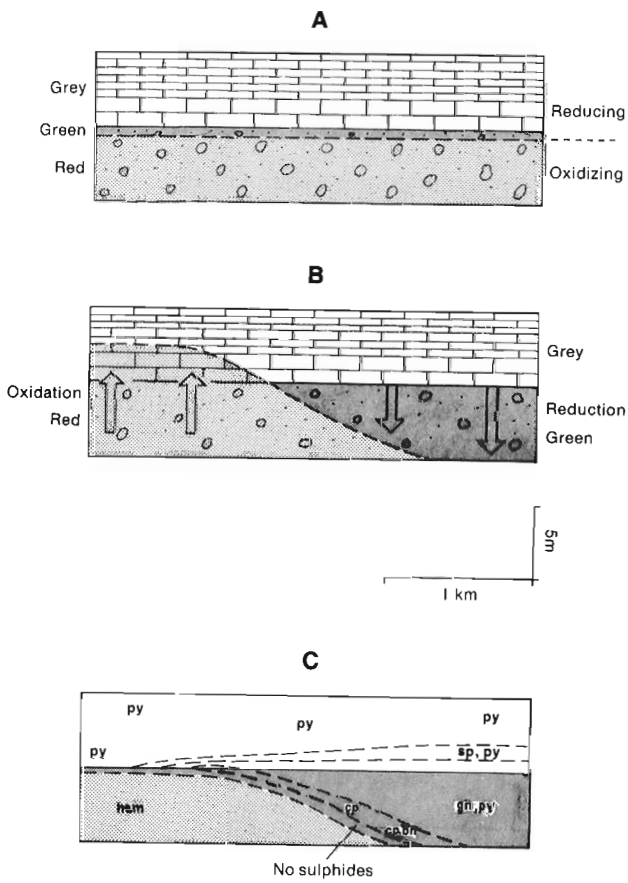

Legend for Figures 21.7, 8, and 9.

- dolomite
- limestone
- argillaceous limestone
- gypsum, anhydrite, salt
- claystone
- siltstone
- sandstone
- conglomerate
- basement; sedimentary, metamorphic, igneous
- direction of fluid flow

A Typical "stable", planar oxidation-reduction boundary a few centimetres to a few metres below the contact;

B depicts oxidation-reduction boundary that migrates either up or down section;

C possible mineral zones in Yankee Line road area. Abbreviations: bn = bornite; cp = chalcopyrite; gn = galena; hem = hematite; py = pyrite, and sp = sphalerite.

Figure 21.8. Diagrammatic sequence through Windsor (A_1 limestone)-Horton contact depicting typical oxidation-reduction boundaries and possible mineral zones.

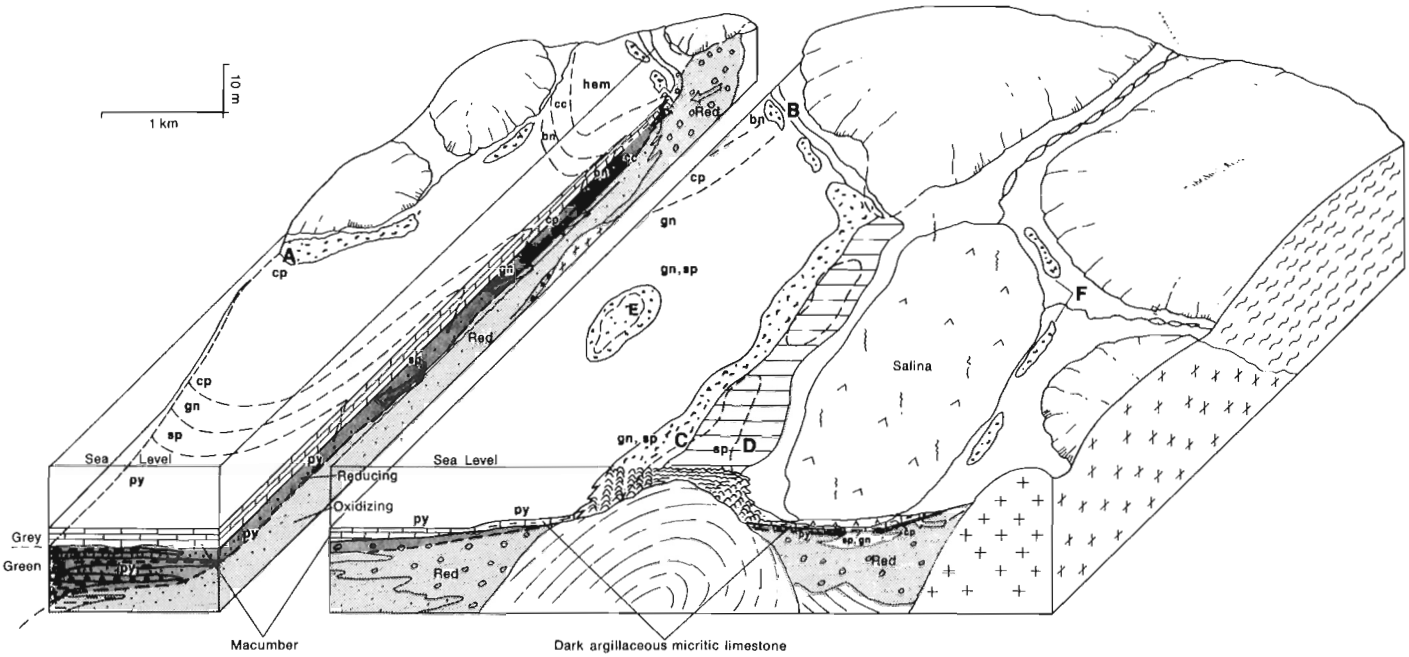

A Black River-type algal "reef", mineralized with chalcopyrite, sitting directly on basement;

B East Bay-type intertidal (?) stromatolites near beach deposits (?) of reworked Horton conglomerate – chalcopyrite and bornite in area;

C Gay's River-type reef formed on sea cliff ridge of basement rocks – extensively dolomitized and mineralized with galena and sphalerite;

D back-reef, planar-bedded, intertidal-supratidal pustular algal mat – extensively dolomitized and mineralized sporadically with sphalerite and galena;

E basinal patch reef on basement high – local galena and sphalerite;

F dead patch reefs formed early in Musquodoboit-type back basin when water levels were high.

Abbreviations are explained in Table 21.1 and Figure 21.8.

Figure 21.9. Block diagram depicting sedimentary environments towards the end of A_1 limestone deposition and idealized sulphide zones.

fact Schenk (1975a) speculated that there should be many A_1 limestones repeated through the section representing a particular lithotope rather than a single stratigraphic unit. Schenk (1969, 1975a) also suggested that the Windsor evaporites were precipitated in supratidal sabkhas and salinas.

The interpretation of the environments of formation of the A_1 limestone and related rocks presented here is a radical departure from Schenk's models. This writer, in basic agreement with Geldsetzer (1977 and 1978), believes that A_1 limestone was deposited in a shallow subtidal environment, i.e. within the photic zone, as a very widespread, single, thin algal unit. Based on broad-scale field examinations and extensive exploration activity no evidence exists to support the contention that there are several A_1 limestones or, in most areas, that conglomerates or other clastic sedimentary rocks sit directly on the A_1 limestone. A_1 deposition was characteristically followed by the accumulation of a very thick sequence of evaporites. Only near the margins of the sedimentary basins are the overlying evaporite units thinner and contain abundant intercalated terrigenous sediments. In these areas a dark, micritic, argillaceous limestone is the basal unit of the Windsor Group. Scour channels, ripple marks, and desiccation cracks, expected of dynamic strand-line environments, have not been observed by the writer in the A_1 limestone.

A single, widespread, low energy, micritic marine carbonate unit deposited directly on continental boulder to pebble conglomerate represents a dramatic change in sedimentary environments. In Figures 21.7 and 21.9 an attempt has been made to portray the sedimentary environments immediately prior to the initial Windsor transgression and towards the end of A_1 limestone deposition, respectively.

Upper Horton sedimentation, as Schenk (1969) and others have proposed, probably occurred in many interconnected, block-faulted, continental, low-latitude desert basins. Thick conglomerate units were probably proximal alluvial-colluvial fans, the product of high energy, intermittent braided streams (Fig. 21.7). In more distal areas, meandering streams with lower gradients gave rise to typical fining-upward fluvial cycles (e.g. a few exist in the Yankee Line road area). These are locally intercalated with lacustrine strata. Extensive lacustrine units, including some evaporitic beds, such as those of the Albert Formation in New Brunswick (Gussow, 1953; Greiner, 1974), indicate that some large, closed desert sedimentary basins existed during Horton time. One of the main sedimentary basins during upper Horton time was probably to the northwest of the central Cape Breton area (Kelley, 1967; Geldsetzer, 1977).

Table 21.2

Basal Windsor Analysis*

Loc. No.[1]	Locality	Sample No.[2]	Cu[3]	Pb[3]	Zn[3]	U[3]	R%Cu[4]	R%Pb[4]	R%Zn[4]	Description[5]
1.	McIntyre Lake									
2.	Big Barren	BB-74-3-705.7'-705.5' (Amax)	100	790	800	1.7	5.9	46.7	47.3	dark grey dolomitic ls; py
		BB-74-23-321.8' (Amax)	50	5900	320	14.4	0.8	94.1	5.1	grey ls; gn, py
3.	Lake Enon	212-1-74A (~194.5') (Noranda)	240	180	520	20.0	25.5	19.1	55.3	grey dolomite; py
		212-2-74-166.7'(Noranda	120	84	11000	4.0	1.1	0.7	98.2	grey-brown, dolomitic ls; py
		L.E.-163-148' (Kaiser)	340	780	780	14.1	17.9	41.0	41.0	dark grey, micritic ls; cp
		L.E.-124-239' (Kaiser)	16	160	1700	2.4	0.9	8.5	90.6	dark grey, micritic ls; cp
		212-11-74-559.8'-560' (Noranda)	30	107	110	0.5	12.1	43.3	44.5	red and yellow, fossiliferous ls
4.	Soldier Cove	KQB-74-66 (+0.1')	413	59	21	1.6	83.8	12.0	4.3	medium to dark grey, micritic ls; cp
5.	Black River	M-2-285' (Imperial)	50	73	16	1.1	35.9	52.5	11.5	medium buff-grey, ls granule cg; py
6.	Sugarcamp	S-1-384.4' (Rio Tinto)	50	482	60	8.1	8.4	81.4	10.1	grey, micritic ls
7.	Diogeness Brook	KQ-77-20B	35	220	435	3.1	5.1	31.9	63.0	dark grey micritic ls; py
		KQ-77-21C	30	165	445	1.7	4.7	25.8	69.5	dark grey micritic ls; py
8.	Huntington Mtn.	KQB-74-98C	30	950	10?	0.7	3.0	96.0	1.0	pale, crystalline ls; gn
9.	Glen Morrison	GM-1-20' (Imperial)	108	50	124	15.4	38.3	17.7	44.0	grey, micritic ls
10.	East Bay	KGB-73-1(7)	190	68	149	4.9	46.7	16.7	36.6	grey, micritic ls
11.	Frenchvale (Coxheath)	KQ-70-459	333	73	680	2.5	30.7	6.7	62.6	dark grey, argillaceous, micritic ls; cp
		67-10-212' (Mar.)	705	380	171	6.7	56.1	30.3	13.6	dark brown-grey, argillaceous, micritic ls;c
		70-4-557' (Cerro)	1280	540	940	4.3	46.4	19.6	34.0	dark grey, argillaceous, micritic ls; cp, py
12.	Christmas Island Pit)	KQB-73-6A	680	40	16	3.3	92.4	5.4	2.2	dark grey, micritic ls
13.	Christmas Is. (Shore)	KQB-73-7A	360	92	18	2.7	76.6	19.6	3.8	light grey, micritic ls
14.	Red Point Road	KQW-75-1D	50	158	90	3.2	16.8	53.0	30.2	grey, micritic ls
15.	Iona Rear	IR-74-2-134' (Amax)	780	210	540	9.3	51.0	13.7	35.3	grey, brachiopod ls; py, cp
16.	Walker Road	KQW-75-4C	40	65	420	3.7	7.6	12.4	80.0	medium grey, micritic ls; py
17.	Cains Mtn.Road	KQW-75-3C	14	133	1000	15.2	1.2	11.6	87.2	dark grey, micritic ls
18.	Jubilee	KQ-75-38	14	54	100	9.9	8.5	32.9	61.0	medium to dark grey micritic ls; petroliferou
		TG-2-40' (Texas Gulf)	38	850	9280	0.9	0.4	8.3	91.3	medium grey, micritic ls; sp, gn (vein)
		TG-14-200.0' (Texas G.)	255	445	520	9.3	20.9	36.5	42.6	medium grey, micritic ls; sp, gn (vein)
		ATG-8-397' (Amax-TG)	13	39	266	1.7	4.1	12.3	83.6	medium grey, micritic ls
19.	Grass Cove Road	KQ-75-45B	350	178	60	12.6?	59.5	30.3	10.2	grey, micritic ls; py
20.	Iona Cross Road	141.3-551.8' (St. Joe)	470	70	20	5.6	83.9	12.5	3.6	grey, micritic ls; py, cp
21.	Washabuck	KQB-73-17C	478	105	54	2.5	75.0	16.5	8.5	black, micritic ls; py, cp
		KQB-73-17C	3100	320	990	2.5	70.3	7.3	22.4	black, micritic ls; py, cp
22.	Whycocomagh	KQB-74-100 (+0')	375	28	16	4.1	89.5	6.7	3.8	dark grey, micritic ls; cp
23.	Hay River	KQB-74-84A	11	<500	110	—	1.8	80.5	17.7	dark grey, micritic ls; py
24.	Glenmore	137.2-328½' (St. Joe)	117	109	3450	3.2	3.2	2.9	93.8	medium grey, micritic ls
25.	East Side Brook	137.1-91 3/4' (St. Joe)	10	15	191	1.4	4.6	6.9	88.4	medium grey, micritic ls
26.	Trout River	KQB-74-86	12	140	340	2.9	2.4	28.5	69.1	dark grey, microcrystalline ls; py
27.	Upper Middle River	KQB-74-76B	105	1300	40	1.1	7.3	90.0	2.8	dark grey, micritic ls; py, gn
28.	McRae Brook	KQB-74-77B	30	569	20	2.2	4.8	91.9	3.2	dark grey, micritic ls; py
29.	Yankee Line	Y.L. 3-206.8' (NSDM)	0960	462	100	4.9	95.1	4.0	0.9	grey, micritic ls; cp, py, mala
30.	Yankee Line (Roadcut)	KQ-77-23D	40	2700	70	3.0	1.4	96.1	2.5	dark grey, micritic ls
		KQB-73-19B	9	192	50	3.8	3.6	76.5	19.9	dark grey, micritic ls
		KQB-73-19B	20	387	103	3.8	3.9	75.9	20.2	dark grey, micritic ls
30.	Yankee Line (Stream)	KQ-77-22EE	40	1290	1370	3.2	1.5	47.8	50.7	dark grey, micritic ls; gn
		KQB-73-18B	13	1400	840	0.7	0.6	62.1	37.3	black, micritic ls; gn
		KQB-73-18B	25	1727	1089	0.7	0.9	60.8	38.3	black, micritic ls; gn
31.	Yankee Line	MR-75-1-145' (Getty)	1340	485	93	7.5	69.9	25.3	4.8	medium to dark grey, micritic ls
		MR-75-2-77' (Getty)	17	875	205	5.4	1.5	79.8	18.7	medium grey, micritic ls
32.	Squire Point	KQB-73-10A	1455	25	13	5.3	97.5	1.7	0.9	dark grey, micritic ls; mala
33.	Englishtown	KQB-74-101	25	750	10?	2.0	3.2	95.5	1.3	light grey, porous ls
		AVERAGE	507	535	795	5.0	27.6	29.1	43.3	

*See Table 21.1 footnotes for explanation.

Table 21.3
Yankee Line Chemical Profiles*

Loc.[1] No.	Locality	Sample No.[2]	Cu[3]	Pb[3]	Zn[3]	U[3]	R%Cu[4]	R%Pb[4]	R%Zn[4]	Description[5]
29.	NSDM D.D.H. #3	Y.L. 3-181'	14	320	222	2.9	2.5	57.6	39.9	medium grey, micritic ls
		Y.L. 3-183'	24	1600	92	3.6	1.4	93.2	5.4	medium grey, micritic ls
		Y.L. 3-187'	20	713	45	4.3	2.6	91.6	5.8	medium grey, micritic ls; gn, py
		Y.L. 3-189'	14	463	63	5.8	2.6	85.7	11.7	medium grey, micritic ls; gn
		Y.L. 3-195'	35	2480	76	4.0	1.4	95.7	2.9	medium grey, micritic ls; gn, py
		Y.L. 3-196'	32	1067	71	4.9	2.7	91.2	6.1	medium grey, micritic ls
		Y.L. 3-200'	24	2300	74	2.7	1.0	95.9	3.1	medium grey, micritic ls; gn, py
		Y.L. 3-202'	35	1920	113	2.0	1.7	92.8	5.5	medium grey, micritic ls
		Y.L. 3-204'	20	667	50	4.3	2.7	90.5	6.8	medium grey, micritic ls; gn, py
		Y.L. 3-206'	242	2060	63	3.4	10.2	87.1	2.7	medium grey, micritic ls; gn, py
		Y.L. 3-206.8'	10960	462	100	4.9	95.1	4.0	0.9	medium grey, micritic ls; cp, mala
		Y.L. 3-207.3'	6540	34	44	3.5	98.8	0.5	0.7	green, ark pebble cg; cp, mala
		Y.L. 3-207.5'	21040	104	34	2.8	99.3	0.5	0.2	green, ark pebble cg; bn
		Y.L. 3-207.7'-207.9'	6660	39	22	1.5	99.1	0.6	0.3	green, ark pebble cg; bn, cp
		Y.L. 3-208.5'	548	38	46	4.9	86.7	6.0	7.3	green ark; cp
30.	Yankee Line Roadcut	KQ-77-23A -3'	480	555	130	1.0	41.2	47.6	11.2	green pebble cg
		KQ-77-23B -4-6"	260	180	100	1.3	48.1	33.3	18.5	green pebble cg
		KQ-77-23C -1'	23000	160	90	3.5	98.9	0.7	0.4	green pebble cg; mala
		KQ-77-23D +0-2"	40	2700	70	3.0	1.4	96.1	2.5	dark grey, micritic ls; py?
		KQ-77-23E +3-4"	40	5000	85	2.2	0.8	97.6	1.7	dark grey, micritic ls; gn, py
		KQ-77-23F +3'	20	1100	120	2.4	1.6	88.7	9.7	dark grey, micritic ls; gn, py
		KQ-77-23G +5'	<10	2105	100	4.3	0.5	95.0	4.5	dark grey, micritic ls; gn, py
30.	Yankee Line Stream Section	KQ-77-22B -230'	20	18	85	2.7	16.3	14.6	69.1	medium grey shale; py
		KQ-77-22E -130'	8	3	25	3.5	22.2	8.3	69.4	buff-grey lacustrine ls
		KQ-77-22F -100'	7	3	21	1.3	22.6	9.7	67.7	red ark
		KQ-77-22G - 70'	5	7	31	1.3	11.6	16.3	72.1	red ark
		KQ-77-22H - 60'	8	10	64	2.5	9.6	12.2	78.1	red pebble cg
		KQ-77-22I - 52'	9	4	45	0.9	15.5	6.9	77.6	red pebble cg; some pale mottles
		KQ-77-22J - 50'	318	4	30	0.6	90.3	1.1	8.5	red and pale green mottled pebble cg
		KQ-77-22K(1)- 48'	31000	20	115	2.5	99.6	0.1	0.4	green pebble cg; mala
		KQ-77-22K(2)- 48'	13000	25	140	6.4	98.7	0.2	1.1	green pebble cg; minor mala
		KQ-77-22L - 45'	6	7	60	0.9	8.2	9.6	82.2	red, ark pebble cg; pale mottles
		KQ-77-22M - 40'	2065	695	130	2.3	71.5	24.0	4.5	green pebble cg; cp, gn
		KQ-77-22N - 39'	220	15	140	2.5	58.7	4.0	37.3	grey ark
		KQ-77-22O - 35'	200	14000	305	2.2	1.4	96.5	2.1	green pebble cg; gn, py
		KQ-77-22P - 35'	14	1095	86	2.1	1.2	91.6	7.2	pale grey ark; py, gn
		KQ-77-22Q - 27'	110	11000	230	2.9	1.0	97.0	2.0	pale green-grey ark; gn, py
30.		KQ-77-22R - 26'	70	1180	135	3.1	5.1	85.2	9.7	green pebble cg; gn, py
		KQ-77-22S - 25'	15	690	142	1.9	1.8	81.5	16.7	pale grey ark; gn, py
		KQ-77-22T - 23'	40	13000	200	1.5	0.3	98.2	1.5	green grey pebble cg; gn, py
		KQ-77-22U - 21'	105	4000	200	3.1	2.4	92.9	4.6	green-grey pebble cg; gn, py
		KQ-77-22V - 20'	70	7000	165	2.6	1.0	96.8	2.3	green-grey pebble cg; gn, py
		KQ-77-22W - 18'	80	6000	180	1.6	1.3	95.8	2.9	green-grey pebble cg; gn, py
		KQ-77-22X - 16'	19	21	121	1.3	11.8	13.0	75.2	pale pebble cg; py
		KQ-77-22Y - 14'	50	870	195	2.3	4.5	78.0	17.5	pale pebble cg; py
		KQ-77-22Z - 12'	39	1265	70	1.0	2.8	92.1	5.1	pale green-grey pebble cg
		KQ-77-22AA - 8'	20	132	132	1.5	7.0	46.5	46.5	green ark and cg; py
		KQ-77-22BB - 5'	50	5000	335	1.9	0.9	92.8	6.2	green-grey pebble cg; py, gn
		KQ-77-22CC - 4'	20	1155	170	1.2	1.5	85.9	12.6	green-grey pebble cg; py
		KQ-77-22DD - 2-4"	120	1420	1900	2.5	3.5	41.3	55.2	green-grey pebble cg; py, gn
		KQ-77-22EE + 1-3"	40	1290	1370	3.2	1.5	47.8	50.7	dark grey, micritic ls; py, gn, sp?
		KQ-77-22FF + 3'	20	470	1050	3.2	1.3	30.5	68.2	dark grey, micritic ls; py, gn, sp?
		KQ-77-22GG + 6'	40	100	840	3.0	4.1	10.2	85.7	dark grey, micritic ls; py
31.		MR-75-1-142'	955	2000	318	4.3	29.2	61.1	9.7	medium to dark grey, micritic ls
		MR-75-1-145'	1340	485	93	7.5	69.9	25.3	4.8	medium to dark grey, micritic ls
		MR-75-1-145'-145.3'	910	125	98	2.0	80.3	11.0	8.6	pale green, ark pebble cg
		MR-75-1-146'	20	10	203	2.1	8.6	4.3	87.1	red, silty cg breccia
		MR-75-1-148'	20	7	88	1.4	17.4	6.1	76.5	pale green pebble cg
		MR-75-1-150'	10	7	174	1.9	5.2	3.7	91.1	red and green-grey, silty cg
		MR-75-1-154'	12	11	108	1.1	9.2	8.4	82.4	grey, ark pebble cg
		MR-75-1-155½'	14	6	84	0.8	13.5	5.8	80.8	grey, ark pebble cg
		MR-75-1-161½'	18	7	91	1.1	15.5	6.0	78.4	grey, ark pebble cg; py
		MR-75-1-166'	19	5	130	5.3	12.3	3.2	84.4	red-grey, silty pebble cg
31.		MR-75-2-68'	15	120	60	4.4	7.7	61.5	30.8	pale grey, micritic ls
		MR-75-2-70'	10	137	234	2.5	2.6	35.9	61.4	medium grey, micritic ls
		MR-75-2-75'	15	220	173	1.4	3.7	53.9	42.4	medium grey, micritic ls
		MR-75-2-77'	17	875	205	5.4	1.5	79.8	18.7	medium grey, micritic ls
		MR-75-2-77½'	230	16	107	4.0	65.2	4.5	30.3	green ark and cg
		MR-75-2-79'	840	35	131	2.1	83.5	3.5	13.0	green pebble cg
		MR-75-2-84'	13	10	128	1.8	8.6	6.6	84.8	grey (red) pebble cg
		MR-75-2-93'	24	10	85	0.9	20.2	8.4	71.4	pale green-grey pebble cg
		MR-75-2-108'	47	10	96	1.3	30.7	6.5	62.7	pale green-grey pebble cg
		MR-75-2-114'	50	8	89	1.6	34.0	5.4	60.5	pale green-grey pebble cg
		MR-75-2-120'	12	7	81	1.3	12.0	7.0	81.0	pale red-grey pebble cg; green mottles
		MR-75-2-127'	17	11	134	0.9	10.5	6.8	82.7	medium red-grey pebble cg
		MR-75-2-134'	10	9	126	1.1	6.9	6.2	86.9	medium red-grey pebble cg
		MR-75-2-141'	12	7	99	1.5	10.2	5.9	83.9	medium red-grey pebble cg

* See Table 21.1 footnotes for explanation.

The extensive, quiet-water, micritic basal carbonates of the Windsor Group indicate an extremely rapid initial transgression of the Windsor sea which completely inundated most areas of Horton sedimentation and the upland, terrigenous sediment source areas. Most of the upper Horton sedimentary basins at the time of transgression were probably below sea level which accounts for the rapid transgression. Tectonic activity, perhaps rifting, during early Windsor time permitted the ingress of the ocean. The entrance to the Windsor basin was probably narrow or shallow and soon became restricted, possibly by reef construction or long shore sediment transport. The initial Windsor sea soon became saline and slightly stagnant. Under these conditions algae thrived but normal marine organisms could not survive. Corals, crinoids, brachiopods, gastropods, and bryozoans in lowermost Windsor carbonates must have lived either shortly after the initial transgression before salinities increased or in the upper less saline layers of the Windsor sea, or flourished during brief influxes of less saline waters. Under these conditions Gay's River-type carbonate banks and reefs could be time-equivalent to the thin, dark, micritic, argillaceous, forereef limestones (e.g. "Frenchvale-Lake Enon facies") and basinal A_1 limestone (Fig. 21.9).

The salinities in these restricted basins soon rose to the point where enormous quantities of sulphate and salt were precipitated. In a sense, these inland seas were gigantic salinas. Considering that these sedimentary basins were products of rift tectonics, and that the climate was arid, it is not unreasonable to expect that very large desert basins below sea level could exist. Presumably if rifting continued eventually the basins would be connected to the nearest ocean. This writer suspects that many of the very large evaporite basins of the world, such as the Upper Permian Zechstein basin of central Europe, formed in a similar manner. Since many important sedimentary copper deposits throughout the world occur below thick evaporite sequences, this type of marine drowning of desert fluvial systems could be instrumental in ore genesis.

Ore Genesis

The prime site of sedimentary copper formation is basal, anoxic sediments of a marine transgressive cycle deposited on continental sediments accumulated in equatorial arid or semi-arid regions (Lombard and Nicolini, 1962; Strakhov, 1962; Kirkham, 1973, 1975). By some means the paleohydrologic regimes established in such environments were instrumental in the release of metals from the underlying, immature oxidized sediments. Under oxidizing conditions these metals were transported in solution until they encountered the basal, reduced marine sediments where the metals were precipitated.

Figure 21.8 schematically illustrates the nature of this oxidation-reduction boundary along the Windsor-Horton contact. In most areas the boundary was apparently stable and only a few centimetres to a few metres of the underlying red beds were reduced (A, Fig. 21.8). However, in some areas, such as Ship Cove in Newfoundland, the oxidation-reduction boundary migrated up into the basal Windsor Limestone (B, Fig. 21.8), while in other regions, such as the Yankee Line road area, the boundary migrated down into the upper Horton sediments (B and C, Fig. 21.8). Base metal sulphides occur associated with both "stable" and "unstable" oxidation-reduction boundaries. The important feature is that the metals are not related directly to a particular sedimentary facies, such as the A_1 limestone, but rather to an early diagenetic boundary. The fact that, in otherwise similar anoxic, carbonaceous A_1 limestone, pyrite occurs invariably above the base metal-bearing limestone indicates that the metals could not have migrated down through the sedimentary column from the overlying evaporites nor in the strictest sense could they be syngenetic. The metal-bearing solutions must have come from below. Nevertheless, the widespread, finely disseminated nature of the base metal sulphides indicates that the metals were in the rocks before any significant loss of permeability.

Idealized zonal patterns of sulphide minerals are illustrated in Figures 21.8 and 21.9. A complete or incomplete, overlapping sequence of mineral zones ranging outwards and upwards from red hematitic areas is chalcocite, bornite, chalcopyrite, galena, sphalerite, and pyrite. The pyrite or originally tetragonal iron sulphide (Berner, 1964) was probably in the unconsolidated sediments before the base metal sulphides were precipitated. This zonal pattern along the Windsor-Horton contact, although less well developed and documented, is very similar to that described for the Kupferschiefer and other basal Zechstein rocks (Jung, 1968; Erzberger et al., 1968; Haranczyk, 1970; Lur'ye and Gablina, 1972; Rentzsch, 1974). Similar processes may have operated in both sedimentary basins. Although lead and zinc are minor, Brown (1971) has documented a similar zonal pattern of sulphides, which cuts the bedding at a gentle angle, in the Proterozoic White Pine copper deposit in Michigan.

In regard to the Kupferschiefer, von Hoyningen-Huene (1963), Lur'ye and Gablina (1972), and Lur'ye (1974) have suggested that the Zechstein sea rapidly flooded many large fluvial systems, but since the fluvial sediments were still very permeable and extended to the south far beyond the new shoreline, the hydraulic head permitted the flow of oxidized groundwaters well out under the Zechstein sea. The regional, lateral facies change from coarse grained permeable conglomerate and sandstone to fine grained impermeable fluvial and lacustrine strata in the underlying Rotliegendes is considered by Lur'ye and Gablina to have caused these oxidized, metal-bearing groundwaters to permeate the basal Zechstein sediments and possibly issue onto the sea floor. In Figure 21.9 an attempt has been made to illustrate a weak hydraulic system of this type but in this case the base metal sulphide zones do not reach the regional facies boundary between the permeable and impermeable underlying strata.

Rose (1976) has emphasized that transport of metals in chloride brines is far more reasonable than transport in dilute, aqueous solutions. In the "paleoacquifer" hydraulic model outlined above it is difficult to envisage how brines could be involved. Renfro (1974) has proposed a sabkha, brine-reflux model to account for copper transport and deposition under sedimentary conditions. Smith (1974, 1976) and others have presented elaborations of this model. Although the sabkha model may help explain some sedimentary copper deposits, it cannot account for base metal sulphide concentrations in sediments that were deposited in other environments, such as the subtidal Kupferschiefer and A_1 limestone or the continental stream channel deposits at Nacimiento in New Mexico (Woodward et al., 1974). Dense brines possibly from the overlying evaporite basins in both the Zechstein and Windsor found their way into the underlying sediments*. Perhaps the base metals migrated by simple ionic transfer in brines or by circulating brines from the oxidized red beds to the reduced sediments near the Zechstein-Rotliegendes and Windsor-Horton contacts where they were precipitated. Pyritic lacustrine sedimentary rocks about 230 feet below the Windsor-Horton contact in the Yankee Line road area indicate that the base metals did not migrate through these beds and conceivably were derived from the red beds much closer to the Windsor-Horton

* As Geldsetzer (pers. comm.) points out, since most of the A_1 limestone has not been dolomitized, such brines probably did not pass through most of the basal Windsor carbonate.

contact. Despite these various proposals on the genesis of the base metals along the Windsor-Horton contact the details of the ore-forming processes remain largely unknown.

A Gay's River-type reef or carbonate bank, heavily mineralized with galena and sphalerite, is depicted in Figure 21.9. Although the galena and sphalerite would generally fall within lead-zinc zones of the A_1 and basinal micritic, argillaceous limestones, the writer does not know whether this potentially economic concentration of metals is related to the widely dispersed, disseminated base metal sulphides that occur along the Windsor-Horton contact. The metal distribution at Gay's River, described to the writer by company geologists, together with the fact that the deposit sits directly on an impermeable basement, support a model of genesis whereby metal-rich brines, perhaps expelled during compaction, moved laterally from adjacent evaporite beds. MacLeod (1975) presented convincing evidence that the galena and sphalerite were deposited during early diagenesis. Such timing is similar to that proposed here for the origin of the dispersed, disseminated sulphides along the Windsor-Horton contact.

Texasgulf Inc. and Amax Exploration Inc. are currently exploring the small, high grade Jubilee zinc-lead showing in central Cape Breton Island (Fig. 21.2, loc. 18). Open-space fillings of abundant sphalerite, galena, barite, and pyrite occur near the top of the A_1 limestone below massive anhydrite. Low grade veins of the same minerals occur in the lower part of the A_1 limestone, and disseminated sulphides occur in green-grey, arkosic pebble conglomerate at the top of the Horton Group. This mineralization occurs adjacent to a fault and dies out abruptly away from the fault. The fault and associated mineralization postdate the upper A_1 limestone. Other than occurring near the Windsor-Horton contact this mineralization displays few similarities to the typical, stratiform, disseminated mineralization and probably is unrelated to it.

Discussion

Anomalous concentrations of base metals occur at many localities scattered along the Windsor-Horton contact in central Cape Breton Island. Geological studies and exploration to date have not identified the existence of viable deposits. Nevertheless, much of the contact remains to be explored and the detailed controls on sulphide distribution are still poorly understood. Available evidence, however, does point to an early diagenetic concentration of base metals related to sedimentary processes.

The fact that base metal sulphide mineralization was found to extend at least 50 feet below the Windsor-Horton contact in the Yankee Line road area, should caution exploration geologists to explore not only the Windsor-Horton contact but, where possible, to trace the base metal sulphides down section to the oxidation-reduction boundary. Drill holes through the contact, where feasible, should be extended through this boundary.

The results of this study do not indicate the existence of major concentrations of uranium along the Windsor-Horton contact in central Cape Breton Island. Processes which led to the concentration of uranium in similar rocks in the South Maitland area were probably very different from those that concentrated base metals in central Cape Breton Island.

Acknowledgments

Many of the localities discussed in this report were sampled and described by W.P. Binney (specimens KQB) and D. Worley (specimens KQW). The excellent co-operation of all mining companies working in the area is very much appreciated. Permission was granted to sample and study all available diamond drill cores through the Windsor-Horton contact and many geological maps and reports were provided for the writer's use. For some areas company maps are a great improvement over existing published geological maps. Numerous company geologists and personnel of the Nova Scotia Department of Mines provided their time, cheerful assistance, and open, friendly discussion. The author also has had many fruitful discussions with H. Geldsetzer of the Geological Survey. M.J. Copeland of the Geological Survey kindly identified fossils collected from the A_1 limestone.

H. Dunsmore, H. Geldsetzer, and R. Thorpe reviewed the manuscript and made many improvements.

References

Bell, W.A.
1929: Horton-Windsor district, Nova Scotia; Geol. Surv. Can., Mem. 155, 268 p.

Bell, W.A. and Goranson, W.A.
1938: Sydney Sheet (west half); Geol. Surv. Can., Map 360A.

Berner, R.A.
1964: Iron sulfides formed from aqueous solution at low temperatures and atmospheric pressure; J. Geol., v. 72, no. 3, p. 293-306.

Brown, A.C.
1971: Zoning in the White Pine copper deposit, Ontonagon County, Michigan; Econ. Geol., v. 66, p. 543-573.

Binney, W.P.
1975a: Copper occurrences in Lower Carboniferous sedimentary rocks of the Maritime Provinces; Geol. Surv. Can., Open File 281, 156 p.

1975b: Lower Carboniferous stratigraphy and base-metal mineralization, Lake Enon, N.S.; unpubl. M.Sc. thesis, Queen's Univ., Kingston, 94 p.

Binney, W.P. and Kirkham, R.V.
1974: A study of copper mineralization in Mississippian rocks of Nova Scotia; in Report of Activities, Part A, Geol. Surv. Can., Paper 74-1A, p. 129-130.

1975: A study of copper mineralization in Mississippian rocks of the Atlantic Provinces; in Report of Activities, Part A, Geol. Surv. Can., Paper 75-1A, p. 245-248.

Charbonneau, B.W. and Ford, K.L.
1977: Ground radiometric investigations Kennetcook area, Nova Scotia; in Geol. Surv. Can., Open File 467.

1978: Uranium mineralization at the base of the Windsor Group, South Maitland, Nova Scotia; in Current Research, Part A, Geol. Surv. Can., Paper 78-1A, p. 419-425.

Clifton, H.E.
1963: The Pembroke Breccia of Nova Scotia; unpubl. Ph.D. thesis, Johns Hopkins Univ., Baltimore, 209 p.

Collins, J.A.
1974: The sedimentary copper universal; from sedimentologic and stratigraphic syntheses of the Proterozoic of Icon, Quebec; Grinnell Formation, Alberta; Nonesuch Shale, Michigan; and the Mississippian Horton-Windsor Formations of Nova Scotia; unpubl. Ph.D. thesis, Queen's Univ., Kingston, 259 p.

Erzberger, R., Franz, R., Jung, W., Knitzschke, G., Langer, M., Luge, J., Rentzsch, H., and Rentzsch, J.
1968: Lithologie, paläogeographie und metallführung des Kupferschiefers in der Deutschen Demokratischen Republik; Geologie, v. 12, p. 776-791.

Geldsetzer, H.H.J.
1977: The Windsor Group of Cape Breton Island, Nova Scotia; in Report of Activities, Part A, Geol. Surv. Can., Paper 77-1A, p. 425-428.

1978: The lower Windsor of Cape Breton Island, Nova Scotia, Canada: An early Carboniferous evaporite basin of a Zechstein-type? (abstract); Geol. Soc. Am., Abstracts with Programs, Northeast Section, p. 43.

Greiner, H.
1974: The Albert Formation of New Brunswick: a Paleozoic lacustrine model; Geologische Rundschau, v. 63, no. 3, p. 1102-1113.

Gussow, W.C.
1953: Carboniferous stratigraphy and structural geology of New Brunswick, Canada; Am. Assoc. Petrol. Geol., Bull., v. 37, no. 37, p. 1713-1816.

Haranczyk, C.
1970: Zechstein lead-bearing shales in the Fore-Sudetian monocline in Poland; Econ. Geol., v. 65, p. 481-495.

Jones, B.E. and Covert, T.G.N.
1972: Geology of Middle River and Baddeck Forks map areas, Victoria County, Nova Scotia; N.S. Dep. Mines and Cape Breton Dev. Corp., Cape Breton Island Min. Res. Surv., 124 p.

Jung, W.
1968: Sedimentary rocks and deposits in Saxony and Thuringia; Guide to Excur. 38AC, XXIII Inter. Geol. Cong., Prague, 33 p.

Kelley,D.G.
1967: Baddeck and Whycocomagh map areas, with emphasis on Mississippian stratigraphy of central Cape Breton Island, Nova Scotia; Geol. Surv. Can., Mem. 351, 65 p.

Kirkham, R.V.
1973: Environments of formation of concordant and peneconcordant copper deposits in sedimentary sequences (abstract); Can. Mineralogist, v. 12, pt. 2, p. 145-146.

1974: A synopsis of Canadian stratiform copper deposits in sedimentary sequences; in Gisements stratiformes et provinces cuprifères, ed. P. Bartholomé, Société Géologique de Belgique, Liège, p. 367-382.

1975: Visit to Kupferschiefer copper deposits in Poland provides data for comparing Canadian occurrences; Northern Miner, Nov. 27, p. A9-A11.

Lombard, J. and Nicolini, P.
1962: Search for the characteristics that are most frequently associated with copper stratiform mineralizations in Africa; Stratiform copper deposits in Africa, Sym. Ass. of African Geol. Surv., p. 205-212.

Lur'ye, A.M.
1974: Copper deposits in marine sediments; Sovetskaya Geologiya, no. 1, p. 20-29 (Internat. Geol. Rev., v. 17, no. 9, p. 1094-1102).

Lur'ye, A.M. and Gablina, I.F.
1972: Source of copper in the formation of Mansfeld-type deposits in the west Ural region; Geochem. Internat., v. 9, p. 56-57 (Geokhimiya, no. 1, p. 75-88).

MacLeod, J.L.
1975: Diagenesis and sulphide mineralization at Gay's River, Nova Scotia; unpubl. B.Sc. thesis, Dalhousie Univ., Halifax, 138 p.

Mamet, B.L.
1970: Carbonate microfacies of the Windsor Group (Carboniferous), Nova Scotia and New Brunswick; Geol. Surv. Can., Paper 70-21, 121 p.

Renfro, A.R.
1974: Genesis of evaporite-associated stratiform metalliferous deposits – a sabkha process; Econ. Geol., v. 69, p. 33-45.

Rentzsch, J.
1974: The "Kupferschiefer" in comparison with the deposits of the Zambian Copperbelt; in Gisements stratiformes et provinces cuprifères, ed. P. Bartholomé; Société Géologique de Belgique, Liège, p. 403-426.

Rose, A.W.
1976: The effect of cuprous chloride complexes in the origin of red bed copper and related deposits; Econ. Geol., v. 71, p. 1036-1048.

Schenk, P.E.
1967a: The Macumber Formation of the Maritime Provinces – A Mississippian analogue to Recent strand-line carbonates of the Persian Gulf; J. Sed. Petrol., v. 37, p. 365-376.

1967b: The significance of algal stromatolites to paleo-environmental and chronostratigraphic interpretations of the Windsorian Stage (Mississippian), Maritime Provinces; Geol. Assoc. Can., Spec. Paper 4, p. 229-243.

1969: Carbonate-sulfate-redbed facies and cyclic sedimentation of the Windsorian Stage (Middle Carboniferous) Maritime Provinces; Can. J. Earth Sci., v. 6, p. 1037-1066.

1975a: Windsorian Stage (Middle Carboniferous), Antigonish basin; Maritime Sediments, v. 11, no. 2, p. 55-68.

1975b: Carbonate-sulfate intertidalites of the Windsor Group (Middle Carboniferous) Maritime Provinces, Canada; in Tidal Deposits, ed. R.N. Ginsburg, Springer-Verlag, p. 373-380.

Smith, G.E.
1974: Depositional systems, San Angelo Formation (Permian)North Texas-Facies control of red bed copper mineralization; Texas Bur. Econ. Geol., Report of Invest. 80, 74 p.

1976: Sabkha and tidal-flat facies control of stratiform copper deposits in North Texas; in Stratiform Copper Deposits of the Midcontinent Region, a Symposium, eds. K.S. Johnson and R.L. Croy, Oklahoma Geol. Surv. Circular 77, p. 25-39.

Strakhov, N.M.
1962: (trans. 1970) Accumulations of Cu-Pb-Zn; their origin and distribution in arid regions; Principles of Lithogenesis, v. 3, New York, Plenum Press, p. 22-81.

Utting, J.
1977: Preliminary palynological investigation of the Windsor Group (Mississippian) of Nova Scotia; in Report of Activities, Part A, Geol. Surv. Can., Paper 77-1A, p. 347-349.

1978: Palynological investigation of the Windsor Group (Mississippian) of Port Hood Island and other localities on Cape Breton Island, Nova Scotia; in Current Research, Part A, Geol. Surv. Can., Paper 78-1A, p. 205-207.

von Hoyningen-Huene, E.
1963: Zur paläohydrogeologie des Oberrotliegenden und des Zechsteins im Harzvorland; Deutsche Gesellschaft für Geologische Wissenschaften, Berichte; v. 8, no. 1, p. 201-220.

Weeks, L.J.
1954: Southeast Cape Breton Island, Nova Scotia; Geol. Surv. Can., Mem. 277, 112 p.

Worley, D.
1975: A petrologic study of the copper sulphide distribution across the Windsor-Horton/Codroy-Anguille contact in parts of the Atlantic Provinces; unpubl. B.Sc. thesis, Queen's Univ., Kingston, 51 p.

Woodward, L.A., Kaufman, W.H., Schumacher, O.L., and Talbot, L.W.
1974: Stratabound copper deposits in Triassic sandstone of Sierra Nacimiento, New Mexico; Econ. Geol., v. 69, p. 108-120.

22. FLUID INCLUSION STUDIES AND GENESIS OF THE REXSPAR URANIUM-FLUORITE DEPOSIT, BIRCH ISLAND, BRITISH COLUMBIA

Project 770024

R.D. Morton[1], A. Aubut[1], and S.S. Gandhi
Regional and Economic Geology Division

Abstract

Morton, R.D., Aubut, A., and Gandhi, S.S., Fluid inclusion studies and genesis of the Rexspar uranium-fluorite deposit, Birch Island, British Columbia; in Current Research, Part B, Geol. Surv. Can., Paper 78-1B, p. 137-140, 1978.

Uranium and fluorite mineralization of the Rexspar deposit occurs in trachytic volcanic rocks. Preliminary observations on primary fluid inclusions in fluorite samples show that a liquid CO_2 phase is present in uranium-rich zones, and this phase is absent in uranium-poor zones. Homogenization temperatures for inclusions in the uraniferous zone are 140 to 230 C.

It is postulated that a hydrothermal solution, genetically related to the trachytic magma and charged with CO_2, transported uranium as carbonate complexes at about 200 C. A rapid drop in partial pressure of CO_2 caused deposition of uranium. Another phase of hydrothermal solution, possibly a subsequent one, lacked CO_2 and hence, the capacity to transport uranium.

Introduction

The Rexspar uranium-fluorite deposit is situated approximately 4 km south of Birch Island, and 130 km north of Kamloops, British Columbia. Fluorite was reported in 1918, and the property was first drilled in 1942-43 to investigate fluorite-celestite mineralization. Studies by the British Columbia Department of Mines and the Geological Survey of Canada revealed low radioactivity in this 'Fluorite' zone. Subsequent prospecting located uranium and thorium bearing zones in its vicinity (Joubin and James, 1956). Three of these, referred to as 'A', 'B' and 'Black Diamond' or 'BD' zones (Fig. 22.1) have been explored intermittently since 1949. They are estimated to contain a total of 1 114 400 tonnes of material grading on the average 0.655 kg U/tonne (Cotter, 1977; Preto, 1978).

Fluorite is abundant in all the mineralized zones. It is deep purple, and is commonly coarse, and thus suitable for fluid inclusion studies. Samples representing the 'A', 'BD' and 'Fluorite' zones were collected along with samples for geochronological studies, during the summer of 1977 by S.S. Gandhi. The fluorite samples were studied in the Fluid Inclusion Laboratory of the Department of Geology, University of Alberta, by A. Aubut and R.D. Morton.

Geology

The Rexspar property is underlain by a sequence of feldspar porphyritic trachytic flows and hypabyssal intrusives, pyroclastics, tuffs, and pyritic schists of rhyolitic composition. The sequence includes lenses of dark grey, pyrite-rich tuffaceous or argillaceous material, which are hosts to the uranium-thorium mineralization.

The trachytic members appear to overlie conformably a metasedimentary sequence of quartz-sericite schists with interbedded carbonaceous and phyllitic units. The trachytic assemblage to a large extent forms the present erosion surface. Overlying metasediments are seen only as a few small remnants.

The beds and schistosity have gentle dips, commonly less than 30° to the northwest. The rocks of the trachytic suite commonly exhibit considerable cataclasis and alteration, such that many are transformed to breccias, mylonites, and sericitic schists, in part carbonate- or albite-rich. Evidence of deformation is also seen in the mineralized zones in such features as elongation of pyroclastic fragments, deformed mica, and brecciated fluorite cemented by later fluorite (Joubin and James, 1957). Several faults and thrusts have been recognized in the area.

Age of 'trachyte'

The precise age of the trachytic rocks is not known. These rocks and the associated metasediments were considered a part of the Eagle Bay Formation by Okulitch and Cameron (1976). This formation is a complex and stratigraphically diverse succession ranging in age from mid-Paleozoic to Late Triassic. Limestone beds of this formation located about 40 km south of the Rexspar deposit, have yielded fossils of Mississippian age.

Radiometric age determinations on phlogopite of two samples from the Rexspar deposit, using K-Ar method are:

Lamprophyric dyke, 'BD' zone adit: 47.1 ± 2.6 Ma
(GSC-2837; unpublished)

Coarse pyrite-mica rock, 'B' zone: 236 ± 8 Ma
(GSC-2810; unpublished)

The pyrite-mica rock sample is a part of the mineralized zone. Gas extraction during its analysis was poor. The result, however, gives a minimum age for the mineralization. This minimum Permian age rules out the Baldy Batholith of Jurassic and/or Cretaceous age, which outcrops less than 6 km south of the Rexspar deposit (Campbell, 1963), as the source of the mineralization. The lamprophyric dyke cuts the 'BD' zone, and is undeformed and unaltered.

A Rb-Sr isochron age on the trachyte is being determined by the Geological Survey of Canada.

Mineralogy

Uranium mineralization is confined largely to dark coloured, tuffaceous or argillaceous lenses which contain between 5 and 20 per cent pyrite (Joubin and James, 1956). An appreciable amount of thorium and traces of rare earths are present. The mineralized zones contain abundant coarse pyrite and fluorphlogopite aggregates, carrying minor fluorite and calcite. These aggregates are variable in size and shape and may be either conformable with the schistosity or discordant to it. Other minerals identified are pitchblende, uranian thorite with minor uranothorianite, bastnaesite, torbernite, and metatorbernite (McCammon, 1954; Joubin and James, 1956, 1957; Lang et al., 1962). The radioactive phases

[1] Department of Geology, University of Alberta, Edmonton.

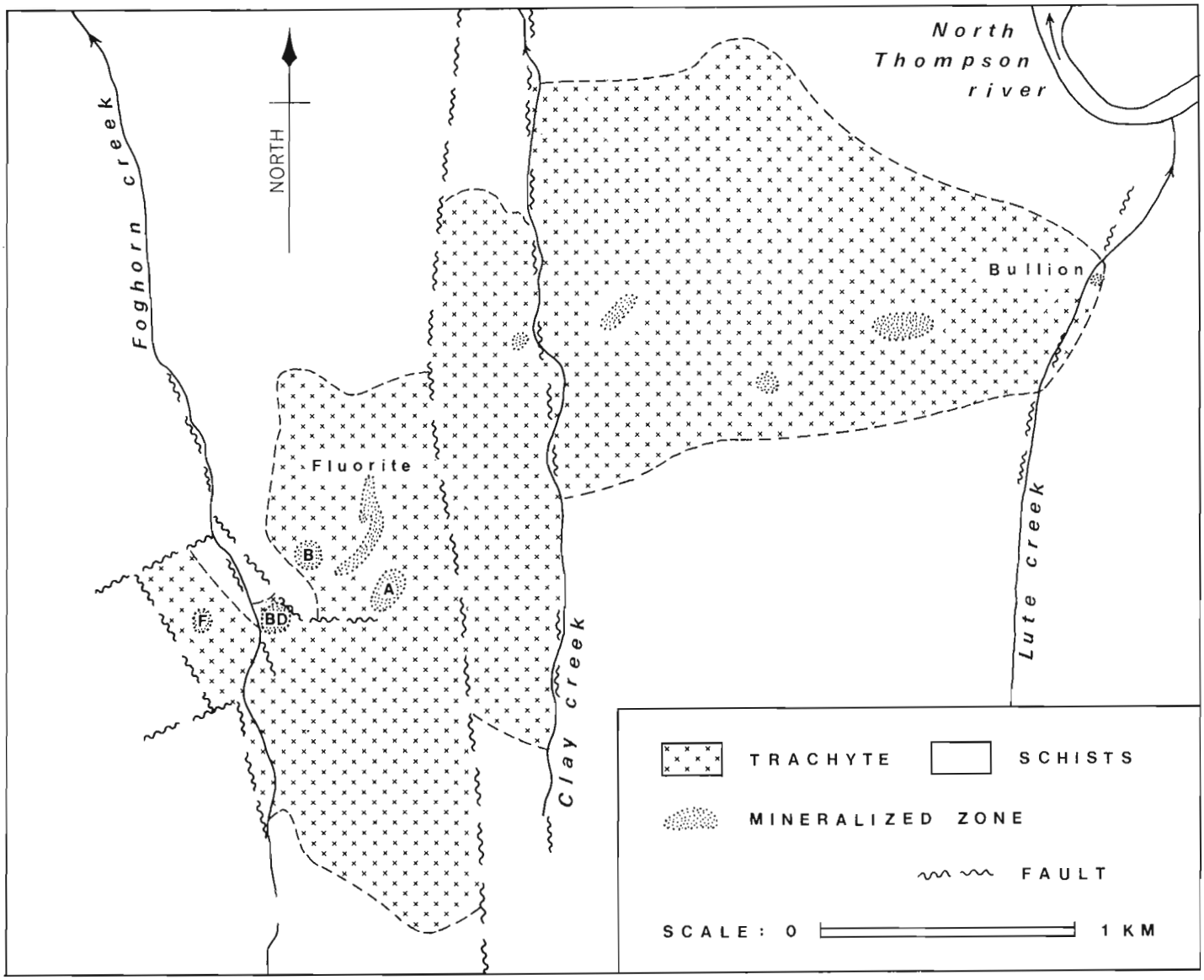

Figure 22.1. General geology of the Rexspar property.

occur as finely disseminated grains within matrices of fluorphlogopite, sericite, pyrite, purple fluorite, celestite, albite, pyrite, and carbonate. Minor zircon, rutile, and monazite are also present. Evidence for multiple stage of mineralization is provided by the presence of zones bearing trachyte fragments in a fine grained mica-pyrite-fluorite matrix that have been cut by a later series of fluorite veins.

The 'Fluorite' zone is a tabular zone about 15 m thick and dipping 35° or so to the northwest subparallel to the schistosity (McCammon, 1949), and consists of massive and disseminated fluorite (15 to 20 per cent) and celestite (10 to 15 per cent), with pyrite (up to 5 per cent), molybdenite and traces of galena in lithic tuff and tuff breccia of the trachyte. It has virtually no uranium or thorium. The relation of fluorite in the 'Fluorite' zone with the two stages of fluorite in the uraniferous zones is not certain. Differences in associated minerals suggest that the 'Fluorite' zone may have formed at a different time than the two stages represented by the fluorite in the uraniferous zones.

Fluid Inclusions

Studies of fluid inclusions were conducted on a television-equipped Chaixmeca VT2120, heating-freezing microscope stage, capable of an accuracy of ±0.1°C within the temperature ranges reported herein (Poty et al., 1976).

Two types of primary fluid inclusions were identified in the lithologies studied:

(i) Aqueous liquid + vapour (code WV)

(ii) Aqueous liquid + liquid CO_2 + vapour (code WCV)

Fluorites from the 'A' and 'BD' uraniferous zones carry WV and WCV primary inclusions 10 to 30 µm in diameter in approximately equal proportions (~ 60 WV: ~ 40 WCV). Those inclusions with visible liquid CO_2 (Fig. 22.2C) have 2 to 20 volume per cent CO_2. In contrast, the uranium-depleted 'Fluorite' zone carries only WV primary inclusions, 5 to 12 µm in diameter (Fig. 22-2A, B).

As anticipated, the fluorite-rich lithologies studied were both difficult to prepare as doubly-polished sections and to work with on the heating-freezing stage. Only specimens from the uraniferous 'BD' zone proved feasible for heating-freezing studies, owing to persistent decrepitation and leakage in the well-cleaved fluorites. In this zone the aqueous fluids in the primary inclusions exhibited freezing temperatures of -0.9°C to -13.0°C (mean -4.8°C) indicating a mean salinity of approximately 7 weight per cent equivalent NaCl, with a range of 2 to 18 weight per cent equivalent NaCl.

Heating experiments on the materials from the 'BD' uraniferous zone yielded uncorrected homogenization temperatures +140°C to +230°C (mean 181.0°C). The question of pressure corrections is difficult to resolve. If one is to assume the uranium mineralization to have been late-stage hydrothermal and of shallow, volcanic-exhalative character, there would be negligible corrections to apply. However, if the data of Takenouchi and Kennedy (1964, 1965) and Klevtsov and Lemmlein (1959) concerning the CO_2-H_2O system and pressure corrections are applied, then a corrected temperature of homogenization of 200°C to 215°C is inferred, and the inferred pressure at the time of mineralization would be 200 to 450 bars.

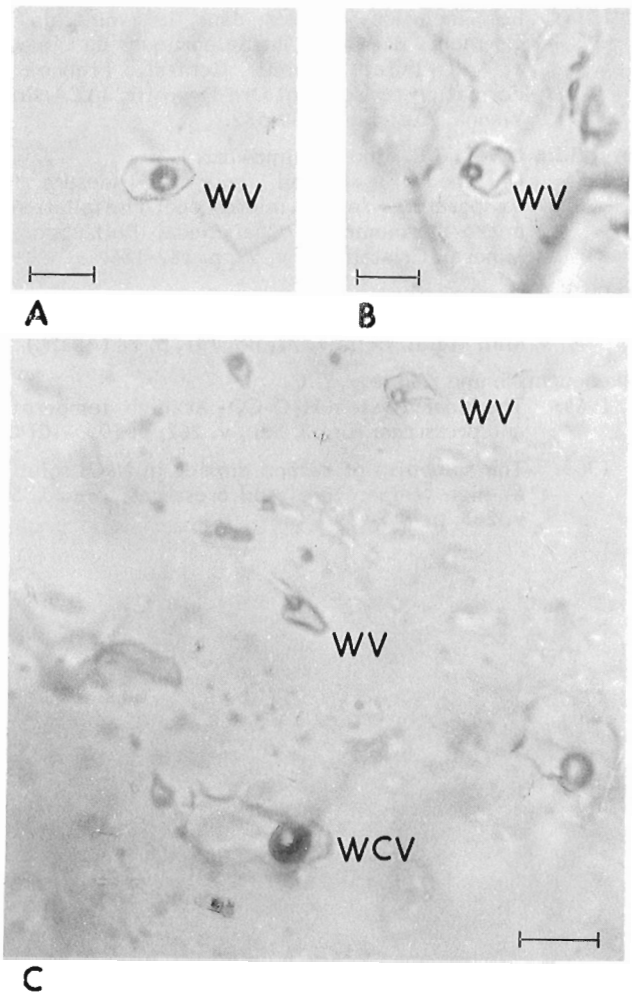

A and B: Typical primary H_2O-vapour inclusions from the 'Fluorite' zone.

C: A typical assemblage of coeval primary inclusions from the uraniferous 'BD' zone. Here inclusions with H_2O- liquid CO_2-vapour (WCV) are associated with H_2O-vapour inclusions (WV).

(Bar scale represents 20 μm)

Figure 22.2. Fluid inclusions from the Rexspar 'BD' and 'Fluorite' zones.

Genesis

Genetic relationships between the trachytic volcanics and the mineralizing fluids are apparent from the nature of the host rocks, the mineralogy of the deposits, and their field relations. Joubin and James (1956) postulated that an initial sulphide-fluorite mineralization was introduced during a synvolcanic exhalative episode and that subsequent cataclasis was followed by the deposition of uraniferous minerals and recementation by fluorite. Preto (1978) suggested that fluorphlogopite, pyrite, fluorite, and uranium-bearing minerals were deposited by late stage, deuteric volatile-rich fluids during the evolution of a highly differentiated intrusive-extrusive igneous suite.

Preliminary observations on fluid inclusions presented here suggest a probable mechanism of uranium transport and deposition.

The presence of coeval WV and WCV inclusions in the fluorites of the 'A' and 'BD' uraniferous zones at the Rexspar property is indicative of effervescence of the saline hydrothermal systems during the uranium mineralization process. It is likely that the uranium (together with thorium and rare-earth elements) was transported as carbonate complexes in a weakly saline aqueous system charged with CO_2 (the CO_2 being of volcanic origin). As the carbonate-rich uranium-bearing, saline solutions resided within the cooling trachytic suite at around 200°C, the fissure systems were vented to the surface. This would have resulted in a sudden pressure drop and in a concomitant effervescence with the release of CO_2 gas, thus drastically lowering the partial pressure of CO_2 in the system. Such a drop in P_{CO_2} could result in a precipitation of uranium minerals, as the uranyl carbonate complexes would no longer be stable in the system.

In contrast, the 'Fluorite' zone, which may have formed at a different time than the uraniferous bodies, appears to bear no evidence of the presence of CO_2. It was apparently formed from a predominantly aqueous hydrothermal system; (perhaps during a subsequent incursion of meteoric waters). This then would explain its relative lack of uranium mineralization, for the system would be unable to support the formation of uraniferous carbonate complexes and thus perhaps unable to mobilize or to transport uranium in any large quantities.

These observations provide an excellent analogy to those of Poty et al. (1974) regarding the granitoid-hosted uranium deposits of Limousin in the Central Massif of France. In both cases the presence of CO_2-bearing fluid inclusions characterizes the uraniferous zones and their absence is characteristic of barren zones. In both cases too, uranium may have been deposited partly as a result of a drop in the CO_2 content of the hydrothermal systems due to venting, rather than to the commonly assumed U^{6+} U^{4+} reduction processes. To some extent too, a reduction in the P_{CO_2} could have been brought about by carbonatization of some of the trachytic wall rocks. As in the case of the Limousin deposit, the mechanisms which might have effected the postdepositional reduction of uranium from U^{6+} to U^{4+} are as yet unknown.

Conclusion

Observations on the primary fluid inclusions in fluorite lead to the conclusion that carbon dioxide played an important role in transportation of uranium in hydrothermal solution and its deposition at the Rexspar deposit.

Acknowledgments

Thanks are due to E.L. Evans of Denison Mines Limited for co-operation in providing information on the Rexspar deposit. Discussions with V. Preto of British Columbia Department of Mines have been valuable, and thanks are also extended to him.

References

Campbell, R.B.
1963: Adams Lake map-area, British Columbia; Geol. Surv. Can., Map 48.

Cotter, N.P.
1977: Rexspar outlines B.C. "U" plans; Northern Miner, v. 63, no. 40.

Joubin, F.R. and James, D.H.
1956: Rexspar uranium deposits; Can. Min. J., v. 77, p. 59-60.

1957: Rexspar uranium deposits; in 'Structural Geology of Canadian Ore Deposits', Can. Inst. Min. Metal., p. 85-88.

Klevtsov, P.V. and Lemmlein, G.G.
1959: Pressure corrections for the homogenization temperatures of aqueous NaCl solutions; Akad. Nauk. SSSR, Dokl., v. 128, no. 6, p. 1250-1253.

Lang, A.H., Griffith, J.W., and Steacy, H.R.
1962: Canadian deposits of uranium and thorium; Geol. Surv. Can., Econ. Geol. Rep. 16, p. 205-207.

McCammon, J.W.
1949: 'Spar 1 and Spar 2 Claims' (Fluorite); British Columbia Minister of Mines Annual Report, p. A250-255.

1954: Rexspar Uranium and Metals Mining Co. Limited; British Columbia Minister of Mines Annual Report, p. A108-111.

Okulitch, A.V. and Cameron, B.E.B.
1976: Stratigraphic revisions of the Nicola, Cache Creek, and Mount Ida Groups, based on conodont collections for the western margin of the Shuswap Metamorphic Complex, south-central British Columbia; Can. J. Earth Sci., v. 13, no. 1, p. 44-53.

Poty, B.P., Leroy, J., and Cuney, M.
1974: Les inclusions fluides dans les minerais des gisements d'uranium intragranitiques du Limousin et du Forez (Massif Central, France); in Formation of Uranium Ore Deposits, IAEA Proc., Vienna, Austria, p. 569-582.

Poty, B.P., Leroy, J.R., and Jachimowicz, L.
1976: Un nouvel appareil pour la mesure des temperatures sons le microscope: l'installation de micro-thermometric Chaixmeca; Bull. Soc. Fr. Mineral. Cristallogr., v. 99, p. 182-186.

Preto, V.A.
1978: Geology of the Rexspar uranium deposit; Can. Min. Metal. Bull., v. 71, no. 791, p. 78 (Abstr.)

Takenouchi, S. and Kennedy, G.C.
1964: The binary system H_2O-CO_2 at high temperatures and pressures; Am. J. Sci., v. 262, p. 1055-1074.

1965: The solubility of carbon dioxide in NaCl solutions at high temperatures and pressures; Am. J. Sci., v. 263, p. 445-454.

23.

GEOLOGICAL OBSERVATIONS AND EXPLORATION GUIDES TO URANIUM IN THE BEAR AND SLAVE STRUCTURAL PROVINCES AND THE NONACHO BASIN, DISTRICT OF MACKENZIE

Project 770024

S.S. Gandhi
Regional and Economic Geology Division

Abstract

Gandhi, S.S., Geological observations and exploration guides to uranium in the Bear and Slave structural provinces and the Nonacho Basin, District of Mackenzie; in Current Research, Part B, Geol. Surv. Can., Paper 78-1B, p. 141-149, 1978.

Over 200 uranium occurrences are known in the study area, and the majority of them are hosted by Proterozoic rocks. They are classified into six groups, namely, hydrothermal veins, late magmatic differentiates, syngenetic sedimentary deposits, disseminations in paragneiss, disseminations in sandstone, and unconformity-related supergene concentrations. Past production came from the hydrothermal veins. In recent years, exploration efforts have been concentrated in the search for sandstone-type and unconformity-related deposits, and have met with encouraging results. The nature and geological setting of the occurrences are reviewed briefly and some geological guides to exploration are suggested.

Introduction

The Bear and Slave structural provinces and the Nonacho Basin immediately to the south of them, in the northwestern part of the Canadian Shield display a variety of geological settings suitable for several different types of uranium mineralization, and thus present favourable targets for exploration. Previous exploration, dating back to about 1940, has revealed over 200 uranium occurrences, and has led to two mining operations, the well-known Eldorado Mine on Great Bear Lake, and the Rayrock Mine about 150 km south of it (Fig. 23.1). These mines produced 5200 and 150 t of uranium metal (13.5 and 0.4 million pounds U_3O_8) respectively prior to 1961. Exploration activities have intensified in recent years and have brought to light some promising prospects.

A brief review of the known occurrences is presented here, based partly on the examination of 45 of them during the 1977 field season. A tentative classification scheme is given, and some geological guidelines in the search for additional deposits are suggested.

General Geology

Tectonic elements of the northwestern part of the Canadian Shield are shown in Figure 23.1 (from Hoffman et al., 1974). Most known uranium occurrences are in Proterozoic rocks (2500 to 600 Ma) of five areas or districts; namely, Great Bear Batholith and volcanic belt; Coppermine Homocline; Bathurst Aulacogen; Athapuscow Aulacogen; and Nonacho Basin. Major rock units of these areas are listed in Table 23.1.

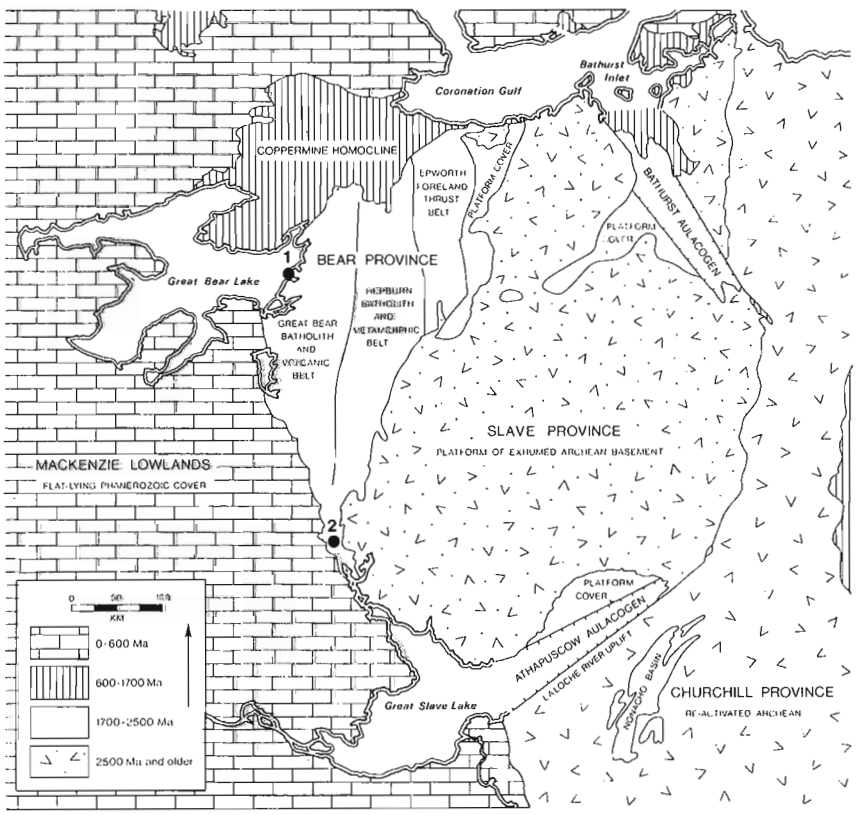

1. Eldorado Mine
2. Rayrock Mine

Figure 23.1.

Tectonic map of northwestern part of Canadian Shield showing Bear and Slave structural provinces and part of Churchill Province (from Hoffman et al., 1974, p. 42).

Table 23.1

Table of Formations: Bear and Slave structural provinces and Nonacho Basin

AGE	Nonacho Lake area (Fault-controlled Basin)	East Arm-Great Slave Lake area (Athapuscow Aulacogen)	Bear Lake Area (Coronation Geosyncline, Bear Province)	Dismal Lakes area (Coppermine Homocline)	Bathurst Inlet area (Bathurst Aulacogen)
CENOZOIC	Recent glacial drift, alluvial sands	Recent deltaic and allvial sands	Recent glacial drift, lake deposits etc.	Recent glacial drift, alluvial sands	Recent glacial drift, alluvial sands
	--ca. 65 Ma--	---unconformity---	---unconformity---		
MESOZOIC			Cretaceous: undivided		
	--ca. 225 Ma--	---unconformity---	---unconformity---		
PALEOZOIC		Devonian: Pine Point sequence, dominantly carbonates	Devonian: Bear Creek Formation Cambro-ordovician: Ronning Group, Saline River Formation, Old Fort Formation		
	--ca. 600 Ma--	---unconformity---	---unconformity---	---unconformity---	
HADRYNIAN				Rae Group	Rae Group (?)
	--ca. 1000 Ma--			---unconformity---	---unconformity---
NEOHELIKIAN				Husky Creek Formation Copper Creek Formation Dismal Lakes Group	Algak Formation Ekalulia Formation Kanuyak Formation
	--ca. 1400 Ma--			---unconformity---	---unconformity---
PALEOHELIKIAN		Mackenzie Dyke swarm	Mackenzie Dyke swarm Hornby Bay Group	Muskox Intrusion Hornby Bay Group	Parry Bay Formation Ellice River Formation
				---unconformity---	---unconformity---
	Gabbro dykes	Et-Then Group			Tinney Cove Formation
	--ca. 1800 Ma unconformity--	---unconformity---	---unconformity---	---unconformity---	---unconformity---
APHEBIAN	(Hudsonian events of folding, faulting and local reactivation of the basement)	'Exotic Breccia' dyke-like intrusives Quartz diorite-monzonite laccoliths and dykes	Bear Batholith and comagmatic acidic volcanics and inter-bedded sediments of Echo Bay (Cameron Bay) Group Hepburn Batholith	Granite (Folding, metamorphism) Akaitcho Group	
				---unconformity (?)---	
	Nonacho Group	East Arm Supergroup Christie Bay Group Pethei Group Kahochella Group Sosan Group	Metamorphosed Snare and Epworth groups Snare Group	Epworth Group Takiyuk Formation Cowles Lake Formation Recluse Formation Rocknest Formation Odjick Formation unnamed Formation	Goulburn Group Amogok Formation Brown Sound Formation Kuuvik Formation Peacock Formation Quadyuk Formation Burnside River Formation Western River Formation
		---unconformity---			
		Union Island Group			
		---unconformity---			
		Diabase dykes Easter Island Dyke Alkaline Complexes Wilson Island Group			
	--ca. 2400 Ma unconformity--	---unconformity---	---unconformity---	---unconformity---	---unconformity---
ARCHEAN	Granite Ortho and paragneiss Tazin Group				
	---unconformity---				
	Granitic Basement	Slave Craton	Gabbro, grandiorite, granite, ortho and paragneiss Yellowknife Supergroup		
			---unconformity---		
			Granitic Basement		

(compiled from Balkwill, 1971; Baragar and Donaldson, 1973; Campbell, 1978; Campbell and Cecile, 1976; Cook and Aitken, 1971; Davidson, 1978; Hoffman, 1968, 1969, 1978; McGlynn, 1977; and Norris, 1965).

The Great Bear Batholith and related effusive rocks form the western part of Coronation Geosyncline, and were developed about 1800 Ma ago during the late stage of Hudsonian orogeny (Hoffman and McGlynn, 1977). To the north it is covered by younger Proterozoic rocks of Coppermine Homocline, consisting of a sequence of sediments and plateau basalts dipping gently to the north (Baragar and Donaldson, 1973). Bathurst Aulacogen, also referred to as Kilohigok Basin of Bathurst Inlet area, is tectonically related to the geosyncline and is filled with sediments and subordinate volcanics (Campbell and Cecile, 1976; Campbell, 1978). It is the least explored of the five areas. Athapuscow Aulacogen along the East Arm of Great Slave Lake is also tectonically related to the geosyncline, and has a thick sequence of sedimentary rocks with minor associated volcanics (Hoffman 1968, 1969; Hoffman et al., 1977). The Nonacho Basin is a fault-controlled intracratonic sedimentary basin (McGlynn, 1971a).

Uranium Occurrences

Classification

The known uranium occurrences are classified into six groups. The classification is a tentative one, but adequate for the remarks made here. The groups are:

1. Hydrothermal veins
2. Late magmatic differentiates
3. Syngenetic sedimentary deposits
4. Disseminations in paragneiss
5. Disseminations in sandstone
6. Unconformity-related supergene concentrations

These are reviewed briefly, citing examples and references to published literature. Geological features useful in further exploration are noted.

(1) Hydrothermal veins

Distribution. Hydrothermal uranium veins are most common in the Bear Batholith area, where they are localized along fractures that are subsidiary to major northeast-trending strike-slip faults. Mapping to date shows that there are about 50 such faults along the 450-km length of the batholith (McGlynn, 1977). The faults can be traced for distances up to 70 km, and some have displacements of several kilometres. The distribution of over 100 known uranium occurrences shows greater concentrations near the western boundary of the batholith. This appears in part to be due to better exposures and access, but it may also indicate that certain parts of the batholith are relatively more favourable than the rest. The extent of the batholith under a thin Phanerozoic cover (Balkwill, 1971; Cook and Aitken, 1971) is not well known, but aeromagnetic maps show patterns similar to those observed over the exposed parts of the batholith, for several kilometres to the west of the boundary of the cover rocks.

Vein-type deposits are also found in other Proterozoic rocks, where they occur along fractures, faults, shears, mylonite zones, and breccia zones, as well as along foliation trends in phyllites and other metasediments. Some of the mineralized faults follow regional fold structures and foliation trends, and because of their great strike lengths and associated mylonitization, they appear to be deep-seated. Those in the western part of the Nonacho basin are good examples (J.C. McGlynn, pers. comm.).

Mineralogical Features. All the veins carry uranium in pitchblende. The associated minerals suggest two natural groupings of the veins, namely 'simple' quartz-hematite veins and 'complex' Ag, Bi, Co-Ni arsenide, Cu-sulphide veins (Lang et al., 1962, p. 59-60).

The simple veins are widely distributed throughout the Bear Batholith area, and are also encountered in the Nonacho Lake area. In the Bear Batholith area, they are commonly associated with 'giant quartz veins' and quartz stockworks, but form only a small part of them. Rayrock Mine is a type example of this mode of occurrence (Lang et al., 1962, p. 193-196; McGlynn, 1971b, p. 88-90). At Rayrock, the late stage pitchblende-bearing hematite-quartz veins occupy fractures and breccia zones within a quartz stockwork and its surrounding alteration zone of epidote-hematite-quartz in the granodiorite country rock.

There are many pitchblende veins of fracture-fillings which carry little or no quartz or other gangue minerals. Some of these are considered hydrothermal, since they grade into or are closely associated with what are regarded as hydrothermal veins. Others are supergene concentrations. An example of such a concentration is a new showing discovered by the writer and S.M. Roscoe, about 32 km east-southeast of Rayrock Mine, on claims held by C. Vaydick. The vein consists of pitchblende seams up to 2 mm thick along a vertical, north-trending fracture traceable for 10 m in a massive andesitic host rock. Similar simple pitchblende veins are observed elsewhere in the Bear Batholith area in other types of host rocks. Examples are acidic volcanics mineralized with widespread copper sulphide mineralization, diabase dykes, and granite. Thus both the simple hydrothermal veins supergene-type fracture-fillings are widespread in the area. In some cases, classification is difficult. The source of uranium in the supergene-type fracture filling is usually not apparent, it could be local or remote, concentrated or disperse. The possibility that it could have come from hydrothermal veins in the vicinity should be kept in mind during exploration.

The complex veins are found in a restricted area of about 1000 km^2 southeast of Great Bear Lake, which may be referred to as the Echo Bay-Camsell River mining camp. This area is underlain by rocks of the basal part of the volcanic sequence related to the Bear Batholith, associated sediments, and granitic plutons of the Bear Batholith (Hoffman and McGlynn, 1977). The volcanics and associated sediments are hosts to the vein deposits. The deposits include the old Eldorado mine, now producing silver, and other currently operating silver mines namely Terra, Norex, and Silver Bay. At the Eldorado mine, silver and uranium occur in the same fracture system but on the scale of mining, silver-rich veins and shoots tend to be separate from those rich in uranium. Mineral paragenesis of this and other mines has been studied by several workers (Kidd and Haycock, 1935; Campbell, 1955; Jory, 1964; Badham et al., 1972; Mursky, 1973; Shegelski, 1973) and five stages are recognized. Much of the uranium was deposited during an early stage of pitchblende-quartz-hematite veining, which preceded the deposition of silver and Co-Ni arsenides. Exploration for silver and uranium in the area has not always gone hand in hand. Thus there are some silver prospects in the vicinity of which additional exploration may prove fruitful. In this respect, a recent announcement by Terra Silver Mines (Northern Miner, Jan.'78, v. 63, No. 43) of intersection of a pitchblende-bearing vein close to silver veins and carrying uranium grades comparable to those mined at the Eldorado mine, provides an incentive for further exploration for uranium. The production figures show that the Echo Bay-Camsell River mining camp as a whole has produced four times as much uranium metal as silver.

Genesis. The origin of the pitchblende-bearing veins of Bear Batholith area has been discussed by many workers (see Kidd and Haycock, 1935; Lang, 1952; Campbell, 1955; Lang et al., 1962; Mursky, 1963, Jory, 1964; Ruzicka, 1971; Robinson and Morton, 1972; Badham et al., 1972; Robinson and Ohmoto, 1973; Shegelski, 1973; Thorpe, 1974; Langford, 1977). Laboratory studies on the complex veins by Badham et al. (1972) showed that ore deposition occurred in dilatant zones from mineralizing solutions at temperatures between 140 and 230°C. The radiometric age determinations converge around 1450 Ma for deposition of pitchblende, and between 1700 and 1850 Ma for the formation of the host rocks (see discussion by Thorpe, 1974). Brief genetic hypotheses considered by various workers are: (a) hydrothermal solutions derived from an acidic magmatic source related to the Bear Batholith (Kidd and Haycock, 1935; Mursky, 1963; Shegelski, 1973); (b) leaching of ore metals from tuffaceous host rocks by heated brines, connate or meteoric water (but not magmatic), and deposition in the veins (Robinson and Morton, 1972; Robinson and Ohmoto, 1973); (c) hydrothermal solutions carrying Ag, Co, Ni, As, Bi, and Cu derived from a gabbroic magma that formed the diabase dykes which intruded the area about 1425 Ma ago (Mursky, 1973; Thorpe, 1974), and (d) supergene concentrations by surface meteoric waters near the paleosurface (Langford, 1977).

Objections arise in all of the above hypotheses. If the radiometric age of the veins is accepted as their true age, then they are much younger than the Bear Batholith, and thus cannot have a direct genetic relationship with the batholith. Leaching of ore metals from tuffaceous host rocks cannot be applied to many occurrences that are remote from such rocks. Gabbroic magma is a likely source for various metals except for uranium and associated silica. Difficulties with supergene concentration as a primary mechanism for the formation of the veins are: lack of extensive weathering or alteration required for such a process, absence of reducing agent, presence of abundant quartz, and depth extension of veins to over 300 m. Supergene concentration has however played a secondary role in deposition of minor amounts of botryoidal pitchblende and other secondary minerals, which is attributed by all workers to the action of the surface waters on the existing deposits. Some pitchblende fracture fillings with little or no gangue minerals can be, as mentioned above, attributed to supergene concentration.

A modified version of the first hypothesis, implied by some of the earlier workers and favoured by the writer, is as follows. Hydrothermal solutions derived from the Bear Batholith are the most likely source of quartz and pitchblende. The simple veins were probably formed soon after the emplacement of the Batholith. Their wide distribution is consistent with such an origin. The Ag, Bi, Co-Ni-arsenide veins formed later, from mineralizing solutions derived from a restricted source related to the diabase intrusions. The solutions followed some of the fractures occupied by earlier veins, which were reopened and extended by fault movements. At places these solutions came in contact with the earlier deposited uranium, which was partly or wholly dissolved, and later redeposited with a polymetallic mineral assemblage. Thus parts of the veins show effects of superimposed mineralization. Fault movements continued well into the Helikian times, and most likely affected the pitchblende-bearing veins so that radiometric equilibrium was readjusted. The younger ages obtained may thus be reconciled under such an hypothesis.

(2) Late Stage Magmatic Differentiates

Proterozoic intrusive rocks represent a wide range of igneous activity. From the standpoint of late stage magmatic differentiates carrying uranium the most important are granites, alkaline complexes, and diorite-monzonite plutons.

Granites. Pegmatites carrying uranium and thorium minerals are associated with both Archean and Aphebian granites. The occurrences are commonly small and low grade in terms of uranium values. Only a few are well studied, such as those in Yellowknife-Beaulieu region (Kretz, 1968).

Some available data suggest that certain granitic bodies and their hypabyssal and effusive equivalents, are enriched in uranium or thorium or both. Examples are parts of Bear Batholith area (Allan and Cameron, 1973) and granitic rocks in the area west of the Nonacho basin (Charbonneau, in prep.). These uranium-enriched rocks are a potential source for primary as well as secondary concentrations of uranium.

Alkaline Complexes. There are only two alkaline complexes found to date in the Bear and Slave structural provinces, but more can be expected. One is the 'Big Spruce' complex located about 40 km east-northeast of Rayrock mine (Martineau and Lambert, 1974; Irving and McGlynn, 1976; Currie, 1976). The other is the 'Blachford' complex, located about 160 km southeast of the mine (Davidson, 1978). Radiometric age determinations on the two complexes gave 2111 ± 40 Ma (Rb-Sr isochron, Martineau and Lambert, 1974) and 2057 ± 56 Ma (K-Ar method; Davidson, 1978) respectively. The Big Spruce complex is a nepheline agpaitic syenite complex, with carbonatite differentiates that carry localized concentrations of U and Th. The Blachford complex is a silica-saturated agpaitic complex and has late differentiates enriched in niobium, uranium, thorium, rare earths, and other metals. Albite, magnetite, and fluorite are common minerals in the late differentiates. The work done to date indicates a niobium-rich zone about 10 m wide and 700 m long, carrying low but significant uranium values (see assays, Davidson, 1978, p. 125).

Diorite-monzonite plutons. These occur as laccoliths in the East Arm of Great Slave Lake. Their late stage differentiates are coarse magnetite-apatite-amphibole veins, which in some cases carry notable amounts of pitchblende. Pitchblende is disseminated along parts of the veins, commonly in close association with magnetite. The veins occur near the margins of the plutons. Field relations and petrological observations show that the vein minerals, including pitchblende, are derived from the plutons. Radiometric age determinations support this genetic connection. A pitchblende-bearing sample (LF-71-29, H.W. Little) from the 'Rex' property (Lang et al., 1962, p. 203-205) gave a Pb^{207}/Pb^{206} ratio that yielded an age of 1750 Ma (Pb^{207}/U^{235} and Pb^{206}/U^{238} ratios gave 1662 and 1550 Ma respectively). The host rock is similar to two other dioritic rocks in the East Arm area, dated at 1845 and 1795 Ma (GSC 61-78 and 67-77; Hoffman, 1969) by K-Ar method. Similar magnetite-apatite-actinolite veins and small pods are described in the Echo Bay-Camsell River area (Badham and Morton, 1976), but no pitchblende was reported in them.

(3) Syngenetic sedimentary deposits

The important sedimentary beds for this type of deposits are quartz-pebble conglomerate, dolomite, and shale.

Quartz-pebble conglomerate. An example of uraniferous quartz-pebble conglomerate of fossil placer type is known on the west shore of the MacInnis Lake area in the Nonacho basin (McGlynn, 1971a, p. 142). Three separate horizons or reefs ranging in thickness from 2 to 10 m are known within a stratigraphic thickness of about 300 m, consisting mainly of arkose and minor shale. Outcrops of quartz-pebble conglomerate also occur northeast and southeast of MacInnis Lake. Uranium values reported to date are low, but are significantly higher than the background. Tin is present along with uranium. No systematic evaluation of the MacInnis Lake subbasin is available.

Quartz-pebble conglomerate horizons are known elsewhere in the Aphebian sequences, but to date no significant uranium values have been reported.

Dolomite. Some algal and arenaceous dolomitic beds in the lower part of the Aphebian sequence along the East Arm of Great Slave Lake contain monazite and uraninite (or pitchblende) concentrations. One example is the McLean Bay occurrence (Lang et al., 1962, p. 201-202) where the host dolomite is interbedded with quartzite. Thorium predominates over uranium. The mineralization is apparently detrital. Other examples of anomalous radioactivity in uranium and thorium, were observed by the writer in dolomitic rocks interbedded with sandstone and siltstone of Wilson Island Group on Wilson Island, and on a small island to the southwest where the unconformity between the granitic basement and the Sosan Group is exposed. Lenses of quartz-pebble conglomerate were also seen in the Sosan Group here. Scintillometer readings indicated a predominance of thorium over uranium.

Shale. Shale beds frequently carry notable concentrations of uranium. Such shale lenses are encountered in sandstones of the Nonacho and Hornby Bay groups. The shales are red, green, or grey. Extensive shale beds, particularly the dark grey graphitic variety such as the Fontana Formation in Epworth Group (Hoffman et al., 1978), are favourable host rocks for uranium, and merit attention during exploration. Another favourable geological setting is where shale is interbedded with tuffs in an area of strongly bimodal, basic and acidic volcanic activity. Such a setting is present in the lower part of the volcanic sequence in the Hottah Lake-Camsell River area (Hoffman and McGlynn, 1976) where basaltic volcanics (Hottah Lake Basalt Unit) are overlain by acidic volcanics (Camsell River Rhyolite Unit) related to the Bear Batholith. This setting resembles that seen in the Aphebian Aillik Group of Labrador where several uranium deposits are hosted by an 'argillite-tuffaceous sediment' horizon (Gandhi, 1977).

(4) Dissemination in paragneiss

There are a number of small uranium occurrences along layers in paragneiss. The most common host rocks are quartzofeldspathic gneisses rich in biotite and/or hornblende, apparently derived from impure siltstone. A typical example is a zone on the north shore of DeVries Lake, about 100 km north of Rayrock mine (Thorpe, 1972, p. 68-72). The host rock is a metasediment of the Snare Group. Pegmatitic quartzofeldspathic veins and patches are common in the highly contorted micaceous paragneiss. Uranium mineralization (uraninite or pitchblende) is disseminated along zones up to 1 m wide and traceable for several tens of metres. These mineralized zones are discontinuous. Magnetite is abundant in the zones, and traces of molybdenite and chalcopyrite are also present.

There are other similar occurrences in the basement gneiss of Nonacho Lake area, where the host rock could be Archean which has been affected by Hudsonian deformation during Aphebian times.

The origin of these occurrences is debatable. The mineralized zones display minor tight folds and crenulations and are cut by pegmatitic veinlets. These features suggest the possibility that mineralization is predeformation and premetamorphism. Uranium may have been originally dispersed through the host rock, and may have been later concentrated by metamorphic segregation. Alternatively, a hydrothermal source may be postulated. The presence of granitic bodies in the vicinity can be inferred from the abundance of pegmatitic dykes, and could have contributed uranium which was deposited in the host rocks prior to the final phase of deformation and metamorphism.

(5) Disseminations in sandstone

General Remarks. Aphebian and Helikian sandstones host several uranium occurrences, and are favourable targets for exploration. Mineralization consists of disseminated pitchblende, with local high grade aggregates. Traces of other metals such as copper and silver are detected, but there is little or no thorium. The mineralized zones vary in shape from irregular to crudely lenticular and are subparallel to bedding. Local fractures carrying higher grade concentrations are common, but they account for only a minor proportion of the mineralization.

There are many variations within this group of deposits, as seen from the well-known deposits in the Phanerozoic sandstones in the western United States (Fischer, 1974). A common feature is that the host rock is continental sandstone. Many of the Proterozoic sandstones of the Bear and Slave structural provinces and the Nonacho basin are continental, and contain red beds. One main point of difference between the latter and the Phanerozoic sandstones is that the Proterozoic sandstones lack remains of land plants, which some investigators believe played a crucial role as a reducing agent in deposition of uranium from the oxidized solutions that transported it. This factor cannot be very critical, however, since uranium does occur in the Proterozoic sandstones, and also in parts of the Phanerozoic sandstones where plant remains are scarce or absent. Other reducing agents such as pyrite, and other forms of organic remains, or chemical factors such as Eh-pH and dissolved CO_2, need to be invoked in the case of Proterozoic sandstones.

The proximity of potential source rocks, such as granites or tuffs containing higher than background concentrations of uranium to continental sandstones, is a useful guide to exploration (see also Rich et al., 1977, p. 64-73). In this regard, sandstones of the Hornby Bay Group are particularly well situated with respect to the Great Bear Batholith and volcanic belt.

Aphebian sandstones. The best known uranium occurrences are in the Sosan Group on the East Arm of Great Slave Lake. The host unit is the basal Hornby Channel Formation consisting mainly of coarse subarkosic sandstone of fluviatile origin (Hoffman, 1968, 1969). There are 20 occurrences along its 200 km strike length. They are described in detail by Morton (1974) and Walker (1977).

The age of uranium mineralization of this type in such ancient sandstones is a topic of considerable interest. Geological evidence bearing on the minimum age is provided by the presence of mineralized sandstone blocks in exotic breccia of Simpson Island in the western part of East Arm of Great Slave Lake. The breccia are older than the Paleohelikian Et-Then Group (Reinhardt, 1972, p. 27) and younger than Stark Formation of Christie Bay Group (Hoffman, 1978). Several radiometric age determinations on the mineralized rocks are now available. One is on a sample collected from 'Vestor Zone 5' on Simpson Island (sample No. LF-71-21, collected by H.W. Little). Analyses done at Teledyne Laboratories for the Geological Survey of Canada, gave a Pb^{207}/Pb^{206} ratio corresponding to an age of 1556 Ma; Pb^{207}/U^{235} and Pb^{206}/U^{238} ratios give 1004 and 766 Ma, respectively, indicating discordance attributable to a loss of lead from the system. Other Pb-U isotopic age determinations were done by Bloy (1978) at the University of Alberta. His analyses of a suite of samples from the 'Vestor Zone 5', and another suite from the 'Toopon Lake Zone' about 130 km to the northeast, yielded ages for the uranium mineralization of 1510± 8 and 2123 ± 60 Ma, respectively (G. Bloy; pers. comm., 1978). The older age is regarded as the age of primary mineralization which is little affected by later geological events, whereas the younger age is interpreted as resulting from remobilization of uranium during later

tectonic movements and/or metamorphism. The age of the host Sosan Group is indicated by the data from Rb-Sr and K-Ar age determinations on the overlying and underlying rocks. The minimum age is defined by the Seton volcanics in the overlying Kahochella Group which gave a Rb-Sr isochron age of 1870 Ma (Baadsgaard et al., 1973). The Sosan Group is younger than the 'Easter Island' dyke, a minor differentiated alkaline complex (Hoffman, 1978). Biotite from the dyke has been dated by the K-Ar method at 2200 Ma (Burwash and Baadsgaard, 1962, p. 28), and 2170 Ma (Leech et al., 1963, p. 61). From these data, it appears likely that uranium mineralization took place soon after the deposition of the host Hornby Channel Formation of the Sosan Group, and has been modified to some extent in those parts of the basin which are affected by tectonic activities.

The possibility of sandstone-type uranium occurrences in other nonmarine Aphebian sandstones of the Bear and Slave structural provinces and the Nonacho basin merits investigation. For example sandstones interbedded with volcanics of the Bear Batholith area are theoretically favourable host rocks. A group of small showings east of Beaverlodge Lake and about 100 km southeast of Great Bear Lake, is of interest in this regard. The showings were discovered in 1977 by D. Arden, a prospector working under the Federal Prospectors' Assistance Program. Mineralization consists of disseminations and local concentrations of pitchblende along narrow linear zones in rusty weathering, rather massive sandstone. Work has not yet progressed enough to establish whether they represent sandstone-type mineralization or are supergene concentrations. These occurrences are however distinguished from the typical hydrothermal veins for which this area has been noted in the past (Lord, 1951, p. 110; McGlynn, 1971b, p. 112-114). The host sandstone has been described as part of the Snare Group in earlier reports. It was observed however that it disconformably overlies a feldspar quartz porphyry north of Beaverlodge Lake. The porphyry has ignimbritic character, a feature common in volcanic rocks coeval with the Bear Batholith plutons. This suggests that the sandstone is younger than the Snare Group.

Helikian sandstones. Uranium was first discovered in these rocks during 1969. The showing is located south of Dismal Lakes, about 115 km north-northeast of Eldorado Mine, in the upper part of the Paleohelikian Hornby Bay Group (Bizard and Salat, 1969). The host unit is white to buff quartzose sandstone, with minor conglomerate interbeds. It correlates with Unit 11 of Baragar and Donaldson (1973). About 2 km northeast of this showing, a promising prospect has been located recently in an overburden covered area. This prospect is also in the same unit (L. Kirwin, Esso Minerals Limited, pers. comm., 1978).

The host unit is extensive between Coppermine River and Great Bear Lake; the published maps of Baragar and Donaldson cover less than 25 per cent of its extent. It is being actively explored by various companies. Other Helikian sandstones have received much less attention to date.

Phanerozoic sandstones. Sandstones of Phanerozoic cover rocks in the vicinity of a known Proterozoic uranium district such as the Bear Batholith area, should be considered for their uranium possibilities. Such possibilities have been suggested for the Mesozoic and Cenozoic rocks of the Southern Interior Plains of Canada by Chamberlain (1960) in view of uranium deposits in South Dakota and Wyoming. In South Dakota, the Precambrian Black Hills form a domal area, about 150 km long and 75 km wide, flanked by outward dipping Phanerozoic strata. Uranium deposits are found in fluvial and fluvial-marine sandstones of the Cretaceous Inyan Kara Group in the vicinity of Black Hills, and in the Paleocene lignite (Hart, 1968; Harshman, 1968; Fischer, 1974).

Phanerozoic rocks of the Great Bear Lake-Great Slave Lake area, are described by Norris (1965), Balkwill (1971) and Cook and Aitken (1971). The most favourable rocks for uranium mineralization are the Cambrian Old Fort Formation and Cretaceous sandstones and associated lignite. The Old Fort Formation is a thin basal unit that occurs discontinuously along the western boundary of the batholith in paleo-depressions of the Precambrian erosional surface. It is a transgressive clastic unit which has some locally derived material. It is overlain by red and green shales, siltstones and dolomite. The Cretaceous sandstones are also thin and poorly exposed, but apparently cover extensive areas north and south of Great Bear Lake. They are interbedded with shales and lignite seams.

It appears from the topography of the area and descriptions of the units, that at least part of the Bear Batholith area remained as a positive feature during the deposition of Phanerozoic rocks. It may have contributed some sediments and also apparently maintained a positive relief after their deposition. The area may also have contributed uranium to the sediments through the action of groundwater flows, which could have deposited the metal at suitable reducing sites.

(6) Unconformity-related supergene concentrations

The most significant and extensive unconformities in the Bear and Slave structural provinces are the Archean-Aphebian, Aphebian-Helikian, and Aphebian-Paleozoic interfaces. Uranium occurrences are found at or near the first two of these unconformities, which are briefly discussed below. The Aphebian-Paleozoic unconformity mentioned earlier with reference to the Cambrian Old Fort Formation is little explored, and is not further discussed here.

Archean-Aphebian unconformity. Nonacho Group consists predominantly of continental fluviatile sediments deposited in a fault-controlled intracratonic basin (Burwash and Baadsgaard, 1962; McGlynn, 1971a). The precise age of the group is not known but it has some structural and lithological similarities with the Martin Formation near Uranium City in Saskatchewan, which is believed to be Late Aphebian or very Early Paleohelikian in age (Koeppel, 1968; Fraser et al., 1970). The basement rocks of the Nonacho basin are Archean, in part remobilized during Aphebian, and include a considerable proportion of metasediments of the Tazin Group that are exposed near the unconformity. Several uranium occurrences are known at or close to the unconformity at the base of the Nonacho Group in the basement as well as in the Nonacho sediments. Their origin is uncertain, and more work is required to arrive at positive conclusions. There is a possibility that supergene processes were active at the unconformity and could have concentrated uranium from either local or distant sources. The most favourable sites appear to be where the unconformity comes in contact with metasediments and/or faults.

Aphebian-Helikian unconformity. The unconformity at the base of the Paleohelikian Hornby Bay Group, is potentially favourable for uranium deposits as it compares in age and geological setting to the one at the base of Athabasca Formation in Saskatchewan (Fraser et al., 1970). A zone of paleosaprolitic alteration related to the unconformity is extensive (Hoffman and McGlynn, 1977). The basal units of the Hornby Bay Group are deep red conglomerate and sandstone (Baragar and Donaldson, 1973). It is believed that the basement relief at the time of deposition of the group may have been as much as 500 m (P. Hoffman, pers. comm., 1977). Some of the Aphebian faults have been active during the deposition of Hornby Bay Group rocks. These faults and basement highs would have a considerable influence on the migration and deposition of uranium.

Several uranium occurrences are known in the Aphebian basement rocks near the unconformity. These are pitchblende fracture fillings in rocks such as granite and mafic dykes. The supergene origin of the occurrences is indicated by such features as limited strike and dip extent, partially weathered granitic host rocks, open fracture filling in fine mafic dykes, and the absence or scarcity of gangue minerals. Some of them may be remnants of formerly larger supergene concentraitons at the unconformity. Their presence is encouraging for further exploration of the unconformity.

Conclusions

The various geological environments suitable for uranium deposition in the Bear and Slave structural provinces and the Nonacho basin, coupled with the presence of a number of uranium occurrences, suggests an optimistic outlook for exploration successes in the region. Of particular interest in this regard are the high grade vein-type, sandstone-type, and unconformity-related uranium mineralization. The search for the last two types has been undertaken only during the last few years, and the results to date have been encouraging.

Acknowledgments

The writer wishes to acknowledge with thanks valuable help and information he received during the 1977 field season from the Federal Department of Indian and Northern Affairs, and various mining and exploration companies active in the area, in particular, Cominco, Noranda, Esso Minerals, Trigg, Woollett and Associates, BP Minerals, Hudson Bay Oil and Gas, Gulf Minerals, Uranerz Explorations, Wyoming Minerals, Canadian Occidental Petroleum, Highwood Resources, Rayrock Mines, Echo Bay Mines, and Terra Mines. The writer was assisted in the field by R.W. Anderson. Part of the writer's fieldwork was conducted with S.M. Roscoe and Y. Maurice of the Geological Survey of Canada, and with W. Gibbins of the Department of Indian and Northern Affairs.

References

Allan, R.J. and Cameron, E.M.
1973: Uranium content of lake sediments, Bear-Slave Operation, District of Mackenzie; Geol. Surv. Can., Map 9-1972.

Baadsgaard, H., Morton, R.D., and Olade, M.A.D.
1973: Rb-Sr isotopic age for the Precambrian lavas of Seton Formation, East Arm of Great Slave Lake, Northwest Territories; Can. J. Earth Sci., v. 10, p. 1579-1582.

Badham, J.P.N. and Morton, R.D.
1976: Magnetite-apatite intrusions and calc-alkali magmatism, Camsell River, N.W.T.; Can. J. Earth Sci., v. 13, p. 348-354.

Badham, J.P.N., Robinson, B.W., and Morton, R.D.
1972: The geology and genesis of the Great Bear Lake silver deposits: 24th Intern. Geol. Congress, Section 4., p. 541-548.

Balkwill, H.R.
1971: Reconnaissance geology, southern Great Bear Plain, District of Mackenzie; Geol. Surv. Can., Paper 71-11.

Baragar, W.R.A. and Donaldson, J.A.
1973: Coppermine and Dismal Lakes map-areas; Geol. Surv. Can., Paper 71-39.

Bizard, C. and Salat, H.
1969: Report on the geological exploration over PEC claim group, Dismal Lakes area, Northwest Territories; unpubl. Report for Aquitaine Oil Limited; Assessment Files, Dep. of Northern and Indian Affairs, Yellowknife, N.W.T.

Bloy, G.
1978: Uranium mineralization in Great Slave Supergroup, N.W.T., Abstract: 14th Annual Western Interuniv. Geol. Conf., Vancouver, B.C.

Burwash, R.A. and Baadsgaard, H.
1962: Yellowknife-Nonacho age and structural relations; in Tectonics of the Canadian Shield, J.S. Stevenson (ed.); R. Soc. Spec. Publ. no. 4, p. 22-29.

Campbell, D.D.
1955: Geology of the Pitchblende deposits of Port Radium, Great Bear Lake, N.W.T.; unpubl. Ph.D. thesis, Calif. Inst. Technol., 323 p.

1957: Port Radium Mine: in Structural Geology of Canadian Ore Deposits, 2nd Edn.; Can. Inst. Min. Metall., p. 177-189.

Campbell, F.H.A.
1978: Geology of the Helikian rocks of the Bathurst Inlet area, Coronation Gulf, Northwest Territories; in Current Research, Part A, Geol. Surv. Can., Paper 78-1A, p. 97-106.

Campbell, F.H.A. and Cecile, M.P.
1976: Geology of the Kilohigok Basin, Goulburn Group, Bathurst Inlet, District of Mackenzie; in Report of Activities, Part A, Geol.Surv. Can., Paper 76-1A, p. 369-377.

Chamberlain, J.A.
1960: On the uranium possibilities of the southern interior plains of Canada; Geol. Surv. Can., Paper 59-16.

Charbonneau, B.W.
Fort Smith radioactive belt, District of Mackenzie, Northwest Territories; Geol. Surv. Can., Paper 78-1A. (in prep.)

Cook, D.G. and Aitken, J.D.
1971: Geology, Colville Lake map-area and part of Coppermine map-area, Northwest Territories; Geol. Surv. Can., Paper 70-12.

Currie, K.L.
1976: The alkaline rocks of Canada; Geol. Surv. Can., Bull. 239, p. 103.

Davidson, A.
1978: The Blachford Lake Intrusive Suite: An Aphebian alkaline plutonic complex in the Slave Province, Northwest Territories; in Current Research, Part A, Geol. Surv. Can., Paper 78-1A, p. 119-128.

Fischer, R.P.
1974: Exploration guides to new uranium districts and belts; Econ. Geol., v. 69, p. 362-376.

Fraser, J.A., Donaldson, J.A., Fahrig, W.F., and Tremblay, L.P.
1970: Helikian basins and geosynclines of the northwestern Canadian Shield; in Symposium on basins and geosynclines of the Canadian Shield, ed. A.J. Baer, Geol. Surv. Can., Paper 70-40, p. 213-238.

Gandhi, S.S.
1977: Geological setting and genetic aspects of uranium deposits in Kaipokok Bay-Big River area, Labrador; Geol. Soc. Amer., Program with Abstracts, Seattle, p. 983.

Harshman, E.N.
1968: Uranium deposits of Wyoming and South Dakota; in Ore Deposits of the United States, 1933-1967, Graton-Sales volume, New York, Am. Inst. Min. Metall. Petrol. Eng., p. 815-831.

Hart, O.M.
1968: Uranium in the Black Hills; in Ore deposits of the United States, 1933-1967, Graton-Sales volume, New York, Am. Inst. Min. Metall. Petrol. Eng., p. 832-837.

Hoffman, P.F.
1968: Stratigraphy of the Great Slave Supergroup (Aphebian), east arm of Great Slave Lake, District of Mackenzie; Geol. Surv. Can., Paper 68-42, 93 p.

1969: Proterozoic paleocurrents and depositional history of the East Arm Fold belt, Great Slave Lake, Northwest Territories; Can. J. Earth Sci., v. 6, p. 441-462.

1978: Age of exotic blocks in diatreme dykes of the Athapuscow Aulacogen, Simpson Islands area, East Arm of Great Slave Lake, District of Mackenzie; in Current Research, Part A, Geol. Surv. Can., Paper 78-1A, p. 145-146.

Hoffman, P.F., Bell, I.R., Hildebrand, R.S., and Thorstad, L.
1977: Geology of Athapuscow Aulacogen East Arm of Great Slave Lake, District of Mackenzie; in Report of Activities, Part A, Geol. Surv. Can., Paper 77-1A, p. 117-129.

Hoffman, P.F., Bell, I.R., and Tirrul, R.
1976: Sloan River map-area (86K), Great Bear Lake, District of Mackenzie; in Report of Activities, Part A, Geol. Surv. Can., Paper 76-1A, p. 353-358.

Hoffman, P.F., Dewey, J.F., and Burke, K.
1974: Aulacogens and their genetic relation to geosynclines, with a Proterozoic example from Great Slave Lake, Canada; in Modern and Ancient Geosynclinal Sedimentation; Dott, R.H., Jr. and Shaver, R.H. (ed.), Soc. Econ. Paleont. Mineral., Spec. Publ. 19, p. 38-55.

Hoffman, P.F. and McGlynn, R.
1977: Great Bear Batholith: a volcano-plutonic depression; in Volcanic Regimes in Canada, W.R.A. Baragar, L.C. Coleman, and J.M. Hall (ed.); Geol. Assoc. Can., Spec. Paper 16, p. 169-192.

Hoffman, P.F., St.-Onge, M., Carmichael, D.M., and de Bie, I.
1978: Geology of the Coronation geosyncline (Aphebian), Hepburn Lake sheet (86J), Bear Province, District of Mackenzie; in Current Research, Part A, Geol. Surv. Can., Paper 78-1A, p. 147-151.

Irving, E. and McGlynn, J.C.
1976: Polyphase magnetization of the Big Spruce complex, N.W.T.; Can. J. Earth Sci., v. 13, p. 476-489.

Jory, L.T.
1964: Mineralogical and isotopic relations in the Port Radium pitchblende deposit, Great Bear Lake, Canada; unpubl. Ph.D. thesis, Calif. Inst. Technology, Pasadena, 275 p.

Kidd, D.F. and Haycock, M.H.
1935: Mineralogy of the ores of Great Bear Lake; Geol. Soc. Am., Bull. 46, p. 879-960.

Koeppel, V.
1968: Age and history of uranium mineralization of the Beaverlodge area, Saskatchewan; Geol. Surv. Can., Paper 67-31.

Kretz, R.
1968: Study of pegmatite bodies and enclosing rocks, Yellowknife-Beaulieu region, District of Mackenzie; Geol. Surv. Can., Bull. 159, 109 p.

Lang, A.H.
1952: Canadian deposits of uranium and thorium; Geol. Surv. Can., Econ. Geol. Rep. 16, 173 p.

Lang, A.H., Griffith, J.W., and Steacy, H.R.
1962: Canadian deposits of uranium and thorium; Geol. Surv. Can., Econ. Geol. Rep. 16, 324 p.

Langford, F.F.
1977: Surficial origin of North American pitchblende and related uranium deposits; Am. Assoc. Petrol. Geol., Bull., v. 51, no. 1, p. 28-42.

Leech, G.B., Lowdon, J.A., Stockwell, C.H., and Wanless, R.K.
1963: Age determinations and geologic studies (including isotopic ages – Report 4); Geol. Surv. Can., Paper 63-17, 140 p.

Lord, C.S.
1951: Mineral industry of District of Mackenzie, Northwest Territories; Geol. Surv. Can., Mem. 261, p. 110-113.

Martineau, M.P. and Lambert, R. St. J.
1974: The Big Spruce Lake nepheline-syenite/carbonate complex, N.W.T. (abstr.); Geol. Assoc. Can. Ann. Meeting Program, p. 59.

McGlynn, J.C.
1971a: Stratigraphy, sedimentology and correlation of the Nonacho Group, District of Mackenzie; in Report of Activities, Part A, Geol. Surv. Can., Paper 71-1A, p. 140-142.

1971b: Metallic mineral industry, District of Mackenzie, Northwest Territories; Geol. Surv. Can., Paper 70-17, 194 p.

1977: Geology of Bear-Slave Structural Provinces, District of Mackenzie, scale 1:1 000 000; Geol. Surv. Can., Open File Map No. 445.

Morton, R.D.
1974: Sandstone-type uranium deposits in Proterozoic strata of northwestern Canada; in Formation of Uranium Ore deposits, Intern. Atom. Energy Agency, Ser. no. STI/PUB/374, p. 255-273.

Mursky, G.
1963: Mineralogy, petrology and geochemistry of Hunter Bay area, Great Bear Lake, Northwest Territories, Canada; unpubl. Ph.D. thesis, Stanford Univ., Calif., 144 p.

1973: Geology of the Port Radium map-area, District of Mackenzie; Geol. Surv. Can., Mem. 374, 40 p.

Norris, A.W.
1965: Stratigraphy of Middle Devonian and older Paleozoic rocks of the Great Slave Lake region, Northwest Territories; Geol. Surv. Can., Mem. 322.

Reinhardt, E.W.
1972: Occurrences of exotic breccias in the Pettitot Islands (85H/10) and Wilson Island (85H/15) map-areas, East Arm of Great Slave Lake, District of Mackenzie; Geol. Surv. Can., Paper 72-25, 43 p.

Rich, R.A., Holland, H.D., and Petersen, U.
1977: Hydrothermal uranium deposits; Elsevier Scientific Publishing Company, New York

Robinson, B.W. and Morton, R.D.
1972: The geology and geochronology of the Echo Bay area, Northwest Territories, Canada; Can. J. Earth Sci., v. 9, p. 158-171.

Robinson, B.W. and Ohmoto, H.
1973: Mineralogy, fluid inclusions, and stable isotopes of the Echo Bay U-Ni-Ag-Cu deposits, Northwest Territories, Canada; Econ. Geol., v. 68, p. 635-656.

Ruzicka, V.
1971: Geological comparison between east European and Canadian uranium deposits; Geol. Surv. Can., Paper 70-48, 196 p.

Shegelski, R.J.
1973: Geology and mineralogy of Terra silver mine, Camsell River, Northwest Territories; unpubl. M.Sc. thesis, University of Toronto, 92 p.

Thorpe, R.I.
1972: Mineral exploration and mining activities, mainland Northwest Territories, 1966 to 1968; Geol. Surv. Can., Paper 70-70, 204 p.

1974: Lead isotope evidence for the genesis of silver-arsenic vein deposits of the Cobalt and Great Bear Lake areas, Canada; Econ. Geol., v. 69, p. 777-791.

Walker, R.R.
1977: The geology and uranium deposits of Proterozoic rocks, Simpson Islands, Northwest Territories; unpubl. M.Sc. thesis, University of Alberta, Edmonton, 193 p.

24.

THE APPLICATION OF AIRBORNE GAMMA-RAY SPECTROMETRY IN THE SEARCH FOR RADIOACTIVE DEBRIS FROM THE RUSSIAN SATELLITE COSMOS 954 (OPERATION "MORNING LIGHT")

Q. Bristow
Resource Geophysics & Geochemistry Division

Abstract

Bristow, Q., The application of airborne gamma-ray spectrometry in the search for radioactive debris from the Russian satellite Cosmos 954 (Operation "Morning Light"); in Current Research, Part B, Geol. Surv. Can., Paper 78-1B, p. 151-162, 1978.

Radioactive debris from the Russian satellite Cosmos 954 was located using airborne gamma-ray spectrometry. An analysis was made of two spectrometric techniques used to detect man-made radiation sources in the presence of a relatively high natural radioactivity background. An experiment was also conducted to determine the atmospheric attenuation of gamma radiation in the 0.7 meV energy region. These data were used to calculate the minimum point source strengths likely to be detected by the Geological Survey of Canada airborne gamma-ray spectrometer under the conditions in which it was used during the search.

Introduction

On 24 January, 1978, the Russian Satellite Cosmos 954, reported to be carrying a nuclear reactor on board, re-entered the Earth's atmosphere and disintegrated, the pieces coming to rest in the Northwest Territories. The probable impact trajectory for the debris was calculated from information based on eye witness accounts of the re-entry and from tracking data which were available. These calculations, from which the search areas shown in Figure 24.1 were established, were made by experts who formed part of a team of scientists and technicians sent in on 24 January by the U.S. Department of Energy (USDOE formely ERDA) to aid in the search.

On the evening of 24 January, R.L. Grasty of the Geological Survey of Canada (GSC) arrived at the Canadian Forces Base in Edmonton (the centre of subsequent operations) to assess the situation. He immediately recommended to Department of National Defence (DND) officials that the GSC airborne gamma-ray spectrometer be used to assist in the airborne search for the radioactive debris. The GSC spectrometer consists of 50 350 cm^3 of sodium iodide detector volume, with associated data acquisition electronics which are mini-computer based. Complete 256 channel gamma ray spectra are recorded on magnetic tape along with identification and navigational data at discrete time intervals which can be as short as 0.25 s. A six channel strip chart recorder allows running profiles corresponding to counts in chosen spectral windows, ratios of such counts, or almost any other algebraic function involving them to be plotted continuously in-flight. On the evening of 25 January the equipment was enroute to Edmonton with the author and P.B. Holman, who acts as field party chief for routine summer operations involving the instrument. Within 2 hours of arrival at C.F.B. Edmonton the spectrometer was installed in a Hercules C-130 aircraft and fully operational. Figure 24.2 gives some idea of the setup. One hour later the aircraft left on its first 12 hour search mission with the author acting as equipment operator. During the second flight with R.L. Grasty and P.B. Holman operating the equipment and with a press party on board, evidence was obtained of a man-made radiation source on the frozen surface of the East Arm of Great Slave Lake. A subsequent study of the accumulated spectra corresponding to the anomaly on the chart record (Fig. 24.4) showed unmistakable evidence of the fission product lanthanum (^{140}La).

The ratio shown on the strip chart record (Fig. 24.4) was used on the advice of Thane Hendriks, a member of the USDOE team, whose experience in searching for man-made radiation sources was of considerable value in this project.

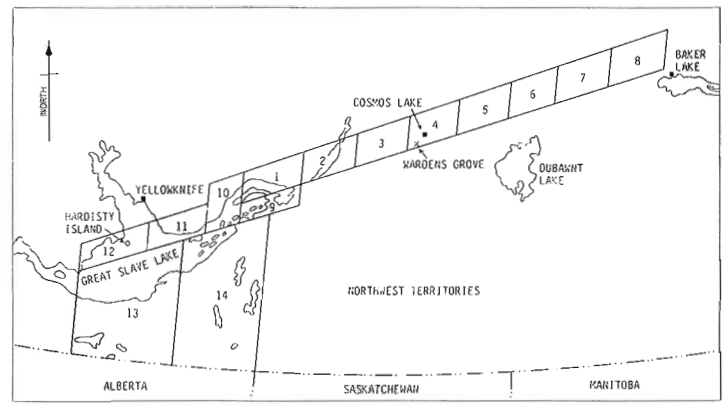

Figure 24.1 The impact trajectory of the satellite stretches from Great Slave Lake northeast toward Baker Lake. Sectors 13 and 14 were established with wind borne material in mind.

Subsequently other functions were tested in an attempt to optimise the signal to noise ratio for detection of man-made radiation sources with spectra of the general shape shown in Figure 24.3. This figure shows the gamma-ray spectrum obtained by subtracting the local background spectrum taken over a few records either side of the anomaly discovered on Great Slave Lake from the accumulated spectra over the anomaly itself. The ^{140}La peak at 1.59 meV is clearly seen along with a low energy continuum up to about 0.78 meV which is due to other fission products. This anomaly was the first piece of hard evidence that any radioactive debris had in fact landed in the area.

Navigation

In the initial stages the most probable areas where radioactive debris was likely to be found were given broad radiometric survey coverage relying on a combination of conventional navigational aids such as doppler and omega, together with visual identification of topographic features from maps of the area. It became clear that systematic detailed coverage of some portions of the trajectory would be required and that this would only be possible with more precise navigation. The USDOE team, for some years, has been using a Microwave Ranging System, (MRS) made by Del Norte Inc., of Texas. The MRS uses two portable land beacons which are positioned about 50 km apart. These beacons communicate automatically with a unit installed in the aircraft to provide the aircrew with the distances from

the beacons in metres, updated every half second. The carrier frequencies are of the order of 3 GHz which restricts the use of the MRS to line-of-sight. Satisfactory signals can be received up to a distance of about 80 km from either beacon. A Hewlett Packard 9825A calculator interfaced with the aircraft distance measuring unit processes the range signals on-line to provide linear grid co-ordinates scaled and oriented to coincide with whatever map frame of reference the operator chooses to use. In order to accomplish this it is first necessary to fly between the two beacons and determine their separation by finding the minimum sum of the two ranges. During this operation the calculator prints the sum of the ranges every half second, so that it is a simple matter for the operator to determine this base line distance. The system must then be geographically referenced by flying directly over two points in the area which are readily identifiable and whose co-ordinates on the chosen map reference frame are accurately known. Once this has been done the calculator has the necessary information to allow the operator to set a course anywhere within the two circles whose two points of intersection coincide with the beacon positions (but not within the area common to both circles). The calculator provides an analogue signal to a centre zero meter in the cockpit which the pilot uses to maintain the aircraft on the chosen flight line. The system is very accurate and especially suitable for flying a series of closely spaced parallel lines.

Figure 24.2 The GSC gamma-ray spectrometer installed in the Hercules CC-130 aircraft, was designed as a single self-contained unit on castor wheels and weighs over half a ton. The MRS navigational units (see text) were conveniently mounted on one end of the spectrometer for operation by a military navigator.

The USDOE team has had considerable experience with the MRS in helicopter surveys over flat terrain in a warm climate, where access by road to suitable beacon locations is the norm. It was with some trepidation therefore that the MRS was tried out with Hercules aircraft at subzero temperatures (as low as -40°C) over the undulating and desolate terrain of the Northwest Territories, where helicopters were the only means of positioning the beacons. Canadian Forces personnel constructed special insulated boxes to contain two beacons each with independent sets of rechargeable batteries for complete double redundancy. Each beacon would operate unattended for at least two days at subzero temperatures. The first tests were sufficiently successful that a detailed plan was worked out to cover a large portion of the search sectors shown in Figure 24.1 at a line spacing of 460 m (1500 ft) and at a flying altitude of 230 m (750 ft) mean terrain clearance. The line-of-sight restriction caused "dropout" problems in some areas but these were overcome by frequent movement of the beacons to cover such regions. The navigational data were recorded on magnetic tape along with the gamma-ray spectrometry data and this enabled the actual track flown to be recovered and plotted to map scale to provide an overlay on a master map at C.F.B. Edmonton.

Subsequently a second MRS was obtained by DND to support the GSC airborne gamma-ray spectrometer in its Hercules aircraft. Fortunately the interfacing of the Hewlett Packard calculator with the spectrometer for recording the data required only minor hardware and software modifications, since both were equipped with industry standard RS232C E.I.A. ports. The USDOE team were using some sophisticated software developed by Thane Hendriks for plotting the recovered track, and this was kindly made available to the GSC personnel by USDOE. By a happy coincidence there was almost complete hardware compatibility between the GSC spectrometer system and the USDOE data processing equipment. This enabled the USDOE software to be run with only minor modification on a ground-based data reduction system consisting of a twin GSC spectrometer system normally used for borehole logging research, together with some other peripherals shipped from the GSC Ottawa headquarters.

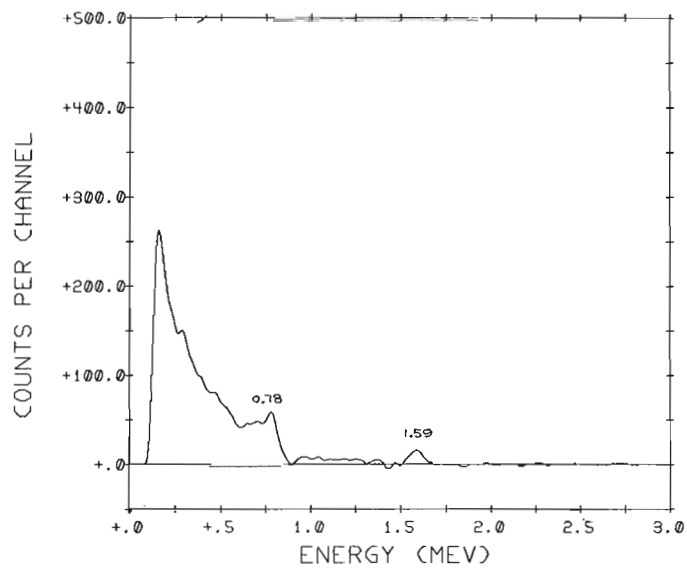

Figure 24.3 The spectrum above is the cumulative addition of individual spectra recorded over the anomaly of Figure 24.4, with local background either side subtracted. The small peak at 1.59 meV is from the fission product ^{140}La and confirmed the evidence of Figure 24.4. The single overflight by the spectrometer thus provided conclusive proof of the presence and the nature of the radioactive debris on the lake.

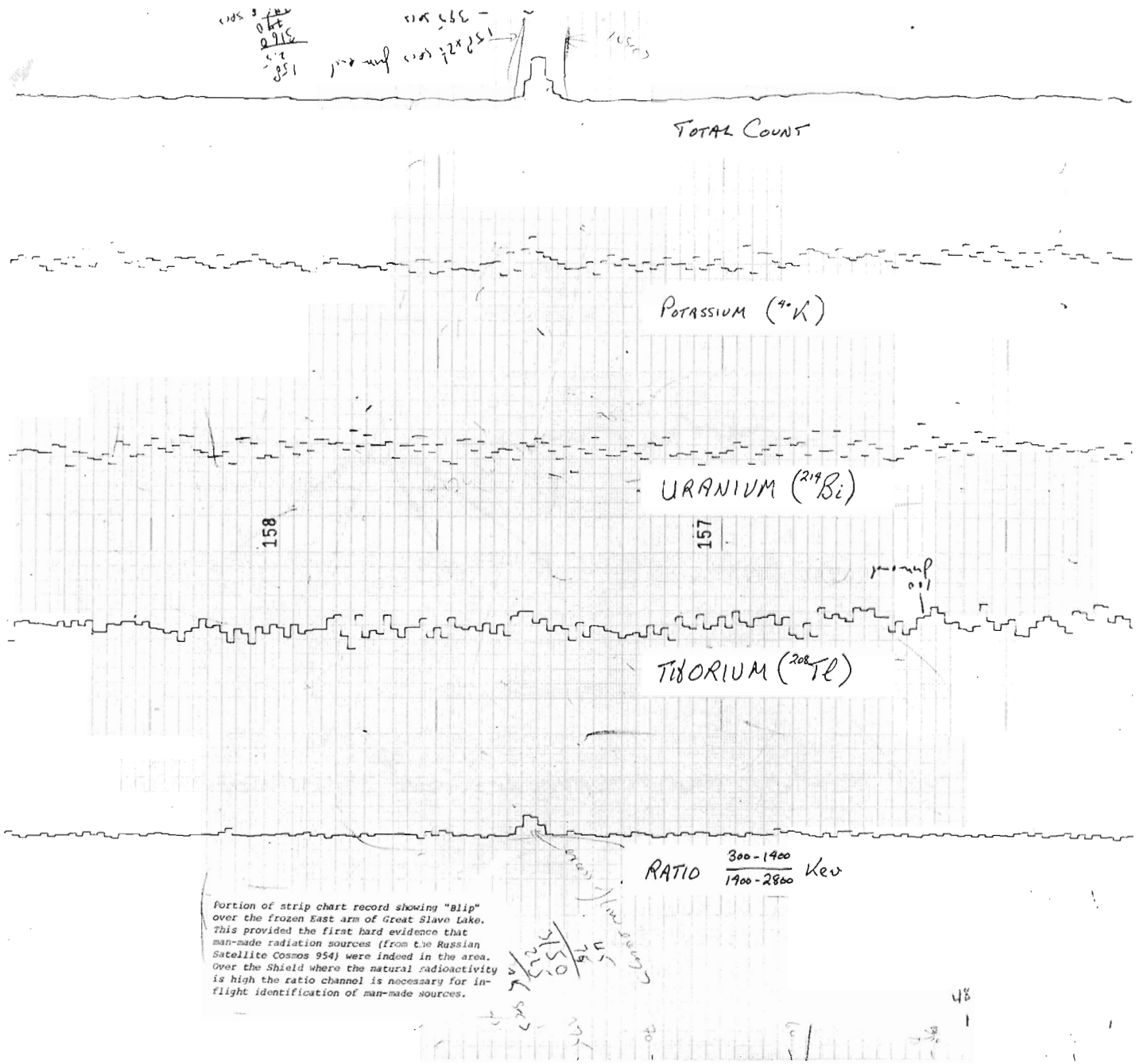

Portion of strip chart record showing "Blip" over the frozen East arm of Great Slave Lake. This provided the first hard evidence that man-made radiation sources (from the Russian Satellite Cosmos 954) were indeed in the area. Over the Shield where the natural radioactivity is high the ratio channel is necessary for in-flight identification of man-made sources.

Figure 24.4 This (rather battered) piece of history is the portion of the strip chart record showing the first evidence of radioactive debris from COSMOS 954 on Great Slave Lake.

Experience has shown that the MRS is accurate (to within a few tens of metres) and is reasonably simple to instal and operate. Under normal circumstances the logistics of beacon placement would be straight forward, however, it was a formidable undertaking in the wintry wilderness of the Northwest Territories in mid-January and February. The success of the MRS operation is due in large measure to the Canadian Forces helicopter crews whose task it was to move the beacons and keep them operative, and to the Hercules flight crews who quickly became very skillful in setting up the airborne part of the system each day and flying the closely spaced lines with little or no deviation from the planned track. The main limitation of the MRS for airborne use is the line-of-sight requirement between the aircraft and both beacons. A secondary limitation is the directionality of the antennae; unless all three are oriented correctly to within about 15° signal dropouts occur, thus limiting the range. For example, whenever the aircraft departs from level flight as in a turn, the signal is temporarily lost.

Navigation has been and continues to be the most intractible problem in any attempt to carry out accurate airborne surveys and the experience of this project was no exception. Without the MRS it would not have been possible to carry out the close grid coverage used in the satellite search.

Detection of man-made radiation sources

The radioactive debris from Cosmos 954 contained both fission and activation products. Of those products having significant gamma activity in the 0.3 meV to 3.0 meV region, almost all produced the major portion at less that 1.0 meV. The high natural radioactivity of some Precambrian granitic rocks in the search area frequently gave rise to small anomalies which were indistinguishable in the total count profiles from those anomalies generated by radioactive debris or "hits" as they were called. Various diagnostic functions designed to discriminate between natural and man-made radiation using different spectral windows were evaluated and the most succesful was a modified version of one used by the USDOE team. The first method was a running profile of the ratio C_1/C_2 where C_1 represents the count rate in the low energy part of the spectrum (300-900)keV (window 1), and C_2 represents the count rate in the high energy region from (900-1500)keV (window 2). The second method was a running profile of the expression C_1-AC_2 where A is the average value of the ratio C_1/C_2 in the absence of anomalies. Note that on the average, in the absence of anomalies, C_1-AC_2 will be zero. These two functions C_1/C_2 and C_1-AC_2 have similar behaviour, and both are reasonably insensitive to natural radiation anomalies due to the varying potassium, uranium, and thorium contents of the terrain.

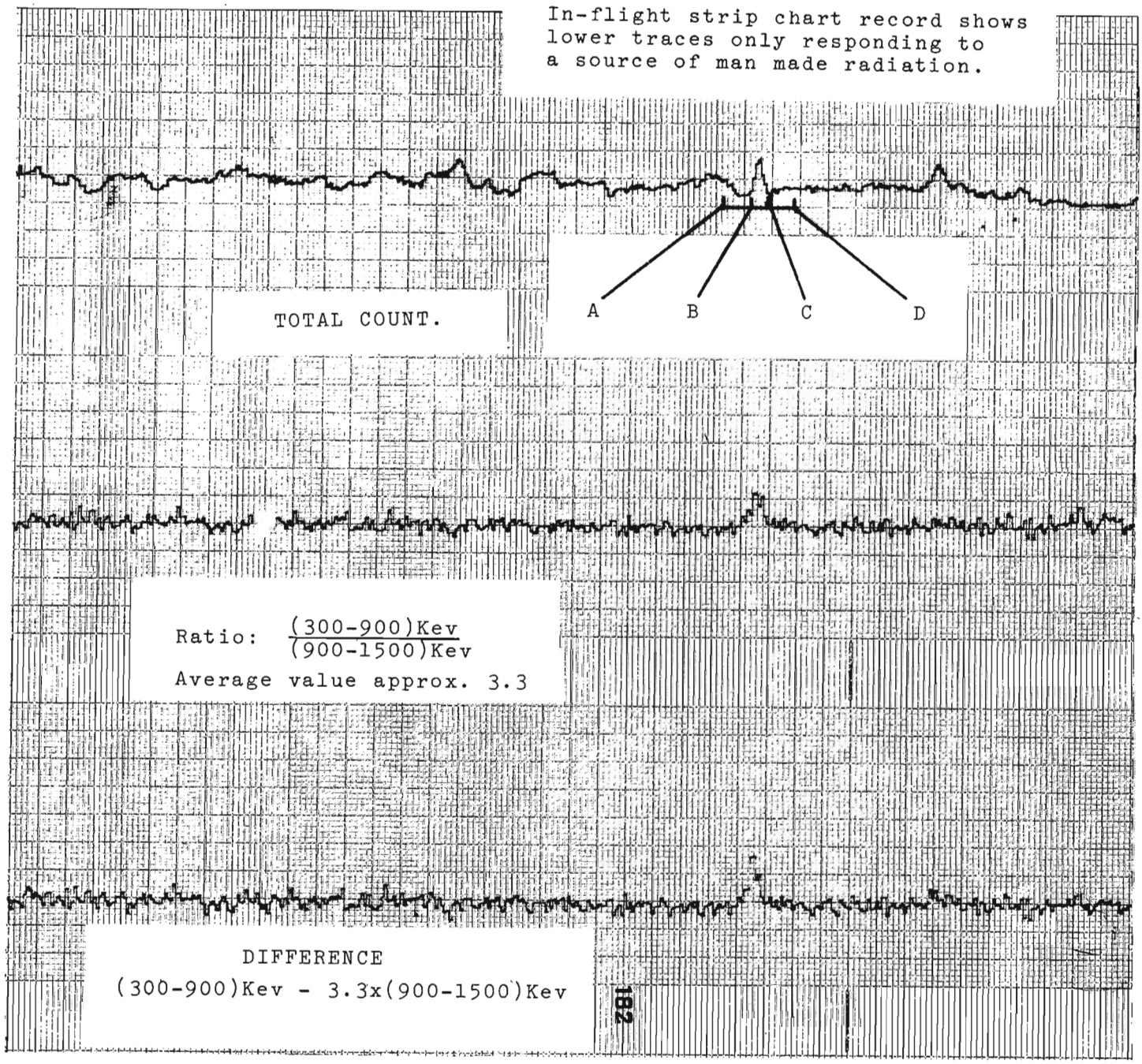

Figure 24.5 The strip chart record shows that the total count profile (top) is incapable of distinguishing between debris and natural anomalies. The spectral diagnostic functions (see text) respond only to debris sources.

Figure 24.5 shows a portion of a strip chart record recreated from the taped data taken on an actual search mission. Several total count anomalies are evident but only one causes the ratio and difference profiles to register significant deflections. A successful recovery was subsequently made of a radioactive satellite fragment at that location.

In the early stages of the project, data from the GSC spectrometer were processed by the USDOE team; subsequently the main operating software for the GSC spectrometer was modified by the author to produce a post flight tape replay and hit analysis system. The system was designed to monitor a specified diagnostic function as the tape was played back in order to extract automatically the anomalous spectra if the predetermined threshold was exceeded and to produce spectral plots on the strip chart recorder. The necessary software for this was developed on the ground based twin data processing system. The resulting addition to the GSC capability allowed the tapes to be analyzed for man-made sources by the airborne spectrometer during the two hour return flight to base from the search area.

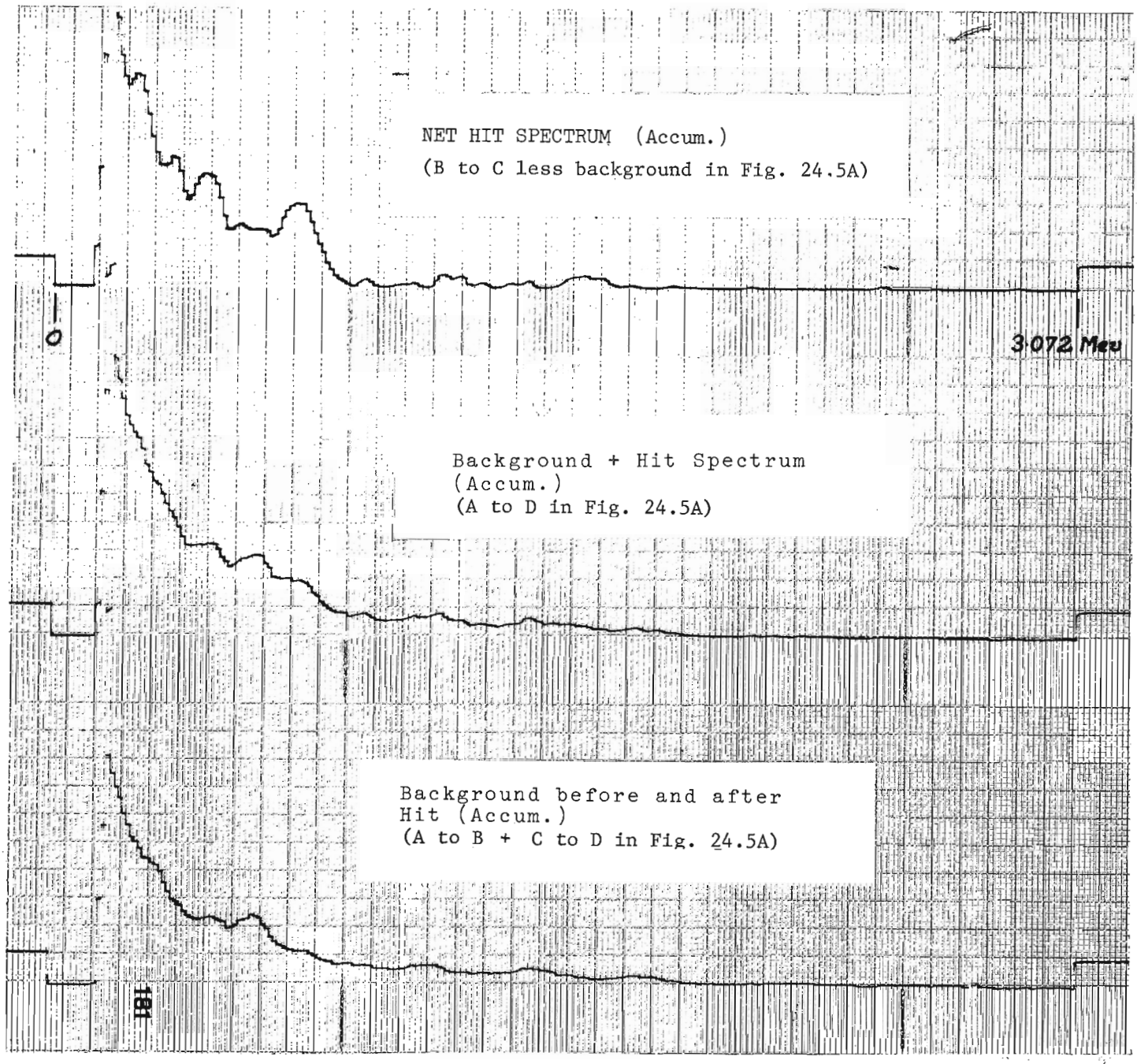

Figure 24.6 These three spectra were generated by the "hit detector" and analysis program (see text) when it encountered the man-made source shown in Figure 24.5.

The method of operation of this off-line analysis or "Hit Detector" program is given below:

- Keyboard entry of a channel number for the strip chart recorder causes the average level on that channel (due to whatever function it is plotting, which is also selectable) to be computed continuously as the tape is replayed. Updates of the average level are made at the end of each set of 16 one second records.
- If an anomaly occurrs which exceeds the critical value (average level plus a constant) for three or more consecutive records, then the criteria for a hit have been met and the program starts the spectrum analysis routine.
- The spectrum analysis routine accumulates successive spectra in a separate block of memory for as long as the hit criteria are being met. This corresponds to the interval BC in Figure 24.5 (top profile) as determined by whichever of the two diagnostic functions (other two profiles) is being monitored. The continuous averaging is suspended during this time to avoid distorting the reference level.
- When the level on the chosen channel once again falls below the critical value the tape reverses for 10 records plus the number of records encountered in the interval BC, stopping at A. It then starts forward again accumulating the spectra over the interval AD which includes intervals AB (10 background records), BC (hit records), and CD (10 more background records) in another block of memory.
- The accumulated spectra for interval BC are then subtracted from the accumulated spectra for interval AD on a channel by channel basis leaving an accumulated background spectrum corresponding to AB + CD.
- The accumulated hit spectra (in the from of a single spectrum) are now multiplied by 20/(number of records in BC) to normalize this spectrum with respect to the background AB + CD.
- The background and hit spectra thus produced are then smoothed once using a simple three point running average, and the background spectrum is subtracted (again on a channel by channel basis) from the hit spectrum. This leaves a net hit spectrum which is again smoothed and which will be (within the statistical accuracy of the data) the spectrum of whatever source was responsible for the anomaly.
- When the above analysis (which is entirely automatic) has been completed, the hard copy terminal prints out the navigational data relating to the position of the hit and sounds a repetitive beep signal to alert the operator that the hit criteria have been met.
- Keyboard entries by the operator then allow three spectra-

  Net Hit
  Hit + Background
  Background

  to be displayed individually on a CRT display (which is a part of the spectrometer hardware) or to be plotted simultaneously on three channels of the strip chart recorder.

Figure 24.6 shows the three spectra generated by the program when it encountered the hit shown in Figure 24.5. The large peak in the net spectrum (Fig. 24.6 top) is approximately 0.8 meV, the small peak at approximately centre scale is almost certainly the 1.59 meV peak of ^{140}La.

A modified version of this hit detector scheme was incorporated into the main in-flight operating software for the spectrometer. This provided an in-flight indication that a hit had occurred by giving a half scale deflection of a formerly unused channel of the chart recorder. The MRS range data for each hit were stored sequentially in a seperate block of memory, and were printed out automatically when the spectrometer was taken out of its autocycle mode for tape changing.

Spectrometer detection limits for man-made radiation sources

To establish a basis for search and recovery criteria, the detection thresholds for airborne gamma-ray spectrometers that were used in the search had to be determined. In the case of the GSC spectrometer a statistical analysis was made of the sensitivity of the ratio and difference diagnostic functions described earlier, to determine the minimum increase in count-rate which would be required for a man-made source to cause a statistically significant signal in the presence of representative natural background count-rate. An experiment was then carried out to determine as accurately as possible the effective attenuation by air of radiation in the 0.7 meV region. It was then possible to make a reasonable estimate of the strength of a source that would only just be detected under the worst condition, i.e. with the source midway between two flight lines.

In the case of two quantities Q_1 and Q_2 with measurement errors e_1 and e_2 having a gaussian distribution, the ratio of these quantities will be given by

$$\frac{Q_1 \pm e_1}{Q_2 \pm e_2} = \frac{Q_1}{Q_2}\left\{1 \pm \left[\left(\frac{e_1}{Q_1}\right)^2 + \left(\frac{e_2}{Q_2}\right)^2\right]^{1/2}\right\} \quad (1)$$

(see e.g. Chase and Rabinowitz, 1968)

In the present case

$$Q_1 = N_1 \text{ and } Q_2 = N_2$$

where N_1 and N_2 are the mean count rates in the low energy (300-900) keV and high energy (900-1500) keV portions of the spectrum respectively. The standard deviations of N_1 and N_2 a are defined as:

$$\sigma_1 = \sqrt{N_1} \text{ and } \sigma_2 = \sqrt{N_2} \quad (2)$$

Letting $e_1 = k\sigma_1$ and $e_2 = k\sigma_2$, equation (1) can now be generalized using the relation in equation (2) to show the variation in "Background Ratio" (R_B), i.e. the ratio of low energy count rate to high energy count rate in the absence of radiation from man-made sources.

$$R_B = \frac{N_1 \pm k\sigma_1}{N_2 \pm k\sigma_2} = \frac{N_1}{N_2}\left\{1 \pm k\left[\frac{N_1+N_2}{N_1N_2}\right]^{1/2}\right\} \quad (3)$$

A man-made radiation source will contribute additional counts to the low energy window, thereby augmenting N_1 by an amount which we will call C_M. In other words the count rate in the lower energy window at a given point along the profile in the absence of man-made radiation sources will be given in statistical terms by

$$C_1 = N_1 \pm \sigma_1 \text{ where } \sigma_1 = \sqrt{N_1}$$

in the higher energy window by

$$C_2 = N_2 \pm \sigma_2 \text{ where } \sigma_2 = \sqrt{N_2}$$

In the vicinity of a man-made source the value of C_2 will be relatively unaffected while C_1 will change to $C_1 = N_1 + C_M \pm \sigma_1$, where now $\sigma_1 = (N_1+C_M)^{1/2}$. The result will be a shift in the ratio to a new value with new confidence limits. If this shift is to be discernible with the confidence level implied by the value of k (e.g. k = 2 for 2σ implies a

confidence level of 95% etc.), then the lower confidence limit of the new ratio (R_M) must coincide with the upper confidence limit of the background ratio (R_B). The addition of C_M to the numerator changes the error e_1 in equation (1) from $k\sqrt{N_1}$ to a new value given by:

$$e_1 = k(N_1+C_M)^{1/2} \tag{4}$$

Equation (3) can now be modified to include C_M in order to give the new ratio R_M which includes the effect of a man-made source:

$$R_M = \frac{N_1+C_M}{N_2}\left\{1 \pm k\left[\frac{N_1+C_M+N_2}{(N_1+C_M)N_2}\right]^{1/2}\right\} \tag{5}$$

We are now in a position to determine the value of C_M in terms of the other quantities in equation (5) all of which are known, by equating:

$$R_B \text{ (upper limit)} = R_M \text{ (lower limit)} \tag{6}$$

The minimum detectable value of C_M will depend on the confidence limit selected as determined by the value used for k. From equations (3), (5), and (6) we have:

$$\frac{N_1}{N_2}\left\{1 + k\left[\frac{N_1+N_2}{N_1N_2}\right]^{1/2}\right\} = \frac{N_1+C_M}{N_2}\left\{1 - k\left[\frac{N_1+C_M+N_2}{(N_1+C_M)N_2}\right]^{1/2}\right\} \tag{7}$$

by making the substitutions:

$$N_1/N_2 = A$$

$$C_M/N_1 = M$$

equation (7) can be reduced to:

$$M^2(N_1-k^2A)-Mk\left\{2\left[N_1(A+1)\right]^{1/2}+k(2A+1)\right\} = 0 \tag{7a}$$

one solution for M is thus zero and the other is:

$$M = \frac{k\left\{2\left[N_1(A+1)\right]^{1/2}+k(2A+1)\right\}}{N_1-k^2A} \tag{7b}$$

In this application $N_1 \gg k^2A$

and thus:

$$C_M = 2k\left[N_1(A+1)\right]^{1/2} + k^2(2A+1) \tag{8}$$

which is the desired expression for the minimum value of C_M which will be detected by the ratio discrimination method.

In the case of the difference discrimination method using the same low and high energy spectral windows the statistical variation is given by:

$$(Q_1 \pm\sigma_1) - (Q_2 \pm\sigma_2) = Q_1-Q_2 \pm \left[\sigma_1^2+\sigma_2^2\right]^{1/2} \tag{9a}$$

A parallel argument to the one given above for the ratio method shows that with the difference method the minimum detectable C_M will be given by:

$$C_M - k(N_1+C_M+A^2N_2)^{1/2} = k(N_1+A^2N_2)^{1/2} \tag{9b}$$

Since $N_1 = AN_2$:

$$C_M - k\left[N_1(A+1)+C_M\right]^{1/2} = k\left[N_1(A+1)\right]^{1/2} \tag{9c}$$

As before one solution to this equation is zero, and the other is:

$$C_M = 2k\left[N_1(1+A)\right]^{1/2} + k^2 \tag{10}$$

which is the desired expression for the minimum value of C_M which will be detected by the difference discrimination method. Equations (8) and (10) indicate that the ratio and difference methods give essentially the same sensitivity provided that the value of N_1 is large compared with A, i.e. the value of C_M required for recognition of a man-made source with a given background is the same for either case.

Experience indicated that the ratio of the two spectral windows being used in this case varied somewhat depending on whether the aircraft was flying over ice (where the background was due primarily to radioactivity from the aircraft itself), or over land. Table 24.1 shows representative background values determined by accumulating spectra from long flights made over ice and over land (1000 one-second records of each).

These were used to evaluate the minimum detectable count rates C_M from equation (8) for confidence levels corresponding to σ to 2σ. The data for these are shown in table 24.2.

The Hercules aircraft has a number of luminous (radium) dials in the cockpit instrumentation, these are a well known source of added ^{214}Bi background in airborne survey work of this type and undoubtedly contributed to the surprisingly high background over ice. It was not until some time later that a small ^{137}Cs source was identified in an igniter unit used to start an auxilliary engine in the Hercules. The radiation from this low level source would have caused a shift in the ratio as the natural background dropped from land to ice, since its entire contribution is in the (300-900) keV portion of the spectrum. This then was a contributing factor in the relatively large change in the ratio of the (300-900) keV and the (900-1500) keV count rates over land and over ice.

Air attenuation measurements at 0.7 meV

The major unknown factor in attempting to determine detection limits for man made sources was the effective attenuation coefficient for energies in the 0.7 meV region when viewed with the (300-900) keV spectral window. This will be different from the readily available data for photopeak attenuation, as scattered radiation will still be counted in such a window.

A ^{137}Cs source (energy 0.662 meV) of the order of 100 mCi was positioned at a clearly marked site while the Hercules carrying the GSC spectrometer made passes over it at altitudes of 152 m, 230 m, and 305 m (500, 750, and 1000 ft), two passes at each altitude. The altitude was measured with a radar altimeter and care was taken to ensure that the chosen altitudes were maintained as precisely as possible. Figure 24.7 shows the (300-900) keV window count rate profiles for the 152 m and 230 m passes. Figure 24.8 shows a portion of strip chart record for a 230 m and 305 m overflight, again the greater sensitivity of the difference trace as compared to the ratio is evident. The statistics of the 305 m data were not in fact good enough to be useful in the subsequent calculation of attenuation.

The aircraft ground speed was 241 km/h (150 mph) so that a correction must be applied to observed peak count rate readings (one-second records) to convert them to values that would be obtained if the aircraft were stationary over the source for the same time. The principle involved in this correction (or more precisely deconvolution), can be seen by reference to Figure 24.9. If the detector in the aircraft were

situated directly over the source at point O, then since the flux intercepted by the detector with an effective area A is a fraction $A/4\pi H^2$ of the total flux emitted by the source, then the count rate registered per second would be:

$$C = C_o \frac{A}{4\pi H^2} K \qquad (11)$$

where:

A = Effective detector area

Co = Total gamma photons/s emitted by the source

K = Constant which includes attenuation due to air path length and aircraft structure; effect of detector efficiency, etc., all of which are assumed to remain constant over the relatively small changes of source detector distances involved.

Suppose that the aircraft moves with velocity, v, from P to Q (Fig. 24.9) in the interval of time from t_1 to t_2. After a time t when it is at a distance r from the source, with the detector area making an angle θ with the tangent to the sphere with radius r and centre the source, the instantaneous count rate will be given by:

$$C = Co \frac{A\text{Cos}\theta}{4\pi r^2} K$$

The total number of counts over the interval from P to Q will then be given by:

$$C_t = \int_{t_1}^{t_2} \frac{CoAK}{4\pi r^2} \text{Cos}\,\theta.\, dt \qquad (12)$$

From Figure 24.9:

$$\text{Tan}\,\theta = \frac{vt + H\,\text{Tan}\,\theta_1}{H}$$

differentiating the above we obtain:

$$H\,\text{Sec}^2\,\theta.d\theta = v.dt$$

giving $dt = \frac{H}{v}\,\text{Sec}^2\,\theta.d\theta$

also from Figure 24.9 $r = H/\text{Cos}\,\theta$

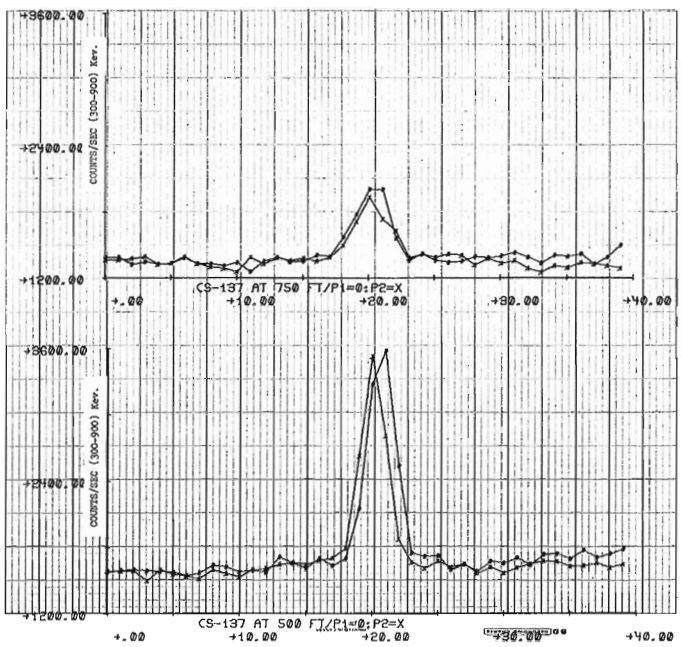

Figure 24.7 Count-rate profiles in the (300-900) keV window are shown against time (one second per point) as the spectrometer was flown over a ^{137}Cs source at two altitudes, two passes at each one.

equation (12) can now be rewritten with θ as the variable of integration giving:

$$C_t = \frac{CoAK}{4\pi} \int_{\theta_1}^{\theta_2} \frac{\text{Cos}\theta}{Hv} .\, d\theta$$

which evaluates to:

$$C_t = \frac{CoAK}{4\pi} . \frac{1}{Hv} (\text{Sin}\,\theta_2 - \text{Sin}\,\theta_1) \qquad (13)$$

The counts which would have been accumulated had the aircraft been stationary over the source for the same time interval (in this case one second) are given by equation (11). The correction factor F which must be applied to observed peak count rates as the aircraft crosses the source, is therefore given by the ratio of equations (11) and (13):

$$F = \frac{v}{H(\text{Sin}\,\theta_2 - \text{Sin}\,\theta_1)} \qquad (14)$$

Since the attenuation due to air is assumed constant in this analysis, the correction can only be applied realistically for the single one second interval during which the crossing was made, or for the two adjacent central intervals if the count rates are approximately equal. Inspection of the profiles in Figure 24.7 gives a fairly good indication in each case of the position of the aircraft with respect to point O in Figure 24.9 during the peak counting intervals.

Table 24.1
Typical background count rates over ice and land
(average over 1000 one-second records)

Window	Energy Range keV	Background Counts/s	
		Over land	Over ice
1	300-900	N_1 = 1047	N_1 = 706
2	900-1500	N_2 = 340	N_2 = 200
		(A = 3.08)	(A = 3.53)

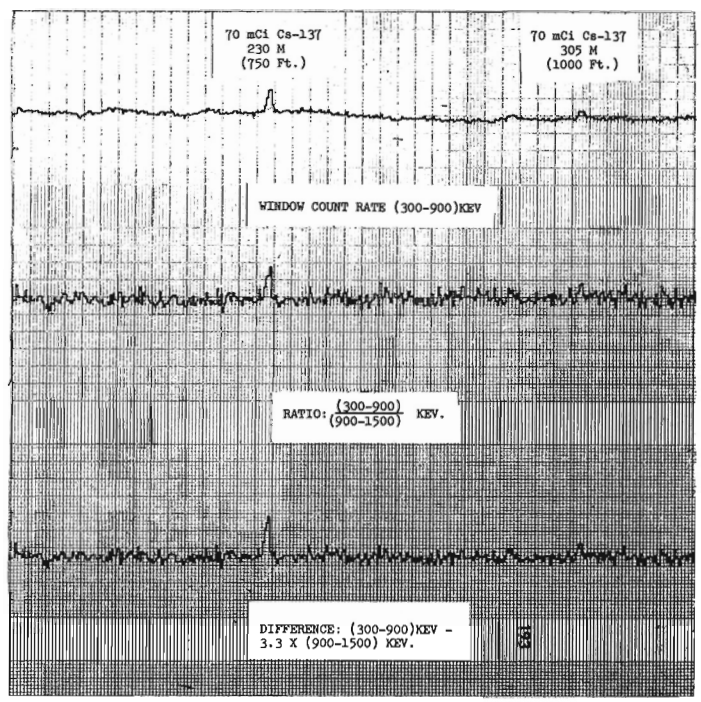

Figure 24.8 Strip chart profiles for consecutive overflights of a ^{137}Cs source at 230 m and 305 m.

The mean background levels for each over flight were estimated by inspection of the Figure 24.7 profiles and subtracted from the peak values which were then corrected by equation (14) above, using values of θ_1 and θ_2 estimated from the shape of each peak profile. The data are tabulated in Table 24.3 below.

The standard relation for atmospheric attenuation of gamma radiation from a point source is given by

$$C = \frac{Cu}{R^2} e^{-\mu r}$$

where C is the radiation intensity at a distance R from a source, Cu is that at unit distance from it and μ is the linear attenuation coefficient. If two count rates C_1 and C_2 (i.e. quantities proportional to radiation intensity) are observed at distances R_1 and R_2 from a source, then it can be shown that:

$$\mu = \frac{1}{R_2 - R_1} \ln \frac{C_1}{C_2} \left(\frac{R_1}{R_2}\right)^2$$

Applying the data from Table 24.3 gives the value of μ at 0°C for the (300-900) keV spectral window as:

$$\mu = 4.66 \times 10^{-3}\ m^{-1}$$

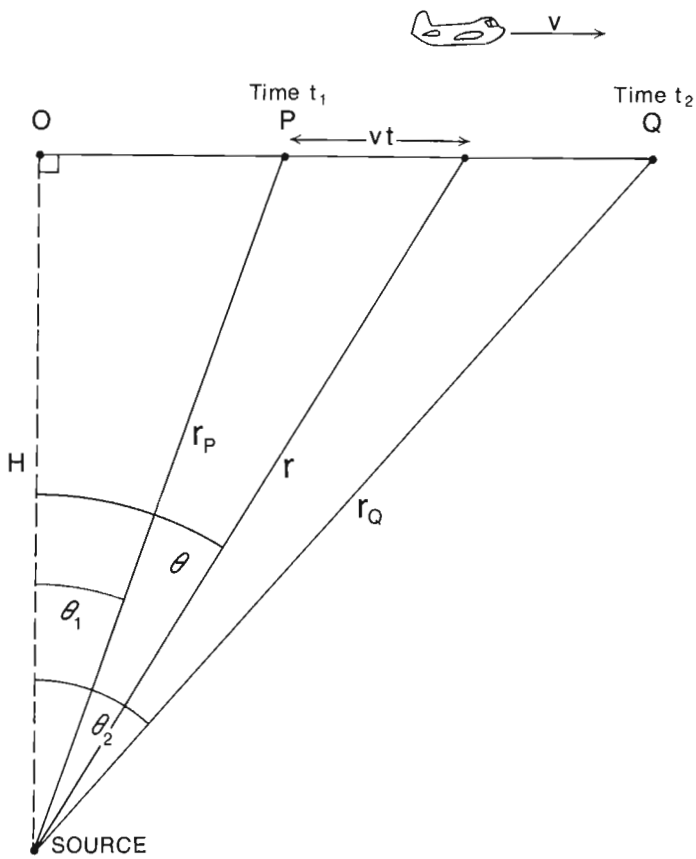

Figure 24.9 The counts accumulated over the time interval from P to Q will be less than would have been obtained by remaining at point O directly above the source for the same time. A correction can be applied to compensate for this.

Table 24.2
Minimum count rates for the successful recognition of radiation from man-made sources using the ratio or difference diagnostic functions with typical background values from Table 24.1

Confidence Limits	Minimum detectable count rate C_M Counts/s	
	Over land	Over ice
σ	139	121
2σ	293	258

Table 24.3
Data obtained from overflights of a ^{137}Cs source at two altitudes

	152 m (500 ft)		230 m (750 ft)	
	Pass 1	Pass 2	Pass 1	Pass 2
Background (c/s)	1680	1620	1438	1356
Net ^{137}Cs (c/s)	2020	1909	650	579
Correction factor F	1.038	1.024	1.040	1.011
Net corrected ^{137}Cs (c/s)	2096	1955	677	585
Mean Corrected ^{137}Cs (c/s)	2025		631	
μ for (300-900) keV @ 0°C=4.66 x 10^{-3} m^{-1} (1.42 x 10^{-3} ft^{-1})				
^{137}Cs source strength calculated from above data = 72 mCi				

Table 24.4

Minimum detectable point source strengths at worst-case survey geometry with 457 m (1500 ft) line spacing and 230 m (750 ft) terrain clearance

Confidence Level	Minimum Point Source Strength Over land		Over ice	
	0°C	-30°C	0°C	-30°C
σ	70 mCi	84 mCi	61 mCi	73 mCi
2σ	147 mCi	176 mCi	129 mCi	155 mCi

The hit detection and analysis programme described earlier was used to produce the net ^{137}Cs spectra of Figures 24.10 and 24.11 (the vertical scales are different). These show that a considerable amount of scattered radiation reaches the detector and bears out the reasoning given earlier that photopeak attenuation coefficients are not applicable to the situation here where a comparatively wide spectral window is being used.

Minimum detectable source strengths

The statistical analysis and experimental determination of air attenuation covered in the preceding sections provide the information necessary for calculation of the man-made source strengths which would just be detected under the worst survey geometry condition. The MRS coverage was at 457 m (1500 ft) line spacing at a nominal altitude of 230 m (750 ft). The worst case therefore is with the source midway between two lines, which involves a slant distance of 323 m (1060 ft) and a projected detector area along this line of $1/\sqrt{2}$ times the actual area.

The scintillation detectors used in the spectrometer consist of twelve square cross section crystals 102 mm on a side by 406 mm long (4x4x16 in). Eleven were operational during this search giving an effective detector area of 0.452 m^2. By definition one curie of activity produces 3.7 x 10^{10} disintegrations/s. Assuming one gamma photon per disintegration, then the counts/s/mCi will be given by:

$$\text{Counts. } s^{-1}. \text{ mCi}^{-1} = \frac{A}{4\pi R^2} 3.7 \times 10^7 \times e^{-\mu R}$$

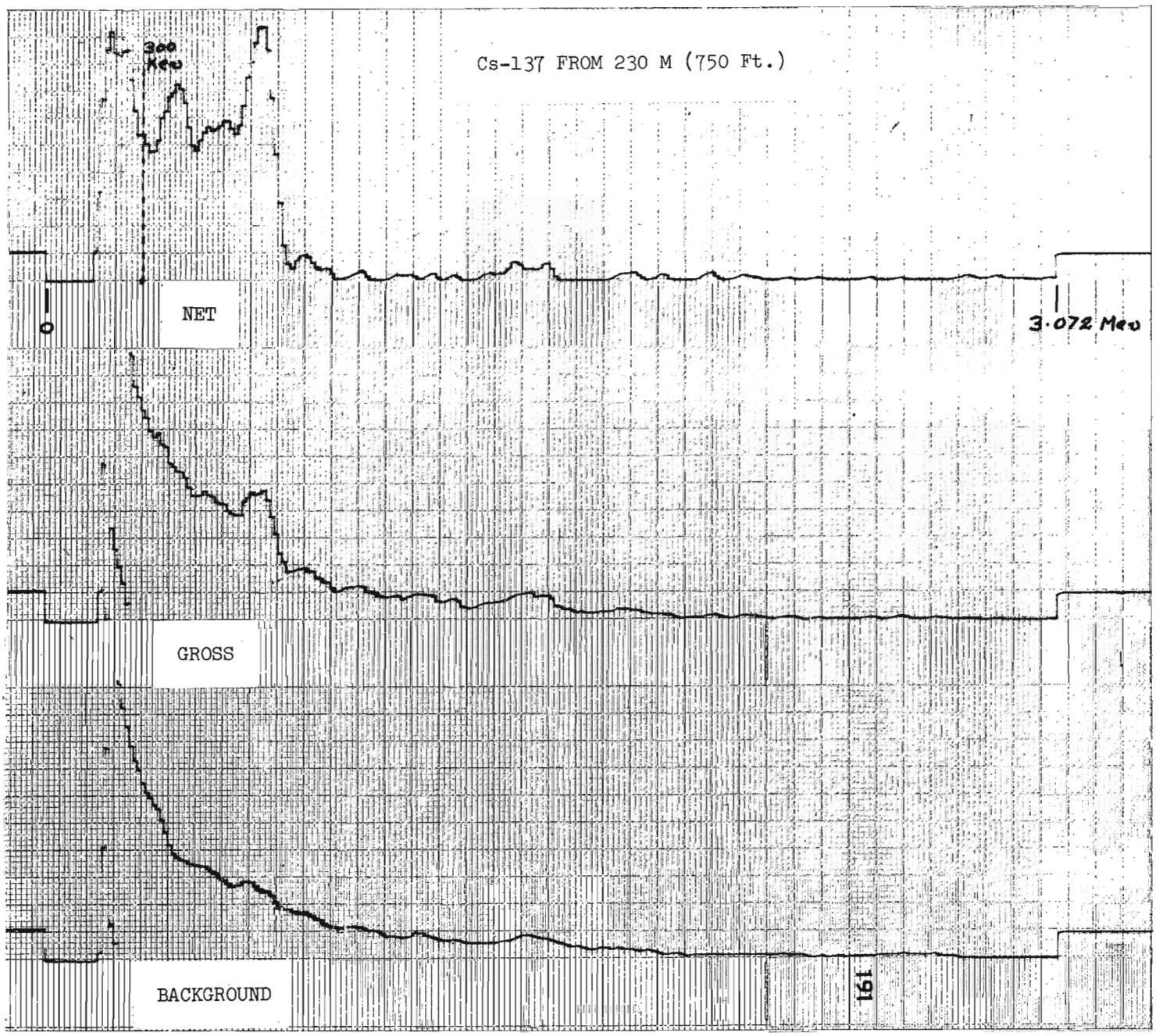

Figure 24.10 The top spectrum shows the scattering of the 662 keV energy of ^{137}Cs by the atmosphere at a source-detector distance of 230 m. The vertical scale is different from that of Figure 24.11. Much of the scattered radiation is still included in a (300-900) keV window.

where:

A = effective detector area tangent to a sphere radius R and centre the source.

R = source-detector distance

The experimental determination of μ was made at an air temperature of 273°K (0°C). The early part of the search operation was carried out in air temperatures of the order of 243°K (-30°C). Since atmospheric pressure variations in absolute terms are negligible, the changes in air density are essentially inversely proportional to absolute temperature. Thus under worst case conditions the value of μ was greater by a factor of 273/243 (ratio of the absolute temperatures).

For a given value C_0 of the counts/s/mCi under worst case conditions, the minimum detectable source strength will be given by C_M/C_0 where C_M is the minimum detectable count rate from a man-made source. Table 24.4 shows minimum detectable source strengths in terms of ^{137}Cs (662 keV) calculated as described above using C_M values from Table 24.2.

These figures tie in reasonably well with the 305 m (1000 ft) pass over the ^{137}Cs source. Figure 24.8 indicates that the difference diagnostic function (lower profile) had less than a 2σ shift at this distance from the source, which was calculated to have a strength of 72 mCi.

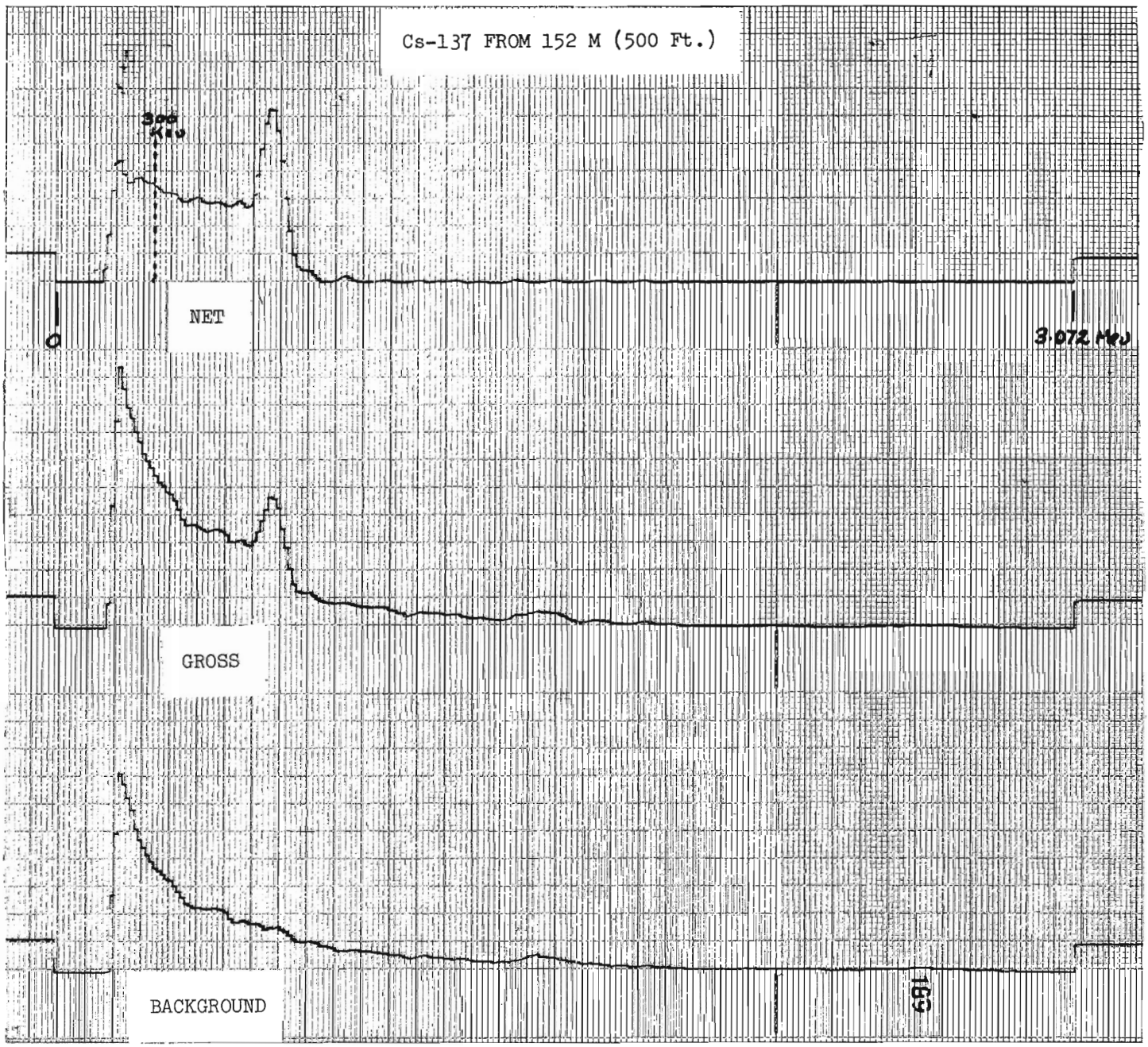

Figure 24.11 The top trace shows a ^{137}Cs spectrum at 152 m source-detector distance. The atmospheric scattering is less severe than in Figure 24.10.

Conclusion

The re-entry of Cosmos 954 represents the first significant "accident" in Canada involving man-made radioactive material. This paper has reported on the experience gained in locating and identifying debris from the air, and provides some reference data, and an analysis of the principles involved in detecting radiation from man-made sources in the event that surveys of this sort should ever be necessary again.

Acknowledgments

The author wishes to make special mention here of the GSC operational group who went back and forth to Edmonton in shifts on a seemingly endless belt. Between them they supported the GSC spectrometer survey for nearly three months on a seven day week basis: Yves Blanchard, Dominique Boucher, George Cameron, Peter Holman, Bill Hyatt, and Jacques Parker, and Keith Richardson who was in overall command of the group. A.G. Darnley, Director of the Resource Geophysics & Geochemistry Division, was actively involved at the interdepartmental level and was responsible for the subsequent participation in the search by Canadian geophysical companies under the supervision of R.L. Grasty.

The author gratefully acknowledges discussions with and helpful advice from Pat Killeen and John Conaway of the G.S.C.; and from many members of the USDOE team, in particular Thane Hendricks and Al Vaillard of EG&G Las Vegas, and Don Goldman of the Lawrence Livermore Laboratory in California.

Reference

Chase, G.D. and Rabinowitz, J.L.
1968: Principles of Radioisotope Methodology; Burgess Pub. Co. Minneapolis.

25.

THE RELATIONSHIP OF URANIUM DEPOSITS TO METAMORPHISM AND BELTS OF RADIOELEMENT ENRICHMENT

Project 740085

P.G. Killeen and K.A. Richardson
Resource Geophysics and Geochemistry Division

Abstract

Killeen, P.G. and Richardson, K.A., The relationship of uranium deposits to metamorphism and belts of radioelement enrichment; in Current Research, Part B, Geol. Surv. Can., Paper 78-1B, p. 163-168, 1978.

The Canadian Uranium Reconnaissance Program routinely produces contour maps which show the distribution of the radioelements potassium, uranium and thorium. Belts of radioelement enrichment have been delineated on compilations of these contour maps. It is suggested that the intersections of belts may be favourable locations for economic concentrations of uranium.

Economic concentrations of uranium, in particular large-volume, low-grade deposits, may be formed by processes of remobilization and granitization associated with metamorphic events.

It is well known that during the formation of granitic rocks, uranium concentrates in the melt until the last stages of cooling and crystallization and is found in associated late-stage pegmatites (Neuerberg, 1956; Rankama and Sahama, 1950). Conversely, there is evidence that uranium is one of the first elements to become remobilized during metamorphism (Heier, 1965). Heier considered regional metamorphism as a potentially active process of element fractionation, involving migration of the elements. He observed that much of the uranium and thorium in rocks appears to be in leachable positions, possibly adsorbed on mineral surfaces rather than in distinct mineral lattice positions. The uranium and thorium would therefore be more easily affected by metamorphic processes. Studies by Killeen and Heier (1974) of radioelement distributions in a small gneiss dome showed evidence that uranium and thorium had become remobilized even though metamorphism was only of sufficient intensity to reset the K-Ar clocks but not the Rb-Sr clocks.

In a broader investigation of 10 granitic plutons in Precambrian terrane of the Telemark area of Norway, Killeen and Heier (1975a) found that the concentrations of the radioelements were directly related to the degree of granitization. Maximum radioelement concentrations in the granites occurred when the source material had been previously enriched by an earlier orogeny. It appeared that the granites were of three types, the result of granitization and remobilization during: (1) the Svecofennian orogeny, (2) the Sveconorwegian orogeny, or (3) both orogenies. They suggested that granites of the third type would have the highest radioelement concentrations resulting from remobilization. The distribution of radioelement values for the granites measured in their investigation suggested the occurrence of three parallel zones and that the three zones were overprinted by a subsequent orogenic event of greater intensity.

One interpretation of Killeen and Heier's (1975c) data is that each belt of remobilization comprised several parallel axes of radioelement enrichment formed by mobilization, separated by zones of depletion out of which the U and Th have probably moved (Fig. 25.1). The lengths of the above mentioned Scandinavian belts are approximately 150 km with about 35 km between belts. One of the belts overprinting these was studied in greater detail by Killeen and Heier (1975b), and was determined to have an exposed length of about 300 km.

Belts of radioelement enrichment of similar dimension in the Canadian Shield have been delineated by airborne gamma-ray spectrometry (Darnley et al., 1971). The significance of the measurements by airborne gamma-ray spectrometry has been discussed by Charbonneau et al. (1976). Richardson et al. (1975a) described four of these belts of radioelement enrichment. The belts included the Wopmay belt (or Great Bear batholith) 240 km long by 80 km wide, the Fort Smith belt (240 km x 80 km), the Wollaston Lake belt (480 km x 70 km), and the Molson Lake-Red Sucker Lake belt (200 km x 40 km). Analysis of lake sediment geochemical data within the Great Bear batholith (Lund, 1973) indicated northeast and northwest trending crest lines on the uranium trend surface separated by 21.5 km and 28 km, respectively. Another zone of radioelement enrichment about 30 km wide and more than 100 km long north of the Elliot Lake uranium deposits was described by Richardson et al. (1975b), and further descriptions of radioelement-enriched zones and belts can be found in Darnley et al. (1975, 1977).

These belts are considered to be possible source rocks for the formation of uranium deposits by secondary enrichment (through erosion and chemical or mechanical concentration for example). Alternatively these belts may also contain a sufficient enrichment in uranium to produce a high-tonnage low-grade uranium deposit without recourse to further secondary enrichment.

One zone of uranium enrichment in the Johan Beetz area of Quebec has been studied extensively by Hauseux (1976). The area is being prospected because of its potential to contain large low-grade uranium deposits. Hauseux indicated that the uranium mineralization could be explained by a remobilization of uranium during regional metamorphism. The uranium moved into granitized areas where concentration occurred probably along strike in the fold axial zones which constituted low-pressure areas. Hauseux concluded that "the entire region once lay in the deeper zones of the Grenvillian Orogenic Belt, acquiring its present state wholly through mountain building processes, and is now exposed thanks to peneplanation".

Little (1974) discussed 'zones' or 'belts' of favourability for uranium exploration which bear some relation to the present discussion. Burwash and Cumming (1976) described a Hudsonian metamorhpic belt in which U and Th have been concentrated. This belt was mapped in the Precambrian basement beneath the sedimentary cover of Western Canada, by using data from deep drillholes.

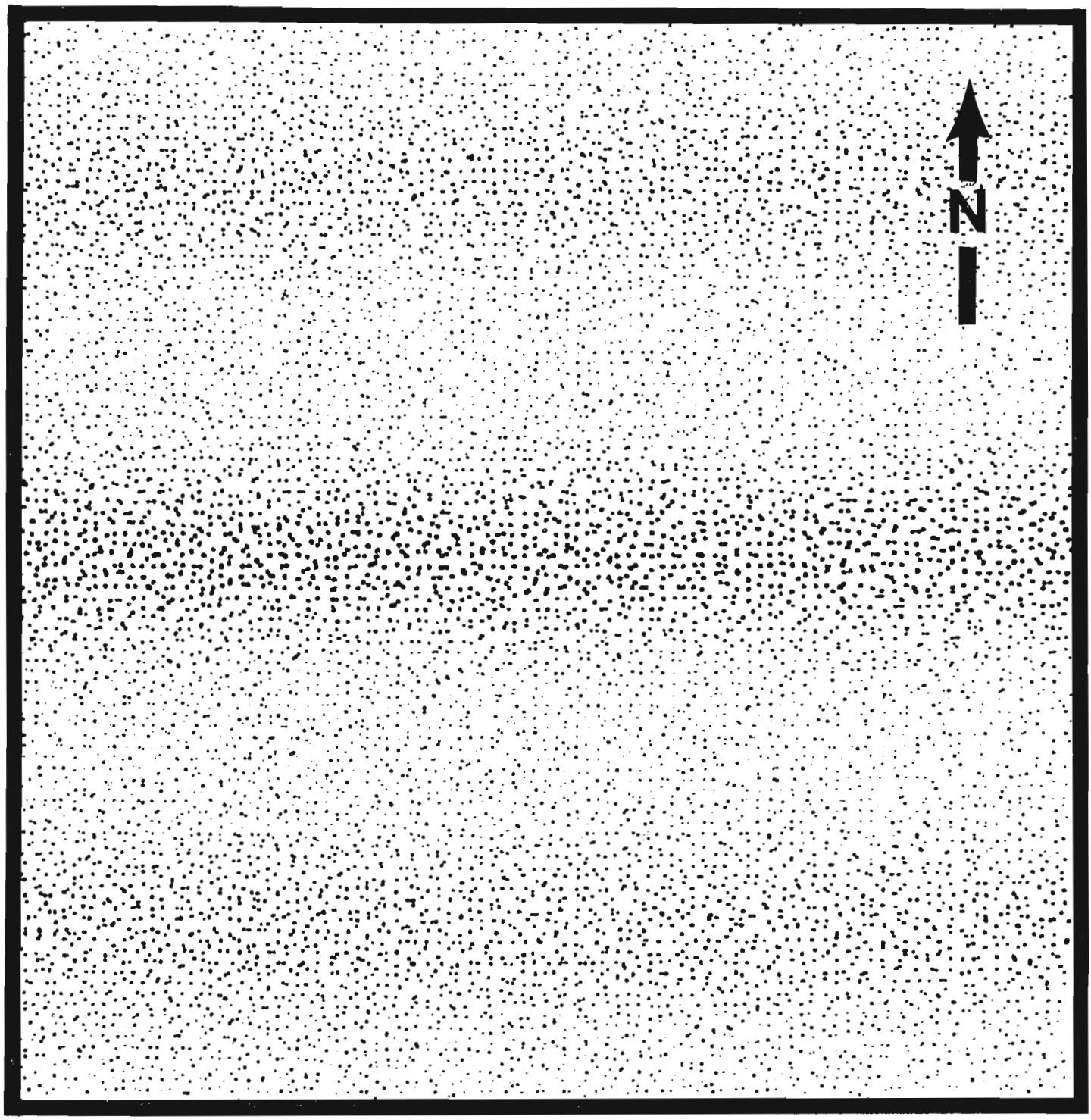

Figure 25.1. Sketch illustrating the concept of parallel belts of radioelement enrichment by remobilization due to metamorphism. The density of dots is proportional to the intensity of metamorphism and thermal remobilization and also radioelement enrichment. The illustration shows three parallel belts (two of minor intensity, one of major intensity) striking in an east-west direction. The centre belt contains the highest degree of radioelement enrichment.

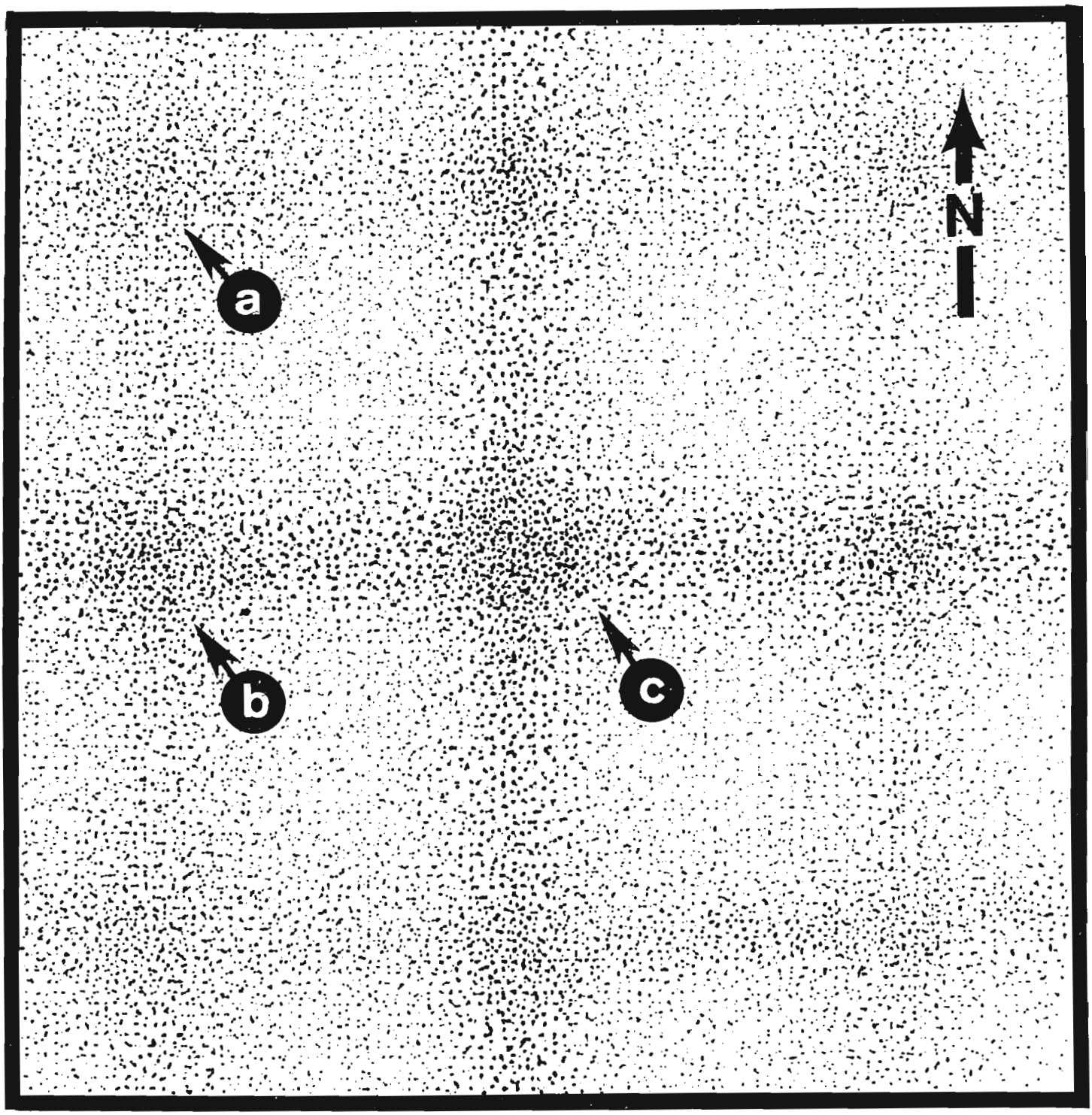

Figure 25.2. Sketch illustrating the concept of intersecting belts of radioelement enrichment due to overprinting of metamorphic events. A similar set of three parallel belts striking in a north-south direction overprint the previous belts described in Figure 25.1. The intersections indicated in the figure show three levels of radioelement enrichment:

a- two minor intensity belts overprinted

b- one major intensity and one minor intensity belt overprinted

c- two major intensity belts overprinted

These points of intersection indicate locations of potential mineral occurrences and deposits, especially at c.

The Norwegian investigations by Killeen and Heier (1975c) suggest that the best possible location for uranium deposits might be at the intersection of belts of radioelement enrichment which are equivalent to zones of orogenic (metamorphic) activity, and consequently zones of remobilization of the radioelements. Figure 25.2 is a diagrammatic sketch of such intersecting belts illustrating where uranium occurrences and potential deposits might be located.

Gabelman (1977) in reviewing orogenic mineralization belts, states "The presence and sequence of metal zones and their geometric conformance to compressive-deformation patterns are so consistent that the writer believes that orogeny stimulates mineralization, which indelibly "fingerprints" the rocks and is erased although incompletely only by higher intensity, superimposed orogeny. The "fingerprints" are useful in deciphering superimposed orogenic belts".

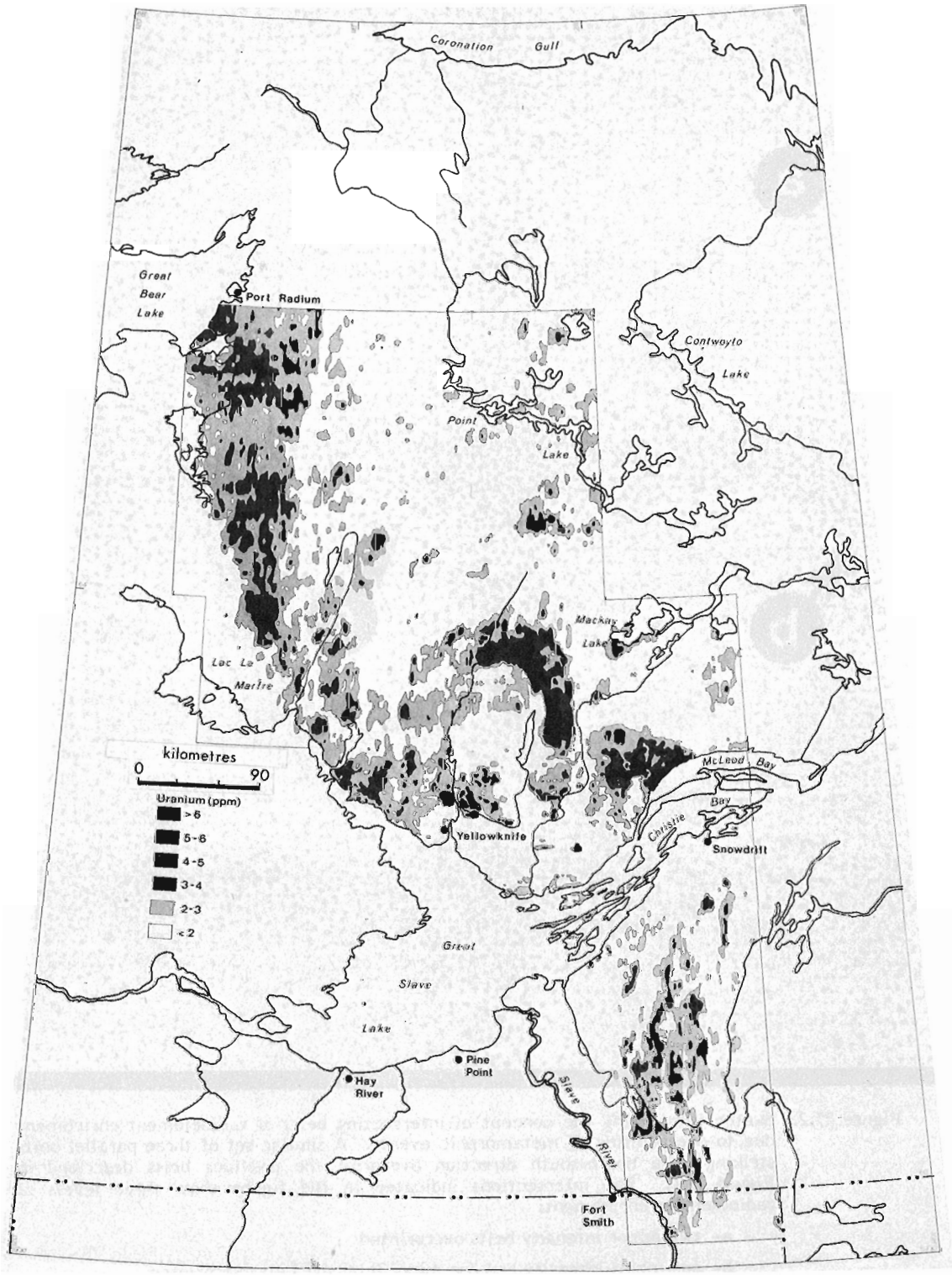

Figure 25.3. Uranium distribution; northwest margin of the Canadian Shield showing belt of uranium enrichment running north from Fort Smith (Fort Smith belt) and curving northwest to Port Radium (Wopmay belt).

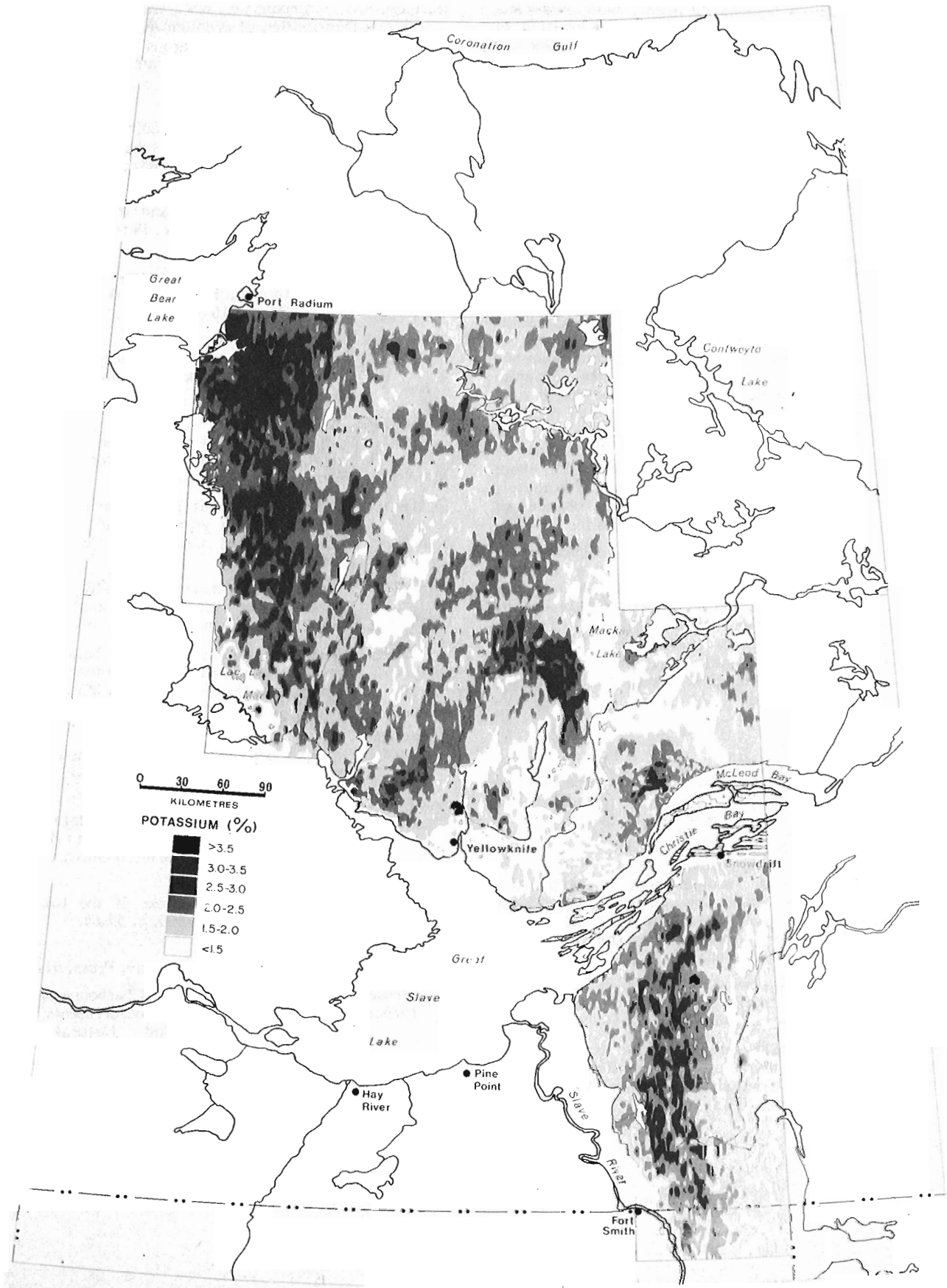

Figure 25.4. Potassium distribution; northwest margin of the Canadian Shield. In addition to a belt of enrichment coinciding with the Fort Smith belt and Wopmay belt shown in Figure 25.3, a series of concentric belts extending east of Wopmay belt can be seen. These parallel, curved belts are centred around the highly enriched semi circular zone centred southwest of Mackay Lake.

These belts are not necessarily linear, and may assume curving or complex sinuous shapes making the location of favourable intersections more difficult. Such a complex belt is shown in Figure 25.3 which is the uranium distribution in an area of about 800 km long and 400 km wide in the northwestern part of the Canadian Shield.

The distribution of potassium, a major element, which may be of some importance in base metal exploration (Davis and Guilbert, 1973) is shown in Figure 25.4, for the same area covered by Figure 25.3. The similar geochemical behaviour of the radioelements is reflected by the areas which show coincident enrichment in uranium and potassium. Particularly striking however, is the pseudo-concentric pattern of potassium enrichment, shown north of the circular zones of enrichment centred southwest of Mackay Lake.

The interpretation of the radioelement distribution patterns as shown on the maps produced by the Canadian Uranium Reconnaissance Program could prove to be of economic significance in the exploration for both uranium and other metals. The Uranium Reconnaissance Program routinely produces contour maps which show the distribution of the radioelements, K, U, and Th. Under this program about 400 000 km^2 are surveyed each year, and coverage of much of the Canadian Shield by airborne gamma-ray spectrometry reconnaissance will be completed by about 1981. Total coverage of the Shield to date is approximately 2×10^6 km^2. As more maps are produced the chances of outlining the belts and locating intersecting belts increase.

Although there is no hard evidence to document the hypothesis that intersecting belts relate to possible economic mineral deposits, it appears plausible. This relation remains to be tested as further survey data are compiled to reveal the overall pattern of radioelement belts within the Canadian Shield. Whether the pattern of radioelement belts is of economic significance or not, such large scale phenomenon should contribute to the geological interpretation of the history of the Canadian Shield.

References

Burwash, R.A. and Cumming, G.L.
1976: Uranium and thorium in the Precambrian basement of western Canada; I. Abundance and Distribution; Can. J. Earth Sci. 13, p. 284-293.

Charbonneau, B.W., Killeen, P.G., Carson, J.M., Cameron, G.W., and Richardson, K.A.
1976: Significance of radioelement concentration measurements made by airborne gamma-ray spectrometry over the Canadian Shield; in Exploration for Uranium Ore Deposits, IAEA Vienna, p. 35-53.

Darnley, A.G., Grasty, R.L., and Charbonneau, B.W.
1971: A radiometric profile across part of the Canadian Shield; Geol. Surv. Can., Paper 70-46.

Darnley, A.G., Cameron, E.M., and Richardson, K.A.
1975: The Federal-Provincial Uranium Reconnaissance Program; in Uranium Exploration 1975; Geol. Surv. Can., Paper 75-26, p. 49-63.

Darnley, A.G., Charbonneau, B.W., and Richardson, K.A.
1977: Distribution of uranium in rocks as a guide to the recognition of uraniferous regions; in Recognition and Evaluation of Uraniferous Areas, IAEA Vienna.

Davis, J.D. and Guilbert, J.M.
1973: Distribution of the radioelements potassium, uranium and thorium in selected porphyry copper deposits; Econ. Geol., v. 68, p. 145-160.

Gabelman, J.W.
1977: Migration of uranium and thorium - exploration significance; Am. Assoc. Petr. Geol., Tulsa.

Hanseux, M.A.
1976: Mode of uranium occurrence in a migmatitic granite terrain, Baie Johan Beetz, Quebec; CIM Bull., v. 70, p. 110-116.

Heier, K.S.
1965: Metamorphism and the chemical differentiation of the crust; Geologiska Föreningens i Stockholm Förhandlingar, v. 87, p. 249-256.

Killeen, P.G. and Heier, K.S.
1974: Radioelement variation in the Levang granite-gneiss, Bamble region, South Norway; Contr. Min. Petrol. 48, p. 171-177.

1975a: Th, U, K, and heat production measurements in ten Precambrian granites of the Telemark area, Norway; Norges Geologiske Undersokelse 319, p. 59-83.

1975b: A uranium and thorium-enriched province of the Fennoscandian shield in southern Norway; Geochim. Cosmochim. Acta, v. 39, p. 1515-1524.

1975c: Radioelement distribution and heat production in Precambrian granitic rocks, southern Norway; Skr. Norske Vidensk. -Akad. i Oslo, Mat. -naturv, p. 1-32.

Little, H.W.
1974: Uranium deposits in Canada - their exploration, reserves and potential; CIM Bull. 67, p. 155-163.

Lund, N.G.
1973: Harmonic analysis of analytical data for uranium in lake sediments in the Great Bear Region, N.W.T.; B.Sc. thesis, Carleton Univ., Ottawa.

Neuerburg, G.J.
1956: Uranium in igneous rocks of the United States; U.S.G.S. Prof. Paper 300, p. 55-64.

Rankama, K. and Sahama, T.G.
1950: Geochemistry; Chicago Univ. Press, 912 p.

Richardson, K.A., Darnley, A.G., and Charbonneau, B.W.
1975a: Airborne gamma-ray measurements over the Canadian Shield; 2nd Natural Radiation Symposium, Rice Univ., p. 681-704.

Richardson, K.A., Killeen, P.G., and Charbonneau, B.W.
1975b: Results of a reconnaissance type airborne gamma-ray spectrometer survey of the Blind River-Elliot Lake area, Ontario; in Report of Activities, Part A; Geol. Surv. Can., Paper 75-1A, p. 133-135.

PICTURE PROCESSING OF GEOLOGICAL IMAGES

A.G. Fabbri and T. Kasvand[1]
Regional and Economic Geology Division

Introduction

A general situation in the field of mineral potential assessment can be imagined as one in which, in addition to a bedrock geology map, there are other maps available for the area of interest, such as a surficial geology map, several geophysical and geochemical contour maps, and a metallogenic map. A geologist is asked to establish correlations and to estimate probabilities for the occurrence of rare geological events, such as economic mineralization. The "pattern recognition" task, effectively, can be so complex that computer techniques, geological knowledge and statistical methods will be essential working tools.

If, for instance, the assumption is made that a specific geological map pattern describes the environment favourable to a particular type of mineral deposit, the geometric probabilities associated with this map pattern can be combined with probabilities associated with the geometry and distribution of mineral deposits and also with the geometric probability associated with a given search pattern. Similar considerations can be made about pictures of microscopic crystalline aggregates in which the pattern obtained by the various crystals during nucleation and growth can be described by the spatial distribution of the boundaries between the crystals.

Studies on geometric probability can be facilitated if map data are more readily captured and quantified for computer processing. Much research has been devoted to these problems in other fields of science but geological patterns have hardly been studied by means of these methods.

Fabbri (1975) and Fabbri et al. (1975) quantified information from maps by overlying a U.T.M. 10 km grid on 1:250 000 specially compiled geological maps and point-counting the different colours corresponding to map units and by constructing data sets for the 10 km cells. Separate data sets were constructed for the occurrence of mineral deposits in these cells. The two data sets represent a data bank which can then be manipulated and analyzed by computer. These methods, which produced results as those in Agterberg et al. (1972), can be improved by minimizing the loss of resolution due to lumping map values into square cell data sets. It is preferable to quantize data from maps so that much of the geometry of the map pattern can be retained.

Some recent techniques of digitization of geological maps have been described by Bouillé (1975) who used a graph theory approach, and by Anuta et al. (1976) who used a polygon technique to digitize geological maps for exploration purposes involving remote sensing and geophysical data.

In 1972 a joint research project between the Geological Survey of Canada and the National Research Council was initiated to investigate the feasibility of quantifying automatically data from geological maps by using a flying spot scanner (Kasvand, 1972). The result of these studies have paved the way for a new project in collaboration with the Electrical Engineering Division of NRC on the development of computer techniques for the digitization and analysis of geological images. Examples of application of interactive programming techniques and subsequent estimation of geometrical probabilities are given in Agterberg and Fabbri (in press).

Digitization and Computer Processing

Picture processing deals with the processing of pictorial information by computer. This field underwent an extensive and rapid development during the last 20 years, in parallel with the growth of computer technology (Rosenfeld and Kak, 1976). Pictures can be analyzed by computers only if they are in digitized form. The computer memory stores the digital representation of pictures in the form of arrays of numbers. To each two- or three-dimensional address a grey level or density value is associated which has a one to one correspondence with a point in the picture. These arrays are the data sets from which programmed algorithms compute measures of the different parameters which describe the patterns contained in the picture. The description of a picture involves properties of the picture or of its parts, and relationships among the parts. Geometrical properties, for example, do not depend on the picture grey levels, but only on the sets of picture points that belong to given picture parts.

The digitization of picture data can be accomplished in several ways. Two common methods are: (a) scanning by means of optical and mechanical devices, and (b) digitizing of contours by means of manual x-y digitizers. In this paper both techniques are applied: (a) a flying spot scanner was used for 25 mm transparencies of black and white tracings of map boundaries; and (b) a graphic tablet was employed for digitizing boundaries of crystal grains from the tracing of an enlarged rock texture from a thin section.

Table 1

Contact length matrix computed for boundaries of sphene, calcic pyroxene, hornblende and plagiolase digitized from a thin section of granulite. Percentage of contact length and area, and number of crystals are also in the table for each crystal type. A transition matrix P has been computed from the contact length matrix

	sphene	pyroxene	hornblende	plagioclase	% contact length	% area	No. of crystals
sphene	0.0000	.0122	.0109	.0208	4.39	.42	25
pyroxene		.0340	.1496	.2578	45.36	20.41	97
hornblende			.0474	.3572	56.51	20.44	139
plagioclase				.1101	74.59	58.72	137

$$P = \begin{pmatrix} .0000 & .2779 & .2483 & .4738 \\ .0269 & .0750 & .3298 & .5683 \\ .0193 & .2647 & .0839 & .6321 \\ .0279 & .3456 & .4789 & .1476 \end{pmatrix}$$

[1] National Research Council, Canada.

From: Scientific and Technical Notes in Current Research, Part B; Geol. Surv. Can., Paper 78-1B .

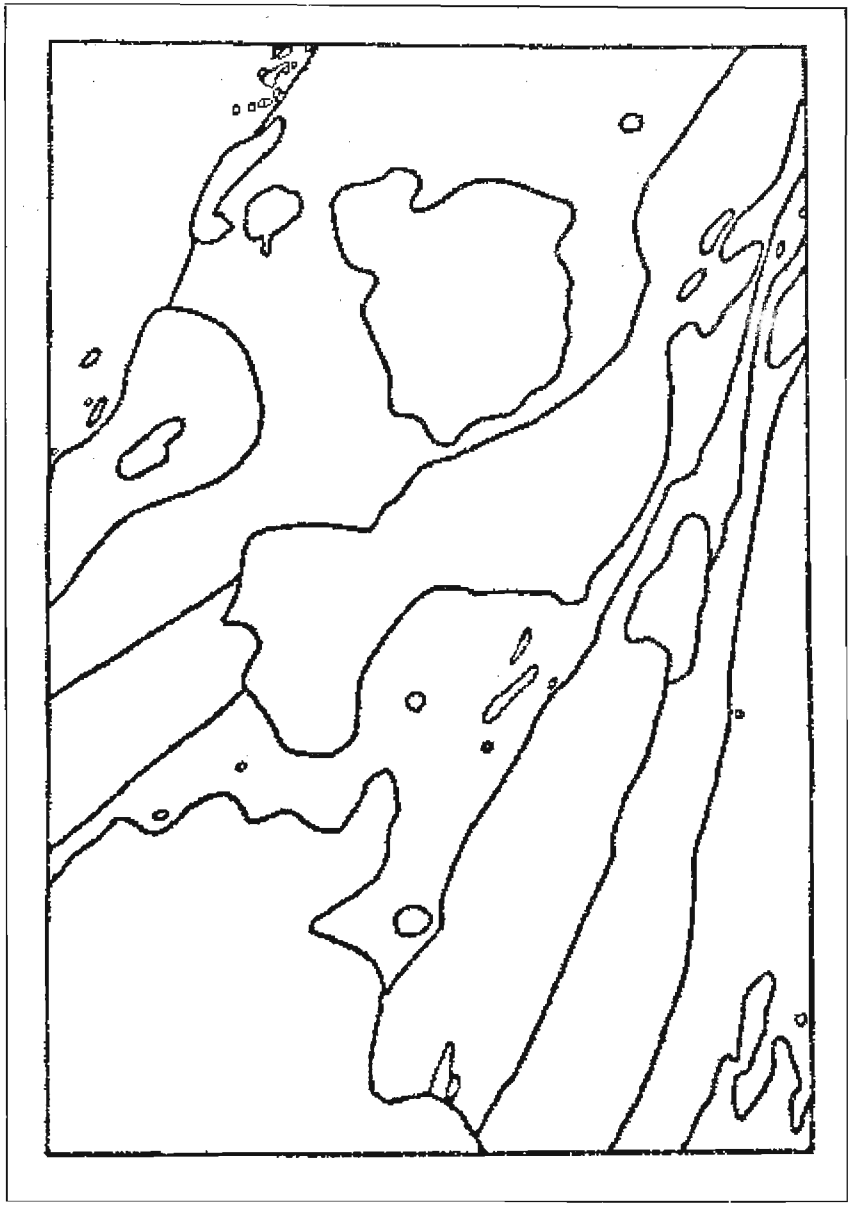

Figure 1. Computer plot of binary image of boundaries of GSC Map 1129A, digitized by means of a flying spot scanner. Picture dimensions are 419 x 600; each picture point corresponds to approximately 190 m.

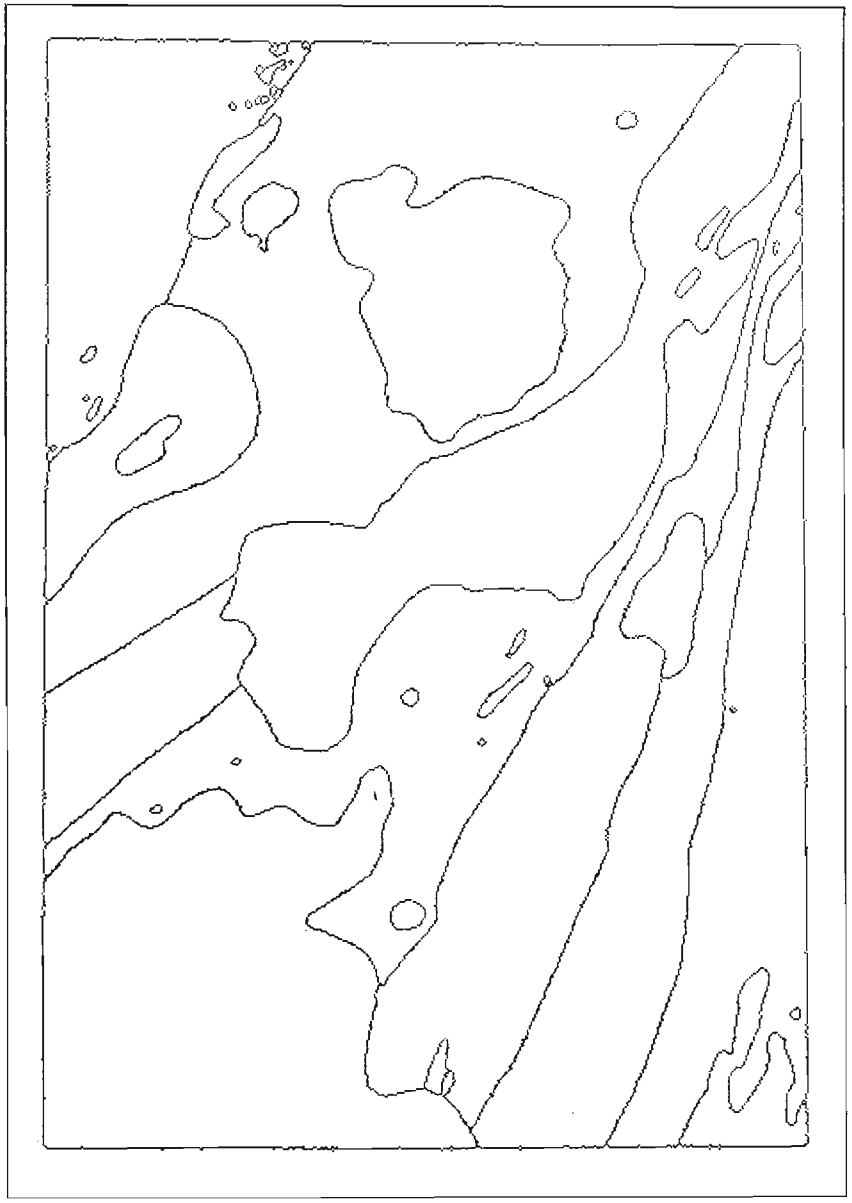

Figure 2. Thinned version of the image of Figure 1.

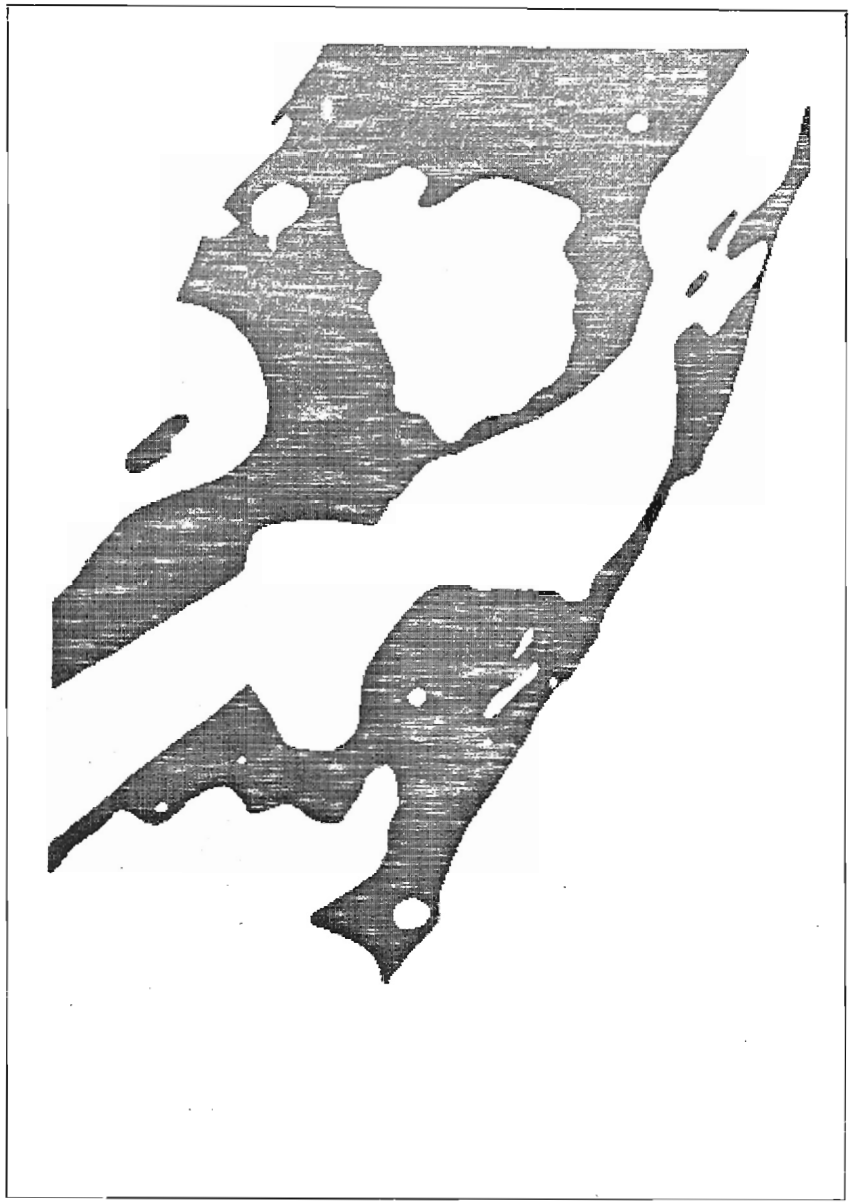

Figure 3. Binary image of Lower Ordovician greywackes, extracted from the image of Figure 2. 61787 picture points correspond to 2231 km^2.

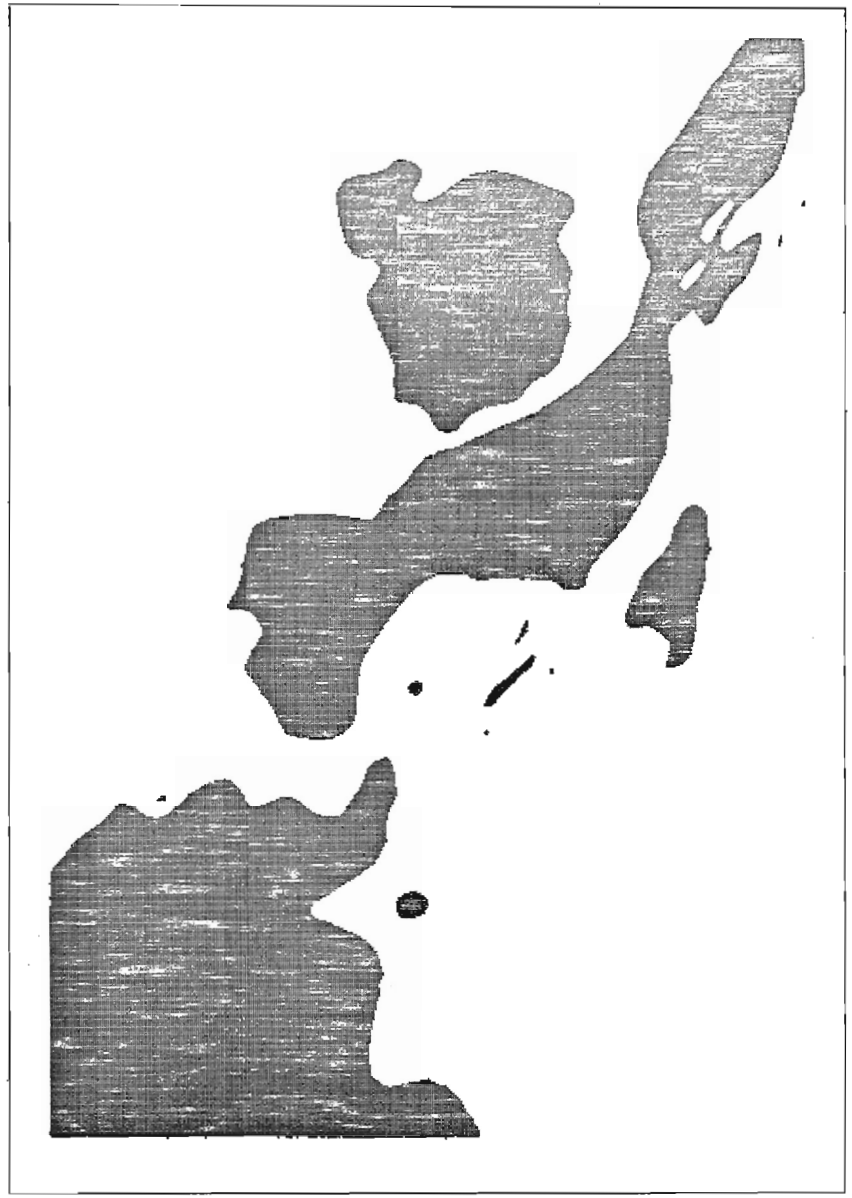

Figure 4. Binary image of Devonian granitic rocks extracted from the image of Figure 2. 71686 picture points correspond to 2588 km^2.

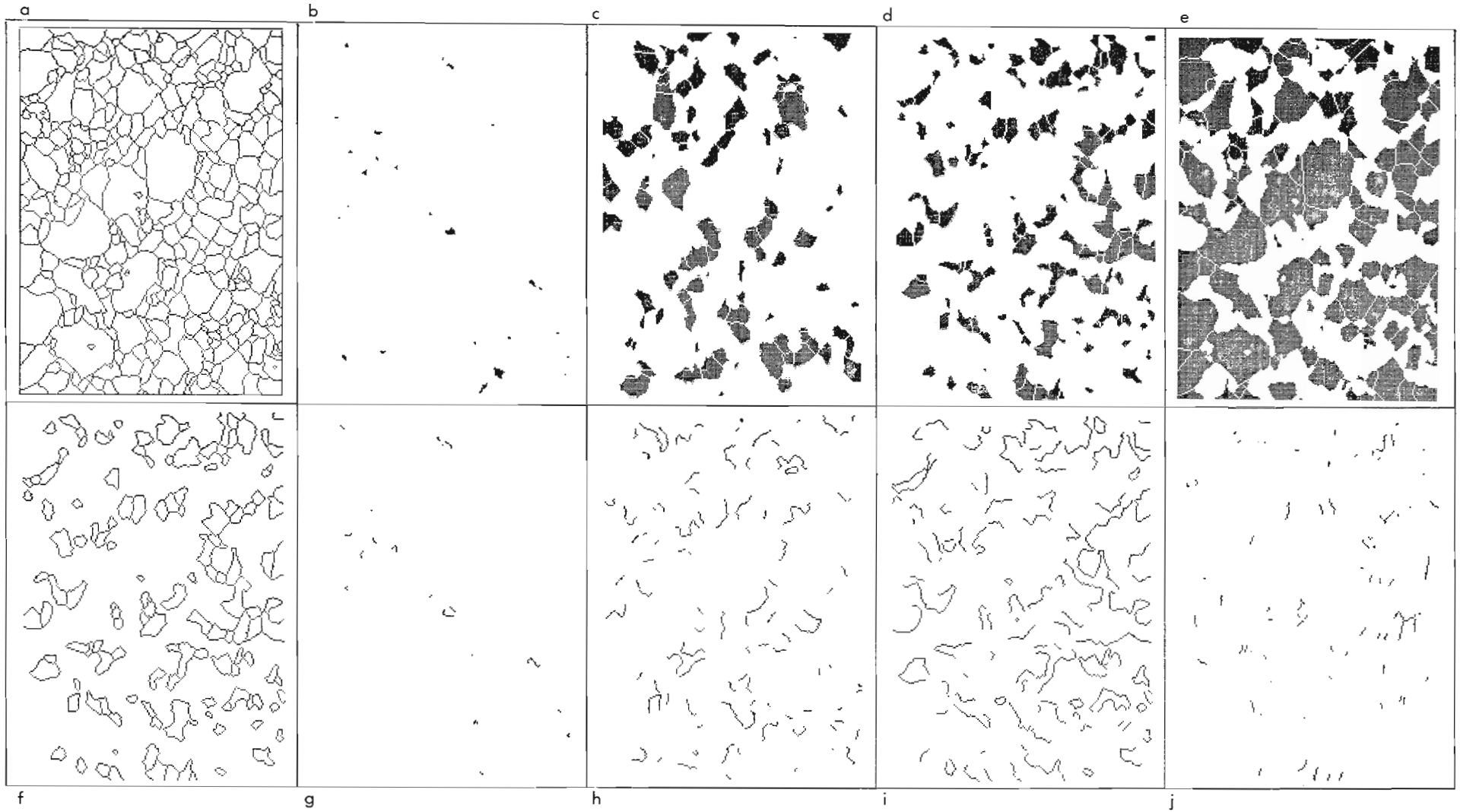

Figure 5. Binary image of a thin section of granulite from Otter Lake, Quebec.

5a: thinned boundary image with rectangular frame added after thinning. Picture dimension is 180 x 252 picture points;

5b to 5e: binary images of sphene, calcic pyroxene, hornblende and plagioclase respectively, extracted from the image in 5a;

5f: image of boundaries of hornblende crystals;

5g: sphene-hornblende boundaries;

5h: calcic pyroxene-hornblende boundaries;

5i: plagioclase-hornblende boundaries;

5j: hornblende-hornblende boundaries.

Applications to Geological Maps

This application describes the following experiment of digitization of a geological map (Geol. Surv. Can., Map 1129A, Terra Nova, Newfoundland, scale 1:253 440). The geological boundaries were drawn in ink on transparent tracing paper, and then photographed on a 35 mm colour transparency. The maximum dimension of the map in the transparency was kept less than 25 mm which is the dimension of the scanner window. This boundary image was scanned by a flying spot scanner at regular intervals in the two perpendicular directions (square raster scanning) to produce a 419 x 600 grey level picture which was recorded on magnetic tape. This picture was filtered by subtracting an image computed by averaging for 15 by 15 arrays of picture points in order to eliminate unevenness in grey level readings (shading) due to scanner. The resulting image was thresholded to obtain a binary image in which 0's correspond to white background, and 1's to points of the black boundary lines. Figure 1 shows the binary image produced, after minor editing for resolving a few of the smaller details. Each picture point in the image can be considered to represent a square cell measuring 190 m on a side.

The geological boundaries of Figure 1 are several picture points in width. They were thinned to the width of a single picture point which maintained the connectivity between points, by means of a line thinning algorithm modified after Tamura (1975). The thinned image is shown in Figure 2 where the boundary width is minimal and from which boundary length can be computed. Separate binary images, one for each map unit, can be extracted from the image of Figure 2 by using a common picture processing technique called component labelling. This algorithm assigns sequential labels to sets of points within each different black boundary. Groups of labels can then be used in order to transform specific geological map units into separate binary images. For example the pattern of Figure 3 is the binary representation of Lower Ordovician greywackes which covers an area of 2231 km^2(61 787 picture points). The pattern of Figure 4 is for Devonian granites which cover an area of about 9588 km^2 (or 71 686 points). From these separate binary images estimates of parameters such as areas, perimeters, and measures of elongation and curvature can be computed. Matching between images results in auto- or cross-correlation functions, which can be used to describe geometrical attributes of the map patterns. Applications of concepts of geometrical probability to map patterns have been exemplified by Agterberg and Fabbri (in press).

Application to Microscopic Textures

Use was made of a graphic tablet for digitizing boundaries of crystal grains. The tablet supplies x-y co-ordinates for the positions of a pen moving on its surface. From these co-ordinates, vectors were computed and transformed into a 180 by 252 binary image of contours. The original drawing (not shown here) of a thin section of a granulite from Otter Lake, Quebec, was obtained from Dr. R. Kretz, University of Ottawa. Minor editing was required for resolving the details of four small crystals.

The line thinning algorithm of the previous application was also applied to the binary image obtained from the tablet. The thinned boundary is shown in Figure 5a. The unit spacing between picture points corresponds to 0.0278 mm. The four minerals occurring in this granulite are sphene, calcic pyroxene, hornblende and plagioclase. The technique of component labelling allowed separation of all grains for each mineral and produced the binary images in Figures 5b to 5e.

Binary image data can be compressed so that a black or white picture point will correspond to an "ON" (1) or "OFF" (0) bit position respectively in a computer word. This data packing drastically decreases storage requirements. Logical or Boolean operations such as "AND", "OR", "NOT" and "AND NOT" on or between binary images can be computed. Bit neighbourhood transformations (Moore, 1968) can also be programmed for packed binary images. A neighbourhood is defined as a small set of picture points surrounding each picture point. For instance, we can consider each point surrounded by 8 neighbours in a rectangular array: 4 points at distance 1 from the centre, and 4 points in diagonal positions at distance $\sqrt{2}$ from the centre point. A bit neighbourhood transformation may consist of making a white centre value black if at least one of the points in the neighbourhood is black. This transformation which can be called dilatation, generates an outgrowth of one picture point for each boundary point of all black shapes in the binary pattern. The reverse transformation is an erosion. Combinations of boolean operations and bit neighbourhood transformations for specially designed neighbourhoods allow the estimation of measures for many geometrical properties of binary images. Theoretical statistical bases and applications of texture analysis techniques have been described by Matheron (1975) and Serra (1975, 1976).

An application is made here on the images of Figures 5a to 5e, in order to produce and display separate images of boundaries between different crystals and also of boundaries between crystals of the same type. As is sometimes done in textural studies in petrology, crystal to crystal transitions are coded for grain sequences along equally spaced linear traverses in order to compute transition matrices which can be compared to Markov chains for texture characterization, as in Kretz (1969) or Whitten et al. (1975).

The approach followed in this application consists of measuring directly the contact length for all contacts of the four minerals of the patterns in Figure 5, and to compute the 4 by 4 transition from these lengths. The images of Figures 5b to 5e were dilatated once, and the resulting images ANDed with the image of boundaries of Figure 5a. This produced a separate boundary image for each crystal type. Figure 5f shows the boundary of hornblende. Each boundary image was then ANDed with any other one, and this produced 6 partial boundary images, one for all possible pairs of crystals. Figures 5g to 5i show the boundaries hornblende-sphene, hornblende-calcic pyroxene and hornblende-plagioclase respectively. The three partial boundaries so obtained for each crystal pair were ORed with each other for every crystal type and the resulting image was complemented (NOT) and ANDed with the boundary image for each crystal type. The results were the images for the boundaries between crystals of the same type. Figure 5j shows all hornblende-hornblende boundaries.

From the different binary images of boundaries so produced, the boundary lengths were computed as multiples of 1 for pairs of black picture points on the same row or column of the binary picture, and as multiples of $\sqrt{2}$ for pairs of diagonal points. The 4 by 4 transition matrix so computed is shown in Table 1, together with the contact length matrix, the percentage of contact length and area for each mineral and the number of grains of each mineral in the images. This type of transition matrix describes fully the texture in two dimensions by expressing the probability for each crystal to be in contact with any other type of crystal and with crystals of the same type. The values in the table show a distinct tendency for unequal contacts over equal contacts. This pattern may provide evidence on genetic relationships between the minerals and on metamorphic recrystallization events of the rock such as interfacial energy and nucleation.

Conclusions

The preceding applications try to exemplify some of the picture processing techniques which can be applied to geological images for facilitating pattern recognition and statistical analysis. Interactive programming methods are being developed by the authors for automating applications of picture processing to mineral exploration problems and analysis of geological textures.

References

Agterberg, F.P., Chung, C.F., Fabbri, A.G., Kelly, A.M., and Springer, J.A.
1972: Geomathematical evaluation of copper and zinc potential of the Abitibi area, Ontario and Quebec; Geol. Surv. Can., Paper 71-41, 55 p.

Agterberg, F.P. and Fabbri, A.G.
Spatial correlation of stratigraphic units quantified from geological map J; Computers and Geoscience (in press).

Statistical treatment of tectonic and mineral deposit data. Bull. Global Tectonics Metallogeny; Am. Univ., Washington, D.C. (in press).

Anuta, P.E., Hauska, H., and Levandowski, D.W.
1976: Analysis of geophysical remote sensing data using multivariate pattern recognition techniques; Proceedings of Symposium on Machine Processing of Remotely Sensed Data, June 25-July 1, 1976, Purdue Univ., West Lafayette, Indiana, Inst. Electr. Electron. Eng., Inc. Catalog No. 76CH1103 MPRSD, p. 1B-11, 1B-14.

Bouillé, F.
1976: Graph theory and digitization of geological map J; Int. Assoc. Math. Geol., v. 8, p. 375-393.

Fabbri, A.G.
1975: Design and structure of geological data banks for regional mineral potential evaluation; Can. Min. Met. Bull., v. 69, p. 91-98.

Fabbri, A.G., Divi, S.R., and Wong, A.J.
1975: A data base for mineral potential estimation in the Appalachian Region of Canada; in Report of Activities, Part C, Geol. Surv. Can., Paper 75-1C, p. 123-132.

Kasvand, T.
1972: Feasibility of automatic measurement of lengths and areas on geological maps; Nat. Res. Counc. Can., Rep. LTR-CS-75,May 1972.

Kretz, R.
1969: On the spatial distribution of crystals in rocks; Lithos, v. 2, p. 39-65.

Matheron, G.
1975: Random sets and integral geometry; New York, John Wiley and Sons, 261 p.

Moore, A.G.
1968: Automatic scanning and computer processes for the quantitative analysis of micrographs and equivalent subjects; in Cheng, G.C., Ledley, R.S., Pollock, D.K., and Rosenfeld, A. (editors): Pictorial Pattern Recognition, Thompson Book Co., Washington, D.C., 521 p.

Rosenfeld, A. and Kak, A.C.
1976: Digital picture processing; New York, Academic Press, 457 p.

Serrà, J.
1975: 15 Fascicules de morphologie mathèmatique appliquée; Centre de Morphologie Mathèmatique. Fontainebleau, France, Jan. 1975 (papers by Chouwe, P.H., Serrà, J., Digabel, H., Klein, J.C., Lorrain, M., and Naert, B.).

1976: Lectures on image analysis by mathematical morphology. Centre de Morphologie Mathèmatique, Fontainebleau, France; Cahier, N-475, July 1976.

Tamura, H.
1975: Further considerations on line thinning schemes; Assoc. Electr. Comm., Japan; Prof. Note 66, 49-56 (in Japanese).

Whitten, E.H.T., Dacey, M.F., and Thompson, K.
1975: Markovian grain relationships of a Grenville granulite; Am. J. Sci., v. 275, p. 1164-1182.

A NEW CASTING TECHNIQUE FOR BELEMNITES AND SIMILARLY SHAPED SMALL FOSSILS

M.F. McLaughlin
Institute of Sedimentary and Petroleum Geology, Ottawa

Introduction and Acknowledgments

The most common method of preparing casts of fossils involves the use of latex rubber and plaster of paris. It is quite satisfactory for most fossils and easy to use if one has some experience. This note attempts to introduce a new, practical and accurate method of preparing casts of a small to minute and sometimes delicate type of fossil — the belemnite. Although the method was not tested on other fossils, it is expected to be usable and advantageous when applied to casting other small, subfusiform fossils (e.g. echinoid spines). The use of silicon rubber is recommended to mould the specimen and epoxy resin is recommended for casting. The advantages of silicon rubber for use with belemnites, are explained in the following text.

The research was done to facilitate belemnite studies of J.A. Jeletzky who supervised the writer's research, provided valuable advice and who critically read and edited this contribution. Special thanks are due to research workers and technicians of the Paleontology Department of the British Museum of Natural History who provided information concerning casting methods used in their paleontological laboratories. The writer is grateful for assistance given by members of the staff of the Archaeological Survey of Canada. Particular benefit was gained from discussions with L. McCarthy on his casting technique.

Table 1

Basic list of equipment

EQUIPMENT	PURPOSE	EQUIPMENT USED
Hot plate/Bunsen burner	To melt wax	
Balance	To measure weight proportions fo silicon rubber and epoxy for catalysis	
Vacuum pump	To remove air bubbles in the silicon rubber	Vactor PV 35 with 1/3 HP motor
Desicator flange	Container for vacuum operation on the silicon rubber	Fisher Bel Art (ID 14-3cm)
Plastic vials	Container for the preparation of the silicon rubber mould (see Fig. 1)	"RIGO" Plasticlear vials by Richards Glass Co. Ltd.
Centrifuge tubes	Container for the mould and liquid epoxy during centrifugation (see Fig. 8)	Polypropylene centrifuge tube with conical bottom (OD 2.9cm, length 13.4cm)
Centifuge facility	To separate air and epoxy in the mould	

From: Scientific and Technical Notes in Current Research, Part B; Geol. Surv. Can., Paper 78-1B .

The Latex Method

The latex and plaster of paris method of casting can be used on delicate spiculate, subfusiform, or mace-shaped belemnites and other similarly shaped fossils. However, the resulting plaster casts do not reproduce faithfully the proportions and shape of belemnite guards and their more subtle external morphological features. Furthermore, the resulting plaster cast is often too delicate for manipulation because of the available grades of plaster of paris. Those features which are reproduced are eventually worn off with extensive handling. In comparison with silicon rubber, latex rubber has a very short life; in fact it begins to shrink from the moment it is pealed off the belemnite and will dehydrate significantly once the volatiles leave. Therefore, unlike the silicon rubber moulds, the latex mould cannot be used repeatedly over a period of time. The latex method does not involve the use of equipment such as a vacuum pump and a centrifuge. Therefore, unlike the silicon rubber method, the quality of the end product will depend largely on subtle intricacies of the technique and experience of the operator.

The Silicon Rubber Method

The equipment and materials needed for the silicon rubber casting technique are listed in Tables 1 and 2. The use of equipment such as a vacuum pump and a centrifuge to do the more difficult precision work allows a technician with little or no experience to use the silicon rubber method with success. It would be possible to do without the pump and centrifuge if a technician is sufficiently skillful, however, the quality of the cast and the rate of success is not encouraging. On the other hand, this variant is the ideal alternative for those who wish to test this technique and keep the costs down during the trial period.

The Technique

Preparation of plastic vials: Use a No 9 tapered plastic vial with a plastic cap. This size is ideal for the average belemnite. Cut off the bottom and smooth the edges, lubricate the inner walls of the vial with petroleum jelly. Put 9 mm of plasticine in the vial's plastic cap, stick 3 mm of the apical end of the belemnite to be cast into this bed of plasticine. Place the plastic cap on the vial containing the belemnite which must be in a vertical position not touching the walls of the vial. Melt some wax and let it run down the inner wall of the vial and up the halfway mark of the specimen (Fig. 1). It is very important that no wax adheres to the upper part of the specimen since any such wax would be reproduced in the casting process.

Preparation of wax surface: As the wax hardens it will cave in around the specimen due to capillary attraction caused by surface tension and the relative value of adhesion between liquid and solid (the vial wall) (Fig. 2). With the rounded end of a slender glass rod or the equivalent, poke four or more small depressions 3 mm deep, in the concave border around the specimen. These are very important relief features in the preparation of the silicon rubber mould since they contribute to the interlocking surface of its two parts. As soon as the wax is hard, apply petroleum jelly once again to the inner surface of the vial and prepare silicon rubber to pour the first half of the mould.

Table 2

Basic list of material

MATERIAL	USE
RTV 41 liquid silicon rubber	Mould material
E.L.R. 2795 epoxy resin	Cast material
Petroleum jelly	Release agent
Oil paint	To color epoxy
Wax (Parowax)	Mounting medium
Plasticine	Mounting medium

The first half of the silcon rubber mould: Mix the recommended amount of silicon rubber by weight with its catalyst, place the mixture in a vacuum for five to ten minutes to remove air bubbles and then pour the rubber slowly into the vial until the specimen is covered. If the belemnite is too long for the vial, adapt an extension using plastic sheeting and tape. A depression must be moulded in the silicon rubber at the tapered end of the vial to within 3 mm of the top of the alveolar end of the belemnite. This depression is used in the later stages of the technique to hold a reserve of epoxy resin (the casting material) used during centrifugation. To make this depression the use of the rubber end of an eyedropper, or the equivalent, suspended above the fossil with a needle is recommended. If the needle is inserted too high or too low, the position of the eyedropper can be varied by simply bending the needle (Fig. 3). The depth of the eyedropper can be determined before the first half of the silicon rubber is poured into the vial. Pour the silicon rubber into the vial to a level which will allow room for the eyedropper. Push the eyedropper into the silicon rubber until both ends of the needle rest on the edge of the vial. When the silicon rubber has cured (usually overnight), remove the plastic cap and the plasticine. Then, by running a lubricated needle between the vial and its contents, it is possible to push the rubber and wax out of the vial. It is very important not to remove or even jar the specimen from its rubber mould; therefore, clean the belemnite and the silicon rubber as one unit.

The silicon rubber interface: As a last step before pouring the second half of the silicon rubber mould, a notch should be cut on the outer circumference of the silicon rubber interface (Fig. 4). This notch will be helpful when the two halves are put together during the casting operation. This is also the time to add any other features to the rubber interface; for example, if one had poured the silicon rubber of the first half of the mould directly onto the hardened wax without making the depressions around the specimen, this omission could be compensated for by carving notches in the silicon rubber interface once the rubber has cured (Fig. 5). Many variations to this technique are possible. The writer leaves it to the reader to develop his own.

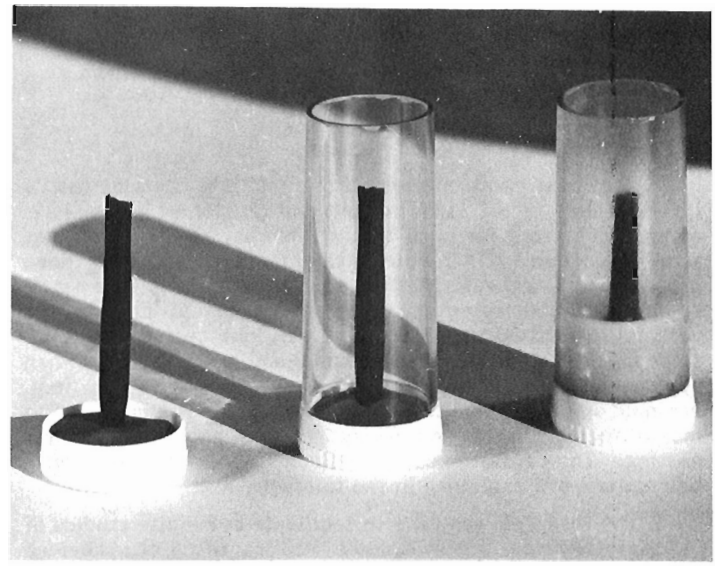

Figure 1. Figures 1a-1c illustrate the correct positioning of the belemnite in the mounting medium and its handling; a) the belemnite is placed in the plasticine; b) the vial is placed over the specimen and pressed into the plastic cap and, c) the wax is carefully poured to the halfway mark of the belemnite.

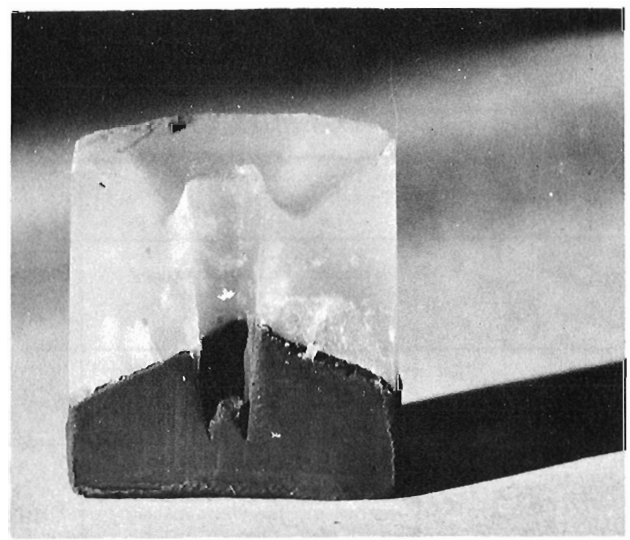

Figure 2. Cross-section of the two mounting mediums the plasticine and the wax. The plasticine holds the belemnite while the wax is being poured. The wax secures the specimen and the depression formed around the specimen during its solidification will be reproduced by the first half of the rubber mould and form the basis for the mould's interface.

Once satisfied with the conditions of the silicon rubber interface, petroleum jelly should be brushed over the interface and into the depressions and notches of the rubber, and lubricate the inside of the vial. Then the first half of the mould and belemnite should be repositioned in the vial. The second half of the silicon rubber mould should be left to catalyse (usually 6 hours).

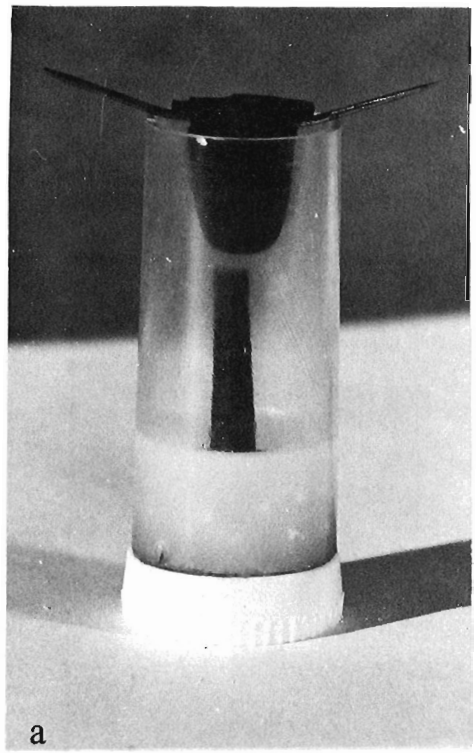

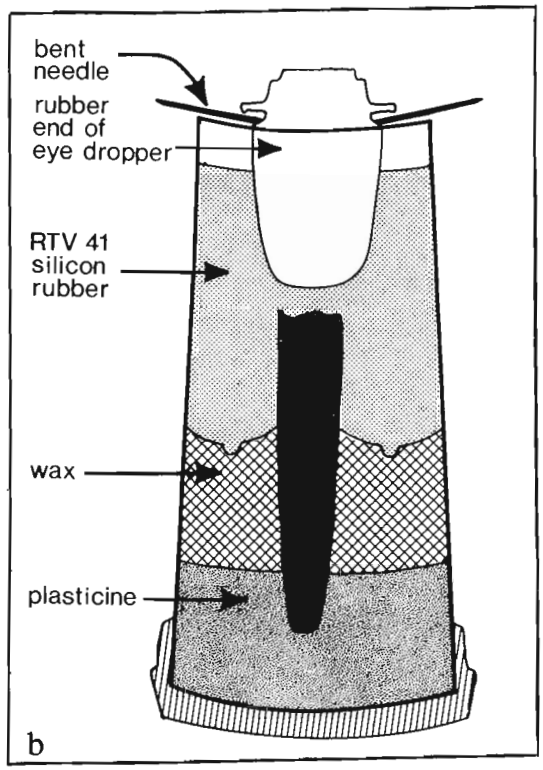

Figure 3. The vial, wax and the belemnite are ready for the pouring of the first half of the silicon rubber mould. But before pouring the rubber, an eyedropper or equivalent is positioned, 3 mm above the belemnite and a needle is pushed through it so as to guarantee its position above the belemnite. The eyedropper is removed during the pouring of the silicon rubber but it can easily be replaced after (Fig. 3b). The cavity created by the eyedropper will hold the reserve epoxy during centrifugation.

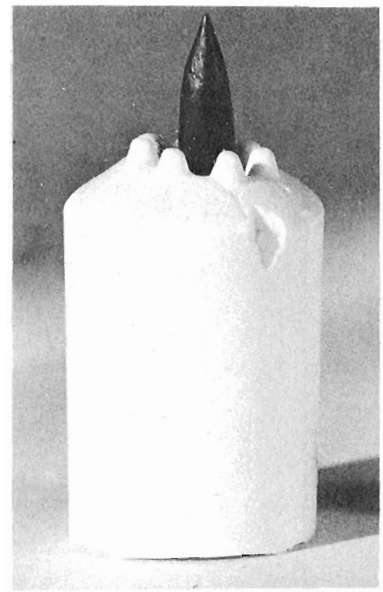

Figure 4.

The first half of the silicon rubber mould is complete. A notch is cut on the outer circumference of the interface. When the two halves of the mould are complete and filled with liquid epoxy, the notch is necessary to obtain a quick merge of the two halves.

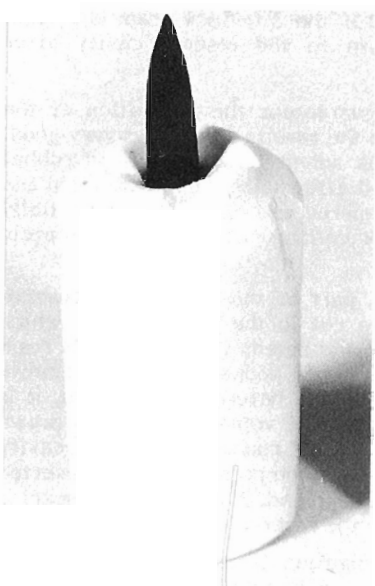

a

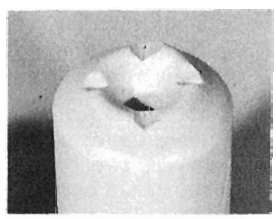

b

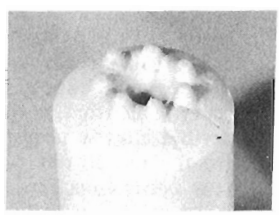

c

Figure 5. In Figure 5a the interface notches are carved with a razor-sharp knife after the silicon rubber and belemnite are removed from the plastic vial. Figures 5b and 5c show the two interface options discussed in the text.

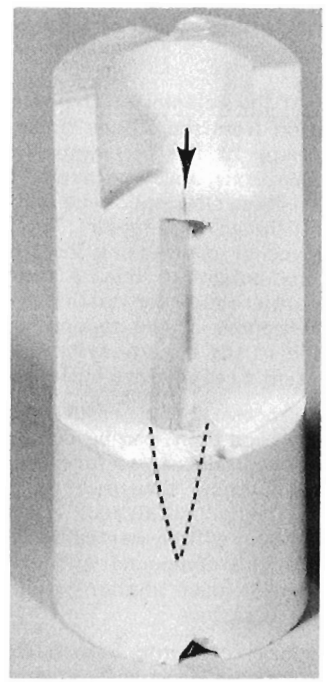

Figure 6. One half of the rubber mould is sectioned and placed over the other half to illustrate clearly how well the silicon rubber will copy all the features set up for it (Fig. 3). In this case a cylindrical flat-bottomed object was used to make the reserve cavity instead of the eyedropper. Notice the slit-cut between the reserve and belemnite cavities.

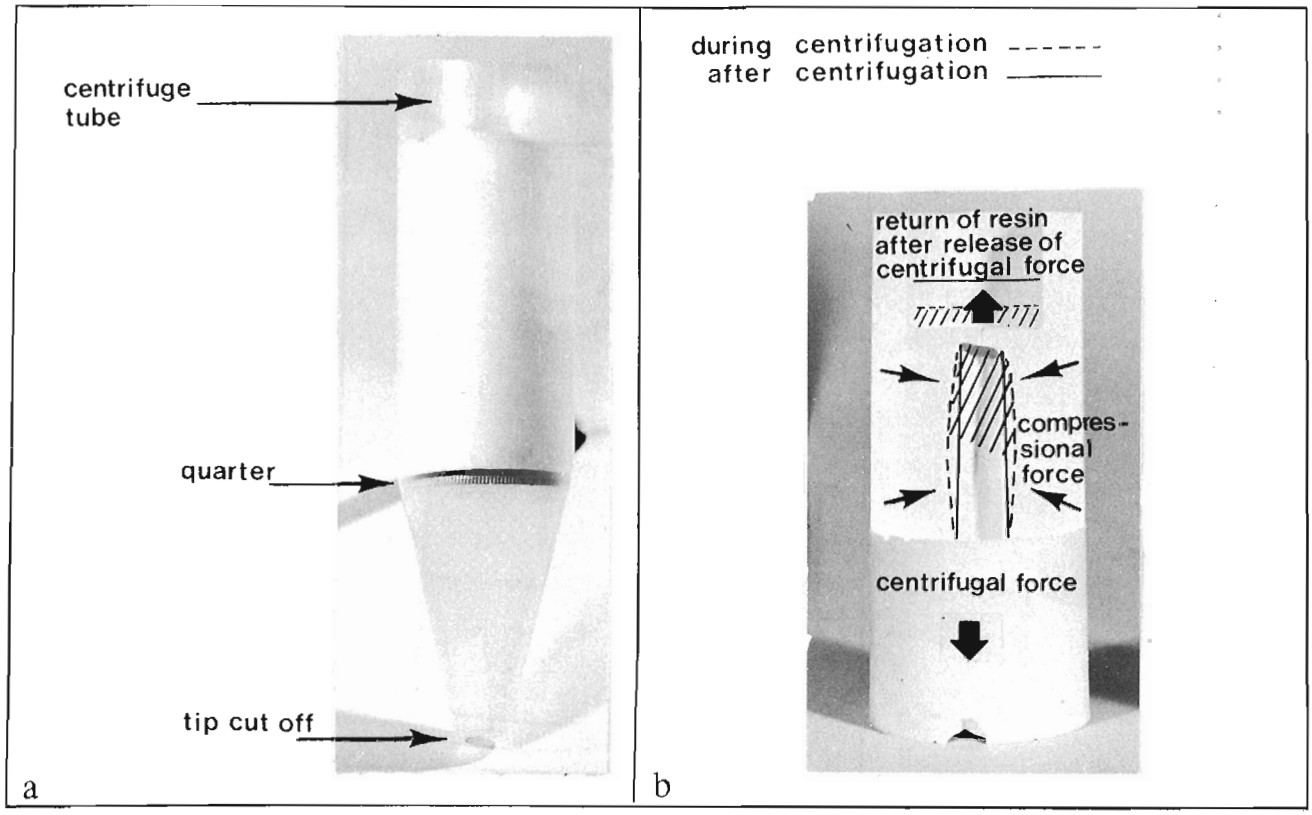

Figure 7. Once the belemnite cavity is filled with epoxy resin, the two halves of the mould are taped together and some epoxy resin is placed in the reserve cavity. A 25 cent piece and the mould are then dropped into a centrifuge tube. The coin which is up against the conical end of the tube gives the mould a solid backing during centrifugation (a) when some of the resin from the reserve cavity is forced into the belemnite cavity. The excess resin is expelled to the reserve cavity after centrifugation. The forces controlling the displacement of resin are centrifugal and compressional (Fig. 7b).

How to extract the belemnite: The belemnite should be removed with caution from the silicon rubber mould. Due to the long slender shape of the belemnite, a force directed across its longitudinal axis, must be avoided. A longitudinal pulling force may cause the specimen to break if it has suffered previous damage and repair. The most successful extraction is achieved by contracting the flexible rubber and literally pushing the belemnite out. After removal of the belemnite, the mould is ready for casting. Finally the cavity created by the eyedropper at the tapered end of the mould should be connected to the mould cavity by means of a slit-cut in the rubber using a razor-sharp knife (Fig. 6).

The casting process: Epoxy resin is the ideal casting compound; it is tough and light, can be coloured, has virtually no shrinkage and reproduces surface detail with great fidelity. A word of warning though; if a large quantity of epoxy (> 35 cc) is being catalyzed, the catalysis will accelerate and the batch will be wasted before it can be used. The technician using this compound will learn with time how to reduce his catalyst or make smaller batches so as to induce milder catalysis of the resin.

Insert the epoxy resin into both halves of the silicon rubber mould; this can be done with a needle drop by drop. Fill each half to the top but it is important not to overfill since this would cause the excess to lodge in the interface when the two rubber mould halves are put together. As a measure of prevention, drainage pits may be carved into the interface to accommodate any overflow of resin. After putting the moulds together, wrap a length of plastic or electrical rubber tape around the interface seam. This is a simple way to hold the mould closed during and after centrifugation since excess resin, if given the chance, will ooze out through the seam. If the interface seam is sealed, the excess resin will return to the reserve cavity after centrifugation (see Fig. 6).

Centrifugation: This guarantees the separation of the air from the epoxy resin and the results are always very good. However, two rules must be adhered to; the silicon rubber mould should be taped closed after being filled with resin and the reserve cavity at the tapered end of the mould partially filled. The time required for centrifugation is approximately 5 minutes.

During centrifugation, part of the resin in the reserve cavity is drawn through the cut in the rubber mould which connects the reserve cavity and belemnite cavity. This resin replaces and expels unwanted air pockets in the belemnite cavity. Due to the highly flexible nature of the mould, it is possible that a larger than normal volume of resin is drawn into the mould cavity. This excess must exit from the cavity after centrifugation, due to the compressional force exerted by the silicon rubber on the resin and, if the interface seam is well sealed, it will return to the reserve cavity (see Fig. 7).

The setup for centrifugation is as follows: place the mould, tapered end up, in a polypropylene centrifuge tube with a conical bottom (O.D. 28.7 mm, length 134 mm). A twenty-five cent coin is placed under the mould as a support for the rubber and to provide a solid backing during centrifugation. Cut off the bottom of the centrifuge tube so that after centrifugation a glass rod or the equivalent may be inserted to remove the mould (see Fig. 7a).

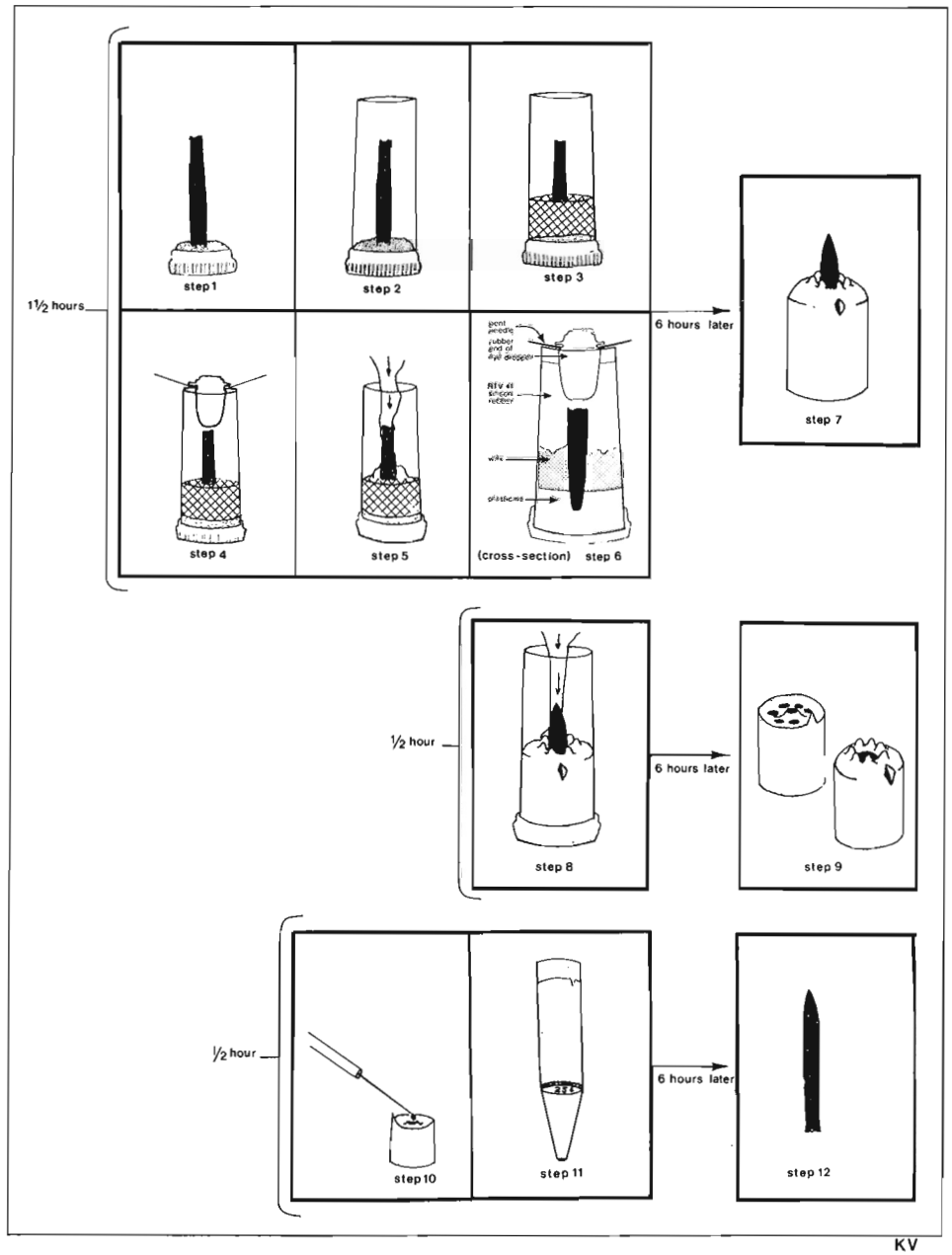

Figure 8. Pictorial guide showing complete casting technique, and time requirements to produce a cast of a belemnite.

The epoxy cast is ready to be removed from the rubber mould when the resin in the reserve cavity has solidified and is brittle. If the epoxy is not brittle, the cast will deform when removed.

Time and Basic Considerations

This technique can be used on as many as fifteen belemnites at one time. In fact, group castings take approximately the same overall time required to make a single cast but they require planning and co-ordination of work routines. Figure 8 is a pictorial guide to the different steps and their time requirements, although the important clues to the successful use of this technique are in the main text.

Many variations may be contemplated but, while these new ideas are being devised and implemented, four basic parameters must be taken into consideration: first, the size and shape of the specimen to be cast; second, adherence to catalyst proportions, curing time, and the proper use of release agents; third, the nature of the rubber mould interface; and fourth, the quality of the cast product.

THE SPACE GROUP OF STRONTIODRESSERITE

A.C. Roberts
Central Laboratories and Administrative Services Division

Introduction

Strontiodresserite is a rare strontium, aluminum carbonate hydrate, $SrAl_2(CO_3)_2(OH)_4 \cdot H_2O$, which occurs in a silicocarbonatite sill exposed at the Francon Quarry, St-Michel, Montreal Island, Québec. It was listed by Sabina (1976) as Francon unknown No. 6 and later characterized by Jambor et al. (1977). The physical characteristics of the strontiodresserite specimens precluded any single crystal study and consequently the powder diffraction pattern was partially indexed on the basis of its similarity to dundasite, $PbAl_2(CO_3)_2(OH)_4 \cdot H_2O$.

Recently, smooth white spheres of strontiodresserite, averaging 0.5 mm in diameter, were identified by powder X-ray diffraction from a specimen (APS 495) collected by A.P. Sabina. These spheres, found on a grouping of weloganite and quartz crystals, are composed of radiating fibers which physically resemble dresserite (Jambor et al., 1969) and were of sufficient size to warrant single crystal examination.

X-ray Crystallography

Two fibers of strontiodresserite, approximately 0.2 mm in length, were isolated from one of the spheres and oriented by precession single crystal photography. The orientation films were virtually free of satellite reflections and displayed minimal spot distortion. Long exposure $h0\ell \rightarrow h3\ell$, $0k\ell \rightarrow 2k\ell$, $hk0$, $hk1$ precession photographs, employing nickel-filtered copper radiation, were then collected parallel and normal to the axis of elongation (c-axis).

Strontiodresserite displays orthorhombic symmetry with measured cell parameters a = 9.176 Å*, b = 16.010 Å and c = 5.602 Å. The space group conditions: (1) $hk\ell$ all orders, (2) $0k\ell$ with k = 2n, (3) $h0\ell$ with $h + \ell = 2n$, and (4) $hk0$ all orders, are consistent with either Pbnm or $Pbn2_1$. These criteria are identical to those obtained by Cocco et al. (1972) for dundasite. They reported, based on a crystal structure analysis, that the true space group was Pbnm. Hence, strontiodresserite and dundasite are isostructural and a complete Sr-Pb solid solution series could theoretically exist between them.

* $1 Å = 10^{-10} m$

X-ray Powder Diffraction

The powder data reported by Jambor et al. (1977) are partially in error because of contamination by a gibbsite-like phase (unknown No. 3 of Sabina (1976)). The line at 4.80 Å should be omitted from their pattern as it is the most intense line of the unnamed mineral. An indexed powder pattern consistent with the single crystal results of this study is presented in Table 1. Calculated spacings derived from least squares refinement of 16 unambiguously indexed lines between 4.41 Å and 1.833 Å yielded the following unit cell dimensions:

a = 9.168 (4) Å
b = 16.037 (6) Å
c = 5.598 (3) Å
V = 823.06 Å^3

The calculated density, assuming a stoichiometric formula with Sr:Ca = 4:1 and Z = 4, is 2.73 g/cm^3; very close to the measured density of 2.71 g/cm^3 reported by Jambor et al. (1977).

Table 1

X-ray powder data for strontiodresserite**

	I_{est}	$d Å_{meas}$	$dÅ_{calc}$	hkl		I_{est}	$dÅ_{meas}$	$dÅ_{calc}$	hkl
	10	7.97	7.96	110	*	2	2.004	2.005	080
	7	6.04	6.04	120	*	1	1.958	1.958	180
	3	4.59	4.59	021		1	1.926	1.926	332
*	5	4.41	4.41	210		1/2	1.888	1.887	081
	1/4	4.08	4.10	121		1/4	1.871	(1.875	441
*	1	3.99	3.98	220				(1.865	450
	1/4	3.67	3.67	140	*	1	1.833	1.833	370
*	5	3.563	3.562	131		1	1.817	1.817	023
*	1	3.482	3.480	230		1B	1.773	1.773	402
*	3	3.245	3.244	221		6	1.738	1.740	460
	8	3.021	(3.027	150		1/4	1.709		
			(3.018	240		1/2	1.684		
*	1/2	2.953	2.955	231		1	1.665		
*	1/2	2.856	2.856	320		1/4	1.649		
*	2	2.799	2.799	002		1B	1.592		
*	5	2.682	2.682	301		1/4	1.560		
	6	2.648	(2.656	241		1/4	1.533		
			(2.643	022		1/2	1.526		
	<1/4	2.568	2.566	160		1/4	1.507		
*	2	2.546	2.544	321		1/4	1.486		
*	3	2.390	2.389	202		<1/4	1.470		
*	2	2.361	2.363	212		1/4	1.461		
*	1	2.289	2.292	400		1/4	1.424		
	2B	2.213	2.213	350		1	1.401		
	<1/4	2.184	2.181	232		1/4	1.383		
	1/2	2.136	2.135	261		1/2	1.364		
	1	2.102	(2.107	430		1/2B	1.333		
			(2.103	411		2	1.272		
	6	2.052	(2.055	152		1/2B	1.241		
			(2.052	242					

** 114.6 mm Debye-Scherrer camera; Cu/Ni radiation. Film no. 57610-2. Intensities estimated visually.
B = broad line
* = lines used in least squares refinement
Indexed with a = 9.168 Å, b = 16.037 Å, c = 5.598 Å

References

Cocco, G., Fanfani, L., and Nanzi, P.F.
1972: The crystal structure of dundasite; Mineral Mag., v. 38, p. 564-569.

Jambor, J.L., Fong, D.G., and Sabina, A.P.
1969: Dresserite, the new barium analogue of dundasite; Can. Mineral., v. 10, p. 84-89.

Jambor, J.L., Sabina, A.P., Roberts, A.C., and Sturman, B.D.
1977: Strontiodresserite, a new Sr-Al carbonate from Montreal Island, Quebec; Can. Mineral., v. 15, p. 405-407.

Sabina, A.P.
1976: The Francon quarry: a mineral locality; in Report of Activities, Part B, Geol. Surv. Can., Paper 76-1B, p. 15-19.

From: Scientific and Technical Notes in Current Research, Part B; Geol. Surv. Can., Paper 78-1B .

APPLICATIONS OF SIDE-SCAN SONAR TO GEOENVIRONMENTAL RESEARCH IN THE COASTAL WATERS OF BRITISH COLUMBIA

J.L. Luternauer, R.H. Linden and R.E. Thomson[1]
Regional and Economic Geology Division, Vancouver

Side-scan sonar has been used in the coastal waters of British Columbia primarily in searches for downed aircraft, cargo lost off barges, navigational hazards and suitable routes for laying of submarine pipelines. The device has only recently been locally applied to marine geologic research and mapping. As reported earlier (Luternauer and Swan, 1978 and Luternauer et al., 1978), the Geological Survey has employed the technique to delineate the extent and surface character of a submarine slump deposit near Kitimat (D. Swan is now preparing a Bachelor's thesis on the subject at the University of British Columbia) and of a field of sand waves on the Fraser Delta slope. A. Hay, a graduate student at the University of British Columbia, is carrying out studies with the side-scan sonar of the geomorphology of a submarine valley which has developed in the course of tailings dumping in Rupert Inlet, northern Vancouver Island.

During January and early February 1978 we have further applied the side-scan sonar (a) to discriminate the major sediment zones on a open continental shelf bank where Environment Canada is investigating groundfish – substrate affinities ("Amphitrite Bank", Fig. 1), (b) to identify sedimentary environments and produce geological evidence supporting the presence of anomalous oceanographic processes in a long, narrow strait (Johnstone Strait, Fig. 1), and (c) to set the stage for a program to monitor the sedimentary responses to tidal currents on a part of a delta slope which may be eroding (Fraser Delta, Fig. 1).

"Amphitrite Bank"

A 160 km^2 bank off Barkley Sound which is considered to be a major cod fish spawning area was surveyed by side-scan sonar and echosounder. A reconnaissance survey was performed along approximately east-west and north-south tracklines (corresponding to Loran C lines) approximately 3 km apart and a detailed survey (of parts of the bank where major schools of fish have been identified) along north-south tracklines approximately 300 m apart. An earlier study established that the bank is blanketed with gravels (Luternauer, 1976). A preliminary compilation of data derived from the side-scan sonar records (Fig. 2) indicates that the sediments on the central part of the bank (bounded on the east by a long, low ridge) generally are coarser and more poorly sorted than those at the periphery. Furthermore, sediment "banding" probably arising from the oscillatory motion of bottom waters induced by southwesterly swells, is generally more prevalent and better developed at the margins of the bank. The side-scan sonar survey suggests that sediments at the centre of the bank are essentially lag deposits from which finer materials at the margins of the bank are or have been washed.

Submarine photographs (obtained on March 24 and 25, 1977; Fig. 3) similarly suggest that the bank is mantled with patches of mobile and static sediments. Sediments, which are probably transported and sorted by waves and currents, are shown in Figure 3.14, 3.16 and 3.17. In the first two photographs there is a suggestion that the gravels have been segregated into bands which could give rise to the features observed principally on the side-scan records obtained over the bank margins (Fig. 2). The heavy encrustation on the sediments pictured in Figure 3.11a, 3.11b and 3.12 suggest these materials are only infrequently moved.

[1] Institute of Ocean Sciences, Patricia Bay, B.C.

From: Scientific and Technical Notes in Current Research, Part B; Geol. Surv. Can., Paper 78-1B .

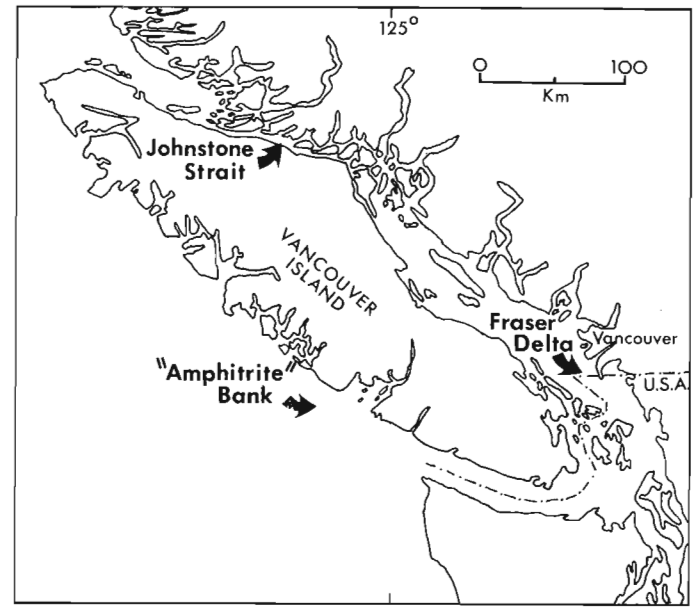

Figure 1. Index map identifying locations of study areas.

Figure 3-11a, 11b represent parts of the seabed which side-scan sonar records indicate have a relatively dense cover of boulders. Sediments in Figure 3.12 lie near the edge of the central blanket of boulders. Sediments in Figure 3.14 lie within the peripheral strip of finer "banded" gravels. Sediments illustrated in Figure 3.16 and 3.17 lie within the central, coarser sediment patch, but where large boulders are not as prevalent. Other photographs (not included) similarly indicate that within the peripheral zone of generally more mobile sediments, patches of what appear to be static sediments also are evident.

The present study would suggest that the sedimentary mosaic on the local shelf can be most effectively mapped by, first, using the side-scan sonar to delineate regional patterns and characteristics of deposits, secondly, obtaining near-bottom photographs of the major sediment types identified and determining general size, sorting and packing characteristics and, thirdly, selecting on the basis of this information the most appropriate sampling device and sampling pattern.

Johnstone Strait

In an earlier report (Thomson and Luternauer, 1978) we described, in a general fashion, the sediment distribution on the floor of Johnstone Strait. In the section of the strait represented in Figure 4 bottom materials include sandy gravels, sands and muddy sandy gravels.

Anomalously fast near-bottom tidal currents and well defined residual (time averaged) eastwardly flows have been observed 3 km to the west of Neville Point (Thomson, 1976, 1977; also Fig. 4). Maximum velocities at depth reach 100 cm/s on the flood and 40 cm/s on the ebb. It is thought that the strong currents in this region are in part due to internal tides, i.e., long internal gravity waves of tidal frequency generated in this case by water ebbing and flooding over the ridge. Internal tidal energy emanating from the area of the ridge would be confined to a "beam" that is bent downward because of the vertical water density structure and the effect of the mean flow. Maximum bottom currents occur where the internal tides would be expected to first impinge on the bottom over an along-channel swath of the order of 1 km.

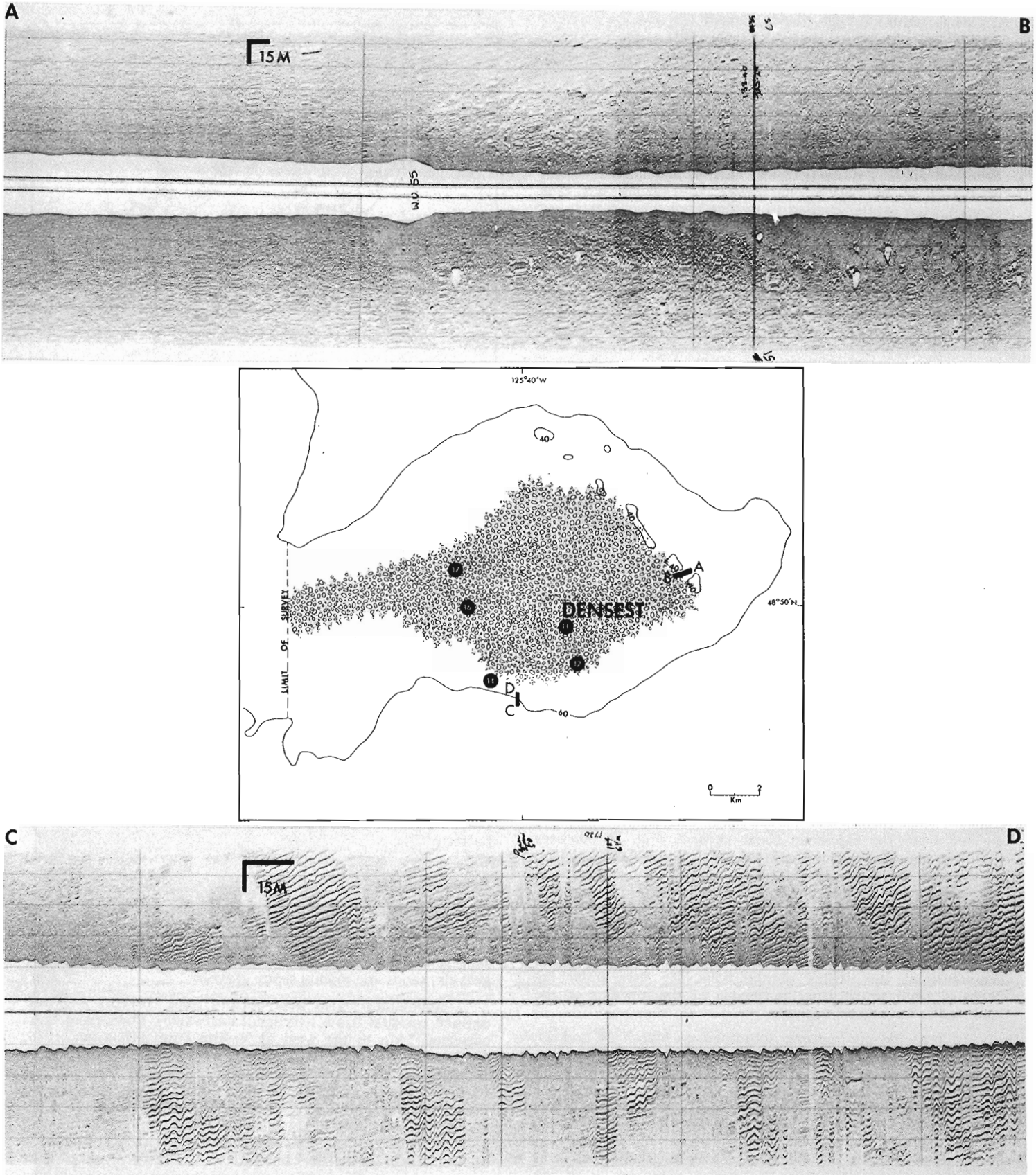

Figure 2. Preliminary compilation of side-scan sonar data obtained Jan. 25-29, 1978 for portion of "Amphitrite Bank" within 60 m contour. Patterned zone represents area within which boulders are prevalent (right half of record A-B). They are most numerous within area marked "densest". In unpatterned peripheral zone sediments are markedly finer and better sorted (left half of record A-B) and commonly exhibit well developed sediment banding (record C-D). It is important to note that the banding is only readily apparent on the north-south oriented tracklines. Thus, any surveys in which the side-scan sonar is employed to define sediment distributions should include tracklines with diverse orientations. Numbers within black dots represent station numbers of photographs in Figure 3.

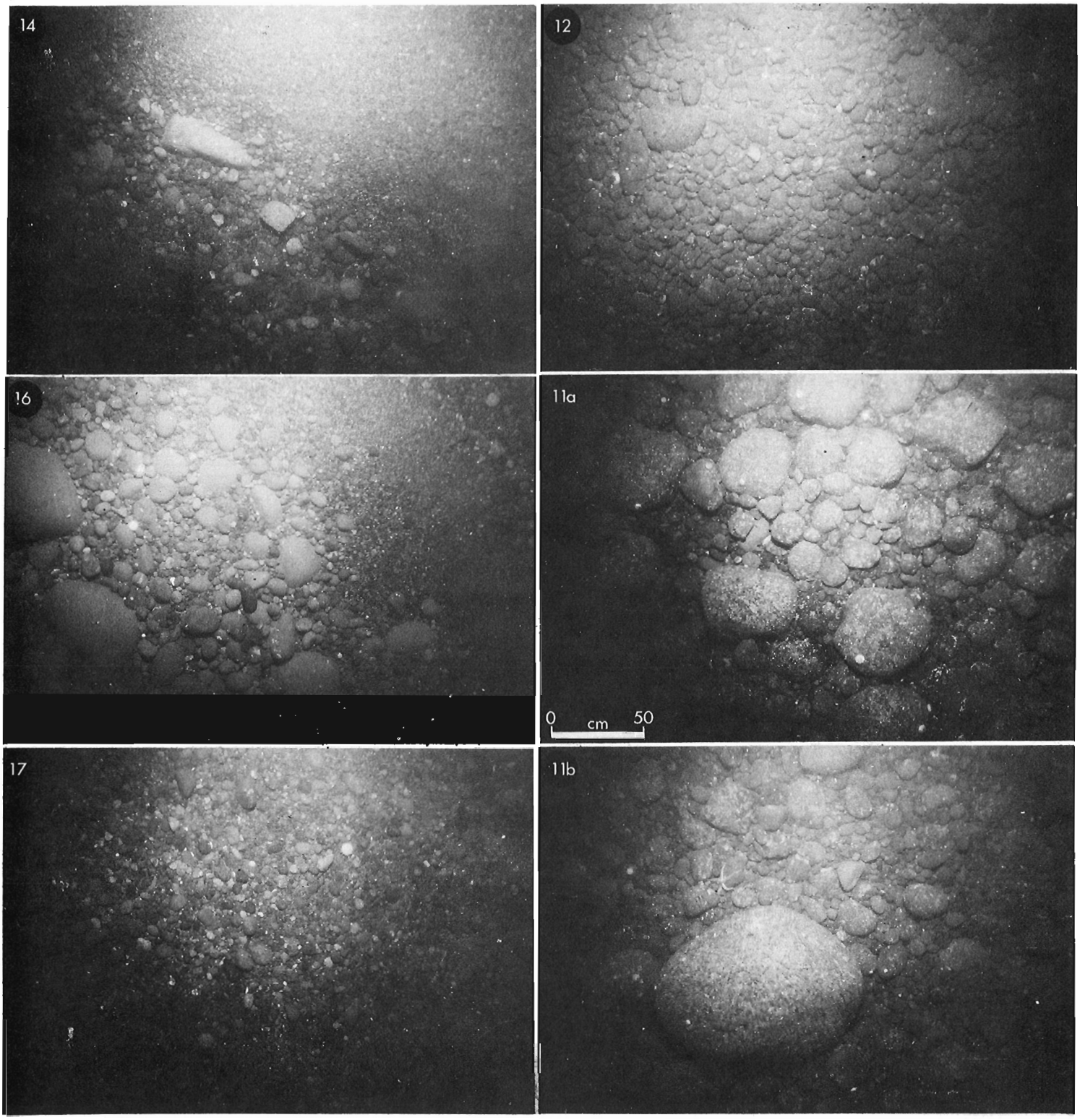

Figure 3. Examples of the sediment character displayed in bottom photographs obtained on March 24, 25 1977 on "Amphitrite Bank". Number on photos represent station numbers whose locations are indicated on Figure 2.

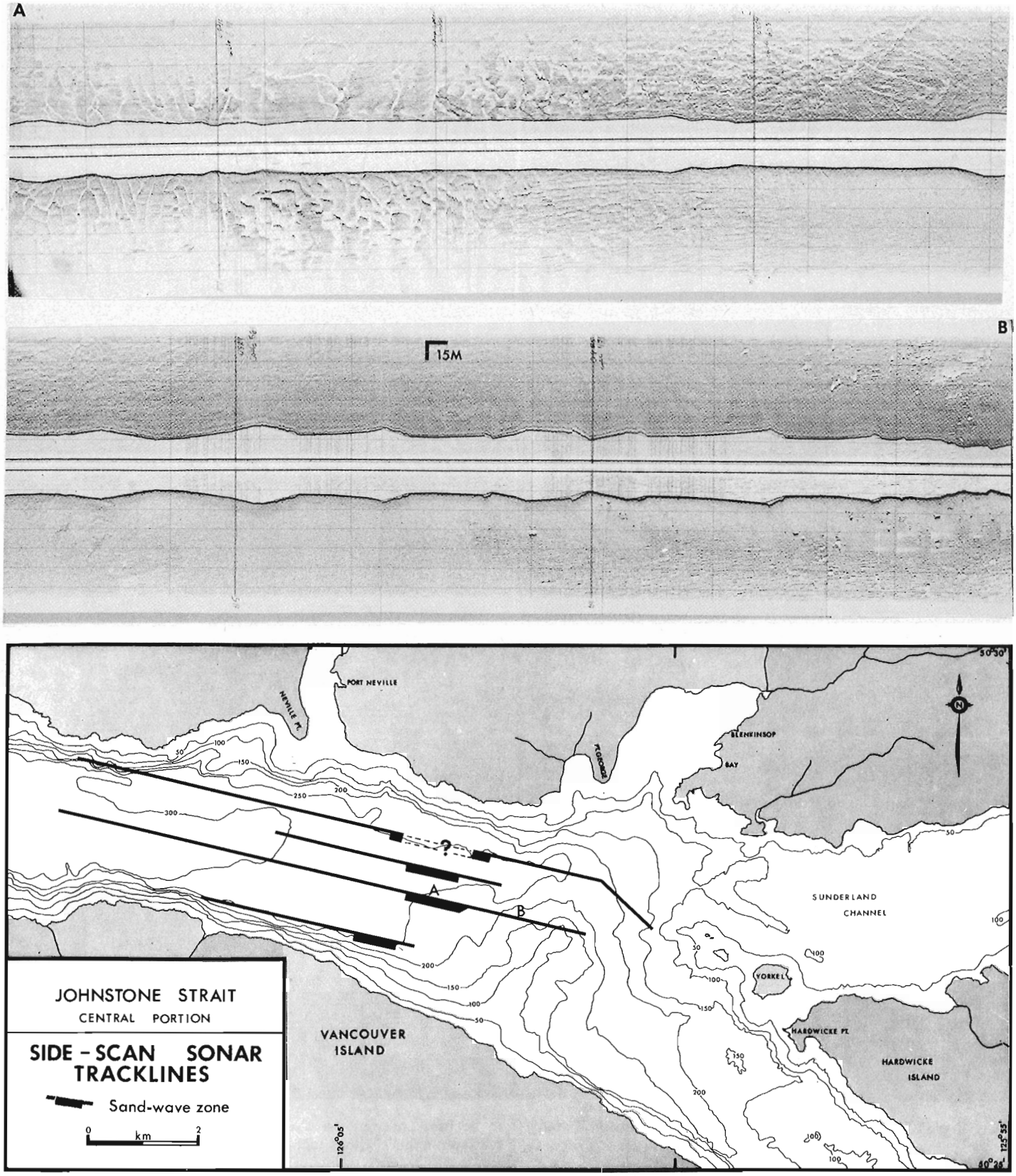

Figure 4. Side-scan sonar tracklines, sand wave zones and bottom morphology central portion Johnstone Strait. The side-scan record A-B was obtained along axial trackline. Bathymetric contours in metres.

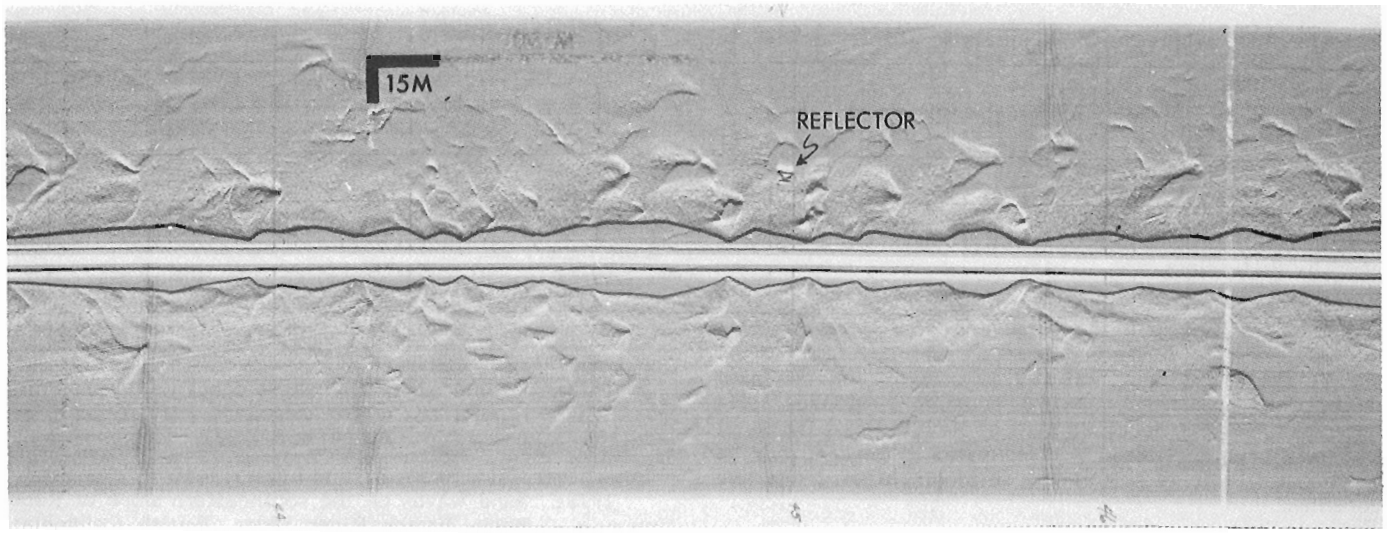

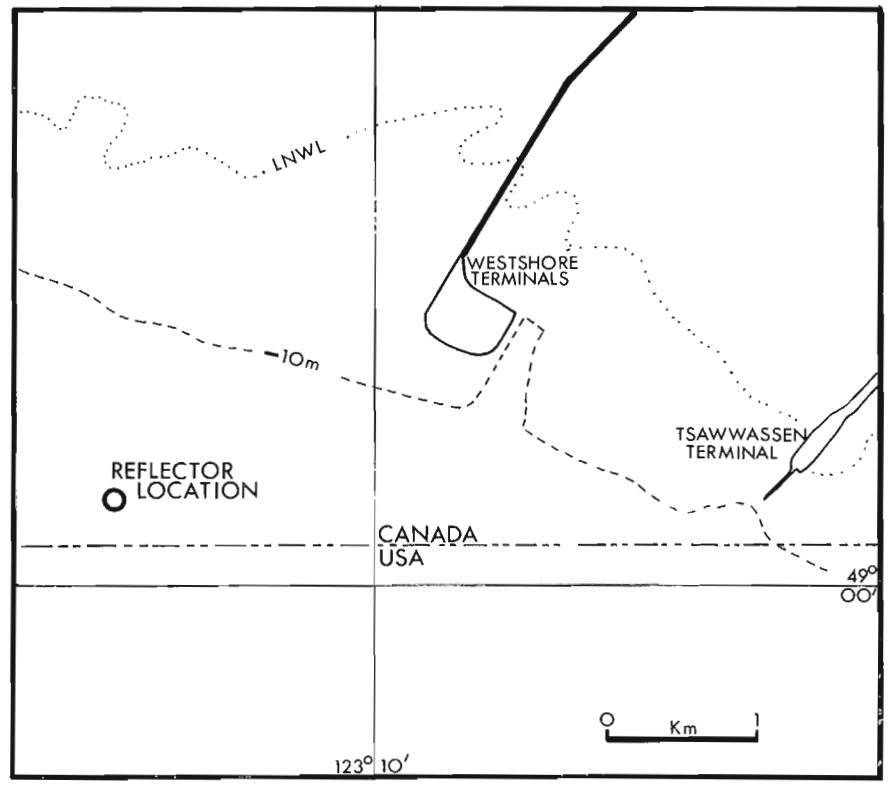

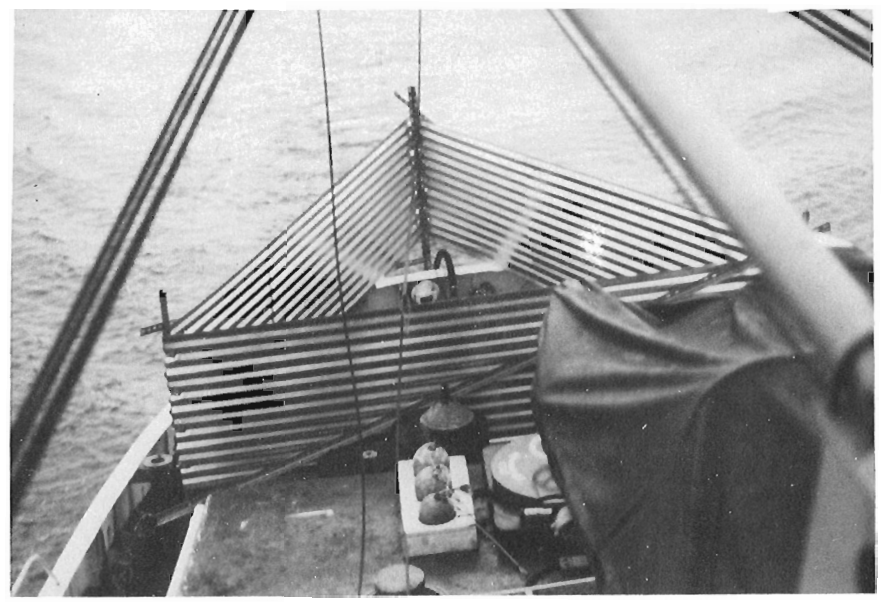

Figure 5.

Location map indicating resting place of acoustic reflector pictured in photograph. The reflector serves as a precise reference target for monitoring morphologic variations of bed forms on Fraser Delta slope (refer to side-scan record). The reflector was assembled from 3 x 10 ft (1x3 m) corrugated aluminum sheeting mounted on an angle iron frame. LNWL = Lowest normal water level.

The floor of the strait was scanned along four lines in November 1977 and February 1978 (Fig. 4). A representative record obtained along the axis of the strait indicates that (a) the flank of the ridge is mantled with coarse, bouldery sediments, (b) for a short distance beyond the base of the ridge sediments become finer and the seafloor lacks distinctive relief, and (c) at approximately 225 m depth along the trackline the seafloor very abruptly becomes rippled with sand waves. Beyond the sand wave zone the bottom is generally featureless.

It is likely that bottom currents along most of the area represented in Figure 4 are capable of transporting clean, well sorted sands. Where bedforms are well developed at the base of the ridge such material is present and sediment transport is occurring. Where anomalous oceanographic processes have been recorded west of Neville Point traces of sand have been recovered but sediments in general may be too coarse or fine to permit the development of distinctive bedforms.

Fraser Delta

During the first two weeks of January 1978 a series of side-scan surveys were performed over the sand wave patch on the Fraser Delta slope identified earlier (Luternauer et al., 1978). Our objective was to define in detail the character of the waves on that part of the field between 80-90 m where they are best developed and where the most severe erosion would be expected to occur. In order to monitor the character of the seabed under varying oceanographic conditions an acoustic reflector was placed within this area (Fig. 5). Several passes were completed over the site with the side-scan sonar. We now have a detailed record of the character of the bedforms on this part of the slope. Subsequent surveys in April and July 1978 should allow us to define morphologic responses to the local hydraulic regime.

Acknowledgments

We thank the Canadian Hydrographic Services for kindly allowing us the use of a Klein Assoc. Inc. side-scan sonar to perform the above studies. R. Currie helped us design the acoustic reflector.

References

Luternauer, J.L.
1976: Geofisheries research off the west coast of Canada; in Report of Activities, Part C, Geol. Surv. Can., Paper 76-1C, p. 157-159.

Luternauer, J.L. and Swan, D.
1978: Kitimat submarine slump deposit(s): A preliminary report; in Current Research, Part A, Geol. Surv. Can., Paper 78-1A, p. 327-332.

Luternauer, J.L., Swan, D., and Linden, R.H.
1978: Sand waves on the southeastern slope of Roberts Bank, Fraser River Delta, British Columbia; in Current Research, Part A, Geol. Surv. Can., Paper 78-1A, p. 351-356.

Thomson, R.E.
1976: Tidal currents and estuarine type circulation in Johnstone Strait, B.C.; J. Fish. Res. Bd. Can., v. 33, n. 10, p. 2242-2264.

1977: Currents in Johnstone Strait, B.C. – supplemental data on the Vancouver Island side; J. Fish. Res. Bd. Can., v. 34, n. 5, p. 697-703.

Thomson, R.E. and Luternauer, J.L.
1978: Tidal regime and sedimentation patterns Johnstone Strait, British Columbia – A preliminary report; Scientific and Technical notes in Current Research, Part A, Geol. Surv. Can., Paper 78-1A, p. 327-332.

THE VOLCANIC-TECTONIC SETTING OF GOLD-QUARTZ VEIN SYSTEMS IN THE TIMMINS DISTRICT, ONTARIO

R.G. Roberts[1], J. Carnevali[1], and J.D. Harris[1]
Regional and Economic Geology Division

Introduction

This note summarizes the principal results of a study of the volcanic and tectonic setting of gold-quartz veins in the Timmins district, Ontario. The study involved surface mapping (Fig. 1) and limited underground mapping at the Dome and Pamour mines.

Periods of Deformation

D_o

The earliest structures are prelithification or slump folds in the bedded, greywacke-argillite turbidites (Fig. 2). Mesoscopic F_o folds occur typically as isolated structures, confined between apparently nonfolded beds. They may be associated with locally brecciated beds, and discontinuities in the bedding that may have the appearance of unconformities, but which are believed to be the result of sliding during the D_o deformation (Fig. 2). The axial surfaces of the folds are oblique to the S_1 foliation of the surrounding rocks.

D_1

The well developed, penetrative, planar and linear fabric of the map area was imprinted on the rocks during this deformation. S_1 is defined by the preferred orientation of chlorite and sericite. It is axial planar to mesoscopic F_1 folds and parallel to the plane of flattening of pillows and variolites. L_1 lineations include the plunge of mesoscopic F_1 fold axes, intersection of S_o (bedding) with S_1, and the elongation of strained pillows and variolites. The attitudes of S_1 and L_1 throughout the map area are shown in Figures 3 and 4.

D_2

The principal mesoscopic structure of this deformation is a crenulation-fracture cleavage, S_1. It strikes north-northeast and dips steeply, predominantly to the northwest. The attitude of S_2 is reasonably constant throughout the map area. Both S_o and S_1 are folded. Mesoscopic F_2 folds include crenulations and open folds with wavelengths of 10 to 15 cm and amplitudes less than 12 cm. Folds are moderately to steeply plunging to the north.

D_3

Fracture-crenulation cleavages with horizontal to gentle dips were developed during this deformation. The S_3 cleavage is axial planar to eastward-trending F_3 folds. The folds, produced by the deformation of S_1 foliation, are open, with axial surfaces 30 to 100 cm apart and amplitudes of less than 30 cm. The structures are best developed in units with a well developed S_1 foliation such as quartz-feldspar porphyry and fine grained tuffs.

D_4

North-northwesterly trending kink planes, and poorly developed fracture cleavage (S_4), parallel to the kink planes, are the youngest mesoscopic fold structures in the area.

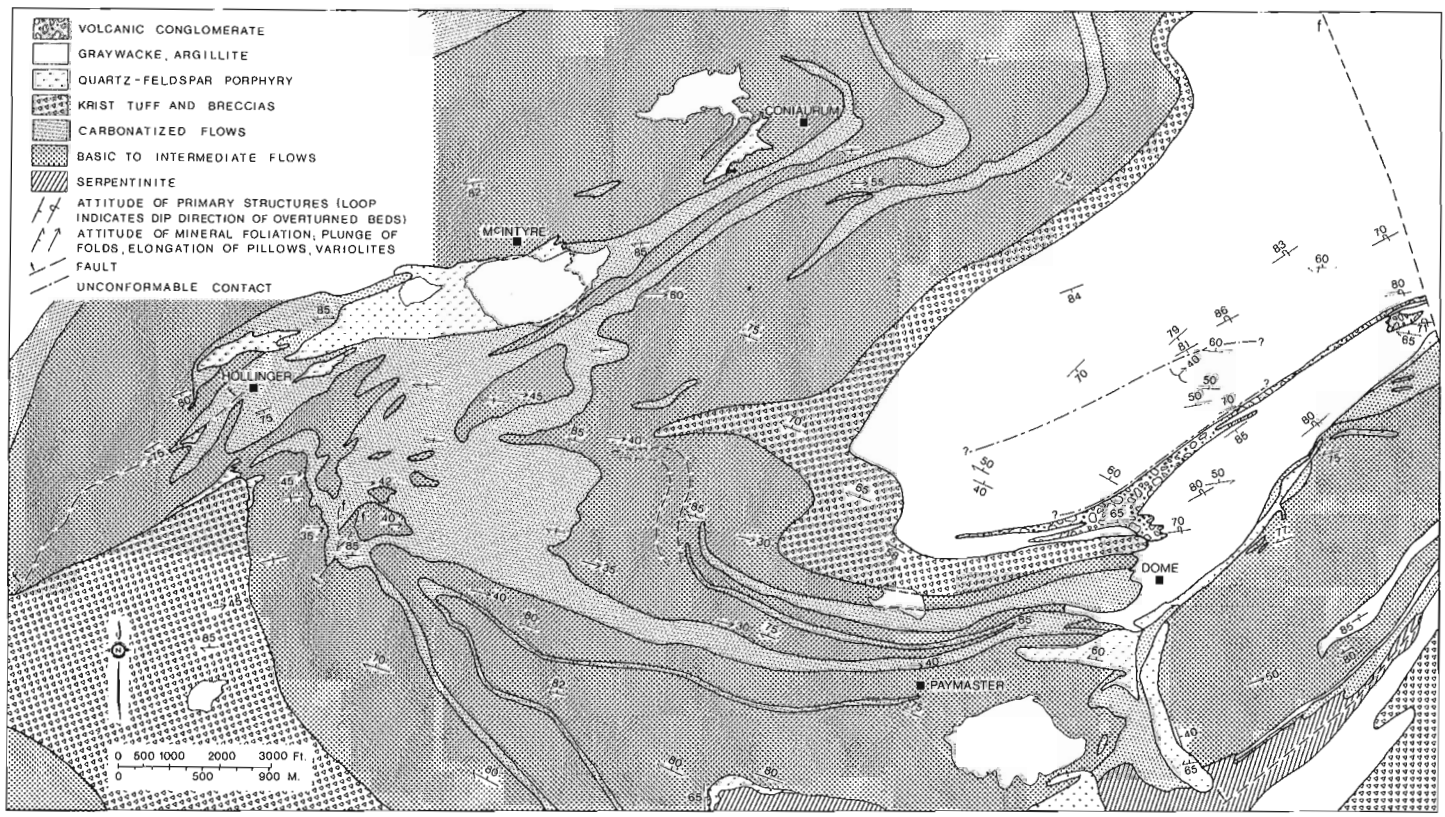

Figure 1. Geological map of the Timmins district.

[1] Department of Earth Sciences, University of Waterloo, Waterloo, Ontario.

From: Scientific and Technical Notes in Current Research, Part B; Geol. Surv. Can., Paper 78-1B .

Timiskaming-Keewatin unconformity

The contact between basic volcanic flows and coarse clastic sediments at the Dome mine has been interpreted in the past as an unconformity and named the Timiskaming-Keewatin unconformity (Ferguson, 1968). An unconformable relationship is also assumed by Pyke (1976) and Davies (1977) in their interpretations of the structural geology of the district. The authors of this note contend that the so-called unconformity is an example of intercalation between essentially contemporaneous flows and sediments at the toe of a volcano.

From southwest to northeast along strike, the rocks at the Dome mine pass from a sequence of basic flows through volcanic conglomerate to greywacke-argillite sediments. Figure 5 illustrates the conformable relationships between basic flows, a unit of laminated tuff, "massive greenstone" (a massive, pyritic greywacke), and volcanic conglomerate in the 1372 stope of the Dome mine. The conglomerate consists of subangular blocks, including blocks of variolitic basalt, up to 0.5 m. All units dip to the north, between 45 and 65 degrees. To the northeast, along strike, there is a transition to argillite-greywacke units. Exposures in the lower levels show that the Krist volcanic unit (a felsic, pyroclastic unit) is overlain and underlain by greywacke-argillite sediments (Ferguson, 1968, Chart D).

The transition to the northeast from volcanic units (flows and felsic pyroclastics) to clastic sedimentary units, through the intercalated sequence, is illustrated in the surface geological map (Fig. 1). This transition plunges to the northeast at 20 to 40 degrees.

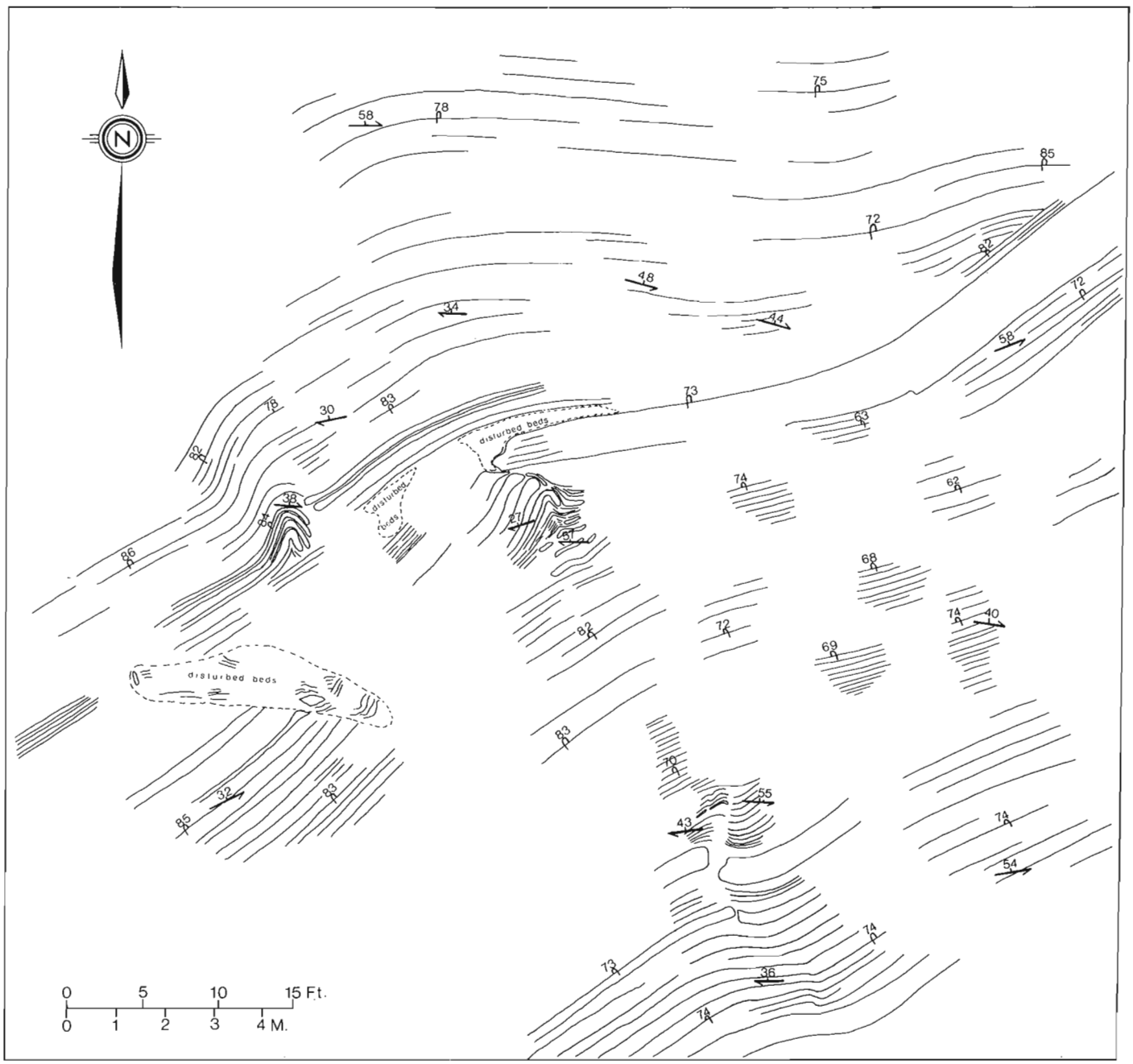

Figure 2. F_0 folds in turbidite, sedimentary rocks 900 m north-northeast of South Porcupine. Attitude of S_1 shown by barbed lines.

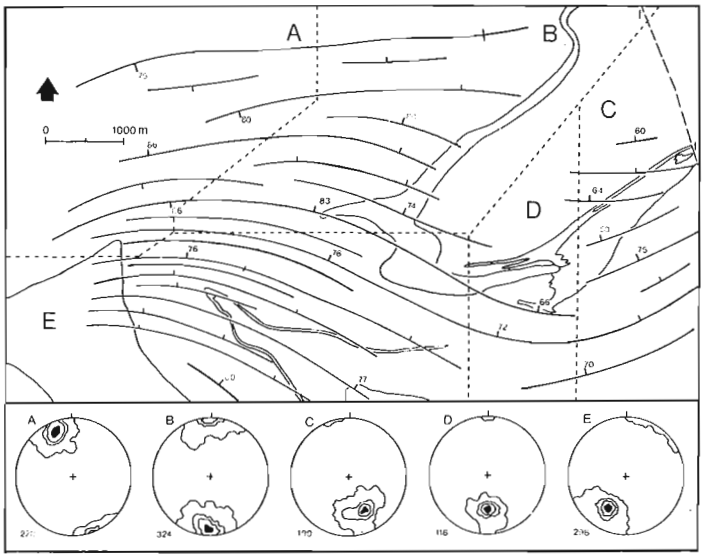

Figure 3. Attitude of the S_1 foliations. Within each domain (A to E) foliation is nearly plane-parallel. Equal area projections of poles to S_1. Contour intervals 1, 11, 21 and 31% per 1% unit area. (After Carnevali, 1976.)

The Porcupine Syncline

From the observations described above, the following may be concluded: (a) The basic flows and the Krist pyroclastic unit are contemporaneous with the sedimentary rocks at the core of the Porcupine syncline, (b) On the north limb of the Porcupine syncline, Krist pyroclastics are overlain by sedimentary rocks (formerly referred to as Keewatin), and on the south limb Krist pyroclastics are interbedded with younger but lithologically similar sedimentary rocks (formerly referred to as Timiskaming).

Clearly, the structure is not a syncline. This conclusion is confirmed when the facing of the rocks is taken into consideration. The sedimentary rocks constitute a turbidite sequence which includes graded beds. The beds are of the order of 20 cm thick and each consists of a lower, graded greywacke overlain by a thin argillite. The evidence from such graded beds is that the sedimentary rocks, with the exception of the block of sediments between the dashed lines in Figure 1, are steeply dipping or overturned, and face south. The units delineated by the dashed lines are bedded greywackes (beds up to 1 m) with tops to the northeast. The attitude of the beds is in marked contrast to the northeast strike and steep dip of underlying and overlying sediments. The block has a limited eastward extent, since on the eastern margin of the map area, sediments across the "Porcupine syncline" are consistently southward facing.

A complete explanation for the structure cannot be given at this time, but the study thus far provides constraints to the interpretation which exclude a simple synclinal structure.

Major Structures

A puzzling aspect of Timmins structural geology has been the fact that although the eastward plunge of the "Porcupine syncline" agrees with the plunge of the mesoscopic structures observed in outcrop, the complementary anticline south of the "Porcupine syncline" closes to the west, thus contradicting the regional eastward plunge. Recently, explanations of this apparent contradiction have been provided by Pyke (1976) and Davies (1977). However, if, as is suggested in this note, the "Porcupine syncline" is not a syncline, the west-closing structure to the south is a southeastwards-plunging syncline. This is strongly supported by the southeast plunge of primary volcanic structures at the Edwards shaft (Ferguson, 1968, Section 10).

The contributions of the various periods of deformation to the structural architecture of the area is still uncertain. The relationship between structures developed during D_0 and the D_1 deformation are presently being studied. The deflection of S_1 throughout the area may be due to rotation about north-northeast folds areas during D_2 (Carnivali, 1976). Deformations D_3 and D_4 had no effect on major structures.

Vein Structures

The gold deposits are associated with carbonatized basic flows (Fig. 1). The carbonatized zones are stratabound, and form mappable units that may be traced from the Schumacher district to the Pamour mine (Karvinen, 1977).

The various types of gold deposits include:

(a) Conformable ankerite "veins" in chemogenic sediments. The form of these "veins" suggests that they are laminated chemogenic sedimentary units (Fig. 5).

(b) Quartz veins, concordant with primary volcanic structures, in carbonatized volcanic rocks, and sedimentary rocks. These veins are characterized by their continuity and persistence along strike, and their thickness which may be greater than 1 m.

(c) Quartz veins discordant to primary volcanic structures; of at least two ages in carbonatized volcanic rocks, and sedimentary rocks. Typically these veins are up to 20 cm thick and persist along strike for less than 10 m (Fig. 5).

On the basis of cross cutting relationships, the discordant veins are younger than the concordant veins. Veins of all groups were emplaced before S_1 was imprinted on the rocks and thus were emplaced before the compressive stage of the D_1 deformation (Fig. 6).

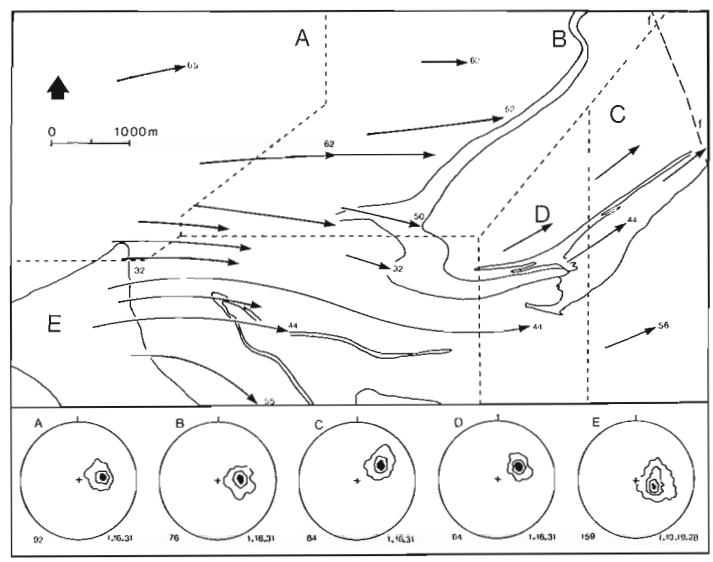

Figure 4. Attitude of the L_1 lineations. Equal area projections of lineations. On each figure, number of data points are shown to the left and contour interval to the right. (After Carnevali, 1976.)

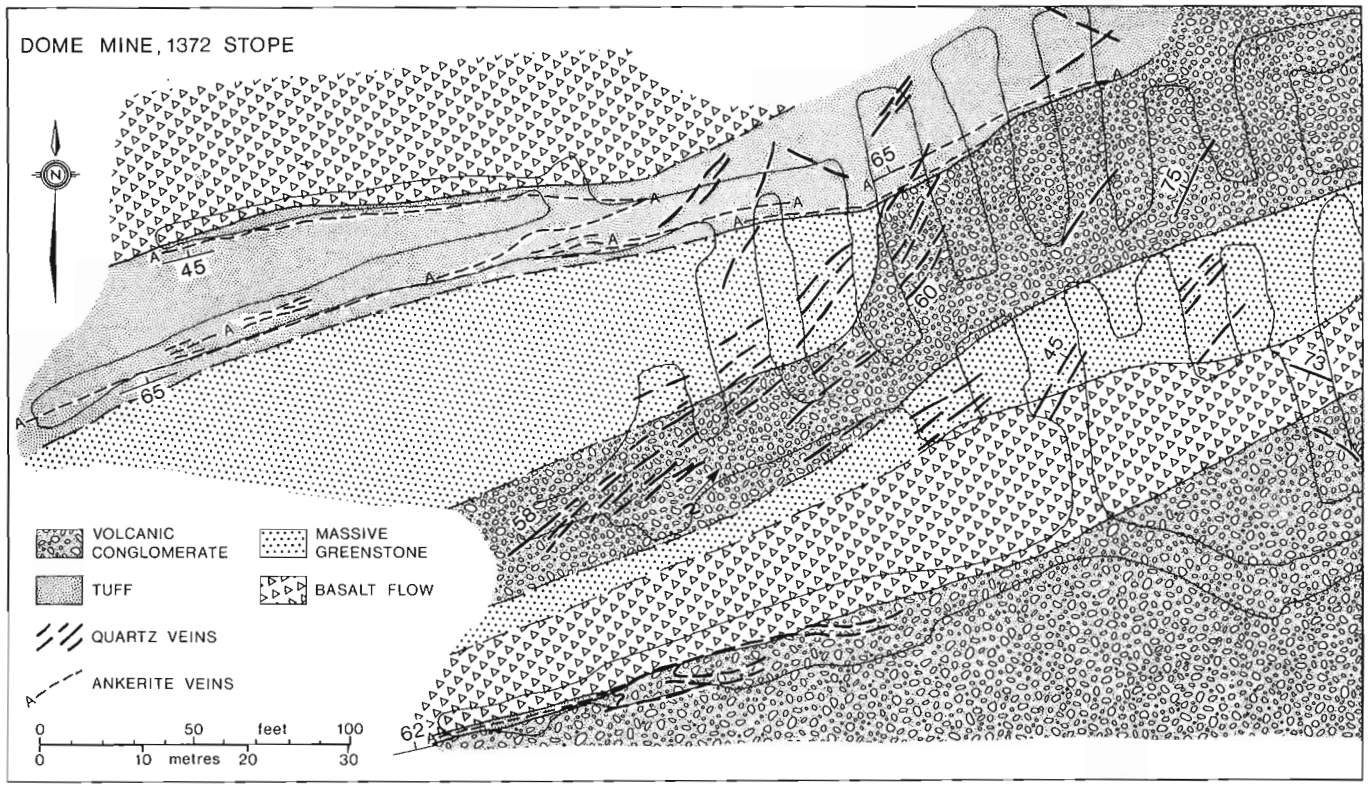

Figure 5. Geological map of part of the 1372 slope, Dome mine.

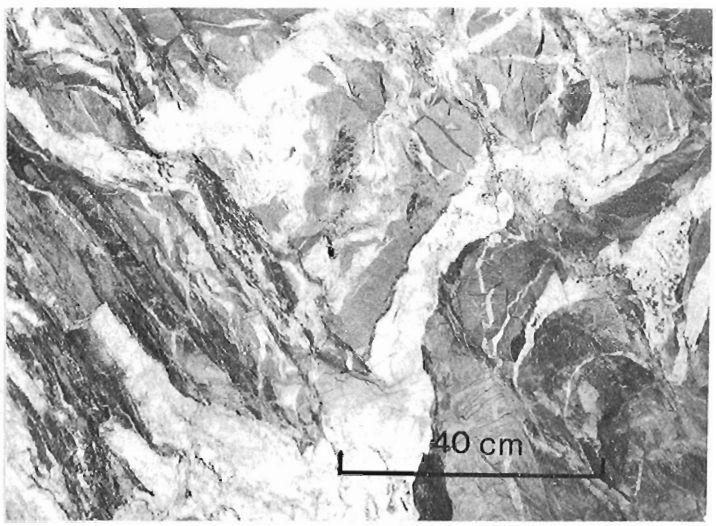

Figure 6. F_1 folds in discordant quartz veins in greywacke, Pamour mine. 1400 level.

Acknowledgments

The authors gratefully acknowledge the kind hospitality and the assistance of mine geologists in the area: Dean Rogers and Dave Bell at the Dome mine, and John Parens at the Pamour mine.

References

Carnevali, J.
1976: Structural analysis of the Timmins-South Porcupine area, Ontario; unpubl. M.Sc. thesis, Univ. Waterloo, 192 p.

Davies, J.F.
1977: Structural interpretation of the Timmins mining area Ontario; Can. J. Earth Sci., v. 14, p. 1046-1053.

Ferguson, S.A.
1968: Geology and ore deposits of Tisdale Township; Ont. Dep. Mines, Geol. Rep. 58, 177 p.

Karvinen, W.O.
1977: Distribution of carbonate-rich rocks, porphyries and gold deposits, Timmins area, Ontario; Geol. Assoc. Can., Ann. Mtg., p. 28 (abstr.).

Pyke, D.R.
1976: On the relationship between gold mineralization and ultramafic volcanic rocks in the Timmins area, northeastern Ontario; Can. Inst. Min. Met. Bull., v. 69, no. 773, p. 79-87.

AN APPROACH TO THE RECORDING, POSITIONING AND MANIPULATION OF COASTAL AND MARINE DATA

Patrick McLaren and Jean-Marie Sempels
Terrain Sciences Division

Introduction

During the last several years the Marine and Coastal Section of Terrain Sciences Division has been asked to advise on such diverse topics as port and harbour planning and oil spill countermeasure programs. Commonly, the lack of data, particularly in the Arctic, has caused difficulties in knowing either the questions or answers necessary in planning for a specific need. Consequently field programs are designed to collect a variety of data including sediment and biologic parameters from the nearshore environments and process measurements of waves and currents. Such data are used to develop coastal models which aid in the understanding of present processes and the resultant coastal characteristics. The model may yield specific data for a specific requirement or, more probably, will enable the proper questions to be formulated for research to meet a specific need.

Coastal models are derived most easily from an understanding of the spatial distribution of data. For example, bathymetry, sediment composition, grain size characteristics, nature and abundance of plant or animal life are all illustrations of variables that are normally spatially dependent. This note describes the development of a system whereby the location, type, and analytical results of nearshore and marine data are recorded in a format suitable for computer mapping. The maps allow both rapid inspection of large amounts of data, and by the judicious use of overlays, relationships between various variables can be assessed quickly.

Nature of Data

There are three related problems associated with the collection and subsequent analyses of nearshore and marine data. First, the sample location must be known with respect to both the shoreline and all other sample locations. Second, each location (and sample) must be identified with a label, and the type of data at that position must be recorded (Fig. 1). In practice the vessel may be running continuous transects with side-scan sonar and subbottom profiling equipment operating, while at the same time plankton nets are being towed. In this case, locations are position fixes which must be recorded in conjunction with the time, ship speed and ship heading. At other locations the ship may remain stationary for a grab sample, core, or current meter installation. Third, maps of the spatial distribution of both the type of data collected and the parameters derived from later analyses of the data must be obtained easily and efficiently.

The system of positioning, data recording, and analyses can be divided into four "levels" as follows:

Level I: Parameters belonging to Level I describe the coastal site, the chosen reference points, and the length and bearing of the baseline if more than one reference point is used (Fig. 1). The reference points may be radar reflectors or transponders set out in known locations or simply prominent features that can be identified with radar or manually surveyed with a sextant. Level I parameters also link the relative position of the fixes with their absolute geographical location.

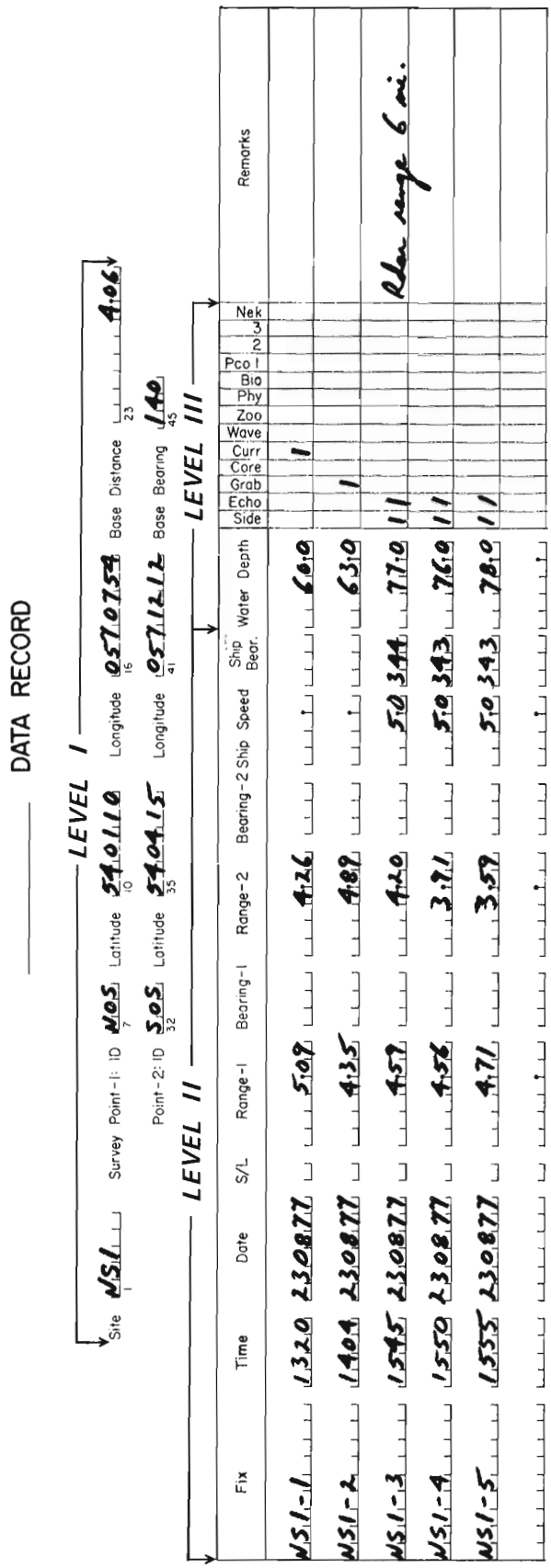

Figure 1. An example of ship's data record identifying three data levels. In this example two ranges are being used for the fix positions.

From: Scientific and Technical Notes in Current Research, Part B; Geol. Surv. Can., Paper 78-1B .

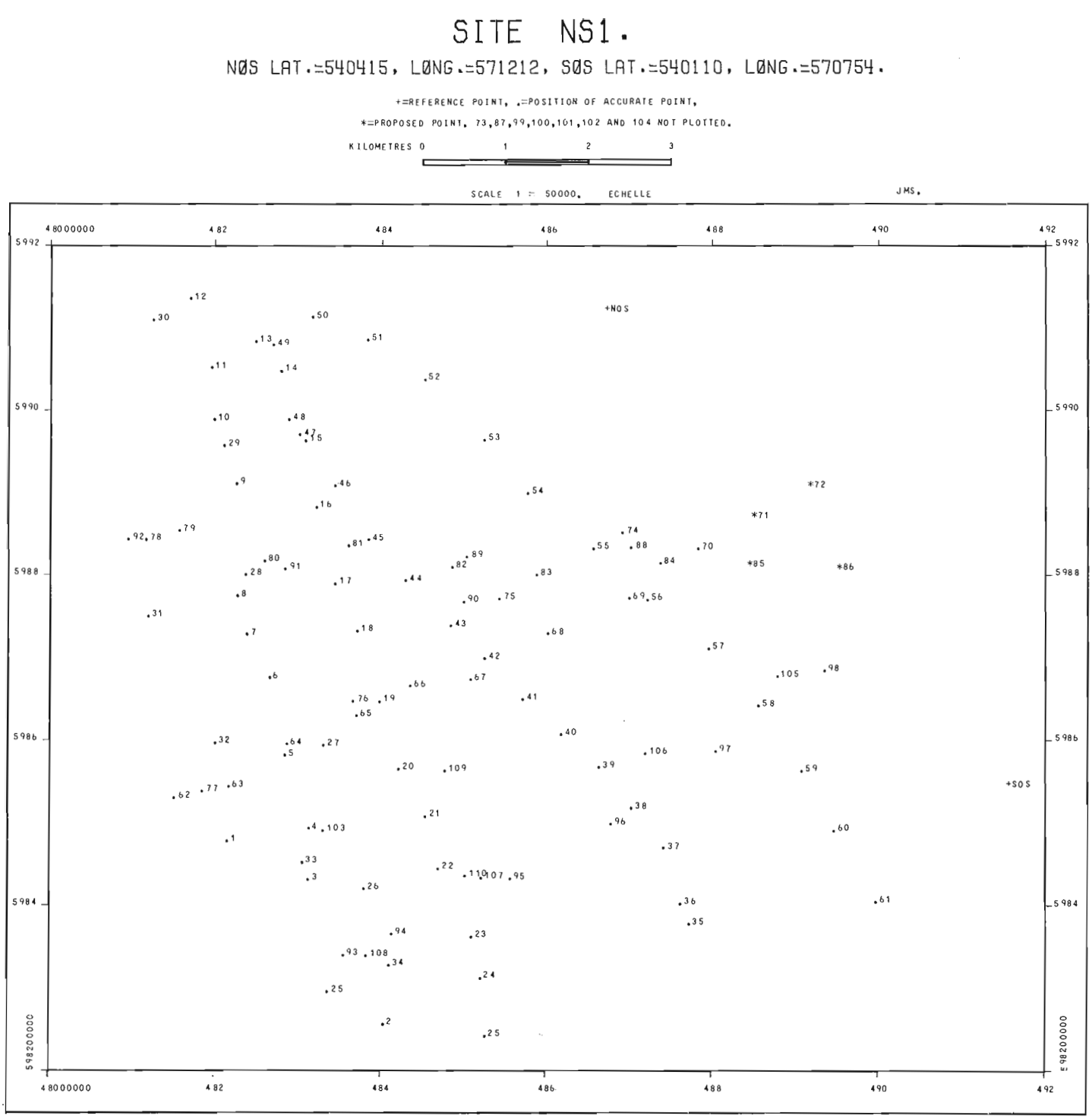

Figure 2. Typical output of all fix positions. Note that fixes 71, 72, 85, and 86 are proposed. This is because they all lie close to the baseline where the radar ranges give poor triangulation. Rather than be unplotted, they are positioned according to the ship's speed, heading, and elapsed time from the last accurate fix. In this case site NS1 is an example of a coastal survey on the Labrador coast using two small islands (NOS and SOS) as reference points.

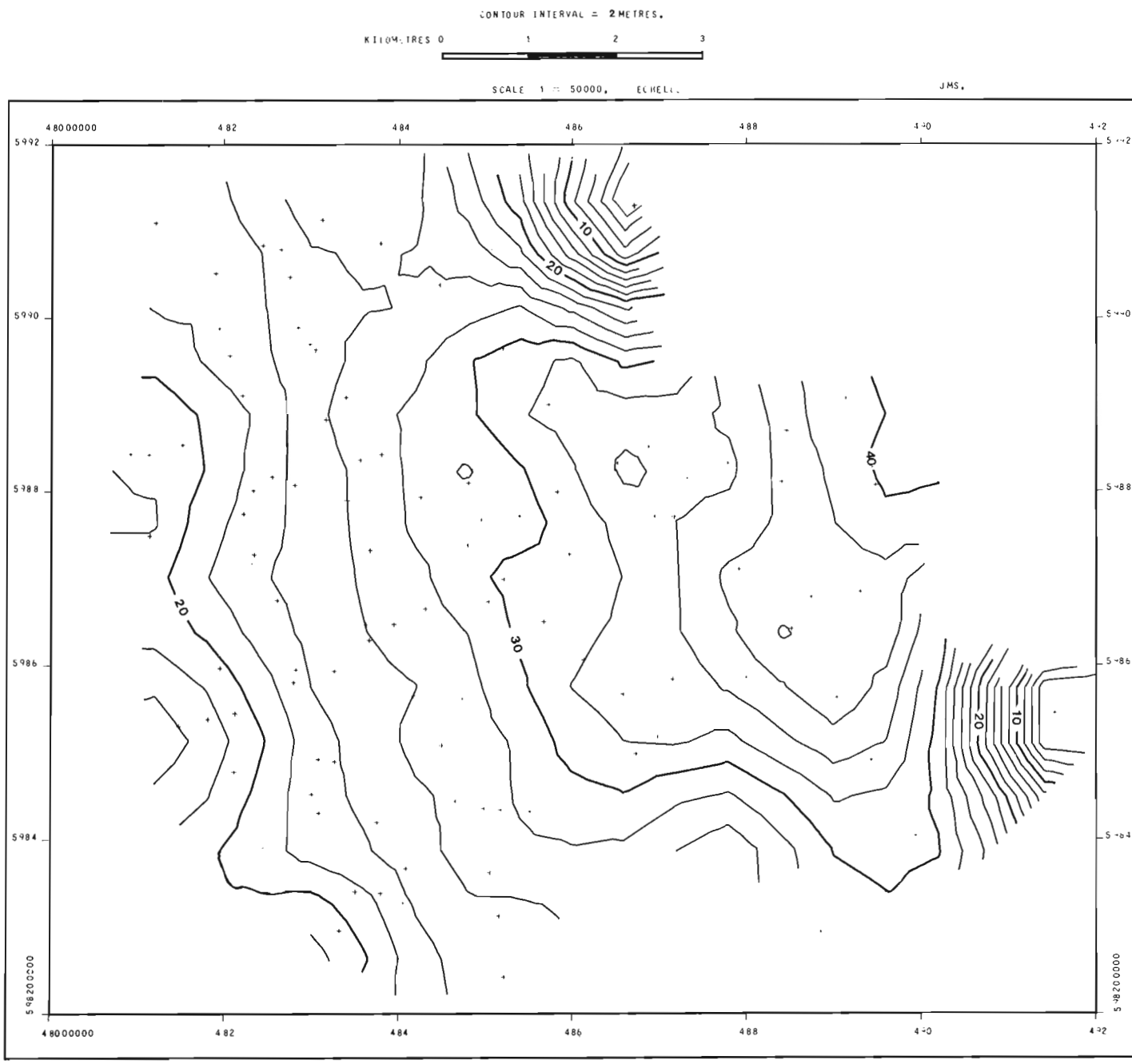

Figure 3. Example of a computer contour plot of water depths using all fix positions.

Level II: Parameters belonging to Level II (Fig. 1) are used directly or indirectly in the positioning of individual sample locations (fixes). These include a label, name, and number for each fix, the heading and speed of the vessel; and two ranges or a range and bearing to either reference point.

Computer methods for obtaining the position of navigational data do exist (Swan et al., 1976), but generally they have a nature that is too specific to be used directly in the present study. In this approach, a computer program was developed to calculate fix positions using Level I and Level II parameters as input. If a coastal site contains only one reference point, a range and a bearing are sufficient. If two reference points are available, the fix position can be calculated from a range and bearing to either reference point, or from two ranges or from two bearings. These contingencies are useful should one reference point become obscured and the position be dependent on a range and bearing to the second reference point. Provisions also are made to derive a proposed position using only ship speed and heading and elapsed time if the range and bearing data are missing or if errors make triangulation impossible (Fig. 2).

Level III and Level IV: Level III parameters identify the kind of data collected at a fix (Fig. 1); as is the case with Level II data, there is considerable flexibility. Different types of information can be added or deleted according to unique or specific characteristics of a coastal site. Level III parameters in the example data record (Fig. 1) include water depth and a system of indicators denoting the presence or absence of side-scan sonar, echo sounding, grab, and core samples, as well as current, wave, and biological measurements. These indicators also may define the presence or absence of analytical results performed on the data they identify. For example, the identification of a grab sample at a particular location also denotes the presence of an array of information of a predetermined nature (per cent gravel, sand, silt and clay; mean grain size, sorting, and skewness) introduced subsequent to field work. The analytical results of Level III parameters are identified as Level IV data.

Nature of Output

The use of Level I, II, and III parameters, combined with available computer programs (Bélanger, 1975, in prep.; Swan and Linden, 1977), enables maps to be produced rapidly (Fig. 2 and 3). Figure 2 is a preliminary computer output of all accurate and proposed fixes relative to two reference points. Useful contingencies include (1) a different symbol for proposed positions, (2) a listing of fixes that are impossible to plot, and (3) a choice of scale. Such a map is helpful for editing purposes. If desired, plots showing the positions of specified data can be obtained. Figure 3 is a contour map of water depth for the same area.

Computer programs currently are being developed that will incorporate Level IV data. When completed, the system will allow maps of any specified data at any level to be constructed with or without contours. The accumulation of field and analytical data, as developed in this approach, also will permit standard mathematical or statistical methods to quantify apparent relationships among variables as determined by the visual assessment of the maps.

References

Bélanger, J.R.B.
1975: ISAMAP User's manual; Geol. Surv. Can., Open File 295, 38 p.

URBIS5 User's reference manual; Geol. Surv. Can., paper. (in prep.)

Swan, D., Frydecky, I., and Currie, R.G.
1976: A library of computer programs for the processing of hyperbolic and range-range navigational data; in Report of Activities, Part B, Geol. Surv. Can., Paper 76-1B, p. 95.

Swan, D. and Linden, R.
1977: Plotting subroutines for the presentation of geological data; in Report of Activities, Part B, Geol. Surv. Can., Paper 77-1B, p. 269-270.

Zn:Cd RATIOS FOR SPHALERITES SEPARATED FROM SOME CANADIAN SULPHIDE ORE SAMPLES

I.R. Jonasson and D.F. Sangster
Resource Geophysics and Geochemistry Division
Regional Economic Geology Division

Introduction

Data are listed in Tables 1 to 3 to permit calculation of Zn:Cd ratio which is independent of the actual Zn content of the ore sample, mineral separate, or zinc concentrate studied. The most common impurity in many of the sphalerite mineral separates analyzed has been identified as pyrite. Other work by Jonasson and Sangster, as yet unpublished, has shown that the Cd content of co-existing pyrites in these zinc ores is very low and therefore it is concluded that pyrite impurities contribute insignificant Cd to the total quantity measured.

The data presented are divided into three separate genetic categories of sulphide deposits: 1) volcanogenic and massive; 2) carbonate-hosted; 3) miscellaneous veins.

Table 1

Zn and Cd content of some Canadian vein sulphide deposits

Name of Occurrence	Location	Rock Type	Ore Type	Code	Zn%	Cd%	Zn/Cd
ARCHEAN							
Severn River	N. Ont.	volcs	Cu-Zn	1	50.0	0.3900	128
				1	44.0	0.3430	128
Berens River	N. Ont.	volcs	Pb-Zn	1	54.0	0.3700	132
				1	46.0	0.3860	119
				1	49.0	0.3700	128
				1	48.0	0.3570	135
North Spirit Lake	N. Ont.	volcs	Pb-Zn	1	41.0	0.2900	169
Homer Lake	Mack.	seds.	Pb-Zn	1	38.0	0.3200	119
				1	50.0	0.1600	313
				1	45.0	0.1600	281
				1	42.0	0.1240	339
PROTEROZOIC							
Cobalt area	N. Ont.	seds.	Pb-Zn,Ag	1	16.0	0.0540	296
				1	34.0	0.1500	227
				1	28.0	0.1000	280
				1	33.0	0.1400	235
				1	33.0	0.1200	275
				1	47.0	0.1600	294
				1	46.0	0.1800	256
Nth. Contact Lake	N. Sask.	volcs	Cu-Zn	1	32.0	0.3400	94
PHANEROZOIC							
Arctic Silver	Yukon	seds.	Pb-Zn-Ag	1	23.0	0.7240	32
Keno Hill	Yukon	seds.	Pb-Zn-Ag	1	41.9	0.5660	74
				1	60.0	0.6000	100
Galkeno	Yukon	seds.	Pb-Zn-Ag	1	59.1	0.7150	83
Keymet	N.B.	volcs	Pb-Zn	1	58.4	0.4070	143
				1	54.4	0.4280	
Louvicourt *	N.B.	volcs	Cu-Zn	1	25.6	0.3350	76
Que. Sturgeon River	N.B.	volcs	Pb-Zn,Cu	1	40.0	0.6700	60
Gaspe Copper	Que.	seds.	Cu, Zn	1	48.0	0.3040	158

Notes: Code 1 signifies a sphalerite or a sphalerite-pyrite separate
2 signifies a monthly mine zinc concentrate
3 signifies a hand specimen ore sample

rylt = rhyolite
ands = andesite
seds = sediments
volc = volcanics * classification in doubt

From: Scientific and Technical Notes in Current Research, Part B; Geol. Surv. Can., Paper 78-1B .

Table 2

Zn and Cd content of some Canadian Massive volcanogenic sulphides

ARCHEAN

Name of Occurrence	Location	Rock Type	Ore Type	Code	Zn%	Cd%	Zn/Cd
East Cleaver Lake	Mack.	meta-rylt	Pb-Zn	3	6.4	0.0315	203
				3	8.9	0.0360	249
				3	3.7	0.0140	261
Hackett River, Camp Lake	Mack.	meta-rylt	Pb-Zn	3	26.0	0.1700	153
				3	16.0	0.1100	145
Hackett River Jo Zone	Mack.	meta-rylt	Pb-Zn	3	11.3	0.0310	368
Hackett River, Watson Lake	Mack.	meta-seds	Pn-Zn	3	18.2	0.0600	303
				3	9.1	0.0290	318
				3	11.3	0.0310	368
Hackett River, Trench three	Mack.	tuffs	Pb-Zn	1	13.4	0.0500	270
				1	18.2	0.0620	291
Yava Syndicate, Agricola Lake	Mack.	meta-volcs	Pb-Zn	1	41.8	0.1400	299
				3	7.5	0.0270	277
				3	5.7	0.0230	248
Takijuq Lake	Mack.	meta-rylt	Cu-Zn	1	38.0	0.1700	224
High Lake	Mack.	meta-rylt	Cu-Zn	1	29.0	0.1100	264
				1	28.0	0.1100	255
				1	21.0	0.0840	250
Indian Mt. Lake	Mack.	meta-rylt	Pb-Zn	1	60.7	0.1910	318
				1	60.0	0.2080	288
				1	58.0	0.1820	319
Spi Lake	Keew.	meta-volcs	Cu-Zn,Pb	1	45.0	0.1400	321
				1	41.9	0.0890	470
				1	38.6	0.0980	394
Mattabi	N. Ont.	tuffs	Cu-Zn	1	40.0	0.1300	308
				1	28.0	0.0880	318
Sturgeon Lake, Falconbridge	N. Ont.	volcs	Cu-Zn	1	55.0	0.1600	344
				1	58.7	0.1330	441
				1	57.5	0.1220	471
South Bay, Uchi Lake	N. Ont.	volcs	Cu-Zn	1	56.0	0.3100	181
				1	56.0	0.2000	280
				1	52.0	0.2600	200
				1	57.0	0.2800	204
				2	51.0	0.2360	216
Geco	N. Ont.	meta-seds	Cu-Zn,Pb	1	36.5	0.2350	155
				1	56.7	0.2380	238
Willecho	N. Ont	meta-seds	Cu-Zn	1	56.8	0.1990	285
				1	51.0	0.1960	260
				1	60.3	0.2600	232
Kam-Kotia	N. Ont.	ands	Cu-Zn	1	54.6	0.1565	349
				1	20.3	0.0520	390
Cdn.-Jamieson	N. Ont.	rylt	Cu-Zn	1	47.7	0.1040	459
				1	59.6	0.1410	423
				1	32.5	0.0480	677
Kidd Creek	N. Ont.	meta-volcs	Cu-Zn,Ag	1	55.7	0.2330	239
				1	53.0	0.3000	177
				1	16.0	0.0600	267
				2	52.0	0.3000	173
				1	32.0	0.2100	152
				1	34.0	0.2200	154
Jameland	N. Ont.	rylt	Cu-Zn	1	25.7	0.2340	756
				1	31.7	0.0660	480

Table 2 (cont.)

Name of Occurrence	Location	Rock Type	Ore Type	Code	Zn%	Cd%	Zn/Cd
Normetal	Que.	volcs	Cu-Zn	2	51.8	0.1370	378
				2	43.1	0.1370	388
				2	52.8	0.1370	385
				2	52.4	0.1330	394
				2	52.9	0.1330	398
				2	50.5	0.1440	351
				2	52.9	0.1420	373
				2	54.8	0.1390	394
Lac Dufault	Que.	rylt-ands	Cu-Zn	2	51.8	0.1150	450
				2	50.5	0.1070	472
				2	49.5	0.1130	438
				2	51.2	0.1110	461
Delbridge	Que.	rylt	Zn	1	61.2	0.1290	474
				1	51.0	0.0590	864
				1	58.3	0.0610	956
				1	37.7	0.0490	769
Coniagas	Que.	tuffs	Pb-Zn, Ag	3	18.2	0.0580	312
				3	14.2	0.0410	343
Manitou-Barvue	Que.	tuffs	Cu-Pb-Zn	2	56.8	0.1650	344
				2	55.4	0.1600	346
				2	55.1	0.1560	353
				2	56.6	0.1670	338
				2	56.0	0.1610	348
				2	18.8	0.0527	357
				2	19.1	0.0565	338
				2	18.3	0.0508	360
				2	12.8	0.0320	400
Mattagami Lake	Que.	tylt	Cu-Zn	1	45.6	0.1000	456
				1	59.6	0.0830	718
				1	55.2	0.1060	521
Orchan	Que.	rylt	Cu-Zn	2	52.9	0.0800	661
				2	53.8	0.0830	648
				2	54.1	0.0850	636
				2	56.5	0.0840	673
Poirier	Que.	rylt	Cu-Zn	1	16.0	0.0360	444
				2	62.9	0.1460	431

All analyses for Zn and Cd in this and accompanying tables were by atomic absorption spectrometry following a total dissolution by a strong HnO_3 – HCl solution.

Notes: Code 1 signifies a sphalerite or sphalerite-pyrite separate
2 signifies a monthly mine zinc concentrate
3 signifies a hand specimen ore sample

rylt = rhyolite
ands = andesite
seds = sediments
volcs = volcanics

Table 2 (cont.)

PROTEROZOIC

Name of Occurrence	Location	Rock Type	Ore Type	Code	Zn%	Cd%	Zn/Cd
Fox Lake	N. Man.	meta-seds	Cu-Zn	2	48.0	0.1500	320
				2	46.0	0.0950	480
Sherridon	N. Man.	meta-seds	Cu-Zn	1	45.0	0.1600	281
				1	47.0	0.1600	294
				1	51.0	0.1800	283
				1	49.0	0.1900	258
				1	47.0	0.1800	261
Ruttan Lake	N. Man.	meta-seds	Cu-Zn,Pb	1	41.0	0.1500	273
				1	35.0	0.1200	292
				1	21.2	0.0700	303
				1	30.8	0.0780	395
Osborne Lake	N. Man.	meta-seds	Cu-Zn	1	20.6	0.0750	275
				1	52.1	0.0290	180
				1	55.4	0.1060	523
Chisel Lake	N. Man.	meta-seds	Pb-Zn,Cu	1	58.7	0.1070	549
				1	60.2	0.1000	602
				1	59.3	0.1600	371
Schist Lake	N. Man.	meta-volcs	Cu-Zn	1	14.4	0.0280	514
				1	45.5	0.0740	615
				1	54.4	0.0860	633
				1	32.5	0.0520	625
Flin Flon	N. Man.	meta-volcs	Cu-Zn	1	55.8	0.1760	317
	N. Sask.			1	28.0	0.1025	273
				1	25.0	0.0940	266
Sulphide Lake	N. Sask.	meta-seds	Cu-Zn	1	34.0	0.1500	227
Western Nuclear	N. Sask.	meta-volcs	Pb-Zn,Cu	1	42.3	0.0420	1007
				1	50.1	0.0510	982
Errington	N. Ont.	tuffs	Cu-Zn,Pb	3	22.0	0.0100	2200
				1	33.0	0.0200	1650
				1	33.0	0.1200	275
				3	25.0	0.1000	250
New Calumet	Que.	meta-seds	Pb-Zn,Ag	1	54.8	0.1220	449
				1	56.0	0.1700	329
				1	48.0	0.1480	324
Tetrault	Que.	paragneiss	Pb-Zn,Ag	1	49.0	0.1800	272
				1	51.0	0.1800	203
Sullivan	B.C.	seds.	Pb-Zn	2	46.0	0.1700	271
				2	53.0	0.1800	294
				2	46.0	0.1660	277

PHANEROZOIC

Name of Occurrence	Location	Rock Type	Ore Type	Code	Zn%	Cd%	Zn/Cd
Faro, Anvil	Yukon	meta-seds	Pb-Zn	1	53.6	0.0570	940
				1	22.8	0.0240	950
				1	62.9	0.0620	1015
				3	28.3	0.0466	607
Western	B.C.	volcs	Pb-Zn,Cu	1	20.0	0.0980	204
Key Anacon	N.B.	meta-volcs	Pb-Zn	1	40.0	0.1100	364
				1	50.8	0.0940	540
				1	51.3	0.1060	484
				1	46.6	0.0740	630
Wedge	N.B.	meta-volcs	Pb-Zn	1	45.0	0.1400	321
Heath Steele	N.B.	meta-volcs	Pb-Zn,Cu	3	11.0	0.0240	458
				1	27.2	0.0360	756
Brunswick No. 12	N.B.	meta-tuffs	Pb-Zn,Cu	3	24.7	0.0310	797
Brunswick No. 6	N.B.	meta-tuffs	Pb-Zn,Cu	3	13.0	0.0280	536
Weedon	Que.	meta-tuffs	Cu-Zn	1	62.7	0.1010	621
				1	50.3	0.1650	305
				1	59.0	0.0620	952
Buchans, McLean	Nfld.	volcs	Pb-Zn,Cu	1	52.0	0.1800	289
				3	21.1	0.0220	959

Notes: Code 1 signifies a sphalerite or sphalerite-pyrite separate
2 signifies a monthly mine zinc concentrate
3 signifies a hand specimen ore sample

rylt = rhyolite
ands = andesite
seds = sediments
volcs = volcanics

Table 3

Zn and Cd content of some Canadian carbonate-hosted massive sulphides

Name of Occurrence	Location	Ore Type	Code	Zn%	Cd%	Zn/Cd
PROTEROZOIC						
Tart Claims	Yukon	Pb-Zn	1	61.0	0.0560	1089
Ug Claims	Yukon	Pb-Zn	3	18.0	0.0295	610
Gayna River Yukon	Yukon	Pb-Zn	3	14.0	0.0320	438
			3	8.6	0.0177	486
			3	4.6	0.0170	271
Odd MacIntyre	Yukon	Pb-Zn	1	46.0	0.0480	958
Tara Claims	Yukon	Pb-Zn	1	48.0	0.0460	1043
Strathcona,	Frnk.	Pb-Zn	1	56.0	0.1900	295
Nanisivik			1	62.8	0.1760	357
			1	58.4	0.1820	321
			1	65.1	0.2290	284
Long Lake	S. Ont.	Pb-Zn	1	61.7	0.1520	406
			1	44.6	0.1250	357
			1	49.0	0.1600	306
PHANEROZOIC						
Jersey	B.C.	Pb-Zn	1	30.0	0.2730	176
Rev, Big Cirque	Yukon	Pb-Zn	1	41.0	0.1700	241
Mt. Tillicum	Yukon	Pb-Zn	3	28.0	0.0900	311
Cypress Bar Claims	Yukon	Pb-Zn	1	68.0	0.2540	268
Ab Claims	Yukon	Pb-Zn	1	47.0	0.0840	560
Goz A Claims	Yukon	Pb-Zn	3	28.0	0.0820	342
Goz E Claims	Yukon	Pb-Zn	3	43.0	0.1220	353
Goz F Claims	Yukon	Pb-Zn	3	17.6	0.0720	244
Goz Ø Claims	Yukon	Pb-Zn	3	28.0	0.0880	318
Goz I Claims	Yukon	Pb-Zn	3	25.0	0.0840	298
Goz J Claims	Yukon	Pb-Zn	3	27.0	0.1160	233
Cab Two Claims	Yukon	Pb-Zn	3	11.0	0.0520	212
Rio Claims	Yukon	Pb-Zn	3	8.0	0.0175	457
Econ Claims	Yukon	Pb-Zn	3	14.0	0.0160	875
Flunk West Claims	Yukon	Pb-Zn	3	12.0	0.0440	273
Arvik, Polaris	Frnk.	Pb-Zn	1	61.5	0.0850	724
Prairie Creek	Mack.	Pb-Zn	1	61.5	0.3200	192
			1	66.5	0.3890	170
Pine Point, Ø-42	Mack.	Pb-Zn	1	64.0	0.1040	615
			1	66.4	0.1770	375
			1	64.0	0.2480	258
			1	64.0	0.2480	258
			1	52.0	0.0960	542
			1	64.0	0.1140	561
			1	58.0	0.0560	1036
Pine Point, N-42	Mack.	Pb-Zn	1	62.0	0.1840	337
			1	59.2	0.1200	493
			1	59.1	0.2440	243
			1	65.2	0.1550	421
			1	52.0	0.1480	351
			1	64.0	0.1040	615
			1	60.0	0.1200	500
			1	62.0	0.1840	337
Pine Point	Mack.	Pb-Zn	2	56.0	0.1200	467

Notes: Code 1 signifies a sphalerite or a sphalerite-pyrite separate
2 signifies a monthly zinc concentrate
3 signifies a hand specimen ore sample

Table 4

Zn and Cd content of copper concentrates from some Canadian mines

ARCHEAN						
Name of Occurrence	Location	Rock Type	Ore Type	Zn%	Cd%	Zn/Cd
Normetal	Que.	volcs	Cu-Zn	3.18	0.0116	274
				4.25	0.0155	274
				3.46	0.0132	262
				3.35	0.0121	277
				3.80	0.0146	260
				3.24	0.0126	257
				3.46	0.0126	274
				3.58	0.0130	275
Lac Dufault	Que.	rylt-ands	Cu-Zn	4.70	0.0120	392
				5.10	0.0132	386
				4.40	0.0111	396
				7.20	0.0183	393
				7.00	0.0183	383
Manitou-Barvue	Que.	tuffs	Cu-Pb-Zn	1.10	0.0047	234
				1.10	0.0047	234
				1.02	0.0045	227
				0.67	0.0030	223
Matagami Lake	Que.	rylt	Cu-Zn	4.59	0.0136	337
				3.29	0.0088	373
				3.58	0.0086	416
				3.35	0.0085	394
				3.24	0.0081	400
				4.55	0.0107	425
				3.93	0.0092	427
				4.46	0.0108	413
Orchan	Que.	rylt	Cu-Zn	8.30	0.0139	597
				7.60	0.0132	576
				6.80	0.0116	410
				3.80	0.0066	576
				4.80	0.0082	585

Notes: 1. rylt = rhyolite, ands = andesite
2. all concentrates are monthly composites
3. all concentrates contain about 30% Cu

Volcanogenic Deposits

The Archean massive volcanogenic category contains some of the largest zinc producers in Canada and includes the mines of the Timmins region of Ontario, the Noranda, and the Matagami Lake camps of Quebec. The deposits of the Manitouwadge area of northern Ontario and those near Ignace, Ontario, are also included.

Significantly, sphalerite from Kidd Creek, the largest known Canadian volcanogenic deposit, contains the highest Cd content and is quite distinct from its immediate neighbours. There are limited data from Geco, another large Zn producer, and it too, along with nearby Willecho, would seem to be enriched in Cd.

On the other hand, the important minis of northwestern Quebec are relatively low in Cd and this is especially true of the Matagami Lake camp. The mines of northwestern Ontario can be regarded as about average with the exception of South Bay which is enriched.

Proterozoic massive volcanogenic deposits form the Flin Flon and Fox Lake camps of northern Manitoba and northern Saskatchewan. Inspection of the data suggests little difference in typical average Zn:Cd ratios from the Archean types. However the Sullivan mine in British Columbia, which is shale-hosted and is one of the largest Zn producers in Canada, is enriched in Cd by comparison. Data quoted here were derived from three-monthly composite concentrates.

Massive volcanogenic ores of Phanerozic age are represented here mainly by the orebodies of the Anvil Range, Yukon and of the Bathurst camp, New Brunswick. Neither group would seem to be enriched in Cd. Some smaller mines in British Columbia, e.g., Western, are somewhat richer in Cd but data are few and too limited in scope to draw reliable conclusions.

Carbonate-hosted Deposits

In general, carbonate-hosted zinc sulphides of all ages are low in Cd. The main zinc producer in Canada for orebodies of this type is at Pine Point, Northwest Territories. Here, Zn:Cd ratios are variable for samples from two deposits but generally indicate that Cd content is low.

Vein Deposits

Direct comparison of vein sphalerites from several regions with neighbouring massive volcanogenic Zn ores reveals that the former are usually enriched by comparison. Age of the orebody does not appear to be a significant factor.

Table 5

Data for Zn:Cd for Zn and Cu concentrates

Name of Occurrence	Location	Cu concentrate			Zn concentrate		
		Zn%	Cd%	Zn/Cd	Zn%	Cd%	Zn/Cd
Normetal	Que.	3.54	0.0132	269	51.4	0.1342	383
Lac Dufault	Que.	5.68	0.0146	390	50.8	0.1115	455
Manitou Barvue	Que.	0.97	0.0042	229	56.0	0.1618	346
Mattagami Lake	Que.	3.87	0.0097	398	53.5	0.0946	565
Orchan	Que.	6.26	0.1114	549	54.3	0.0829	655
Contribution of Cd to Cu concentrate by Cu sulphides (chalcopyrite)							
Normetal	Que.	30% of total Cd					
Lac Dufault	Que.	15% of total Cd					
Manitou Barvue	Que.	33% of total Cd					
Mattagami Lake	Que.	30% of total Cd					
Orchan	Que.	16% of total Cd					

The largest Zn producers of this type are from the Keno Hill area, Yukon, wherein cadmium sulphide minerals have been identified. As might be expected, these Zn sulphides are highly enriched in Cd.

Copper Concentrates

From the accompanying tables it is possible to estimate the quantities of Cd which would find their ways into Zn reduction smelters in various locations in Canada. However, in orebodies which also produce a Cu concentrate, there is commonly a carryover of up to 5 per cent Zn into those concentrates. Cd accompanies these Zn impurities in proportions indicated by Zn:Cd ratios for zinc concentrates.

Table 4 presents Zn:Cd data for Cu concentrates for a number of Cu-Zn producers in Quebec. In each case the main Cu bearing mineral is chalcopyrite. Table 5 presents comparative data for Cu and Zn concentrates for these same deposits. It can be seen from an inspection of respective Zn:Cd ratios that there is apparently a small but significant contribution of Cd from Cu-Fe sulphides. Calculations based on averaged Zn contents and averaged Zn:Cd ratios for a series of monthly composite concentrates (1970-1971) show that Cu-Fe sulphides contribute between 15 and 33 per cent of contained Cd to a Cu concentrate. This Cd may eventually find its way to a copper reduction smelter at Noranda.

Acknowledgments

Zn and Cu analyses were performed by Bondar-Clegg and Company, Ottawa and by the analytical chemistry staff of the Geochemistry Section, Geological Survey of Canada.

DEVELOPMENT OF ANALYTICAL METHODS

Sydney Abbey and Others[1]
Central Laboratories and Administrative Services Division

Two non-dispersive infrared-absorption instruments were acquired and operated in conjunction with a small resistance tube furnace. On heating rock powders with a suitable flux in a stream of oxygen, the water vapour and carbon dioxide evolved can be measured by their infrared absorptions at characteristic wavelengths. Preliminary tests indicate satisfactory performance, but full quantitative applications await the acquisition of a two- or three-channel digital integrator. By means of a third infrared instrument, it may be possible to determine sulphur as the dioxide at the same time. It may also be possible to connect the carbon-dioxide detector to an acid-evolution train and thereby distinguish carbonate from non-carbonate carbon. The new system is so much simpler than those now in use that it may be possible for one operator to analyze twice as many samples per day for three constituents than three operators can do now. (J.-L. Bouvier)

A new automatic recording titrator has been acquired for application to a new method for ferrous iron (Kiss, 1977). The method involves simultaneous decomposition of a large number of samples in a stream of nitrogen in a heated aluminum block. The resulting solutions are titrated in the fluoride medium under constant current conditions between polarized electrodes in the automatic titrator. End-points are indicated by sharp voltage peaks. Published information suggests that the method is more rapid than the classical procedure, more accurate than our present "rapid" method and less susceptible to interferences than either of them. (J.-L. Bouvier)

Despite repeated instrumental breakdowns, the X-ray fluorescence spectrometer continues to provide excellent results (when it is working). Disc preparation has been improved by changing from a lithium tetraborate-metaborate to a lithium tetraborate-fluoride flux. Experiments are underway to improve sensitivity, precision and accuracy in rubidium and strontium determinations for geochronology. (G.R. Lachance and R.M. Rousseau)

Current developments on the direct-reading optical-emission spectrometer include automatic print-out of reports for client scientists on a new high-speed printer and installation of new monitoring channels to detect interference from uranium and other elements. (W.H. Champ and C.F. Meeds)

All methods on the photographic spectrograph are undergoing major revisions because the plates formerly used are no longer available. Development of two new procedures for low concentrations of volatile trace elements is nearing completion (W.H. Champ and P.G. Bélanger), as is an updated semiquantitative method. (W.H. Champ and L.J. Clugston)

New developments applicable to both optical emission systems include modification of arc stands to provide automatic control of arc gap and studies in the use of argon-oxygen mixtures to replace the air-jet in general methods for trace elements. (W.H. Champ and K.A. Church)

A review paper (Abbey et al., 1977) appeared on recent developments in the analysis of silicates.

References

Abbey, Sydney, Aslin, G.E.M., and Lachance, G.R.
1977: Recent developments in the analysis of silicate rocks and minerals; Rev. Anal. Chem., v. 3, p. 281-348.

Kiss, E.
1977: Rapid potentiometric determination of the iron oxidation state in silicates; Anal. Chim. Acta, v. 89, p. 303-314.

ANALYSIS OF INTERNATIONAL REFERENCE SAMPLES

Sydney Abbey and Others[1]
Central Laboratories and Administrative Services Division

Staff of the Analytical Chemistry Section contributed a large volume of analytical data for the eight newest reference samples from the U.S. Geological Survey – a basalt, a marine mud, a quartz latite, a rhyolite, a schist, two shales and a syenite. To date, no master compilation of analytical data nor assigned compositional values have been published by the originator.

Using a recently published method (Sen Gupta, 1976), concentrations of a number of rare-earth elements were determined in 24 international reference rock samples and published (Sen Gupta, 1977).

Analytical data from our own laboratories were combined with those from the Centre de Recherches Pétrographiques et Géochimiques, France, and compared with values assigned by the originators of three reference samples from the Institute of Geochemistry, Irkutsk, U.S.S.R. (Abbey and Govindaraju, in press).

As a result of the availability of additional analytical data, a new set of calculations was conducted to derive new "usable" values for many constituents in the six reference rocks from the National Institute for Metallurgy, South Africa. Those values and many others have been embodied in a new edition of usable values for reference samples of rocks and related materials (Abbey, 1977).

Work is underway on a "gel" method (Date, in press) for preparing synthetic homogeneous standard powders, but difficulties have been encountered with volatile trace elements. (J.G. Sen Gupta.)

References

Abbey, Sydney
1977: Studies in "standard samples" for use in the general analysis of silicate rocks and minerals, Part 5, 1977 edition of "usable" values; Geol. Surv. Can., Paper 77-34.

Abbey, Sydney and Govindaraju, K.
Analytical data on three rock reference samples from the Institute of Geochemistry, Irkutsk; Geostds. Newslett. (in press)

Date, A.R.
Preparation of trace element reference materials by a co-precipitation gel technique; The Analyst. (in press)

Sen Gupta, J.G.
1976: Determination of lanthanides and yttrium in rocks and minerals by atomic absorption and flame-emission spectrometry; Talanta, v. 23, p. 343-348.

1977: Determination of traces of rare-earth elements, yttrium and thorium in several international geological reference samples and comparison of data with other published values; Geostds. Newslett., v. 1, p. 149-155.

[1] Names of other participants given with individual items.

From: Scientific and Technical Notes in Current Research, Part B; Geol. Surv. Can., Paper 78-1B .

RATES OF MOVEMENT ASSOCIATED WITH MUD BOILS, CENTRAL DISTRICT OF KEEWATIN

P.A. Egginton and W.W. Shilts
Terrain Sciences Division

Glacial and marine muds of central Keewatin are rigid or slightly plastic under average field conditions. Because of their low liquid limits (<25%) and limited plasticity indices (<8%), however, they become plastic or liquid with a slight increase in moisture content or porewater pressure. These materials are commonly in motion even on relatively low angle slopes, and in this region the downslope movement of muds (solifluction) is closely related to, if not inseparable, from mud boil activity. This note reports some measurements of magnitudes of mud movement associated with mud boils in central Keewatin.

Initial study sites were located at Victory and Kaminak lakes in 1973; additional sites were added in 1977 at Ferguson and Henik lakes (Fig. 1). The original study sites were located here: 1) for logistical reasons as the project originated as an offshoot of a terrain mapping program in central Keewatin (viz. Shilts et al., 1976) and 2) because mud boils are particularly well developed on the relatively clay-rich red till of a large glacial dispersal train (Klassen and Shilts, 1977; Shilts, in press). In addition, the removal of the hematite-bearing clay fraction by slope wash or deflation causes red till exposed at the surface to become pink, grey, or brown, creating colour contrasts that facilitate the study of mud boil structures.

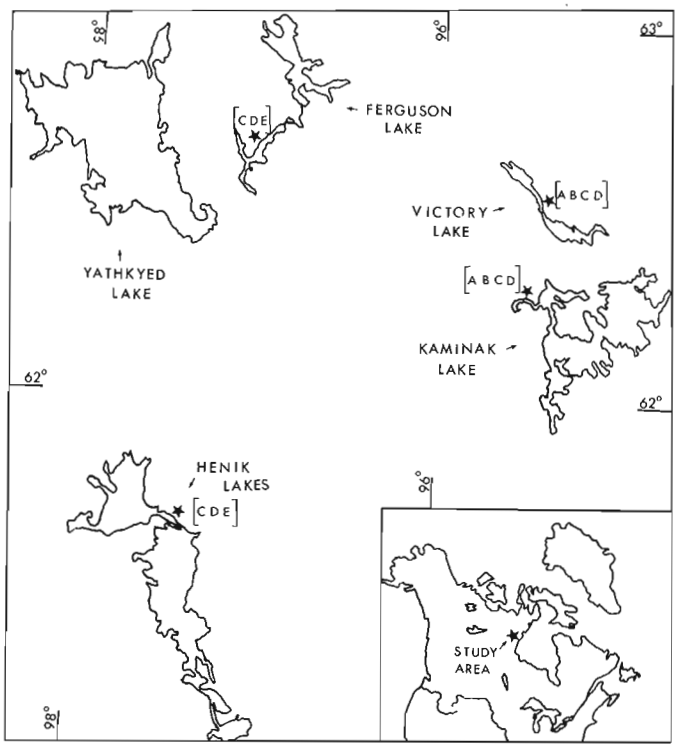

Figure 1. The location of mud boil study sites, central Keewatin. The letters refer to the type of instrumentation used:

A – aluminum tags; C – theodolite and targets;
B – tubing; D – circuits;
E – thermistors, soil moisture cells, and pressure gauges (see text).

From: Scientific and Technical Notes in Current Research, Part B; Geol. Surv. Can., Paper 78-1B .

Figure 2. A mud boil in the Victory Lake area, 1973. The aluminum tags used to monitor horizontal displacement of the mud are located under the rocks. (GSC 203165-H)

Instrumentation

A variety of techniques are being employed to provide information on active layer movement associated with mud boils. Specific clusters of mud boils were chosen for study if they appeared to be active, and an effort was made to include mud boils under a wide range of slope and textural conditions. The type of instrumentation and the location of study sites is illustrated in Figure 1.

In 1973, approximately 30 numbered aluminum tags (2 x 0.5 cm), held in place by small nails, were placed in predetermined patterns and spacings on the surface of several mud boils. In subsequent years any horizontal component of surface movement was measured relative to the position of other aluminum tags on the same mud boil (Fig. 2).

At nine sites (in 1973) clear plastic tubes, 10 cm in diameter and 183 cm in length, were buried vertically so that the bases were at or near the bottom of the active layer in the centre of a mud boil. The plastic tubes were slotted at the bottom to permit the intrusion of mud. Large boulders weighing 20 kg or more were placed on top of each tube to permit easy field identification, to protect the tubes from precipitation, and to keep the tube positioned at the bottom of the active layer.

Benchmarks were installed in 1977 and a theodolite was used in conjunction with the benchmarks to facilitate controlled measurement of the horizontal or vertical position of targets placed on the mud boils. The benchmarks are 2 cm diameter, copper-clad rods and are the type commonly used by the Geodetic Survey. Where possible the rods were cemented into holes drilled in bedrock outcrops (Fig. 3); where this was not possible the rods were driven to some depth (>1.5 m) into the permafrost by means of a portable jackhammer.

In addition, more than 300 simple "make or break" circuits were installed in mud boils at various sites. The circuits serve as simple event records. Depending upon the initial installation, the circuits record the occurrence of either a horizontal or vertical disturbance. In several places the circuits were nested in order to record the occurrence of movement at various depths within the mud boil. The majority of circuits were designed for hand testing; however,

several were attached to long term recorders so that the time of the soil displacements could be recorded.

At the Henik Lakes and Ferguson Lake sites nested thermistors, soil moisture cells, and pressure gauges were installed in mud boil centres and borders to provide additional information on soil conditions during periods of activity. In 1978 and subsequent years, it is planned to visit sites where benchmarks, circuits, and thermistors have been installed to ascertain modes and amounts of movement; the older sites also will be monitored.

Table 1

The relative horizontal displacement of marker tags on the surface of two mud boils over time

Mud boil no. 6			
Tag number	Distances apart (cm)		
	1973	1976	1977
28-29	40	42	42
29-30	40	43	43.5
30-31	40	37.5	37.0
31-32	40	41	41
32-33	40	39.5	40
33-34	40	44.5	44
34-35	40	43	44
35-36	40	38	37
36-37	40	X } 76	X
37-38	400	X }	X
Total	400	320/404.5	320*
48-49	30	30.5	28
49-50	30	29	30
50-51	30	31.5	33
51-52	30	32	33
52-53	30	29.5	30
53-54	30	30	30
54-55	30	31.5	31.5
Total	210	214	215.5
39-40	20	X	X
40-41	20	X	X
41-42	20	X	X
42-43	20	X } 42.5	X
43-44	20	X }	X } 85
44-45	20	22	X }
45-46	20	22	X }
46-47	20	18	17
Total	120	123.5	121

Note:

X – Sites where tags could not be relocated.
* – 320 cm represents the distance between tags 28 to 36.

Mud boil no. 8			
Tag number	Distances apart (cm)		
	1973	1976	1977
108-109	20	18	17
109-110	20	15.5	16.5
110-111	20	24	X } 47
111-112	20	22	}
111-113	20	20	20.3
113-114	20	22.5	24
114-115	20	19.5	20
115-116	20	21.5	22
116-117	20	18	X } 37
117-118	20	20	X }
118-119	20	21	X } 61
119-120	20	X	X }
120-121	20	X } 40	X
121-122	20	X }	18
122-123	20	X	23
123-124	20	X	29
124-125	20	X	19
125-126	20	19	21.5
Total	260	NA	375.3
128-129	20	19.5	X
129-130	20	18.5	16.5
130-131	20	24.5	X } 47 } 68
131-115	20	18.5	} }
115-132	20	22	21
132-133	20	23.5	24
133-134	20	17	18
Total	140	143.5	146.5
135-136	20	19	18.5
136-137	20	20	26
137-138	20	22	26
138-139	20	19	X }
139-118	20	19	X }
118-140	20	25	X } 106
141-141	20	18	X }
Total	140	142	145.5

Table 2

Vertical movements associated with mud boils

	Victory Lake				Kaminak Lake				
Site	104	105	106	107	3	4	2A	2B	5
Tube heave 1973-1977 (cm)	12.5	54.0	31.0	52.0					
Upward movement of mud 1973-1977 (cm)	9.5	54.5	37.0	52.0					
Mud intrusion 1973-1977 (cm)	-3.0	0.5	6.0	0.0	13.0	13.0	32.0	10.0	18.0
Depth to free water surface 1977 (cm)	84.5	33.0	61	49.0	*	*	*	*	*
Depth to tube bottom 1977 (cm)	112.5	96.0	89	85.0					

* no free water

Discussion of Results

Aluminum Surface Markers

The distances between aluminum surface markers on mud boils no. 6 (Kaminak Lake) and no. 8 (Victory Lake) for the years 1973, 1976, and 1977 are presented in Table 1. The information is incomplete because some tags had been buried and could not be found. Buried tags were recovered from beneath as much as 5 cm of mud. Such burial is common, particularly on steeper slopes where vegetation generally is overridden by extruded mud. Where tags could not be relocated, distances were measured between the two remaining tags (indicated by open parenthesis, Table 1).

The difference between the total widths of surface marker strips over the years gives an indication of the apparent rate of mud boil expansion. For example, tags numbered 135 to 141 were located in a straight line across the middle of mud boil no. 8. The total width increased from 140 to 145.5 cm from 1973 to 1977, representing an expansion of 4% (5.5 cm). These values are typical for those recorded.

Plan views of six mud boils, four located on low angle slopes (<2°) at Victory Lake (mud boils nos. 8, 8A, 10, 11) and two located on higher angle slopes (>6°) at Kaminak Lake (mud boils nos. 5 and 6) are presented in Figure 4. The position of aluminum tags and the areas of expansion or contraction over the period 1973 to 1977 are illustrated. Total expansion values and the percentage of expansion are given for each row of tags.

The morphology of individual mud boils appears to be related to slope angle. Elongate, step-like forms are typical of high angle slopes whereas more subdued and regular circular polygonal patterns are associated with low angle slopes (cf. mud boils no. 10 and 6, Fig. 4).

The level of activity and the rates of displacement are thought to be related to soil texture, moisture content, and slope angle. Although movements in excess of 4 cm were measured at all sites, the most active slopes were in the Victory Lake area where mud boils on slopes of less than 2° expanded by as much as 15 cm over the period of measurement. These high rates of activity result in part from the relative abundance of silt and clay in the red till of the Victory Lake area.

Figure 3. A typical benchmark installation on a bedrock outcrop, used to provide the control for accurate measurement of the vertical and horizontal movement of targets placed on mud boils. (GSC 203165-G)

Plastic Tubes

Nine of the mud boils instrumented with plastic tubing were revisited during the 1977 field season. Five sites were located near Kaminak Lake and four at Victory Lake (Fig. 1). The large rocks that had been placed on top of the tubes as caps were found in place only at one site. The others had presumably been dislodged by high winds or browsing caribou.

At Victory Lake in 1977, water was found in the tubes 33 to 84.5 cm below the ground surface (Table 2). The top of the water columns was 20 to 62 cm above the top of the mud at the bottoms of the tubes, depths greater than expected from the accumulation of precipitation. The water levels are interpreted as local water tables within the mud boils, because the depth to the water table is variable, ranging from 33 to 84.5 cm in two mud boils less than 5 m apart (Table 2, sites 104 and 105).

By 1977 the plastic tubes in the Victory Lake area were found to have been extruded or heaved 12.5 to 54 cm from

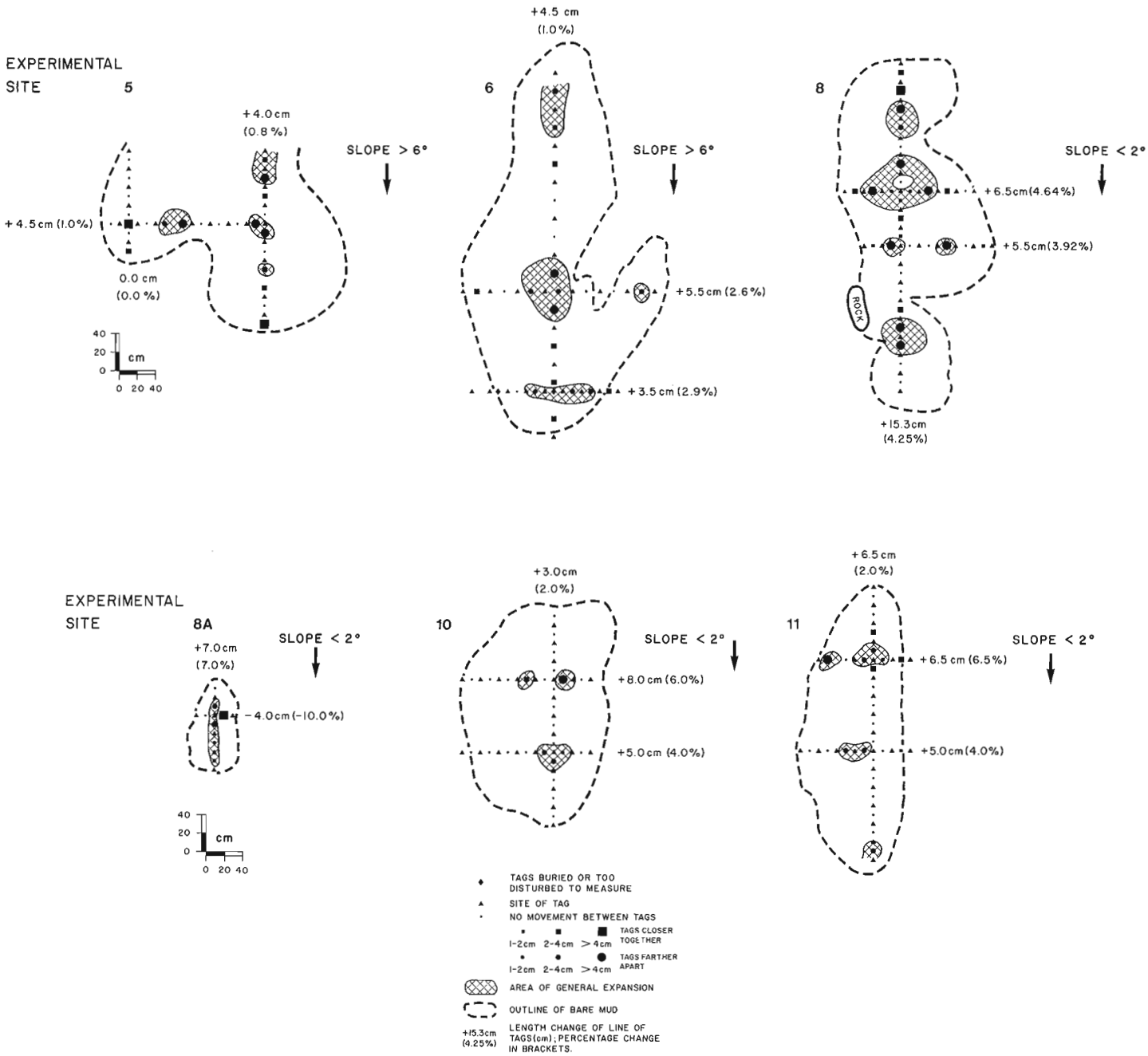

Figure 4. A plan view of mud boils found in the vicinity of Victory and Kaminak lakes. Areas of expansion and contraction are illustrated and values of expansion and percentage of expansion over the period 1973 to 1977 are shown (see text).

their 1973 positions (Table 2). Over the same period mud was forced upward into the space vacated by the tubes, and in some cases mud had intruded several centimetres into the tubes (Table 2). The intrusion of the mud and the ejection of the tube from the mud boils may be synchronous. Considerably greater levels of mud injection were recorded in the tubes at Kaminak Lake in 1977 (up to 32 cm, Table 2) in comparison to those at Victory Lake (up to 6 cm, Table 2).

Summary

The rate of surface activity of mud boils on both high and low angle slopes was more than 4 cm in four years. In some cases surface markers were recovered from beneath 5 cm of mud extruded from injection points in the mud boil. Plastic tubes buried vertically in the centres of mud boils had up to 32 cm of mud injected into them over the same period. It is probable that, in the central Keewatin region, the general downslope movement of mud is accompanied by mud boil activity and is affected by that activity in ways that are as yet poorly understood.

References

Klassen, R.A. and Shilts, W.W.
1977: Uranium exploration using till, District of Keewatin; in Report of Activities, Part A; Geol. Surv. Can., Paper 77-1A, p. 471-477.

Shilts, W.W., Kettles, I.M., and Arsenault, L.
1976: Surficial geology, southeast Keewatin (55E, F, L, 65H); Geol. Surv. Can., Open File 356, legend, maps.

Shilts, W.W.
Nature and genesis of mudboils, Central Keewatin, Canada; Can. J. Earth Sci. (in press)

ROCK WEATHERING FORMS ABOVE CORY GLACIER, ELLESMERE ISLAND, DISTRICT OF FRANKLIN

W. Blake, Jr.
Terrain Sciences Division

Introduction

Early in the 1977 field season, while travelling by helicopter between Makinson Inlet and Coburg Island, a brief stop was made on the plateau to the west of Cory Glacier, southeastern Ellesmere Island (Fig. 1 and 2). W.C. Morgan had noted the presence of tors and deep rock weathering during a landing there earlier in the summer. A revisit was considered imperative because such features had not been reported previously from southern Ellesmere Island. The Cory Glacier area had been reconnoitred by the writer in 1968 and 1970 (Blake, 1975, 1977a), but on those occasions operations with a Piper Super-Cub aircraft restricted landings to the area of raised beaches west of the glacier snout, and the plateau had never been visited.

Relatively little could be accomplished in the time available on July 10th except to gain a general impression of a type of landscape that was most unusual in the author's experience. The purpose of this note is to record the location of this interesting site, to provide some illustrations of the type of features occurring there, and to discuss their implications.

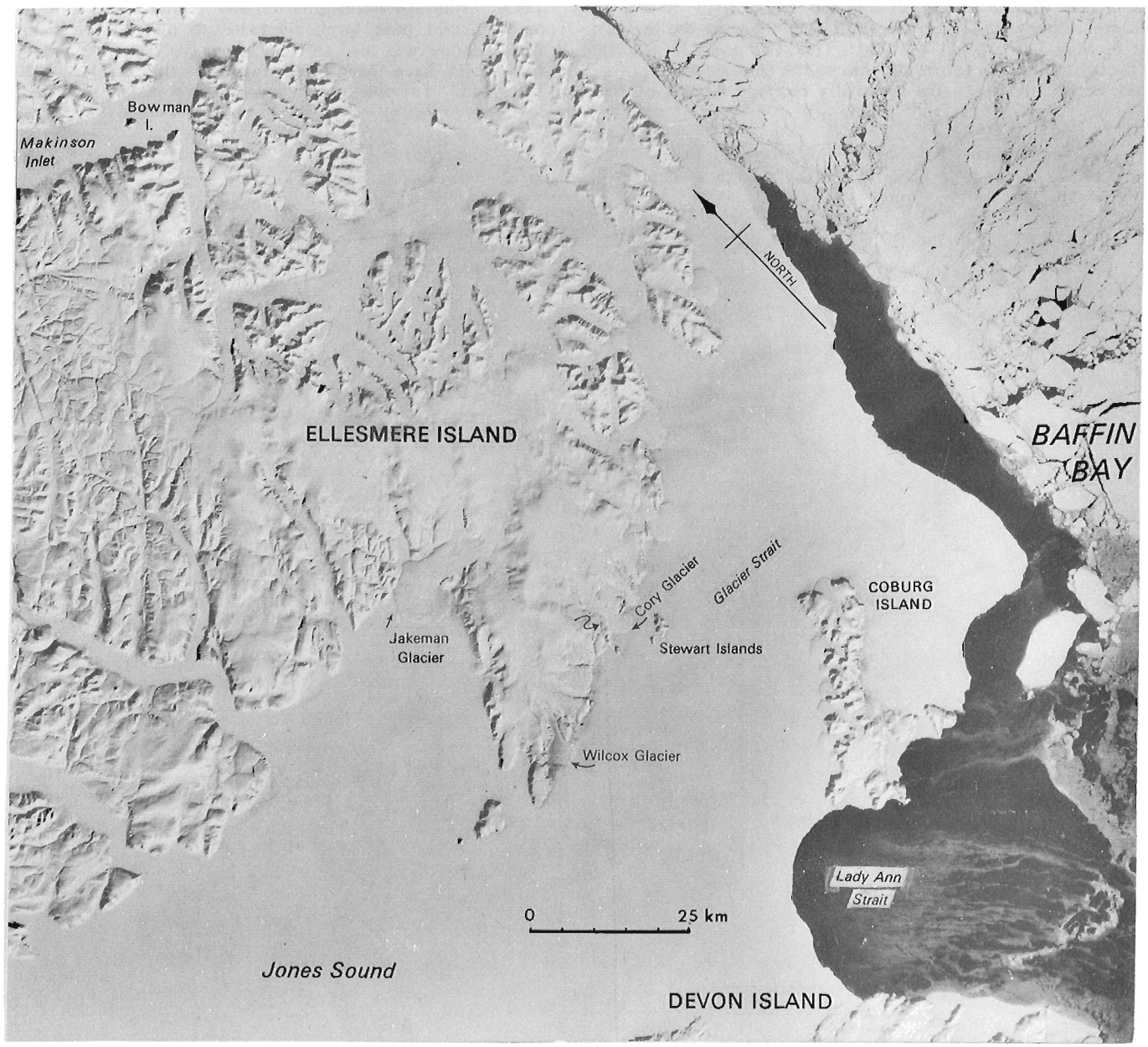

Figure 1. LANDSAT image of southeastern Ellesmere Island showing the location of sites referred to in the text, the extent of present day glaciers, and the development of the North Water on April 26, 1975. The site described in the text is indicated by the arrow to the west of Cory Glacier (image E-11007-17232, spectral band 7).

From: Scientific and Technical Notes in Current Research, Part B; Geol. Surv. Can., Paper 78-1B.

Site Description

The landing site adjacent to the tors was some 415 m a.s.l., according to a determination by stereotope plotter, and the ridge on which the tors are developed rises approximately 60 m above the general level of the plateau surface. The ridge overlooks an unnamed subsidiary tongue of Cory Glacier (Fig. 2). The tors are more than 300 m above the glaciers on either side, although the surface of the ice cap rises above the plateau within a distance of 5 km to the north and west. The tors are developed in a massive, coarse grained, foliated biotite granite.

Figures 3 to 5 illustrate the type of landscape that has developed along this ridge of the plateau. It is obvious that much material has been removed along joints, and many whole blocks have disintegrated. The outcrops are well rounded, deeply weathered, and aprons of grus are ubiquitous. Figure 6 shows a typical large weathering pit. The largest pits attain 15 cm in depth and are more than 30 cm in diameter, dimensions that are similar to those of the largest pits recorded by Sugden and Watts (1977) in gneissic granite on Broughton Island, some 1100 km to the southeast along the coast of Baffin Bay. The generally rounded nature of the rock surfaces and the development of weathering pits is reminiscent, also, of the examples given as being representative of weathering zone I (the oldest) in the Maktak-Quajon-Narpaing Fiord areas of Baffin Island (close to Broughton Island) by Pheasant and Andrews (1972) and Boyer and Pheasant (1974).

Chronology

As reported earlier (Blake, 1977a) the snout of Cory Glacier is now somewhat more extensive than it was 6490 ± 140 years ago (GSC-1170), when organic material was accumulating in a lagoon close to sea level. This deposit is now 10 m a.s.l., and the highest raised beaches attain elevations of more than 50 m. In addition, thick fragments of **Mya truncata** shells, which had washed out of the till where the moraine ridges on the west side of Cory Glacier are breached by the river (Fig. 2) are >37 000 years old (GSC-1223). This age determination shows that some time in the more distant past (probably prior to mid-Wisconsin time), Cory Glacier was also far less extensive than it is today, for the shells have been picked up by the glacier when it advanced. Yet the lateral moraines on either side of Cory

Figure 2. Vertical aerial photograph showing the location of the ridge (black arrow) to the west of Cory Glacier on which the tors and weathering pits shown in Figures 3 to 6 are developed. Photograph A16682-171 taken from an altitude of ca. 9100 m, July 16, 1959. National Air Photographic Library, Department of Energy, Mines and Resources, Ottawa.

Figure 3. General view northward along the granite ridge on which tors are developed west and south of Cory Glacier (visible in middle right distance). Note the disintegrated bedrock and grus aprons in the foreground. On the tor in the background, material has been removed along joints to a depth of at least 4 m. July 10, 1977 (GSC-173351).

Figure 4. View north at another section of the deeply weathered granite ridge shown in Figure 2. Note the rounded form of the outcrops in the foreground and the surrounding aprons of grus. July 10, 1977 (GSC-173343).

Figure 5. More detailed view of weathered granite along the ridge above Cory Glacier. The hammer handle is 33 cm in length. July 10, 1977 (GSC-173341).

Glacier, east of the ridge on which the tors have developed, rise up to 45 m above the present ice surface, indicating that the glacier also has been thicker, probably most recently in post-Hypsithermal time (cf. Koerner, 1977).

Discussion

The type of landscape present above Cory Glacier, characterized by deeply weathered bedrock, stands in marked contrast to exposures in Makinson Inlet and farther north along the east coast of Ellesmere Island where intense action by glaciers has polished and sculptured granite bedrock at similar elevations (Blake, 1977b, 1978). Unless the rates of weathering in southeastern Ellesmere Island are vastly different from those reported, for example, by Dyke (1978) on granitic gneiss from southwestern Cumberland Peninsula, Baffin Island, it seems extremely unlikely that actively eroding ice flowed across this ridge in late Wisconsin time. In fact, it may well be that such an event has not occurred for a much longer period of time; in this connection the reader is referred to Dyke (1976) for a discussion of the development of tors on Somerset Island.

During the last glaciation, or perhaps during several glaciations, ice draining towards the sea was channelled through the valleys on either side of the ridge. The ridge itself may have had only a carapace of relatively thin, cold-based ice, which presumably would not have affected the underlying bedrock surface other than to inhibit further weathering. Despite the fact that Paleozoic rocks outcrop within 13 km to the west-southwest and 24 km to the northwest (Christie, 1962) and that a few dark grey carbonate boulders were noted during a traverse across the moraines on the west side of Cory Glacier in 1968 (although crystalline rocks predominated), no carbonate erratics were noticed among the tors during the course of this brief visit. One fragment of charnockite was discovered, as was a piece of garnet gneiss; these rocks are foreign to the granite, but they may have travelled only a short distance to reach the ridge. The same is true on the summit plateau of the larger of the Stewart Islands, visited briefly on the return trip from Coburg Island. No limestone or dolomite boulders were observed in the vicinity of the landing site, at an elevation of more than 300 m and approximately 4.5 km to the southeast of the snout of Cory Glacier.

Blake (1970, 1975) noted that data relating to the tilt of Holocene shorelines around Jones Sound were in agreement with Pelletier's (1966) hypothesis, based on an analysis of bathymetric information, that a large outlet glacier had drained eastward to Baffin Bay via Lady Ann Strait (Fig. 1). The information presented here with regards to deep weathering on the plateau above Cory Glacier is an indication that, in the Jones Sound region, only Lady Ann Strait was a major drainageway for ice derived from Devon Island and southern Ellesmere Island, as well as from the Innuitian Ice Sheet farther west. The deepest parts of this strait, in the triangle between Wilcox Glacier (Ellesmere Island), Coburg Island, and northeastern Devon Island, attain depths of more than 180 m (Fig. 1). By contrast, a portion of Glacier Strait between the Stewart Islands and Coburg Island is less than 60 m deep; hence this area would have been dry land when sea level was lower during the maximum of any glaciation. Perhaps glaciers such as Cory Glacier, Wilcox Glacier, and those on the northwest side of Coburg Island merely enlarged their expanded-foot lobes, and perhaps the deeper parts of Glacier Strait – i.e., to the northeast and southwest – sustained ice shelves. In any event it seems certain that considerable time has elapsed since actively flowing ice built up in Glacier Strait, or on the highlands to the northwest, to a thickness that was sufficient to inundate ridges such as that west of Cory Glacier where the tors are found.

Acknowledgments

I am indebted to W.C. Morgan, Regional and Economic Geology Division, for drawing my attention to the tors and for providing information on the bedrock. Logistical support during the field season was furnished by the Polar Continental Shelf Project (G.D. Hobson, Director) and by T. Frisch of

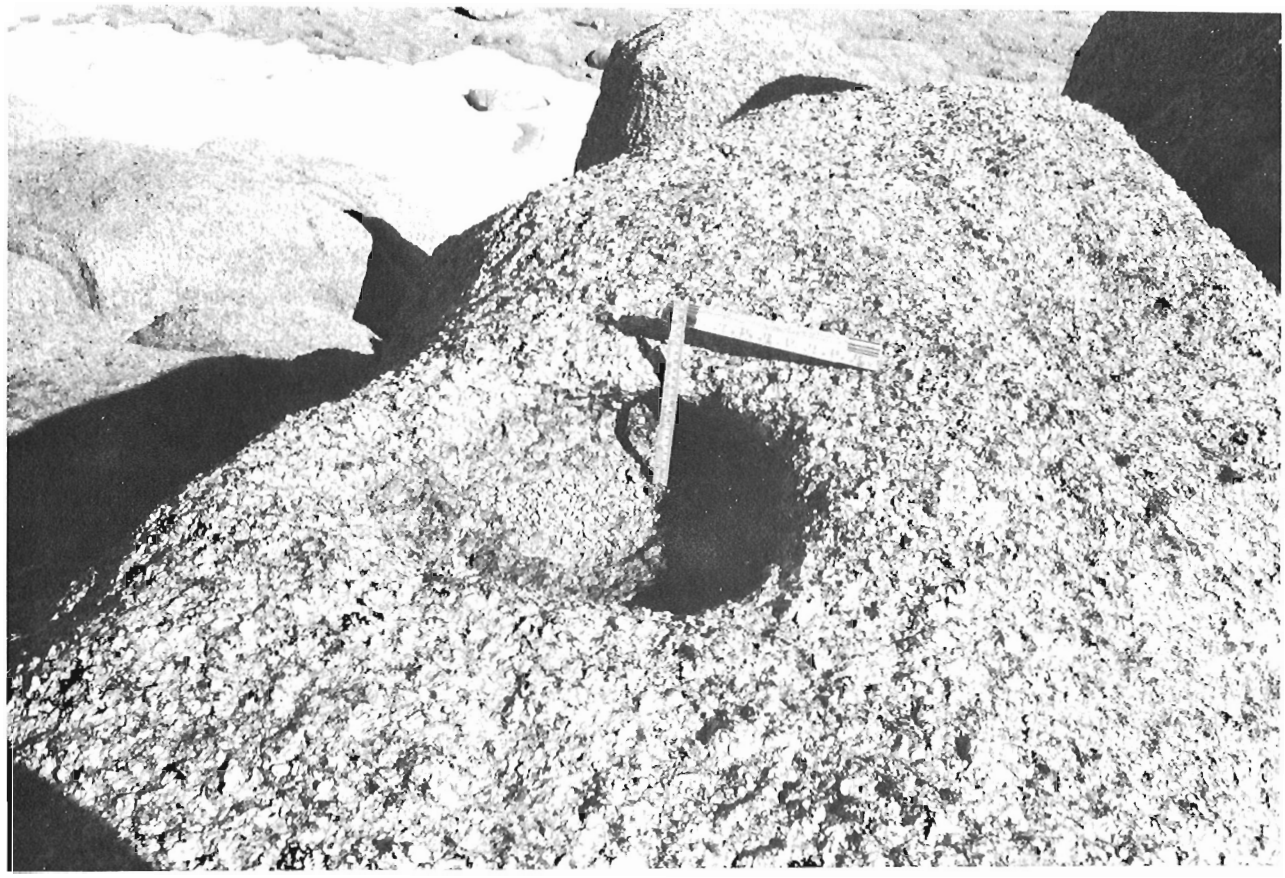

Figure 6. Detail of a weathering pit in the coarse grained granite of the tors. This pit is over 12 cm deep and more than 25 cm in diameter. July 10, 1977 (GSC-173345).

Regional and Economic Geology Division. Mrs. G. Mizerovsky assisted by determining elevations in a stereotope plotting instrument. Comments and suggestions which have helped to clarify various points in the manuscript have been provided by A. MacS. Stalker and R.J. Richardson.

References

Blake, W., Jr.

1970: Studies of glacial history in Arctic Canada. I. Pumice, radiocarbon dates, and differential postglacial uplift in the eastern Queen Elizabeth Islands; Can. J. Earth Sci., v. 7, p. 634-664.

1975: Radiocarbon age determinations and postglacial emergence at Cape Storm, southern Ellesmere Island, Arctic Canada; Geogr. Ann., Ser. A, v. 57, p. 1-71.

1977a: Iceberg concentrations as an indicator of submarine moraines, eastern Queen Elizabeth Islands, District of Franklin; in Report of Activities, Part B; Geol. Surv. Can., Paper 77-1B, p. 281-286.

1977b: Glacial sculpture along the east-central coast of Ellesmere Island, Arctic Archipelago; in Report of Activities, Part C; Geol. Surv. Can., Paper 77-1C, p. 107-115.

1978: Aspects of glacial history, southeastern Ellesmere Island, District of Franklin; in Current Research, Part A; Geol. Surv. Can., Paper 78-1A, p. 175-182.

Boyer, S.J. and Pheasant, D.R.

1974: Delimitation of weathering zones in the fiord area of eastern Baffin Island, Canada; Geol. Soc. Am., Bull., v. 85, p. 805-810.

Christie, R.L.

1962: Geology, southeast Ellesmere Island, District of Franklin; Geol. Surv. Can., Map 12-1962.

Dyke, A.S.

1976: Tors and associated weathering phenomena, Somerset Island, District of Franklin; in Report of Activities, Part B; Geol. Surv. Can., Paper 76-1B, p. 209-216.

1978: Qualitative rates of frost heaving in gneissic bedrock on southeastern Baffin Island, District of Franklin; in Current Research, Part A; Geol. Surv. Can., Paper 78-1A, p. 501-502.

Koerner, R.M.

1977: Ice thickness measurements and their implications with respect to past and present ice volumes in the Canadian High Arctic ice caps; Can. J. Earth Sci., v. 14, p. 2697-2705.

Pelletier, B.R.

1966: Development of submarine physiography in the Canadian Arctic and its relation to crustal movements; in Continental Drift, ed. G.D. Garland; R. Soc. Can., Spec. Publ. 9, p. 77-101.

Pheasant, D.R. and Andrews, J.T.

1972: The Quaternary history of the northern Cumberland Peninsula, Baffin Island, N.W.T.: Part VIII, Chronology of Narpaing and Quajon Fiords, during the past 120,000 years; in 24th Int. Geol. Congr. (Montreal, 1972), Sect. 12, Quaternary Geology, p. 81-88.

Sugden, D.E. and Watts, S.K.

1977: Tors, felsenmeer and glaciation in northern Cumberland Peninsula, Baffin Island; Can. J. Earth Sci., v. 14, p. 2817-2823.

ATV-DRILL PERFORMANCE: A CASE STUDY, FORT SIMPSON, DISTRICT OF MACKENZIE

Mark Nixon
Terrain Sciences Division

Introduction

During late March and April 1977 Terrain Sciences Division and the Department of Geology, University of Alberta took part in a joint project about 40 km south of Fort Simpson, Northwest Territories (Fig. 1). The purpose of the field work was to gather ground ice and groundwater data on a distinctive, widespread organic terrain type in upper Mackenzie Valley.

Drilling through seasonal frost and permafrost into the unfrozen material below was necessary for installation of piezometers and thermistor strings. Holes were located along previously surveyed profiles. Cores were taken, and maintained in the frozen state, in order to log detailed stratigraphy and to provide undisturbed samples for determination of geotechnical properties and ground ice geochemistry.

The ATV-drill (Veillette and Nixon, 1975) used for this drilling and sampling is a light soil auger mounted on a 3 m mast and carried by an eight wheel drive all terrain vehicle (ATV) (Fig. 2). The project provided an opportunity for further evaluation of the equipment.

This report deals with the performance of the ATV-drill and related equipment and the implications for future use.

Site Location and Description

The study area covers less than 1 km^2 of raised peatland and low fen and ponds south of the confluence of Liard and Mackenzie rivers and north of Jean Marie Creek in map sheet 95H (Fig. 1). It is within the southern fringe of the discontinuous permafrost zone (Brown, 1967).

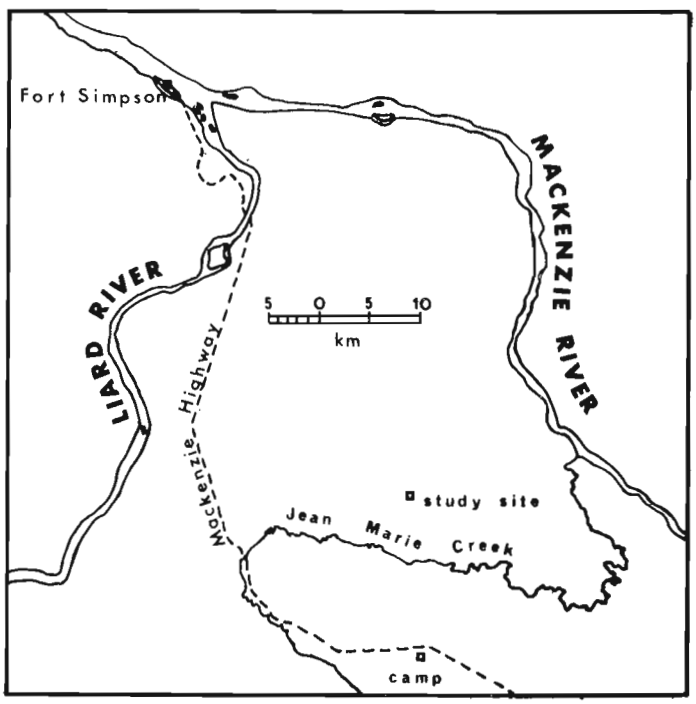

Figure 1. Location map for the study site, south of Fort Simpson, Northwest Territories.

Relief on the glaciolacustrine plain may be more than 3 m and commonly consists of steep banks of raised peat plateaus. The plateau surfaces are irregular with hummocks, closed depressions, and frost fissures. Vegetation is an open spruce wood of generally small trees.

The general stratigraphy of the raised peatland includes up to 3.5 m of peat over glaciolacustrine silty clay. Permafrost extends to a maximum depth of 9 m. In possible collapse structures within the plateaus the peat is thinner and only seasonal frost was encountered.

Access to the site from a camp at the highway was via an overgrown seismic line for 13 km and over frozen ponds and fen for another 5 km. The seismic line crosses two steep beach bluffs and the moderately steep banks of Jean Marie Creek. Across areas of marshy ground, the surface is extremely rough.

Equipment

The ATV-drill was conceived as a self-contained mobile permafrost coring auger for rapid drilling to 3 m depth, but can be used to greater depths, and has considerable drill tool flexibility, including diamond drilling equipment and continuous flight augers.

Two major modifications were tested. A drill head (power and transmission unit) that provided higher torque and lower speed (49 kg-m and 50 rpm) than that originally mounted was employed, and optional snow tracks were fitted over the standard low pressure tires. Modified CRREL core augers (Veillette, 1975a) for 5 and 7.5 cm diameter cores were used. These consist of core barrels with carbide cutters and double helical flights to carry cuttings to the top; they were developed by U.S. Army Cold Regions Research and Engineering Laboratory (Geotest, 1974). A continuous flight auger stem, producing a 7.5 cm diameter hole, also was used.

Figure 2. ATV-drill in drilling position; note the Stihl 4308 drill head (GSC 203314-F).

From: Scientific and Technical Notes in Current Research, Part B; Geol. Surv. Can., Paper 78-1B .

Drilling Results

The maximum depth reached (7.5 cm diameter coring) was 11.6 m; the average depth of 11 holes was 7.6 m. In total 66.9 m of core was taken and 17 m of augering was completed in 8 drilling days. About 70 per cent of the planned drilling was completed. Average drilling and sampling rates indicated that 5 cm diameter cove could be taken to 8 m in just over 3 hours, and 7.5 cm diameter coring could be achieved to the same depth in slightly less than 5 hours. These rates will vary but give a general idea of expected production.

Drill Transport

Evaluation of cold season performance of the ATV-drill was hampered by a dearth of snow and by high temperatures that melted the small accumulation. Despite these factors, some impression of the utility of the tracks was gained. In heavy, wet snow up to 45 cm deep and in lighter snow to 60 cm (both were maximum depths encountered), the tracks provided adequate floatation (Fig. 3). None of the surface conditions, which ranged from light, dry snow to hard packed, wet snow and mud, presented a traction problem for the track equipped vehicle.

Maximum relief on the bog and fen test site is 3.6 m and consists of steep, in places vertical, peat banks bounding raised bogs. In addition, 5 m high, steep, former beach bluffs and the banks of Jean Marie Creek strike across the access route. Parts of the seismic line were overgrown with willow and poplar brush with trunks up to 5 cm in diameter (Fig. 4). Vehicle progress was not impeded by terrain or vegetation.

When the site profiles were surveyed the previous summer, a path was cleared for passage of the ATV-drill. Because a deeper snow cover was anticipated, many stumps protruded up to 30 cm; although high amplitude microrelief features such as these have been specifically identified by the vehicle manufacturer as hazardous to the vehicle tracks, no failure occurred.

Given the various snow conditions and terrain and vegetation types described, the ATV proved to be as fast and manoeuverable as the motorized toboggans used for daily transport. It was far superior to the snowmobiles in terms of personnel comfort over hummocky surfaces and through brush.

Useful fuel consumption was impossible to determine because of an erratic fuel system problem in the engine. The manufacturer gives a figure of 17 km/L for average conditions.

Figure 3.

ATV-drill in transport position; the arrow points to the snow tracks (GSC 203314-E).

Problems

Only one problem arose during use of the CRREL augers. Ice ring buildup on the core barrel shoe (bottom of barrel) stopped penetration in frozen peat. Ice and organic material accumulated around the cutters and adhered to the face of the shoe so that the cutting edges did not contact the peat. Slow rotation of the drill tool did not generate enough frictional heat to melt the ice, but by increasing and maintaining initial feed (pressure on the drill tool) the cutters were forced into the bottom of the hole and the problem was alleviated.

Flight augers were used when undisturbed samples and close stratigraphic control were not required. With the limited feed and bit types available they were not effective in fine grained or organic frozen materials. Coring through the frozen zone was found to be faster than use of the flight augers.

A more serious problem appeared when continuous flight augers were used in closed depressions not underlain by permafrost. Peat and clay situated below the seasonally frozen peat were saturated and fluid. As plastic clay cuttings moved up the auger flights into a zone of unfrozen, nearly liquid peat, they accumulated and expanded below the rigid section of hole in frozen surface peat and made hoisting extremely slow and difficult. Time taken to remove the tools increased the probability that the wet material would swell or flow into the borehole. Usually this problem meant that the target depth for instrumentation was not achieved even though drilling had proceeded well beyond it. Casing of the hole would solve the problem but this may not be practical for very light operations. Possibly a larger hole drilled through the frozen material would relieve the constriction.

Discussion

The drill head, identical to that used on the Stihl 4308 earth auger (Veillette and Nixon, 1976), had not been tested on the ATV-drill in frozen ground. A considerable potential was indicated by previous trials to 9 m depth in stiff clay of Ottawa Valley, Ontario and by extensive use in the Arctic as a hand held auger to 6 m depth.

Performance and reliability during spring 1977 were generally excellent, although the slow rotation – normally a distinct advantage in frozen materials (Veillette, 1975, p. 425) – may have contributed to the formation of ice rings on the barrel shoe. It has been observed, however, that frozen clays in the discontinuous permafrost zone may be sensitive to disturbance by rotating drill tools. High unfrozen water contents and relatively high ground temperatures result in rapid liquification of some materials. Success in drilling the clays at the test site can be attributed, in part at least, to the very slow rotation of the drill tools.

Figure 4.

ATV-drill passing through brush on the access route (GSC 203314-G).

Previous testing of the ATV-drill in frozen ground was limited to use of the CRREL equipment to a depth of 3 m in marine silts of northern Somerset Island, Northwest Territories; flight augers to 3 m in stony fill and rubble at Resolute Bay, Northwest Territories; and N size diamond core barrel (drillhole diameter 7.62 cm) to 2.5 m in sand and gravel at Resolute Bay (Veillette and Nixon, 1975). The drill was used with flight augers to drill organic materials, sand, and clay to a maximum depth of 20 m in Ottawa Valley, Ontario (P.B. Fransham, pers. comm., 1976). Successful drilling of frozen peat and silty clay to depths of more than 9 m in the warmer permafrost of the discontinous zone increases the range of material types investigated with the ATV-drill.

Part of the research program involved installation of piezometers below permafrost, which required drilling at least 1 m into unfrozen silty clay. The lower boundary of a permafrost body is gradational, and coring commonly continued into the unfrozen zone. Although samples of unfrozen clay certainly were disturbed by torsion that twisted the core into a tight helix, the barrel continued to perform well in this material. The major manufacturer of CRREL coring augers clearly specifies their use in snow, ice, and fine grained frozen soils (Geotest, 1974, p. 99), and experience has indicated that use in unfrozen material is often unsatisfactory. Perhaps in this case a combination of texture and moisture content produced a cohesion compatible with CRREL auger function. Beak Consultants Ltd., Calgary report some success from modifications to CRREL barrels to allow their use in unfrozen unconsolidated material (W.J. Stephen, pers. comm., 1977).

Drill production figures must be viewed in light of the nature of the study and the limited manpower (2 man crew). It was necessary to install piezometers and thermistor strings as work progressed which reduced drilling efficiency. Nevertheless, the fact that only 70 per cent of the planned drilling was completed can be attributed in large part to the mild weather and the scarcity of snow. Access to the site became increasingly difficult and with the failure of ice on Jean Marie Creek, the project was terminated. Maintaining the core in a frozen state required considerable time and effort.

The scarcity of snow did not permit thorough testing of the track equipped vehicle for winter use, but performance indicated that normal snow conditions and most brush vegetation would present no significant obstacle to mobility. Negotiation of steep, slippery slopes and hummocky terrain reinforced previous indications that the ATV maintains exceptional traction and stability on steep slopes and over rough ground.

Conclusions

The outstanding feature of the ATV-drill is its light weight mobility. Performance on this project has demonstrated its main advantages of inexpensive positioning and rapid, convenient movement on site. Helicopter support to move a drill from borehole to borehole at this small site would have been more expensive and less efficient and flexible than using the ATV carrier.

Although considerable time was spent in sampling and instrumentation, drilling rates of 1.7 holes per day averaging 7.6 m per hole were achieved. This is more than twice the production of a similar site study on the Involuted Hill near Tuktoyaktuk, Northwest Territories (Annan et al., 1975) and supports previous observations suggesting that a small drill with relatively low torque can produce results in permafrost, both in terms of depth and sampling capability, that may be of use for a wide range of investigations.

Manual feed and hoisting are limiting factors, especially considering the greater depth of drilling required by this project. The recently completed conversion to hydraulic functions with increased capabilities should markedly improve the efficiency of this machine and allow a safer operation by providing closer control and reducing personnel fatigue.

Acknowledgments

The author would like to recognize the tolerance and extra effort of staff at Technical Field Support Services in Hull and District Supply Office, Calgary during preparation for and following field work. Able site direction and assistance with drilling were provided by S. Chatwin, University of Alberta, Edmonton. The manuscript was read and useful suggestions were offered by J.J. Veillette, P.B. Fransham, and S. Chatwin.

References

Annan, A.P., Davis, J.L., and Scott, W.J.
1975: Impulse radar profiling in permafrost; in Report of Activities, Part C; Geol. Surv. Can., Paper 75-1C, p. 343-51.

Brown, R.J.E.
1967: Permafrost in Canada; Geol. Surv. Can., Map 1246A; Natl. Res. Counc. Can., Div. Bldg. Res., Publication No. NRC 9769.

Geotest Instrument Corp.
1974: Ice, snow and permafrost testing equipment; Geotest Instrument Corp., Bull. 274 ISP, Illinois, p. 99-107.

Veillette, J.
1975: Modified CRREL ice coring augers; in Report of Activities, Part A; Geol. Surv. Can., Paper 75-1A, p. 425-26.

Veillette, J.J. and Nixon, F.M.
1975: A modified ATV-drill for shallow permafrost coring; in Report of Activities, Part C; Geol. Surv. Can., Paper 75-1C, p. 323-24.

1976: Permafrost coring equipment; in Report of Activities, Part A; Geol. Surv. Can., Paper 76-1A, p. 269.

INDICATIONS OF NEOGLACIERIZATION ON SOMERSET ISLAND, DISTRICT OF FRANKLIN

Arthur S. Dyke
Terrain Sciences Division

Two well known types of evidence document expansion of glaciers and semipermanent firn or thin ice caps in the Canadian Arctic during the Little Ice Age, i.e. the last 500 years. These are the presence of ice-cored moraines downice from active glaciers (cf. Denton and Karlén, 1973; Miller, 1973) and the occurrence of areas of "lichen kill" – areas of restricted lichen cover. The latter is especially evident on Baffin Island (Ives, 1962; Locke and Locke, 1977) where such areas have been shown to mark the locations of extensive thin snow or ice fields that accumulated about 300 to 350 years ago; smaller areas have been mapped in northern Labrador (Andrews et al., 1975). From maps of former snowbanks, Neoglacial snowline elevations, an important parameter in the reconstruction of the climate of that period, can be determined. Mapping of Neoglacial snow and ice cover is important also because such glacierization likely is an analogue for the inception of a full-scale glaciation (Andrews et al., 1975). Indeed, such data have been used in experimental computer modelling of the inception and growth of the Laurentide Ice Sheet (Andrews and Mahaffy, 1976; Barry et al., 1975).

Lichen-kill areas, as well as miniature eskers and meltwater channels, indicate neoglacierization of parts of Somerset Island. These are the subject of this note.

Lichen-kill Areas

Extensive areas of Somerset Island are nearly free of lichens and vegetation. For the most part, however, this is not attributable to neoglacierization. About half the island is underlain by limestones and dolostones and supports few lichens, bryophytes, and vascular plants because of its inherent toxicity and/or lack of nutrients. Hence, if that area was extensively snow covered during the Neoglacial, no evidence in the form of lichen-kill could have been left.

On the southern peninsula of the island, gneissic bedrock is masked extensively by till. Over several hundred square kilometres the active layer of the till is mobile because it is saturated beyond its liquid limit. The result of this is a nearly unvegetated surface, but again not because of neoglacierization. Other smaller areas underlain by gneissic bedrock in the northwest quarter of the island are almost lichen-free due to high active layer mobility.

One 30 to 40 km^2 "lichen-free" summit area (location A, Fig. 1; Fig. 2), however, is underlain by gneissic bedrock and cannot be explained in terms of active layer processes, soil toxicity, or any other obvious characteristic. It does not support late-lasting snowbanks today. Apart from its lichen-free nature, it appears identical to surrounding terrain. One must conclude, therefore, that it has not been available for colonization for as long as the surrounding terrain. In other words, until recently it was snow or ice covered.

Numerous much smaller lichen-free areas occur along the escarpments of cryoplanation terraces (Fig. 3) which are common features in the vast tor-dotted areas of the gneissic plateau (Dyke, 1976) and are the sites of late-lasting snowbanks today. This indicates that during the Little Ice Age much larger snowbanks lasted throughout the summer.

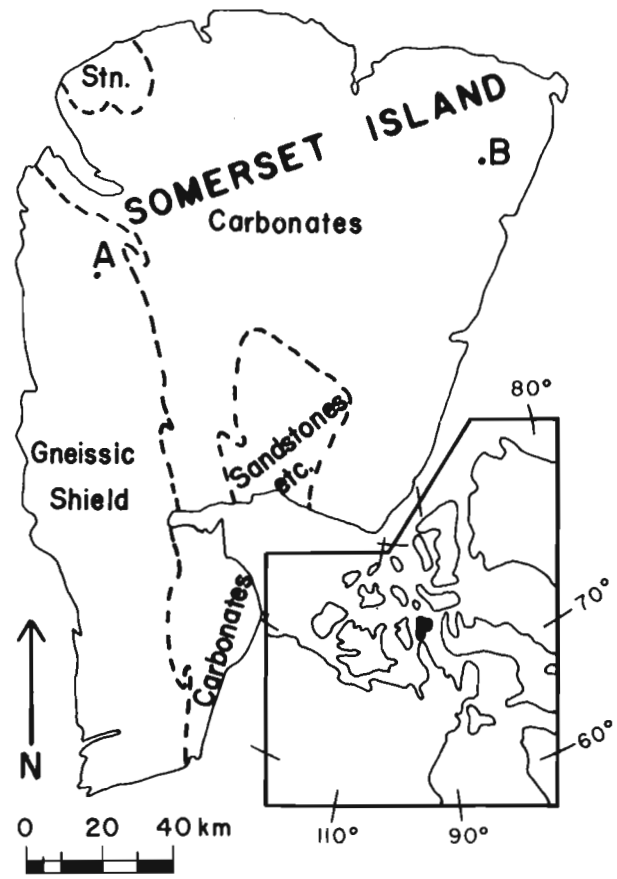

Figure 1. A map of Somerset Island showing the major bedrock units and the locations of Neoglacial features (A and B) discussed in the text.

Meltwater Features

Near the northeastern corner of the island evidence of two Neoglacial ice caps is in the form of tiny lateral and subglacial meltwater channels and eskers (location B, Fig. 1; Fig. 4). Two eskers at the point indicated by the arrow in Figure 4 extend across an ice-filled minor gully, and the gravels overlie the ice. The site was inspected in August 1977. The bedrock exposed in meltwater channels is essentially unweathered, which is different from usual outcrops of carbonates elsewhere on the island. The lack of chemical weathering and the fact that the eskers postdate not only the minor gully but also the ice that fills it indicate that they date from a very recent period such as the Neoglacial when climate was more severe than at present.

In this vicinity about ten glaciers, some of which are 30 m or more thick, survive today on the walls of deep canyons (Fig. 4). These exist because of enhanced accumulation of snow in the canyons by wind drift and protection from ablation by shadowing by the adjacent canyon walls. They have caused little, if any, sculpture of the canyons, and hence are essentially inactive or cold based. The pattern of eskers and channels indicates that the Neoglacial ice caps retreated to stagnant ice plugs in the canyons. Maps of older meltwater features (Craig, 1964; Netterville et al., 1976) indicate that larger former ice caps retreated in a similar fashion.

From: Scientific and Technical Notes in Current Research, Part B; Geol. Surv. Can., Paper 78-1B .

Paleoclimatic Implications

The lichen-kill area (location A, Fig. 1) is centred on a summit at 405 m elevation; the margin of the area, the edge of the former snowbank, lies at about 335 m elevation. Both former ice caps (location B, Fig. 1) occupied the plateau surface at 335 m elevation. Thus, at these sites the Neoglacial snowline on northern Somerset Island was at about 335 m, although large areas of the island above this elevation do not appear to have been glacierized. The three sites in question, for some reason, must have had relatively enhanced snow accumulation, although they are by no means topographically favoured.

Miller et al. (1975) placed the modern glaciation level (the level above which most summits should be ice covered) over northwestern Baffin Island and southwestern Devon Island at 400 to 500 m with the 400 m isoline curving across Barrow Strait towards Somerset Island. This is not much above the Neoglacial snowline elevation. On north-central Baffin Island the paleoglaciation level, calculated from maps of lichen-kill areas, varies from 500 m west of the axis of the island to 800 m over the east coast fiord terrain; the majority of lichen-free terrain lies between 450 and 600 m elevation (Locke and Locke, 1977). Somerset Island data, although sparse, indicate a decline of the paleoglaciation level northwestward from Baffin Island. They also indicate that the high plateau surface is glacialogically sensitive to relatively short-term variations of the present interglacial climate.

Acknowledgments

Logistical support for field work was provided by the Polar Continental Shelf Project, Department of Energy, Mines and Resources. The manuscript was read by S.A. Edlund, D.R. Grant, and R.J. Fulton.

Figure 2.

Low-angle aerial view of the "lichen-free" summit area on northwestern Somerset Island (location A, Fig. 1). The dark patches are lichen covered and projected through the former snowbank. View is northwestward with Aston Bay in the background. GSC 203014-K.

Figure 3.

Low-angle aerial view of "lichen-free" areas (light patches) and late-lasting snowbanks along escarpments of cryoplanation terraces on the gneissic plateau of west-central Somerset Island. The middle ground is about 3 km wide. GSC 203014-L.

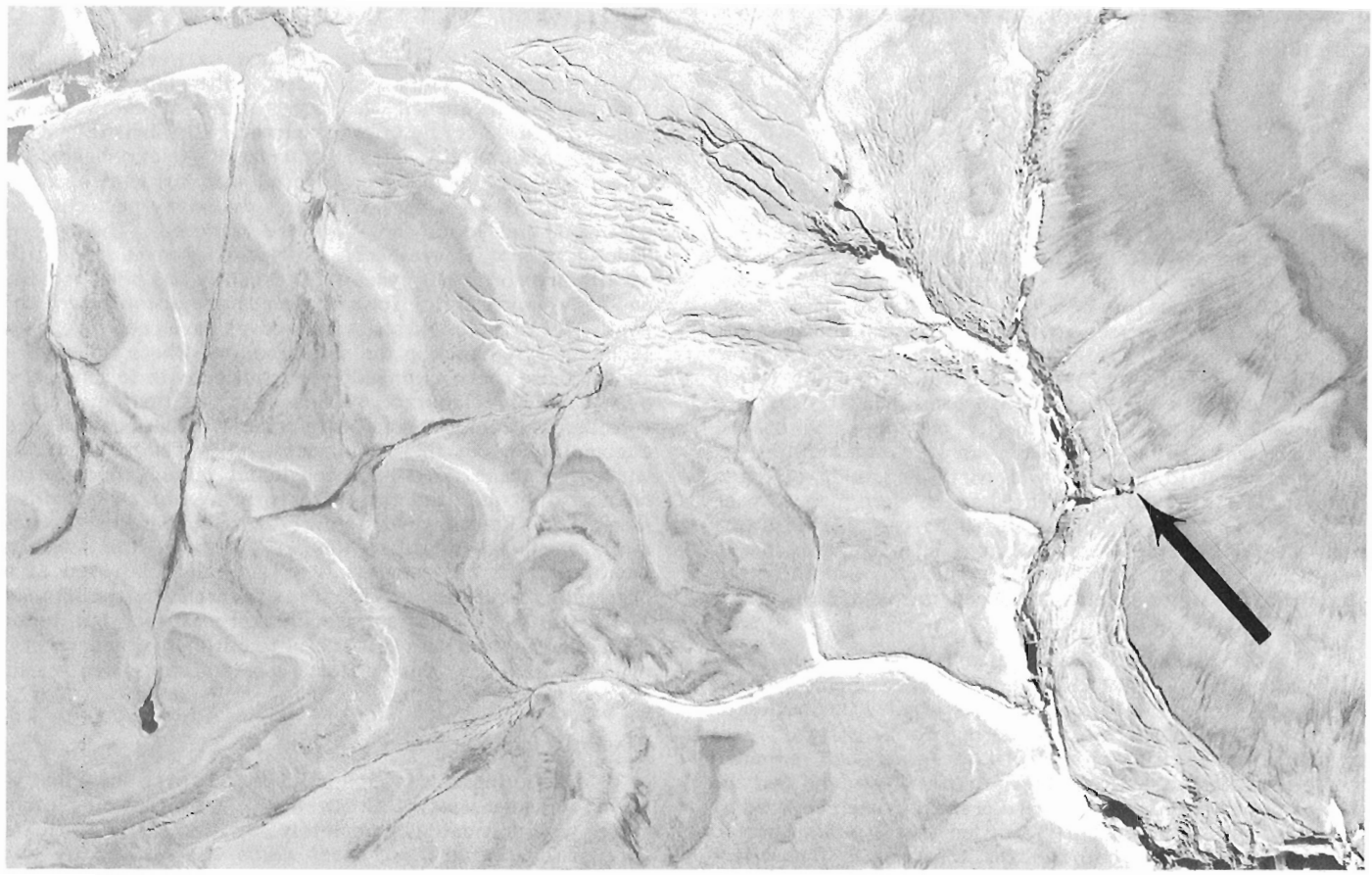

Figure 4. An enlargement of a part of airphoto A16331-149 (National Airphoto Library, Canada) showing the larger of the two areas of miniature meltwater channels and eskers at location B, Figure 1. The arrow indicates the location of two eskers which cross an ice-filled gully. The larger white features are cold-based glaciers occupying canyons, and the body of water in the upper left-hand corner is a small proglacial lake. The field of view is about 5 km wide.

References

Andrews, J.T., Barry, R.G., Davis, P.T., Dyke, A.S., Mahaffy, M., Williams, L.D., and Wright, C.
1975: The Laurentide Ice Sheet: problems of mode and speed of inception; World Meteorol. Org., Pub. No. 421, p. 87-94.

Andrews, J.T. and Mahaffy, M.A.
1976: Growth rate of the Laurentide Ice Sheet and sea level lowering (with emphasis on the 115,000 B.P. sea level low); Quat. Res., v. 6, p. 167-184.

Barry, R.G., Andrews, J.T., and Mahaffy, M.A.
1975: Continental ice sheets: conditions for growth; Science, v. 190, p. 979-981.

Craig, B.G.
1964: Surficial geology of Boothia Peninsula and Somerset, King William, and Prince of Wales Islands, District of Franklin; Geol. Surv. Can., Paper 63-44, 10 p.

Denton, G.H. and Karlén, W.
1973: Holocene climatic variations: their pattern and probable cause; Quat. Res., v. 3, p. 144-205.

Dyke, A.S.
1976: Tors and associated weathering phenomena, Somerset Island, District of Franklin; in Report of Activities, Part B; Geol. Surv. Can., Paper 76-1B, p. 209-216.

Ives, J.D.
1962: Indications of recent extensive glacierization in north-central Baffin Island, N.W.T.; J. Glaciol., v. 4, p. 197-205.

Locke, C.W. and Locke, W.W. III
1977: Little Ice Age snow-cover extent and paleoglaciation thresholds: north-central Baffin Island, N.W.T., Canada; Arct. Alp. Res., v. 9, p. 291-300.

Miller, G.H.
1973: Late Quaternary glacial and climatic history of northern Cumberland Peninsula, Baffin Island, N.W.T., Canada; Quat. Res., v. 3, p. 561-583.

Miller, G.H., Bradley, R.S., and Andrews, J.T.
1975: The glaciation level and lowest equilibrium line altitude in the high Canadian Arctic: maps and climatic interpretation; Arct. Alp. Res., v. 7, p. 155-168.

Netterville, J.A., Dyke, A.S., and Thomas, R.D.
1976: Surficial geology and geomorphology of Somerset and northern Prince of Wales Islands; Geol. Surv. Can., Open File 357, 5 photomosaic maps at 1:125 000 scale.

GLACIAL HISTORY OF AND MARINE LIMITS ON SOUTHERN SOMERSET ISLAND, DISTRICT OF FRANKLIN

Arthur S. Dyke
Terrain Sciences Division

Introduction

The question of the extent of Laurentide and local ice masses and the age of the major glacial features on Somerset Island has proven difficult to answer. Jenness (1952) considered that northeastern Somerset Island had never been touched by Laurentide ice, whereas the western and southern parts may have been. Craig and Fyles (1960) made a similar distinction, but following additional field work Craig (1964) concluded that the whole island had been inundated by late Wisconsin Laurentide ice, primarily on the basis of the ubiquitous distribution of gneissic erratics. Laurentide ice was considered to have flowed northward and retreated southward. A few easterly oriented striae were mapped near the west coast and were interpreted as probably resulting from "lateral movement adjacent to a late tongue of ice in Peel Sound" (Craig, 1964, p. 5). This is essentially the interpretation which seems favoured today (Prest, 1969; Bryson et al., 1969; CLIMAP, 1976).

In 1975 the author was a member of the field party which mapped the surficial geology of Somerset Island (Netterville et al., 1976a); on the basis of the distribution of tors and other advanced weathering forms, Dyke (1976) suggested that significant areas of the island had remained ice free throughout at least the late Wisconsin (and perhaps the whole Wisconsin) or that these areas had been covered by cold-based ice. Subsequently, Sugden (1976) has supported the cold-based ice hypothesis for the area. The writer returned to the island in 1977 in an attempt to clarify the major elements of the glacial history. The most definitive data have come from the southern part of the island (Fig. 1) and are the subject of this paper.

Two distinct terrains, one of glacial and one of nonglacial character, are recognized. Within the glacial terrain two sets of marine limit features are mapped and dated. The older marine limit was formed upon deglaciation, and the younger apparently by a transgression in an ice-free area.

Nonglacial Terrain

The gneissic terrain, which northwest of Creswell Bay lies higher than approximately 330 m (Fig. 1), is characterized by broad valleys and summits and a well integrated drainage system with a virtual absence of lakes. The summits have a felsenmeer and grus cover which is interrupted by tors; the hillslopes have cryoplanation terraces with felsenmeer and grus cover, and the valleys are choked with vast soliflual accumulations of fines, the source of which is upslope grus. In short, this landscape is the product of long continued denudation, planation, and megascale slope sorting by periglacial processes (Fig. 2, 3). During two days of foot traversing in this terrain no erratics or other signs of glaciation were found. Farther north in a similar landscape, however, Dyke (1976) reported the presence of a few highly weathered limestone erratics; thus it is likely that at some time the area, along with the remainder of the island (Netterville et al., 1976b), was inundated by an ice sheet. Indeed, this nonglacial terrain may be a relict from preglacial time having survived under a series of nonerosive Quaternary ice sheets. This is the interpretation invoked for many similar areas in Scotland, Greenland, and Canada by Sugden (1968, 1974) and Sugden and Watts (1977). The processes that have shaped the terrain, however, are active today, and this makes it difficult to accept the "pre-glacial relict" hypothesis.

Glacial Terrain

There is a profound difference between the terrain discussed above and the remainder of the map area (Fig. 1). The boundary between the two terrain types is sharply deliniated at 330 m by lateral meltwater channels (Fig. 1, 4). On the proximal side of the boundary, gneissic bedrock is ubiquitously ice moulded or covered with till with abundant and easily recognized erratics, drainage patterns are deranged, and ponds and lakes are numerous. The gneissic bedrock is not unweathered as glacial grooves and striae usually are found only where till recently has been removed and heavy-mineral rich folia commonly are disintegrated to a depth of 2 to 3 cm. No striae or grooves have been mapped on sedimentary bedrock in the map area, and where till cover is absent these rocks commonly are mantled with felsenmeer or a silty rubbly diamicton produced by weathering. Thus, a considerable amount of postglacial weathering has been accomplished, but this is miniscule when compared to that which has occurred on the nonglacial terrain. Because the boundary between the two differently weathered terrains is marked by ice-marginal features, these features probably mark a glacial limit. If this is the case, the advanced weathering of the nonglacial terrain might be used as an argument that it has been ice free at least since the Illinoian. The data below substantiate this proposition, but before discussing the age data it is useful to outline the general style of glaciation as this differs substantially from earlier concepts.

Glaciation and Recession

Till flutings and glacial grooves and striae show that the area south and west of Creswell Bay and Stanwell-Fletcher Lake was inundated completely by an eastward-flowing foreign (Laurentide?) ice sheet which was sufficiently thick to overtop the highest summits (ca. 500 m) without noticeable topographic channelling of flow (Fig. 1). This flow direction is also spectacularly recorded by large fiords and U-shaped troughs such as Fitz Roy Inlet (Fig. 5). The pervasive eastward flow requires a significant ice dispersal area west of the island rather than to the south as suggested by earlier workers.

The ice sheet thinned northward as indicated by efficient topographic channelling of flow in the Stanwell-Fletcher Lake area and by the above mentioned trimline at 330 m marking the limit of glacial erosion and deposition. North of the head of Creswell Bay, southward oriented roches moutonnée and meltwater channels indicate that the foreign ice coalesced with a local ice cap situated east of the nonglacial terrain. Obviously, only part of the local ice cap features has been mapped on Figure 1. Other areas with meltwater channels (Craig, 1964; Netterville et al., 1976a) indicate that the ice cap may have covered much or all of the northeastern carbonate plateau.

The nested side-hill meltwater channels show that a lobe of ice retreated northwestward in the Stanwell-Fletcher Lake area and that the local ice cap retreated generally northward with ice remaining in broad shallow valleys later than on interfluves.

Pre-Holocene Marine Sediments

As the ice retreated from Creswell Bay, deltaic sediments were deposited at the mouths of meltwater channels, some of which are presently dry or carry misfit streams. The highest such delta lies at 205 m a.s.l. at the head of Creswell Bay.

On the north side of Creswell Bay, near its mouth, a delta whose top is at 180 m a.s.l. occupies the headwaters of the modern drainage system (Fig. 1, 6). The delta overlies sandstone bedrock but its topset gravels contain numerous

From: Scientific and Technical Notes in Current Research, Part B; Geol. Surv. Can., Paper 78-1B .

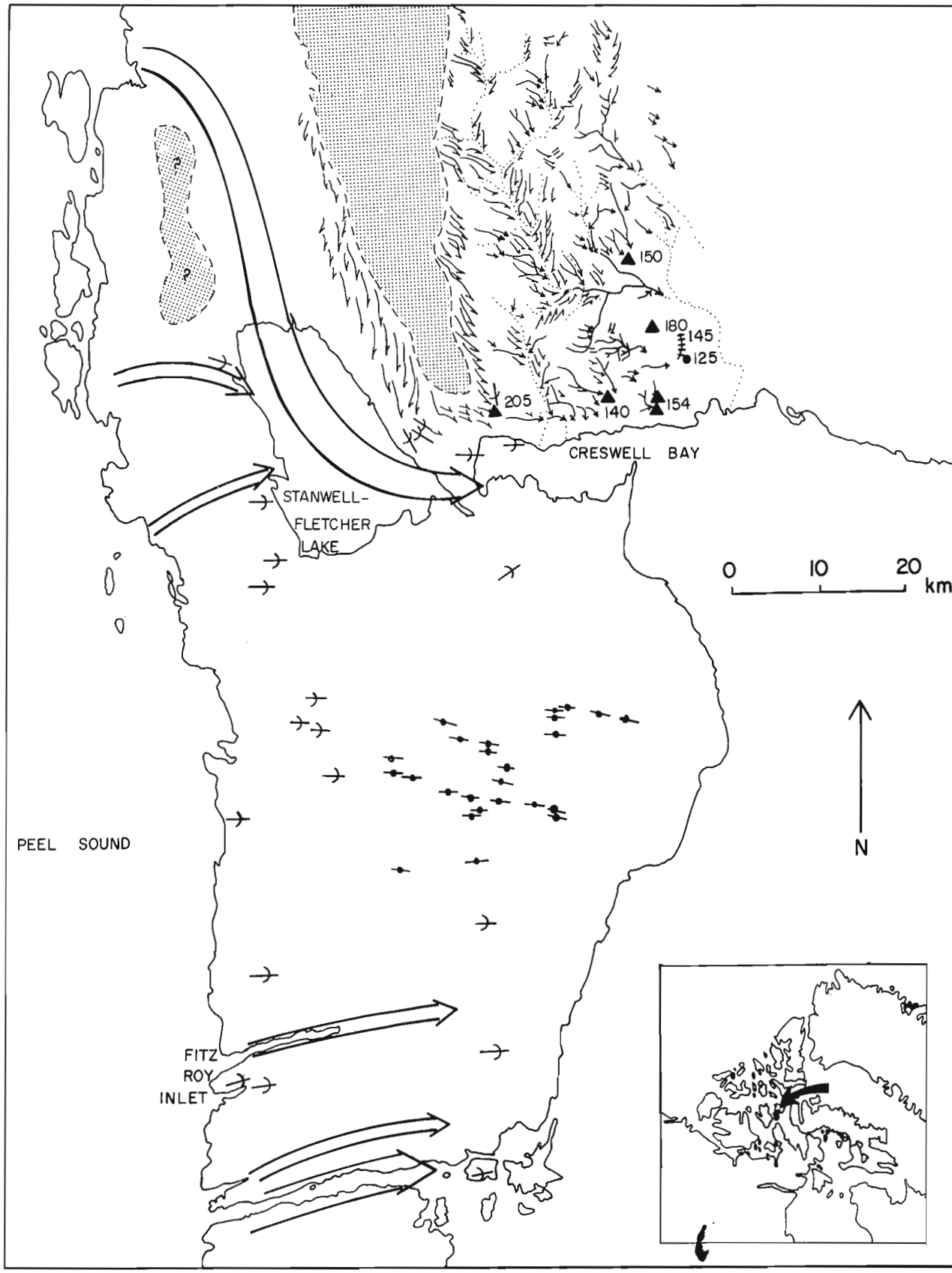

Figure 1. A map of southern Somerset Island showing nonglacial terrain (dotted areas), lateral meltwater channels (arrows with single barbs which indicate the down-ice side), subglacial meltwater channels (arrows with double barb), glacial grooves and striae (arrows with crescentic barbs), flutings in till (shafts with dots), fiords and troughs (large open arrows), pre-Holocene marine deltas (black triangles), a pre-Holocene marine beach (hachured line), a delta marking the Holocene marine limit (black dot), and the elevations of raised marine deposits in metres (numbers beside symbols).

Figure 2.

Ground view of a summit in the nonglacial terrain. The dominant features are felsenmeer (foreground) and tors (on skyline). GSC 203014-Q.

Figure 3.

Ground view of the headwaters of a broad valley in the nonglacial terrain. The valleys are being filled with large soliflual accumulations consisting mainly of sand and finer material derived from grus on the surrounding slopes. GSC 203014-N.

Figure 4.

Low angle aerial view of lateral meltwater channels (snow-filled linear depressions) in gneiss just east of the nonglacial terrain north of Creswell Bay. GSC 203014-R.

Figure 5.

Low angle aerial view eastward along Fitz Roy Inlet. The sidewalls are about 300 m high. GSC 203014-T.

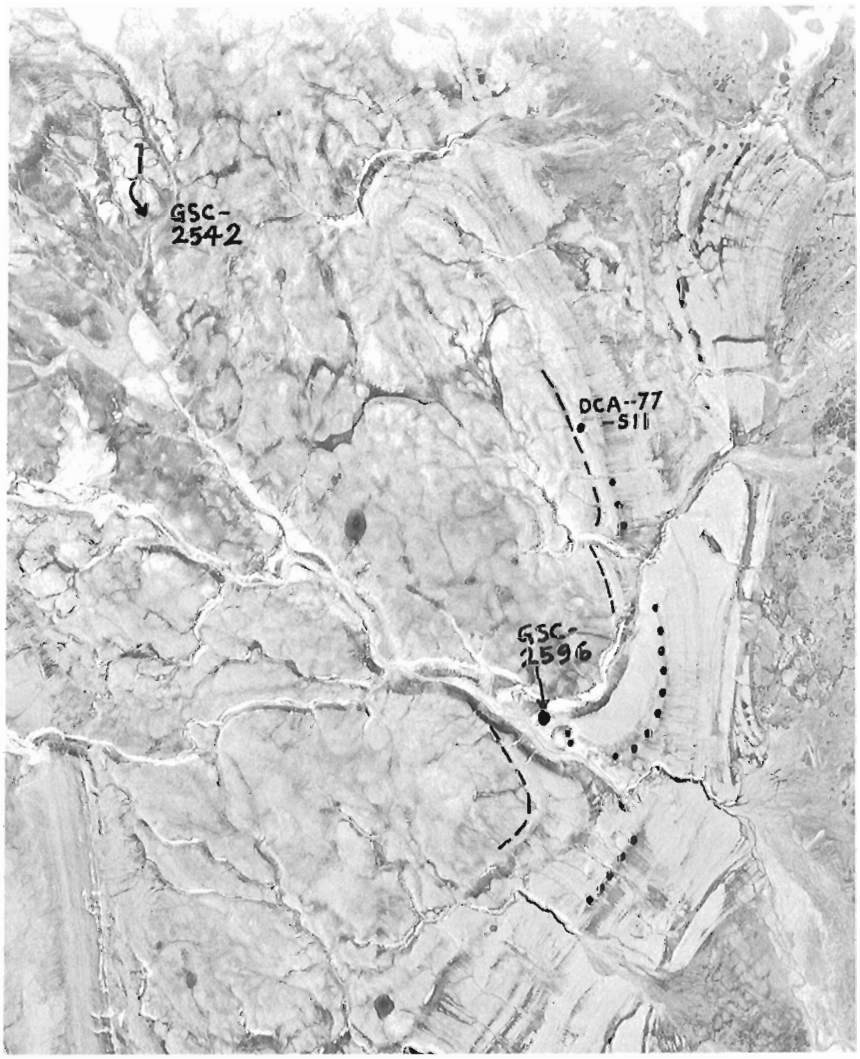

Figure 6.

Part of airphoto A16080-104 (National Airphoto Library, Canada) showing features and sample sites in an area north of the mouth of Creswell Bay. Site 1 is a delta whose top is 180 m a.s.l. The arrow near it locates the collection site of the wood dated at >38 000 years old (GSC-2542). The broken line marks the highest beach ridge at 145 m a.s.l.; DCA-77-S11 is a shell sample from this beach. The dotted line marks a wave-cut notch at 125 m a.s.l.; GSC-2596 is a shell sample from this level. Scale is approximately 1:60 000.

granitic boulders. These could have been transported either from the shield of western Somerset Island by the foreign ice or from the conglomerate facies of the local bedrock, which outcrops 3 km west of the delta, by the local ice cap. Their well rounded nature favours the latter as the source.

Splintered wood identified as spruce by L.D. Farley-Gill (GSC Wood Identification Report 77-43) but as Siberian Larch by H. Zalasky (Northern Forest Research Centre, Department of Fisheries and Environment, Edmonton) was collected from the eroded slope of this delta at 160 m a.s.l. and was dated at >38 000 years (GSC-2542). The wood could only have moved down from its original position of deposition. Hence, assuming the material is driftwood, it relates to a relative sea level stand higher than 160 m.

The highest beach gravels in this area form a distinct line at 145 m a.s.l. (Fig. 6). A large sample (DCA-77-S11) of **Hiatella arctica**, consisting mostly of whole valves, was collected from an area of a few square metres on the foreslope of the highest beach ridge. The shells were abundant around the entrances to lemming burrows, which indicates that they originally were embedded in the material. The shells were analyzed by the amino-acid method and were estimated to be >40 000 years old; they probably are early Wisconsin in age (G.H. Miller, pers. comm., 1977). The shells have not been dated radiometrically but are almost certainly beyond the range of the radiocarbon dating method. The samples indicate that deglaciation and emergence occurred prior to the late Wisconsin. An alternative explanation is that both the wood and shells were transported to the area by late Wisconsin ice and were incorporated into Holocene marine sediments. However, the preservation of the shells as whole valves and the unlikelihood of discovering erratic wood make this alternative much less attractive.

Holocene Marine Limit

The highest marine sediments locally which have yielded fossils of Holocene age coincide in elevation with a pronounced wave-cut notch in the sandstone bedrock at 125 m a.s.l. (Fig. 1 and 6). Shells (**Mya truncata** and **Hiatella arctica**) collected from highly fossiliferous upper foreset sands of a small delta graded to this level were dated at 9270 ± 90 years (GSC-2596). The presence of the notch indicates that the sea stood at this level for a considerably longer period than it did at others. The age of this sample is similar to those of seven other samples from high level Holocene marine features on other parts of the island.

A pit excavated at 100 m a.s.l. at a site downslope from the wave-cut notch showed that thin fossiliferous beach gravels overlie decomposed sandstone bedrock in which the original bedding is still recognizable; a natural stream cut at 13 m a.s.l. exposes Holocene marine sediments overlying 1 m of weathered carbonate bedrock which grades downward to in place bedrock. These buried paleosols presumably record a subaerial weathering interval of considerable duration that likely followed deglaciation and emergence and that preceded a later marine transgression, possibly to the Holocene marine limit. If relative sea level fell below 13 m a.s.l. following deglaciation and later transgressed to 125 m a.s.l.to form the Holocene marine limit, both the initial unloading of early or middle Wisconsin ice and subsequent re-loading of the region (though not necessarily the island) by late Wisconsin ice were separate major events.

Summary

Southern and western Somerset Island were inundated by a foreign ice sheet that flowed onto the island from a major but undefined, and hitherto unrecognized, area of ice dispersal to the west. On the southernmost part of the island this ice was sufficiently thick to inundate summits rising to 500 m elevation and to defy topographic channelling of flow. The ice sheet thinned northward, and in the Stanwell-Fletcher Lake basin ice flow was severely topographically channelled. The ice margin, which is marked by lateral meltwater channels, lay against the western side of the gneissic plateau along the 330 m contour. A lobe of foreign ice flowed into Creswell Bay where it coalesced with the southern edge of the ice cap centred on the northeastern carbonate plateau. The western margin of this latter ice cap, which also is marked by lateral meltwater channels, lay against the eastern side of the gneissic plateau approximately along the 330 m contour. Nested side-hill meltwater channels show that the foreign ice margin receded northwestward in the Stanwell-Fletcher Lake basin and that the local ice cap receded generally northward.

During retreat proglacial deltas were deposited in the sea which was as much as 205 m above present sea level in Creswell Bay. Driftwood from 160 m a.s.l. and shells from a beach ridge at 145 m are beyond the range of radiocarbon dating and are probably of early or middle Wisconsin age — i.e. related to retreat of an early Wisconsin ice load. This is a significant revision of the earlier, and still prevalent, concept that the last major glaciation of the island occurred during the late Wisconsin. If the area was covered by late Wisconsin ice both the wood and shells must be glacial erratics that have been incorporated into marine sediments.

The apparent Holocene marine limit at the mouth of Creswell Bay is marked by a wave-cut notch in bedrock and dates from 9270 ± 90 years B.P. The Holocene marine gravels overlie deeply weathered (disintegrated) bedrock indicating that a marine transgression followed a substantial period of subaerial weathering.

Acknowledgments

Field Work during 1975 and 1977 was supported by the Polar Continental Shelf Project, Department of Energy, Mines and Resources. Capable field assistance was rendered by Robert Helie and Steven Black. The manuscript was read by D.A. Hodgson and R.J. Fulton.

References

Bryson, R.A., Wendland, W.M., Ives, J.D., and Andrews, J.T.
1969: Radiocarbon isochrones on the disintegration of the Laurentide Ice Sheet; Arc. Alp. Res., v. 1, p. 1-14.

CLIMAP
1976: The surface of the ice-age earth; Science, v. 191, p. 1131-1137.

Craig, B.G.
1964: Surficial geology of Boothia Peninsula and Somerset, King William, and Prince of Wales Islands, District of Franklin; Geol. Surv. Can., Paper 63-44, 10 p.

Craig, B.G. and Fyles, J.G.
1960: Pleistocene geology of Arctic Canada; Geol. Surv. Can., Paper 60-10, 21 p.

Dyke, A.S.
1976: Tors and associated weathering phenomena, Somerset Island, District of Franklin; in Report of Activities, Part B; Geol. Surv. Can., Paper 76-1B, p. 209-216.

Jenness, J.L.
1952: Problem of glaciation in the western islands of Arctic Canada; Geol. Soc. Am., Bull., v. 63, p. 939-952.

Netterville, J.A., Dyke, A.S., and Thomas, R.D.
1976a: Surficial geology and geomorphology of Somerset and Northern Prince of Wales Islands; Geol. Surv. Can., Open File 357, 5 photomosaic maps at 1:125 000 scale.

Netterville, J.A., Dyke, A.S., Thomas, R.D., and Drabinsky, K.A.
1976b: Terrain inventory and Quaternary geology Somerset, Prince of Wales and adjacent islands; in Report of Activities, Part A; Geol. Surv., Can., Paper 76-1A, p. 145-154.

Prest, V.K.
1969: Retreat of Wisconsin and Recent ice in North America; Geol. Surv. Can., Map 1257A.

Sugden, D.E.
1968: The selectivity of glacial erosion in the Cairngorm Mountains, Scotland; Inst. Br. Geogr., Trans., v. 45, p. 79-92.

1974: Landscapes of glacial erosion in Greenland and their relations to ice, topographic and bedrock conditions; in Progress in Geomorphology – Papers in honour of D.L. Linton, ed. E.H. Brown and R.S. Waters; Inst. Br. Geogr., Spec. Publ., no. 7, p. 177-193.

1976: Glacial erosion by the Laurentide Ice Sheet and its relationship to ice, topographic and bedrock conditions; Dep. Geogr., Univ. Aberdeen, 86 p.

Sugden, D.E. and Watts, S.H.
1977: Tors, felsenmeer, and glaciation in northern Cumberland Peninsula, Baffin Island; Can. J. Earth Sci., v. 14, p. 2817-2823.

NOTE TO CONTRIBUTORS

Submissions to the *Discussion* section of *Current Research* are welcome from both the staff of the Geological Survey and from the public. Discussions are limited to 6 double-spaced typewritten pages (about 1500 words) and are subject to review by the Chief Scientific Editor. Discussions are restricted to the scientific content of Geological Survey reports. General discussions concerning branch or government policy will not be accepted. Illustrations will be accepted only if, in the opinion of the editor, they are considered essential. In any case no redrafting will be undertaken and reproducible copy must accompany the original submissions. Discussion is limited to recent reports (not more than 2 years old) and may be in either English or French. Every effort is made to include both *Discussion* and *Reply* in the same issue. *Current Research* is published in January, June and November. Submissions for these issues should be received not later than November 1, April 1, and September 1 respectively. Submissions should be sent to the Chief Scientific Editor, Geological Survey of Canada, 601 Booth Street, Ottawa, Canada, K1A 0E8.

TWO MAJOR PROTEROZOIC UNCONFORMITIES, NORTHERN CORDILLERA: DISCUSSION

G.M. Yeo, G.D. Delaney, and C.W. Jefferson
Department of Geology
University of Western Ontario, London, Ontario, N6A 5B7

Manuscript received April 3, 1978

A recent paper "Two major Proterozoic unconformities, northern Cordillera" (Eisbacher, 1978), while presenting valuable new information about the regional stratigraphy of the northern Cordillera and a stimulating "working synthesis" of it, invites a number of important criticisms. In the following discussion we shall comment, first, on the Proterozoic stratigraphy and tectonics of the Wernecke Mountains region, second, on that of the Mackenzie Mountains, and, third, on the nature and significance of the two major Proterozoic unconformities recognized by Eisbacher. Finally we shall propose an alternative correlation between the Proterozoic succession seen in Wernecke Mountains and that of the Mackenzie Mountains.

The Wernecke Assemblage

Both Green (1972) and Bell and Delaney (1977) recognized a threefold subdivision of the lowermost Proterozoic sequence exposed in the Wernecke Mountains (cf. Eisbacher, 1978, p. 54). The lowest subdivision, the Fairchild Lake Group (Delaney, in Young et al., in press; Delaney, in prep.) consists of at least 4000 m of light grey-weathering siltstones which are locally carbonate rich. Conformably overlying the Fairchild Lake Group is the Quartet Group (ibid.) which comprises at least 5000 m of dark grey-weathering shales and siltstones with some sandstone intercalations near the top. The Gillespie Lake Group (ibid.) overlies the Quartet Group with an apparently transitional contact. The Gillespie Lake Group consists of approximately 3000 m of orange to buff weathering dolostone. This sequence has been informally named the "Wernecke supergroup" (ibid.).

Structural trends are north-northeast in the easternmost exposures of the "Wernecke supergroup"; however, the dominant structural trend of these rocks in the Wernecke and Ogilvie mountains is west-northwest (Green, 1972; Delaney, in prep.). Norris and Hopkins (1977) suggested that the local north-northeast trend may be related to differential movement and subsequent rotation along splays or the Knorr Fault. Hence although the structural trend in the type area of the Racklan orogeny (Wheeler, 1954; Gabrielse, 1967; Eisbacher, 1978) is north-northeast, that is not the characteristic structural trend of the "Wernecke Assemblage".

Other features of the "Wernecke supergroup" relevant to regional correlation are: 1) the entire sequence is cut by immense heterolithic breccia complexes (Fig. 1) containing U, Cu, Co, Fe, and Ba mineralization (Bell and Delaney, 1977; Bell, 1978; Delaney et al., in press); 2) most of the "Wernecke supergroup" has been metamorphosed to lower greenschist facies and locally (near the margins of breccia complexes and along fault zones) is at the upper greenschist grade (Young et al., in press; Delaney, in prep.); 3) copper mineralization occurs throughout the Wernecke succession.

Mackenzie Mountains

Proterozoic strata in the Mackenzie Mountains constitute two major sequences informally named (as shown in Fig. 1) the "Mackenzie Mountains supergroup" and the "Ekwi supergroup" (Young et al., in press; Jefferson, in press; Yeo, in press; Young et al., in prep.). The regional stratigraphy and tectonic framework of the sequence have been described by Gabrielse et al. (1973), Aitken et al. (1973), Aitken and Cook (1974a, b), Eisbacher (1976, 1977, 1978), Aitken (1977), Aitken et al. (1978), Young et al. (in press), Young et al. (in prep.) and others. Only those aspects of Eisbacher's recent paper requiring clarification will be discussed below.

The contact between the Redstone River Formation and the underlying Little Dal Formation does not appear to be a major stratigraphic break. A conformable relationship is widely observed (Jefferson, in Young et al., in press; Jefferson, in press). This contact, indicated by Eisbacher (1978, p. 53 and Fig. 12.1) to be an unconformity, is locally "abrupt". We agree with Eisbacher (1978, p. 53) that "contemporaneous faulting and regional arching along northerly to northeasterly trends probably account for most of the rapid facies changes and suggest a pronounced change in tectonic setting in the region during deposition of the Redstone". However, because conformable contacts have been documented between the Little Dal Group and Redstone River Formation, we suggest that the change in sedimentary style and the tectonic phenomena related to this merely reflect the initiation and early pulses of the event which culminated in the Racklan orogeny which is indicated by the major stratigraphic break between the "Mackenzie Mountain supergroup" and the "Ekwi supergroup".

Eisbacher (1978, p. 54) suggested that the major unconformity separating the "Mackenzie Mountains supergroup" and the "Ekwi supergroup" locally occurs within the Sayunei Formation. In the Nite Creek area in Sekwi Mountains he reported that "carbonate strata of the Coppercap Formation and basal buff maroon siltstone of the Sayunei Formation are deformed into large folds and broken by faults...". This is in accord with our observations. We are not convinced however, that "the folds are truncated and overlain with angular unconformity by sharpstone conglomerates...". The crucial feature, the orthoconglomerate that is supposed to truncate the folds, appears to be deformed as well, although not to the same extent. Exposure of this unit is very poor, but it does not appear to be the continuous, sheet-like marker inferred. Rapitan orthoconglomerates are typically lenticular (Eisbacher, 1976, 1978). Two alternative interpretations are offered here. These could be younger (Laramide?) folds involving a more competent carbonate sheet between relatively homogenous, less competent rocks: gypsum below and siltstone above. Eisbacher (1976) described evidence for minor tectonic shear within the silty matrix of Shezal Formation mixtites, a widespread phenomenon. Large amounts of strain could be accommodated in Rapitan sediments by such shearing. This style of deformation is discussed by Johnson (1970) and Johnson and Ellen (1974). They might also be penecontemporaneous, large scale, slump folds. Both large and small scale intraformational folds and slump features are common in all of the units of the Rapitan in which beds competent to act as strain markers can be recognized. In any case, it is difficult to reconcile the dilational tectonic regime proposed by Eisbacher (1976, 1977), and supported by our own observations, with compressional features (Eisbacher, 1978).

From: Discussions and Communications in Current Research, Part B; Geol. Surv. Can., Paper 78-1B.

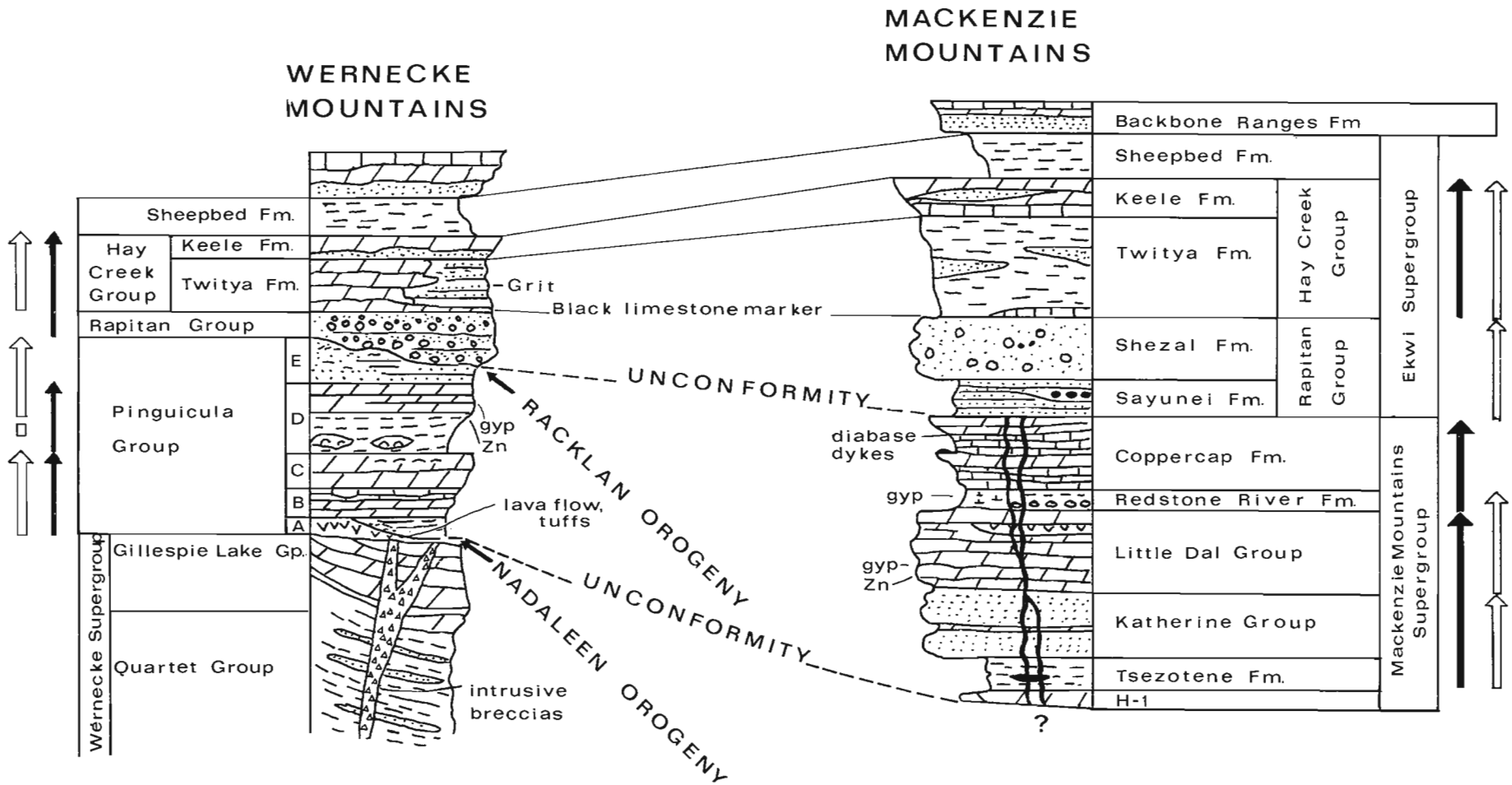

Figure 1. Schematic stratigraphy (after Eisbacher, 1978) of the Proterozoic in Mackenzie Mountains and eastern Wernecke Mountains showing the suggested revised correlation between the two areas. Solid arrows are shallowing upward cycles; open arrows are clastic to carbonate cycles. Note that there are at least two of each of these in both the Pinguicula Group and the "Mackenzie Mountains supergroup".

The Sayunei Formation is defined (Eisbacher, 1978, p. 53) as "a monotonous argillite-siltstone sequence interlayered with lenticular bodies of sharpclast siltstones". Are the maroon mixtites reported earlier (Eisbacher, 1977) from the Lower Rapitan to be excluded? Greenish mixtites occur below the rhythmic argillites in Thundercloud Range (Yeo, in Young et al., in press). It is not made clear that the homotaxial equivalent of the Sayunei Formation in the Snake River area (informally named the Snake River Formation by Yeo, in Young et al., in press) is not at all like the Sayunei described by Eisbacher (1978) but comprises massive and crudely laminated stratified mixtites with minor orthoconglomerate (commonly with rounded clasts), sandstone, and iron formation. These are interpreted as glacial-marine tillites and flow tillites (Ziegler, 1959, Yeo in Young et al., in press; Yeo, in press). It should be emphasized that this is the original type area of the Rapitan Group (Green and Godwin, 1963) although nearly all subsequent descriptions (e.g. Gabrielse et al., 1973; Aitken et al., 1973; Eisbacher, 1976, 1977) and stratigraphic nomenclature are derived from the equivalent rocks far to the southeast.

No convincing evidence for subaerial exposure in the lower Rapitan has ever been reported (polygonal structures found south of the North Redstone River and believed by Gabrielse et al. (1973) to be mudcracks are probably infilled synaeresis cracks similar to structures seen north of the North Redstone). It therefore seems unlikely that sandstone and conglomerate lenses in the lower Rapitan south of Rapitan Creek "could represent environments of braided rivers" (Eisbacher, 1978, p. 55), especially when these occurrences are down-basin (Eisbacher, 1977, Fig. 46.9) from the glacial marine mixtites mentioned above. A submarine channel origin is preferred.

In his discussion of the Rapitan basin, Eisbacher (1978, p. 57) indicated that the Shezal Formation represents a regional glaciation. Nowhere is it made clear that the Sayunei Formation was also deposited under glacial conditions as is indicated by a host of features including glacial-marine tillites, dropstones, striated clasts, till pellets, and till balls (Ziegler, 1959; Young 1976; Yeo in Young et al., in press).

Although it is not impossible that the eustatic sea level changes recorded in the Keele and Sheepbed formations might be due to glaciation (perhaps the second late Precambrian glacial event reported in Australia, Scandinavia, and other parts of the world), it strains credulity to call upon a glacial mechanism to explain this without any lines of supporting evidence (e.g. glacial features in stratigraphically equivalent rocks). By this argument any sea level changes might reflect the waning and waxing of glaciers and the entire stratigraphic record could be one of continuous glaciation somewhere else!

The reasoning behind Eisbacher's (1977; 1978, Fig. 12.1) inclusion of the Keele Formation within the Rapitan Group has not been made explicit. We concur that since the Twitya siltstones and the Keele Formation interfinger and are at least partly facies-equivalent, it is reasonable to group them together. We suggest, however, that a new group be created for this purpose and the name "Rapitan Group" be used in its original sense (Green and Godwin, 1963) to include only the mixtites, mudstones, conglomerates, and iron formation. We suggest that the Twitya and Keele formations (and their equivalents, if any, to the west) be included in the Hay Creek Group (Yeo, in press). Examination of the development of stratigraphic nomenclature for the youngest Proterozoic sequence of Mackenzie Mountains (Table 1) makes it apparent that the Twitya siltstones were included in the Rapitan for mapping convenience (Grabrielse et al., 1973, p. 20) since no other explanation for the expansion of the Rapitan Group from Green and Godwin's (1963) original usage was given. If Eisbacher's proposed second expansion of the Rapitan Group is accepted we shall have an unusual sequence comprising two very distinctive and unrelated sedimentary assemblages, one representing a glaciation and the other a shallowing upwards cycle, in which at least local unconformity separates every formation, but excluding the Sheepbed Formation which lies conformably above it!

Proterozoic unconformities

The type area for the Racklan orogeny is in the northeastern part of the Rackla Range of the Wernecke Mountains, where the Pinguicula Group (Eisbacher, 1978) unconformably overlies the "Wernecke supergroup". This unconformity was first described by Wheeler (1954) but he was uncertain of the ages of the units concerned and did not name it. Gabrielse (1967, p. 275) equated the stratigraphic discordance described by Wheeler with the unconformity between the Rapitan and older strata in the Mackenzie Mountains. He named the event associated with both unconformities, the Racklan orogeny. In all subsequent usage, the unconformity below the Rapitan is considered to be the expression of the Racklan orogeny (Douglas, 1970; Wheeler and Gabrielse, 1972; Stewart, 1972, 1976; and others). The equating of the Racklan orogeny with the East Kootenay orogeny, the tectonic event preceding deposition of the glaciomarine Toby Formation in the southern Canadian Cordillera, is also firmly entrenched in the literature (Douglas, 1970; Gabrielse, 1972; Monger et al., 1972; Harrison et al., 1974; Stewart, 1976; and others). Thus, although the type locality of the Racklan orogeny is an area in which the Pinguicula Group unconformably overlies deformed "Wernecke supergroup" rocks, the term "Racklan orogeny" has always been used to denote a younger tectonic event marked by the unconformity between rocks of the Rapitan Group and the "Mackenzie Mountains supergroup". Since this is firmly entrenched usage, we advocate retaining the term "Racklan orogeny" in its accepted sense. We suggest the name "Nadaleen orogeny" (Young et al., in prep.) for the tectonic disturbance responsible for the older unconformity between the Pinguicula Group and the "Wernecke supergroup" which is exposed in the Nadaleen map area (Blusson, 1974).

Regional correlation

Based upon the preceding discussion, a revised stratigraphic correlation between the Proterozoic sequences of the Wernecke and Mackenzie mountains is proposed in Figure 1. The lowest succession in the Wernecke Mountains, the "Wernecke supergroup", consists of fine grained clastics conformably overlain by dolostones. These rocks have been metamorphosed to at least lower greenschist facies. Heterolithic, mineralized breccias cut the entire "Wernecke supergroup". The main structural trend of this succession is west-northwest and the event responsible for this deformation, which includes overturned strata, is the "Nadaleen orogeny". In the eastern Wernecke Mountains, rocks of the "Wernecke supergroup" are unconformably overlain by those of the Pinguicula Group (Eisbacher, 1978). We support Blusson's proposal (pers. comm. to Jefferson, 1978) that the Pinguicula Group can be correlated with the entire "Mackenzie Mountains Supergroup", rather than just the Redstone River and Coppercap formations. Unlike the "Wernecke supergroup", the "Mackenzie Mountains supergroup" is virtually unmetamorphosed; it is not cut by mineralized intrusive breccia complexes; nor does it exhibit the intense structural deformation of the "Wernecke supergroup". In addition, the Pinguicula Group has many characteristics which support comparison with the "Mackenzie Mountains supergroup". Both contain sulphates and zinc-bearing carbonates and both contain at least two shallowing upwards cycles of the sort described by Eisbacher (1976) for the "Mackenzie Mountains supergroup". The major fold event, here called the "Nadaleen orogeny", which separates

Table 1
Development of stratigraphic nomenclature for the Upper Proterozoic
Mackenzie Mountains, Yukon, and Northwest Territories

Lithologic Unit (Thickness)	Ziegler (1959)	Green and Goodwin (1963)	Gabrielse et al. (1965)	Upitis (1966)	Gabrielse (1967)	Gabrielse et al. (1973)	Eisbacher (1976)	Eisbacher (1978)	Yeo (in press)	
Shale (760 m)			Unit 9	Unit 9		Sheepbed	Sheepbed	Sheepbed	Sheepbed	
Ss., ls., dol., sh., cgl. (610 m)			Unit 8	Unit 8		Keele	Keele	Keele	Keele (Hay Creek Group)	Ekwi Supergroup
Shale (1170 m)			Unit 7	Upper (Rapitan Group)	?—?	Upper (Rapitan Group)	"Shale" (Rapitan Group)	Twitya (Rapitan Group)	Twitya (Hay Creek Group)	
Grey Mixtite (775 m+)	Bonnet Plume R. Tillite	Rapitan Group		Middle	Rapitan Formation	Middle	"Diamictite"	Shezal	Shezal (Rapitan Group)	
Maroon Mixtites etc. (750 m+)	Snake River Tillite			Lower		Lower	"Maroon"	Sayunei	Sayunei	

Historical development of the stratigraphic nomenclature for the Upper Proterozoic sequence in Mackenzie Mountains.
It is suggested here and elsewhere (Yeo, in press) that

1. the "Rapitan Group" be restricted, following Green and Godwin's (1963) original usage, to include only the glacigene units,
2. a new group, the Hay Creek Group, to include the Keele and Twitya formations, be recognized, and
3. that the entire upper Proterozoic sequence of Mackenzie Mountains be included in the "Ekwi supergroup" (Young et al., in press; Yeo, in press).

This revised stratigraphic nomenclature corresponds to the principal natural subdivisions, both stratigraphic and tectono-stratigraphic, of the uppermost Proterozoic in Mackenzie Mountains.

the "Wernecke supergroup" and the Pinguicula Group in the Wernecke Mountains can hardly be equated with the local unconformity between the Redstone River Formation and the Little Dal Group in the Mackenzie Mountains, especially since the latter must lie closer to the basin margin!

Eisbacher (1978, p. 57) suggested that the presence of copper in the lower part of the Pinguicula Group (Hart River showing) and in the Redstone and Coppercap formations supported his correlation. He also noted, however, the occurrence of "copper mineralization in Little Dal Group, ...Sayunei Formation, and Keele Formation...". Copper mineralization is also known in the Katherine Group (Blusson, pers. comm. to Jefferson, 1978) and Shezal Formation, and throughout the Wernecke supergroup". The widespread copper mineralization in Proterozoic rocks of the northern Cordillera does not support any particular correlation. The comment that the Redstone copper showings are "stratabound only in a very broad sense" (Eisbacher, 1978, p. 57), since copper occurs throughout the Proterozoic succession, makes a mockery of the term, "strata-bound" (A.G.I. Glossary, 1972) and the relevance of this though to the rest of the paper is unclear. Not only are the principal Redstone showings strata-bound, but they are stratiform (Jefferson in Delaney et al., in press; Jefferson, in press).

The correlation given here is a tentative one pending more detailed description of the Pinguicula Group.

Conclusion

Reasonable alternative interpretations can be made of the Proterozoic succession in the northern Cordillera. There appear to be three major sequences (Young et al., in prep.) separated by two major unconformities as observed by Eisbacher (1978). The sequences from oldest to youngest are: the "Wernecke supergroup", the Mackenzie Mountains supergroup-Pinguicula Group, and the "Ekwi supergroup". It is suggested that the events separating them be called the Nadaleen and Racklan orogenies respectively. It is recommended that the Rapitan be redefined to include only the lower two glacigene formations (Sayunei and Shezal formations) and that the Twitya and Keele formations be included in a new group, the Hay Creek Group.

Acknowledgments

Each of the authors has been involved in a stratigraphic study of a part of the Proterozoic succession discussed above for the past two or more years: G.D. Delaney on the Wernecke Supergroup, C.W. Jefferson on the Redstone and Coppercap formations and Little Dal Group, and G.M. Yeo on the Rapitan Group. We thank J.D. Aitken, R.T. Bell, S.L. Blusson, G.E. Eisbacher, D.K. Norris, J. Ruelle, and G.M. Young for past discussions which have led us to our present views.

References

Aitken, J.D.
1977: New data in correlation of the Little Dal Formation and a revision of Proterozoic map-unit "H5"; in Report of Activities, Part A, Geol. Surv. Can., Paper 77-1A, p. 131-135.

Aitken, J.D. and Cook, D.G.
1974a: Geology of parts of Mount Eduni (106A) and Bonnet Plume (106B) map-areas, District of Mackenzie; Geol. Surv. Can., Open File Report 221.

1974b: Carcajou Canyon map-area (96D), District of Mackenzie; Geol. Surv. Can., Paper 74-13.

Aitken, J.D., Macqueen, R.W., and Usher, J.L.
1973: Reconnaissance studies of Proterozoic and Cambrian stratigraphy, lower Mackenzie River area (Operation Norman), District of Mackenzie; Geol. Surv. Can., Paper 73-9, 178 p.

Aitken, J.D., Long, D.G.F., and Semikhatov, M.A.
1978: Progress in Helikian stratigraphy, Mackenzie Mountains; in Current Research, Part A, Geol. Surv. Can., Paper 78-1A, p. 481-484.

Bell, R.T.
1978: Breccias and uranium mineralization in the Wernecke Mountains, Yukon Territory - a progress report; in Current Research, Part A, Geol. Surv. Can., Paper 78-1A, p. 317-322.

Bell, R.T. and Delaney, G.D.
1977: Geology of some uranium occurrences in Yukon Territory; in Report of Activities, Part A, Geol. Surv. Can., Paper 77-1A, p. 33-37.

Blusson, S.L.
1974: Nadaleen River map-area of Operation Steward; Geol. Surv. Can., Open File no. 205.

Delaney, G.D.
Stratigraphy of the Wernecke Supergroup, Yukon Territory. (in prep.)

Delaney, G.D., Jefferson, C.W., Yeo, G.M., McLennan, S.M., Bell, R.T., and Aitken, J.D.
Some Proterozoic sediment-hosted metal occurrences of the northeastern Canadian Cordillera; Society of Economic Geologists, Couer d'Alene Field Conference, Wallace, Idaho, Nov. 3-5, 1977. Idaho Bureau of Mines Special Publication. (in press)

Douglas, R.J.W.
1970: Geology and Economic Minerals of Canada; Geol. Surv. Can., Econ. Geol. Rep. 1, 838 p.

Eisbacher, G.H.
1976: Proterozoic Rapitan Group and related rocks, Redstone River area, District of Mackenzie; in Report of Activities, Part A, Geol. Surv. Can., Paper 76-1A, p. 117-125.

1977: Tectono-stratigraphic framework of the Redstone Copper belt, District of Mackenzie; in Report of Activities, Part A, Geol. Surv. Can., Paper 77-1A, p. 229-234.

1978: Two major Proterozoic unconformities, northern Cordillera; in Current Research, Part A, Geol. Surv. Can., Paper 78-1A, p. 53-58.

Gabrielse, H.
1967: Tectonic evolution of the northern Canadian Cordillera; Can. J. Earth Sci., v. 4, p. 271-298.

1972: Younger Precambrian of the Canadian Cordillera; Am. J. Sci., v. 272, p. 521-536.

Gabrielse, H., Roddick, J.A., and Blusson, S.L.
1965: Flat River, Glacier Lake, and Wrigley Lake, District of Mackenzie and Yukon Territory; Geol. Surv. Can., Paper 64-52, 30 p.

Gabrielse, H., Blusson, S.L., and Roddick, J.A.
1973: Geology of Flat River, Glacier Lake, and Wrigley Lake map-areas, District of Mackenzie and Yukon Territory; Geol. Surv. Can., Mem. 366, 153 p.

Green, L.H.
1972: Geology of Nash Creek, Larsen Creek and Dawson map-areas, Yukon Territory; Geol. Surv. Can., Mem. 364, 157 p.

Green, L.H. and Godwin, C.I.
1963: Snake River area. Mineral industry of the Yukon Territory and southwestern District of Mackenzie; Geol. Surv. Can., Paper 63-38, p. 15-18.

Harrison, J.E., Criggs, A.B., and Wells, J.D.
1974: Tectonic Features of the Precambrian Belt Basin and their Influence on Post Belt Structures; U.S. Geol. Surv. Prof. Paper 866, 15 p.

Jefferson, C.J.W.
Stratigraphy and sedimentology, Upper Proterozoic Redstone Copper Belt, Mackenzie Mountains, N.W.T. - a preliminary report; in Mineral Industry Report 1975, Northwest Territories. Indian and Northern Affairs Economic Geology Series 1979.

Johnson, A.M.
1970: Physical Processes in Geology; Freeman, Cooper and Co., San Francisco, 577 p.

Johnson, A.M. and Ellen, S.D.
1974: A theory of concentric, kink, and sinusoidal folding and of monoclinal flexuring of compressible elastic multilayers; Tectonophysics, v. 21, p. 301-339.

Monger, J.W.H., Souther, J.G., and Gabrielse, H.
1972: Evolution of the Canadian Cordillera: a plate tectonic model; Am. J. Sci., v. 272, p. 577-602.

Norris, D.K. and Hopkins, W.S.
1977: The Geology of the Bonnet Plume Basin, Yukon Territory; Geol. Surv. Can., Paper 76-8, 20 p.

Stewart, J.H.
1972: Initial deposits in the Cordilleran geosyncline: evidence of a late Precambrian (850 m.y.) continental separation; Geol. Soc. Am., Bull., v. 83, p. 1345-1360.

1976: Late Precambrian evolution of North America: plate tectonics implications; Geology, v. 4, p. 11-15.

Upitis, U.
1966: The Rapitan Group, southwestern Mackenzie Mountains, Northwest Territories; unpubl. M.Sc. thesis, McGill University, Montreal, 70 p.

Wheeler, J.O.
1954: A Geological Reconnaissance of the Northern Selwyn Mountains Region, Yukon and Northwest Territories; Geol. Surv. Can., Paper 53-7.

Wheeler, J.O. and Gabrielse, H.
1972: The Cordilleran structural province; in Price, R.A. and Douglas, R.J.W. (ed.), Variations in Tectonic Styles in Canada, Geol. Assoc. Can., Spec. Paper 11, p. 1-81.

Yeo, G.M.
Iron-formation in the Rapitan Group, Mackenzie Mountains, Yukon and Northwest Territories; in Mineral Industry Report 1975, Northwest Territories. Indian and Northern Affairs Economic Geology Series 1979.

Young, G.M.
1976: Iron-formation and glaciogenic rocks of the Rapitan Group, Northwest Territories, Canada; Precam. Res., v. 3, p. 137-158.

Young, G.M., Jefferson, C.W., Long, D.G.F., Delaney, G.D., and Yeo, G.M.
Upper Proterozoic stratigraphy of northwestern Canada and Precambrian history of North American Cordillera; Society of Economic Geologists, Couer d'Alene Field Conference, Wallace, Idaho, Nov. 3-5, 1977. Idaho Bureau of Mines Special Publication. (in press)

Young, G.M., Jefferson, C.W., Delaney, G.D., and Yeo, G.M.
Precambrian evolution of the North American Cordillera. (in prep.)

Ziegler, P.A.
1959: Fruhpalaozoische tillite im ostlichen Yukon-Territorium (Kanada); Eclogae Geologicae Helvetiae, v. 52, p. 735-741.

AUTHOR INDEX